Ghent University
Faculty of sciences
Department for Organic Chemistry
Laboratory for Organic and Bio-organic Synthesis

Mimicking 1,5-benzodiazepine-2,4-diones, a modular approach on solid-phase

Fréderique Backaert

Promotor: Prof. Dr. Johan Van der Eycken

Academic year: 2015-2016

Dissertation submitted in fulfillment of the requirements for the degree of
Doctor of Philosophy in Science: Chemistry

Members of the examination committee

Reading committee

Dr. Jurgen Caroen (Ghent University)
Prof. Dr. Annemieke Madder (Ghent University)
Prof. Dr. Igor Opsenica (University of Belgrade)

Examination committee

Chair:
Prof. Dr. José Martins (Ghent University)

Other members:
Dr. Jurgen Caroen (Ghent University)
Prof. Dr. Annemieke Madder (Ghent University)
Prof. Dr. Igor Opsenica (University of Belgrade)
Prof. Dr. Kourosch Abbaspour Tehrani (University of Antwerp)
Prof. Dr. Erik Van der Eycken (Catholic University of Leuven)
Prof. Dr. Johan Van der Eycken (Ghent University)

Dankwoord

Dit werk kwam tot stand na vele jaren hard werken, sommige periodes verliepen vlot, andere periodes wat minder. Toch kwam dit werk niet alleen tot stand door “hard werk” van de auteur, maar is dit werk een samenspel van heel wat mensen die hier rechtstreeks of onrechtstreeks aan meegeholpen hebben. Naast een persoonlijke *dankjewel* verdienen al deze mensen om in dit werk vereeuwigd te worden.

Eerst en vooral gaat een woord van dank uit naar mijn ouders. Dankzij jullie ondernemende ingesteldheid ben ik in staat geweest dit project aan te vangen én te volbrengen. Bovendien hebben jullie mij steeds gesteund in mijn studies en hebben jullie me *alle* kansen gegeven om deze tot een succes te brengen.

Professor Johan Van der Eycken wil ik uiteraard ook bedanken voor de steun en kansen die ik kreeg bij aanvang én gedurende dit doctoraatsonderzoek. Doch enkel het *harde* resultaat van mijn onderzoek vervat is in het werk hiernavolgend, is er ook een groot aandeel aan *zacht* resultaat, die mij een volledig ander en completer persoon heeft gemaakt.

Uiteraard verdient Pieter meer dan één woord van dank! Het mag gezegd dat zonder Pieter dit werk en onderzoek nooit zou tot stand gekomen zijn, zeker omdat hij net de connectie tussen prof. Van der Eycken en mezelf mogelijk maakte. Naast de ontelbare gezamenlijke werkuren in het labo zullen me de pauzes en bijhorende gesprekken bijblijven. Deze waren een moment van decompressie, creëerden oplossingen voor grote of kleine problemen, waren gewoon een klein moment van ontspanning,… Daarnaast leerde je me de lat steeds opnieuw hoger te leggen en zorgde dat ik mijn focus (of “dé kern van de zaak”) niet uit het oog verloor! Bedankt!

De vele collega’s van het labo An, Ine, Rosa, Jelle, Karel-Simon, Timoty, Katrien, Timothy, Dries, Nick, Bo, Sam, Pieter, Xenia, Heba én Mohammed creëerden een ontspannen sfeer en uiterst aangename werkomgeving. In het bijzonder wil ik Jurgen bedanken voor de

vele inspirerende gesprekken, peptalk (bij mindere momenten) en leuke samenwerking gedurende de vele jaren. Daarnaast wil ook alle master en bachelor studenten, vanuit binnen- en buitenland bedanken voor hun bijdrage aan dit werk. Bovendien verdient ook Jan Goeman een expliciete vermelding voor de behandeling van de vele (lees: oneindig vele) LC-MS stalen. Vaste-fase synthese zonder LC-MS analyse is uitermate moeilijk én tijdrovend. Jouw flexibiliteit gecombineerd met een no-nonsense aanpak en technische kennis zorgde voor vlotte resultaten én een *continu* werkend machinepark.

Daarnaast wil ik ook Veerle, Paul, Karine, Tom D. en Tom P. bedanken voor jullie administratieve en immer belangrijke ondersteunde diensten. Bovendien werp ik graag Dieter, Tim en prof. José Martins een woord van dank toe voor hun knap werk rond atropoisomerie. Vele experimenten zijn voorafgegaan aan wat in dit werk voorgesteld wordt. Nogmaals dank voor deze fijne samenwerking.

Als laatste wil ik vrienden en vriendinnen, (schoon)familie, huidige collega's én in het bijzonder, mijn partner Frederick bedanken voor het geduld en steun van de voorbije maanden én jaren. Vooral jij, Frederick, mag nu gerust ademhalen, het waren lastige en vermoeiende laatste maanden met weinig tijd voor elkaar maar deze zijn eindelijk voorbij. Dank je om vol te houden, we kunnen nu terug samen leukere dingen doen!

Fréderique Backaert

februari 2016

Preface

The work here presented, entitled "Mimicking 1,5-benzodiazepine-2,4-diones, a modular approach on solid-phase", represents the result of a four and a half year research project initiated in September 2008 at the laboratory for organic and bio-organic synthesis of prof. dr. Johan Van der Eycken at Ghent University, Belgium.

After tossing the idea of a new scaffold design in the initial days of the project, which was based on the well-known class of 1,5-benzodiazepine-2,4-diones with an incorporated 1,2,3-triazole as a mimick of a *cis*-amide. Shortly afterwards, an ambitious strategy for a solid-phase synthesis was established. This approach encompassed three crucial steps including firstly a broad applicable azide introduction on solid-phase, secondly a regioselective introduction of an 1,5-disubstituted 1,2,3-triazole moiety and thirdly a clean and efficient release of the cyclized final product from the resin.

This manuscript consists of five parts whereas the introduction provides an thorough study of the relevant literature on the four major topics of this research project including medicinal chemistry, combinatorial chemistry, bioisosterism and click chemistry. The aim and strategy part encompasses a concise description of the proposed solid-phase strategy and possible diversifications. The third part discusses, thematically, the performed research both the successes and concurrent failures of this work. The final chapter of the third part comprises the conclusion of this work which allows the reader to have a clear view on the entire work and clear links for further detailed reading.

If the reader would like to verify experimental procedures or reproduce parts of this work practically, the fourth part contains the supporting information to this work. Still, I would like emphasize specific safety aspects with respect to the explosive nature of azides, especially in dichloromethane containing solvent systems. Additionally, possible formation of hydrazoic azide should always to be taken into account. Proper literature

reading, careful handling of azide derivatives and treatment of azide solutions in fume hoods is strongly recommended.

The final, fifth, part of this work focusses on conformational aspects of the molecules synthesized throughout this work. I decided to categorize these two chapters as an appendix, as the work was only initiated at the end of the research and only initial steps were taken into this specific research field. Additionally, the work illustrated in these chapters is the result of extensive NMR spectra recording by the NMR and Structure Analysis research group of prof. dr. José Martins.

At last, I hope that you will enjoy reading this manuscript and that I may inspire other young chemists, after reading this work, to continue further exploration of the chemical space around the benzodiazepine motif based on a solid-phase chemistry approach.

Fréderique Backaert

February 2016

Content

Part 1: Introduction

PART 1: INTRODUCTION

I. Medicinal chemistry

A. History of drug discovery – privileged structures

Until the 1980s, information on drug targets at the molecular level was scarce and drug development was mostly driven by data obtained from pharmacological screenings. These tests were performed on a relatively small scale leading to only few pharmacological models with (if successful) an eventual outcome of one single clinical candidate. Screening, either random or directed, was a low throughput, labor-intensive process and usually directed to the identification of drug rather than lead candidates. At the end of the 1980s, a screening capacity of hundred samples a week was considered as high-throughput.[1] Overall, the process of drug discovery 'then' was slow and operated from a relatively small knowledge.

In the last decades, drug discovery moved to another focus due to advances in molecular biology, molecular informatics, combinatorial chemistry and automation of synthesis methods. Furthermore, tools including advances in synthetic, analytical and purification technologies are available. Therefore many thousands of compounds can be synthesized and screened rapidly, yielding more leads which eventually give rise to a higher number of clinical candidates.[1]

Despite the theoretically appealing image of the concurrence of new synthetic approaches and high-throughput screening (HTS), it became rapidly clear that these techniques did not fulfill the highly anticipated results. More specifically, the disappointment was the final outcome of the applied techniques, due to their immaturity and inability to make the right compounds[2,3]. Moreover, as the library members lacked structural diversity and had poor physicochemical properties, some might conclude that there was no rational library design[4].

> *"In general, the libraries were produced with an eye towards overall quantity, rather than quality."*[4]

Libraries, containing bioactive natural product-based members, overcame the low hit-rate problem but failed however generating a novel biological response, as these natural product-based collections were simple analogues or homologs of the parent natural product[4,5].

An alternative for the latter could be provided by creating collections of unique, highly potent small molecules addressing biological targets and therefore managing new and already existing diseases. The initial step towards this alternative approach was given by Ariëns and co-workers[6], who noted the presence of hydrophobic double-ring systems in many biogenic amine antagonists. Furthermore, they observed multiple actions of those frameworks and related this effect to the inherent conformational flexibility, therefore recognizing the presence of recurring structural units in many receptor ligands.

Almost a decade later, in 1988, Evans and colleagues[7] studied intensively the 1,4-benzodiazepine scaffold as selective and orally effective cholecystokinin antagonists. Apart from this activity, they found the ability of these structures to bind to gastrin and central benzodiazepine receptors. The diversity in observed biological activity was the launch of a quest towards an easier discovery of lead compounds by using the principles of *privileged structures*. This term was introduced by Evans defining privileged structures as motifs which:

> *"are capable of providing useful ligands for more than one receptor and that judicious modification of such structures could be a viable alternative in the search for new receptor agonists and antagonists."*[7]

The exploration of privileged structures in drug discovery is a rapidly emerging theme in medicinal chemistry. Molecules described as privileged structures are structural motifs capable of interacting with a variety of unrelated molecular targets and are typically constrained, heterocyclic multi-ring systems capable of orienting varied substituent patterns in a well-defined 3D space.[7,8,9] As the medicinal chemist needs to provide more hits in a reasonable time, the privileged structure framework, allows him to discover more biologically active compounds across a broad range of therapeutic targets.

B. Drug-likeness vs. lead-likeness

Another problem of the designed libraries in the late 1980s is the drug-likeness of the synthesized compounds. *In vitro* HTS allowed assays to be performed in solvents like DMSO therefore ignoring the insoluble nature of the specific compound in aqueous media. This tends to shift the HTS hits towards more lipophilic and generally less soluble profiles, whereas the majority of drugs are intended for oral therapy and hence need to be water soluble. Introducing oral availability in the library design is not straightforward nor predictable and hit optimization towards oral availability is time- and resource-consuming.

To counteract this downside of high-throughput screening, a computational analysis of more than 2000 existing drug and candidate drugs in clinical trials towards several physico-chemical parameters was performed by Lipinski.[10] The results illustrated in most cases a strong relation between oral availability and the studied physicochemical parameters. Moreover, a clear preference for oral bioavailability was found towards small, lipophilic compounds. These findings were formulated by the Lipinski's "rule of five" for small molecular frameworks as[i]:

> *"Poor absorption or permeation are more likely when:*
> *There are more than 5H-bond donors;*
> *The molecular weight is over 500;*
> *The clogP is over 5;*
> *There are more than 10 H-bond acceptors."*

This famous mnemonic provides a guideline for medicinal chemists in order to make a prevalidation of the proposed synthetic library which can prevent compound failure during clinical trials. Generally, library members are avoided which violate at least two of the above rules of five.

Further adjustments needed to be made as medicinal chemists tend to increase molecular weight and lipophilicity during the lead optimization[11], giving rise to final drug candidates which do not fulfill the rule of five anymore. Therefore a scaled-down "rule of three" creates freedom for lead optimization within the (orally available) druggable space. This rule of three aims to select hits which obey to the following guidelines:

> *"a molecular weight lower than 300;*
> *the number of H-bond donors and acceptors for both is lower or equal to three;*
> *a clogP value is smaller than three."* [12]

C. Examples of privileged structures

1. 1,4-Benzodiazepine-2-ones

Benzodiazepines, more specifically 1,4-benzodiazepine-2-ones have been the subject of study for over more than 70 years and have been the key example of privileged structures. Although Evans first coined the term "privileged structures" in 1988, the philosophy of this concept started a few years earlier with the synthesis of nonpeptidal antagonists of the cholecystokinin peptide hormone.[13] Metabolically stable peptide analogs had already been designed but lacked physicochemical properties such as oral bioavailability. Evans based his research on the naturally occurring asperlicin **I.1** which was reported as a modest CCK-antagonist.[14] By looking for the elements in asperlicin **I.1** which might be responsible for the

[i] This rule of thumb is derived from results which can be associated with 90% of orally active drugs that have achieved phase II clinical phase.

activity, Evans recognized constructive elements including a 1,4-benzodiazepine moiety (Diazepam, **I.2**) and an L-tryptophan **I.3** side chain.

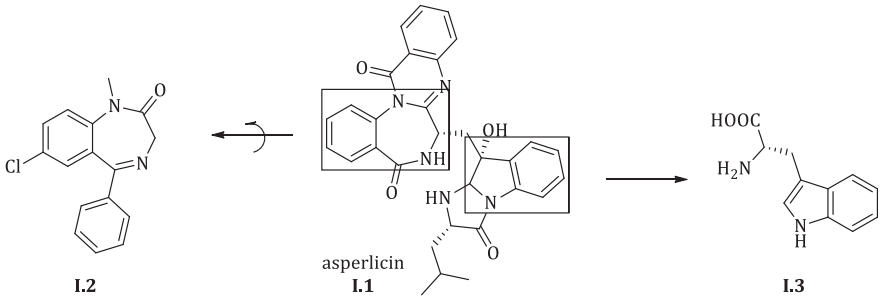

Figure I-1:Natural compound asperlicin (I.1) and its composed elements suggested by Evans

The benzodiazepine scaffold was earlier profoundly reported by Sternbach[15] as an anxiolytic, hypnotic and antiepileptic agent. This comprehensive study lead to the commercialization of multiple drugs such as diazepam **I.2**, oxazepam **I.4**, flurazepam **I.5**, clorazepate **I.6**, clonazepam **I.7**, lorazepam **I.8** and prazepam **I.9**.

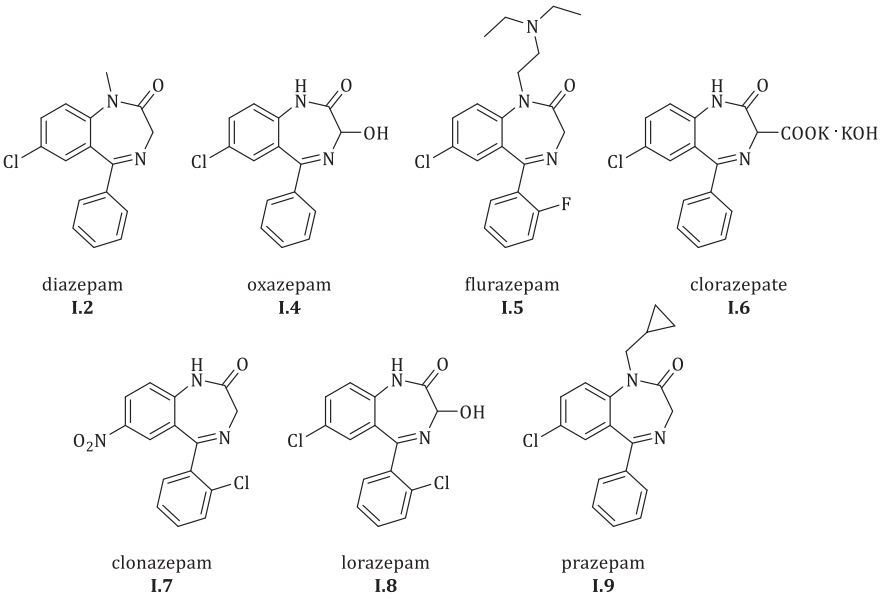

Figure I-2: Sternbach's initial library of benzodiazepines

Besides this report, others[16] also stressed the versatility and high effectiveness of this moiety as a peptide receptor ligand. Based on this ability and the assumption that there are common features of structure and conformation among peptides, Evans pursued the development of the improved CCK-antagonist with the 1,4-benzodiazepine template. Therefore acknowledging this framework for the first time as a "privileged structure". Eventually, this

research lead successfully to the synthesis of a library containing more than 120 members of 3-substituted 1,4-benzodiazepine-2-ones with **I.10** as a promising, highly potent, orally effective, non-peptidic antagonist for CCK-A peptide hormone.[7,17]

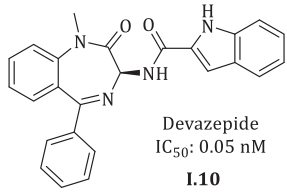

Devazepide
IC_{50}: 0.05 nM
I.10

Besides the pioneering work and vision of Evans, other groups also contributed to the exploration of the benzodiazepine scaffold and its privileged abilities.[3,18] Additionally to the mentioned anxiolytic, hypnotic and antiepileptic activities[15], highly selective cholecystokinin (CCK) receptor subtype A[13,19] **I.10**, and subtype B[18,20] **I.11** antagonists, *κ*-selective opiate agonists[21] **I.12**, HIV Tat antagonists[22] **I.13**, ras farnesyltransferase inhibitors[23] **I.14**, endothelin receptor antagonists[24] (ERA) **I.15**, platelet-activating factor (PAF) antagonists[25] **I.16**-**I.17**, HIV-1 reverse transcriptase inhibitors[26] **I.18** and glycoprotein (IIbIIIa) inhibitors[27] **I.19** were discovered.

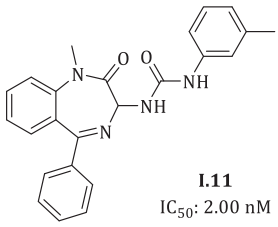

I.11
IC_{50}: 2.00 nM

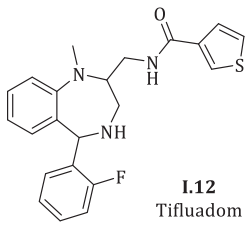

I.12
Tifluadom

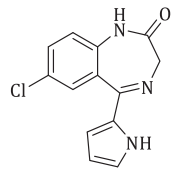

I.13
Ro5-3335

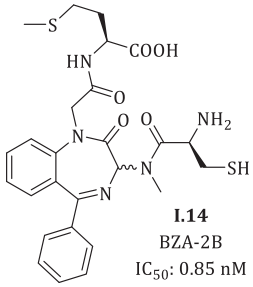

I.14
BZA-2B
IC_{50}: 0.85 nM

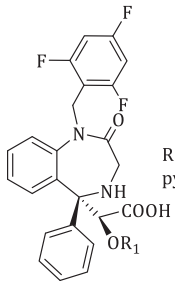

R_1 = 4,6-$(H_3C)_2$-2-pyrimidine
I.15

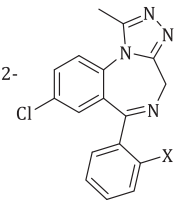

I.16
X=H
Alprazolam

I.17
X=Cl
Triazolam

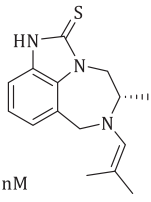

I.18
R82150
IC_{50}: 0.028 nM

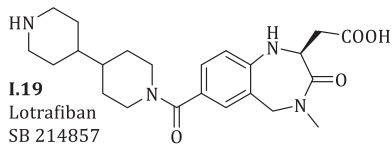

I.19
Lotrafiban
SB 214857

Figure I-3: Examples of the 1,4-benzodiazepine framework as privileged structure I.11 - I.19

2. 1,4-Benzodiazepine-2,5-diones

Another subset of the benzodiazepine class are the collection of the 1,4-benzodiazepine-2,5-diones. This second class shows interesting diverse biological activity as anxiolytics, antitubercular agents[28] **I.20**, histone deacetylase (HDAC) inhibitors[29] **I.21**, antithrombotics[30] **I.22**. Even more, they function as opiate receptor antagonists[31], anticonvulsant agents[32], CCK antagonists[33] or as promising herbicides[34] **I.23**.

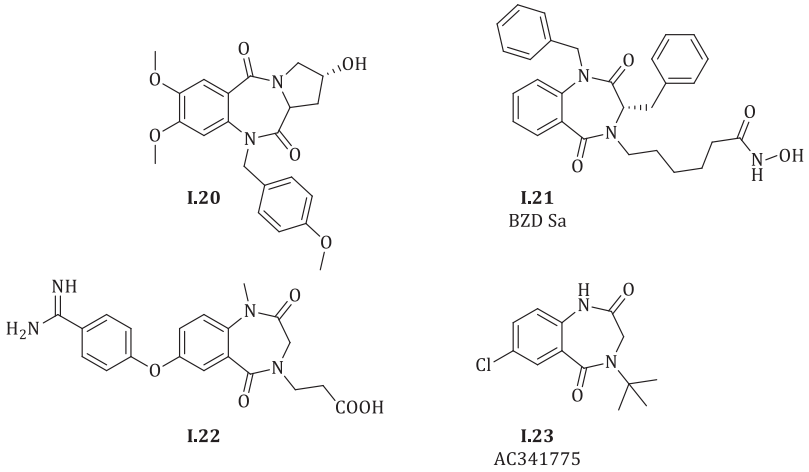

I.20 **I.21** BZD Sa

I.22 **I.23** AC341775

Figure I-4: Examples of the 1,4-benzodiazepin-2,5-dione framework as privileged structure I.20 – I.23

3. 1,5-Benzodiazepine-2,4-diones

A third, much less studied class based on the benzodiazepine motif are the 1,5-benzodiazepine-2,4-diones, also seen as a privileged scaffold. For example, clobazam[35] **I.24** and triflubazam[36] **I.25** have been used clinically as anxiolytic agents, 3-phenyl-1,5-dihydrobenzo[*b*]1,5-diazepin-2,4-dione **I.26** as inhibitor of HIV-1 capsid assembly[37] and 1-adamantyl-1-methyl-3-(arylaminocarbonyl)amino-2,4-dioxo-5-phenyl-2,3,4,5,-tetrahydro-1*H*-1,5-benzodiazepine **I.27** as cholecystokinin-B receptor antagonist[38].

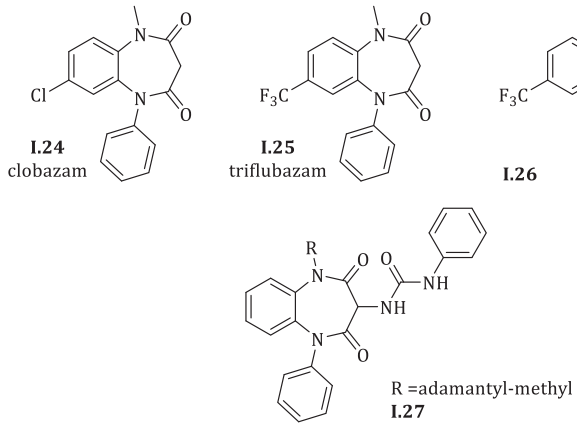

Figure I-5: Examples of the 1,4-benzodiazepin-2,5-dione framework as privileged structure I.24 – I.27

Apart from the three classes mentioned above, other classes have been synthesized by varying the positions of the nitrogen within the seven-membered ring such as 2,3-benzodiazepines[39] **I.28**. Furthermore, replacements of benzene moiety creates new classes with active members, doing so thieno-[40] **I.29**, pyrido-[41], imidazolobenzodiazepines[42] **I.30** were synthesized leading to new active compounds.

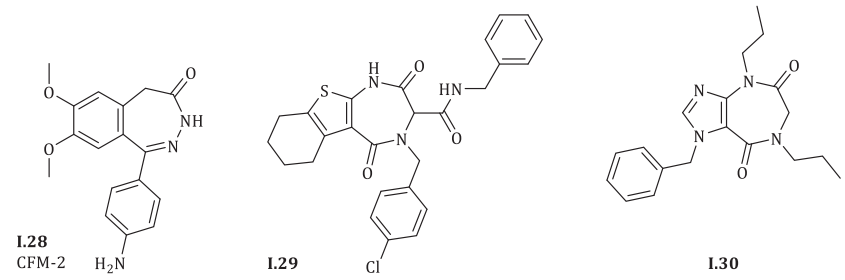

Figure I-6: 2,3-Benzodiazepine I.28 and isosteric replacement of benzene moieties I.29 – I.30

From a synthesis point of view, numerous synthesis methods have been developed, yet Bunin and Ellman[43] were the first to prepare benzodiazepines on solid-phase. Besides the novelty of creating a library of benzodiazepines using a solid support, they also extended the scope of solid-phase chemistry from peptide-like compounds to small organic molecules. Initially, they were able to construct a library containing 192 members.

D. Privileged structures based on natural products

Detailed study of active natural product skeletons have led to the identification of synthetically straightforward template molecules, which could be elaborated in a combinatorial way to create diversity oriented libraries in solution- or on solid-phase. For example, the 2,2-dimethylbenzopyran moiety **I.31** is claimed as a privileged structure as this

subunit is present in more than 4000 compounds including natural products and designed structures with diverse biological activity.[8] The advances in chemical biology demand increased collections of natural product-like small molecules. Due to the complexity, difficult isolation and extensive structure elucidation of natural products as such, these libraries based on a natural product motif could be a solution to provide rapidly the demanded compounds for high-throughput screening. Even more, the idea of using natural product-like libraries for finding new ligands for known or recently discovered targets is justified by the fact that natural products have undergone evolutionary selection for binding to specific protein domains which might enhance the hit rate hence the quality of the libraries.[3]

> *"the natural product-like compounds produced in diversity oriented synthesis have a much better shot at interacting with the desired molecular targets and exhibiting interesting biological activity."*[3]

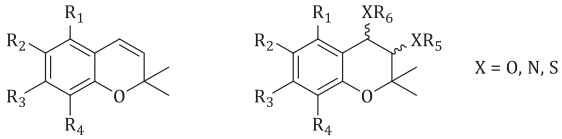

Figure I-7: Benzopyran I.31 as privileged structure and late-stage modification possibilities I.32

Nicolaou and co-workers presented in a trilogy of reports[8,44a,44b] the synthesis of a 10000-membered natural product-like library based on the benzopyran moiety **I.31** paying attention to diversity and biological applications. Not only the numerous occurrence of this moiety with a wide range of corresponding biological activities but also the degree of functionalization and rigidity of the scaffold made this *the* privileged structure to work on. As the solid-phase synthesis included incorporation of multiple aromatic rings and a wide range of functional groups, good physicochemical and drug-like properties (*vide supra*) can be addressed to the produced compounds. Thanks to the present olefin, post modification could lead to further functionalized compounds **I.32**.

An initial high-throughput antibacterial screening of one of the libraries showed that a number of members were found to be active towards several Methicillin-Resistant *Staphylococcus aureus* (MRSA)[ii] strains. Further modification led to compound **I.33** which demonstrated to be a novel benzopyran-based antibacterial agent, highly active towards MRSA strains.[45]

Apart from the antibacterial screening, other testing results discovered a farnesoid X receptor[iii] (FXR) activation for certain hits[46]. After a full SAR study, four different classes of

[ii] Methicillin-Resistant *Staphylococcus aureus* or multi-drug resistant *Staphylococcus aureus* (MRSA) are bacteria responsible for disease which are difficult to treat due to the resistivity of these strains towards β-lactam antibiotics.

[iii] Farnesoid X Receptor (FXR) is a transcriptional sensor for bile acids which are the primary product of cholesterol metabolism.

new FXR agonists were introduced, among them the most potent to FXR activators reported to date. An example of a lead structure for FXR activation is **I.34**, based on the benzopyran moiety named by Nicolaou as *fexachloramide*.

Both examples presented in **Figure I-8** clearly illustrate the importance and effectiveness of natural product-based collections of compounds able to show affinity towards a diverse field of biological targets.

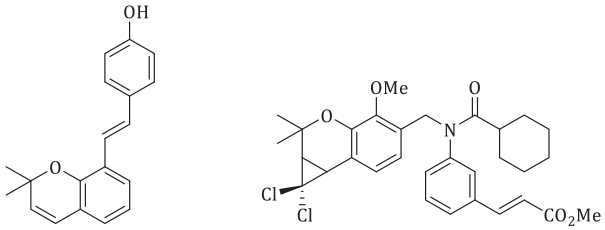

I.33 **I.34**
ED_{50}: 0.188 μM

Figure I-8: Benzopyran based antibacterial agent I.33 and fexachloramide I.34

Other examples[47] of natural product-based libraries include synthesis of olomoucine-based compounds **I35**, in general a purine template collection, leading to a potent cyclin-dependent kinase (CDK) inhibitor **I.36** by Norman[48a] and Gray[48b]; the sesterpene dysidiolide **I.37** is a natural product found in marine sponge *Dysidea etheria* and was the first known natural inhibitor of the dual-specificity phosphatase enzyme Cdc25A[49]. Several groups[50] were able to establish libraries of this compound using this specific molecular framework. Compound **I.38**, synthesized by Waldmann,[50b] is a 6-fold more potent Cdc25A inhibitor than **I.37**.

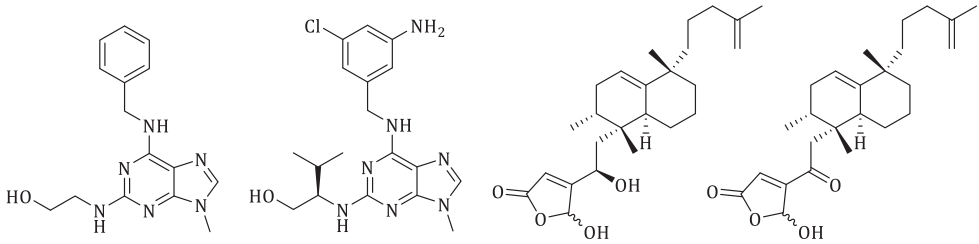

I.35 Olomoucine **I.36** **I.37** Dysidiolide **I.38**

Figure I-9: Other examples of natural product-based libraries

REFERENCES

[1] a) Proudfoot, J. R. High-Throughput Screening and Drug Discovery. In *The practice of Medicinal Chemistry*; Wermuth, C. G., Ed.; Elsevier: London, **2008**; pp. 144-155. b) Triggle, D. J. Overview: The Search for Biologically Useful Chemical Space. In *The practice of Medicinal Chemistry*; Wermuth, C. G., Ed.; Elsevier: London, **2008**; pp. 517-531.

[2] Horton, D. A.; Bourne, G. T.; Smythe, M.L. *Chem. Rev.* **2003**, *103*, 893-930.

[3] Breinbauer, R.; Vetter, I.; Waldmann, H. *Angew. Chem. Int. Ed.* **2002**, *41*, 2878-2890.

[4] Welsch, M. E.; Snyder, S. A.; Stockwell, B. R. *Curr. Opin. Chem. Biol.* **2010**, *14*, 1-15.

[5] Burke, M.D.; Schreiber, S. L. *Angew. Chem. Int. Ed.* **2004**, *43*, 46-58.

[6] Ariëns, E. J.; Beld, A. J.; Rodrigues de Miranda, J. F.; Simonis, A. M. In *The Receptors A Comprehensive Treatise*; O'Brien, R. D., Ed.; Plenum Press: New York, **1979**; p 33.

[7] Evans, B. E.; Rittle, K. E.; Bock, M. G.; DiPardo, R. M.; Freidinger, R. M.; Whitter, W. L.; Lundell, G. F.; Veber, D. F.; Anderson, P. S.; Chang, R. S. L.; Lotti, V. J.; Cerino, D. J.; Chen, T. B.; Kling, P. J.; Kunkel, K. A.; Springer, J. P.; Hirshfieldt, J. *J. Med. Chem.* **1988**, *31*, 2235-2246.

[8] Nicolaou, K. C.; Pfefferkorn, J. A.; Roecker, A. J.; Cao, G.-Q.; Barluenga, S.; Mitchell H. J. *J. Am. Chem. Soc.* **2000**, *122*, 9939-9953.

[9] Polinsky, A. Lead-likeness and Drug-likeness. In *The practice of Medicinal Chemistry*; Wermuth, C. G., Ed.; Elsevier: London, **2008**; pp. 244-253.

[10] Lipinksi, C. A.; Lombardo, F.; Dominy, B. W.; Feeney, P. J. *Adv. Drug. Del. Rev.* **1997**, *23*, 3-25.

[11] Teague, S. J.; Davis, A. M.; Leeson, P. D.; Oprea T. *Angew. Chem. Int. Ed.* **1999**, *38*, 3743-3748.

[12] Congreve, M.; Carr, R.; Murray C.; Jhoti H. *Drug. Disc. Today* **2003**, *8*, 876-877.

[13] Evans, B. E.; Bock, M. G.; Rittle, K. E.; DiPardo, R. M.; Whitter, W. L.; Veber, D. F.; Anderson, P. S.; Freidinger, R. M. *Proc. Natl. Acad. Sci. U.S.A.* **1986,** *83*, 4918-4922.

[14] Chang, R. S.; Lotti, V. J.; Monaghan, R. L; Birnbaum, J.; Stapley, E. O.; Goetz, M. A.; Albers-Schönberg, G.; Patchett, A. A.; Liesch, J. M.; Hensens O. D. *Science* **1985**, *230*, 177-179.

[15] Sternbach, L. H. *J. Med. Chem.* **1979**, *22*, 1-7.

[16] a) Guidotti, A.; Furchetti, C. M.; Corda, M. G.; Konkel, D.; Bennett, C. D.; Costa, E. *Proc. Natl. Acad. Sci. USA* **1983**, *80*, 3531-3533. b) Alho, H.; Costa, E.; Ferrero, P.; Fujimoto, M.; Cosenza-Murphy, D.; Guidotti, A. *Science* **1985**, *229*, 179-182.

[17] Josselyn, S.A.; Franco, V.P.; Vaccarino, F.J. *Physicopharmacology* **1996**, *123*, 131-143.

[18] Kees, K. L.; Cheeseman, R. S.; Prozialeck, D. H.; Steiner, K. E. *J. Med. Chem.* **1989**, *32*, 13-16.

[19] Bunin, B. A.; Plunkett, M. J.; Ellman, J. A. *Proc. Natl. Acad. Sci. U.S.A.* **1994**, *91*, 4718-4712.

[20] Bock, M. G.; DiPardo, R. M.; Evans, B. E.; Rittle, K. E.; Whitter, W. L.; Veber, D. F.; Anderson, P. S.; Freidinger, R. M. *J. Med. Chem.* **1989**, *32*, 13-16.

[21] Römer, D.; Buschler, H. H.; Hill, R. C.; Maurer, R.; Petcher, T. J.; Zeugner, H.; Benson, W.; Finner, E.; Milkowski, W.; Thies, P. W. *Nature* **1982**, *298*, 759-760.

[22] a) Hsu, M. C.; Schutt, A. D.; Holly, M.; Slice, L. W.; Sherman, M. I.; Richman, D. D.; Potash, M. J.; Volsky, D. J. *Science* **1991**, *254*, 1799-1802. b) Hsu, M.-C.; Schutt, A. D.; Holly, M.; Slice, L. W.; Sherman, M. I.; Richman, D. D.; Potash M. J.; Volsky, D. J. *Biochem. Soc. Trans.* **1992**, *20*, 525-531.

[23] James, G. L.; Goldstein, J. L.; Brown, M. S.; Rawson, T. E.; Somers, T. C.; McDowell, R. S.; Crowley, C. W.; Lucas, B. K.; Levinson, A. J.; Masters, J. C. *Science* **1993**, *260*, 1937- 1942.

[24] Bolli, M. H.; Marfurt, J.; Grisostomi, C. *J. Med. Chem.* **2004**, *47*, 2776–2795.

[25] Kornecki, E.; Ehrlich, Y.H.; Lenox. R. H. *Science* **1984**, *226*, 1454-1456.

[26] a) Pauwels, R.; Andries, K.; Desmyter, J.; Schols, D.; Kukla, M. J.; Breslin, H. J.; Raeymaeckers, A.; Van Gelder, J.; Woestenborghs, R.; Heykants, J.; Schellekens, K.; Janssen, M. A. C.; Clercq, E. D.; Jansen, P. A. J. *Nature* **1990**, *343*,

470-474. b) Pauwels, R.; Andries, K.; Debyser, Z.; Kukla, M.J.; Schols, D.; Desmyter, J.; Clercq, E. D.; Jansen, P. A. J. *Biochem. Soc. Trans.* **1992**, *20*, 509-512.

[27] Samanen, J. M.; Ali, F. E.; Barton, L. S.; Bondinell, W. E.; Burgess, J. L.; Callahan, J. F.; Calvo, R. R.; Chen, W.; Chen, L.; Erhard, K.; Feuerstein, G.; Heys, R.; Hwang, S.-M.; Jakas, D. R.; Keenan, R. M.; Ku, T. W.; Kwon, C.; Lee, C.-P.; Miller, W. H.; Newlander, K. A.; Nichols, A.; Parker, M.; Peishoff, C. E.; Rhodes, G.; Ross, S.; Shu, A.; Simpson, R.; Takata, D.; Yellin, T. O.;Uzsinskas, I.; Venslavsky, J. W.; Yuan, C.-K.; Huffman, W. F. *J. Med. Chem.* **1996**, *39*, 4867–4870.

[28] Kamal, A.; Reddy, K. L.; Devaiah, V.; Shankaraiah, N.; Reddy, G. S. K.; Raghavan, S. *J. Comb. Chem.* **2007**, *9*, 29–42.

[29] Loudni, L.; Roche, J.; Potiron, V.; Clarhaut, J.; Bachmann, C.; Gesson, J.-P.; Tranoy-Opalinski, I. *Bioorg. Med. Chem. Lett.* **2007**, *17*, 4819-4823.

[30] a) McDowell, R. S.; Blackburn, B. K.; Gadek, T. R.; McGee, L. R.; Rawson, T.; Reynolds, M.; Robarge, K. D.; Somers, T. C.; Thorsett, E. D.; Tischler, M.; Webb, R. R.; Venuti, M. C. *J. Am. Chem. Soc.*, **1994**, *116*, 5077-5083. b) Robarge, K.D.; Dina, M.S.; Somers, T.C.; Lee, A.; Rawson, T. E.; Olivero, A.G.; Tischler, M.H.; Webb II, R. R.; Weese, K. J.; Aliagas, I.; Blackburn B. K.; *Bioorg. Med. Chem.* **1998**, *6*, 2345-2381.

[31] Carabateas, P. M.; Harris, L. S. *J. Med. Chem.* **1966**, *9*, 6-10.

[32] Cho, N. S.; Song, K. Y.; Parkanyi, *J. Heterocycl. Chem*. **1989**, 26, 1807-1810.

[33] Aquino, C. J.; Dezube, M.; Sugg, E. E.; Sherrill, R. G.; Willson, T. M.; Szewczyk, J. R. *Int. Pat. Appl.* WO 9528399.

[34] a) Karp. G. M. *J. Org. Chem.* **1995**, *60*, 5814-5819. b) Singh, B.K.; Szamosi, I. T.; Dahlke, B. J.; Karp, G. M.; Shaner, D. L. *Pestic. Biochem. Physiol.* **1996**, *56*, 62-68.

[35] Kruse, H. *Drug Dev. Res.* **1982**, *2*, 145-151.

[36] Nicholson, A. N.; Stone, B. M.; Clarke, C. H. Br. *J. Clin. Pharmacol.* **1977**, *4*, 567-572.

[37] Fader, L. D.; Bethell, R.; Bonneau, P.; Bös, M.; Bousquet, Y.; Cordingly, M. G.; Coulombe, R.; Deroy, P.; Faucher, A.-M.; Gagnon, A.; Goudreau, N.; Grand-Maître, C.; Guse, I.; Hucke, O.; Kawai, S.H.; Lacoste, J.-E.; Landry, S.; Lemke, C. T.; Malenfant, E.; Mason, S.; Morin, S.; O'Meara, J.; Simoneau, B.; Titolo, S.; Yoakim, C. *Bioorg. Med. Chem. Lett*. **2011**, *21*, 398-404.

[38] Ursini, A.; Capelli, A. M.; Carr, R. A. E.; Cassara, P.; Corsi, M.; Curcuruto, O.; Curotto, G.; Cin, M. D.; Davalli, S.; Donati, D.; Feriani, A.; Finch, H.; Finizia, G.; Gaviraghi, G.; Marien, M.; Pentassuglia, G.; Polinelli, S.; Ratti, E.; Reggiani, A.; Tarzia, G.; Tedesco, G.; Tranquillini, M. E.; Trist, D. G.; Van Amsterdam, F. T. M. *J. Med. Chem.* **2000**, *43*, 3596-3613.

[39] a)Bevacqua, F.; Basso, A.; Gitto, R.; Bradley, B.; Chimirri, A. *Tetrahedron Lett.* **2001**, *42*, 7683-7686. b) Rosaria, G.; Barreca, M. L.; De Luca, L.; De Sarro, G.;Ferreri, G.; Quartarone, S.; Russo, E.; Constanti, A.; Chimirri, A. *J. Med. Chem.* **2003**, *46*, 197-200.

[40] Huang, Y.; Wolf, S.; Bista, M.; Meireles, L.; Camacho, C.; Holak, T. A.;Dömling, A. *Chem. Biol. Drug. Des.* **2010**, *76*, 116-129.

[41] El Bouakher, A.; Laborie, H.; Aadil, M.; El Hakmaoui, A.; Lazar, S.; Akssira, M.; Viaud-Massuard, M. C. *Tetrahedron Lett.* **2011**, *52*, 5077-5080.

[42] Daly, J. W.; Hide, I.; Brindson, B. K. *J. Med. Chem.* **1990**, *33*, 2818-2821.

[43] Bunin, B. A.; Ellman, J. A. *J. Am. Chem. Soc.* **1992**, *114*, 10997-10999.

[44] a) Nicolaou, K. C.; Pfefferkorn, J. A.; Mitchell, H. J.; Roecker, A. J.; Barluenga, S.; Cao, G.-Q.; Alleck, R. L.; Lillig, J. E. *J. Am. Chem. Soc.* **2000**, *122*, 9954-9967. b) Nicolaou, K. C.; Pfefferkorn, J. A.; Barluenga, S.; Mitchell H. J.; Roecker, A. J.; Cao, G.-Q. *J. Am. Chem. Soc.* **2000**, *122*, 9968-9976.

[45] Nicolaou, K. C.; Roecker, A. J.; Barluenga, S.; Pfefferkorn, J. A.; Cao, G.-Q. *ChemBioChem* **2001**, *2,* 460-465.

[46] Nicolaou, K. C.; Evans, R. M.; Roecker, A. J.; Hughes, R.; Downes, M.; Pfefferkorn, J. A. *Org. Biomol. Chem* **2003**, *1,* 908-920.

[47] Koch, M. A.; Waldemann, R. *Drug. Discov. Today* **2005**, *10*, 471-483.

[48] a) Norman, T. C.; Gray, N. S.; Koh, J.; Schultz, P. G. *J. Am. Chem. Soc.* **1996**, *118*, 7430-7431. b) Gray, N. S.; Wodicka, L.; Thunnissen, A.-M. W. H.; Norman, T. C.; Kwon, S.; Espinoza, F. H.; Morgan, D. O.; Barnes, G.; LeClerc, S.; Meijer, L.; Kim, S. H.; Lockhart, D. J.; Schultz, P. G. *Science* **1998**, *281*, 533-538.

[49] Demeke, D.; Forsyth, C. J.; *Tetrahedron* **2002**, *58*, 6531–6544.

[50] a) Brohm, D.; Metzger, S.; Bhargava, A.; Müller, O.; Lieb, F.; Waldmann, H. *Angew. Chem. Int. Ed.* **2002**, *41*, 307-311. c) Brohm, D.; Philippe, N.; Metzinger, S.; Bhargava, A.; Müller, O.; Lieb, F.; Waldmann, H. *J. Am. Chem. Soc.* **2002**, *124*, 13171-13178. b) Lyon, M. A.; Ducruet, A. P.; Wipf, P.; Lazo, J. S. *Nat. Rev. Drug. Discov*. **2002**, *1*, 961-976 (and references therein).

II. Combinatorial chemistry

A. Introduction

In the last decades, medicinal chemistry changed tremendously. More than thirty years ago, the medicinal chemist and his pharmacologist counterpart were the main drivers of the research project. The potential lead compounds, based on creativity and intuition, were synthesized in solution in gram quantities to be provided to the pharmacologist. As only little was known about the detailed biological targets and mechanisms involved in most diseases, the pharmacologist generally used animal *in vivo* models, therefore needing a large amount of product. Apart from this lack of knowledge, commercially available starting materials and methodology related to synthesis, analysis and purification were limited, leading to very time-consuming syntheses with a confined number of products that could be screened. As the biological evaluation took only a short time, the rate to discover new chemical entities was completely determined by the more time-consuming synthesis[1] (**Figure II-1).**

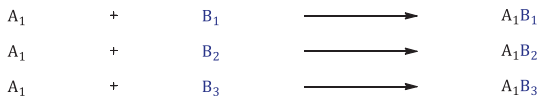

Figure II-1: Conventional synthesis

The development of a high-throughput synthesis method could supply this entreated higher input of new compounds. Geysen[2] encountered this problem in 1984 with an innovative method for peptide and oligonucleotide synthesis *via* a pin shaped solid support. Based on this approach, other groups continued and expanded this idea towards other chemistries such as proteins, synthetic oligomers, small molecules and oligosaccharides. It was not until the early 1990s that the term “combinatorial chemistry” was first used.

The basic principle of a combinatorial based synthesis is a simultaneous preparation of a large number of different compounds. Comparing to the conventional method, a combinatorial approach enables synthesis of collections within a short time (**Figure II-2**).

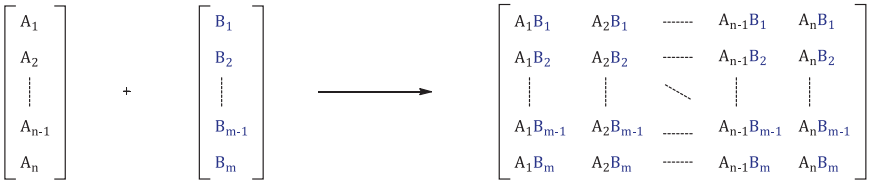

Figure II-2: Combinatorial synthesis

As can be seen in **Figure II-2**, a simple combinatorial synthesis results in a large matrix or library with *n* x *m* members by assembling all possible combinations of building blocks A and B. New lead compounds can be prepared either as *one compound* in *one vessel* by "*parallel synthesis*"[3,4] or as mixtures in the same reaction vessel with the "*split-mix*"[5] method.

Parallel synthesis introduced by Lam[3], applicable for both in solution and for solid-phase bound strategies, comprises a straightforward sequence of steps yielding a compound which identity is easy tractable and predictable due to the spatial separation (*one compound – one vessel*).

Using a *split-mix* or *split-pool* method, specifically designed for solid-phase chemistry (**Figure II-3)**, several compounds are made in one reactor. The synthesis starts with splitting up the resin bound starting material in *n* equal portions and each of these are individually reacted with a different single reagent. After completion of the reaction and work-up, the individual portions are recombined. Subsequently, the *n* resin bound intermediates are mixed again and divided in equal portions, whereas the following reaction can start. The whole process may then be repeated until all reaction steps are completed. The size of the library is easily determined as the product of the number of building blocks of each type that are used in each synthesis step.

Notwithstanding the high speed synthesis of a large number of compounds *via* parallel synthesis or a split-mix method, the screening can be performed with a single compound or with the whole mixture. If a mixture is used and whenever a hit is found, the characterization of the actual active compound is compulsory, yet somewhat sluggish. This includes a time-consuming deconvolution process, which involves iterative rounds of retrosynthesis and screening of library subsets to find the active compound. Even more, it could be possible that the observed activity is an accumulation of weak activities of all compounds present in the mixture, in which case the deconvolution process leads to a disappointing result. Another possibility to identify the lead compound is tagging[i,6].

[i] The information which directly related to the identity of the active compound is present on the resin in the form of a tag or label. This tag can be based on an oligonucleotide or peptide sequence which has orthogonal

It can be concluded that the combination of privileged structures with the power of combinatorial chemistry to prepare large sets of diverse compounds around a common chemical motif should allow a faster identification of new agonists, antagonists or inhibitors for new members of a known receptor or enzyme biological family[7].

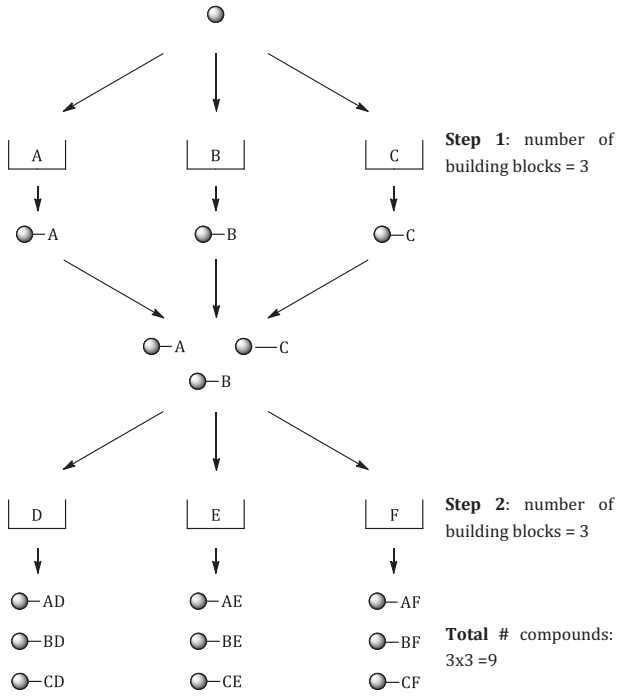

Figure II-3: Split-mix or split-poolmethod

B. Solid-phase chemistry

> *"I have never been able to reconstruct the moment when the idea came to me, but probably it was at night, just as other ideas often come into one's head. It was obviously a result of having recognized a direct need and having thought about the general problems for some weeks. ... Although I cannot recall the exact time I had the idea, I do know when I recorded the basic concept in my notebook: May 26th 1959..."*
>
> *Bruce Merrifield*

In the 1940s-1960s, solution-phase techniques and reagents for the synthesis of small biologically active peptides were well established. Nevertheless, the synthesis of longer peptide chains dealt with a lot of difficulties. Solubility of the reactants and purification of the

chemistry compared to the desired library members. Additionally, tags based on 'unique' mass encoding or radiofrequency encoding are known.

intermediates or final product, became more and more challenging with a growing peptide chain. Bruce Merrifield reported in 1963, a new ground-breaking and Nobel-prize winning method for peptide synthesis, introducing solid-phase peptide synthesis[ii] as:

> *"the stepwise addition of protected amino acids to a growing peptide chain which is bound by a covalent bond to a solid resin particle. This provides a procedure whereby reagents and by-products are removed by filtration, and the recrystallization of intermediates is eliminated."* [8a]

This new concept of chemical synthesis was refreshing by means of purification as simply dissolving excess reagents or by-products was required and time-consuming recrystallization steps were avoided. Moreover, this approach created a new view on chemistry in general as solid-phase synthesis enables an automation process, which can be subdivided as:

- attachment of starting material;
- repetitive or consequent reactions;
- cleavage of final product.

To perform an efficient solid-phase synthesis two elements have to be chosen rationally, the solid support and the linker which connects the substrate and the solid-phase *via* a connection point (**Figure II-4**). A spacer, which creates a defined distance between the solid support and the linker to avoid sterical hindrance, can also be incorporated, but will not be discussed further as this element can be comprised in the linker.

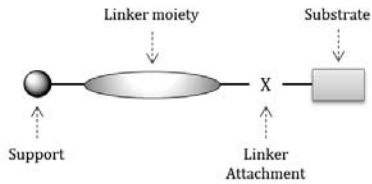

Figure II-4: Schematic representation of a solid-phase structure.

1. Solid support

The choice of solid-phase or solid support is crucial for a successful solid-phase strategy. Since Merrifield introduced solid-phase peptide synthesis (SPPS), by using a chloromethylated polystyrene lightly cross-linked with divinylbenzene, the use of polymers to facilitate synthesis and product purification has become widespread. Even more, types of non-organic solid supports (such as cotton[9], glass[10],…) and non-cross-linked (PEG, PE, PS,…) polymers have been developed. In this work only the cross-linked polymer-based solid-supports will be discussed in more detail.

[ii] Despite the fact that the term "solid-phase synthesis" is commonly used, "matrix-assisted synthesis" is suggested to be more precise as the polymers used are not generally solids. Nevertheless, within this work the term solid-phase chemistry will be used as such.

Solid-phase synthesis, an efficacious course of chemical transformations on an inert polymeric support, is influenced by the physicochemical nature of the polymer at the following five levels:[11]

a) Microscopic structure and morphology

As the chemical modifications of the substrate occur within the polymer-matrix, an efficient penetration of the reagents to the reactive sites is compulsory. This accessibility is mainly determined by the pore-size and porosity of the polymer-matrix. These aspects of microscopic structure and morphology are controlled during the manufacturing process (e.g. suspension polymerization). Pore-size and porosity combined with the swelling degree (*vide infra*) of a polymer in a specific solvent will have an important effect on the reaction rate.

b) Cross-linking and matrix structure

The frequency of cross-linking bridges between the polymer chains determines, in the first instance, the mechanical strength and to which extent the cross-linked polymer swells in the solvent of choice for a specific chemical transformation. However, the overall polymer robustness and swelling degree are also strongly related to the noncovalent interactions (e.g. aromatic π - π stacking, H-bonding), the equivalent length of un-cross-linked polymer chains, and matrix morphology.

As purification of the reactions is performed *via* a washing procedure, thus by using solvents which only dissolve excess reagents and possible by-products, the resin has to remain solid at all times. Even more, a stable physical form and mechanical stability are required to enable automation and to circumvent filtration problems. As most polymers are soluble in a selected range of organic solvents, the use of cross-linked polymers is therefore a must for a good practice of solid-phase chemistry. A frequently used cross-linking agent for polyalkene-based resins is divinylbenzene.

c) Polymer-solvent compatibility

Expansion of the polymeric network or swelling degree in a specific solvent is pivotal for the reaction rate occurring in the heart of the cross-linked matrix, as it enables accessibility towards the reactive sites. Insights of the swelling degree are obtained by looking at the relationship between the chemical structure of the polymer and the solvent. Polystyrene-based resins form a very tight network of aromatic interactions within the matrix, and the swelling in a given solvent is determined by the feasibility of the solvent to interrupt these aromatic interactions in the matrix. For polystyrene, mostly apolar solvents such as dichloromethane give arise to an optimal swelling. In **Table II-1**, a representation of commonly used polymer resins and their corresponding swelling degree in specific solvents is made.[11,12]

d) Polymer-substrate compatibility

As mentioned in previous paragraphs, the polystyrene matrix is held together by aromatic, nonpolar interactions, which have an effect on the reaction rates of the chemical transformations. In the case of peptide synthesis on polystyrene resin, constructing a relatively nonpolar sequence (e.g. leucine, valine, phenylalanine) will proceed smoothly, however amino acids bearing polar residues (e.g. glycine, asparagine) will suffer difficulties while approaching the reactive site(s). This problem rises as strongly polar sequences have no effective compensating H-bonding or aromatic interactions, eventually leading to a low degree of peptide-polymer interactions. Accordingly, strong polar peptide sequences on polystyrene can only interact with themselves, which leads to folding of the sequence and eventually to inaccessible reactive sites. Extensive research has been performed to create grafted polymers in order to provide amphiphilic characteristics (TentaGel, ArgoGel, …).[13]

e) Presence of attachment points

As a solid-phase synthesis strategy implies reagents modifying a substrate or intermediate on a resin an attachment point for a first building block onto the matrix is required. During the manufacturing process, a comonomer is added to impose a diversity in the polymer sequence, which enables future reactivity. In order to fine-tune this reactivity according to the applied strategy, a linker is attached to increase the specificity of the resin.

Table II-1: Swelling properties for four resins (volume in mL/g dry resin)

Solvent	**Wang**[a] (low loading)	**TentaGel**[b] S RAM	**MBHA**[c] neutralized	**PDMA**[d]
NMP	6.4	4.4	7.2	-
THF	6.0	4.0	7.2	-
CH_2Cl_2	5.4	5.6	7.6	9.5
DMF	5.2	4.4	5.6	9.1
Toluene	4.0	3.6	6.4	-
THF/H_2O (1/1)	2.8	5.2	4.4	-
MeOH	1.6	3.6	1.2	12
H_2O	1.6	3.6	2.2	9

[a]*p*-hydroxybenzyl alcohol functionalized PS resin. [b]amphiphilic resin: PS derivatized with PEG units combined with rink amide linker. [c] PS modified with 4-MethylBenzHydrylAmine [d]polydimethyl-acrylamide

2. Linkers

Apart from the choice of solid support, the choice for an appropriate linker is pivotal for a successful solid-phase synthesis strategy. Although there is a wide diversity in solid supports, the variety in attachment points is restricted (mostly limited to aliphatic or benzylic -OH, $-NH_2$ or -Cl). The attachment of a linker to the solid-phase prior to substrate could overcome this problem and create a wide range of custom-made solid-phase resins tailored to the applied strategy. This linker or adapter will allow attachment of all kinds of starting material and guarantee an efficient release whenever needed. As a requirement, the linker must resist all applied conditions during the synthesis to avoid premature cleavage.

a) Linker as a bifunctional protecting group

The connection between the solid-phase and the linker is obviously permanent during the synthesis and the cleavage step of the final product. Therefore, the unit resin – linker can be seen as an insoluble, immobilizing, protecting group for solid-phase synthesis. The bond between the linker and the substrate or final product has to be cleaved in a selective manner, without final product degradation.

b) Types of linkers

Since solid-phase chemistry was originally designed for peptide synthesis using a *limited* number of possible coupling conditions and side-chain deprotection reactions on solid-phase, a *limited* number of linkers was sufficient in order to create a lot of different peptides. When solid-phase peptide synthesis evolved towards organic synthesis of (small) non-peptidic molecules, the available linkers were incompatible with the broad range of chemical transformations. Therefore, new linkers were developed in order to cover a wide range of chemical reactions on solid-phase.[14] In **Figure II-5**, an attempt for classification according to the remaining functionality on the released product is made. Doing so, a division between classical, traceless, multifunctional linker units and cleavage *via* cyclization/release is achieved.[15] Due to the broad nature of multifunctional linkers (including photocleavable linkers, safety-catch linkers, ...) only classical, traceless and cleavage *via* cyclization/release will be discussed.

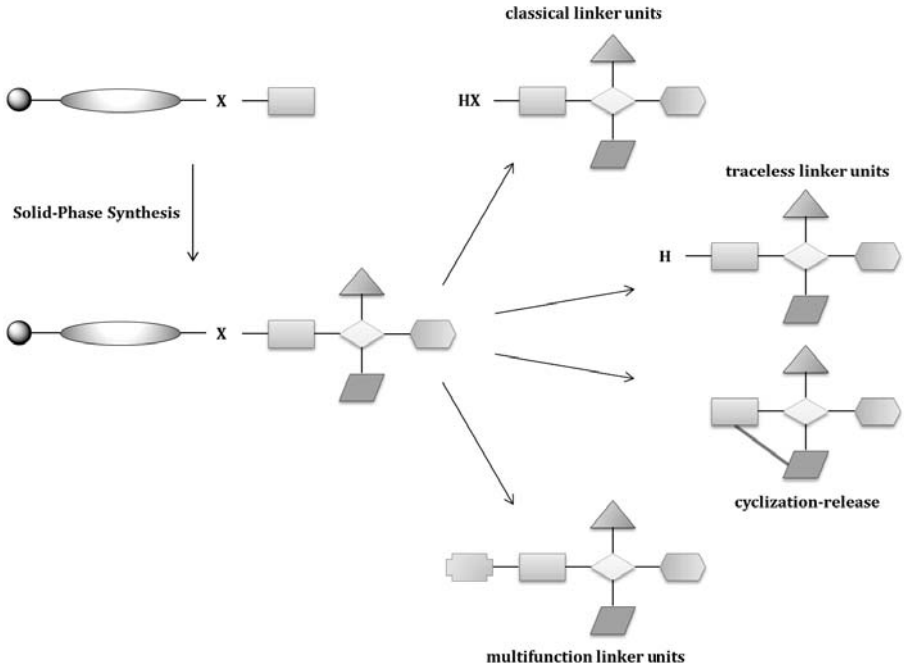

Figure II-5: Overview of linker strategies

- **Classical linker units**

A classical linker strategy can be employed when a (pharmacophore) group on the substrate does not require modification during the synthesis and will be released as such upon cleavage. In these cases, the linker acts as protecting group for the specific functional group. Many of these innumerable linker types have been developed and mainly have a specific acid or base lability. After release, the mostly polar functionality is protonated, leading to amines, alcohols or carboxylic acids. A common cleavage method for solid-phase synthesis uses volatile strong acids such as HF and TFA as they are easily removed *via* evaporation. The specificity for applied conditions is dependent on the relative stability of the protonated linker *versus* the benzyl cation formed upon cleavage. Within the same class of linkers, the more stable the benzyl cation formed, the weaker the acid that can be used for cleavage. It is easy to understand that electron-donating groups will increase the stability of the benzyl cation.

Apart from acid promoted cleavage, classical linkers can also be susceptible to nucleophiles and bases. A nucleophilic replacement of the linker moiety *via* hydroxide, methoxide or unhindered amines could lead to release of the desired product in solution. Strictly basic conditions are applied when the cleavage mechanism involves elimination or cyclization.

Most commonly, linkers which are sensitive for acid cleavage, also might undergo undesired nucleophilic displacement. In order to avoid the latter, sterically hindered linkers can be applied.

- **Traceless linker units**

In most cases, after employing a classical linkage strategy, a polar functional group remains present in the final compound. The latter can have adverse effects on the pharmacokinetic or binding properties of the desired compound. As a compensation, traceless linkers were developed in order to release compounds with no apparent *memory* of the solid-phase. Practically, only a hydrogen or halogen atom is added to the final product upon release. This work was pioneered by Ellman[16] in 1995 *via* the introduction of silicon-based linkers, whereas protosilation yields a protonated product.[17]

Further development, by Ellman[18], was made *via* the introduction of germanium-based linkers which undergo similar chemistry but are more labile. An alternative for this silicon- or germanium-based linker strategy is an immobilization occurring through a transition metal carbonyl linker (e.g. cobalt, chromium, manganese) and an arene bond.

- **Cyclization/release**

One of the early objectives of solid-phase chemistry was the ability to synthesize compounds in high purity. Despite of the promoted synthesis with large excesses of reagents and easy intermediate purification by filtration, the formation of by-products cannot be avoided. A solution for the synthesis of cyclic compounds is given when a cyclization/release strategy is used with a specific and well-chosen linker. Cyclization and cleavage are combined in a single step, which results in the following benefits:

- no polar functionality remains on the final product (in contrast to a classical linker);
- only the linear counterparts of the final product are able to cyclize.

The latter results in an enhanced purity as an *in situ* purification is performed. Non-cyclizable by-products remain attached to the resin when specific cyclization/release conditions are applied. In this sense, the linker has a dual function: besides connecting the substrate to the solid support, the linker moiety acts as an activating group to enable cyclization upon applying the well-chosen, linker-dependent conditions.

In recent literature, many procedures have been developed for creating carbon-nitrogen or carbon-oxygen bonds for cyclic compounds including hydantoins,[19] ureas[20], phthalimides,[21] pyrimidinones,[22] quinazolinones,[23] (spiro)diketopiperazines,[24] 1,4-benzodiazepine-2,5-diones,[25] benzodiazepinones,[26] dihydropyrimidine-2,4-diones,[27] lactones,[28] pyrazolones,[29]...

Besides the successful synthesis of above mentioned cyclic compounds *via* lactam or lactone formation, recent developments also include carbon-carbon bond formation *via* addition of carbanions to susceptible atoms, and ring closing olefin metathesis. The latter is a very

efficient tool to create species with different ring sizes, from seven-membered lactams[30] to sixteen-membered lactones such as the epothilone[31] derivatives.

REFERENCES

[1] Lombardino, J. G.; Lowe III, J. A. *Nat. Rev. Drug Discov.* **2004**, *3*, 853-862.

[2] Geysen, H. M.; Meloen, R. H.; Barteling, S. J. *Proc. Natl. Acad. Sci. U.S.A.* **1984**, *81*, 3998-4002.

[3] Lam, K. S.; Salmon, S. E.; Hersh, E. M.; Hruby, V. J.; Kazmierski, W. M.; Knapp, R. J. *Nature* **1991**, *354*, 82-84.

[4] Thompson, L. A.; Ellman, J. A. *Chem. Rev.* **1996**, *96*, 555-600.

[5] a) Sebestyen, F.; Dibo, G.; Kovacs, A.; Furka, A. *BioMed. Chem. Lett.* **1993**, *3*, 413-418. b) Furka, A.; Sebestyen, F.; Asgedom, M.; Dibo, G. *Int. J. Pept. Protein Res.* **1991**, *37*, 487-493. c) Nefzi, A.; Ostresh, J. M.; Houghten, R. A. *Chem. Rev.* **1997**, *97*, 449-472 and references therein.

[6] Hinzen, B. Encoding Strategies for Combinatorial Libraries. In *Combinatorial Chemistry, from theory to application* Bannwarth, W.; Hinzen, B. ; Eds. Wiley-VCH: Weinheim, **2006**, pp 513-516.

[7] Mason, J. S.; Morize, I.; Menard, P. R.; Cheney, D. L.; Hulme, C.; Labaundiniere R. F. *J. Med. Chem.* **1999**, *42*, 3251-3264.

[8] a) Merrifield, B. R. *J. Am. Chem. Soc.* **1963**, *85*, 2149-2154. b) Merrifield, R. B. *Science* **1986**, *232*, 341-347.

[9] Eichler, J.; Bienert, M.; Stierandova, A.; Lebl, M. *Pept. Res.* **1991**, *4*, 296-307.

[10] Albericio, F.; Pons, M.; Pedroso, E.; Giralt, E. *J. Org. Chem*. **1989**, *54,* 360-366.

[11] Hudson, D. *J. Comb. Chem.* **1999**, *1*, 333-360.

[12] Santini, R.; Griffith, M. C.; Qi, M. *Tetrahedron Lett.* **1998**, *39*, 8951-8954.

[13] Bayer, E. *Angew. Chem. Int. Ed. Engl*. **1991**, *30*, 113.

[14] Reviews: a) Guillier, F.; Orain, D.; Bradley, M. *Chem. Rev*. **2000**, *100*, 2091-2157. b) Lloyd-Williams, P.; Albericio, F.; Giralt, E. *Tetrahedron* **1993**, *49,* 11065-11133. c) Backes, B. J.; Ellman, J. A. *Curr. Opin. Chem. Biol.* **1997**, *1*, 86. d) Blackburn, C. *Pept. Sci.* **1998**, *47*, 311-360. e) James, I. W. *Tetrahedron* **1999**, *55*, 4855-4946.

[15] Scott, P. J. H. Linker Strategies in Modern Solid-Phase Organic Synthesis. In *Solid-Phase Organic Synthesis: Concepts, Strategies, and Applications* Toy, P. H.; Lam, Y.; Eds. Wiley: New York, **2012**, pp 14-48.

[16] Plunkett, M. J.; Ellman, J. A. *J. Org. Chem.* **1995**, *60*, 6006-6007.

[17] a) Gil. C.; Bräse, S.; *Curr. Opin. Chem. Biol.* **2004**, *8*, 230-237. b) Comely, C. A.; Gibson, S. E. *Angew. Chem. Int. Ed.* **2001**, *40*, 1012-1032. c) Bräse, S.; Dahmen, S. *Chem. Eur. J.* **2000**, *6*, 1899-1905.

[18] Plunkett, M. J.; Ellman, J. A. *J. Org. Chem.* **1997**, *62*, 2885-2893.

[19] a) Colacino, E.; Lamaty, F.; Martinez, J.; Parrot, I.; *Tetrahedron Lett.* **2007**, *48,* 5317-5320. b) Wilson, L. J.; Li, M.; Portlock, D. E. *Tetrahedron Lett.* **1995**, *39*, 5135-5138. c) Staldwieser, J.; Ellmerer-Muller, E. P.; Tako, A.; Maslouh, N; Bannwarth, W. *Angew. Chem. Int. Ed.* **1998**, *37*, 1402-1404.

[20] Bonnet, D.; Ganesan, A. *J. Comb. Chem.* **2002**, *4*, 546-548.

[21] Martin, B.; Sekljic, H.; Chassaing, C. *Org. Lett* **2003**, *5*, 1851-1853.

[22] Pathak. R.; Roy, A. K.; Kanojia, S.; Batra. S.; *Tetrahedron Lett*. **2005**, *46*, 5289-5293.

[23] Kesarwani, A. P.; Srivastava, G. K.; Rastogi, S. K.; Kundu, B. *Tetrahedron Lett.* **2002**, *43*, 5579-5581.

[24] a) Habashita, H.; Kokubo, M.; Hamano, S.; Hamanaka, N.; Toda, M.; Shibayama, S.; Tada, H.; Sagawa, K.; Fukushima, D.; Maeda, K.; Mitsuya, H.; *J. Med. Chem.* **2006**, *49*, 4140-4152. b) Bray, A. M.; Lagniton, L. M; Valerio, R. M.; Maeji, N. J. *Tetrahedron Lett.* **1994**, *35*, 9079-9082. c) Bray, A. M.; Maeji, N. J.; Geysen, H. M. *Tetrahedron Lett.* **1990**, *31,* 5811-5814. d) Bray, A. M.; Maeji, N. J.; Valerio, R. M.; Campbell, R. A.; Geysen, H. M. *J. Org. Chem.* **1991**, *56*, 6659-6666. e) Szardenings, A. K.; Burkoth, T. S. *Tetrahedron* **1997**, *53,* 6573-6593. f) van Loevezijn, A.; van Maarseveen, J. H.; Stegman, K.; M, V. G.; Koomen, G. *Tetrahedron Lett.* **1998**, *39,* 4737-4740.

[25] Mayer, J. P.; Zhang, J.; Bjergarde, K.; Lenz, D. M.; Gaudino, J. J. *Tetrahedron Lett.* **1996**, *37,* 8081-8084.

[26] DeWitt, S. H.; Kiely, J. S.; Stankovic, C. J.; Schroeder, M. C.; Cody, D. M. R.; Pavia, M. R. *Proc. Natl. Acad Sci. U. S. A.* **1993**, *90,* 6909-6913.

[27] Kolodziej, S. A.; Hamper, B. C. *Tetrahedron Lett.* **1996**, *37*, 5277-5280.

[28] a) Le Hete, C.; David, M.; Carreaux, F.; Carboni, B.; Sauleau, A. *Tetrahedron Lett.* **1997**, *38,* 5153-5156. b) Matthews, J.; Rivero, R. A. *J. Org. Chem.* **1998**, *63,* 4808-4810. c) Moon, H. S.; Schore, N. E.; Kurth, M. *J. Org. Chem.* **1992**, *57,* 6088-6089.

[29] a) Tietze, L. F.; Steinmetz, A.; Balkenhohl, F. *Bioorg. Med. Chem. Lett.* **1997**, 7, 1303-1306. b) Tietze, L. F.; Steinmetz, A. *Synlett* **1996**, 667-668.

[30] a) Piscopio, A. D.; Miller, J. F.; Koch, K. *Tetrahedron Lett.* **1997**, *38*, 7143-7146. b) Piscopio, A. D.; Miller, J. F.; Koch, K. *Tetrahedron Lett.* **1998**, *39*, 2667-2670.

[31] a) Nicolaou, K. C.; Winssinger, N.; Pastor, J.; Ninkovic, S.; Sarabia, F.; He, Y.; Voufloumis, D.; Yang, Z.; Li, T.; Giannakakou, P.; Hamel, E. *Nature* **1997**, *387*, 268-272. b) Nicolaou, K. C.; Vourloumis, D.; Li, T.; Pastor, J.; Winssinger, N.; He, Y., Ninkovie, S.; Sarabia, F.; Vallberg, H.; Roschangar, F.; King, N. P.; Ray, M.; Finlay, V.; Giannakakou, P.; Verdier-Pinard, P.; Hamel, E. *Angew. Chem. Int. Ed.* **1997**, *36*, 2097-2103.

III.Bioisosterism

A. Introduction

"The properties of elements are the periodic function of their atomic masses"

Dmitri Mendeleev

Mendeleev's periodic table (1869) was the first way of organizing elements in such a fashion that chemical and physical properties could be predicted. This was accomplished by assuming that these characteristics were determined by a returning pattern or *periodic system*, in the peripheral layer of electrons resulting in an arrangement of atoms in periods (horizontal) and groups (vertical). In a period, certain trends can be noticed related to the atomic radius, electron affinity, ionization potential and electronegativity. Nevertheless, within one period neighboring elements have very different chemical properties. On the other hand, groups are considered to be more important for classifying elements. Similar physical properties but also reactivity of elements in one group can be anticipated as they all have the same number of valence electrons. Mendeleev's approach was innovative and a start for others to pursue the study on similarities regarding elements, groups of atoms and molecules.[1,2]

Allen (1918) composed the *molecular number N* of a compound A as:

$$N_A = aN_1 + bN_2 + \ldots + zN_i$$

With N_1, N_2, N_3, …, N_i the respective atomic numbers of each element present in the molecule and a, b, c, …, z the numbers of atoms present in the molecule. An evaluation of two compounds can be made by a simple calculation. For example, Na^+ and NH_4^+ having both a molecular number of 11, which could lead to the assumption that both have similar physical properties.[2]

One year later, Langmuir (1919) introduced the term *isosterism* to categorize ions or molecules with the same number of electrons in the same arrangement, defining groups of isosteres containing electronic and steric arrangements of atoms, groups, radicals with the same number of atoms and valence electrons.

> *"Comolecules are thus isosteric if they contain the same number and arrangement of electrons. The comolecules of isosteres must, therefore, contain the same number of atoms. The essential differences between isosteres are confined to the charges on the nuclei of the constituent atoms."* [3]

Langmuir compared the physical properties of various molecules such as N_2 and CO, N_2O and CO_2, and found them to be similar. By extension, he identified a list of 21 groups of isosteres (**Table III-1**).[1] This classification was later coincidentally acknowledged by the resemblance of biological properties of CO_2 and N_2O as both gases were capable of acting as reversible anesthetics to the slime mold *Physarum polycephalum*.[4] Furthermore, both gases have similar physical properties such as viscosity, density, refractive index in liquid, dielectric constant en solubility in ethanol.[5]

Table III-1: Groups of isosteres as identified by Langmuir

Groups	Isosteres
1	H^-, He, Li^+
2	O^{2-}, F^-, Ne, Na^+, Mg^{2+}, Al^{3+}
3	S^{2-}, Cl^-, Ar, K^+, Ca^{2+}
4	Cu^{2-}, Zn^{2+}
↓	↓
8	N_2, CO, CN^-
9	CH_4, NH_4^+
10	CO_2, N_2O, N^{3+}, CNO^-
↓	↓
20	MnO_4^-, CrO_4^{2-}
21	SeO_4^{2-}, AsO_4^{3-}

Grimm (1925) extended the concept of isosterism by defining his *hydride displacement law:*

> *"Atoms anywhere up to four places in the periodic system before an inert gas change their properties by uniting with one to four hydrogen atoms, in such a manner that the resulting combinations behave like pseudoatoms, which are similar to elements in the groups one to four places respectively, to their right."*[6]

Thus, the addition of a *hydride* to an element from the periodic group 4A, 5A, 6A, 7A and 0 creates a 'pseudoatom' which properties are strongly related to the element next to the original element in the periodic table.[7] Grimm's hydride displacement law is depicted in

(**Table III-2**), wherein each column the original element is followed by its isosteric and isoelectric pseudoatom. Differently from Langmuir, Grimm allows isosteres to have a different number of atoms yet the same valence electrons. This law also imposes a clear link between similarities in size between the groups, based on the elements in the same period of the periodic system. However, Grimm's approach does not take into account the actual location, movement or resonance of the electrons within the orbitals of the functional group replacements. Moreover, this law fails regarding some physical characteristics among electronegativity, polarization, binding angles, size, shape of molecular orbitals, electron density and partition coefficient which all determine physicochemical properties of a molecule.[5]

Table III-2: Grimm's Hydride Displacement Law

Groups of pseudoatoms					
C	N	O	F	Ne	Na^+
	CH	NH	OH	FH	
		CH_2	NH_2	OH_2	FH_2^+
			CH_3	NH_3	OH_3^+
				CH_4	NH_4^+

After a series of studies related to the applications of isosteres towards biological problems, Erlenmeyer (1935) formed a second extension to the concept of isosterism and postulated that:

> *"isosteres are atoms, ions and molecules in which the peripheral layers of electrons are considered as identical"* [8]

In extension, Erlenmeyer added the following to the work of Grimm:[2]

- Groups in the periodic system act isosteric.
- Regarding the definition of 'pseudoatoms': include compounds with similar characteristics although there is no direct relation to the periodic system, i.e. -Cl = -CN = -SCN.
- Introducing ring equivalents: $-CH_2=CH_2-$ en -S- share resemblances and therefore benzene and thiophene act as isosteres (**Figure III-1**)[9].

Table III-3: Isosterism by Erlenmeyer

No. of peripheral electrons				
4	5	6	7	8
N^+	P	S	Cl	ClH
P^+	As	Se	Br	BrH
S^+	Sb	Te	I	IH
As^+		PH	SH	SH_2
Sb^+			PH_2	PH_3

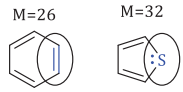

Figure III-1: Benzene and thiophene act as ring equivalents

While acknowledging the usefulness of the isosteric concept for designing biologically active compounds, Friedman (1951) introduced *bioisosteres* initially as:

> *"atoms and molecules which fit the broadest definition of isosteres and have the same type of biological activity"* [10]

This description implies that agonists and antagonists, interacting with the same receptor site, are bioisosteres. Although this does not rely on the structure, only the interactions have to be similar and therefore, both molecules are seen as bioisosteres.

The current and most accepted meaning of bioisosterism was given by Thornber (1979).

> *"Bioisosteres are groups or molecules which have chemical and physical similarities producing broadly similar biological effects"* [11]

According to the degree of electronic and steric alikeness, Burger (1970) created two subcategories within isosterism: *classical* or *non-classical bioisosteres*.[12] The first subcategory is related to size equivalency whereas the second is most related to the biological effect and thus used interchangeable with bioisosteres. Moreover, classical isosteres can be divided in five distinct categories:

- Univalent atoms or groups (substituting halogens by other electron withdrawing substituents such as $-CF_3$ en -CN);
- Divalent atoms or groups (mutual replacement of -O-, -S-, -NH- and $-CH_2-$);
- Trivalent atoms or groups (replacing $R_1R_2R_3$**N** by $R_1R_2R_3$**CH**);
- Tetravalent atoms or groups (substituting =C= by $=N^+=$ or =Si=);
- Ring equivalents (replacing benzene by a thiophene, a pyridine or a furan moiety).

Figure III-2 presents a simple classical isosteric replacement of divalent atoms, where Clozapine (**III.1**, antagonist, interacting with D_4 receptors in the central nervous system) is shown together with two commercially available isosteric analogues Quetiapine **III.2** and Loxapine **III.3**.

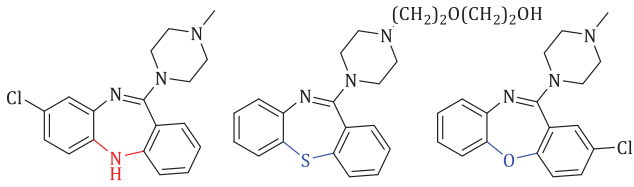

Figure III-2: Classical isosteric replacement of -NH- by -O- or -S-

Non-classical bioisosteric replacements aim greater selectivity, less side effects, lower toxicity, improved pharmacokinetics, increased stability, simplified synthesis and circumventing intellectual property restrictions. **Figure III-3** shows an example of bioisosteres where the *cis*-amide bond in diazepam is substituted by a 1,2,4-triazole (Alprazolam, **I.16**) or an imidazole moiety (Midazolam, **III.4**).[2]

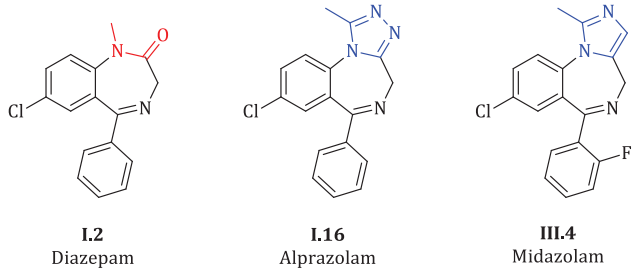

Figure III-3: Example of bioisosteric replacement in the benzodiazepine series

Another form of bioisosterism, *scaffold hopping*, includes the substitution of the initial molecular scaffold by a different central core retaining biological activity. The new scaffold should ideally be comparable in size, shape and make similar interactions with the binding site[13].

In this work, the focus lays on the replacement of a *cis*-amide bond by a 1,2,3-triazole moiety. In the following paragraphs, a more profound discussion will be made regarding the validity of this replacement.

B. Triazoles as non-classical bioisosteres

1,2,3-Triazoles[14,15], as planar five-membered ring systems with an aromatic character, are π-electron-deficient and have both basic and acidic properties. At physiological pH, the triazole moiety is not protonated due to poor basicity. Furthermore, they exhibit a strong dipole

moment (~ 5 Debye)[i,14,16] and show a good hydrogen-bond-acceptor ability. Even more, they are stable towards metabolic and chemical degradations and show inertness towards severe hydrolytic, oxidizing and reducing conditions even at high temperatures. Thanks to these characteristics they become interesting tools for bioisosteric replacements for amide bonds or double bonds *(vide infra)*.

1. 1,2,3-Triazoles as bioisosteres of amides

The similarities between the 1,4-regioisomer of a 1,2,3-triazole and a *trans*-amide bond can be defined as follows:

- the lone pair of N(3) mimics the carbonyl oxygen lone pair and acts as a H-bond acceptor.
- the strongly polarized C(5) hydrogen can act as H-bond donor, corresponding with the *trans*-amide proton.
- the polarized and electrophilic C(4) is equivalent to a carbonyl carbon.

Apart from these similarities some differences are found in:

- the dipole moment of a triazole (~ 5 D) is larger than for a *trans*-amide (~ 3.5 D) resulting in H-bond donor and acceptor properties which are more expressed, therefore creating an enhanced peptide mimicry.
- the distance between both substituents R_1 and R_2 is higher due to a difference in the number of bridging atoms (three vs. two), leading to 1.1 Å distance difference.

Taking into account the similarities and differences, it can be concluded that the 1,4-regioisomers mimic a *trans*-amide bond.

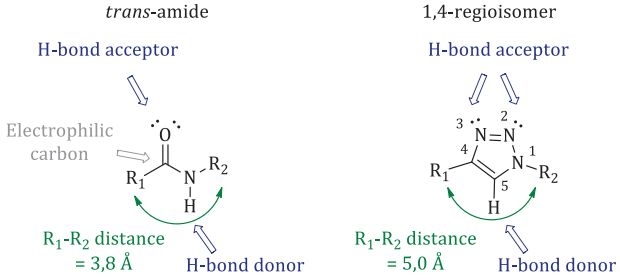

Figure III-4: Structural and electronic evaluation of a *trans*-amide bond *versus* the 1,4-regioisomer of a 1,2,3-triazole moiety

[i] Calculated value: 4.76 ± 0.17 D

A complementary mimic for a *cis*-amide bond can be found in the 1,5 regioisomer as:

- the distance between both side chains R_1 and R_2 is identical.
- the lone pair of N(2) mimics the carbonyl oxygen lone pair and acts as a H-bond acceptor.
- the strongly polarized C(4) hydrogen can act as H-bond donor.

The only difference is a higher dipole moment for the triazole moiety and a lack of carbonyl carbon in the case of the triazole.

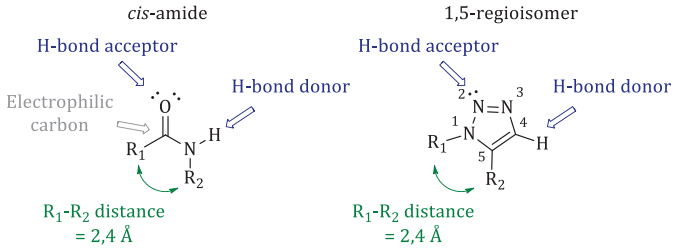

Figure III-5: Structural and electronic evaluation of a *cis*-amide bond versus the 1,5-regioisomer of a 1,2,3-triazole moiety

2. 1,2,3-Triazoles as bioisosteres of double bonds

In **Figure III-6**, Combrestatin A-1 (**III.5**) and Combrestatin A-4 (**III.6**) (anti-cancer and anti-angiogenic agents) are represented, where the *cis*-conformation of the double bond is essential for interaction with the colchicine binding site of α,β-tubulin. Hansen and co-workers[17] published 1,5-disubstituted 1,2,3-triazole modified analogues **III.7** – **III.9** which retains partially the same mode of action comparing to **III.5** and **III.6**. Another example of a double bond bioisostere is given by Genazzani and co-workers[18], where a *trans* double bond is replaced by a 1,4-disubstituted 1,2,3-triazole moiety. In this case, this double bond is mimicked and a 72-membered library of analogues was successfully synthesized in a combinatorial fashion.

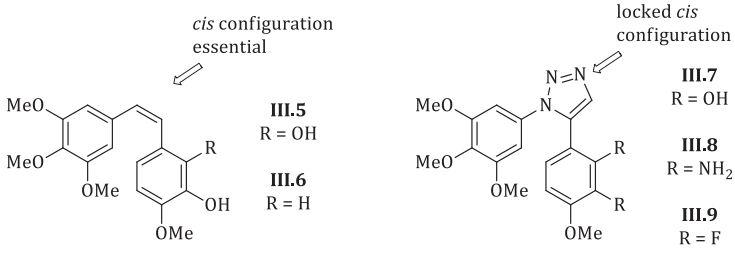

Figure III-6: Combrestation A-1 (III.5), A-4 (III.6) and 1,5-disubstituted 1,2,3-triazole analogues III.7-III.9.

3. Bioisosteric applications of 1,4-disubstituted 1,2,3-triazoles

a) Macrocyclization

Van Maarseveen and co-workers[19] studied the synthesis of the naturally occurring cyclotetrapeptide cyclo-[Pro-Val-Pro-Tyr] (**III.10, Figure III-7**), a potent tyrosinase inhibitor isolated from *L. Helveticus.* All synthesis attempts failed to yield the natural product **III.10** due to the problematic ring closing step at all possible positions.[20] Taking advantage of an amide bond mimicry by a 1,4-disubstitued 1,2,3-triazole moiety and by employing the corresponding ring closure *via* Cu(I)-assisted 1,3-dipolar cycloaddition affords macrocycle **III.11** in good efficiency. The resulting amide bond mimick **III.11** retains tyrosinase inhibitory activity[21,22].

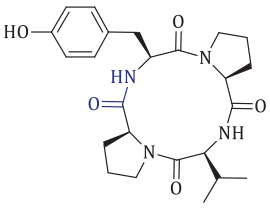

III.10

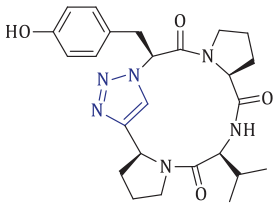

III.11

entry	Tyrosinase activity IC_{50} [mM][a]
III.10	1.5
III.11	0.5

[a] Concentration for 50% reduction in tyrosinase activity from mushroom tyrosinase extract.

Figure III-7: Cyclotetrapeptide cyclo-[Pro-Val-Pro-Tyr] (III.10) and triazole analogue III.11.

b) Peptide bond surrogates

Wong and co-workers demonstrated that the 1,4-disubstituted 1,2,3-triazole moiety can be used as an effective replacement for a peptide bond in HIV-1 protease inhibitors (e. g. amprenavir (**III.12**)). Interestingly, docking studies of two synthesized structures **III.13** and **III.14** show that the triazole ring is an excellent amide surrogate which retains all hydrogen bonds in the active site[23].

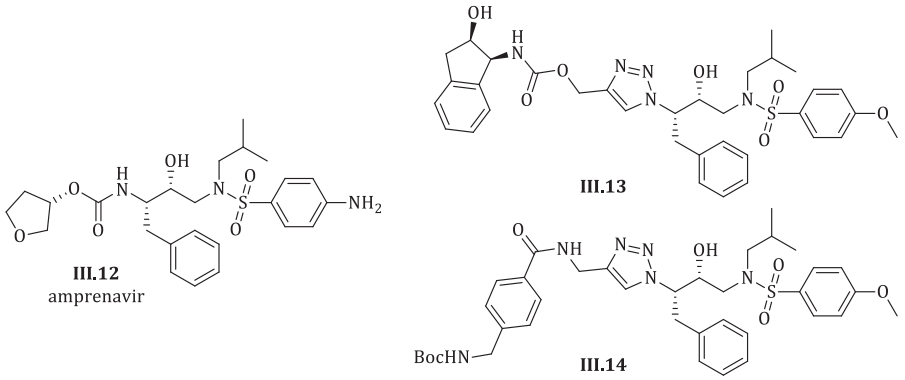

Figure III-8: Amprenavir (III.12, HIV-1 protease inhibitor) and two active peptide surrogate analogues

c) Linkers

As click chemistry is highlighted by its modularity, high efficiency and tolerance towards a broad range of functional groups, stability under physiological conditions as well as its biocompatibility, the formed 1,2,3-triazole moiety becomes a favorable linker. In this sense, the triazole functionality can be used to generate twin drugs (homo/heterodimer) to produce more potent and/or more selective drug candidates comparing the single entity[24]. Even more, a linker strategy can be used if the active site of the target consists of two different binding pockets.[25]

d) Bioconjugation

The properties of the 1,2,3-triazole, such as good solubility in water, stability in typical biological conditions, rigidity and mimicry of the amide bond, make it an ideal linker to immobilize fluorescent tags or small molecules to biomolecules.[26].

4. Bioisosteric applications of 1,5-disubstituted 1,2,3-triazoles

a) Locking the configuration

Ghadiri and co-workers[27] studied the synthesis of the natural cyclic tetrapeptide apicidin (**Figure III-9**) where the most predominant conformation in solution 'all *trans*' **III.15** does not correspond to the active conformation (**III.16**, *cis-trans-trans-trans*). Therefore, 1,4- (**III.17**) and 1,5-disubstituted 1,2,3-triazole surrogates **III.18** were used for fixing respectively the desired *trans*- and *cis*-conformation. Moreover, by comparing the activity of both analogues, it became clear that the *cis-trans-trans-trans* conformation **III.16** is the most active one[28].

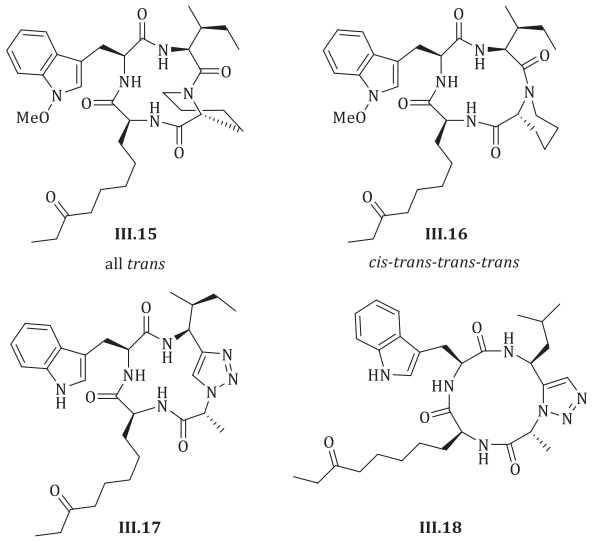

Figure III-9: Apicidin configurations III.15 / III.16 and 1,4 – III.17 /1,5-disubstituted-1,2,3-triazole mimick III.18.

Kubik and co-workers[29] also presented the facile synthesis of a hexapeptide mimick wherein challenging proline amide bond formations can be replaced *via* a Ru(II)-facilitated synthesis of a 1,5-disubstituted 1,2,3-triazole moiety[30] at several positions yielding the desired cyclic hexapeptidomimetic structure.

Extensive efforts have been made to develop deoxyuridine triphosphatase (dUTPase) inhibitors, leading to hit compound **III.20** with potent inhibitory activity and drug-like properties. This tertiary amide is 12 times more active than the corresponding secondary amide **III.19**, whereas conformational NMR analysis confirmed that only the *cis*-conformation **III.20** contributes to its higher potency. 1,5-Disubstituted 1,2,3-triazole derivative **III.22**, replacing the *cis* tertiary amide, was synthesized to create a restricted surrogate of the *cis*-amide bond to further improve the inhibitory potency. After SAR study improvements, compounds were reported with desirable pharmacokinetic profiles in mice and a clearly enhanced antitumor activity of a thymidylate synthase inhibitor *in vivo*.

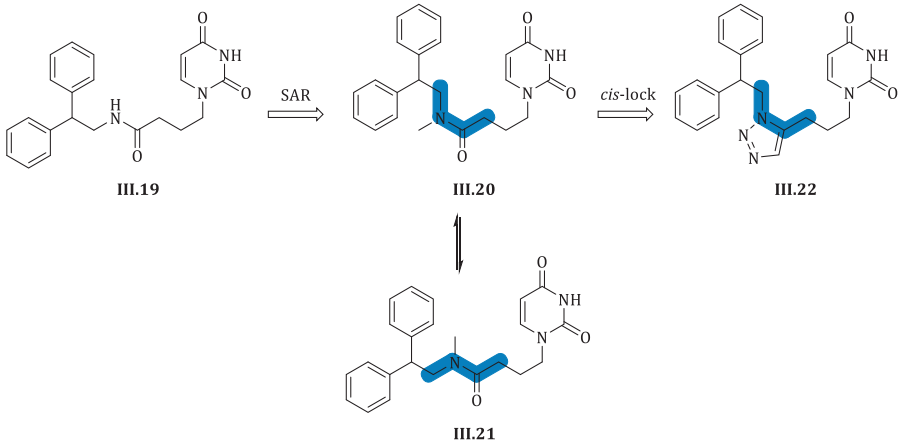

Figure III-10: dUTPase inhibitors enhancement by including 1,5-disubstituted triazoles as *cis*-lock

b) Inducing turn motifs

Rademann and co-workers[31] published a *cis* peptide mimetic by introduction of a 1,5-disubstituted 1,2,3-triazole moiety, leading to products with carefully controlled conformations. This work allows to study the exploitation of the effects of *cis* peptide geometry, either for open-chain conformations (**III.24**) or for peptide turns (**III.23** and **III.25**). Moreover, Appella[32] stated that introducing a 1,5-disubstituted 1,2,3-triazole moiety affords peptoids containing hairpins in aqueous solutions.

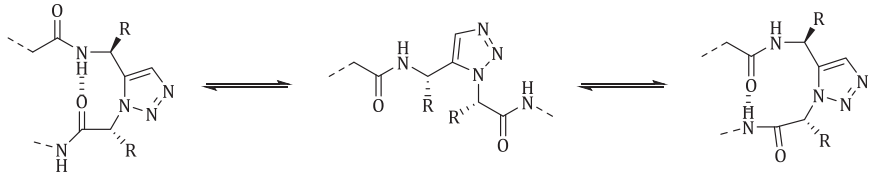

III.23 **III.24** **III.25**

cis peptide mimetic

Figure III-11: Controlling peptide conformation by employing 1,5-disubstituted 1,2,3-triazole moieties.

REFERENCES

[1] Patani, G. A.; LaVoie, E. J. *Chem. Rev.* **1996**, *96*, 3147-3176.

[2] Ciapetti, P.; Gietlen, B. Molecular Variations Based on Isosteric Replacements. In The practice of Medicinal Chemistry; Wermuth, C. G., Ed.; Elsevier: London, **2008**; pp. 290-334.

[3] Langmuir, I. *J. Am. Chem. Soc.* **1919**, *41*, 1543-1559

[4] Seifriz, W. *Science* **1948**, *107*, 15-16

[5] Knittel, J. J.; Zavod, R. M. Drug Design and Relationship of Functional Groups to Pharmacologic Activity. In Foye's Principles of Medicinal Chemistry, 6th edition; Williams, D. A.; Foye, W.O.; Lemke T.L.; Eds.; Lippincott Williams & Wilkins: Philadelphia , **2008**, pp 59.

[6] (a) Grimm, H. G. *Z. Electrochem.* **1925**, *31*, 474-480. (b) Grimm, H. G. *Naturwissenschaften* **1928**, *17*, 557-564.

[7] Lima, L. M.; Barreiro, E. J. *Curr. Med. Chem.* **2005**, *12*, 23-49.

[8] Erlenmeyer, H.; Leo, M. *Helv. Chim. Acta* **1932**, *15*, 1171-1186.

[9] Nobles, W. L.; Dewitt Blanton, C. *J. Pharm. Sci.* **1964**, *53*, 115-129.

[10] Friedman, H. L. *NASNRS* **1951**, *206*, 295-358.

[11] Thornber, C. W. *Chem. Soc. Rev.* **1979**, *8*, 563-580.

[12] Burger, A. In Burger's Medicinal Chemistry, 3rd edition; Burger, A.; Ed.; Wiley-Interscience: New York, **1970**; pp. 64-80.

[13] Brown, N. In Bioisosters in Medicinal Chemistry, Mannhold, R.; Kubinyi, H.; Folkers, G.; Ed.; Wiley-VCH: Weinheim, **2012**; pp. 38

[14] Tron, G. C.; Pirali, T.; Billington, R. A.; Canonico, P. L.; Sorba, G.; Genazzani, A. A. *Med. Res. Rev.* **2008**, *28*, 278-308.

[15] Hou, J.; Liu, X.; Shen, J.; Zhao, G.; Wang, P. G. *Expert Opin. Drug. Discov*. **2012**, *7*, 489-501.

[16] El-Bakali Kassimi, N.; Doerksen, R. J.; Thakkar, A. J. *J. Phys. Chem.* **1995**, *99*, 12790-12796.

[17] a) Akselsen, O. W.; Odlo, K.; Cheng, J.-J.; Maccari, G.; Botta, M.; Hansen, T. V. *Bioorg. Med. Chem.* **2011**, *20*, 234-242. b) Odlo, K.; Fournier-Dit-Chabert, J.; Ducki, S.; Gani, O. A. B. S. M.; Sylte, I.; Hansen, T.V. *Bioorg. Med. Chem.* **2010**, *18*, 6874-6885.

[18] Pagliai, F.; Pirali, T.; Del Grosso, E.; Di Brisco, R.; Tron, G. C.; Sorba, G.; Genazzani, A. A. *J. Med. Chem*. **2006**, *49*, 467-470.

[19] Bock, V. D.; Perciaccante, R.; Jansen, T. P.; Hiemstra, H.; van Maarseveen, J. H. *Org. Lett.* **2006**, *8*, 919–922.

[20] Schmidt, U.; Langner, J. *J. Pept. Res.* **1997**, *49*, 67–73.

[21] White, C.J.; Yudin, A. K. *Nature Chem.* **2011**, *3*, 509-524.

[22] Bock, V. D.; Speijer, D.; Hiemstra, H.; van Maarseveen, J. H. *Org. Biomol. Chem.* **2007**, *5*, 971–975.

[23] a) Brik, A.; Alexandratos, J.; Lin, Y.-C.; Elder, J. H.; Olson, A. J.; Wlodawer, A.; Goodsell, D. S.; Wong, C.-H. *ChemBioChem* **2005**, *6*, 1167-1169. b) Whiting, M.; Muldoon, J.; Lin, Y.-C.; Silverman, S. M.; Lindstrom, W.; Olson, A.J.; Kolb, H. C.; Finn, M. G.; Sharpless, K. B.; Elder, J. H.; Fokin, V. V. *Angew. Chem.* **2006**, *118*, 1463-1467.

[24] a) Kuhhorn, J.; Hubner, H.; Gmeiner,P. *J. Med. Chem*. **2011**, *54*, 4896-4903. b) Roy, B.; Chakrabortry, A.; Ghosh, S. K.; Basak, A.; *Bioorg. Med. Chem. Lett.* **2009**, *19*, 7007-7010. c) Singh, P.; Singh, P.; Kumar, M.; Gut, J.; Rosenthal, P. J.; Kumar, K.; Kumar, V.; Mahajan, M.P.; Bisetty, K. *Bioorg. Med. Chem.* **2012**, *22*, 57-61.

[25] a) Wang, J.; Uttamchandani, M.; Li, J. Hu, M.; Yao, S. Q. *Org. Lett.* **2006**, *8*, 3821-3824. b) Trabocchi, A.; Menchi, G.; Cini, N.; Bianchini, F.; Raspanti, S.; Bottoncetti, A.; Pupi, A.; Calorini, L.; Guarna, A. *J. Med. Chem.* **2010**, *53*, 7119-7128. c) Shen, J.; Woodward, R.; Kedenburg, J. P. Liu, X. W.; Chen, M.; Fang, L. Y.; Sun; D. X.; Wang. P. G. *J. Med. Chem.* **2008**, *51*, 7417-7427. d) Brik, A.; Wu, C.-Y.; Wong, C.-H. *Org. Biomol. Chem.* **2006**, *4*, 1446-1457. e) Lipinski, C.; Hopkins, A. *Nature* **2004**, *432*, 855-861.

[26] Wang, Q.; Chan, T. R.; Hilgraf, R.; Fokin, V.V.; Sharpless, K. B.; Finn, M. G. *J. Am. Chem. Soc.* **2003**, *125*, 3192-3193.

[27] Horne, W. S.; Olsen, C. A.; Beierle, J. M.; Montero, A.; Ghadiri, M.R. *Angew. Chem. Int. Ed.* **2009**, *48*, 4718-4724.

[28] Miyakoshi, H.; Miyahara, S.; Yokogawa, T.; Endoh, K.; Muto, T.; Yano, W.; Wakasa, T.; Ueno, H.; Chong, K. T.; Taguchi, J.; Nomura, M.; Takao, Y.; Fujioka, A.; Hashimoto, A.; Itou, K.; Yamamura, K.; Shuto, S.; Nagasawa, H.; Fukuoka, M. *J. Med. Chem.* **2012**, *55*, 6427-6437.

[29] Krause, M. R.; Goddard, R.; Kubik. S. *J. Org. Chem.* **2011**, *76*, 7084-7095.

[30] Tam, A.; Arnold, U.; Soellner, M. B.; Raines, R. T. *J. Am. Chem. Soc.* **2007**, *129*, 12670-12671.

[31] Ahsanullah, Schmieder, P.; Kühne, R.; Rademann, J. *Angew. Chem. Int. Ed.* **2009**, *48*, 5042-5045.

[32] Pokorski, J. K.; Miller Jenkins, L. M.; Feng, H.; Durell, S. R.; Bai, Y.; Appella, D. H. *Org. Lett.* **2007**, *9*, 2381-2383.

IV. Click chemistry

A. Introduction

Click chemistry describes a set of powerful, highly trustworthy and selective reactions to generate new substances quickly and reliably by joining units in a "spring-loaded" fashion together through heteroatom links. Moreover, in order to be accepted as click chemistry,

> *"the reaction must be modular, wide in scope, give very high yields, generate only inoffensive byproducts that can be removed by nonchromatographic methods, and be stereospecific. The required process characteristics include simple reaction conditions, readily available starting materials and reagents, the use of no solvent or a solvent that is benign (such as water) or easily removed, and simple product isolation"*[1].

These spring-loaded reactions proceed rapidly to completion and form selectively one product thanks to a highly thermodynamic driving force, usually greater than 20 kcal/mol. Among many examples of this kind of reactions, cycloadditions beautifully represent the ideals of click chemistry. In particular, the thermal 1,3-dipolar cycloaddition between azides and alkynes defined by Huisgen[i,2] are known to be the

> *"cream of the crop"*[1].

Despite their ideal reactivity, starting material availability, selectivity and orthogonality, this reaction got left behind due to the potential explosive nature of azides at the (required) high reaction temperatures. Moreover, the 1,2,3-triazoles formed were a mixture of inseparable 1,4- and 1,5-regioisomers, so being synthetically unattractive.

---

[i] Note: The formation of a 1,2,3-triazole was first discovered by Michael in 1893 after a reaction of phenyl azide with dimethyl acetylene dicarboxylate. In the 1950s and 1960s, Rolf Huisgen systematically investigated a group of [3+2] cycloadditions, recognized their common features and classified them as *1,3-dipolar cycloadditions.*

Thanks to the independent introduction of the copper catalyzed azide-alkyne cycloaddition (CuAAC) by Sharpless[3] and then shortly after by Meldal[4], resulting in the regioselective synthesis of the 1,4-regioisomer, this reaction became a *hot topic* in organic and bioorganic chemistry. Moreover, in the last years, many research groups provided (besides the CuAAC) other safe 1,3-dipolar cycloaddition methods such as the ruthenium-catalyzed azide-alkyne cycloaddition (RuAAC), the silver-catalyzed azide-alkyne cycloaddition (AgAAC) and the strain-promoted [3+2] cycloaddition. Each of them will be discussed in the following paragraphs, including general properties, mechanistic concerns, catalyst sources and an example of a recent striking research application.

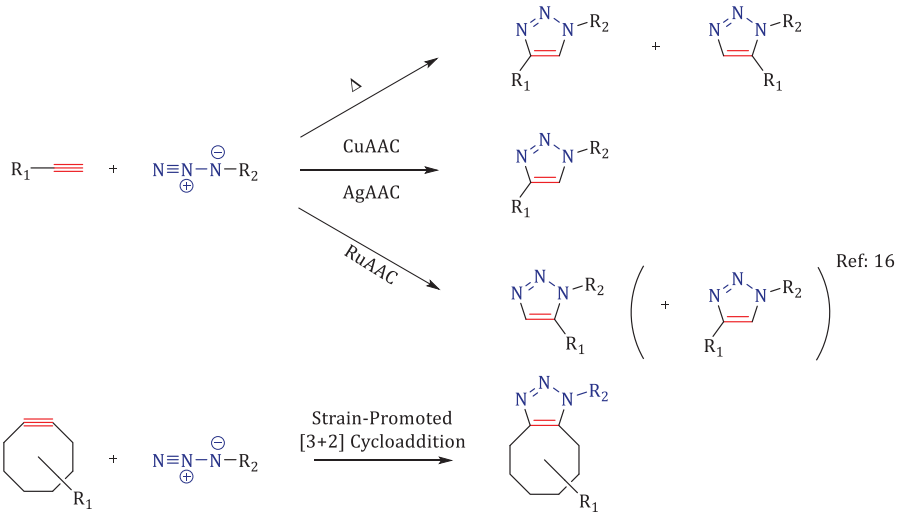

Figure IV-1: Overview of the most important click chemistry procedures

B. CuAAC

As already mentioned above, the copper-catalyzed azide-alkyne cycloaddition (CuAAC) was independently introduced by Sharpless[3] and Meldal[4]. Thanks to the use of Cu(I) as catalyst, the relatively high activation energy barrier[ii,5] could be decreased, leading to a rate acceleration of the 1,2,3-triazole formation in a regioselective way.

1. Mechanism

In 2002, the intermediacy of Cu(I) acetylides in CuAAC was postulated by Sharpless and Meldal based on the lack of reactivity of internal alkynes[3,6]. Soon thereafter, a computational

[ii] For hydrazoic acid and acetylene the calculated free energy of activation is 29.9 kcal/mol (calcultated according to mPW1K.

study of elementary steps of the sequence was performed by Sharpless. The initial computations focused on the possible reaction pathways between Cu(I) acetylides and organic azides. The key bond-making steps are shown in **Scheme IV–1** and the energy diagram is presented in **Figure IV-2**. The formation of the Cu(I) acetylides **IV.3** (Step **A**) was calculated to be exothermic by 11.7 kcal/mol with H_2O as a ligand (slightly endothermic with acetonitrile as a ligand 0.6 kcal/mol[iii]). This is consistent with the well-known facility of this step, which probably occurs through the intermediate step of a π-alkyne–copper complex **IV.2**. The π coordination of an alkyne to copper is calculated to reduce the pK_a of the alkyne proton by almost 10 units, resulting in pK_a values within the deprotonation range in aqueous media[7]. A concerted 1,3-dipolar cycloaddition of the azide to the copper acetylide has a high calculated potential energy barrier (23.7 kcal/mol), thus the metal must play an additional role. In the proposed sequence, the azide **IV.4** is activated by coordination to copper (Step **B**), leading to the intermediate **IV.5**. The key bond-forming event takes place in the next step (Step **C**), when **IV.5** is converted to the unusual six-membered copper metallacycle **IV.6**.

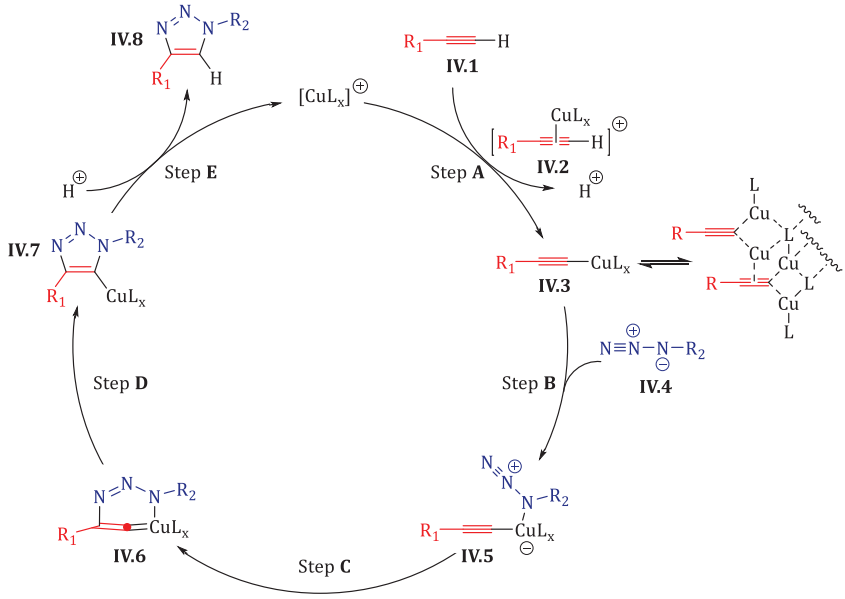

Scheme IV–1: Mechanism of the CuAAC proposed by Sharpless[6] and adjusted according to Fokin[8]

This step is endothermic by 12.6 kcal/mol in H_2O with a calculated barrier of 18.7 kcal/mol, which is significantly lower than the barrier for the uncatalyzed reaction (25.7 kcal/mol for

[iii] This agrees with experimental data as the CuAAC is much faster in H_2O and does not require an amine base.

the 1,4-regioisomer) thus accounting for the enormous rate acceleration of 10^5 accomplished by Cu(I)[iv].

The CuAAC reaction is therefore not a concerted cycloaddition, and its regioselectivity is explained by the binding of both azide and alkyne to copper prior to the formation of the C–C bond. The energy barrier for the ring contraction of **IV.6** (step **D**), which leads to the triazolyl–copper derivative **IV.7**, is quite low (3.2 kcal/mol). Protonation of **IV.7** (step **E**) releases the final 1,4-regioisomer of the triazole product **IV.8**, thereby completing the catalytic cycle. The proposed mechanism accounts for the key experimental observations. First, the dramatic rate increase observed is in agreement with the 11 kcal/mol lower activation barrier compared to the concerted cycloadditions. Secondly, the exclusive regioselectivity of the Cu(I)-catalyzed processes is both predicted computationally and observed experimentally.

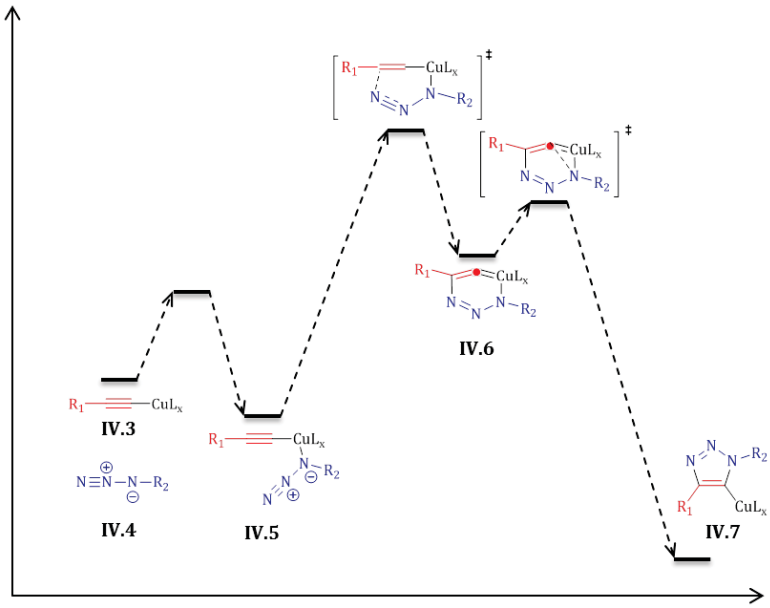

Figure IV-2: Energy diagram of the key bond making steps in the CuAAC.[6]

Recent studies by density functional theory (DFT) calculations found a second-order dependence in copper, leading to the assumption that a second copper atom might be present in the metallacycle-forming step.[9]

[iv] Calculations for the concerted 1,5-regioisomer formation give arise to an activation barrier of 26.0 kcal/mol. The low energy barrier difference between both regioisomers explains the almost 1:1 mixture if purely thermal, uncatalyzed conditions are used.

2. Copper catalyts

Different sources of Cu(I) catalytic active species can be used[10]:

- Copper(I) halides (CuBr, CuI): due to their low solubility in organic solvents, the use of copper(I) halides requires an amine base or elevated temperatures[4]. Coordination complexes (i.e. $[Cu(CH_3CN)_4]PF_6$) are very effective in organic solvents. In accordance to the thermodynamic instability of Cu(I) and low standard potential of Cu^{2+}/Cu^{+}, oxygen-free conditions have to be employed to prevent oxidation and loss of active catalyst.
- *In situ* preparation of Cu(I) by the use of copper(II) salts (i.e. $CuSO_4.5H_2O$) and a reducing agent (i.e. sodium ascorbate) do not require addition of a base. This method prevents the oxidation of Cu(I) to Cu(II) by oxygen[3].
- Introducing Cu(I) by comproportionation of Cu(II) and Cu(0). A simple piece of copper metal and the copper oxide on the surface are sufficient to initiate the catalytic cycle.

C. AgAAC

Despite many initial efforts to involve silver(I) species in the azide-alkyne reaction[11], no triazole formation was observed. The copper(I) salt was found to be essential for the cycloaddition. Vemula and co-workers[12] reported a novel silver(I)-catalyzed regioselective azide-alkyne cycloaddition. Vemula used a well-defined copper-free, silver(I) complex which catalyzes selectively the azide-alkyne cycloaddition (AgAAC) leading to the 1,4-disubstituted regioisomer in excellent yields. The proposed mechanism corresponds to the copper-mediated pathway (**Scheme IV–1**), still after formation of the silver acetylide further activation is necessary to obtain cycloaddition products. Therefore, a well-defined P,O-ligand **IV.9**, created by Vemula, is necessary. The hemilabile nature of this ligand could, after breaking the silver-oxygen bond, return electron density through the metal to the alkyne to afford cyclization.

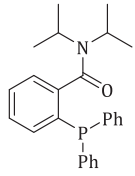

IV.9

Figure IV-3: *N,N*-diisopropyl-2-diphenylphosphinobenzamide (IV.9) as proposed ligand to AgOAc by Vemula mediating AgAAC.

D. RuAAC

The discovery of the Cu(I) catalysis of the Huisgen's dipolar cycloaddition in a selective and regiospecific way was the start of the *click-era*. Terminal alkynes and azides react with the formation of 1,4-disubstituted 1,2,3-triazoles under mild conditions. This powerful click reaction has quickly found many applications in chemistry, biology and material sciences. This success highlighted the need for selective, high yielding access to the complementary 1,5-disubstituted triazoles.

In 2005, Fokin and co-workers[13] introduced a ruthenium(II)-catalyzed azide-alkyne "fusion" reaction. As catalytic transformations of alkynes by ruthenium complexes were already well-known[14], ruthenium seemed to be a logical choice for catalyzing this azide-alkyne cycloaddition. Several Ru(II) complexes were evaluated and a conclusion could be made that C_p* (pentamethylcyclopentadienyl) decorated catalysts gave a selective formation of the desired 1,5-regioisomer, using a broad range of aromatic and aliphatic alkynes. Moreover, internal alkynes participate in the triazole formation, therefore excluding ruthenium acetylides as reactive intermediates. Regarding the azide substitution degree, primary and secondary azides get involved well and only tertiary azides give rise to low yields.[13,14]

A solvent study revealed that benzene, toluene, 1,2-dichloroethane and dioxane perform equally well but protic solvents have a detrimental effect on yield and selectivity. [13]

1. Mechanism

A possible mechanism proposed by Fokin is shown in **Scheme IV–2**. The C_p*RuL_2 **IV.10** complex displaces two spectator ligands forming the activated complex **IV.11**. The unstable 14-electron intermediate **IV.11** undergoes an oxidative coupling with alkyne **IV.1** and azide **IV.4** to form **IV.12** (step **A**). The latter is converted into a ruthenacycle **IV.13** (step **B**), which controls the regioselectivity of the overall process as the new C-N is formed between the more electronegative and less sterically-hindered carbon of the alkyne and the terminal nitrogen of the azide. The metallacycle then undergoes reductive elimination (step **C**) to intermediate **IV.14**. The catalytic cycle is closed by releasing the aromatic 1,5-regioisomer of the 1,2,3-triazole **IV.15** (step **D**) whilst regenerating complex **IV.10**[15].

The spectator ligands L and C_p* ligand are of crucial importance for the efficiency and regioselectivity of the cycloaddition. The lability of the spectator ligands determines the formation of the activated complex **IV.11** and the sterically-demanding C_p* facilitates the reductive elimination (step **C**).

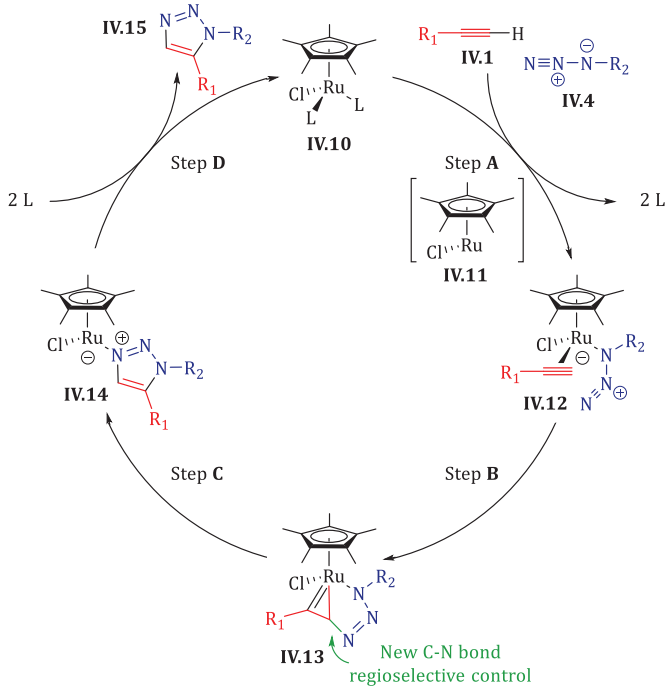

Scheme IV–2: Mechanism of RuAAC proposed by Fokin[15]

In order to determine the experimentally observed regioselectivity of the Ru(II)-promoted azide-alkyne cycloaddition, DFT studies were executed[15]. By using methyl azide, propyne and [C_pRuCl] as a complex, the computational study provided information about the probable pathways. Taking into account all different possibilities regarding the oxidative addition, four distinct situations (**IV.16**, **Scheme IV-4**) with minimal energy difference (< 1 kcal/mol) can be investigated[v].

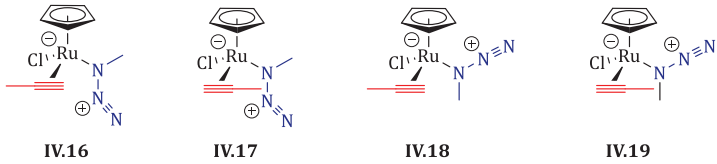

Figure IV-4: Four distinct situations with minimal energy difference regarding the oxidative addition.

In **Figure IV-5**, the energy profile for the RuAAC of one distinct situation **IV.16** is shown. The oxidative addition (step **B**, **Scheme IV–2**), results in a six-membered metallocycle **IV.21** which is 13.2 kcal/mol more stable than **IV.16** with a small activation barrier of 4.3 kcal/mol.

[v] The azide **IV.4** can react with the metal via the proximal or distal nitrogen and the alkyne **IV.1** can also coordinate to the metal in a π-fashion in two discrete situations. In total four different possibilities, two of which give arise to the 1,5-regioisomer, while the other two lead to the 1,4-regioisomer.

Intermediate **IV.21** undergoes a reductive elimination *via* transition state **IV.22** (RDS, E_a: 13 kcal/mol) forming the Ru-triazole complex **IV.23**. Alternatively **IV.21** relaxes to a more stable six-membered ring **IV.25** (E_a: 1.6 kcal/mol). The overall process is therefore influenced by the relative energies and the ease of interconversion of the intermediates **IV.21** and **IV.25**. Fokin proposes that in the case of C_p*RuCl complexes, the formation of **IV.25** is disfavored due to an amplified steric repulsion of the methyl groups of the C_p* moiety with the alkyl moiety of the alkyne. Eventually, **IV.21** is directly converted into **IV.23** with an overall activation energy barrier of 13 kcal/mol accounting for the observed rate acceleration compared to the 1,3-dipolar cycloaddition by Huisgen. Other possible discrete active catalyst species **IV.17**-**IV.19** are disfavored in the oxidative addition step.

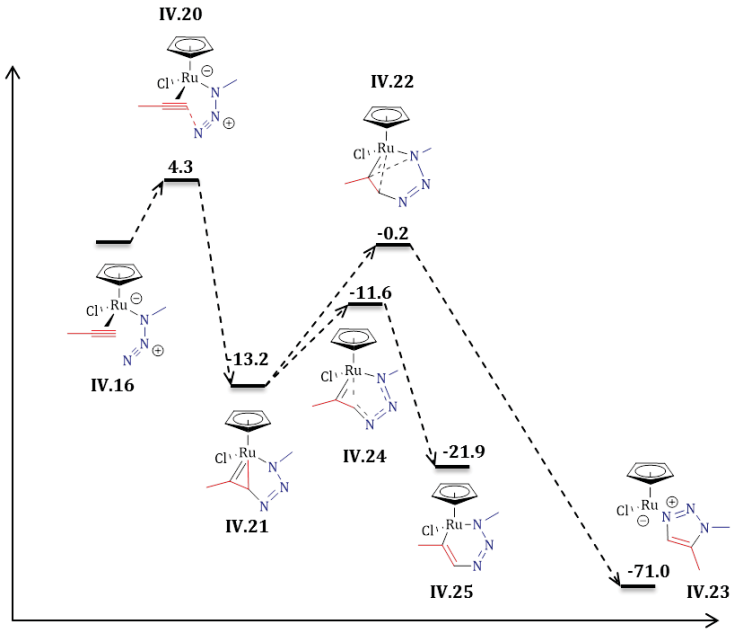

Figure IV-5: Energy diagram of the key bond making steps in the RuAAC

2. Ruthenium Catalysts:

- [C_p*RuCl] complexes are excellent and selective catalysts for RuAAC purposes. Thanks to the bulkiness and the high electron density of the C_p* ligand, these complexes are able to stabilize the intermediates as well as to orientate the oxidative addition of alkyne and azide to the desired conformation. Expecially C_p*RuCl(PPh_3)$_2$ **IV.26** and C_p*RuCl(COD) **IV.27** (**Figure IV-6**) are very thankful examples as they are superior to other [C_p*RuCl] complexes in terms of efficiency, stability and synthetic availability.[16] As the cyclooctadiene ligand in **IV.27** is more labile than phosphine ligands in **IV.26**, the former is more easily displaced resulting in a higher activity of **IV.27** even at room temperature.

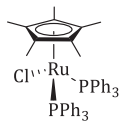

IV.26

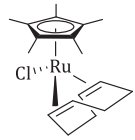

IV.27

Figure IV-6: Commonly used [Cp*RuCl] for RuAAC purposes

- [C_pRuCl] complexes are moderately active and give arise to mixtures of 1,4- and 1,5-triazoles.
- [RuCl] complexes are found to be very ineffective towards the RuAAC: the lack of the electron-rich C_p or C_p* ligand is detrimental to the stabilization of the higher oxidation states of the metal center. Depending on the type of [RuCl] catalyst, no or only marginal effectiveness was observed. Even more, the use of some ruthenium complexes lacking the C_p or C_p* ligand (i.e. $RuH_2(CO)(PPh_3)_3$ and $Ru(C{\equiv}CPh)_2(CO)(PCy_3)$ catalysts) leads to the selective formation of the 1,4-regioisomer[17].

E. Strain-promoted [3+2] cycloaddition

All the methods previously described, deal with cycloadditions which involve metals as catalysts. As copper, silver and ruthenium are toxic to both mammalian and bacterial cells, applications wherein the cells need to remain viable are excluded. Even more, the catalyst-free Huisgen [3+2] cycloaddition only occurs at high temperatures due to the high activation energy barrier. An alternative way to promote the azide-alkyne cycloaddition could be the release of ring strain[18].

Bertozzi and co-workers[18], published the strain promoted click reaction, based on the work of Wittig and Krebs[19] which established an 'explosive' reaction between cyclooctyne and phenyl azide. The origin for this extraordinary reactivity of this reaction can be assigned to the bond angle deformation of the triple bond to 163°[20], which accounts for nearly 18 kcal/mol of ring strain[21]. This destabilization of the starting material reduces the activation energy barrier and therefore a substantial rate acceleration is observed comparing to unstrained alkynes. Taking advantage of this ring strain, the cycloaddition occurs readily under physiological conditions in the absence of auxiliary reagents. Employing the strain-promoted [3+2] azide-alkyne cycloaddition reaction enables the selective chemical modification of biomolecules and living cells without any apparent physiological harm. In the last years, this reaction has been used *interalia* for real-time imaging of azide labelled biomolecules[22], radiolabelling of antibodies[23] and peptides related to diagnosis and imaging of cancer[24].

The reactivity and regioselectivity of this reaction was studied by Houk and co-workers[25] by means of a computational study with benzyl azide (**Figure IV-7**, **IV.4**) and substituted (OMe, Cl, F, CN) cyclooctynes **IV.28**. They determined that fluorine substitution decreases the free

activation energy barrier and therefore turns out to have the most dramatic effect on the reactivity by enhancing the reaction rate.

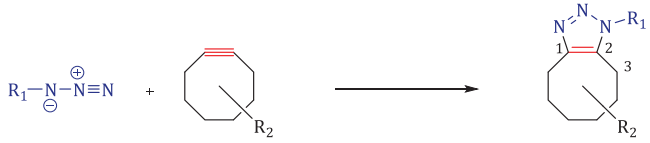

IV.4 **IV.28** **IV.29**

Figure IV-7: Strain-promoted [3+2] azide-alkyne cycloaddition.

Regarding the regioselectivity, gas-phase calculations for 3-substituted cyclooctynes **IV.28** were performed resulting in a calculated activation free energy difference of 1.5 kcal/mol in favor for the 1,5-regioisomer **IV.29**. Nevertheless, solvation free energy corrections reduced this energy difference resulting in a decreased regioselectivity[vi]. Therefore, it can be concluded that both regioisomers are formed in a nearly equivalent ratio.

F. Miscellaneous formation of 1,5-disubstituted 1,2,3-triazole

Next to the ruthenium(II)-catalyzed azide-alkyne cycloaddition, few other examples of 1,5-regioisomer formation have been reported. In the lead of the discovery of ruthenium as an excellent catalyst, Sharpless and Fokin[26] revisited an existing method of Akimova and co-workers[27] for the synthesis of 1,5-disubstituted regioisomers by using azides and lithium or magnesium acetylides (**Figure IV-8**, **IV.30**). After re-establishing the procedure of Akimova for the synthesis of 1,5-regiomers, Sharpless and Fokin explored this reaction further by trapping the 4-bromomagnesium-1,2,3-triazole **IV.31** with electrophiles other than protons, therefore creating 1,4,5-trisubstituted 1,2,3-triazoles **IV.32** in moderate to good yields. Despite, these interesting results, the stoichiometric amount of magnesium or lithium acetylide reagents imposes compatibility limitations to the functional groups present.

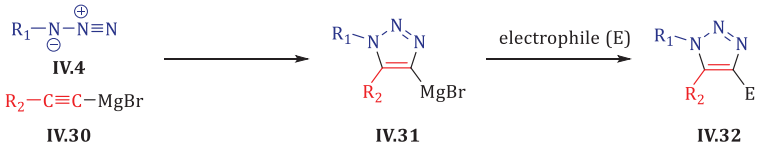

IV.31 **IV.32**

Figure IV-8: Procedure for 1,4,5-trisubstituted triazole synthesis proposed by Akimova and further elaborated by Sharpless and Fokin.

In 2004, Hlasta and co-workers[28] described a method for the synthesis of 1,5-disubstituted triazoles by the use of 1-trimethylsilylacetylenes (**Figure IV-9**, **IV.33**). The regioselectivity is

[vi] This could be explained by taking into account electrostatic potential surfaces and dipole moments of the resulting 1,4- and 1,5-regioisomers. As the dipole moment for the 1,4-regioisomer is higher (5.5D compared to 2.0D for the 1,5-regioisomer in gas phase and 7.0D compared to 2.8D in H_2O), solvation hence stabilizes the 1,4-regioisomer more strongly than the 1,5-regioisomer, leading to a loss of regioselectivity.

controlled by a combination of steric hindrance and the ability of silicon to stabilize a partial positive charge at the acetylene β-carbon in the transition state. Desilylation of triazole intermediate **IV.34** can be obtained by treatment with 50% TFA/dichloromethane. Doing so, a small library of 1,5-disubstituted 1,2,3-triazoles **IV.15** was obtained in moderate yields.

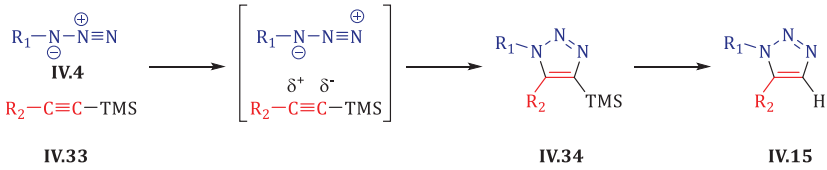

Figure IV-9: Hlasta's procedure for 1,5-disubstituted triazole moieties.

In 2010, Fokin and co-workers[29] presented a transition-metal-free synthesis of 1,5-diaryl-1,2,3-triazoles by using a catalytic amount of tetramethylammonium hydroxide. This mild and experimentally simple catalytic method for the generation of the reactive acetylides reacts readily with aryl azides (**IV.36**, **Figure IV-10**) resulting in the exclusive formation of 1,5-disubstituted triazole moieties in good to excellent yields.

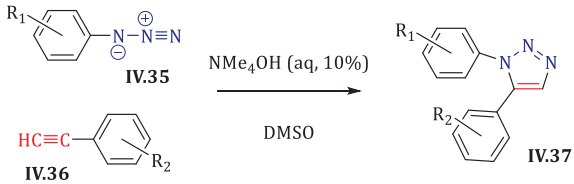

Figure IV-10: Fokin's transition-metal-free procedure for 1,5-disubstituted triazole moieties

REFERENCES

[1] Kolb, H. C.; Finn, M. G.; Sharpless, K. B. *Angew. Chem. Int. Ed*. **2001**, *40*, 2004-2021.

[2] a) Lwowski, W. In *1,3-Dipolar Cycloaddition Chemistry*, Vol. 1, Ed.: A. Padwa, Wiley: New York, **1984**, pp. 559-560. b) Huisgen, R. *Pure Appl. Chem.* **1989**, *61*, 613-628.

[3] Rostovtsev, V. V.; Green, L. G.; Fokin, V. V.; Sharpless, K. B. *Angew. Chem. Int. Ed.* **2002**, *41*, 2596.

[4] Tornøe, C. W.; Cristensen, C.; Meldal, M. *J. Org. Chem.* **2002**, *67*, 3057-3064.

[5] Jones, G.O.; Ess. D.H.; Houk, K.N. *Helv. Chim. Acta* **2005**, *88*, 1702-1710.

[6] Himo, F.; Lovell, T.; Hilgraf, R.; Rostovtsev, V. V.; Noodleman, L.; Sharpless, K. B.; Fokin, V. V. *J. Am. Chem. Soc.* **2005**, *127*, 210.

[7] a)Hein, C. D.; Liu, X.-M.; Wang, D. *Pharm.Res.* **2008**, 25, 2216-2230. b) Bock, V. D.;Hiemstra, H.; van Maarseveen, J H. Eur. *J. Org. Chem.* **2006**, *1*, 51-68.

[8] Hein, J. E.; Fokin, V. V. *Chem. Soc. Rev.* **2010**, *39*, 1302-1315.

[9] a) Rodionov, V. O.; Fokin, V. V.; Finn, M. G. *Angew. Chem. Int. Ed.* **2005**, *44*, 2210-2215. b) Rodionov, V. O.; Presolski, S. I.; Diaz, D. D.; Fokin, V. V.; Finn M. G. *J. Am. Chem. Soc*. **2007**, *129*, 12705-12712.

[10] Tornøe, C. W.; Meldal, M. *Chem. Rev.* **2008**, *108*, 2952-3015.

[11] a) Silvestri, I. P.; Andemarian, F.; Khairallah, G. N.; Yap, S. W.; Quach, T.; Tsegay, S.; Williams, C. M.; O'Hair, R. A. R.; Donnelly, P. S.; Williams, S. J. *Org. Biomol. Chem.* **2011**, *9*, 6082-6088. b) Aucagne, V.; Leigh, D. A. *Org. Lett.* **2006**, *8*, 4505-4507.

[12] McNulty, J.; Keskar, K.; Vemula, R.; *Chem. Eur. J.* **2011**, *17*, 14727-14730.

[13] Zhang, L.; Chen, X.; Xue, P.; Sun, H. H. Y.; Williams, I.D.; Sharpless, K. B.; Fokin, V. V.; Guochen, J. *J. Am. Chem. Soc.* **2005**, *127*, 15998-15999.

[14] a) Dixneuf, P. H.; *Pure Appl. Chem.* **1989**, *61*, 1763-1770. b) Murahashi, S.-I.; Takaya, H.; Naota, T. *Pure Appl. Chem.* **2002**, *74*, 19-24.

[15] Boren, B. C.; Narayan, S.; Rasmussen, L. K.; Zhang, L.; Zhao, H.; Lin, Z.; Jia, G.; Fokin, V. V. *J. Am. Chem. Soc*. **2008**, *130*, 8923-8930.

[16] Dixneuf, P. H.; Bruneau, C.; Derien, S. *Pure Appl. Chem.* **1998**, *70*, 1065.

[17] a) Liu, P. N.; Li J.; Su, F. H.; Ju, K. D.; Zhang, L.; Shi, C.; Sung, H. H. Y.; Williams, I. D.; Fokin, V. V.; Lin, Z.; Jia G. *Organometallics* **2012,** *13*, 4904-4915. b) Liu, P. N.; Siyang, H. X.; Zhang, L.; Tse, K. S. K.; Jia, G. *J. Org. Chem.* **2012**, *13*, 5844-5849.

[18] Agard, N. J.; Prescher, J. A.; Bertozzi, C. R. *J. Am. Chem. Soc.* **2004**, *126*, 15046-15047.

[19] Wittig, G.; Krebs. A. *Chem. Ber.* **1961**, *94*, 3260-3275.

[20] Meier, H.; Petersen, H.; Kolshorn, H. *Chem. Ber.* **1980**, *113*, 2398-2409.

[21] Turner, R.; Jarrett, A. D.; Goebel, P.; Mallon, B. J. *J. Am. Chem. Soc.* **1973**, *95*, 790-792.

[22] Jewett, J. C.; Bertozzi, C. R. *Org. Lett.* **2011**, *13*, 5937-5939.

[23] Carpenter, R. D.; Hausner, S. H.; Sutcliffe, J. L. *ACS Med. Chem. Lett.* **2011**, *2*, 885-889.

[24] Campbell-Verduyn, L. S.; Mirfeizi, L.; Schoonen, A. K.; Dierckx, R. A.; Elsinga, P. H.; Feringa, B. L. *Angew. Chem. Int. Ed.* **2011**, *50*, 11117-11120.

[25] Schoenebeck, F.; Ess, D. H.; Jones, G. O.; Houk, K. N. *J. Am. Chem. Soc.* **2009**, *131*, 8121-8133.

[26] Krasinski, A.; Fokin, V. V.; Sharpless K. B. *Org. Lett.* **2004**, *6*,1237-1240.

[27] a) Akimova, G. S.; Chistokletov, V. N.; Petrov, A. A. *Zh. Org. Khim.* **1967**, *3*, 968. b) Akimova, G. S.; Chistokletov, V. N.; Petrov, A. A. *Zh. Org. Khim.* **1967**, *3*, 2241. c) Akimova, G. S.; Chistokletov, V. N.; Petrov, A. A. *Zh. Org. Khim.* **1968**, *4*, 389.

[28] a) Coats, S. J.; Link, J. S.; Gauthier, D.; Hlasta, D. J. *Org. Lett.* **2005**, *7*, 1469-1472. b) Hlasta, D. J.; Ackerman, J. H. *J. Org. Chem.* **1994**, *59*, 6184-6189.

[29] Kwok, S. W.; Fotsing, J. R.; Fraser, R. J.; Rodionov, V. O.; Fokin, V. V. *Org. Lett.* **2010**, *12*, 4217-4219.

PART 2:
AIM & STRATEGY

V. Aim & Strategy

The aim of this research project is to synthesize new potent biologically active scaffolds based on the previously studied 1,5-benzodiazepine-2,4-diones (**V.1**, **Figure V-2**), which also show privileged structure capacities. This [1,2,3]triazolo[1,5-*d*]-1,4-benzodiazepin-2-one scaffold **V.2** mimics structures **V.1** as stated by the principles of bioisosterism. The privileged capacity of the 1,5-benzodiazepine-2,4-diones **V.1** and the principles of bioisosterism are respectively depicted in section **I.3** and **III.1**, yet the latter are briefly summarized in **Figure V-1.**

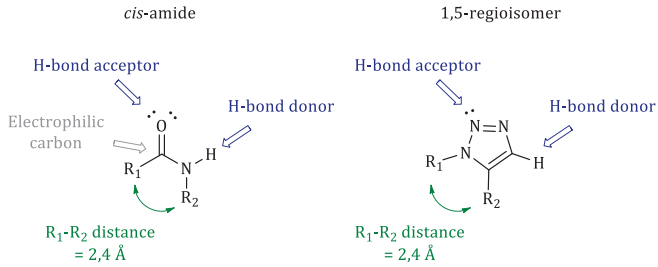

Figure V-1: Structural and electronic evaluation of a *cis*-amide bond versus the 1,5-regioisomer of a 1,2,3-triazole moiety

Thanks to these similarities depicted in **Figure V-2**, this 1,2,3-triazole fused benzodiazepine **V.2** can be regarded as a mimic for the 1,5-benzodiazepine-2,4-diones **V.1**.

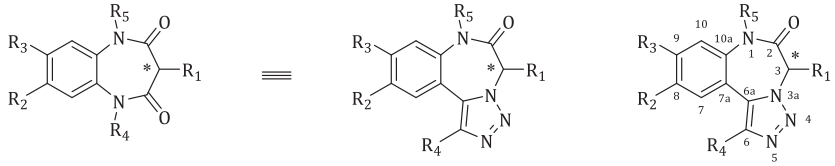

Figure V-2: Fundamental concept of this research applying bioisosterism to 1,5-benzodiazepine-2,4-diones V.1

This scaffold consisting of a tricyclic system, built up *via* a seven-membered ring, a triazole and an aryl moiety, needs to be constructed *via* a solid-phase strategy in an efficient and short way. Moreover, the applied reaction conditions should enable a feasible introduction of five different diversity points, therefore allowing a vast and rational exploration of the chemical space around this new scaffold molecule.

In **Figure V-3**, a retrosynthetic approach is presented showing that the desired seven-membered ring will be constructed *via* a lactam formation in the last step. Preferably, this amide bond formation will be part of a cyclization/release strategy, wherein cyclization of the seven-membered ring and simultaneous release from the resin will be pursued. This cyclization/release strategy can be achieved *via* an attack of the aniline nucleophile onto the carboxyl functionality present in **V.4**.

The next step in the retrosynthesis involves the introduction of the fifth diversity point, which can be introduced *via N*-monoalkylation of resin-bound aniline **V.5**. Several procedures can be employed, i.e. Mitsunobu-Fukuyama conditions or a reductive alkylation.

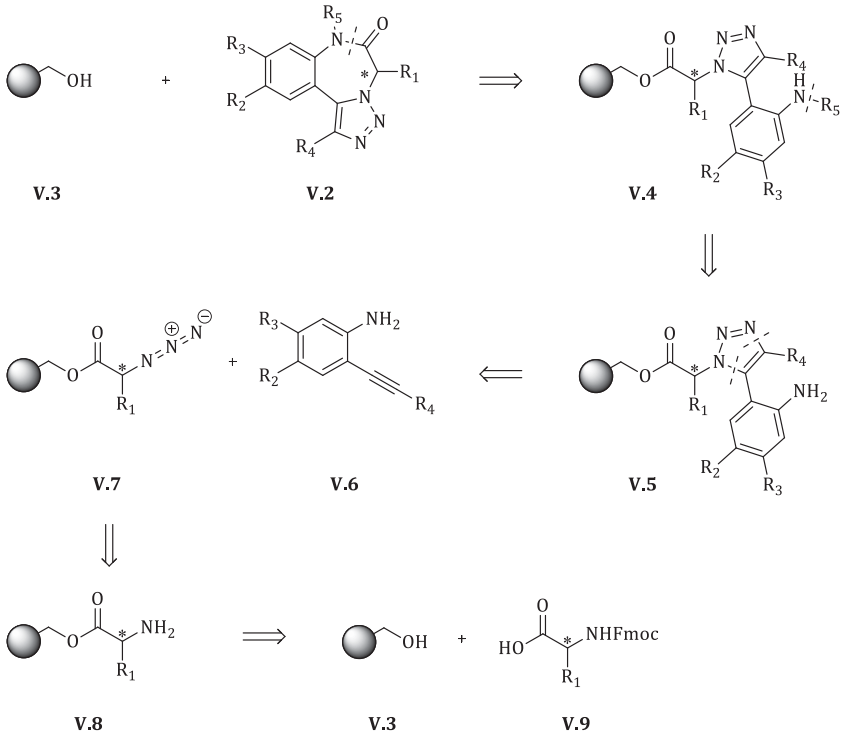

Figure V-3: Retrosynthetic approach toward desired scaffold molecule V.2

The required solid-phase bound aniline **V.5** needed for the incorporation of the R_5 side chain and subsequent cyclization/release is introduced by a 1,3-dipolar cycloaddition of 2-ethynylaniline building blocks **V.6** and a solid- phase bound α-azido acid **V.7**. The

ethynylaniline building blocks can be synthesized in solution starting from commercially available 2-iodoanilines (**V.10**, **Figure V-4**). Thanks to the diversity among these available starting products a range of various building blocks can be made, therefore allowing the introduction of three diversity points during the 1,3-dipolar cycloaddition step.

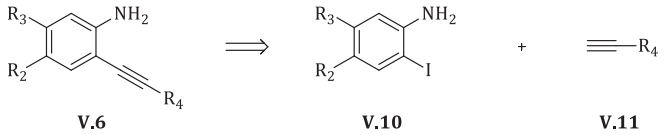

Figure V-4: Retrosynthesis of 2-ethynylaniline building block V.6

Apart from the incorporation of the aniline functionality, the 1,3-dipolar cycloaddition selectively needs to yield the desired 1,5-disubstituted regioisomer of the triazole moiety, as the 1,4-regioisomer does not allow cyclization to the desired seven-membered products.

The other reaction partner for this 1,3-dipolar cycloaddition, a solid-phase bound azide **V.7**, will be formed by a diazotransfer procedure on solid-phase starting from a resin-bound amine **V.8**. The choice for commercially available enantiomerically pure α-amino acids as amine source was made by the presence of the required carboxylic acid function and by the importance of amino acid side chains as pharmacophore groups. Moreover, a well-understood knowledge of amino acid coupling procedures on the solid-phase **V.3** is available in literature.

A modular approach for the synthesis of this new triazole-fused benzodiazepine (**V.2, Figure V-5**) can be claimed as:

- one diversity point is introduced *via* commercially available α-amino acids **V.9**.
- a straightforward synthesis and introduction of 2-ethynylaniline building blocks bearing three different sites of diversity **V.6** is possible.
- *N*-monoalkylation procedures using alkylating agents **V.12** facilitating the incorporation of the last diversity point are available.
- a cyclization/release strategy will generate the desired molecules with an enhanced purity.

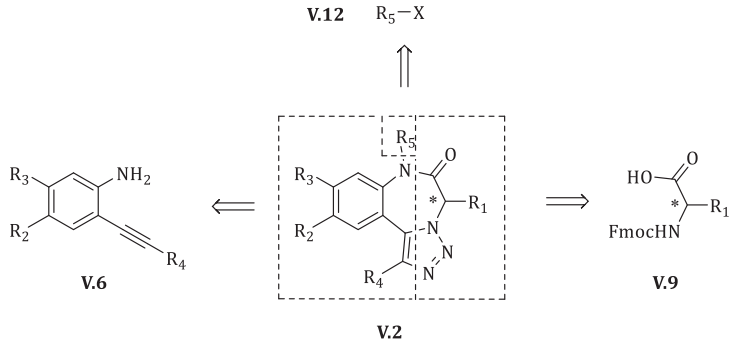

Figure V-5: Modular synthesis affording the desired 1,2,3-triazole fused benzodiazepine V.2.

PART 3: RESULTS & DISCUSSION

VI. Coupling

A. Introduction

The coupling of an α-amino acid **V.9** to Wang resin **V.3** comprises a condensation reaction between an alcohol moiety, present on the polymer matrix and a carboxylic acid represented by the *N*-protected α-amino acid **V.9**. As this condensation reaction yields an ester bond, the equilibrium of this reaction needs to be shifted to the desired direction. The latter can be achieved upon activation of the carboxylic acid, more specifically by converting the hydroxyl of the carboxylic acid into a better leaving group. This activation procedure should be fast, quantitative and should be carried out under mild conditions without affecting stereogenic centers present in the substrate. Several procedures which generate active compounds such as (mixed) anhydrides, activated esters[1], acyl halides[2], acyl azides, acylimidazoles[3] have been developed in order to give an answer to these demands. Among the wide range of available coupling methods, one of the most established and traditional ways for activating carboxylic acids is the carbodiimide method generating (mixed) anhydrides or active esters. This method will be discussed in the following paragraphs.

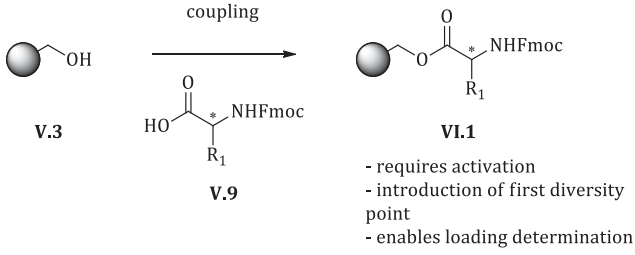

Figure VI-1: Coupling step of the amino acid (V.9) to Wang resin (V.3)

B. Carbodiimides activation procedure

N,N'-Dicyclohexylcarbodiimide (DCC, **VI.2**) was the first coupling reagent to be synthesized and used as coupling reagent and was reported by Sheehan in 1955[4]. Since this discovery, many variations have been developed for case-specific applications. In **Figure VI-2**, three examples are given: *N,N'*-dicyclohexylcarbodiimide (DCC, **VI.2**), *N,N'*-diisopropylcarbodiimide (DIC, **VI.3**) and the water-soluble *N*-ethyl-*N'*-(3-dimethylaminopropyl)carbodiimide hydrochloride (EDC.HCl, **VI.4**).

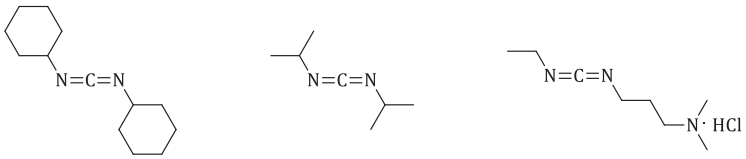

VI.2 **VI.3** **VI.4**

Figure VI-2: Commonly used carbodiimide based coupling reagents

1. Mechanism

a) Possible pathways upon activation

Carbodiimides can be used for activating carboxylic acids towards symmetrical anhydrides, activated esters, or many serve as a direct coupling agent. Upon addition of the carbodiimide to a carboxylic acid **VI.5** solution, the weakly alkaline nitrogen present in carbodiimide **VI.6** readily deprotonates the acid affording **VI.7** and **VI.8**. The next step involves addition of deprotonated carboxylic acid **VI.7** to protonated diimide **VI.8** forming the *O*-acylisourea **VI.9**. As the latter is the most reactive species present, **VI.9** can readily undergo attack of a nucleophile **VI.10** (alcoholysis or aminolysis) to form the desired ester **VI.11** or amide bond respectively along with the urea byproduct (pathway **A**). Possible enolization in the presence of a base could lead to a loss of enantiomeric purity of the coupled amino acid (*vide infra*).

Another possibility is the formation of the symmetrical anhydride **VI.12** upon reaction of the *O*-acylisourea **VI.9** with a second carboxylate **VI.7** (pathway **B**). This side reaction (desired or unintentionally) leads to the anticipated final compound **VI.11**, yet the use of a second equivalent of carboxylic acid gives rise to lower coupling yields and if desired, this strategy is not ideal for coupling expensive and non-natural amino acids.

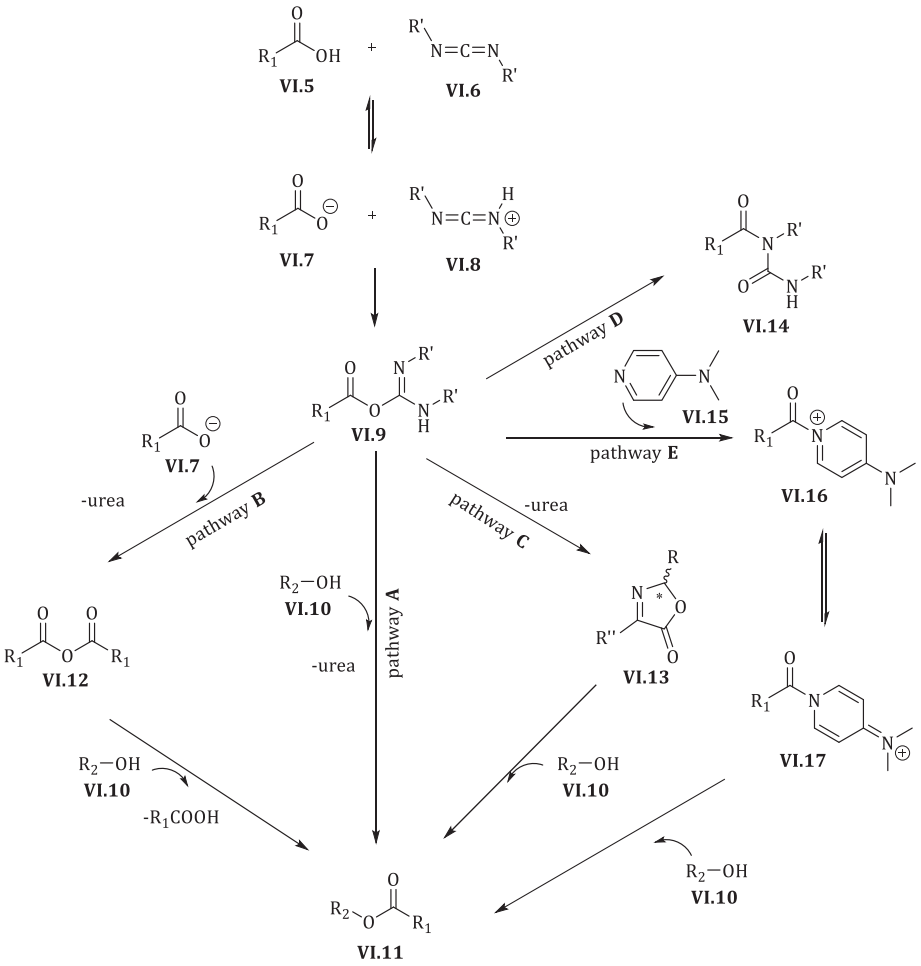

Scheme VI–1: Possible pathways upon carboxylic acid activation with carbodiimides.

Pathway **C** involves the cyclization of the *O*-acylisourea **VI.9** into oxazolones **VI.13**, the formation of which is detrimental for the coupling rate with nucleophiles, as oxazolones are far less reactive towards ring opening. Even more, as the α-H present in this five-membered ring is extremely prone to racemization, the enantiomeric purity of the coupling product decreases tremendously (see **Figure VI-3**). This oxazolone formation can be avoided by choosing the appropriate *N*-protecting group, such as carbamate groups, decreasing the likelihood of oxazolone **VI.13** formation.

Pathway **D** shows the irreversible formation of *N*-acylurea derivatives **VI.14** by a rearrangement. An intramolecular addition/elimination of the nitrogen to the carbonyl group generates stable *N*-acylurea and therefore loss of activated species. This side reaction can be

avoided by addition of *N*-hydroxybenzotriazole (HOBt), *N*-hydroxy-7-aza-benzotriazole (HOAt) or *N,N*-dimethylaminopyridine (DMAP, **VI.15,** pathway **E**). A fast addition of HOBt creates an activated ester, which can be readily alcoholyzed. In case of DMAP as nucleophilic catalyst, the regeneration of the aromaticity is the driving force of the coupling reaction. Generally, these additives increase the reaction rate of the coupling step therefore reducing the epimerization levels.[5] Taken into account the explosive nature of the discussed benzotriazoles[6], our preference goes to DMAP.

b) Racemization

As mentioned before, the strong activation of a carboxyl function by carbodiimides could provoke side reactions. The intramolecular attack of a carbonyl oxygen to the strongly polarized *O*-acylisourea **VI.9** leads to the formation of oxazolones **VI.13** which are quite unreactive and hence hardly opened with nucleophiles (**Figure VI-3**). Mild basic conditions enable abstraction of the α-hydrogen, giving rise to **VI.19**. As the rate of racemization is higher than the rate for ring opening[7], racemization in the α-position takes place.

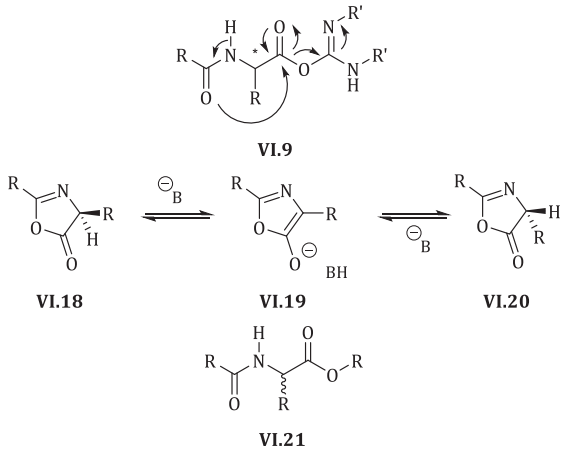

Figure VI-3: Racemization *via* oxazolone formation

Another pathway for racemization while using carbodiimides as coupling agents is represented in **Figure VI-4**, and occurs *via* an intermolecular proton abstraction from the *O*-acylisourea intermediate **VI.22**. The resulting enol form **VI.23** is further stabilized by an intramolecular hydrogen bond presented in structure **VI.24**.

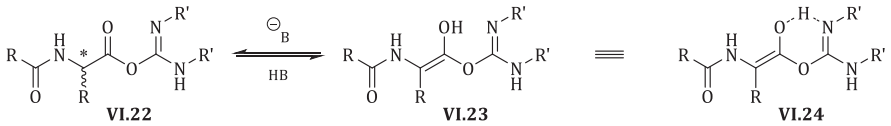

Figure VI-4: Racemization *via* keto-enol tautomerization

Generally, the rate of racemization depends on temperature, reaction conditions and specific substituents present in the substrate.

C. α-Amino acid coupling on Wang

The α-amino acids used are *N*-carbamate protected as this reduces likelihood of racemization, moreover, homocoupling between two amino acids is avoided. As a protecting group, the fluorenylmethoxycarbonyl group (Fmoc) or tert-butoxycarbonyl group (Boc) can be chosen. The latter can be cleaved under acidic conditions (50% TFA/dichloromethane),[8] while the Fmoc-group requires basic conditions (20 v/v% 4-methylpiperidine/DMF)[8] for removal. As these basic deprotecting conditions are orthogonal with our applied Wang resin, the Fmoc-protecting group will be chosen for this work. Additionally, the UV-active dibenzofulvene-piperidine adduct enables a loading determination of the resin loading with amino acid.

As illustrated in **Scheme VI-2**, during this research, the coupling of eight commercially available enantiomerically pure α-amino acid derivatives was performed. DIC/DMAP was chosen as the appropriate activation procedure in order to minimize racemization and to increase the reaction rate (pathway **E**, **Scheme VI-1**). Wang resin was treated twice with activated amino acid, followed by a capping procedure in order to deactivate the residual alcohol moieties. The efficiency of the coupling step (**Table VI-1**) was determined *via* a quantitative Fmoc determination method upon extensive drying of the beads. The outcome of these measurements provide the loading of α-amino acid on the resin and is necessary to have a clear sight in the amount of reagents needed in the next reaction steps.

The quantitative Fmoc method test relies on the determination of the concentration of dibenzofulvene adduct which is released upon treatment of the solid-phase bound Fmoc-protected amino acid with a piperdine base ($t_{1/2}$ = 6s in 20% piperidine/DMF[9]). If the Lambert-Beer applicability is justified (concentration < 0.15mM), a UV measurement of the obtained solution at 300nm allows a concentration determination according to [1].[10]

$$A = \varepsilon . l . c \qquad [1]$$

A= measured absorbance [/]
ε = emission coefficient (8358,5) [$M^{-1}.cm^{-1}$]
l = path length [cm]
c = concentration of dibenzofulvene adduct [M]

As can be seen from **Table VI-1** coupling efficiencies, determined by the UV-quantitation of released dibenzofulvene adduct, vary between 88-97% after two consecutive treatments with actived species.

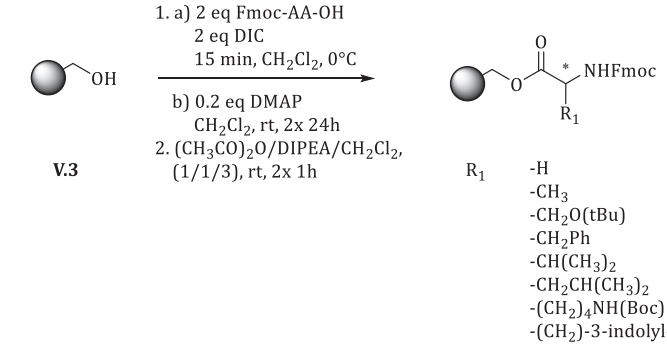

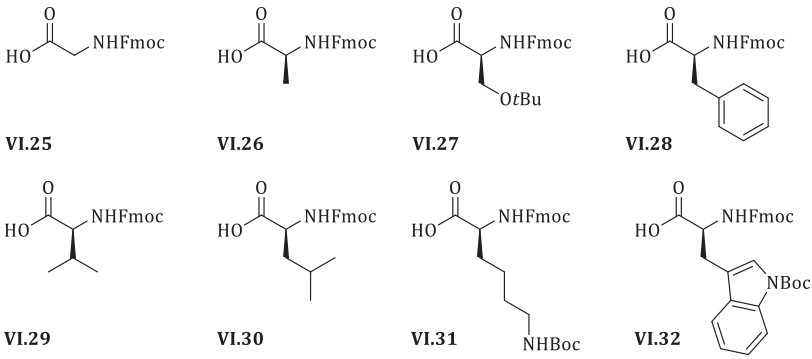

Scheme VI–2: Coupling of VI.25 – VI.32 to Wang's resin V.3

Table VI-1: Coupling efficiency

entry	compound	coupling efficiency (%)[a]
1	**L-VI.33**	96
2	**L-VI.34**	88
3	**L-VI.35**	91
4	**L-VI.36**	93
5	**L-VI.37**	93
6	**L-VI.38**	96
7	**L-VI.39**	97
8	**L-VI.40**	92

[a] determined *via* UV- spectroscopy

REFERENCES

[1] Excellent reviews: a) Valeur, E.; Bradley, M. *Chem. Soc. Rev.* **2009**, *38*, 606-631 (and references therein). b) El-Faham, A.; Albericio, F. *Chem. Rev.* **2011**, *111*, 6557-6602 (and references therein). c) Han, S.-Y.; Kim, Y.-A. *Tetrahedron* **2004**, *60*, 2447-2467.

[2] Zhang, L.-H.; Chung, J. C.; Costello, T. D.; Valvis, I.; Ma, P.; Kauffman, S.; Ward, R. *J. Org. Chem.* **1997**, *62*, 2466.

[3] a) Paul, R.; Anderson, W. *J. Am. Chem. Soc.* **1960**, *82*, 4596. b) Dale, D. J.; Draper, J.; Dunn, P. J.; Hughes, M. L.; Hussain, F.; Levett, P. C.; Ward, G. B.; Wood, A. S. *Org. Process Res. Dev.* **2002**, *6*, 767.

[4] Sheehan, J.C.; Hess, G.P.; *J. Am. Chem. Soc.* **1955**, *77*, 1067-1068.

[5] a) Koenig, W.; Geiger, R. *Chem. Ber*. **1970**, *103*, 788-798. b) Koenig, W. Geiger, R. *Chem. Ber.* **1970**, *103*, 2024-2033. c) Carpino, L. A. *J. Am. Chem. Soc.* **1993**, *115*, 4397-4398.

[6] a) Malow, M.; Wehrstedt, K. D.; Neuenfeld, S. *Tetrahedron Lett* **2007**, *48*, 1233-1235. B) Wehrstedt, K. D.; Wandrey, P. A.; Heitkamp, D. *Hazard. Mater.* **2005**, *126*, 1-7.

[7] Griehl, C.; Kolbe, A.; Merkel, S. *J. Chem. Soc., Perkin. Trans. 2* **1996**, 2525.

[8] Mergler, M.; Durieux, J. *The Bachem practice of SPPS*; Bachem AG, **2005**; pp 43–46.

[9] Atherton, E.; Logan, C.J.; Sheppard, R.C. *J. Chem. Soc. Perkin Trans. 1* **1981**, 538-546.

[10] Caroen, J. Analysemethoden in de vastefasesynthese. In *Ontwikkeling van een vastefasestrategie voor 1,2,3,4,5,6-hexahydro-1,5-benzodiazocine-2,6-dionen voor toepassing in combinatorische bibliotheken*, Universiteit Gent, **2012**, p.71-72.

VII. Diazotransfer

A. Introduction

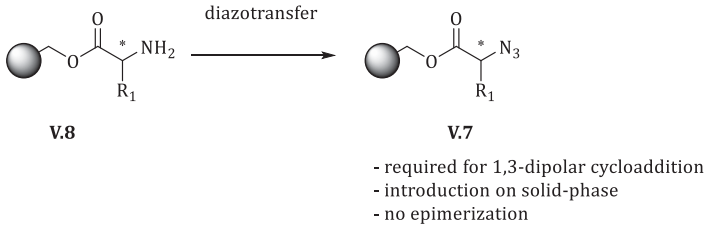

Figure VII-1: Diazotransfer reaction step

The usefulness of azides in organic synthesis extends far beyond their purpose in 1,3-dipolar cycloadditions aimed in this work. Organic azides[1] are used to mask amines, as strategic synthetic tool,[2] in photoaffinity labelling,[3] in drugs,[4] etc… Azides have found their application in sensitive substrates such as oligosaccharides,[5] aminoglycoside antibiotics,[1,6] glycoaminoglycans,[7] peptidonucleic acids (PNA)[8], as well as in solid-phase peptide synthesis.[9]

Introducing azides in organic molecules can be accomplished by several ways; most of them rely on direct displacement reaction (S_N2-fashioned) with an azide anion.[10] However, such reactions at an sp^3 carbon may cause inversion[11], epimerization[12] or concurrent elimination[13] and when performed in solvents like DMF or DMSO product isolation can be difficult. Other possibilities are reactions of aryldiazonium salts with inorganic azides (diazotization)[14], cleavage of triazenes,[15] among others[1b], lacking to a certain extent orthogonality. An alternative preparation of azides is given by a *di-nitrogen-transfer* from a diazotransfer reagent to an amine. This strategy avoids epimerization, inversion and elimination. Thanks to the readily commercially available α-amino acids, the incorporation of azides in this work will rely on the diazotransfer reaction.

An ideal diazotransfer reagent should be crystalline (for purification, handing and stability), non-explosive, easily prepared and effective for diazotransfer reactions. In the early days of the azide research field, many diazotransfer reactions were performed with trifluoromethanesulfonyl azide or triflyl azide (**VII.1**). Although many reports state the first synthesis by Cavender and Shiner in 1972[16], it was Ruff who prepared this reagent for the first time in 1965[17]. Treating trifluoromethanesulfonyl anhydride with sodium azide in sulfolane resulted in the formation of trifluoromethanesulfonyl azide, which was roughly purified *via* a *vacuum* distillation. Initially, this reagent was synthesized for the purpose of a reactivity study dealing with nucleophiles and the fluorosulfonyl group.

The work provided by Shiner initiated with the observation of Regitz[18], where *p*-toluenesulfonyl azide reacts with active methylene functionalities with the formation of diazocompounds as a result of a diazotransfer reaction. The sulfonyl azide reagents explored were not active enough to convert less active compounds such as alkyl amines. Therefore, Shiner reported the first conversion of alkyl amines into alkyl azides with trifluoromethanesulfonyl azide (**VII.1**) and, even more gave a first clue of the unstable nature of this diazotransfer reagent by describing:

> *"After experiencing an explosion…"*

Shiner suggest to use this reagent in solution, including solvents like dichloromethane, DMF, THF, DMSO, dioxane and acetonitrile, therefore enabling the use without decomposition of the trifluoromethanesulfonyl azide for the first 24 hours. Due to the moderate yields combined with the unstable and dangerous nature of this particular diazotransfer reagent, this procedure was only reported scarcely for the conversion of amines present in amino acids[19] and amino sugars[20]. A typical procedure for the preparation of triflyl azide (**VII.1**) is presented in **Scheme VII–1.**

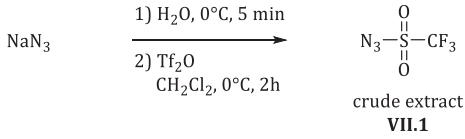

Scheme VII–1: Common preparation of trifluoromethanesulfonyl azide (VII.1) proposed by Shiner

Meanwhile, Hassner published the explosive nature upon upconcentration of dichloromethane mixtures containing sodium azide due to the presence of diazidomethane. Therefore it is strongly discouraged to concentrate reaction mixtures of the azide anions and dichloromethane.[21]

B. Diazotransfer mechanism

Wong[22] reinforced the diazotransfer reaction by using transition metals as catalysts for alkyl azide formation, initially for protecting amines as azides, especially in glycosides. A tremendous reaction rate increase was observed when 1 mol% of divalent copper was added to the reaction mixture. Later, Wong and co-workers[23] improved this procedure by stating that the solvent ratio had a dramatic influence on the rate and reproducibility of this diazotransfer reaction. A specific ratio of H_2O, CH_3OH and CH_2Cl_2 was found to give the best results as an approximate ratio of 1:2.5:1 tends to be a monophasic system. Apart from Cu(II), other transition metals such as Zn(II) and Ni(II) were found to be effective for catalyzing the reaction, resulting in a significant rate acceleration.

From a mechanistic point of view, Fisher and Anselme suggested a dianionic tetrazene intermediate (stabilized by two sodium ions) as key elements in the mechanism[24]. Nyffeler and Wong further extended this mechanism by incorporation of a divalent metal acting as a Lewis acid shown in **Figure VII-2**.[23]

The conversion initiates with the complexation of amine **VII.2** and the transition metal (Cu(II) or Zn(II)), which under basic conditions provides **VII.3**. Due to the extreme electrophilicity of the triflyl azide (**VII.1**), a nucleophilic attack by the amine **VII.3** occurs on the highly electrophilic triflyl azide yielding intermediate **VII.4**. Deprotonation and attack of the negatively charged nitrogen atom onto the metal forms a metal-stabilized mixed tetrazene **VII.5**. A reverse [3+2] dipolar cycloaddition gives rise to the desired alkyl azide **VII.6** and metal-triflyl imido complex **VII.7**. According to the computational work of Brandt *et al.*[25] it is suggested that **VII.7** forms an equilibrium with **VII.9**. Another transimination of **VII.7** could also yield transient metal-imido complex **VII.8** which upon addition of triflyl azide could form the mixed tetrazene **VII.5**. A full investigation of this mechanism is still under development, yet the proposal of Nyffeler and Wong explains the catalytic activity of the transition metals.

Further refinements of the procedure of Wong were done by Ye *et al.* who reported a triflyl azide preparation in CH_3CN or pyridine. The latter resulted in a stock solution which can be added directly to the amine solution for the subsequent diazotransfer reaction[26]. This procedure leads to a higher efficiency as hydrolysis can be avoided, therefore reducing the amounts of Tf_2O and NaN_3. Ernst *et al.*[27] reported a replacement of dichloromethane as solvent of choice by toluene, therefore circumventing the formation of hazardous side products as azidochloromethane and diazidomethane (*vide supra*).

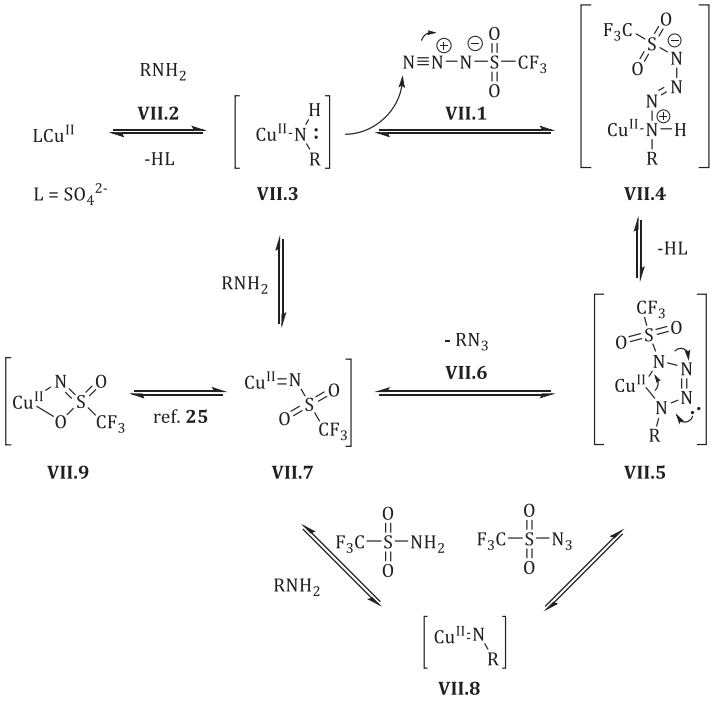

Figure VII-2: Diazotransfer mechanism proposed by Wong[23]

A report provided by Liskamp[28], illustrated a solid-phase application of a diazotransfer reaction by using freshly prepared triflyl azide (**VII.1**). α-Amino acids and short peptides bound onto ArgoGel with a Wang linker were converted into respectively the corresponding azido acids and azido peptides. This strategy enabled the synthesis of peptides with an N_3-terminus, therefore offering an alternative for the preparation of azido acids in solution and subsequent coupling to the solid support. The latter has to be avoided as activated azide species are extremely sensitive[i,29] to harmful decomposition.

In **Scheme VII-2**, the procedure is shown where solid-bound Fmoc-protected L-phenylalanine (**VI.36**) is converted into the desired azido acid **VII.10** in 84% yield, with full preservation of the chirality.

[i] In general, organic azides are considered sensitive when the azido content is exceptionally high. There is no sharp threshold at which the explosive hazard starts. However, as a rule of thumb, violent decomposition reactions are expected for azido compounds having a (C+O)/N ratio of < 3.

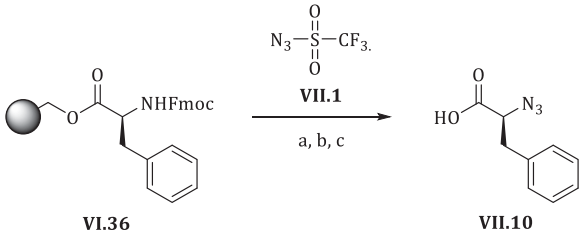

a) 20 v/v% piperidine/NMP, rt, 3x 8 min b) 16.7 eq **VII.1**, 10 mol% $CuSO_{4.5}H_2O$, TEA, CH_2Cl_2/MeOH (9/1) c) TFA/CH_2Cl_2 (1/1), rt, 1h

Scheme VII–2: Liskamp's procedure towards solid-phase synthesis of azido acids.

As mentioned before, a certain *azidophobia*[30] hampered the research concerning azides, due to the related specific explosive and impact sensitive characteristics. Triflyl azide (**VII.1**) is an example of a diazotransfer reagent which needs to be handled with caution, therefore impeding this reagent to be used extensively as diazotransfer reagent in solid-phase syntheses.

In 2007, Goddard-Borger and Stick[31] reported a new, efficient, inexpensive and - more importantly - a shelf-stable diazotransfer reagent imidazole-1-sulfonyl azide hydrochloride (**VII.11**). This was based on the idea that replacing the trifluoromethyl group by another electron withdrawing group would preserve the reactivity, whilst however inducing crystallinity and therefore stability. Goddard-Borger found that this reagent is effective for solution-phase amine to azide conversion with retention of the stereogenic centra. Moreover, **VII.11** can be used for diazotransfer to active methylene compounds.

In **Scheme VII–3**, a typical solution phase procedure for diazotransfer of L-phenylalanine (**VII.12**) is shown, where 1.2 equivalents of imidazole-1-sulfonyl azide hydrochloride (**VII.11**) with 2 equivalents of potassium carbonate and catalytic amount of Cu(II) in methanol gives rise to (*S*)-2-azido-3-phenylpropanoic acid (**VII.10**) in 75% yield.

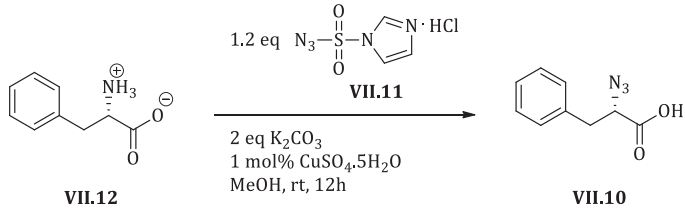

Scheme VII–3: Proposed conditions by Goddard-Borger for in solution diazotransfer

Taken into account the inexpensive, harmless[ii] nature of this reagent, we dedicated to continue our research continued with this promising diazotransfer reagent. Moreover, its crystallinity would enable an easy practice of parallel solid-phase chemistry. Unfortunately, the conditions provided by Goddard-Borger were not applicable to polystyrene based solid-phase chemistry as methanol is an unsuitable solvent for this apolar resin (swelling degree of Wang in MeOH: 1.6 mL/g dry resin, see section § **I.2.B.1**). Secondly, as potassium carbonate is only partially soluble in MeOH, the accessibility of the base to the reactive sites would be low, therefore being ineffective.

C. Optimization procedure towards a solid-phase diazotransfer reaction

The procedure started by preparing imidazole-1-sulfonyl azide hydrochloride (**VII.11**, **Scheme VII–4**) *via* the procedure reported by Goddard-Borger.[31] The diazotransfer reagent was formed in 82% yield, in correspondence with the reported synthesis by Goddard-Borger. Only an adjusted work-up was performed in order to remove the excess of imidazole.

[ii] In 2011, Goddard-Borger and Stick[31b] added a correction to their original paper, stating that their shelf-stable reagent certainly had some safety issues regarding the preparation, storage and use of imidazole-1-sulfonyl azide hydrochloride (**VII.11**).

- Concentration of the mother liquors of **VII.11** resulted in an explosion, most probably due to present side products like diazido sulfonyl[31c] and/or hydrazoic acid.
- Storage of **VII.11** needs to be done under dry and inert conditions as **VII.11** reacts slowly with water to form hydrazoic acid.
- Heterogenous reactions should be avoided as localized heat could initiate explosive thermal decomposition.
- Impact tests indicated that **VII.11** has an impact sensitivity of 6 J. In accordance with the *UN Recommendations on the Transport of Dangerous Goods*, **VII.11** should be considered a "sensitive" material.

Further developments perfomed by Goddard-Borger and co-workers[31d], introduced other imidazole-1-sulfonyl azide salts, preserving the diazo donation capacity and improving the impact stability. Hydrogen sulphate salts appeared to be the recommended alternative for **VII.11** taken into account stability, preparation and costs. As a response to this, Wang and co-workers published an alternative route to prepare imidazole-1-sulfonyl azide hydrochlorides by avoiding the azidosulfonyl chloride intermediate[31e]. However, during the research performed in this work, no problems occurred while preparing or using imidazole-1-sulfonyl azide hydrochloride **VII.11** Storage in the freezer under Ar atmosphere prevented decomposition.

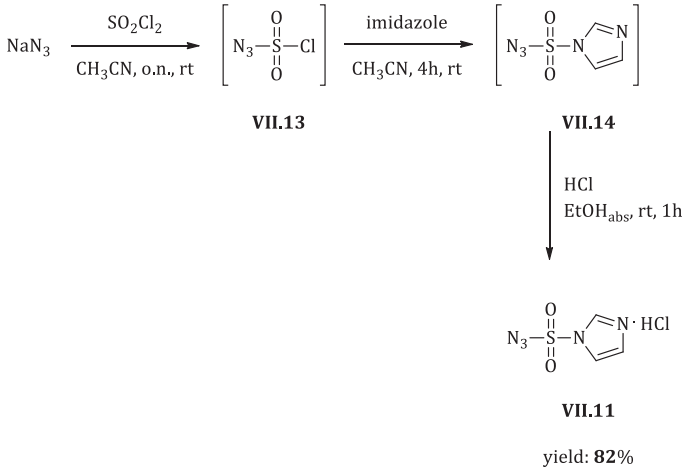

Scheme VII–4: Synthesis of imidazole-1-sulfonyl azide hydrochloride (VII.11)

The solid-phase diazotransfer procedure was optimized by varying (a) the solvent system, (b) the base, (c) the number of equivalents and (d) the reaction temperature. Initially, different solvent systems were employed in order to obtain good swelling properties of the polymer matrix in combination with an optimal conversion into the desired solid-phase bound azide. Secondly, as solid-phase synthesis requires an excellent solubility of the reagents in the chosen solvent, the inorganic potassium carbonate was replaced by an organic, nitrogen containing base.

1. Influence of the solvent system

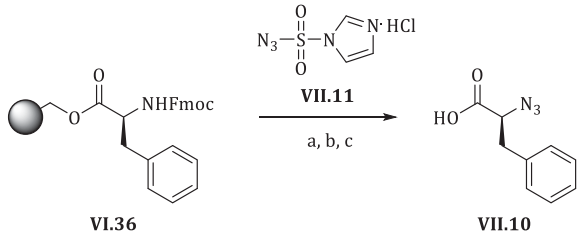

a) 20 v/v% 4-Me-piperidine/DMF, rt, 3x 10 min b) 1.2 eq **VII.11**, 2 eq TEA, 1 mol% $CuSO_4.5H_2O$, solvent (**Table VII-1**), rt, 24h c) TFA/H_2O (95/5), rt, 2h.

Scheme VII–5: Diazotransfer optimization procedure by employing different solvent systems.

To a first extent, solid-phase bound L-phenylalanine (**VI.36**) was treated with imidazole-1-sulfonyl azide hydrochloride (**VII.11**), after removal of the Fmoc protecting group, in different solvent systems in the presence of triethylamine for 24 h with a Cu(II)-source as catalyst. Considering the safety aspects of reactions with azides dissolved in dichloromethane and the

possible formation of the dangerous and instable diazomethane (*vide infra*), the optimization reactions were executed on a minimalistic scale (~ 0.065 mmol). The inherent technical features of LC-MS analysis (at 214 nm) allow obtaining insights in the 'amine-to-azide conversion' or crude yield upon small-scale reactions. The crude yield was monitored by LC-MS analysis after cleaving an aliquot of resin with TFA/H_2O (95/5). The choice for L-phenylalanine was made by its apparent UV-activity which enables detection of both the azide **VII.10** formed and the remaining amine **VII.12**. A qualitative IR analysis was done in order to verify the presence of the characteristic azide peak in the IR-spectrum at ±2100 cm^{-1}. In **Table VII-1**, the crude yield is illustrated for the tested solvent systems. This amine-to-azide conversion was evaluated by integrating peaks present in the whole chromatogram at 214 nm. Therefore this amine-to-azide conversion is considered to be a percentage of the formed azide present in the mixture assuming the presence of 100% amine before the diazotransfer. Taking into account the well-established amino-acid coupling procedures, consequent capping step and Fmoc-deprotection, this is fulfilled. Additionally, integration of the whole chromatogram was performed upon evaluation of specificity of the analytical HPLC method and equal extinction coefficients at 214 nm for all peaks present. Specificity can be verified by comparing the corresponding UV spectrum of the peak of interest at base, mid-height (both up- and downslope) and its maximum or by evaluating the corresponding mass spectrometer channel of the specific peak (if available). The azide peak of interest was identified as specific and, additionally, at 214 nm excitation with consequent detection is considered to be non-discriminative.

Table VII-1: Solvents applied in Scheme VII–5 and corresponding amine-to-azide conversions

entry	solvent	VII.10 (%)[a]
1	CH_2Cl_2	23
2	CH_2Cl_2/MeOH (9/1)	43
3	CH_2Cl_2/MeOH/H_2O (8/1/1)	46
4	DMF	54
5	DMF/CH_2Cl_2 (9/1)	42
6	THF	3
7	THF/H_2O (9/1)	49

[a] Crude yield determined via LC-MS analysis (214 nm) after 24h reaction (see **Scheme VII-5**)

Reactions using dichloromethane (**Table VII-1**, entries **1**-**3**) as part of the solvent system show a very low yield of the amine into the azide after 24 h of reaction. More specifically, entry **2**, which simulates the conditions of Rijckers *et al.*,[28] results in a disappointing yield to the desired azide. Taking into account the safety aspects of azides dissolved in

dichloromethatne, further investigation is strongly discouraged. DMF (**Table VII-1**, entries **4**-**5**), as main solvent, gives rise to a moderate formation of the solid-phase bound azide. As the amine is not present in the mixture we conclude that 46% of the mixture are side products. Experiments using THF as the sole solvent (**Table VII-1**, entry **6**) showed almost no amine – to-azide conversion due to low solubility of the diazotransfer reagent and Cu(II)-catalyst in THF; however addition of water (**Table VII-1**, entry **7**) increased the solubility and therefore raised the yield drastically from 3% to 49% after a 24h reaction, with remaining starting material. Moreover, the chromatographic profile of the specific mixture indicated a clean reaction step.

A second set of test reactions was performed by taking a closer look at the influence of the amount of H_2O on the diazotransfer reagent solubility and the corresponding amine-to-azide conversion. **Table VII-2** illustrates the results of diazotransfer reactions performed with increasing amount of H_2O in the solvent system.

Table VII-2: Amine-to-azide conversion with increasing amount of water ratio in the solvent system

entry	solvent	VII.10 (%)[a]
6	THF	3
7	THF/H_2O (9/1)	49
8	THF/H_2O (8/2)	51
9	THF/H_2O (7/3)	62
10	THF/H_2O (6/4)	71
11	THF/H_2O (1/1)	81
12	THF/H_2O (4/6)	70
13	THF/H_2O (3/7)	45
14	THF/H_2O (2/8)	42
15	THF/H_2O (1/9)	40
16	H_2O	0

[a] Crude yield determined via LC-MS analysis (214 nm) after 24h reaction according to principle described on p.72.

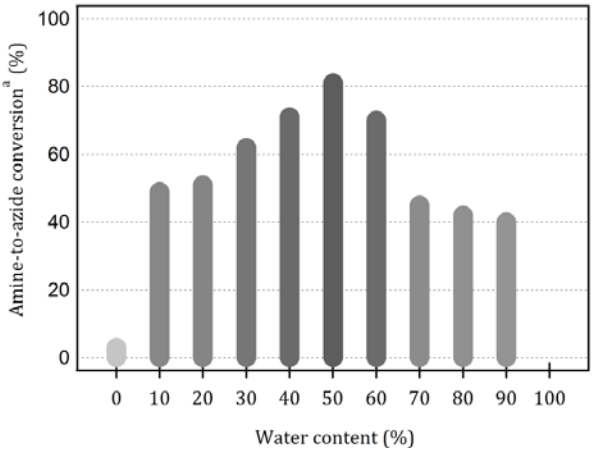

Figure VII-3: Graphical representation of the amine-to-azide conversion with varying THF/H_2O ratios as solvent system.

As can be seen in **Table VII-2** and **Figure VII-3** the yield increases upon addition of H_2O to the solvent mixture. An equal ratio of THF and H_2O (**Table VII-2**, entry **11**) gives rise to a maximal amine-to-azide conversion or yield of 81% without presence of starting material. Further increasing the amount of water, decreases the swelling of the polymer matrix, therefore reducing the accessibility of the reactive sites leading eventually to 0% amine-to-azide conversion if 100% water is used. The solvent system of choice applied for all following diazotransfer reactions will be THF/H_2O (1/1).

2. Influence of the base

In order to verify any influence of the base added to the reaction mixture, DIPEA and TEA were tested with conditions as presented in **Scheme VII–6.**

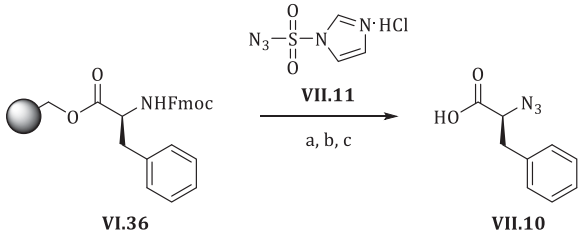

a) 20 v/v% 4-Me-piperidine/DMF, rt, 3x 10 min b) 1.2 eq **VII.11**, 2 eq base (**Table VII-3**), 1 mol% $CuSO_4.5H_2O$, THF/H_2O, rt c) TFA/H_2O (95/5), rt, 2h.

Scheme VII–6: Optimization of the diazotransfer procedure by employing different bases.

Table VII-3: Conditions applied in Scheme VII–6 and corresponding amine-to-azide conversion

entry	base		VII.10 (%)[a]
	TEA	DIPEA	
1	2 eq	-	81
2	-	2 eq	72

[a] Crude yield determined via LC-MS analysis (214 nm) after 24h according to principle described on p.72.

As DIPEA (entry **2**) gave a lower conversion compared to TEA (entry **1**), we continued with TEA as a base.

3. Influence of the amount of diazotransfer reagent VII.11, the base and the reaction temperature

In order to increase the amine-to-azide conversion of the diazotransfer reaction, different amounts of diazotransfer reagent were added combined with increasing amounts of base (i.c. TEA) to release the free amine from its hydrochloride. The last parameter which could influence the conversion of amine to azide was found to be the temperature which was varied from room temperature to 50°C.

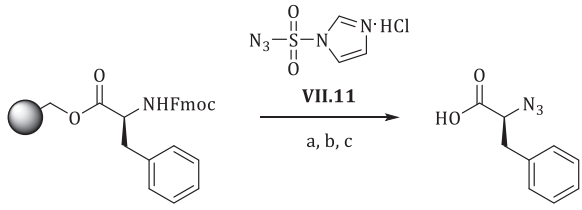

a) 20 v/v% 4-Me-piperidine/DMF, rt, 3x 10 min b) **VII.11** (**Table VII-4**), TEA (**Table VII-4**), 1 mol% $CuSO_4.5H_2O$, THF/H_2O, T °C (**Table VII-4**) c) TFA/H_2O (95/5), rt, 2h.

Scheme VII–7: Optimization of the diazotransfer procedure by employing different equivalents of VII.11 and base

Table VII-4: Conditions applied in Scheme VII–7 and corresponding amine-to-azide conversion

entry	VII.11	TEA	T (°C)	VII.10 (%)[a]
1	1.2 eq	2 eq	25	81
2	2 eq	3 eq	25	72
3	1.2 eq	2 eq	50	54
4	2 eq	3 eq	50	51

[a] Crude yield determined via LC-MS analysis (214 nm) after 24h according to principle described on p.72.

Of all conditions tested, taken into account the amount of azide formed compared to remaining amine and side product formation, 1.2 equivalents of diazotransfer reagent and 2 equivalents of TEA at room temperature gave the best results. Possible degradation of the diazotransfer reagent at elevated temperatures could explain the lower yield found for entries **3** - **4** in **Table VII-4**.

4. Determination of the epimerization ratio during diazotransfer reaction

In order to determine the ratio of epimerization occurring during the diazotransfer reaction, eight solid bound tripeptides (**VII.20-VII.23**, **Figure VII-4**) were synthesized in order to subject them to the diazotransfer reaction conditions described above.

The first amino acid in the tripeptide was the achiral glycine **VI.25** which is not sensitive to racemization during the coupling step on Wang resin by employing a DIC/DMAP coupling procedure. For the second unit, eight L- and D-α-amino acids were chosen: Fmoc-Ala-OH (**VI.26**), Fmoc-Phe-OH (**VI.28**), Fmoc-Leu-OH (**VI.30**) and Fmoc-Glu(O*t*Bu)-OH (**VII.15**).

For the third amino acid, L-Fmoc-Phe-OH (**L-VI.28**) was used, as the optimization procedure was performed with this α-amino acid. The idea behind this strategy is that if epimerization of the stereogenic center occurs at the position of the terminal α-amino acid, diastereoisomers will be formed which can be separated by means of conventional HPLC techniques.

In **Scheme VII–8**, the synthesis of the tripeptides is illustrated. As the diazotransfer reaction and possible racemization were the only subject of interest, no intermediate coupling efficiencies were determined. After the synthesis, the Fmoc group was removed from the eight tripeptides and the resulting free amines were converted into the corresponding azidotripeptides by using the optimized procedure as determined above (1.2 equivalents of imidazole-1-sulfonyl azide hydrochloride (**VII.11**), 2 equivalents of TEA, 1 mol% $CuSO_4.5H_2O$ in THF/H_2O (1/1) for 24 h at room temperature). The last step of the synthesis involved

cleavage of the azidopeptides from the solid-support by using TFA/H_2O (95/5) for two hours at room temperature.

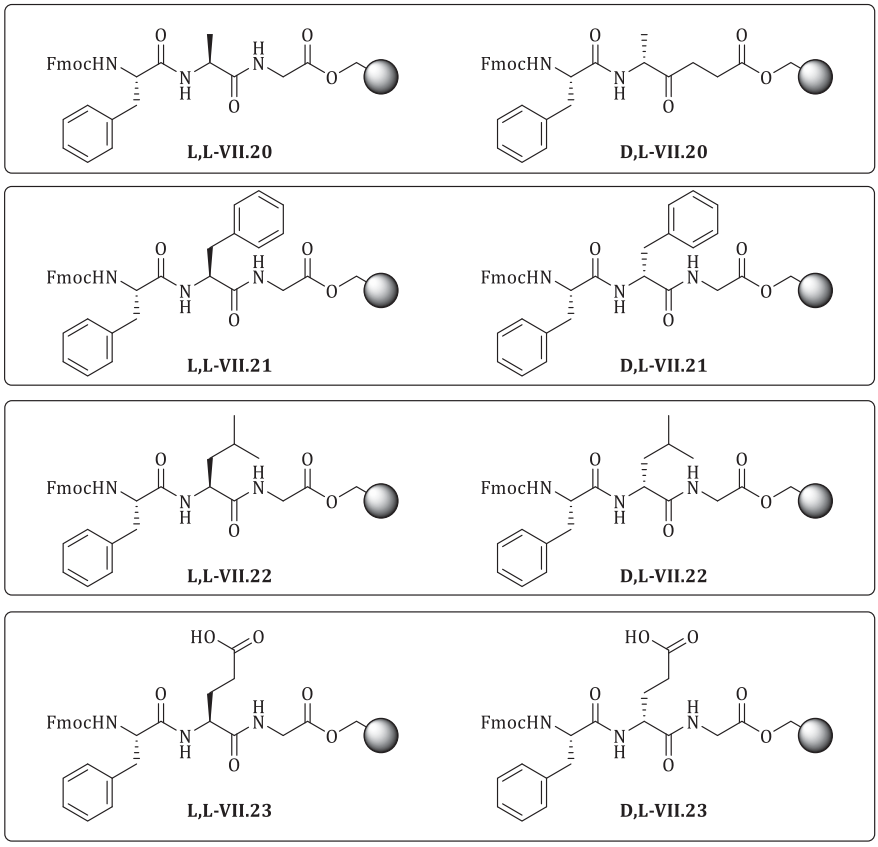

Figure VII-4: Synthesized tripeptides (VII.20-VII.23)

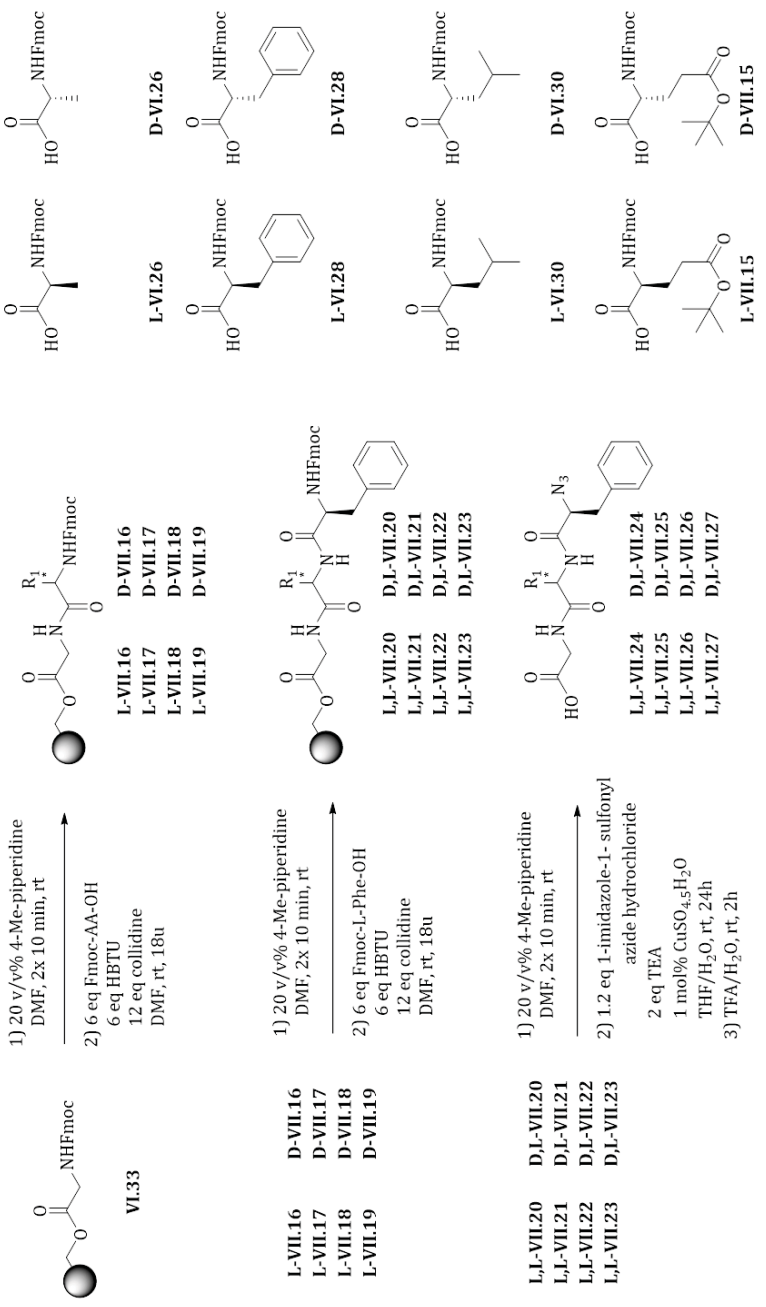

Scheme VII–8: Solid-phase synthesis of azidotripeptides (VII.24-VII.27)

After cleavage of the azidopeptides obtained (**Figure VII-5**), an HPLC separation of artificial mixtures of each pair of diastereomeric tripeptides was pursued. Four 1:1 diastereomeric mixtures were composed and conditions for separation investigated. Unfortunately, only for **L,L-VII.26** and **D,L-VII.27** baseline separation *via* HPLC could be achieved.

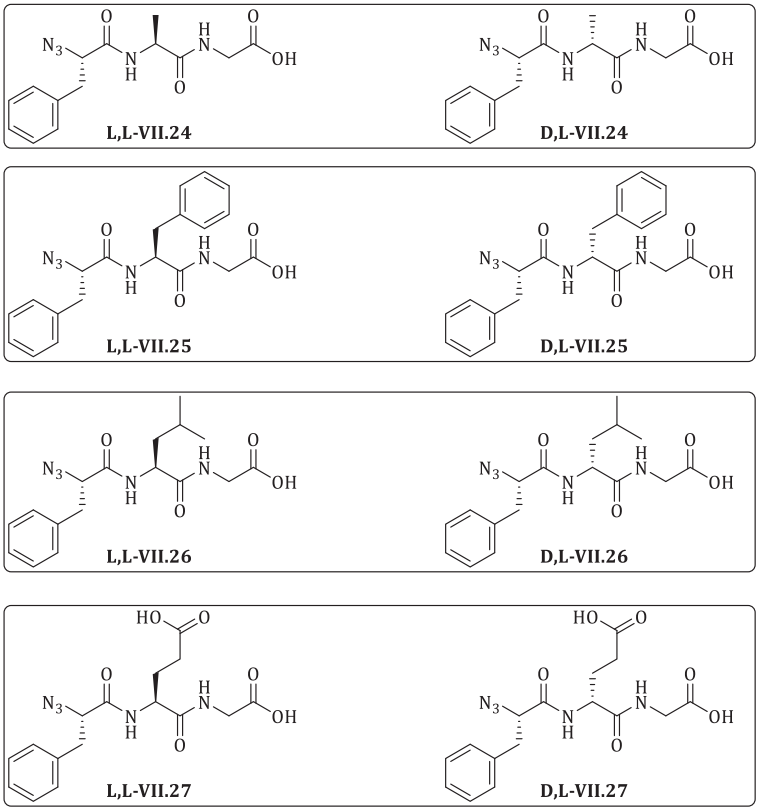

Figure VII-5: Overview of the synthesized azidotripeptides (VII.24-VII.27)

If epimerization occurs during the diazotransfer reaction, the possible enantiomers are shown in **Figure VII-6**. **L,L-VII.26** and **D,L-VII.26** are the outcome of the separate reactions, whereas an artificial mixture of both, acting as diastereoisomers, was used to optimize the HPLC separation. **L,D-VII.26** and **D,D-VII.26** are the epimers of respectively **L,L-VII.26** and **D,L-VII.26**, also acting as diastereoisomers. Even more, there is an enantiomeric relation between, **L,L-VII.26** and **D,D-VII.26** and **D,L-VII.26** and **L,D-VII.26**, logically the latter will have the same retention time when HPLC analysis is performed.

If the azidopeptides **L,L-VII.26** and **D,L-VII.26** are injected separately for HPLC analysis, the possible corresponding enantiomer should elute separately with a retention time comparing to the other diastereoisomer.

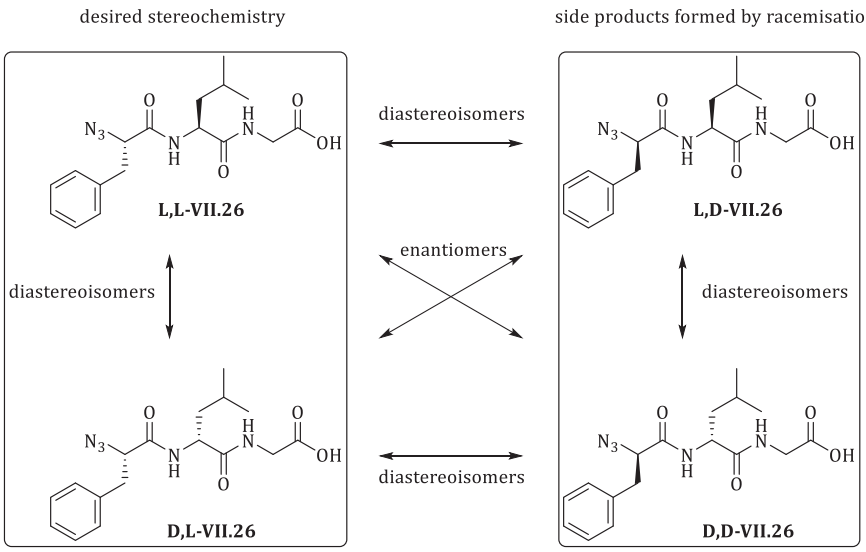

Figure VII-6: All possible stereoisomers which could be formed during a diazotransfer reaction.

Figure VII-7 shows the optimized HPLC separation, of an artificial diastereoisomeric mixture of **L,L-VII.26** and **D,L-VII.26** where both peaks are baseline separated. **Figure VII-8** shows the injection of **L,L-VII.26** under the same chromatographic conditions, where the complete absence of a peak with a retention time associated to **D,L-VII.26** or **L,D-VII.26** proves that no racemization occurred during the diazotransfer procedure.

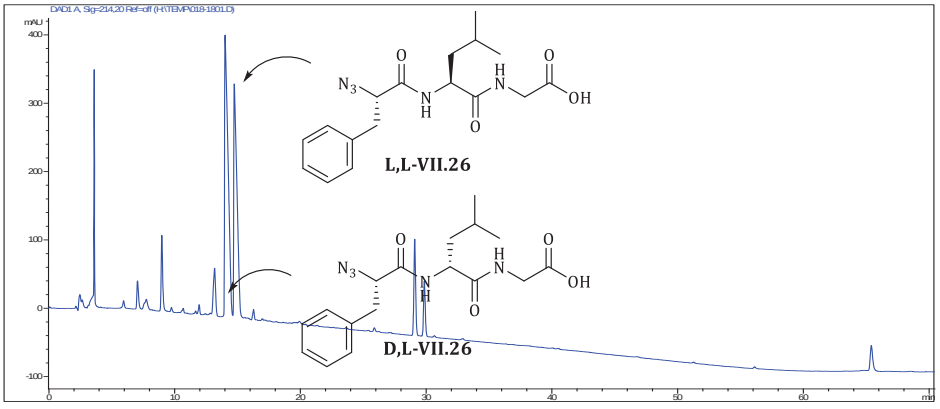

Figure VII-7: HPLC co-injection chromatogram of an artificial mixture of L,L-VII.26 and D,L-VII.26

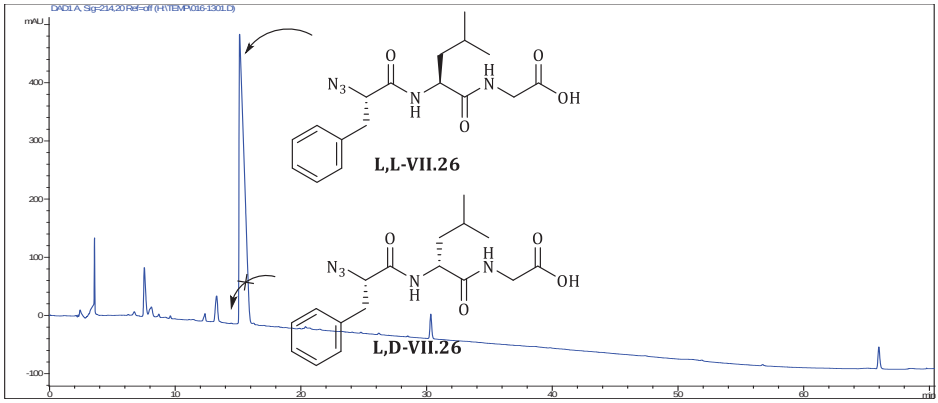

Figure VII-8: HPLC chromatogram of the sole injection of L,L-VII.26

5. Combinatorial chemistry

In order to synthesize the proposed compounds **V.2**, nine solid-phase bound Fmoc-protected α-amino acids (**VI.33-VI.40**) were converted into the corresponding solid-phase bound α-azido acids (**VII.28-VII.35**).

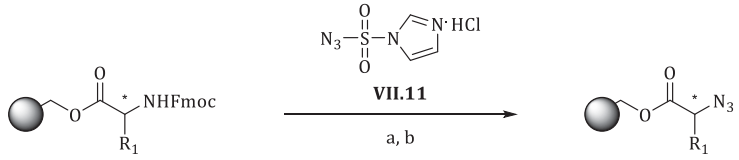

R_1	H	**L-VI.33**	R_1	H	**L-VII.28**
	(S)-CH_3	**L-VI.34**		(S)-CH_3	**L-VII.29**
	(S)-$CH_2O(t\text{Bu})$	**L-VI.35**		(S)-$CH_2O(t\text{Bu})$	**L-VII.30**
	(S)-Bn	**L-VI.36**		(S)-Bn	**L-VII.31**
	(R)-Bn	**D-VI.36**		(R)-Bn	**D-VII.31**
	(S)-$CH(CH_3)_2$	**L-VI.37**		(S)-$CH(CH_3)_2$	**L-VII.32**
	(S)-$CH_2CH(CH_3)_2$	**L-VI.38**		(S)-$CH_2CH(CH_3)_2$	**L-VII.33**
	(S)-$(CH_2)_4NHBoc$	**L-VI.39**		(S)-$(CH_2)_4NHBoc$	**L-VII.34**
	(S)-CH_2(NBoc)-3-indolyl	**L-VI.40**		(S)-CH_2(NBoc)-3-indolyl	**L-VII.35**

a) 20 v/v% 4-Me-piperidine/DMF, rt, 2x 10 min b) 1.2 eq imidazole-1-sulfonyl azide hydrochloride **(VII.11)**, 2 eq TEA, 1 mol% $CuSO_4.5H_2O$, THF/H_2O, rt, 24h.

Scheme VII–9: Overview of the α-amino acids submitted to a diazotransfer reaction

6. Recent and ongoing important developments

a) Towards safety

In 2010, Katritzky and co-workers[32], reported a new diazotransfer reagent for solution phase amine-to-azide conversion, benzotriazole-1-sulfonyl azide (**VII.36**). This reagent has the advantage of being stable, crystalline, safe to handle with a long shelf life and soluble in both organic and aqueous solvents. Moreover, it ensures a convenient synthesis of enantiomerically pure α-azido acids.

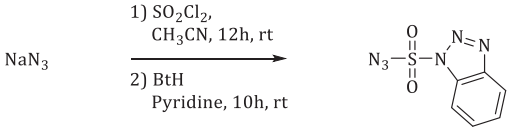

VII.36

Scheme VII–10: Synthesis of benzotriazole-1-sulfonyl azide (VII.36)

b) Towards a higher efficiency

More importantly, Löwik and co-workers[33] published in 2012, a solid-phase diazotransfer procedure using imidazole-1-sulfonyl azide hydrochloride (**VII.11**). In particular, this procedure was optimized for NovaPEG and polystyrene based polymer supports. According to this paper, the optimal conditions for diazotransfer were achieved by using water and DMF as solvent for respectively NovaPEG and polystyrene resin. More strikingly, Löwik achieves diazotransfer after 30 minutes with excellent conversions (>95%) without addition of $CuSO_4.5H_2O$, therefore questioning the proposed mechanism by Nyffeler[23].

During the optimization procedure performed in this work, the use of DMF as solvent of choice (**Table VII-2**, entry **4**) was rejected due to a sluggish reaction. After a reaction time of 24 h, 54% yield along with side product formation was observed. Therefore, it might be concluded that the optimization procedure performed is incomplete and a further study on the progress of the conversion and metal necessity is appropriate.

c) Late stage optimization

Upon publication of the work of Löwik and co-workers, our optimizated procedure of the diazotransfer reaction was revisited at a late stage of this research project. Additional experiments were performed in order to verify the robustness of the conditions provided by Löwik and to determine the role of the divalent copper catalyst. Therefore, three batches of solid-phase bound L-phenylalanine were treated with 3 eq imidazole-1-sulfonyl azide hydrochloride (**VII.11**) and 4.5 eq DIPEA in DMF for respective reaction times of 15, 30 and 60 minutes. Secondly, to another three batches, 1 mol% $CuSO_4.5H_2O$ was added to the reaction mixture. After cleavage with TFA/H_2O (95/5), LC-MS analysis provided the following results concerning amine-to-azide conversion (**Table VII-5**).

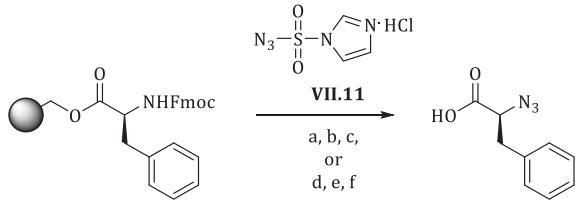

a) 20 v/v% 4-Me-piperidine/DMF, rt, 2x 15 min b) 3 eq **VII.11,** 4.5 eq DIPEA, DMF c) TFA/H_2O (95/5), rt, 2h.
d) 20 v/v% 4-Me-piperidine/DMF, rt, 2x 15 min e) 3 eq **VII.11,** 4.5 eq DIPEA, 1 mol% $CuSO_4.5H_2O$, DMF f) TFA/H_2O (95/5), rt, 2h.

Scheme VII–11: Late stage optimization protocol

Table VII-5: Results of the late stage optimization protocol

entry	reaction time (min)	$CuSO_{4.5}H_2O$	VII.10 (%)[a]
1	15	-	55%
2	30	-	48%
3	60	-	49%
4	15	1 mol%	38%
5	30	1 mol%	53%
6	60	1 mol%	45%

[a] Crude yield determined via LC-MS analysis (214 nm)

The results presented in **Table VII-5** clearly do not reach the excellent yields obtained by Löwik and co-workers[33]. The achieved amine-to-azide conversions are within the range of earlier experiments obtained during the initial optimization process. Apart from a full consumption of the starting material, many side products were formed. Still, it is noteworthy that the diazotransfer in DMF proceeds smoothly without addition of Cu(II)-catalyst and is finished after 15 minutes.

REFERENCES

[1] Excellent reviews on this topic: a) Bräse, S.; Gil, C.; Knepper, K.; Zimmermann, V. *Angew. Chem. Int. Ed.* **2005**, *44*, 5188-5240. b) Pinho e Melo, T. M. V. D. Synthesis of Azides. In *Organic Azides, Syntheses and Applications*; Bräse, S.; Banert, K., Eds.;John Wiley & Sons: West Sussex, 2009; pp 53-90.

[2] a) Sugimori, T.; Okawa, T.; Eguchi, S.; Kakehi, A.; Yashima, E.; Okamoto, Y. *Tetrahedron* **1998**, *54*, 7997–8008. b) Airiau, E.; Spangenberg, T.; Girard, N.; Breit, B.; Mann, A. *Org. Lett.* **2010**, *12*, 528–531. c) Snider, B. B.; Zhou, J. *J. Org. Chem.* **2005**, *70*, 1087–1088. d) Seo, J. H.; Liu, P.; Weinreb, S. M. *J. Org. Chem.* **2010**, *75*, 2667–2680. e) Cassidy, M. P.; Özdemir, A. D.; Padwa, A. *Org. Lett.* **2005**, *7*, 1339–1342.

[3] a) Teixeira-Clerc, F.; Michalet, S.; Menez, A.; Kessler, P. *Bioconjugate Chem.* **2003**, *14*, 554–562. b) Radominska, A.; Drake, R. R. *Methods Enzymol.* **1994**, *230*, 330–339. c) Buchmueller, K. L.; Hill, B. T.; Platz, M. S.; Weeks, K. M. *J. Am. Chem. Soc.* **2003**, *125*, 10850–10861. d) Pinney, K. G.; Mejia, M. P.; Villalobos, V. M.; Rosenquist, B. E.; Pettit, G. R.; Verdier-Pinard, P.; Hamel, E. *Bioorg. Med. Chem.* **2000**, *8*, 2417–2425. e) Chambers, J. J.; Gouda, H.; Young, D. M.; Kuntz, I. D.; England, P. M. *J. Am. Chem. Soc.* **2004**, *126*, 13886–13887. f) Voskresenska, V.; Wilson, R. M.; Panov, M.; Tarnovsky, A. N.; Krause, J. A.; Vyas, S.; Winter, A. H.; Hadad, C. M. *J. Am. Chem. Soc.* **2009**, *131*, 11535–11547. g) Sechi, M.; Carta, F.; Sannia, L.; Dallocchio, R.; Dessi, A.; Al-Safi, R. I.; Neamati, N. *Antiviral Res.* **2009**, *81*, 267–276. h) Okada, M.; Matsubara, A.; Ueda, M. *Tetrahedron Lett.* **2008**, *49*, 3794–3796.

[4] Piantadosi, C.; Marasco, C. J., Jr.; Morris-Natschke, S. L.; Meyer, K. L.; Gumus, F.; Surles, J. R.; Ishaq, K. S.; Kucera, L. S.; Iyer, N.; Wallen, C. A.; Piantadosi, S; Modest, E. J. *J. Med. Chem.* **1991**, *34*, 1408–1414.

[5] Dudkin, V. Y.; Crich, D. *Tetrahedron Lett.* **2003**, *44*,1787-1789.

[6] a) Chan, T. R.; Hilgraf, R.; Sharpless, K. B.; Fokin, V. V. *Org. Lett.* **2004**, *6*, 2853–2855. b) Kalisiak, J.; Sharpless, K. B.; Fokin,V. V. *Org. Lett.* **2008**, *10*, 3171–3174.

[7] Orgueira, H. A.; Bartolozzi, A.; Schell, P.; Seeberger, P. H. *Angew. Chem. Int. Ed.* **2002**, *41*, 2128–2131.

[8] Debaene, F.; Winssinger, N. *Org. Lett.* **2003**, *5*, 4445–4447.

[9] Lundquist, J. T., IV; Pelletier, J. C. *Org. Lett.* **2001**, *3*, 781–783.

[10] Excellent reviews on this topic: a) L' abbé, G. *Chem. Rev.* **1969**, *69*, 345–363 . b) Scriven, E.F.V.; Turnbull, K. *Chem. Rev*. **1988**, *88*, 297–368. c) Grashey R.; In *Comprehensive Organic Synthesis*, Trost B. M.; Fleming, I.; Eds; Pergamon Press, 1991, Vol. 6, pp. 225. d) Binder, W.H.; Kluger, C. *Curr. Org. Chem.* **2006**, *10*, 1791–1815. e) Palacios, F.; Aparicio, D.; Rubiales, G.; Alonso, C.; de los Santos, J.M. *Curr. Org. Chem.* **2006**, *10*, 2371–2392.

[11] Righi, G.; D'Achille, C.; Pescatore, G.; Bonini, C. *Tetrahedron Lett.* **2003**, *44*, 6999-7002.

[12] Evans, D. A.; Britton, T. C.; Ellman, J. A.; Dorow, R. L. *J. Am. Chem. Soc.* **1990**, *112*, 4011–4030.

[13] Chiappe, C.; Pieraccini, D.; Saullo, P. *J. Org. Chem.* **2003**, *68*, 6710-6715.

[14] a) Das, J.; Patil, S. N.; Awasthi, R.; Narasimhulu, C. P.; Trehan, S. *Synthesis* **2005**, 1801–1806. b) Joucla, M.F.; Rees, C. W.; *Chem. Commun.* **1984**, 374-375. c) Melhado, L. L.; Leonard, N. J. *J. Org. Chem.* **1983**, *48*, 5130-5133. d) Cismas, C.; Gimisis, T. *Tetrahedron Lett.* **2008**, *49*, 1336-1339. e) Capitosti, S. M.; Hansen, T. P.; Brown, M. L. *Org. Lett.* **2003**, *5*, 2865-2867. f) Colasson, B.; Save, M.; Milko, P.; Roithova, J.; Schröder, Reinhaud, O.; *Org. Lett*. **2007**, *9*, 4987-4990. g) Li, L.; Han, J.; Nguyen, B.; Burgess, K. *J. Org. Chem.* **2008**, *73*, 1963-1970.

[15] a) Avemaria, F.; Zimmerman, V.; Bräse, S. *Synlett*, **2004**, 1163-1166. b) Gil. C.; Bräse, S. *Chem. Eur. J.* **2005**, *11*, 2680-2688. c) Liu, C.-Y.; Knochel, P. *J. Org. Chem.* **2007**, *72*, 7106-7115.

[16] Cavender, C. J.; Shiner, V. J. *J. Org. Chem.* **1972**, *37*, 3567-3569.

[17] Ruff, J. K. *Inorg. Chem.* **1965**, *4*, 567-570.

[18] Regitz, M. *Angew. Chem. Int. Ed.* **1967**, *6*, 733-749.

[19] Zaloom, J.; Roberts, D.C. J. Org. Chem **1981**, *46*, 5173-5176.

[20] a) Vasella, A.; Witzig, C.; Chiara, J.-L.; Martin-Lomas, M. *Helv. Chim. Acta* **1991**, *74,* 2073-2077. b) Buscas, T.; Garegg, P. J.; Konradsson, P.; Maloisel, J.-L. *Tetrahedron Asymm.* **1994**, *5*, 2187-2194. c) Ludin, C.; Sehwesinger, B.; Schwesinger, R.; Meier, W.; Seitz, B.; Weller, T.; Hoenke, C.; Haitz, S.; Erbeck, S.; Prinzbach, *H. J. Chem. Soc. Perkin Trans. 1* **1994**, 2685-2701.

[21] Hassner, A.; Stern, M.; Gottlieb, H. E.; Frolow, F. *J. Org. Chem.* **1990,** 55, 2304–2306.

[22] Alper, P.B.; Hung, S.C.; Wong, C. H. *Tetrahedron Lett.* **1996**, *37*, 6029-6032.
[23] Nyffeler, P. T.; Liang, C. H.; Koeller, K. M.; Wong, C. H. *J. Am. Chem. Soc.* **2002**, *124*, 10773-10778.
[24] Fisher, W.; Anselme, J.-P. *J. Am. Chem. Soc.* **1967**, *89*, 5284-5285. b) Anselme, J.-P.; Fisher, W. *Tetrehedron* **1969**, *25*, 855-859.
[25] Brandt, P.; Söergren, M. J.; Andersson, P. G.; Norrby, P.-O. *J. Am. Chem. Soc.* **2000**, *122*, 8013-8020.
[26] Yan, R.-B., Yang, F.; Wu, Y.; Zhang, L. - H.; Ye, X. - S. *Tetrahedron Lett.* **2005**, *46*, 8993–8995.
[27] Titz, A.; Radic, Z.; Schwardt, O.; Ernst B. *Tetrahedron Lett* **2006**, *46*, 2383–2385.
[28] Rijkers, D. T. S.; van Vugt, H. H. R.; Jacobs H. J. F.; Liskamp R. M. J. *Tet Lett.* **2002**, *43*, 3657–3660.
[29] P.A.S. Smith, The Chemistry of Open - Chain Organic Nitrogen Compounds, Vol. 2 , 1966 , W.A. Benjamin Inc. , New York, USA , pp. 211 – 256 .
[30] Rostovtsev, V. V.; Green, L. G.; Fokin, V. V.; Sharpless, K. B. *Angew. Chem. Int. Ed.* **2002**, *41*, 2596-2599.
[31] a) Goddard-Borger, E. D.; Stick, R. V. *Org. Lett* **2007**, *9*, 3797-3800. b) correction: Goddard-Borger, E. D.; Stick, R. V. *Org. Lett* **2011**, *13*, 2514. c) Zeng, X. Q.; Beckers, H.; Bernhardt, E.; Willner, H. *Inorg. Chem.* **2011**, *50*, 8679-8684. d) Fisher N.; Goddard-Borger, E. D.; Greiner, R.; Klapötke, T. M.; Skelton, B. W.; Stierstorfer, J. *J. Org. Chem.* **2012**, *77*, 1760-1764. e) Ye, H.; Liu, R.; Li, D.; Liu, Y.; Yan, H.; Guo, W.; Zhou, L.; Cao, X.. Tian, H.; Shen,J; Wang, P. G. *Org. Lett.* **2013**, *1*, 18-23.
[32] Katritzky, A. R.; El Khatib, M.; Bol'shakov, O.; Khelashvili, L.; Steel, P. J. *J. Org. Chem.* **2010**, *75*, 6532-6539.
[33] Hansen, M. B.; van Gurp, T. H. M.; van Hest, J. C. M.; Löwik, D. W. P. M. *Org Lett.* **2012**, *14*, 2330-2333.

VIII. 1,3-Dipolar cycloaddition

A. Introduction

In order to mimick the aimed 1,5-benzodiazepine-2,4-diones by the synthesis of a [1,2,3]-triazolo[1,5-*d*][1,4]benzodiazepine-2-one scaffold **V.2**, the incorporation of a 1,2,3-triazole moiety is the next challenge in this work. Moreover, the 1,2,3-triazole moiety requires a 1,5-disubstitution pattern to mimick successfully the *cis*-amide bond. In the following paragraphs, the optimization procedure towards this incorporation is presented by performing a 1,3-dipolar cycloaddition on solid-phase by using commercially available 2-ethynylaniline (**VIII.2**) as building block.

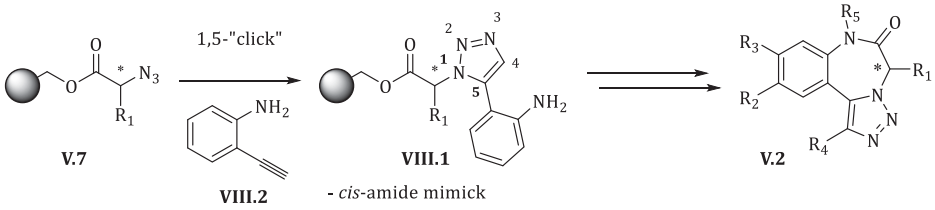

Figure VIII-1: Aimed 1,5-regioselectivity during formation of the 1,2,3-triazole moiety

B. Test case: Introduction of the 1,5-disubstituted triazole moiety

The literature study presented in section **IV.D** revealed a feasible strategy to incorporate the required 1,5-disubstituted 1,2,3-triazole moiety from azides and terminal alkynes by using a Ru(II)-catalyst. More specifically, $C_p^*RuCl(PPh_3)_2$ **IV.26** and $C_p^*RuCl(COD)$ **IV.27** have proven to be very selective in the formation of the desired regioisomer.[1]

IV.26 **IV.27**

Figure VIII-2: $C_p^*RuCl(PPh_3)_2$ (IV.26) and $C_p^*RuCl(COD)$ (IV.27)

In order to introduce the 1,5-disubstitutued 1,2,3-triazole moiety on solid-phase, the solid-phase bound azide formed according to procedures introduced in section **VII.3** is subjected to a ruthenium(II)-catalyzed azide-alkyne cycloaddition with a terminal alkyne and commercially available $C_p^*RuCl(PPh_3)_2$ (**IV.26**)or $C_p^*RuCl(COD)$ (**IV.27**). More specifically, 3 eq of 2-ethynylaniline (**VIII.2**) and various loadings of Ru(II)-catalyst were tested in toluene for 6h at different temperatures[1,2] (**Table VIII-1**). A possible side reaction might be the non-catalyzed thermal click reaction occurring between solid-phase bound azide **VII.45** and terminal alkyne **VIII.2** leading to a mixture of the desired 1,5-regioisomer **VIII.3** and undesired 1,4-regioisomer **VIII.4** (**Scheme VIII-1**). The ratio of both regioisomers, under thermal conditions, is determined by the inherent sterical hindrance present in the reacting substrates, favoring the more stable regioisomer.

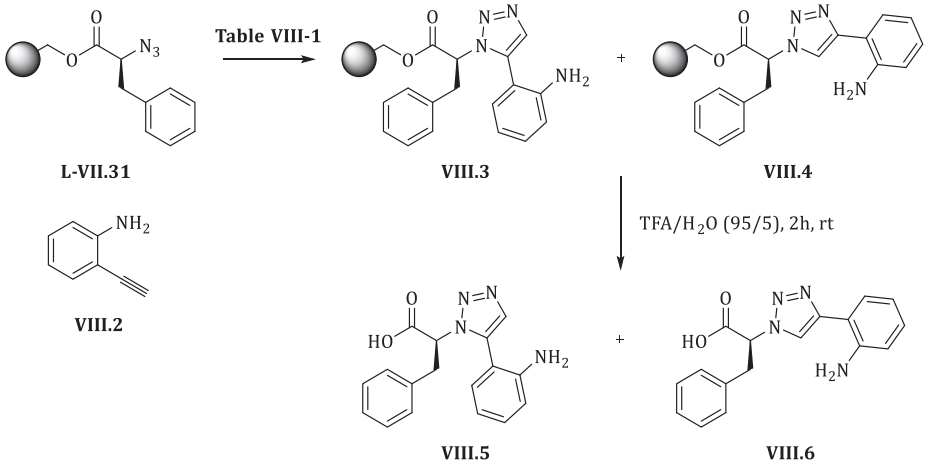

L-VII.31 **VIII.3** **VIII.4**

VIII.2

VIII.5 **VIII.6**

Scheme VIII–1: Possible formation of 1,4- and 1,5-regioisomer of the 1,2,3-triazole moiety upon RuAAC and thermal click reaction induced by elevated temperatures

Table VIII-1: Conditions applied in Scheme VIII–1

entry	conditions					Crude yield (%)[a]
	loading	catalyst	solvent	T	reaction time	
1	5 mol%	$C_p^*RuCl(PPh_3)_2$	toluene	60°C	6h	46%
2	10 mol%	$C_p^*RuCl(PPh_3)_2$	toluene	60°C	6h	56%
3	5 mol%	$C_p^*RuCl(PPh_3)_2$	toluene	rt	6h	<5%
4	10 mol%	$C_p^*RuCl(PPh_3)_2$	toluene	rt	6h	<5%
5	5 mol%	$C_p^*RuCl(COD)$	toluene	rt	6h	46%
6	10 mol%	$C_p^*RuCl(COD)$	toluene	rt	6h	45%

[a] Crude yield determined by *via* LC-MS analysis (214 nm) after 6 h. Calculated upon full integration of the peaks in the chromatogram. Peak corresponding with 291 Da ($M+H^+$) is presented.

After six hours, the reaction was stopped and the beads were isolated. An extensive washing procedure (3x toluene (60°C), 3x DMF, 3x MeOH and 3x CH_2Cl_2) needed to be performed to ensure a full removal of catalyst traces. Preliminary onresin IR analysis proved that the characteristic IR peak for an azide (approx. 2100 cm^{-1}) disappeared, supporting the idea of the formation of a triazole moiety.

Cleaving an aliquot of the resin with 95% TFA/H_2O for 2h at room temperature and subsequent LC-MS analysis gave surprising results. The expected open product **VIII.5** (molecular weight: 308.33 Da) was not present in the mass spectra corresponding to any peak in the chromatograms, only the dehydrated mass (molecular weight: 290.32 Da) was found.

These findings suggested that an acid-catalyzed ring closure occurred during the TFA cleavage step, therefore not yielding the expected open product **VIII.5** but the cyclized seven-membered ring **VIII.7**. Moreover, the exclusive presence of cyclized product **VIII.7** in the absence of any open product (**VIII.5** or **VIII.6**) proved the specific 1,5-regioselectivity of the Ru(II)-catalyzed azide-alkyne cycloaddition. As, the 1,4-regioisomer **VIII.6** is unable to cyclize under any conditions.

Therefore, it can be concluded that the applied RuAAC conditions succeed in selectively generating the desired cycloadduct **VIII.3** and acid-mediated cleavage conditions result in cyclized product **VIII.7**. The redefined reaction scheme is represented in **Scheme VIII–2**.

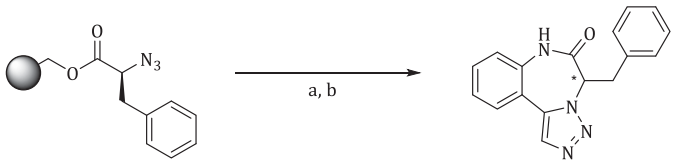

(L)-VII.31 **VIII.7**

a) 3 eq 2-ethynylaniline, 10 mol% $Cp^*RuCl(PPh_3)_2$, toluene, 6h, 60°C b) TFA/H_2O (95/5), 2h, rt

Scheme VIII–2: Revised reaction outcome after standard cleavage

Due to the harsh cleavage conditions, the purity of the crude seven-membered ring **VIII.7** remains certainly less than satisfactory. Nevertheless, as cyclization/release was the initial and anticipated cyclization strategy, new options for the seven-membered ring formation arise.

C. Test case: ring closure

The last step in this synthesis of this new scaffold molecule include the formation of the seven-membered ring and simultaneous release from the resin. By taking advantage of the ester function as the solid-phase anchoring point, a so-called 'cyclization/release' strategy (see section **I.B.2**), which combines both steps, is pursued.

A clear view on the scope of the desired cyclization/release was provided by a set of test reactions to yield the cyclized product **VIII.7**.

Based upon two ring closure mechanisms presented in **Figure VIII-3** and **Figure VIII-4**, respectively both basic and acidic conditions were tested.

1. Base-promoted cyclization/release

Upon addition of a strong base, followed by a proton abstraction of **VIII.8**, the anilide anion attacks the ester carbonyl in an addition/elimination fashion to yield cyclized product **VIII.7**. A possible drawback or pitfall for this mode of action might be racemization of the chiral center (**Figure VIII-3**).

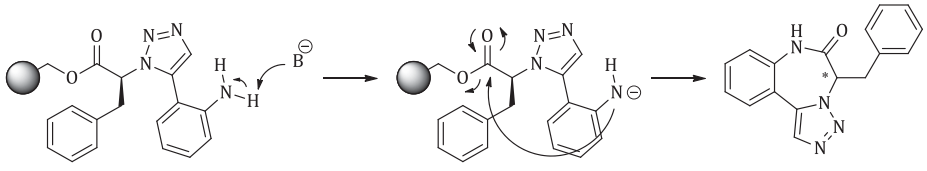

VIII.8 **VIII.9** **VIII.7**

Figure VIII-3: Base-promoted cyclization/release

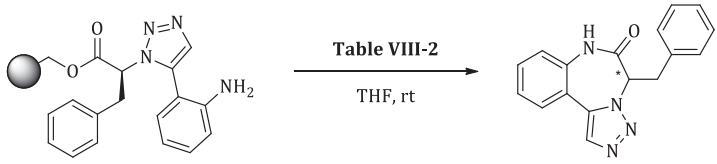

VIII.3 **VIII.7**

Scheme VIII–3: Test reactions towards base-promoted cyclization/release

Table VIII-2: Base-promoted cyclization/release conditions

entry	conditions	crude purity (%)[a,b]	remaining VIII.3 on resin[c]
1	0.1 M KOtBu, THF, rt, 12h	76	yes
2	0.2 M KOtBu, THF, rt, 12h	58	yes
3	1 M KOtBu, THF, rt, 24h	47	yes
4	1 M KOtBu, THF, 60°C, 24h	13	yes

[a] A washing step with 5% $NaHCO_3$ in H_2O and extraction with EtOAc was performed prior to LC-MS analysis.

[b] Crude purity determined via LC-MS analysis (214 nm)

[c] Upon cleavage with 95% TFA/H_2O, rt, 2h

In **Table VIII-2**, four entries for base-catalyzed ring closure and release from the resin are presented. Potassium tert-butoxide was the base of choice in THF in different concentrations, for enabling deprotonation of the aniline hydrogen. After indicated reaction time, an acidic work-up is necessary to neutralise the excess of KOtBu. LC-MS analysis and crude purity determination shows formation of the desired product **VIII.7** in moderate to good purities. Notably, due to the extraction step possible water soluble side products are removed *prior* to analysis and hence not taken into account. Subsequently, the base-treated resin was subjected to standard cleavage conditions with TFA/H_2O (95/5) in order to verify the effectiveness of this base-promoted cyclization/release. The last column of **Table VIII-2** qualitatively shows that intermediate **VIII.3** is still present on the solid-phase and that the cyclization/release is not completed yet after 24 h for all base-promoted conditions.

2. Acid-catalyzed cyclization/release

For the acid-catalyzed procedure, activation *via* protonation of the carbonyl oxygen enables attack of the aniline nitrogen on the carbonyl carbon, triggering an addition/elimination and subsequent release of the cyclized product **VIII.7** (**Figure VIII-4**).

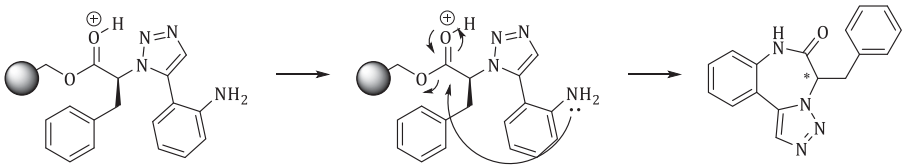

Figure VIII-4: Acid-catalyzed cyclization/release

Section **VIII.A** showed that standard cleavage conditions with TFA/H_2O (95/5) result in cyclization/release, instead of in the anticipated cleavage as carboxylic acid **VIII.5**, yet the crude purities obtained need improvement. Therefore, a set of test reactions for acid-catalyzed ring formations were performed. Different acids and temperatures were tested in order to achieve more insights and to improve the crude yield.

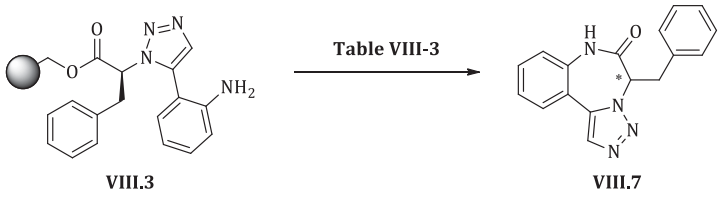

Scheme VIII–4: Test reactions towards acid-catalyzed cyclization/release

Table VIII-3: Acid-catalyzed cyclization/release conditions

entry	conditions	crude purity (%)[a]	remaining VIII.3 on resin[b]
4	TFA/CH_2Cl_2 (1/99), rt, 24h	55	yes
5	TFA/ CH_2Cl_2 (2/98), rt, 24h	24	yes
6	TFA/ CH_2Cl_2 (5/95), rt, 24h	15	yes
7	TFA/ CH_2Cl_2 (10/90), rt, 24h	11	trace
8	TFA/DCE (1/99), 60°C, 24h	56	yes
9	TFA/DCE (2/98), 60°C, 24h	34	yes
10	TFA/DCE (5/95), 60°C, 24h	21	yes
11	TFA/DCE (10/90), 60°C, 24h	13	trace
12	HOAc/CH_2Cl_2, (1/1), rt, 24h	93	trace
13	HOAc/CH_2Cl_2, (60/40), rt, 24h	69	no
14	HOAc/CH_2Cl_2, (70/30), rt, 24h	52	no
15	HOAc/CH_2Cl_2, (80/20), rt, 24h	72	no

[a] Crude purity determined via LC-MS analysis (214 nm)

[b] Upon cleavage with 95% TFA/H_2O, rt, 2h

From **Table VIII-3** it can be concluded that the use of TFA in CH_2Cl_2 or DCE at room temperature or at 60°C (entries **4**-**11**) yields final product **VIII.7** in low to moderate crude purities and that in most cases cyclization/release is not complete (identified upon cleavage with TFA/H_2O 95/5). As these crude purities were low, a weaker acid (entries **12**-**15**) was tested in order to *fine-tune* the cyclization/release. Acetic acid gave excellent results (entry **12**, 93% crude purity) in a 1:1 ratio in dichloromethane for 24h. Subsequent cleavage with TFA/H_2O showed that only trace amounts of intermediate **VIII.3** were still present on the resin. Taken into account the results presented above, the optimal cyclization/release conditions were HOAc/CH_2Cl_2 (1/1) for 24h at room temperature. In **Figure VIII-5**, an LC-MS chromatogram is presented to illustrate the crude purity and **Figure VIII-6** illustrates the remaining resin content upon cleavage with 95% TFA/H_2O after the cyclization/release step wherefrom can be seen that no residual **VIII.7** is present.

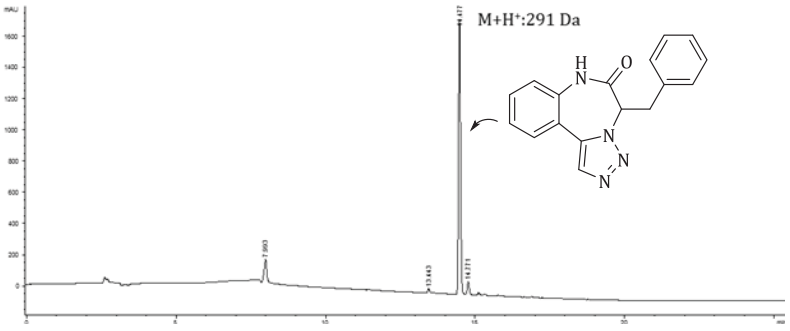

Figure VIII-5: Crude LC-MS of VIII.7 upon cyclization/release with HOAc/CH_2Cl_2, (1/1) at room temperature for 24h.

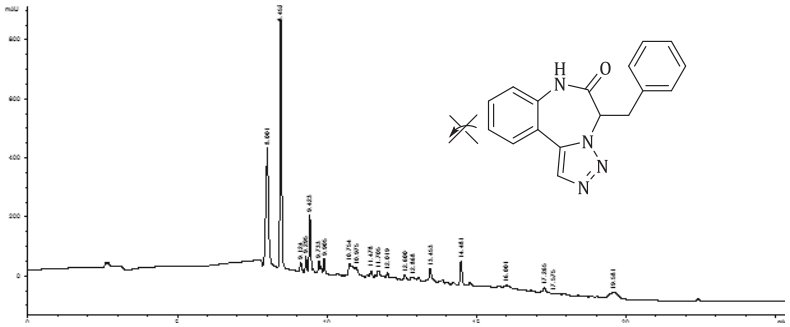

Figure VIII-6: Remaining resin content upon standard cleavage conditions with 95% TFA/H_2O for 2h at room temperature after applying cyclization/release with HOAc/CH_2Cl_2, (1/1) at room temperature for 24h.

D. Proof of principle library

A proof of principle library was synthesized in order to verify the optimized conditions for a broader range of α-amino acids.

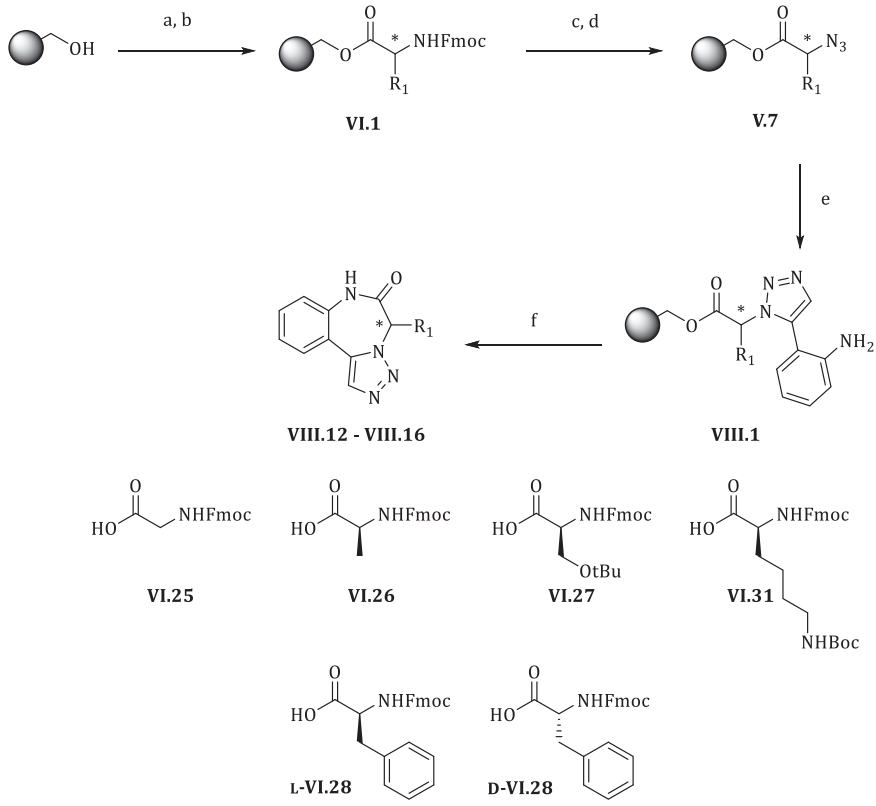

a) 2 eq Fmoc-AA-OH, 2 eq DIC, 0,2 eq DMAP, CH_2Cl_2, rt, 2x 24h b) Ac_2O, CH_2Cl_2, DIPEA (1/1/3) c) 20 v/v% 4-Me-piperidine/DMF, rt, 2x 10 min. d) 1,2 eq imidazole sulfonyl azide hydrochloride, 2 eq TEA, 1 mol% $CuSO_4.5H_2O$, THF/H_2O (1/1), rt, 24h. e) 3 eq 2-ethynylaniline, 10 mol% C_p*$RuCl(PPh_3)_2$, toluene, 60°C, 6h. f) HOAc/CH_2Cl_2 (1/1), rt, 24h.

Scheme VIII–5: Proof of principle library synthesis

Wang resin was successfully coupled with commercially available Fmoc-protected glycine and five Fmoc-protected enantiomerically pure α-amino acids, including L-alanine, L-serine, L-lysine, L- and D-phenylalanine. After loading quantitation *via* the Fmoc-deprotection method, subsequent removal of the Fmoc protecting group resulted in the corresponding resin-bound amines. The latter were converted into the resin-bound azides **V.7** *via* the optimized procedure (section **VII.C**) By employing the Ru(II)-catalyzed azide/alkyne dipolar cycloaddition with commercially available 2-ethynylaniline (**VIII.2**) as building block, a 1,5-disubstituted triazole moiety was formed giving rise to intermediates **VIII.1**. A

cyclization/release strategy was used to perform ring formation and simultaneous cleavage from the solid support affording final products **VIII.12 – VIII.16**. In **Table VIII-4**, the crude purities upon cyclization/release are presented next to the isolated yields. It can be concluded that all compounds are obtained in moderate to good yields.

Table VIII-4: Results of the proof of principle library for compounds VIII.12 – VIII.16

entry	compound	crude purity (%)[a]	isolated yield (%)
1	**VIII.12**	91	44
2	**VIII.13**	93	39
3	**VIII.14**	89	57
4	**VIII.15**	96	45
5	**(*S*)-VIII.16**	94	54
6	**(*R*)-VIII.16**	93	55

[a] Crude purity determined via LC-MS analysis (214 nm)

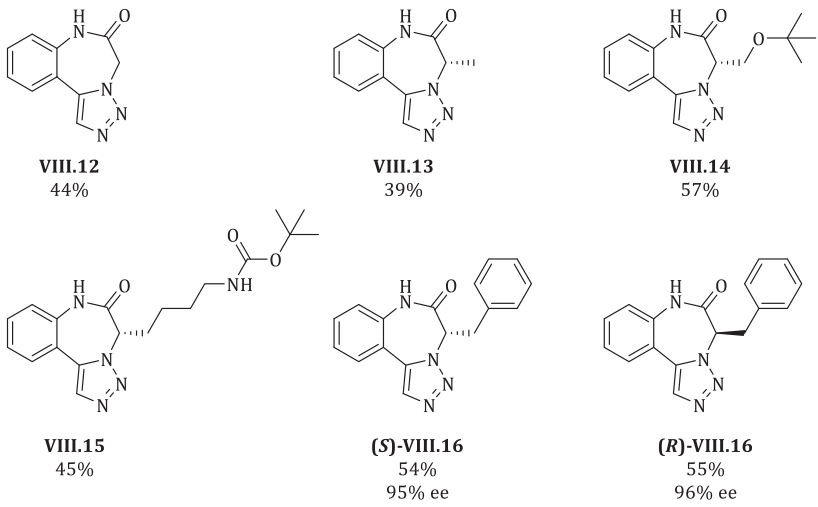

Figure VIII-7: Proof of principle library members

By incorporating L- and D-phenylalanine, a chiral HPLC analysis could determine the ratio of enantiomeric purity of this synthesis strategy. In **Figure VIII-8** an optimized HPLC separation is presented of an artificial mixture of both enantiomers. **Figure VIII-9** represents the HPLC run under the optimized condition where can be seen that the compound has an enantiomeric purity of 95%. This minimal loss of chirality could be explained by the non-racemization free method for α-amino acid coupling to the solid-phase.

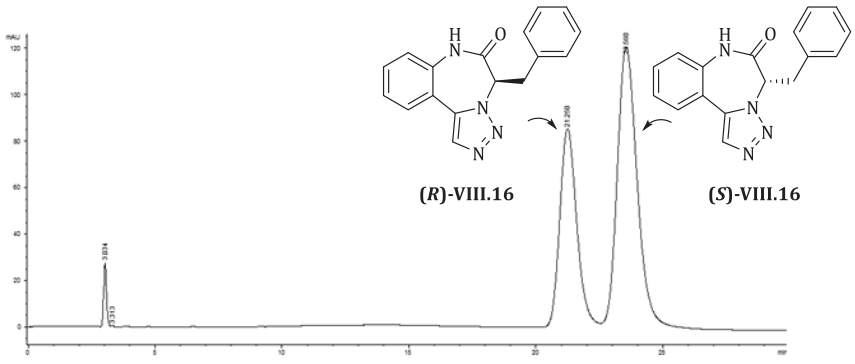

Figure VIII-8: Optimized chiral separation of an artificial mixture of (*S*)-VIII.16 and (*R*)-VIII-16

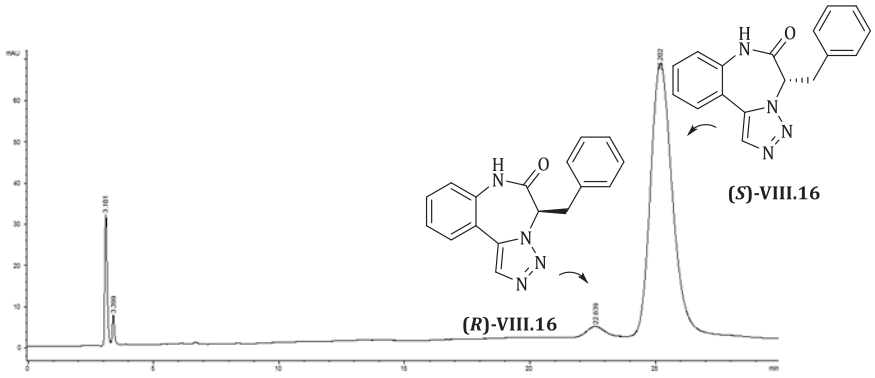

Figure VIII-9: Chiral chromatogram of (*S*)-VIII.16 under optimized conditions

E. Sonogashira cross coupling

As indicated by the proof of principle library in section **VIII.C**, the present synthesis allows for the introduction of various α-amino acids, therefore providing the incorporation of one diversity point. In the quest for further exploration of the chemical space around this scaffold molecule, changes to the aromatic moiety could increase diversity exponentially (see **Figure VIII-10**).

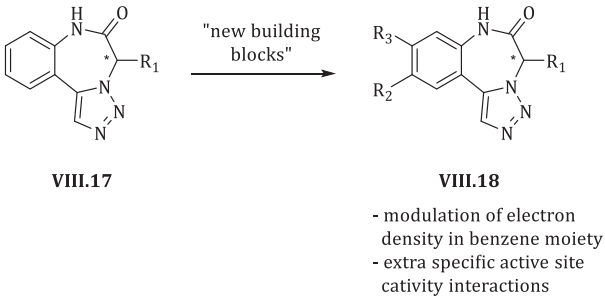

Figure VIII-10: Proposed diversification of the aromatic moiety

1. Building block synthesis

New building blocks **VIII.19** need to be synthesized bearing the required amino and alkyne function with additional diversity points on the aromatic moiety. Because of the readily commercially available 2-iodoanilines **V.10**, it was chosen to introduce the alkyne moiety *via* a Sonogashira cross-coupling reaction with TMS-protected acetylene **VIII.20** in order to create a terminal alkyne building block which could be subjected to Ru(II)-catalyzed 1,3-dipolar cycloaddition.

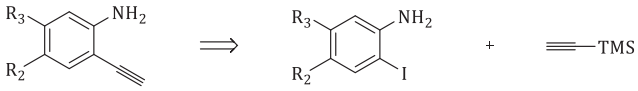

Scheme VIII–6: Retrosynthetic approach towards building block synthesis with extra substituents

Five different 2-iodoanilines **VIII.21** – **VIII.25**, bearing respectively halogen, cyano and nitro functionalities were used as starting product for a large scale Sonogashira cross-coupling reaction. After a short optimization procedure, the optimal conditions were found to be: 4 equivalents of TMS-protected acetylene in diethylamine at room temperature. No dried nor degassed solvents are necessary to perform this conversion. The reaction was completed for all starting products within six hours.

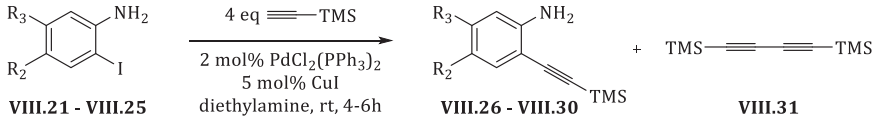

Scheme VIII–7: Sonogashira cross-coupling reaction

Table VIII-5: Results of the Sonogashira cross-coupling reaction

entry	starting product	R_2	R_3	compound	yield (%)
1	**VIII.21**	Cl	H	**VIII.26**	95
2	**VIII.22**	H	Cl	**VIII.27**	92
3	**VIII.23**	Br	H	**VIII.28**	99
4	**VIII.24**	CN	H	**VIII.29**	91
5	**VIII.25**	NO_2	H	**VIII.30**	94

All Sonogashira cross-coupling products were obtained in excellent yields (**Table VIII-5**, 91-99%). Only the formation of a considerable amount of homocoupled TMS-protected acetylene **VIII.31** (so-called Glaser coupling product[3,4]) was observed during this reaction. As this side reaction did not affect the yield of the desired cross-coupled product and the homocoupled product did not interfere with the purification of compounds **VIII.26 – VIII.30**, no further optimization (by working under oxygen-free or reducing atmosphere[5]) was done to minimize this side reaction.

Moreover, it can be seen that when applying these conditions to dihalogenated anilines (enties **1-3, Table VIII-5**), only the iodide is engaged into the Sonogashira reaction leading to mono-cross-coupled product for entry **1**, **2** and more particularly even for entry **3**, which bears a bromine (**Scheme VIII–8**). Therefore, the applied conditions enable a regioselective cross-coupling in the presence of a chlorine or bromine on the aromatic moiety next to an iodine.

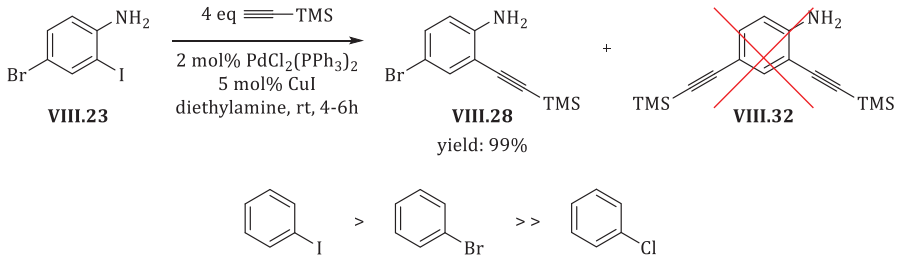

Scheme VIII–8: Selective monoalkynylation during Sonogashira cross-coupling and leaving group capacity

The next step in the building block synthesis involves the removal of the TMS group to afford terminal alkynes **VIII.33 – VIII.37** (**Scheme VIII-9**). A wide range of methods is available for this transformation, from fluoride ion rich solutions ($KF.H_2O$ in DMF or MeOH[6], TBAF in THF[7]) or deprotection upon applying basic conditions (K_2CO_3[8], $CaCO_3$[9], KOH[10] or methoxides[11] in MeOH). Thanks to its ease and efficiency, it was chosen to perform the reaction by adding 1 eq K_2CO_3 in MeOH. The full deprotection of the TMS-alkyne proceeds within few minutes.

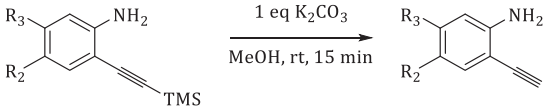

VIII.26 - VIII.30 **VIII.33-VIII.37**

Scheme VIII–9: TMS-deprotection step of VIII.26-VIII.30

As can be seen in **Figure VIII-11** and **Table VIII-6**, all compounds can be deprotected in high yields (84-96%). The overall yields (Sonogashira cross-coupling and desilylation) for building blocks **VIII.33 – VIII.37** are presented in **Table VIII-6**, illustrating that all building blocks are obtained in good overall yields.

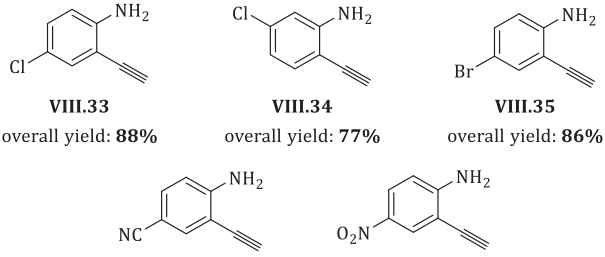

VIII.33 overall yield: **88%**

VIII.34 overall yield: **77%**

VIII.35 overall yield: **86%**

VIII.36 overall yield: **87%**

VIII.37 overall yield: **82%**

Figure VIII-11: Overview of five new building blocks VIII.33 – VIII.37

Table VIII-6: Overview of five new building blocks VIII.33 – VIII.37

entry	compound	R_2	R_3	deprotection yield (%)	overall yield (%)
1	**VIII.33**	Cl	H	93	88
2	**VIII.34**	H	Cl	84	77
3	**VIII.35**	Br	H	87	86
4	**VIII.36**	CN	H	96	87
5	**VIII.37**	NO_2	H	87	82

Many reports[12] have suggested the possibility for cycloisomerization of obtained 2-alkynylanilines (Scheme **VIII-20**) starting from **VIII.18** or **VIII.19**. Thanks to the mild applied conditions, no proof of indole **VIII.38** formation was found.

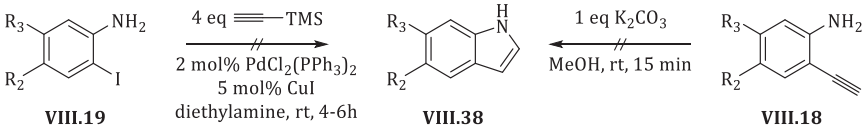

Scheme VIII–10: Possible indole VIII.38 formation

As can be seen from **Table VIII-6**, five building blocks **VIII.33** – **VIII.37** bearing electron withdrawing groups can be readily synthesized in excellent yield on a large scale in solution phase. Apart from a halogen, a cyano or a nitro functionality, also our interest went out to an electron donating group, initially fulfilled by an alkoxy moiety (e.g. methoxy). As 3- or 4-(hydroxy or alkoxy)-2-iodoaniline starting products are not commercially available or too expensive for large scale building block synthesis, the decision was made to start from 3-iodophenol **VIII.39** and perform a strategy presented in **Scheme VIII–11**.

The synthesis initiated with 3-iodophenol which was nitrated[13] with fuming nitric acid to yield 3-iodo-4-nitrophenol **VIII.40** in 35% yield. Unfortunately, the preferential nitration occurred at the less-sterically hindered 2-position giving rise to 5-iodo-2-nitrophenol **VIII.41** in 47% yield. This reaction was not further optimized.

Subsequently, the free alcohol moiety in **VIII.40** was derivatized with a methyl group, affording compound **VIII.42** in 81% yield. As this step induces a new point of diversity, methyl iodide could be replaced by other alkylating agents. The Sonogashira cross-coupling step was performed with trimethylsilylacetylene in order to introduce the necessary alkyne moiety yielding **VIII.43** in 87%. The mandatory aniline function was created by reducing the nitro functionality *via* mild reduction conditions in order not to affect the previously incorporated alkyne function. These mild conditions encompass the *in situ* formation of H_2 by acetic acid and Fe in an EtOH/H_2O mixture. Heating to 60°C is advised to start the hydrogen gas formation. A low yield of 43% for intermediate **VIII.44** was achieved due to the formation of insoluble aggregates which were formed with iron. However, no alkyne reduction to the corresponding alkane was noticed. To increase the combined yield of Sonogashira and nitro-reduction step, the reaction order was switched, yet the nitro-reduction step remained problematic.

The last step included the removal of the TMS-protecting group with conditions provided in section above, giving rise to the building block **VIII.45** in quantitative yield. The overall yield of the synthesis of 2-ethynyl-4-methoxyaniline **VIII.45** starting from 3-iodophenol **VIII.39** was 11%, whereas there is room for further optimization in the nitration and nitro-reduction step.

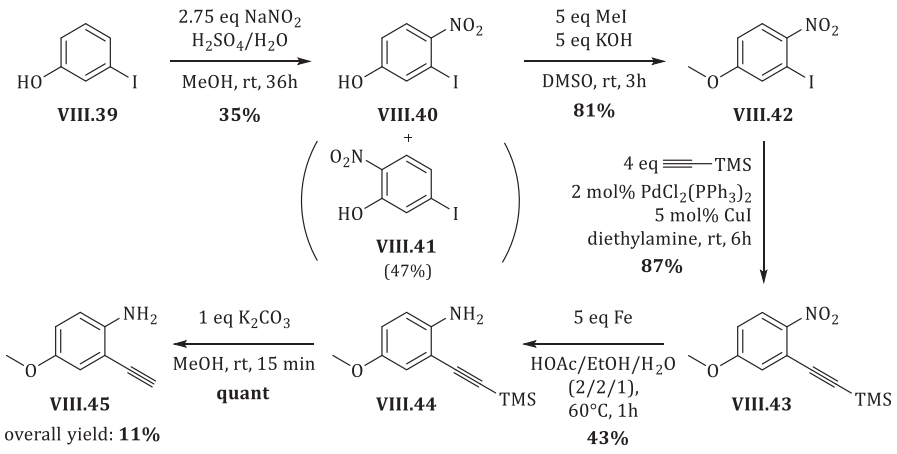

Scheme VIII–11: Synthesis 2-ethynyl-4-methoxyaniline building block VIII.45

2. Combinatorial synthesis

The newly synthesized building blocks **VIII.33** – **VIII.37** and **VIII.45** were validated for their effectiveness in a library synthesis. By a combinatorial synthesis (**Scheme VIII–12**) with seven Fmoc-protected α-amino acids, a library of 36 compounds was synthesized. Due to practical constraints (e.g. availability of building blocks), not all mathematical combinations of the feasible matrix were pursued. In **Table VIII-7** till **Table VIII-13**, the synthesized compounds are presented separately for each α-amino acid **VI.25** and **VI.27-VI.32** with the corresponding crude purities[i] after cyclization/release and the isolated yields.

In extension to section **VIII.C**, randomly selected compounds (**VIII.53**, **VIII.65**, **VIII.68** and **VIII.75**) were assessed for enantiomeric purity by chiral HPLC analyses. Despite a troublesome method optimization, a chiral separation could be obtained for three of four compounds[ii]. The results are presented along with the selected compounds in **Figure VIII-15** and **Figure VIII-17**, wherefrom can be concluded that no racemization occurred. The careful assumption is made that this is representative for the whole library.

[i] For some compounds these crude purities were not determined.
[ii] The chiral separation was accomplished by ing. Jan Goeman from our laboratory.

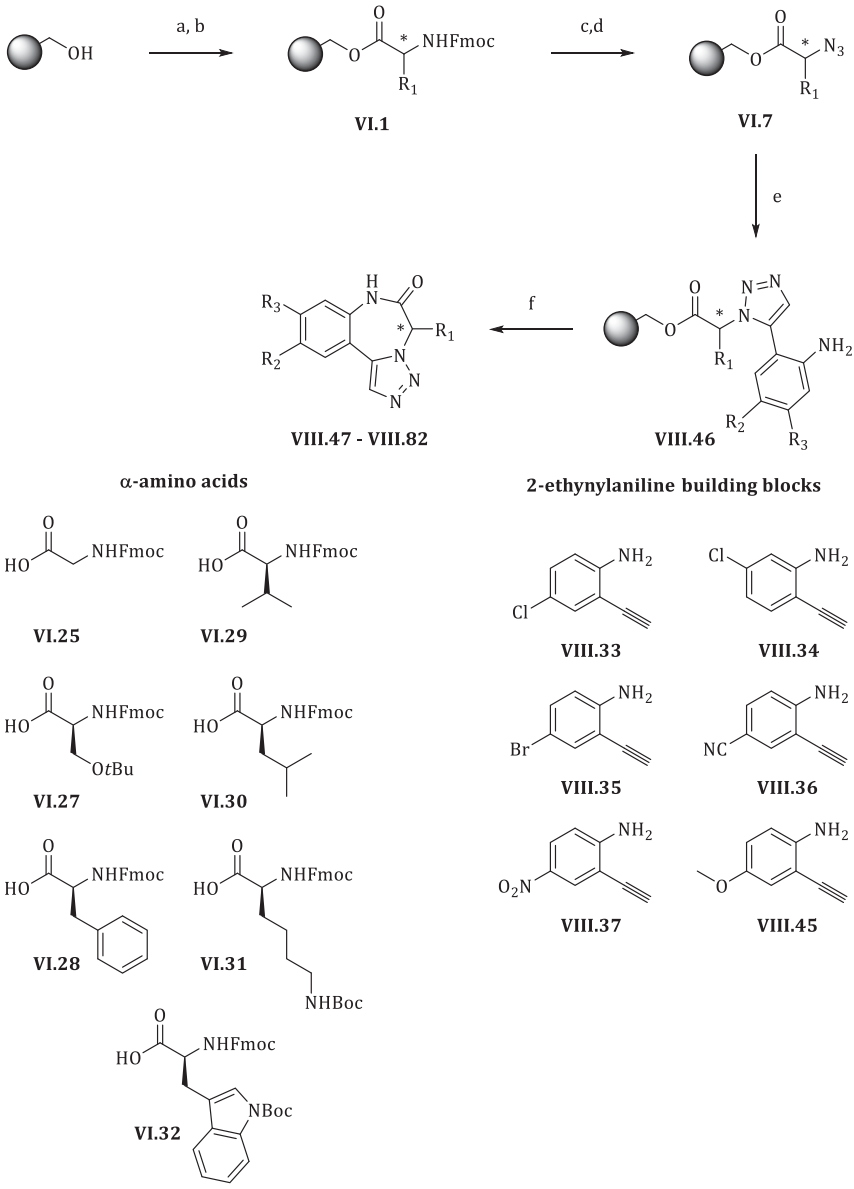

a) 2 eq Fmoc-AA-OH, 2 eq DIC, 0,2 eq DMAP, CH_2Cl_2, rt, 2x 24h b) $(AcO)_2O$, CH_2Cl_2, DIPEA (1/1/3) c) 1) 20 v/v% 4-Me-piperidine/DMF, rt, 2x 10 min. d) 1,2 eq 1-imidazole sulfonyl azide hydrochloride, 2 eq TEA, 1 mol% $CuSO_{4.5}H_2O$, THF/H_2O (1/1), rt, 24h. e) 3 eq **VIII.33 - VIII.37 or VIII.45**, 10 mol% C_p*$RuCl(PPh_3)_2$, toluene, 60°C, 6h. f) HOAc/CH_2Cl_2 (1/1), rt, 24h.

Scheme VIII–12: Combinatorial synthesis towards incorporation of three diversity points.

Table VIII-7: Library members VIII.47 – VIII.51 based on glycine as α-amino acid

entry	compound	R_1	R_2	R_3	crude purity (%)	yield (%)
1	**VIII.47**	H	Cl	H	93	61
2	**VIII.48**	H	H	Cl	90	60
3	**VIII.49**	H	Br	H	-	51
4	**VIII.50**	H	CN	H	74	53
5	**VIII.51**	H	NO_2	H	-	37

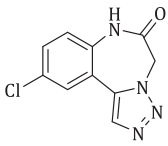

VIII.47
crude purity: **93%**
yield: **61%**

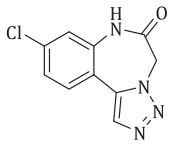

VIII.48
crude purity: **90%**
yield: **60%**

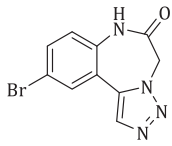

VIII.49
crude purity: **-**
yield: **51%**

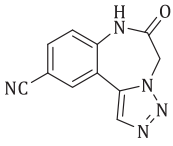

VIII.50
crude purity: **74%**
yield: **53%**

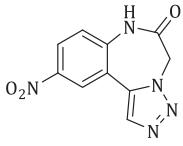

VIII.51
crude purity: **-**
yield: **37%**

Figure VIII-12: Library members VIII.47 – VIII.51 based on glycine as α-amino acid

Table VIII-8: Library members VIII.52 – VIII.57 based on L-phenylalanine as α-amino acid

entry	compound	R_1	R_2	R_3	crude purity (%)	yield (%)
6	**VIII.52**	Bn	Cl	H	95	75
7	**VIII.53**	Bn	H	Cl	96	57
8	**VIII.54**	Bn	Br	H	92	52
9	**VIII.55**	Bn	CN	H	95	56
10	**VIII.56**	Bn	NO_2	H	96	47
11	**VIII.57**	Bn	OMe	H	-	63

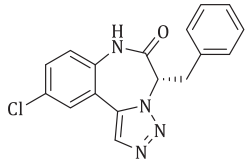

VIII.52

crude purity: **95%**
yield: **75%**

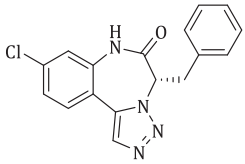

VIII.53

crude purity: **96%**
yield: **57%**
%ee (N/A)

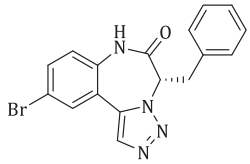

VIII.54

crude purity: **92%**
yield: **52%**

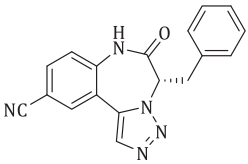

VIII.55

crude purity: **95%**
yield: **56%**

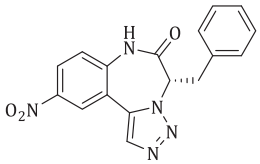

VIII.56

crude purity: **96%**
yield: **47%**

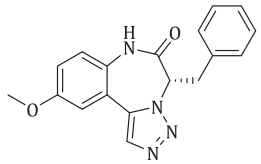

VIII.57

crude purity: **-**
yield: **63%**

Figure VIII-13: Library members VIII.52 – VIII.57 based on L-phenylalanine as α-amino acid

Table VIII-9: Library members VIII.58 – VIII.62 based on L-serine as α-amino acid

entry	compound	R_1	R_2	R_3	crude purity (%)	yield (%)
1	**VIII.58**	$CH_2O(t\text{Bu})$	Cl	H	96	73
2	**VIII.59**	$CH_2O(t\text{Bu})$	H	Cl	96	73
3	**VIII.60**	$CH_2O(t\text{Bu})$	Br	H	95	53
4	**VIII.61**	$CH_2O(t\text{Bu})$	CN	H	91	50
5	**VIII.62**	$CH_2O(t\text{Bu})$	NO_2	H	94	25

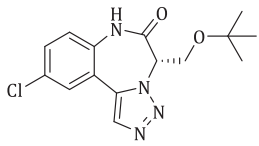

VIII.58
crude purity: **96%**
yield: **73%**

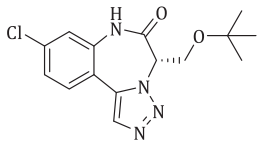

VIII.59
crude purity: **96%**
yield: **73%**

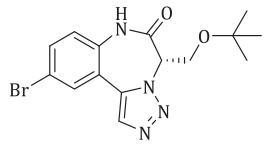

VIII.60
crude purity: **95%**
yield: **53%**

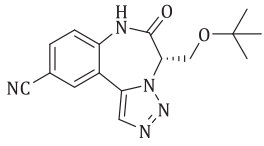

VIII.61
crude purity: **91%**
yield: **50%**

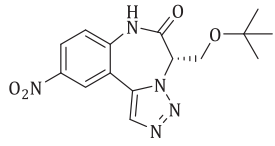

VIII.62
crude purity: **94%**
yield: **25%**

Figure VIII-14: Library members VIII.58 – VIII.62 based on L-serine as α-amino acid

Table VIII-10: Library members VIII.63 – VIII.67 based on L-tryptophane as α-amino acid

entry	compound	R_1	R_2	R_3	crude purity (%)	yield (%)
1	**VIII.63**	*N*-Boc-3-indolylmethyl	Cl	H	92	86
2	**VIII.64**	*N*-Boc-3-indolylmethyl	H	Cl	96	94
3	**VIII.65**	*N*-Boc-3-indolylmethyl	Br	H	91	75
4	**VIII.66**	*N*-Boc-3-indolylmethyl	CN	H	90	35
5	**VIII.67**	*N*-Boc-3-indolylmethyl	NO_2	H	90	13

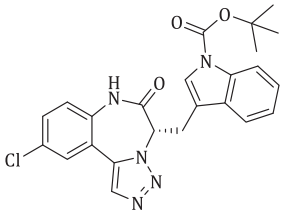

VIII.63
crude purity: **92%**
yield: **86%**

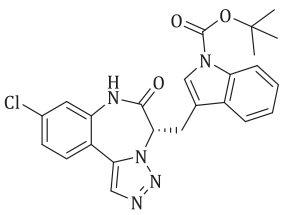

VIII.64
crude purity: **96%**
yield: **94%**

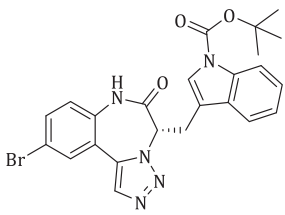

VIII.65
crude purity: **91%**
yield: **75%**
99%ee

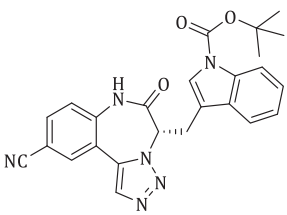

VIII.66
crude purity: **90%**
yield: **35%**

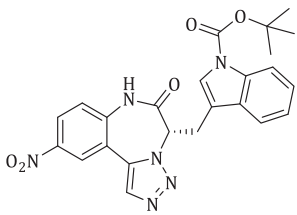

VIII.67
crude purity: **90%**
yield: **13%**

Figure VIII-15: Library members VIII.63 – VIII.67 based on L-tryptophane as α-amino acid

Table VIII-11: Library members VIII.68 – VIII.72 based on L-leucine as α-amino acid

entry	compound	R_1	R_2	R_3	crude purity (%)	yield (%)
1	**VIII.68**	$CH_2CH(CH_3)_2$	Cl	H	93	63
2	**VIII.69**	$CH_2CH(CH_3)_2$	H	Cl	87	75
3	**VIII.70**	$CH_2CH(CH_3)_2$	Br	H	-	60
4	**VIII.71**	$CH_2CH(CH_3)_2$	CN	H	91	59
5	**VIII.72**	$CH_2CH(CH_3)_2$	NO_2	H	-	32

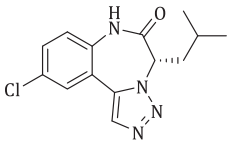

VIII.68

crude purity: **93%**
yield: **63%**
97%ee

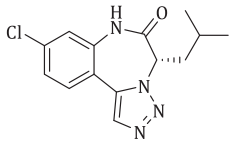

VIII.69

crude purity: **87%**
yield: **75%**

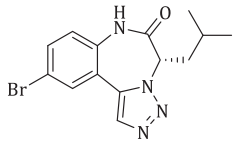

VIII.70

crude purity: **-**
yield: **60%**

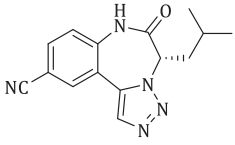

VIII.71

crude purity: **91%**
yield: **59%**

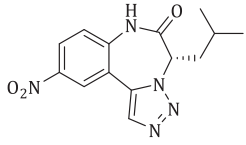

VIII.72

crude purity: **-**
yield: **32%**

Figure VIII-16: Library members VIII.68 – VIII.72 based on L-leucine as α-amino acid

Table VIII-12: Library members VIII.73 – VIII.78 based on L-valine as α-amino acid

entry	compound	R_1	R_2	R_3	crude purity (%)	yield (%)
6	**VIII.73**	$CH(CH_3)_2$	Cl	H	94	68
7	**VIII.74**	$CH(CH_3)_2$	H	Cl	93	69
8	**VIII.75**	$CH(CH_3)_2$	Br	H	-	73
9	**VIII.76**	$CH(CH_3)_2$	CN	H	76	26
10	**VIII.77**	$CH(CH_3)_2$	NO_2	H	-	9
11	**VIII.78**	$CH(CH_3)_2$	OMe	H	-	38

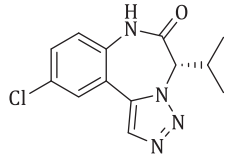

VIII.73
crude purity: **94%**
yield: **68%**

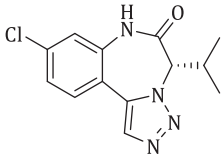

VIII.74
crude purity: **93%**
yield: **69%**

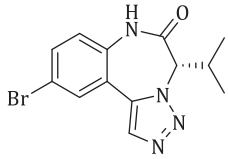

VIII.75
crude purity: **-**
yield: **73%**
>99%ee

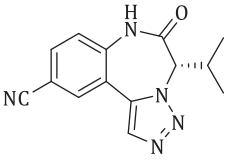

VIII.76
crude purity: **76%**
yield: **26%**

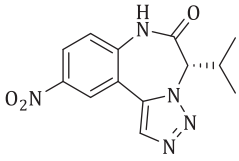

VIII.77
crude purity: **-**
yield: **9%**

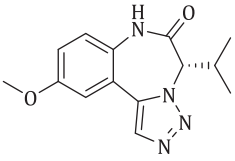

VIII.78
crude purity: **-**
yield: **38%**

Figure VIII-17: Library members VIII.73 – VIII.78 based on L-valine as α-amino acid

Table VIII-13: Library members VIII.79 – VIII.82 based on L-lysine as α-amino acid

entry	compound	R_1	R_2	R_3	crude purity (%)	yield (%)
6	**VIII.79**	$(CH_2)_4NHBoc$	Cl	H	94	55
7	**VIII.80**	$(CH_2)_4NHBoc$	H	Cl	93	69
10	**VIII.81**	$(CH_2)_4NHBoc$	Br	H	-	55
11	**VIII.82**	$(CH_2)_4NHBoc$	NO_2	H	-	27

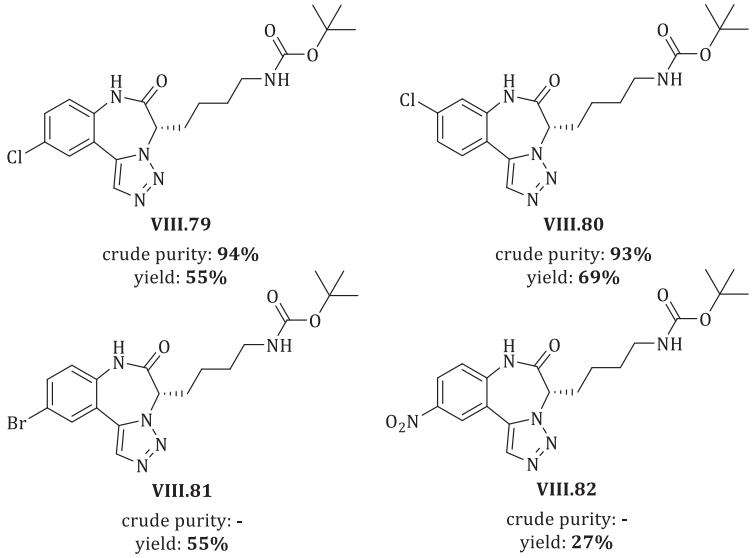

Figure VIII-18: Library members VIII.82 – VIII.85 based on L-lysine as α-amino acid

As can be seen from **Table VIII-7** – **Table VIII-13** and **Figure VIII-12** – **Figure VIII-18**, all compounds can be synthesized in acceptable yields and in an efficient way. Only compounds bearing strong electron withdrawing groups at the para-position from the aniline amine (i.c. nitro, cyano) render the cyclization/release more difficult hence resulting in lower yields.

Generally from the in the sections above, we can conclude that a total of 40 compounds were synthesized by means of a modular approach on solid-phase. These compounds were established by varying two diversity points on the newly designed scaffold, which is in accordance to the proposed aim and objectives discussed in Chapter V. It can be clearly seen that modular approach combined with the cyclization/release strategy enables a straightforward and concise synthesis of the proposed scaffold.

As during this research no concurrent publications of the [1,2,3]triazole[1,5-*d*][1,4]benzodiazepine-2-one motif were found, a reference can be made to Mayer *et al.*[14]

describing a solid-phase synthesis of a 1,4-benzodiazepine-2,5-dione scaffold upon cyclization/release from Wang resin. As this work comprises the synthesis of 11 library members with a yield varying from 45% to 80% (crude purity of max. 90%), the work presented in this manuscript reaches the same level of both efficiency and efficacy, whereas the efficiency is related to the obtained yield and the efficacy is determined by the cyclization/release strategy to liberate cyclized product *only*.

REFERENCES

[1] a) Zhang, L.; Chen, X.; Xue, P.; Sun, H. H. Y.; Williams, I. D.; Sharpless, K. B.; Fokin, V. V.; Jia, . *J. Am. Chem. Soc.* **2005**, *127*, 15998-15999. b) Boren, B. C.; Narayan, S.; Rasmussen, L. K.; Zhang, L.; Zhao, H.; Lin, Z.; Jia, G.; Fokin, V. V. *J. Am. Chem. Soc.* **2008**, *130*, 8923-8930.

[2] Majireck, M. M.; Weinreb, S. M. *J. Org. Chem.* **2005**, *71*, 8680-8683. c) Oppilliart, S.; Mousseau, G.; Zhang, L.; Jia, G.; Thuéry, P.; Rousseau, B.; Cintrat, J.-C. *Tetrahedron* **2007**, *63*, 8094-8098.

[3] a) Siemsen, P.; Livingston, R. C.; Diederich, F. *Angew. Chem., Int. Ed.* **2000**, *39*, 2632-2657. b) Vilhelmsen, M. H.; Jensen, J.; Tortzen, C. G.; Nielsen, M. B. *Eur. J. Org. Chem.* **2013**, 701-711.

[4] a) Glaser, C. *Ber. Dtsch. Chem. Ges.* **1869**, *2*, 422-424. b) Glaser. C. *Ann. Chem. Pharm* **1870**, *154*, 137-171.

[5] Elangovan, A.; Wang, Y.-H.; Ho, T.-I. *Org. Lett.* **2003**, *5*, 1841-1844.

[6] Bellina, F.; Carpita, A.; Mannocci, L.; Rossi, R. *Eur. J. Org. Chem.* **2004**, *12*, 2610–2619.

[7] a) Kraus, G. A.; Bae, J. *Tetrahedron Lett.* **2003**, *44*, 5505–5506. b) Gueugnot, S.; Alami, M.; Linstrumelle, G.; Mambu, L.; Petit, Y.; Larchevêque, M. *Tetrahedron Lett.* **1996**, *52*, 6635–6646. c) Clive, D. L. J.; Tao, Y.; Bo, Y.; Hu, Y.-Z.; Selvakumar, N.; Sun, S.; Daigneault, S.; Wu, Y.-J. *Chem. Commun.* **2000**, 1341–1350. d) Mukai, C.; Nomura, I.; Kitagaki, S. *J. Org. Chem.* **2003**, *68*, 1376–1385.

[8] a) Shin Shun, A. L. K.; Tykwinski, R. R. *J. Org. Chem.* **2003**, *68*, 6810–6813. b) Garcia, J.; López, M.; Romeu, J. *Synlett* **1999**, 429–431. c) Austin, W. B.; Bilow, N.; Kelleghan, W. J.; Lau, K. S. Y. *J. Org. Chem.* **1981**, *46*, 2280–2286; d) Taylor, E. C.; Ray, P. S. *J. Org. Chem.* **1988**, *53*, 35–38; e) Kozawa, Y.; Mori, M. *J. Org. Chem.* **2003**, *68*, 8068–8074. f) Kusaka, S.-I.; Dohi, S.; Doi, T.; Takashi, T.; *Tetrahedron Lett.* **2003**, *44*, 8857–8859.

[9] Fujiwara, J.; Fukutani, Y.; Sano, H.; Maruoka, K.; Yamamoto, H. *J. Am. Chem. Soc.* **1983**, *105*, 7177-7179.

[10] a) Nishinaga, T.; Miyata, Y.; Nodera, N.; Komatsu, K. *Tetrahedron* **2004**, *60*, 3375–3382. b) Nakanishi, H.; Sumi, N.; Aso, Y.; Otsubo, T. *J. Org. Chem.* **1998**, *63*, 8632–8633.

[11] a) Perlman, M. E.; Watanabe, K. A.; Schinazi, R. F.; Fox, J. J. *J. Med. Chem.* **1985**, *28*, 741–748. b) Casara, P.; Danzin, C.; Metcalf, B.; Jung, M. *J. Chem. Soc., Perkin Trans. 1,* **1985**, 2201–2207.

[12] Yudin, A. K. Transition Metal-Catalyzed Synthesis of Fused Five-Membered Aromatic Heterocycles. In *Catalyzed Carbon-Heteroatom Bond Formation*; Yudin, A. K., Ed.; Wiley-VCH, Weinheim, **2011**, pp. 340 - 379.

[13] Banwell, M. G.; Jones, M. T.; Loong, D. T. J.; Lupton, D. W.; Pinkerton, D. M.; Ray, J. K.; Willis A. C. *Tetrahedron*, **2010**, *66*, 9252-9262.

[14] Mayer, J.P.; Zhang, J.; Bjergarde, K.; Lenz, D.M.; Gaudino, J.J.; *Tetrahedron Lett.* **1996**, *37*, 8081-8084.

IX. Synthesis of 1,4,5-trisubstituted triazole moiety

A. Introduction

In the next step towards the synthesis of a full mimick of the 1,5-benzodiazepine-2,4-dione scaffold (e.g. biologically active clobazam **I.24**), a pharmacophoric group at the C4-position of the 1,2,3-triazole moiety needs to be introduced.

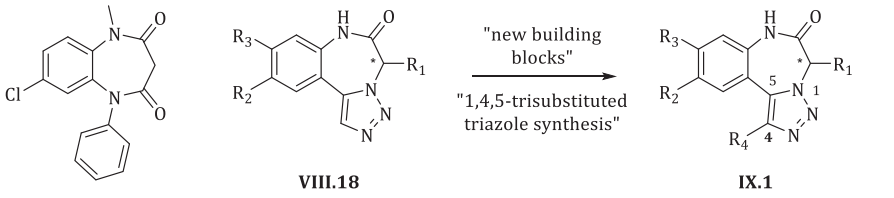

I.24
Clobazam

VIII.18

IX.1

Figure IX-1: **Aimed introduction of the 1,4,5-trisubstituted triazole moiety.**

In order to create this additional diversity in the desired triazole-fused benzodiazepine scaffold **VIII.18** with the preconceived solid-supported synthesis strategy including cyclization/release, a method for solid-phase synthesis of the 1,4,5-trisubstituted 1,2,3-triazole moiety needs to be achieved. As the thermal Huisgen-'click' reaction fails in high reaction rate due to the high activation energy barrier (see section **IV.A**) and only allows strongly deactivated (i.e. electron-poor) alkynes, the Cu(I)- or Ru(II)-catalyzed modifications of this reaction might be potential alternatives.

The mechanism of the CuAAC has proven to proceed *via* a stepwise non-concerted process (see **Scheme IV-1**, **IV.B.1**). Moreover, one of the key steps in the mechanism is the formation

of a terminal copper acetylide, which eventually limits the alkyne scope to terminal alkynes[1], hence, excluding the formation of 1,4,5-trisubstituted 1,2,3-triazoles.

In contrast with the CuAAC, the catalytic cycle of the RuAAC allows internal alkynes to be used, therefore affording 1,4,5-trisubstituted triazoles. Fokin and co-workers[2] initially investigated symmetrical internal alkynes for their use in the RuAAC, resulting in a complete conversion of the azide into symmetrical 1,4,5-trisubstituted triazoles. In a second paper[3], Fokin *et al.* studied a small set of asymmetrical alkynes in the Ru(II)-catalyzed azide-alkyne cycloaddition. In specific cases, a directing effect could be observed related to electronic and steric effects. Alkynes containing a hydrogen bond donor group **IX.3** (e. g. propargylic amines **IX.3a** and alcohols **IV.3b**) exhibit exclusive regioselectivity towards 1,4,5-trisubstituted triazoles **IX.4**. The latter could be attributed to the formation of a strong H-bond between the amine or alcohol and the chlorine ligand present in the active species of the catalyst (**IX.5a** and **IX.5b**, **Figure IX-2**).

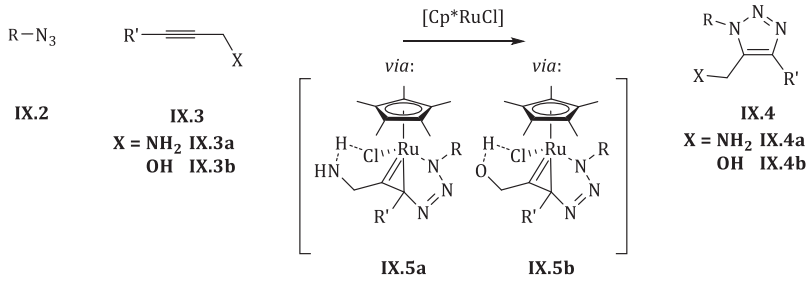

Figure IX-2: Propargylic H-bond donor directing capacities for RuAAC

A more extensive study on internal alkynes has been performed by Weinreb[4] *et al.*, investigating a more diverse set of asymmetric internal alkynes **IX.6** (**Figure IX-3**). Apart from propargylic H-bond donor bearing functionalities, other specific regioselectivities were found, yet (at that time) no compelling mechanistic relevance was provided. In **Table IX-1**, a short list of alkyne substituents and their directing capacities are presented.

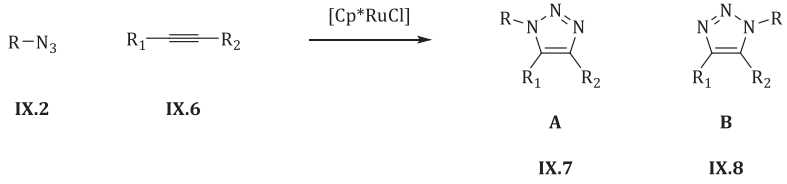

Figure IX-3: Regioselectivity study for internal alkynes performed by Weinreb[4]

From **Table IX-1** can be seen that (a) strong electron withdrawing groups (EWG) (entries **2** and **6**), (b) propargylic H-bond donating groups (entries **3** and **7**) and (c) tertiary azides (entry **9**) have the capacity to create regioselectivity in the Ru(II)-catalyzed dipolar cycloaddition of internal alkynes.

Table IX-1: Summary of the experiments performed by Weinreb[4]

entry	R	R_1	R_2	Result
1	CH_2Ph	Ph	Pr	mixture A/B[1]
2	CH_2Ph	Ph	EWG[2]	A
3	CH_2Ph	Ph	CH_2OH	B
4	CH_2Ph	Ph	TMS	no reaction
5	CH_2Ph	alkyl	alkyl	mixture A/B
6	CH_2Ph	alkyl	EWG[2]	A
7	CH_2Ph	alkyl	CH_2OH	B
8	$CHPh_2$	Ph	Me	mixture A/B
9	1-adamantyl	Ph	Me	B

[1] for R_2 = Pr A:B ratio of 13:87 (for R_2 = Me A:B ratio of 38:62)

[2] such as COOMe or C(=O)Me

Huang and co-workers[5] tested various symmetric and asymmetrical diarylalkynes in order to verify their individual reactivity and secondly, for asymmetrical alkynes, the regioselectivity of the RuAAC.

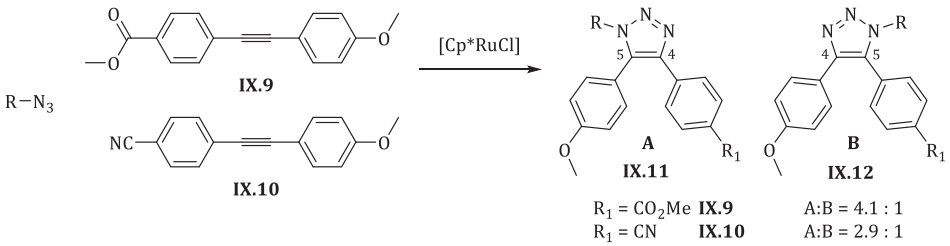

Figure IX-4: Regioselectivity study for internal alkynes performed by Huang[5]

By using para-substituted aryl moieties **IX.9** – **IX.10**, the sterical effects of asymmetric diarylalkynes at the position of the triple bond were nullified, therefore providing a clearer view of the electronic effects in the Ru(II)-catalytic cycle. Furthermore, the alkyne was asymmetrically substituted with an electron-rich and an electron-poor aromatic moiety. After employing the RuAAC it was found that the electron-rich aromatic moiety preferably takes the C5-position of the triazole (**A**, **Figure IX-4**), which is in full correspondence with the mechanistic study provided by Fokin[3] (see section **IV.D.1**).

If sterical and electronic considerations are taken into account, it is proven that the Ru(II)-catalyzed azide-alkyne cycloaddition can be a tool to include 1,4,5-trisubstituted 1,2,3-triazole moieties into our synthetic approach.

In order not to exclude other possibilities towards the synthesis of 1,4,5-trisubstituted 1,2,3-triazole moieties, a short overview is given:

- direct Pd-catalysed[6]- or Cu-catalysed[7]-arylation of 1,4-disubstituted 1,2,3-triazoles;
- Pd-assisted diversification of 5-iodo-1,2,3-triazoles[8];
- reaction of chloromagnesium[9] or bromomagnesium[10]-1,2,3-triazoles with an electrophile;
- one-pot reaction between dicarbonyl derivatives, amines and azides[11];
- proline-catalyzed formation of 1,4,5-trisubsituted 1,2,3-triazoles from ketones and aryl azides[12];
- thermal dipolar cycloadditions with internal alkynes which afford 1,4,5-trisubstituted triazoles[13].

The methods above are not taken into account as these strategies would be unfavorable and inapplicable in combination with the proposed the solid-phase strategy (see Chapter **V**).

B. Retrosynthetic approach

In order to introduce the pharmacophoric group on the triazole moiety in scaffold molecule **IX.1**, the RuAAC will be performed with a solid-phase bound azide **V.7** and an internal alkyne **V.6** to afford the solid-phase bound 1,4,5-trisubstituted triazole intermediate **V.5**. A cyclization/release strategy will be employed to obtain the desired scaffold **IX.1**. The internal alkynes **V.6** will be prepared *via* a Sonogashira cross-coupling between terminal alkynes **V.11** and commercially available 2-iodoanilines **V.10**.

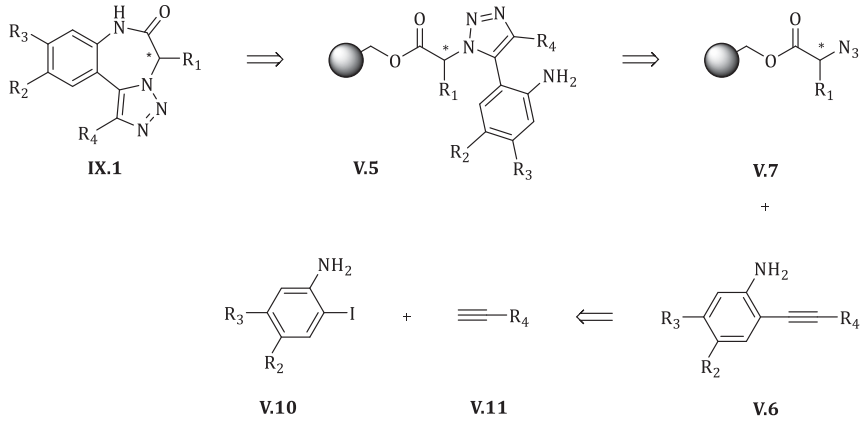

Scheme IX–1: Retrosynthetic approach towards the introduction of a 1,4,5-trisubstituted 1,2,3-triazole moiety.

As illustrated in **Scheme IX–1**, asymmetric alkynes will be used for the synthesis of the 1,4,5-trisubstituted triazole moiety. In a first stage, we will focus on four building blocks presented in **Figure IX-5**. All building blocks will be based on structure **V.6** bearing a 2-aniline moiety required for the ring closure and various side chains R_4. The latter vary from an alkyl chain

(**IX.13**) to a more sterically demanding phenyl ring (**IX.16**). From recent publications[4,5], we could assume that the aniline functionality will provide the required electron density to the alkyne in order to direct, to a certain extent, the RuAAC towards the desired regioisomer **V.5**. More specifically in the case of **IX.13**, this aniline could overrule the low regioselectivity found by Weinreb[4] (**Table IX-1**, entry **1**) for phenyl/alkyl substituents on the alkyne. After initial optimization, a homopropargylic alcohol moiety **IX.17** will also be incorporated as side chain. As, in this case, no H-bond formation with the chlorine ligand in $C_p^*RuCl(PPh_3)_2$ is expected[3], we do not foresee the regioselectivity induced by the aniline group to be affected.

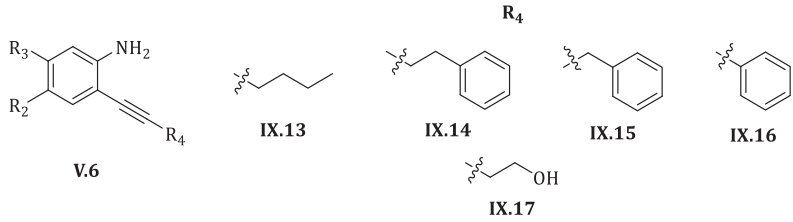

Figure IX-5: Proposed building blocks V.6

Initially four building blocks (**IX.13 – IX.16**) were synthesized in order to verify the regioselectivity in the Ru(II)-catalyzed azide-alkyne cycloaddition. Using the Sonogashira cross-coupling reaction, building blocks **IX.13**, **IX.15** and **IX.16** could be synthesized in excellent yields (94%-98%). Only **IX.14** gave rise to lower yield (82%) as the cross-coupling reaction proceeded sluggish.

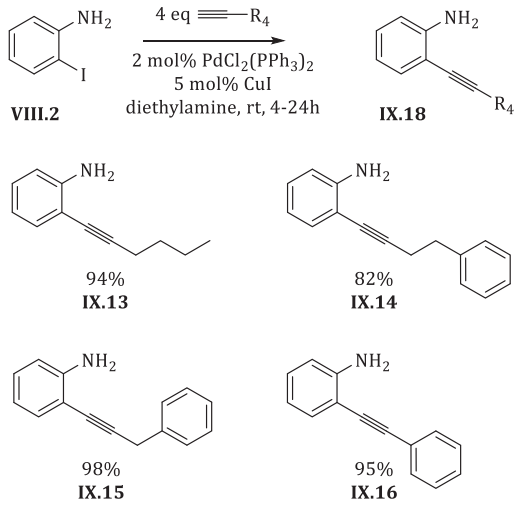

Scheme IX–2: Internal alkyne building block IX.13 – IX.16 synthesis

Table IX-2: Isolated yields for building blocks IX.13 – IX.16

entry	compound	R_4	reaction time	yield (%)
1	**IX.13**	$(CH_2)_3CH_3$	5h	94
2	**IX.14**	$(CH_2)_2Ph$	24h	82
3	**IX.15**	CH_2Ph	24h	98
4	**IX.16**	Ph	4h	95

C. Test case: Synthesis of 1,4,5-trisubstituted triazole moiety

In the following paragraphs, a discussion will be made regarding the solid-phase synthesis of 1,4,5-trisubstituted 1,2,3-triazoles by performing the RuAAC. As internal alkynes can give rise to the formation of two regioisomers (**V.5** and **IX.19**, **Scheme IX–3**), a detailed analysis is required in order to assign and determine the ratio of both regioisomers.

Both regioisomers will be quantified *via* an integration of the crude HPLC-chromatogram, obtained after cleaving an aliquot of the reacted beads **V.5** and **IX.19** with TFA/H_2O (95/5) *via* the standard protocol. Although both 1,4,5-trisubstituted regioisomers **IX.20** and **IX.22** have identical masses, a distinction between both can be made thanks to cyclization/release of the desired solid-phase bound regioisomer **V.5** under acidic conditions (i.e. TFA/H_2O 95/5, see section **VIII.A**). As the cyclized, dehydrated product **IX.21** has a 'molecular weight minus eighteen' as compared to the undesired regioisomer **IX.22**, which will be released from the resin as the uncyclized carboxylic acid, a coupled MS spectrum will enable an unambiguous assignment of the peaks in the HPLC-chromatogram to the corresponding regioisomer. Hence, the cyclization/release strategy facilitates a study of the regioselectivity of the Ru(II)-catalyzed azide-alkyne cycloaddition for internal alkynes bearing an *o*-aniline moiety.

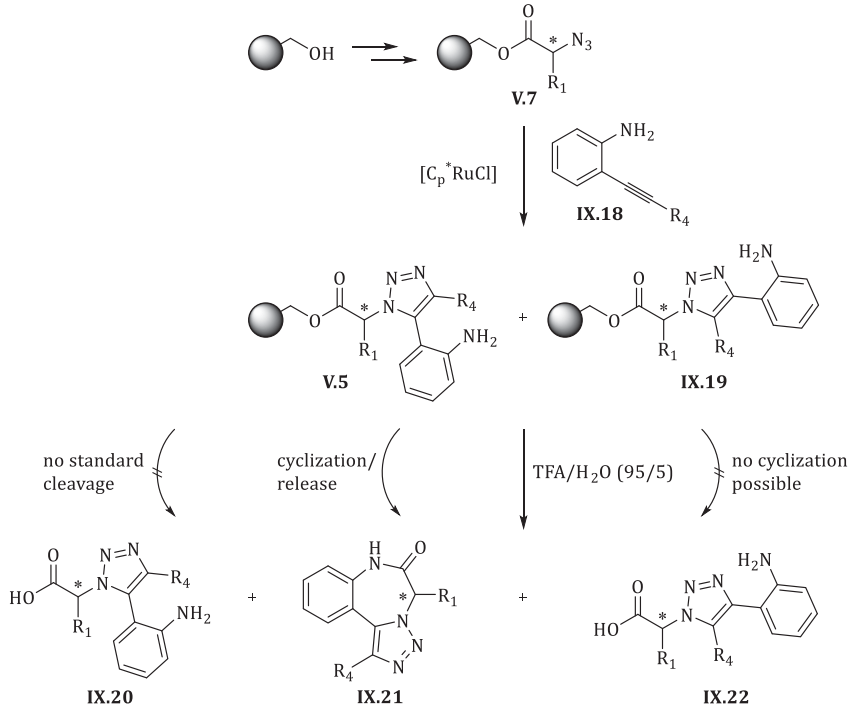

Scheme IX–3: Strategy to determine the ratio of regioisomers V.5 : IX.19

In order to determine the effectiveness and regioselectivity, test reactions were executed while varying the temperature, the Ru(II)-catalyst and the solvent. Furthermore, blank runs (without catalyst) were performed in order to determine whether the thermal Huisgen-'click' reaction has an influence on the ratio of both regioisomers **V.5** and **IX.19**. This reaction could occur at elevated temperatures if the Ru(II)-catalyzed reaction fails or is too slow under the specified conditions. Yet, it can already be mentioned that for blank test reactions (section **IX.C.1** to **IX.C.5**) no (or <1%) thermal Huisgen-'click' reaction took place. Therefore, these results are excluded from **Table IX-3** to **Table IX-7**.

1. Regioselectivity of the cycloaddition with IX.13

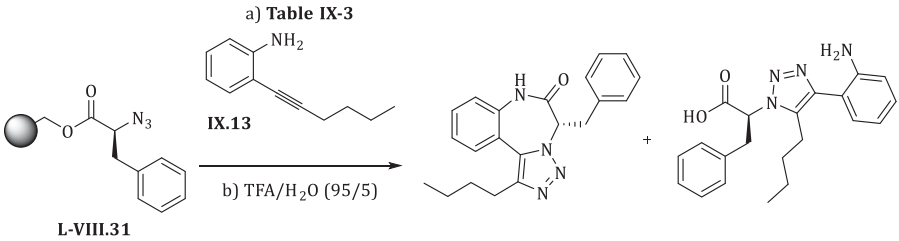

Scheme IX–4: Regioselectivity test reactions for IX.13 after a reaction time of 6h

Table IX-3: Ratio[a] of IX.23 : IX.24

entry	toluene			
	$Cp^*RuCl(PPh_3)_2$		$Cp^*RuCl(COD)$	
	rt	60°C	rt	60°C
1	> 99:1	> 99:1	> 99:1	> 99:1
	dioxane			
	$Cp^*RuCl(PPh_3)_2$		$Cp^*RuCl(COD)$	
	rt	60°C	rt	60°C
2	> 99:1	> 99:1	> 99:1	> 99:1

[a] Ratio determined via LC-MS analysis (214 nm), conversion 100%

As can be seen in **Table IX-3**, all performed test reactions in both solvents give rise to formation of the desired regioisomer in a ratio of 99:1, as only cyclized product **IX.23** is observed. The absence of the open product for the desired regioisomer also illustrates that cyclization/release readily takes place with TFA/H_2O (95/5) without cleaving the product as the carboxylic acid.

More interestingly, comparing to the experiments performed by Weinreb[4] (**Table IX-1**, entry **1**), the electron donating capacity of the aniline enables full formation of the desired regioisomer whereas Weinreb found a 87:13 ratio for asymmetric phenyl/alkyl alkynes with a combined yield of 80%.

2. Regioselectivity of the cycloaddition with IX.14

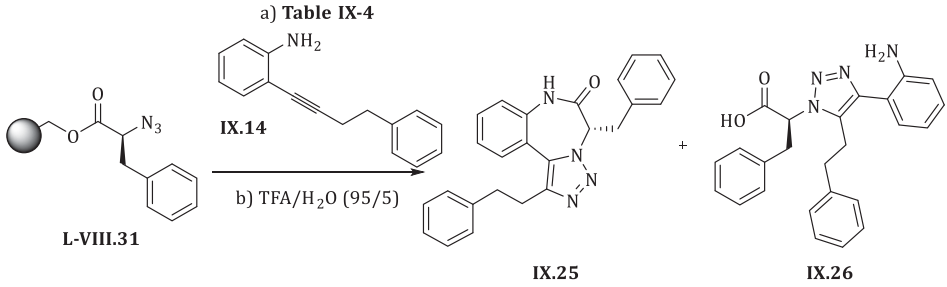

Scheme IX–5: Regioselectivity test reactions for IX.14 after a reaction time of 6h

Table IX-4: Ratio[a] of IX.25 : IX.26

entry	toluene			
	$C_p^*RuCl(PPh_3)_2$		$C_p^*RuCl(COD)$	
	rt	60°C	rt	60°C
1	88:12	89:11	97:3	75:25
	dioxane			
	$C_p^*RuCl(PPh_3)_2$		$C_p^*RuCl(COD)$	
	rt	60°C	rt	60°C
2	85:15	80:20	85:15	72:28

[a] Ratio determined via LC-MS analysis (214 nm), conversion 100%

As can be seen in **Table IX-4**, the results for **IX.14** are different from those for **IX.13** discussed in the previous paragraph. In toluene as solvent, $C_p^*RuCl(COD)$ gives rise to the highest ratio of the desired regioisomer at room temperature. Taken into account the highest activity of this catalyst and/or highest stability, this can explain the high conversion.

In dioxane, generally the ratio is lower, but identical trends can be noticed compared to toluene.

3. Regioselectivity of the cycloaddition with IX.15

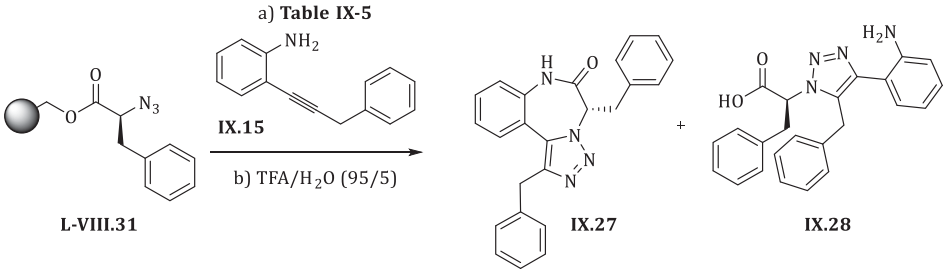

Scheme IX–6: Regioselectivity test reactions for IX.15 after a reaction time of 6h

Table IX-5: Ratio[a] of IX.27 : IX.28

entry	toluene			
	$Cp^*RuCl(PPh_3)_2$		$Cp^*RuCl(COD)$	
	rt	60°C	rt	60°C
1	73:27	85:15	82:18	68:32
	dioxane			
	$Cp^*RuCl(PPh_3)_2$		$Cp^*RuCl(COD)$	
	rt	60°C	rt	60°C
2	39:61[b]	63:37	71:29	70:30

[a] Ratio determined via LC-MS analysis (214 nm)

[b] Effectiveness of RuAAC (75%).

Table IX-5 represents the results of the RuAAC with **IX.15**. Generally, toluene yields again the highest ratio for all applied conditions, with the highest ratio of 85:15 for $Cp^*RuCl(PPh_3)_2$ at 60°C. Comparing to **IX.14**, where $Cp^*RuC(COD)$ yielded the highest ratio, we might assume that conclusions regarding 'the best catalyst' are inadequate and vary upon the substrate. Still, these experiments illustrate clearly the higher activity and regioselectivity of $Cp^*RuCl(PPh_3)_2$ at elevated temperatures comparing with the lower stability of $Cp^*RuCl(COD)$ at those temperatures.

Moreover, dioxane seems to give rise to lower selectivity for the desired regioisomer, indicating that the catalytic process is solvent dependent.

In an attempt to explain the higher scrambling ratio comparing to the results obtained in experiments with **IX.13** and **IX.14** (**Table IX-3** and **Table IX-4**), there might be the possibilty that (a) sterical interactions and (b) stabilizing phenyl – Ru interactions interfere with the proposed/desired catalytic process, therefore influencing the ratio of both regioisomers.

4. Regioselectivity of the cycloaddition with IX.16

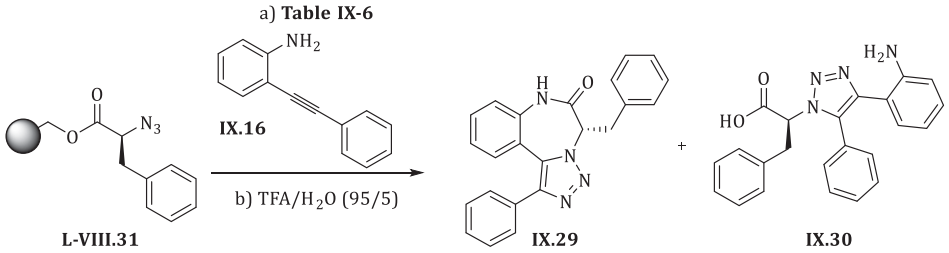

Scheme IX–7: Regioselectivity test reactions for IX.16 after a reaction time of 6h

Table IX-6: Ratio[a] of IX.29 : IX.30

entry	toluene			
	$Cp^*RuCl(PPh_3)_2$		$Cp^*RuCl(COD)$	
	rt	60°C	rt	60°C
1	60:40	79:21	98:2	77:23
	dioxane			
	$Cp^*RuCl(PPh_3)_2$		$Cp^*RuCl(COD)$	
	rt	60°C	rt	60°C
2	72:28	88:12	93:7	89:11

[a] Ratio determined via LC-MS analysis (214 nm)

In **Table IX-6**, the results for the test reactions related to the building block **IX.16** are presented. In contrast with previous results, in this case, dioxane tends to give generally better ratios compared to toluene, except for the best result (i.e. $Cp^*RuCl(COD)$ at room temperature in toluene 98:2). More strickingly, for this nearly symmetrical building block a directing capacity is observed (98:2) due to the electron donating ortho-amino group.

In order to verify the latter assumption a fifth building block was synthesized **IX.31** (**Scheme IX–8**) which bears an additional amine function. The idea of synthesizing **IX.31** came from the need to synthesize a building block that has an identical sterical appearance at the position of the triple bond for the catalyst, but has a different electron density in the second phenyl ring. In order to verify the influence of the second aniline function, test reactions were perfomed (**Scheme IX–9, Table IX-7**).

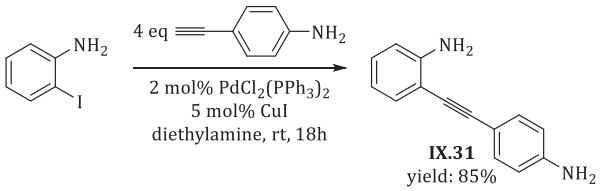

Scheme IX–8: Synthesis of building block IX.31

5. Regioselectivity of the cycloaddition with IX.31

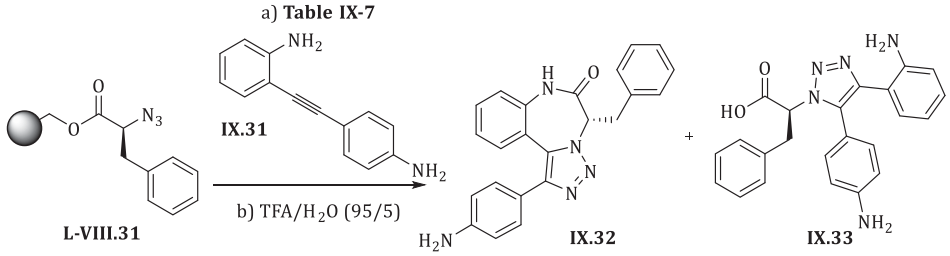

Scheme IX–9: Regioselectivity test reactions for IX.31 after a reaction time of 6h

Table IX-7: Ratio[a] of IX.32 : IX.33

entry	toluene			
	$C_p^*RuCl(PPh_3)_2$		$C_p^*RuCl(COD)$	
	rt	60°C	rt	60°C
1	67:33	78:22	67:33	66:34

[a] Ratio determined via LC-MS analysis (214 nm)

Table IX-7 represents the influence of an additional electron donating group on the second phenyl ring, therefore leading to an increased electron density in the triple bond. The results presented clearly show a lower regioselectivity for $C_p^*RuCl(COD)$, therefore proving the importance of the electronic effects during the catalytic cycle.

By further exploiting the elegant quantification strategy relying on the cyclization/release of one specific regioisomer, more building blocks could be investigated in order to verify and/or quantify the electronic influences of ortho-aniline bearing internal alkynes.

6. Proof of principle library

In order to verify the large-scale synthesis of the desired scaffold molecule and the efficacy of the aimed cyclization/release, a proof of principle library was constructed. A different α-amino acid (i.c. Fmoc-Lys(Boc)-OH **VI.31**) was chosen in order to verify the scope of the α-

amino acid substitution (R_1). Taken into account the best conditions for each alkyne obtained from the test reactions, the 1,3-dipolar cycloaddition will be performed with conditions presented in **Table IX-8**.

Table IX-8: Optimized conditions for 1,4,5-triazole moiety incorporation

entry	alkyne	conditions
1	**IX.13**	10 mol% $C_p^*RuCl(PPh_3)_2$, 60°C, toluene, 6h
2	**IX.14**	10 mol% $C_p^*RuCl(COD)$, rt, toluene, 6h
3	**IX.15**	10 mol% $C_p^*RuCl(PPh_3)_2$, 60°C, toluene, 6h
4	**IX.16**	10 mol% $C_p^*RuCl(COD)$, rt, toluene, 6h

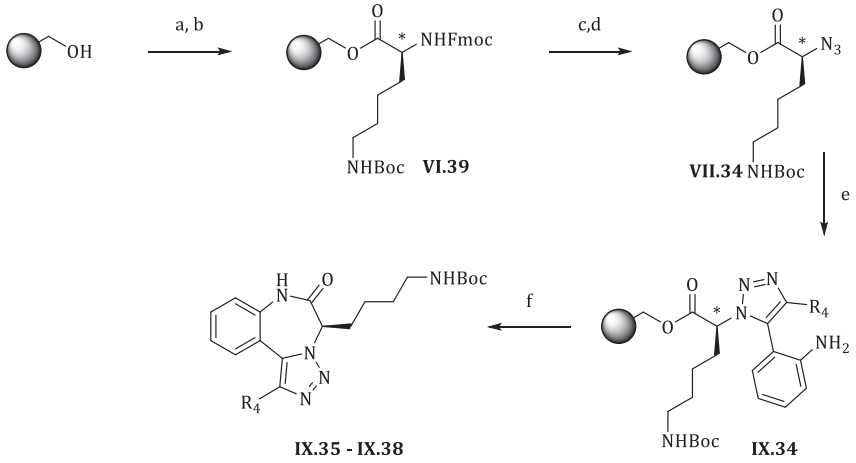

internal alkyne building blocks

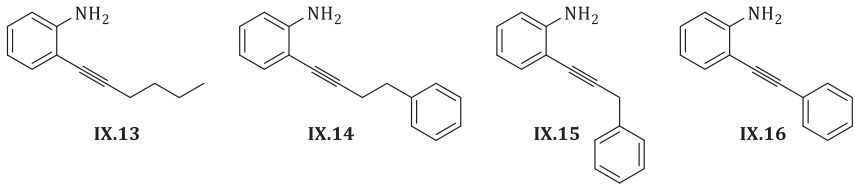

a) 2 eq Fmoc-AA-OH, 2 eq DIC, 0,2 eq DMAP, CH_2Cl_2, rt, 2x 24h b) Ac_2O, CH_2Cl_2, DIPEA (1/1/3) c) 1) 20 v/v% 4-Me-piperidine/DMF, rt, 2x 10 min. d) 1,2 eq imidazole-1-sulfonyl azide hydrochloride, 2 eq TEA, 1 mol% $CuSO_4.5H_2O$, THF/H_2O (1/1), rt, 24h. e) 3 eq **IX.13 - IX.16**, **Table IX-8**. f) HOAc/CH_2Cl_2 (1/1), rt, 24h.

Scheme IX–10: Proof of principle library incorporating a 1,4,5-triazole moiety.

Table IX-9: Proof of principle library incorporating a 1,4,5-triazole moiety.

entry	compound	R_1	R_4	crude purity[a] (%)	yield (%)
1	**IX.35**	$(CH_2)_4NHBoc$	$(CH_2)_3CH_3$	>90%	51%
2	**IX.36**	$(CH_2)_4NHBoc$	$(CH_2)_2Ph$	>90%	83%
3	**IX.37**	$(CH_2)_4NHBoc$	CH_2Ph	>90%	20%
4	**IX.38**	$(CH_2)_4NHBoc$	Ph	>90%	84%

[a] Crude purity could not be exactly quantified due to presence of toluene (added for azeotropic evaporation). Integration @214 nm cannot be trusted as compounds and toluene have identical retention time.

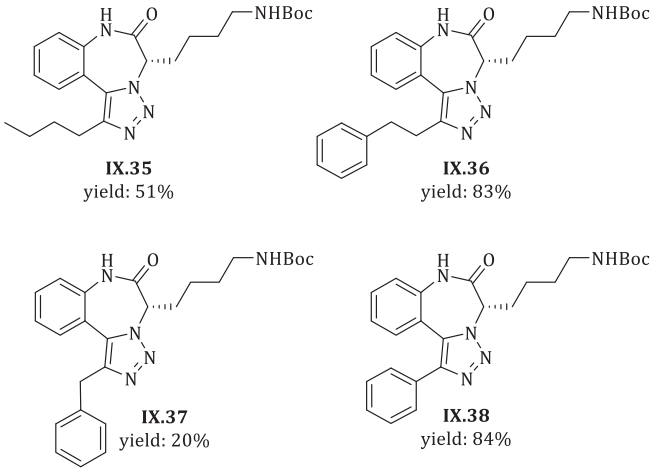

Figure IX-6: Four initial obtained scaffold with a 1,4,5-triazole moiety.

From **Table IX-9** and **Figure IX-6** it can be seen that the aimed synthesis strategy including the cyclization/release step enables the synthesis of compounds bearing a C4-triazole modification. Despite the lower yield for **IX.37**, all other compounds were synthesized in good yields. Furthermore, the cyclization/release gave rise to high crude purities. Apart from toluene, which was added during the work-up, no other peaks were detected in the HPLC-chromatogram. This synthesis as presented in **Scheme IX–10** was further expanded by including two other α-amino acids: Fmoc-Phe-OH **VI.28** and Fmoc-Ser(*t*Bu)-OH **VI.27** leading to a library of six compounds **IX.23, IX.25, IX.29** and **IX.39-IX.41**. Compounds constructed with building block **IX.15** give rise to low yields whereas characterization was not possible, therefore they are excluded from the library.

Table IX-10: Extended proof of principle library incorporating a 1,4,5-triazole moiety.

entry	compound	R_1	R_4	yield (%)
1	**IX.23**	CH_2Ph	$(CH_2)_3CH_3$	57%
2	**IX.25**	CH_2Ph	$(CH_2)_2Ph$	58%
3	**IX.29**	CH_2Ph	Ph	64%
4	**IX.39**	$CH_2O(t\text{Bu})$	$(CH_2)_3CH_3$	63%
5	**IX.40**	$CH_2O(t\text{Bu})$	$(CH_2)_2Ph$	32%
6	**IX.41**	$CH_2O(t\text{Bu})$	Ph	46%

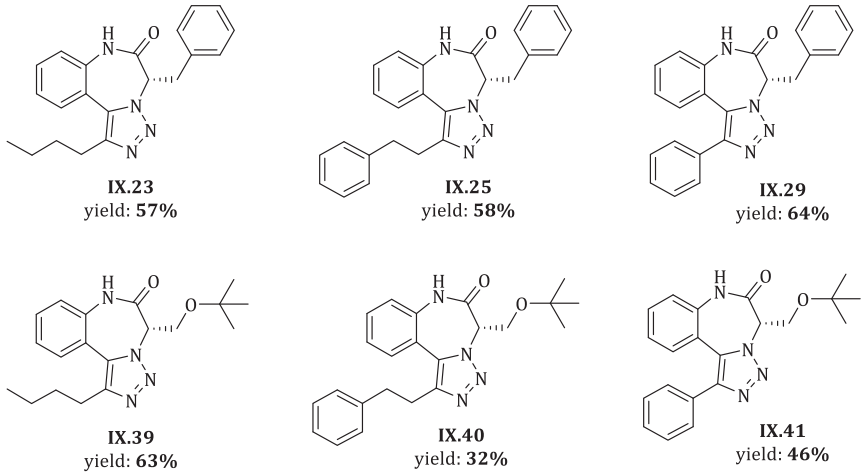

Figure IX-7: Extended proof of principle library incorporating a 1,4,5-triazole moiety.

7. Combinatorial library

In order to this expand library synthesis, a range of new building blocks **V.5** were constructed by subjecting commercially available 2-iodoanilines **V.10** to a Sonogashira cross-coupling reaction with terminal alkynes, including homopropargylic alcohol. As can be seen in **Scheme IX–11** and **Table IX-11**, all building blocks **IX.42** – **IX.47** were synthesized in excellent yields.

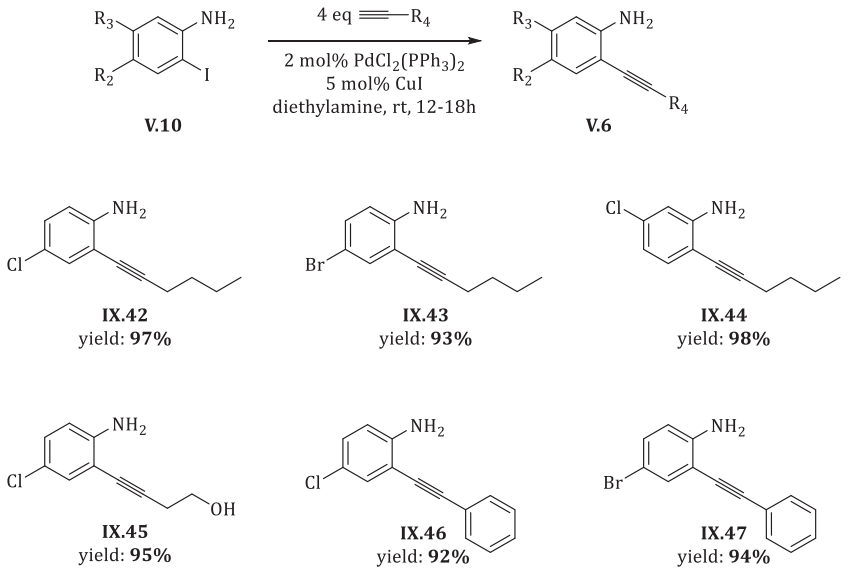

Scheme IX–11: Internal alkyne building block IX.42 – IX.47 synthesis

Table IX-11: Isolated yields for building blocks IX.42 – IX.47

entry	compound	R_2	R_3	R_4	yield (%)
1	**IX.42**	Cl	H	$(CH_2)_3CH_3$	97%
2	**IX.43**	Br	H	$(CH_2)_3CH_3$	93%
3	**IX.44**	H	Cl	$(CH_2)_3CH_3$	98%
4	**IX.45**	Cl	H	$(CH_2)_2OH$	95%
5	**IX.46**	Cl	H	Ph	92%
6	**IX.47**	Br	H	Ph	94%

Moreover, our interest went out to building blocks with electron donating functionalities. 2-Iodo-4-methoxy-1-nitrobenzene (**VIII.42,** synthesized in section **VIII.D.1**) and commercially available 2-iodo-5-methoxy-1-nitrobenzene (**IX.48**) were used in a Sonogashira cross-coupling reaction with 1-hexyne affording respectively 2-(hexynyl)-4-methoxy-1-nitrobenzene (**IX.49**) and 2-(hexynyl)-5-methoxy-1-nitrobenzene (**IX.50**) in excellent yields.

Subsequent reduction of the nitro functionality present in **IX.49** and **IX.50** with Fe and acetic acid give arise to fast reduction to the amine for compound **IX.51** in 52% yield. Unfortunately, for compound **IX.50** the alkyne moiety was instantly reduced into the corresponding alkyl derivative **IX.52** in 65% yield. Most probably this is due to higher electron density in the aromatic ring and by extent in the triple bond given the *p*-methoxygroup.

In order to avoid overreduction, the reaction sequence was inverted. A reduction of intermediate **IX.48** afforded 2-iodo-5-methoxyaniline (**IX.53**) in 63% yield. Further, **IX.53** was used in the Sonogashira reaction with 1-hexyn therefore yielding the desired building block **IX.54** within 12 h in 92% yield.

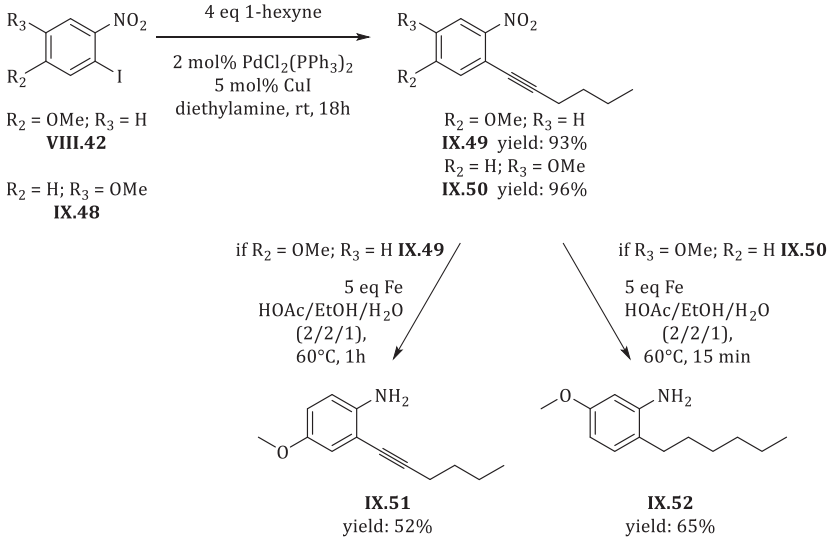

Scheme IX–12: Synthesis of IX.51

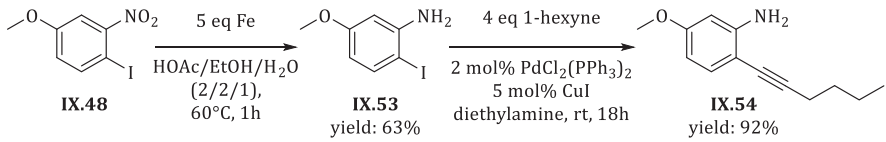

Scheme IX–13: Synthesis of IX.54

The library synthesis was performed by subjecting eight α-amino acids and seven building blocks bearing internal alkynes to generally applied conditions. The isolated yields for this library synthesis are presented in **Table IX-12** - **Table IX-15** and **Figure IX-8** - **Figure IX-11**.

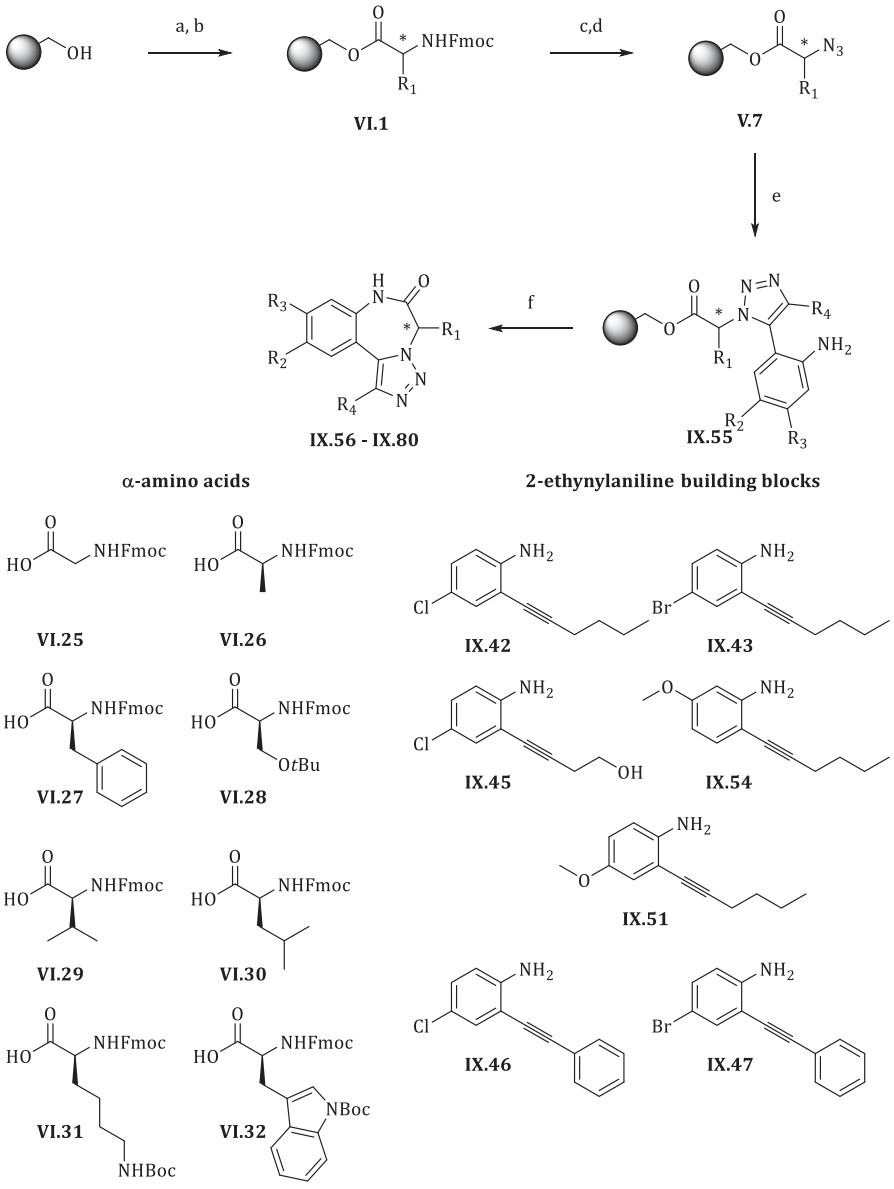

a) 2 eq Fmoc-AA-OH, 2 eq DIC, 0,2 eq DMAP, CH_2Cl_2, rt, 2x 24h b) Ac_2O, CH_2Cl_2, DIPEA (1/1/3) c) 1) 20 v/v% 4-Me-piperidine/DMF, rt, 2x 10 min. d) 1,2 eq imidazole-1-sulfonyl azide hydrochloride, 2 eq TEA, 1 mol% $CuSO_4.5H_2O$, THF/H_2O (1/1), rt, 24h. e) 3 eq alkyne, **Table IX-8** f) $HOAc/CH_2Cl_2$ (1/1), rt, 24h.

Scheme IX–14: Synthesis scheme for a combinatorial library incorporating a 1,4,5-triazole moiety.

Table IX-12: Library members IX.56 – IX.62 based on IX.42 as building block (R_3 = H)

entry	compound	R_1	R_2	R_4	yield (%)
1	**IX.56**	CH_3	Cl	$(CH_2)_3CH_3$	59
2	**IX.57**	CH_2Ph	Cl	$(CH_2)_3CH_3$	34
3	**IX.58**	$CH_2O(t\text{Bu})$	Cl	$(CH_2)_3CH_3$	31
4	**IX.59**	*N*-Boc-3-indolylmethyl	Cl	$(CH_2)_3CH_3$	36
5	**IX.60**	$CH_2CH(CH_3)_2$	Cl	$(CH_2)_3CH_3$	75
6	**IX.61**	$CH(CH_3)_2$	Cl	$(CH_2)_3CH_3$	61
7	**IX.62**	$(CH_2)_4NHBoc$	Cl	$(CH_2)_3CH_3$	58

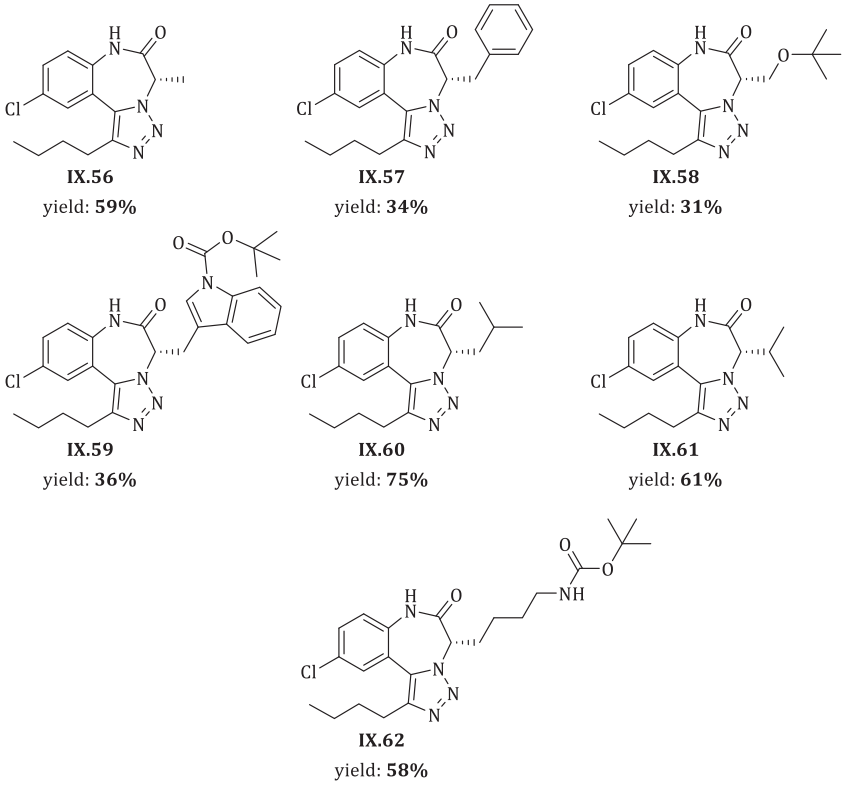

Figure IX-8: Library members IX.56 – IX.62 based on IX.42 as building block

Table IX-13: Library members IX.63 – IX.69 based on IX.43 as building block (R_3 = H)

entry	compound	R_1	R_2	R_4	yield (%)
1	**IX.63**	CH_3	Br	$(CH_2)_3CH_3$	69
2	**IX.64**	CH_2Ph	Br	$(CH_2)_3CH_3$	33
3	**IX.65**	$CH_2O(t\text{Bu})$	Br	$(CH_2)_3CH_3$	29
4	**IX.66**	*N*-Boc-3-indolylmethyl	Br	$(CH_2)_3CH_3$	45
5	**IX.67**	$CH_2CH(CH_3)_2$	Br	$(CH_2)_3CH_3$	74
6	**IX.68**	$CH(CH_3)_2$	Br	$(CH_2)_3CH_3$	53
7	**IX.69**	$(CH_2)_4NHBoc$	Br	$(CH_2)_3CH_3$	63

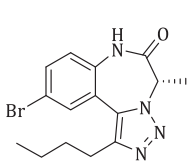

IX.63
yield: **69%**

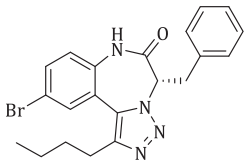

IX.64
yield: **33%**

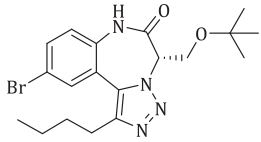

IX.65
yield: **29%**

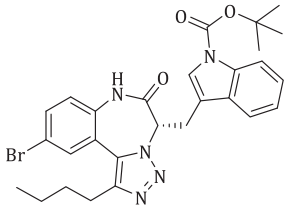

IX.66
yield: **45%**

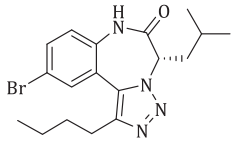

IX.67
yield: **74%**

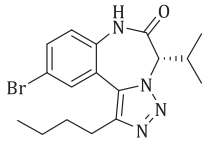

IX.68
yield: **53%**

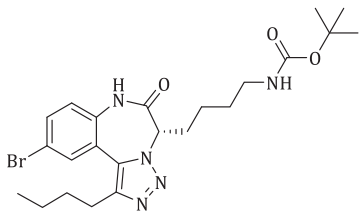

IX.69
yield: **63%**

Figure IX-9: Library members IX.63 – IX.69 based on IX.43 as building block

Table IX-14: Library members IX.70 – IX.76 based on IX.45 as building block (R_3 = H)

entry	compound	R_1	R_2	R_4	yield (%)
1	**IX.70**	CH_3	Cl	$(CH_2)_2OH$	62
2	**IX.71**	CH_2Ph	Cl	$(CH_2)_2OH$	51
3	**IX.72**	$CH_2O(t\text{Bu})$	Cl	$(CH_2)_2OH$	34
4	**IX.73**	*N*-Boc-3-indolylmethyl	Cl	$(CH_2)_2OH$	43
5	**IX.74**	$CH_2CH(CH_3)_2$	Cl	$(CH_2)_2OH$	70
6	**IX.75**	$CH(CH_3)_2$	Cl	$(CH_2)_2OH$	51
7	**IX.76**	$(CH_2)_4NHBoc$	Cl	$(CH_2)_2OH$	62

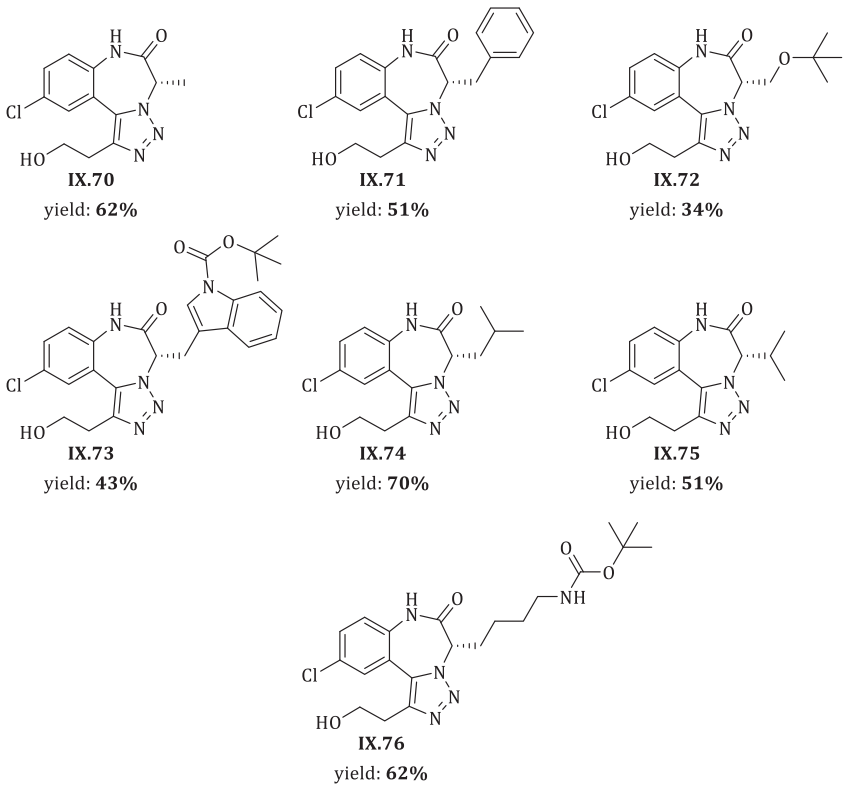

Figure IX-10: Library members IX.70 – IX.76 based on IX.45 as building block

Table IX-15: Library members IX.77 – IX.80 based on IX.46-IX.47, IX.51 and IX.54 as building block

entry	compound	R_1	R_2	R_3	R_4	yield (%)
22	**IX.77**	H	Cl	H	Ph	46
23	**IX.78**	H	Br	H	Ph	49
24	**IX.79**	$CH(CH_3)_2$	OMe	H	$(CH_2)_3CH_3$	40
25	**IX.80**	$CH(CH_3)_2$	H	OMe	$(CH_2)_3CH_3$	67

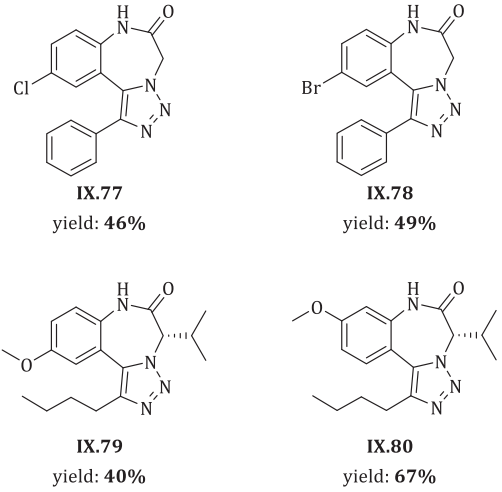

Figure IX-11: Library members IX.77 – IX.80 based on IX.46-IX.47, IX.51 and IX.54 as building block

The tables above (**Table IX-12** - **Table IX-15**), clearly indicate that compounds **IX.56 – IX.80** were synthesized with in moderate to good yields and that 1,4,5-trisubstituted 1,2,3-triazole moieties can be incorporated into our aimed scaffold motif.

REFERENCES

[1] Himo, F.; Lovell, T.; Hilgraf, R.; Rostovtsev, V. V.; Noodleman, L.; Sharpless, K. B.; Fokin, V. V. *J. Am. Chem. Soc.* **2005**, *127*, 210-216.

[2] Zhang, L.; Chen, X.; Xue, P.; Sun, H. H. Y.; Williams, I. D.; Sharpless, K. B.; Fokin, V. V.; Jia, G. *J. Am. Chem. Soc.* **2005**, *127*, 15998-15999.

[3] Boren, B.C.; Narayan, S.; Rasmussen, L. K.; Zhang, L.; Zhao, H.; Lin, Z.; Jia, G.; Fokin, V. V. *J. Am. Chem. Soc.* **2008**, *130*, 8923-8930.

[4] Majireck, M. M.; Weinreb, S. M. *J. Org. Chem.* **2006**, *71*, 8680-8683.

[5] Hou, D.-R.; Kuan, T.-C.; Li, Y.-K.; Lee, R.; Huang, K.-W. *Tetrahedron* **2010**, *66*, 9415-9420.

[6] Chuprakov, S.; Chernyak, N.; Dudnik, A. S.; Gevorgyan, V. *Org. Lett.* **2007**, *9*, 2333-2336. b) Ackermann, L.; Vicente, R. *Org. Lett.* **2009**, *11*, 4922–4925.

[7] Ackermann, L.; Potukuchi, H. K.; Landsberg D.; Vicente R. *Org. Lett.* **2008**, *10*, 3081-3084.

[8] a) Hein, J. E.; Tripp, J. C.; Krasnova, L. B.; Sharpless, K. B.; Fokin, V. V. *Angew. Chem. Int. Ed.* **2009**, *48*, 8018–8021. b) Spiteri, C.; Moses, J. E. *Angew. Chem. Int. Ed.* **2010**, *49*, 31–33. c) Kuijpers, B. H. M.; Dijkmans, G. C. T.; Groothuys, S.; Quaedflieg, P. J. L. M.; Blaauw, R. H.; van Delft, F. L.; Rutjes, F. P. J. T. *Synlett* **2005**, 2059–3062. d) Bogdan, A. R.; James, K. *Org. Lett.* **2011**, *13*, 4060–4063.

[9] Shu, H.; Izenwasser, S.; Wade, D.; Stevens, E. D.; Trudell, M. L. *Bioorg. Med. Chem. Lett.* **2009**, *19*, 891-893.

[10] Krasinski, A.; Fokin, V. V.; Sharpless, K. B. *Org. Lett.* **2004**, *6*, 1237–1240.

[11] a) Niu, T. F., Gu, L., Yi, W. B.; Cai, Ch. *ACS Comb. Sci.* **2012**, *14*, 309–315. b) Pokhodylo, N. T.; Matiychuk, V. S.; Obushak, M. D. *J. Comb. Chem.* **2009**, *11*, 481–485. c) Jin, G.; Zhang, J.; Fu, D.; Wu, J.; Cao. S. *Eur. J. Org. Chem.* **2012**, 5446-5449

[12] a) Wang, L.; Peng, S.; Danence, L. J. T.; Gao, Y.; Wang. J *Chem. Eur. J.* **2012**, *18*, 6088-6093. b) Belkheira, M.; El Abed, D.; Pons, J.-M.; Bressy, C. *Chem. Eur. J.* **2011**, *17*, 12917-12921.

[13] a) McIntosh, M. L.; Johnston, R. C.; Pattawong, O.; Ashburn, B. O.; Naffziger, M. R.; Cheong, P. H.-Y.; Carter, R. H. *J. Org. Chem.* **2012**, *77*, 1101-1112. b) Hou, D.-R.; Alam, S.; Kuan, T.-C.; Ramanathan, M.; Lin, T.-P.; Hung, M.-S. *Bioorg. Med. Chem. Lett.* **2009**, *19*, 1022-1025.

X. Synthesis of [1,2,3]triazolo[1,5-*d*] pyrido[1,4]diazepin-2-ones

A. Introduction

As bioisosteric replacement of ring systems has played a key role in drug design,[1] initial steps towards the introduction of a pyridine moiety over a benzene moiety present in molecule **IX.1** were investigated. The pyridine moiety is seen as a ring equivalent of benzene moiety (see section **III.A**), therefore classifying this diversification as a bioisosteric replacement. Moreover, pyridodiazepines have proven to be an important class of compounds for their versatile use in biological and therapeutic purposes[2], as the introduction of a nitrogen atom in the ring creates an additional hydrogen bond acceptor available for interaction with a receptor. Initially, we chose to investigate the synthesis of pyridodiazepines of type **X.1**.

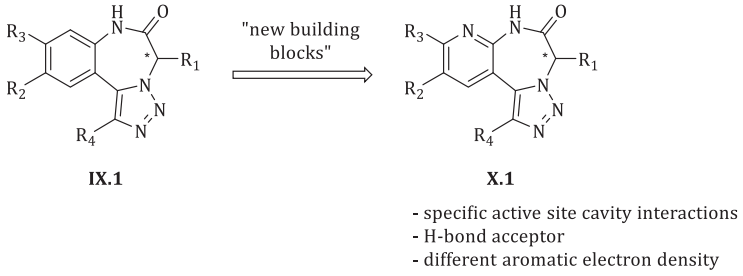

Figure X-1: Bioisosteric replacement of a benzene moiety for a pyridine ring.

B. Building block synthesis

In order to synthesize this [1,2,3]triazolo[1,5-*d*]pyrido[3,2-*f*][1,4]diazepin-2-one (**X.1**) scaffold, new pyridine building blocks **X.6 – X.9** were synthesized starting from commercially available 2-amino-3-iodopyridines **X.2 – X.3** which were subjected to a Sonogashira cross-coupling reaction with TMS-protected acetylene **Scheme X-1** or terminal alkynes **Scheme X-2**.

In the case of trimethylsilylacetylene as alkyne source, a subsequent TMS deprotection step with K_2CO_3 affords the desired terminal alkyne **X.6 – X.7** in good yields.

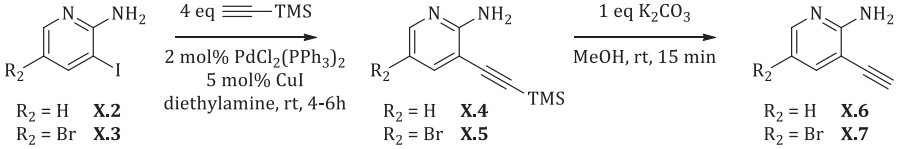

Scheme X–1: Synthesis of 3-ethynyl-2-aminopyridine building blocks.

Table X-1: Results for the synthesis of synthesis of 3-ethynyl-2-aminopyridine building blocks.

entry	compound	R_2	yield (%)
1	**X.4**	H	94
2	**X.5**	Br	90
3	**X.6**	H	76
4	**X.7**	Br	92

If terminal alkynes are used in the Sonogashira reaction, direct formation of the 3-alkynyl-2-aminopyridine **X.8** – **X.9** is achieved with the purpose of obtaining 1,4,5-trisubstituted 1,2,3-triazole moieties.

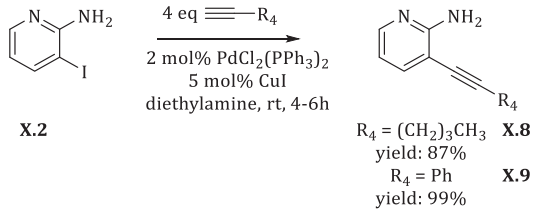

Scheme X–2: Synthesis of 3-alkynyl-2-aminopyridine building blocks X.8 – X.9.

C. Proof of principle library

In order to verify the synthesis strategy for the obtained 3-alkynyl-2-aminopyridine building blocks **X.6** - **X.9**, the latter were used in a proof of principle library synthesis presented in **Scheme X-3.** By varying the α-amino acid from Fmoc-Ser-OH **VI.27**, Fmoc-Leu-OH **VI.30**, Fmoc-Lys-OH **VI.31** and the very sterically hindered Fmoc-Val-OH **VI.29** combined with the alkyne building blocks a small library of five [1,2,3]triazolo[1,5-*d*]pyrido[3,2-*f*][1,4]diazepin-2-ones **X.11 - X.15** were synthesized.

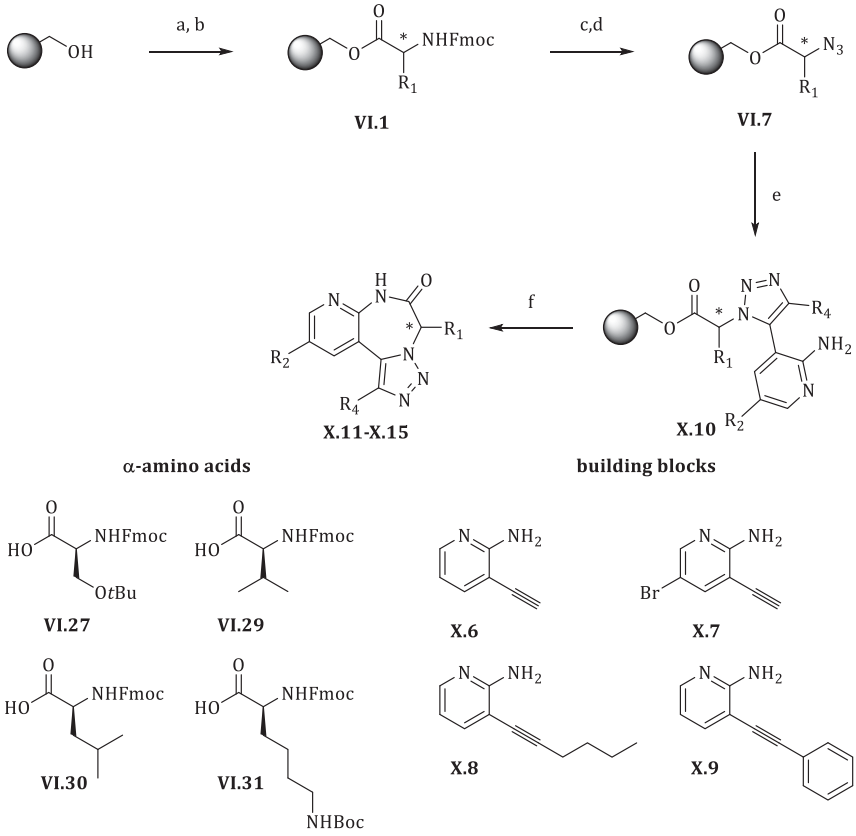

a) 2 eq Fmoc-AA-OH, 2 eq DIC, 0,2 eq DMAP, CH_2Cl_2, rt, 2x 24h b) Ac_2O, CH_2Cl_2, DIPEA (1/1/3) c) 1) 20 v/v% 4-Me-piperidine/DMF, rt, 2x 10 min. d) 1,2 eq imidazole-1-sulfonyl azide hydrochloride, 2 eq TEA, 1 mol% $CuSO_4.5H_2O$, THF/H_2O (1/1), rt, 24h. e) 3 eq **X.6 - X.9**, 10 mol% C_p*$RuCl(PPh_3)_2$, toluene, 60°C, 6h. f) $HOAc/CH_2Cl_2$ (1/1), rt, 24h.

Scheme X–3: Proof of principle library for the synthesis of [1,2,3]triazolo[1,5-d]pyrido[3,2-f][1,4]diazepin-2-ones

In **Table X-2** and **Figure X-2**, the results are presented for the proof of principle library were can be seen that the yields of all library members are substantially lower comparing to their [1,2,3]triazolo[1,5-*d*]benzo[1,4]diazepin-2-one analogues (see section **VIII.D.2**).

Table X-2: Results for the proof of principle library presented in Scheme X-3

entry	compound	R_1	R_2	R_4	yield (%)
1	**X.11**	$CH_2O(tBu)$	H	H	9%
2	**X.12**	$(CH_2)_4NHBoc$	H	H	13%
3	**X.13**	$CH_2CH(CH_3)_2$	Br	H	26%
4	**X.14**	$CH_2CH(CH_3)_2$	H	$(CH_2)_3CH_3$	22%
5	**X.15**	$CH(CH_3)_2$	H	Ph	19%

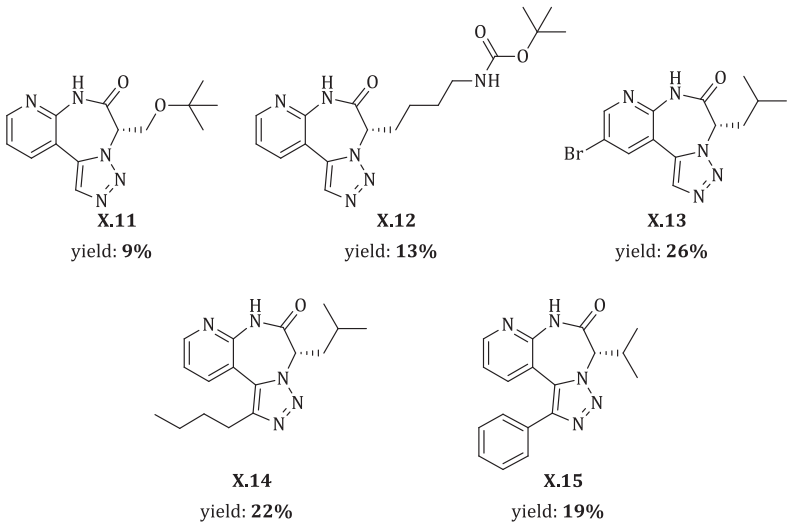

Figure X-2: [1,2,3]triazolo[1,5-*d*]pyrido[3,2-*f*][1,4]diazepin-2-ones (X.1) proof of principle library members

The 'yield determining'-step for the synthesis of these [1,2,3]triazolo[1,5-*d*]pyrido[3,2-*f*][1,4]diazepin-2-ones is the cyclization/release. Although crude purities are within an acceptable range, a subsequent cleavage under standard conditions revealed the presence of open product. From the latter, we can conclude that acid-catalyzed cyclization is tremendously slow comparing to the aniline intermediates, which could be explaned by the protonation of the 2-aminopyridine intermediate **X.16** in acid media (pKa ~ 6.9). Stabilization of the latter leads to the formation of an unreactive derivative, visualized by resonance structure **X.18**.

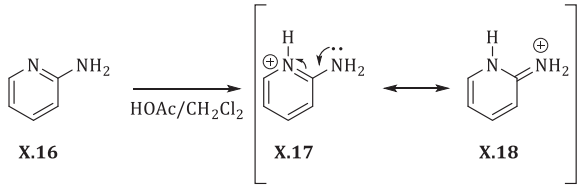

Figure X-3: Stabilization of protonated 2-aminopyridine derivative X.17

In order to avoid this stabilization by electron donation of the amine functionality, future experiments can be performed with isosteric replacements of the aromatic nitrogen. More specifically, 4-alkynyl-3-aminopyridines **X.19** or 2-alkynyl-3-aminopyridines **X.20** (**Figure X-4**) can be used. If 3-alkynyl-4-aminopyridine **X.21** building blocks will be used, stabilization occurs again *via* the *p*-substituted amine.

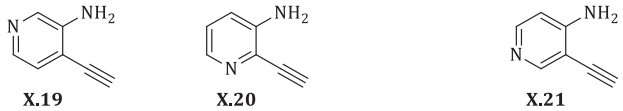

Figure X-4: Alternatives for 2-aminopyridine X.17 aiming an acid-catalyzed cyclization/release strategy

REFERENCES

[1] Ciapetti, P.; Gietlen, B. Molecular Variations Based on Isosteric Replacements. In The practice of Medicinal Chemistry; Wermuth, C. G., Ed.; Elsevier: London, **2008**; pp. 290-334.

[2] a) Goswami, S.; Hazra, A.; Jana, S. *J. Heterocyclic Chem.* **2009**, *46*, 861-865. b) Geng, B.; Basarab, G.; Comita-Prevoir, J.; Gowravaram, M.; Hill, P.; Kiely, A.; Loch, J.; MacPherson, L.; Morningstar, M.; Mullen, G.; Osimboni, E.; Satz, A.; Eyermann, C.; Lundqvist, T. *Bioorg. Med. Chem. Lett.* **2009**, *19*, 930-936. c) Fiakpvi, C. Y.; Phillips, O. A.; Murthy, K. S. K.; Knavs, E. E. *Drug Des. Discovery* **1993**, *10*, 45–55.

XI. *N*-alkylation

A. Introduction

Replacing a hydrogen in a potentially active molecule can have drastic effects on the potency, the duration and even on the nature of the pharmaceutical effect.[1] The amide bond present in the [1,2,3]triazolo[1,5-*d*][1,4]benzodiazepin-2-one scaffold **IX.1** creates an opportunity for further modification. In order to achieve a tertiary amide in the final molecule **V.2**, a monoalkylation needs to be pursued during the synthesis as overalkylated intermediates are unable to undergo cyclization/release in the final step. Initially, two possible pathways for incorporation of a diversity point by replacing one aniline hydrogen are proposed: Mitsunobu-Fukuyama alkylation (section **XI.B**) and reductive alkylation (section **XI.E**).

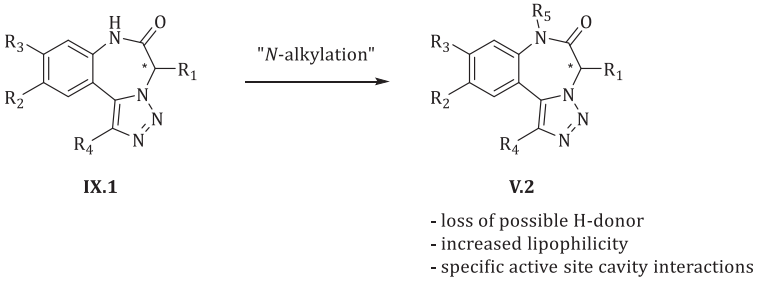

Figure XI-1: *N*-alkylation step

B. First approach: Mitsunobu-Fukuyama alkylation

1. Retrosynthesis

Pathway A (**Scheme XI–1**) represents a Mitsunobu-Fukuyama strategy to synthesize the solid-phase bound fully diversified intermediate **V.4**, bearing a side chain R_5. The final product will be released from the resin *via* the proposed cyclization/release strategy which is performed on intermediate **V.4**. This monoalkylated aniline intermediate **V.4** is achieved after cleavage of a nosyl group (Ns, nitrobenzenesulfonyl) bound onto the anchored monoalkylated aniline **XI.1**. Generally, the nosyl group serves as a protecting group as one aniline hydrogen is temporarily replaced. In the case of a Mitsunobu-Fukuyama alkylation, the nosyl group has a dualistic role and acts additionally as an activating group. The latter is explained by the strong electron withdrawing nature of the nosyl group which promotes the acidic properties of the remaining aniline hydrogen in intermediate **XI.2.** This is illustrated by a pKa decrease of 10 units upon nosyl protection. The pursued Mitsunobu-Fukuyama alkylation step can be done *via* treatment of the solid-phase bound intermediate **XI.2** with alcohols as alkylating agents, PPh_3 and DIAD to afford **XI.1**. The necessary nosyl (Ns) activating group is introduced *via* a sulfonamide bond formation on intermediate **V.5**, the latter being readily synthesized *via* the procedures presented in chapter **VIII.** Thanks to a broad diversity of commercially available alcohols, a wide range of side chains can be incorporated *via* this approach[2].

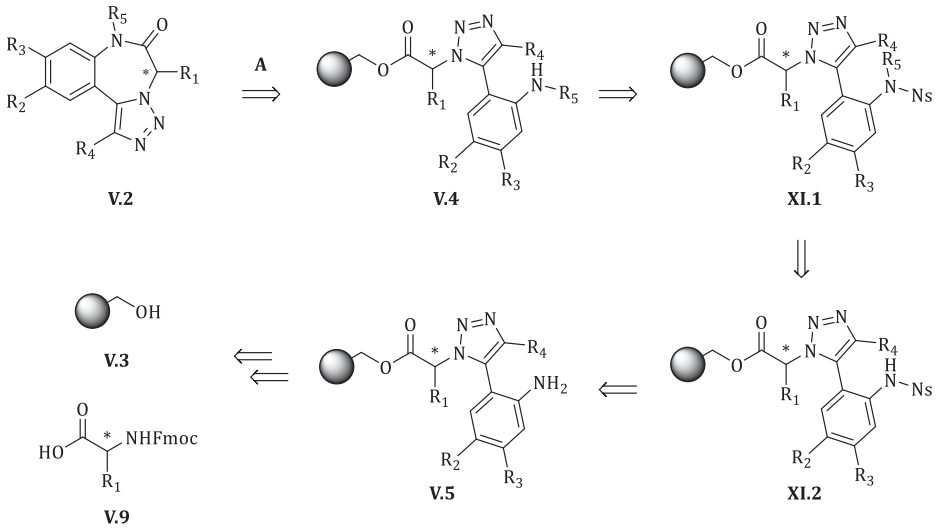

Scheme XI–1: Retrosynthetic approach for the Mitsunobu-Fukuyama alkylation procedure.

2. Nosyl protection

The first step towards *N*-monoalkylation involves the introduction of a Nosyl group onto the solid-phase bound aniline **V.5**. The choice for a nosyl group as protecting/activating group over other related protecting groups (**XI.6**, tosyl group) was made for its mild and orthogonal cleavage method as tosylates require harsh conditions[3] incompatible with Wang resin. In **Figure XI-2**, three possible nosyl derivatives are presented with an alternating nitro substitution pattern resulting in 2-nitrobenzenesulfonylchloride (**XI.3**, *o*-NsCl), 4-nitrobenzenesulfonylchloride (**XI.4**, *p*-NsCl) or 2,4-dinitrobenzenesulfonylchloride (**XI.5**, DNBS-Cl). After *N*-protection, the sulfonamide bond formed is stable and can be cleaved under selective conditions. Moreover, for specific synthetic purposes a DNBS protected amine can be deprotected orthogonally next to a mono-Nosyl-protected amine.[2h]

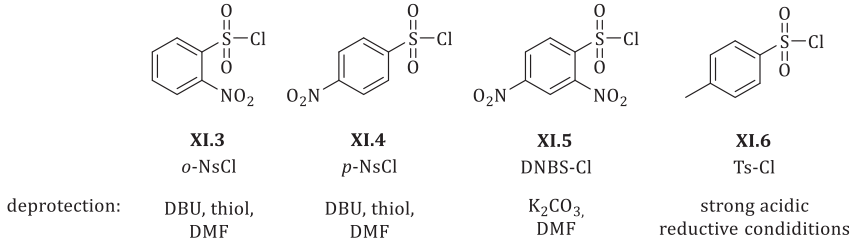

Figure XI-2: Possible nosyl- and tosyl-based protecting group and corresponding standard deprotection methods for tertairy amines.

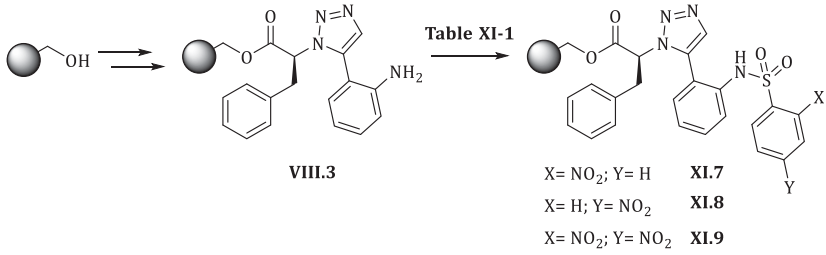

Scheme XI–2: Nosyl protection of VIII.3

The introduction of three nosyl-based protecting groups started by applying general conditions (**Table XI-1**) to intermediate **VIII.3**. More specifically, the solid-phase bound aniline was treated with 5 eq of *o*-NsCl (entry **1**), 5 eq *p*-NsCl (entry **2**) or 5 eq DNBS-Cl (entry **3**) combined with 10 eq of a sterically demanding base (i.e. collidine) in dry dichloromethane for one hour. After an intermediate washing step, these conditions were applied a second time. The reaction was monitored by means of an LC-MS analysis, after treating an aliquot of the reacted beads with TFA/H_2O (95/5).

Table XI-1: Conditions applied in Scheme XI–2

entry	conditions					yield (%)[a]
	reagent	base	solvent	T	reaction time	
1	5 eq *o*-NsCl	10 eq collidine	CH_2Cl_2	rt	2x 1h	<1%
2	5 eq *p*-NsCl	10 eq collidine	CH_2Cl_2	rt	2x 1h	<1%
3	5 eq DNBS-Cl	10 eq collidine	CH_2Cl_2	rt	2x 1h	<1%

[a] Yield determined via LC-MS analysis (214 nm)

Unfortunately, these conditions did not yield the nosyl-protected intermediates (**Scheme XI–2, XI.7-XI.9**). For all three protecting groups, only trace amounts of the Ns-protected aniline were found with a substantial amount of remaining starting material present in the mixture[i]. This lack of reactivity could be explained by the low nucleophilicity of the solid-phase bound aniline. As an answer, DMAP was added to the reaction mixture. This nucleophilic catalyst creates an activated nosyl intermediate which is more susceptible towards nucleophilic attack by the solid-phase bound aniline **VIII.3**. Apart from adding DMAP, equivalents of reagents (*o*-NsCl and base) and temperature were varied in order to find the optimal conditions for nosyl protection. An overview of applied test conditions for exclusively introducing an *o*-Nosyl group is represented in **Table XI-2**.

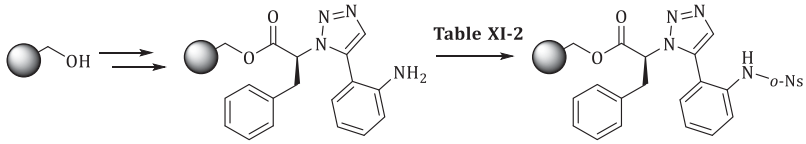

VIII.3 **XI.7**

Scheme XI–3: *o*-Nosyl protection of VIII.3

[i] Due to the acidic cleavage conditions (TFA/H_2O 95/5, 2h, rt), cyclisation/release occurred and the starting material was detected as cyclized product.

Table XI-2: Conditions applied in Scheme XI–3

entry	conditions						yield (%)[a]
	o-NsCl	base	additive	solvent	T	reaction time	
1	2 eq	2 eq pyridine	0.2 eq DMAP	CH_2Cl_2	rt	1h	<1%
2	2 eq	2 eq pyridine	0.2 eq DMAP	DCE	70°C	1h	4
3	5 eq	5 eq pyridine	0.5 eq DMAP	DCE	70°C	1h	10
4	5 eq	10 eq pyridine	0.5 eq DMAP	DCE	rt	5h	8
5	5 eq	10 eq collidine	0.5 eq DMAP	DCE	rt	5h	7
6	10 eq	20 eq pyridine	1 eq DMAP	DCE	rt	5h	20
7	10 eq	20 eq collidine	1 eq DMAP	DCE	rt	5h	10
8	5 eq	10 eq pyridine	0.5 eq DMAP	DCE	70°C	5h	15
9	5 eq	10 eq collidine	0.5 eq DMAP	DCE	70°C	5h	18
10	10 eq	20 eq pyridine	1 eq DMAP	DCE	70°C	5h	44
11	10 eq	20 eq collidine	1 eq DMAP	DCE	70°C	5h	34
12	10 eq	20 eq pyridine	1 eq DMAP	DCE	70°C	2x 5h	61

[a] Yield determined via LC-MS analysis (214 nm)

As can be seen for entries **1** - **3** (**Table XI-2**), adding catalytic amount of DMAP does not afford a straightforward and complete conversion into the desired intermediate **XI.7**. A further increase (entries **7** – **14**, **Table XI-2**) of the amount of reagents and elevated temperatures are required to achieve an acceptable ratio of the desired intermediate **XI.7**. Generally, it can be seen that as more equivalents of *o*-NsCl are used, a higher conversion is achieved. The protection proceeds better at elevated temperatures and the use of pyridine over collidine is preferred. Overall, entry **10** gave the most promising result with a yield of 44% into the desired nosylated aniline intermediate **XI.7**, while 21% of **VIII.3** was recovered. Entry **12** represents a repeated treatment of solid-phase bound aniline **VIII.3** under the conditions found in entry **10**, resulting in a yield of 61% of nosylated compound **XI.7**. HPLC-MS analysis proved that the protection step was complete, as only traces of **VIII.3** were detected.

Taken into account the side product formation, the conditions found in entry **12** give rise to a complete protection of the aniline. Still, these conditions demand a high excess of reagents therefore questioning the atom efficiency of this reaction.

An alternative strategy to introduce the required nosyl protecting and activating group onto the solid-phase will be discussed in section **XI.C**.

3. Mitsunobu-Fukuyama alkylation

The actual alkylation step proceeds *via* conditions provided by Fukuyama, who modified the initial Mitsunobu procedure for alcohol inversion[4]. This technique ensures monoalkylation of the activated (i.e. nosylated) amine/aniline and has been extensively used for the synthesis of polyamines.[2] Addition of an alcohol, diisopropyl azodicarboxylate (DIAD) and triphenylphosphine (PPh_3) to the protected substrate affords alkylation *via* a mechanism presented in **Scheme XI–4**.

a) Mechanism

After an attack of PPh_3 to DIAD (**XI.10**), the protected amine **XI.11** can be deprotonated to give rise to **XI.12** and intermediate **XI.13**. An attack of the alcohol onto the positively charged phosphorous atom results in the formation of a reactive alkoxyphosphonium intermediate **XI.15** and a hydrazine byproduct **XI.16**. The deprotonated **XI.12** attacks intermediate **XI.15** in an S_N2-like fashion[ii] forming the desired *N*-alkylated product **XI.17** and triphenylphosphine oxide as a byproduct. Thanks to the advantages of solid-phase chemistry, byproducts **XI.16** and triphenylphosphine oxide can be removed easily and the reaction can be monitored and repeated until completion.

[ii] Due to this S_N2-like attack, there is a restriction related to the bulkiness of added alcohols. Preferably, primary alcohols are used.

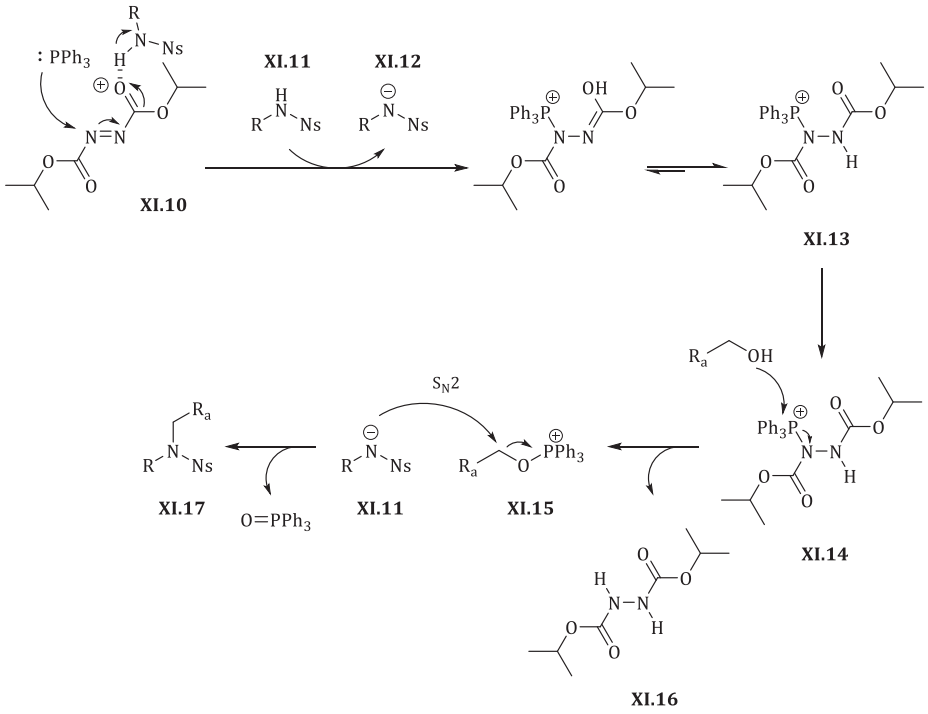

Scheme XI–4: Mitsunobu-Fukuyama *N*-alkylation mechanism

b) Test cases

After retaining the optimal conditions for aniline protection with *o*-NsCl (entry **12**, **Table XI-2**), this Mitsunobu-Fukuyama alkylation is tested in the proposed solid-phase synthesis strategy. Upon addition of 10 equivalents of three alcohols (MeOH, EtOH and iPrOH), 5 equivalents of triphenylphosphine and 5 equivalents of diisopropyl azodicarboxylate to intermediate **XI.7 (Scheme XI-5)**, the reaction proceeds for two hours at room temperature in dry dichloroethane. After applying intermediate washing procedures, this reaction is repeated twice. In **Table XI-3** and **Figure XI-3** the cumulative conversion of the *N*-alkylated intermediate **XI.18 – XI.20** relative to intermediate **XI.7** is presented.

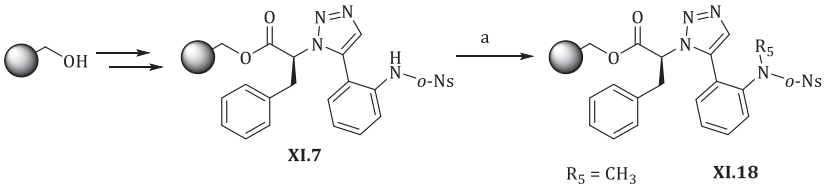

a) 10 eq R_5OH, 5 eq DIAD, 5 eq PPh_3, DCE, rt, 3x 2h.

Scheme XI–5: Mitsunobu-Fukuyama *N*-alkylation

Table XI-3: Obtained conversion after repetitive Mitsunobu-Fukuyama alkylation

entry	ROH	Crude yield[a] (%) after alkylation cycles (#)		
		1	2	3
1	MeOH	67	81	89
2	EtOH	48	69	80
3	iPrOH	29	40	49

[a] Crude yield determined via LC-MS analysis (214 nm)

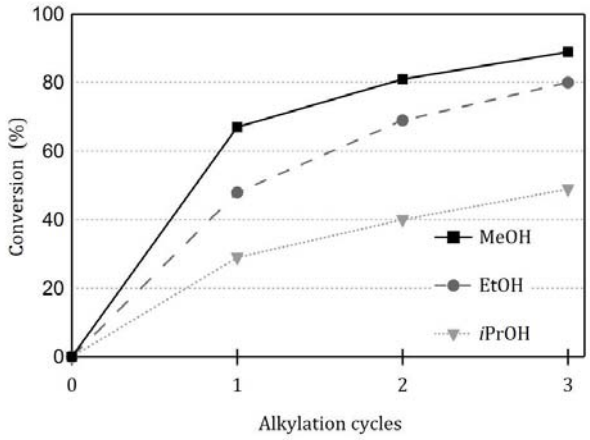

Figure XI-3: Progress of the Mitsunobu-Fukuyama alkylation for each alkylation cycle.

Figure XI-3 illustrates nicely, that for entries **1** and **2** using respectively MeOH and EtOH, the alkylation proceeds smoothly yet a fourth iteration would be advisable. For the secondary alcohol (iPrOH, entry **3**), the alkylation step is, as expected, not completed after three treatments due to the arduous S_N2-step. Further repetitions or other trialkylphosphine

additives are advisable to complete the alkylation procedure for secondary alcohol alkylating reagents[2e].

4. Nosyl cleavage

In order to liberate the secondary aniline intermediate **XI.24**, the nosyl protecting group needs to be removed. Thanks to the strong electron withdrawing capacity of the nitro group on the aromatic moiety, this can be done *via* a nucleophilic aromatic substitution with thiolates[2b] (e.g. *in situ* deprotonated β-mercaptoethanol[5] **XI.22**, thiophenol[2i] or 2-mercaptoacetic acid[6]). Deprotonation is performed with DBU or carbonates, whereas DBU has proven to accelerate the reaction compared to carbonate.

a) Mechanism

The mechanism for this deprotection is shown in **Scheme XI–6** where can be seen that thiolate attack at the *ipso*-position of the aromatic ring of **XI.21** leads to an intermediate stabilized Meisenheimer complex **XI.23**. Re-establishment of the aromatic moiety furnishes the desired secondary amine **XI.24**, gaseous SO_2 and a nitrophenyl thioether as cleavage product which can be removed easily *via* the designated washing procedure.

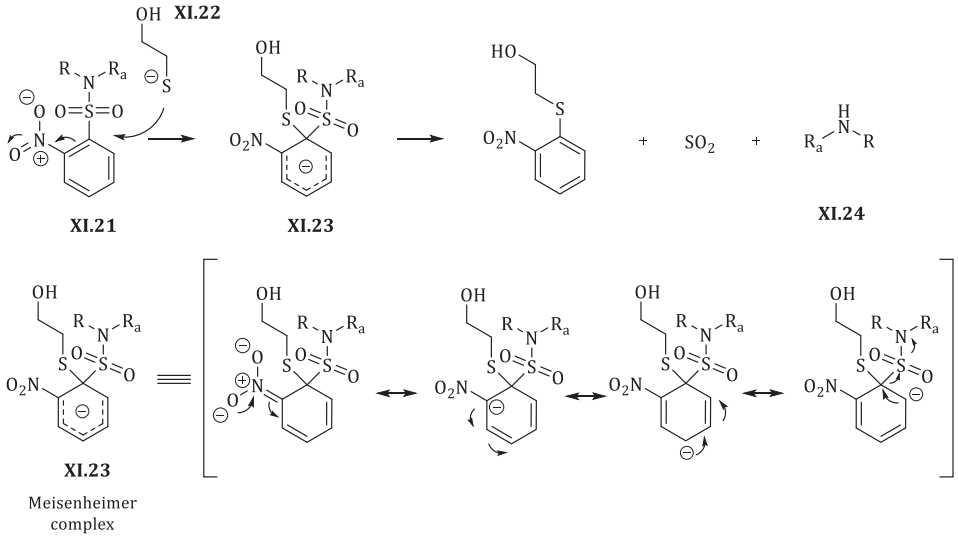

Scheme XI–6: Nosyl deprotection mechanism

b) Test cases

Scheme XI–7 shows the reaction of the nosyl deprotection for intermediates **XI.18** - **XI.20** upon addition of 2.5 equivalents of β-mercaptoethanol and 5 equivalents DBU in DMF, applied twice for 30 minutes. LC-MS analysis showed quantitative conversion of all compounds under these conditions.

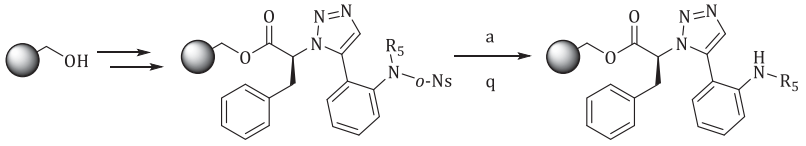

$R_5 = CH_3$	**XI.18**	$R_5 = CH_3$	**XI.25**
$R_5 = CH_2CH_3$	**XI.19**	$R_5 = CH_2CH_3$	**XI.26**
$R_5 = CH(CH_3)_2$	**XI.20**	$R_5 = CH(CH_3)_2$	**XI.27**

a) 2.5 eq DBU, 5 eq β-mercaptoethanol, DMF, rt, 2x 30min.

Scheme XI–7: Nosyl deprotection

5. Cyclization/release with secondary amines: a test case

The next step in the synthesis towards *N*-alkylated [1,2,3]triazolo[1,5-*d*]benzo[1,4]diazepin-2-ones **V.2** involves the optimization of the aimed cyclization/release strategy. Although the Mitsunobu-Fukuyama alkylation did not lead to a complete conversion of the aniline into the monoalkylated product (see section **XI.B.3**, 89% for methyl **XI.18**, 80% for ethyl **XI.19** and 49% for isopropyl **XI.20**), the decision was made to continue despite this incomplete conversion. In fact, the latter deficiency can give an idea on the feasibility of the cyclization/release of intermediates **XI.25** – **XI.27** compared to the already established reaction with non alkylated primary anilines (intermediate **VIII.3**).

In a first stage, 'standard' and optimized conditions (see section **VIII.B.2**) were applied in order to obtain an initial idea on the cyclization/release possibilities for *N*-monoalkylated intermediates **XI.25 – XI.27**.

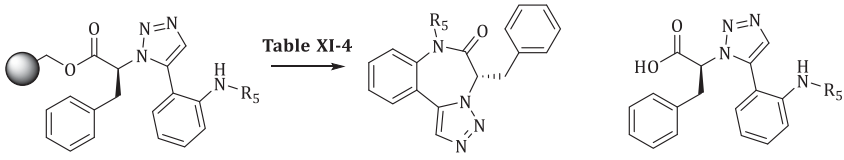

$R_5 = H$	**VIII.3**	$R_5 = H$	**VIII.7**	$R_5 = H$	**VIII.5**
$R_5 = CH_3$	**XI.25**	$R_5 = CH_3$	**XI.28**	$R_5 = CH_3$	**XI.31**
$R_5 = CH_2CH_3$	**XI.26**	$R_5 = CH_2CH_3$	**XI.29**	$R_5 = CH_2CH_3$	**XI.32**
$R_5 = CH(CH_3)_2$	**XI.27**	$R_5 = CH(CH_3)_2$	**XI.30**	$R_5 = CH(CH_3)_2$	**XI.33**

Scheme XI–8: Cyclization/release of *N*-alkylated secundary amines

Table XI-4: Conditions applied in Scheme XI–8

entry	compound	conditions	result (%)[a]
1	**XI.28**	TFA/H_2O (95/5), rt, 2h	open product **XI.31** + trace **XI.28**
2	**XI.29**	TFA/H_2O (95/5), rt, 2h	open product **XI.32** + trace **XI.29**
3	**XI.30**	TFA/H_2O (95/5), rt, 2h	open product **XI.33** + trace **XI.30**
4	**XI.28**	HOAc/CH_2Cl_2 (1/1), rt, 24h	<5% **XI.28**
5	**XI.29**	HOAc/CH_2Cl_2 (1/1), rt, 24h	<5% **XI.29**
6	**XI.30**	HOAc/CH_2Cl_2 (1/1), rt, 24h	<5% **XI.30**

[a] Crude yield determined via LC-MS analysis (214 nm)

As can be seen from **Table XI-4**, entries **1** - **3** represent the standard cleavage conditions for Wang based solid-phase synthesis (TFA/H_2O 95/5). For these entries, almost no cyclization/release occurs, and the open product is isolated **XI.31-XI.33** hence failing in the seven-membered ring formation. This is in contrast with non-alkylated intermediate **VIII.3**, in which case TFA/H2O (95/5) gave only cyclized product (**VIII.7**, see section **VIII.A**). Entries **4** - **6** show the application of the optimal conditions (HOAc/CH_2Cl_2 1/1) for non-alkylated substrates determined in section **VIII.B.2**, resulting in a very low conversion into the desired cyclized product. Hence, although ring closure seems to be possible, sterical hindrance renders the attack of the secondary aniline more difficult, therefore disabling the cyclization.

A new optimization procedure needs to be developed (*vide infra*, see section **XI.E.4**). Furthermore, as it is expected that harsher (acidic) conditions will be necessary to promote the cyclization/release step, another resin will be used in order to maintain orthogonality with the standard cleavage strategy for the chosen linker. The latter will be discussed in section **XI.F.**

C. Mitsunobu-Fukuyama: Second strategy

As the optimized conditions for nosyl protection fail in atom efficiency (2x 10 eq *o*-NsCl, 2x 20 eq pyridine and 2x 1 eq DMAP) and involve an excess of base which could lead to racemization of the used solid-phase bound α-amino acid, an alternative approach for this procedure might be expedient. A strategy including the nosyl group introduction in solution-phase is explored, therefore creating an *N*-(2-ethynylphenyl)-2-nitrobenzenesulfonamide (**XI.34**) which can be used in the RuAAC affording **VIII.3**. The synthesis of building block **XI.34** is presented in **Scheme XI–9**.

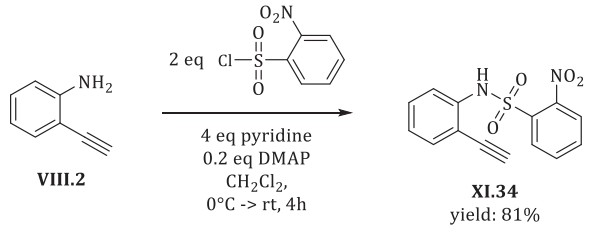

Scheme XI–9: Synthesis of XI.34

After subjecting the 2-ethynylaniline **VIII.2** to the conditions presented in **Scheme XI–9**, the nosyl bearing building block **XI.34** is synthesized in good yield (81%). Afterwards, **XI.34** can be introduced onto the solid-phase *via* the Ru(II)-promoted 1,3-dipolar cycloaddition (**Scheme XI–10**).

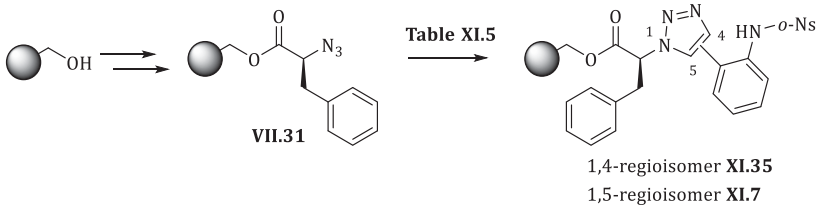

Scheme XI–10: Introducing *o*-Ns group on solid-phase *via* RuAAC

Table XI-5: Conditions applied in Scheme XI–10

entry	conditions					result[a]
	XI.37	catalyst	solvent	T	reaction time	
1	5 eq	0.1 eq $C_p^*RuCl(PPh_3)_2$	toluene	60°C	3h	A
2	5 eq	0.1 eq $C_p^*RuCl(PPh_3)_2$	toluene	60°C	14h	A
3	5 eq	0.1 eq $C_p^*RuCl(COD)$	toluene	rt	3h	A
4	5 eq	0.1 eq $C_p^*RuCl(COD)$	toluene	rt	14h	A

[a] Analysis performed via LC-MS analysis (214 nm)

A: complex mixture: azide **VII.31**, cycloaddition products **XI.7** and **XI.35**

For this reaction, four conditions were tested by varying catalyst, temperature and reaction time (**Table XI-5**). Entry **1** yields a complex mixture including untreated azide **VII.31**, both 1,4- (**XI.35**) and 1,5-cycloaddition (**XI.7**) products and undefinable side-products. An explanation for the formation of both regioisomers could be found in the low electron density of the alkyne of the sulfonamide-diversified building block, therefore interfering with the proposed catalytic cycle. Moreover, at elevated temperatures, the thermal 1,3-dipolar Huisgen

cycloaddition enables the formation of both regioisomers, therefore counteracting the desired regioselectivity. In entry **2**, a prolonged reaction time did not effectively yield the 1,5-cycloadduct **XI.7**.

In order to avoid formation of both regioisomers, another catalyst was used in entry **3** and **4** (i.c. $C_p^*RuCl(COD)$) This catalyst has a higher reactivity/lower stability at room temperature compared to $C_p^*RuCl(PPh_3)_2$ (see section **VIII.A**), therefore enabling reaction at room temperature. Despite these efforts, LC-MS analysis showed a high degree of complexity, as azide **VII.31** and, to a lower extent, both regioisomers were present.

Taking into account the extra protection step in solution, the low conversion of the RuAAC and the complexity of the reaction mixtures, the decision was taken not to continue with this strategy.

D. Mitsunobu-Fukuyama approach: Preliminary conclusion

First, the introduction of the required nosyl-activating group was problematic; a maximum conversion into the desired nosylated intermediate of 61% was achieved. The latter considered too low for incorporation of a temporary activating group. Moreover, the atom efficiency of this protecting step was poor. Therefore, a solution-phase protection strategy was used but the latter failed in regioselectivity during the RuAAC.

The alkylation step and subsequent removal of the nosyl protecting group proceed smoothly, yet the maximum conversion of non-alkylated aniline is determined by the introduction of the nosyl group (61%). Therefore, an alternative strategy for alkylation will be employed in order to increase the conversion and atom efficiency of the reaction.

E. Second approach: Reductive alkylation

1. Retrosynthesis

Pathway B (**Scheme XI–11**) represents the synthesis strategy for *N*-monoalkylation *via* a reductive alkylation procedure[7]. The proposed monoalkylated intermediate **XI.36** is synthesized *via* an *in situ* reduction of an imine **XI.37** formed upon addition of an aldehyde to the solid-phase bound aniline **V.5**. A broad diversity of commercially available aldehydes could enable a fast and straightforward synthesis of a library of *N*-alkylated intermediates **XI.36**. A possible drawback of this reaction includes overalkylation which is known to occur for non-sterically hindered amines.

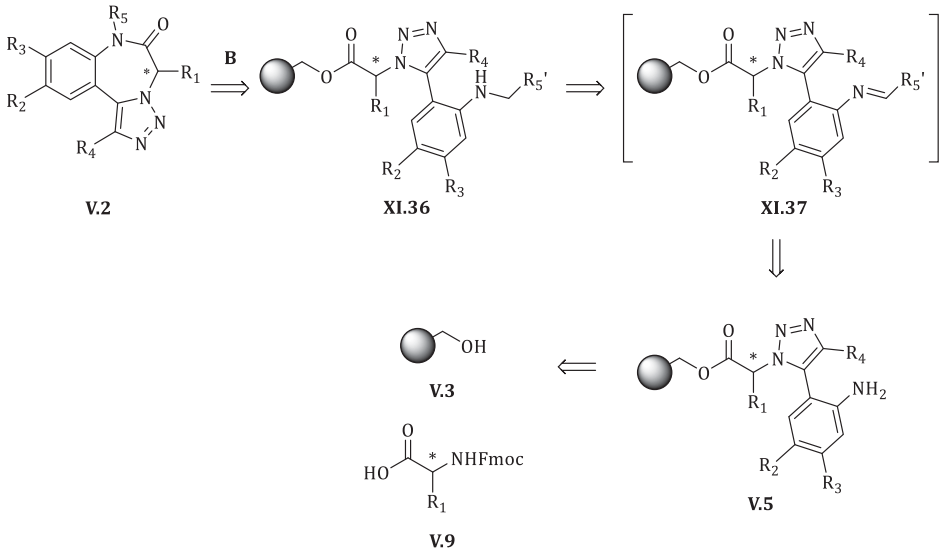

Scheme XI–11: Retrosynthetic approach for the reductive alkylation procedure.

2. Test case: Reductive alkylation with benzaldehyde

The first step towards the reductive alkylation strategy encompasses preliminary and explorative experiments with benzaldehyde. For the *in situ* reduction of the imine, the choice was made for $NaBH(OAc)_3$, as this reagent has proven to be a mild, selective, convenient and superior reducing agent for reductive alkylations tolerating a wide variety of substrates[8,9].

Another possible and popular reducing agent is $NaBH_3CN$[10]. Besides many publications describing successful use of this reagent in the field of reductive alkylations, also some limitations are reported, such as are the requirement to use a large excess of reagent, the sluggish reaction in combination with aromatic ketones (not in scope for this work) and with weakly basic amines, and at last the possibility of contamination of the product with cyanide.[8] Moreover, this reagent is highly toxic and may form HCN and NaCN if an improvident procedure is applied during workup. Taken into account the above argumentation, our decision to use $NaBH(OAc)_3$ as reducing agent seems justified.

Initial test reactions where performed with varying equivalents of benzaldehyde and sodium triacetoxyborohydride in dry dichloroethane for 18h at room temperature (**Scheme XI–12**). The different reaction conditions and corresponding conversions into the monoalkylated intermediate **XI.38** are presented in **Table XI-6**.

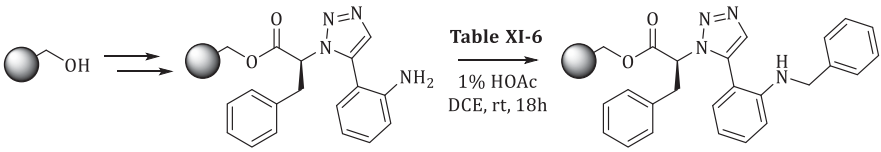

VIII.3 **XI.38**

Scheme XI–12: Reductive alkylation with benzaldehyde

Table XI-6: Conditions applied in Scheme XI–12

entry	conditions		XI.38 (%)[a]
	benzaldehyde	$NaBH(OAc)_3$	
1	3 eq	2 eq	72
2	6 eq	2 eq	67
3	10 eq	2 eq	56
4	3 eq	4 eq	96
5	6 eq	4 eq	92
6	10 eq	4 eq	89
7	3 eq	6 eq	95
8	6 eq	6 eq	95
9	10 eq	6 eq	92

[a] Crude yield determined via LC-MS analysis (214 nm)

From **Table XI-6**, it can be seen that as the equivalents of aldehyde increase (entries **1**-**3**, **4**-**6** and **7**-**9**), the yield of the desired monoalkylated intermediate **XI.38** decreases. This is related to the increasing formation of overalkylated product, as monoalkylation promotes the nucleophilicity of the aniline, which in the presence of an excess of benzaldehyde leads to overalkylation. Comparing entries with identical equivalents of the aldehyde but increasing equivalents of the reducing agent (e.g. entries **1**, **4**, **7**; entries **2**, **5**, **8** and entries **3**, **6**, **9**), the conversion towards monoalkylation **XI.38** increases. Overall, it can be seen that the optimal conditions were found for 3 equivalents benzaldehyde, 4 equivalents $NaBH(OAc)_3$ to obtain 96% conversion into the desired monoalkylated intermediate **XI.38** (entry **4**) without any trace of overalkylation. During this optimization procedure, an earlier observation (section **XI.B.5**) related to the problematic cyclization/release of intermediate **XI.38** was reaffirmed, as cleavage with TFA/H_2O (95/5) yielded to a major extent the open product. A more detailed study on this cyclization will be provided in section **XI.E.4.**

3. Scope of the reductive alkylation

As mentioned earlier, a drawback of this reductive alkylation is the risk for overalkylation. In order to verify if the reductive alkylation as such and the specific conditions determined in previous section are sufficient for a general use as an alkylation strategy, a series of commercially available aldehydes were tested under the conditions from section **XI.E.2**.

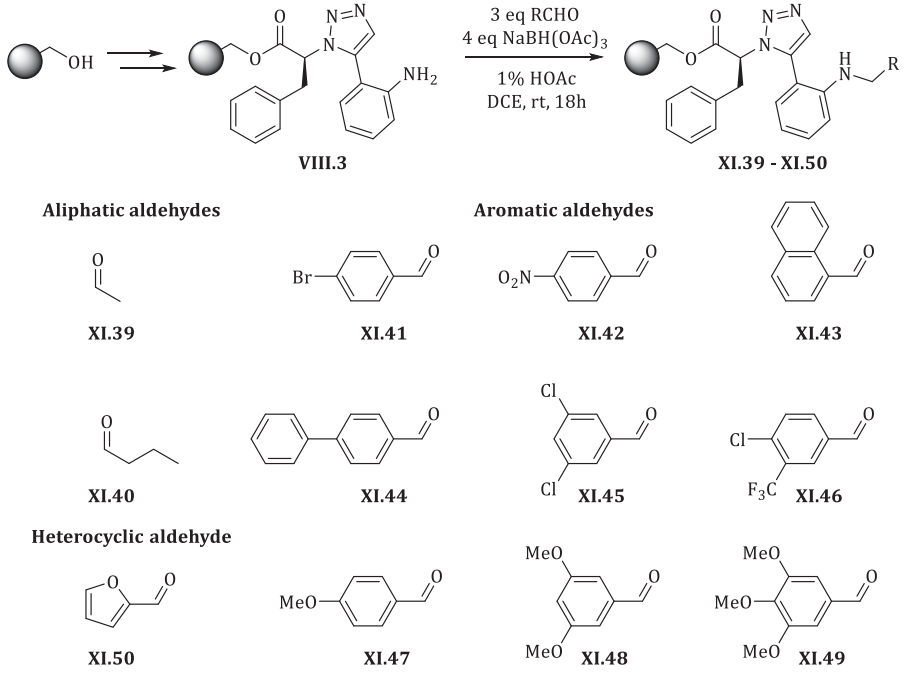

Scheme XI–13: Scope of the reductive alkylation

As can be seen in **Scheme XI–13**, three types of aldehydes were subjected to the conditions found in section **§XI.E.2**, aliphatic aldehydes (**XI.39** - **XI.40**), arylaldehydes (**XI.41** – **XI.49**) and a heteroaromatic aldehyde (**XI.50**). More specifically, electron-rich and electron-poor arylaldehydes were used.

For aliphatic aldehydes, as anticipated, respectively complete and partial overalkylation was found for **XI.39** and **XI.40**. Further optimization is necessary in order to introduce small aliphatic side chains.

The reductive alkylation with arylaldehydes (**XI.41** - **XI.46**) proceeds smoothly with acceptable yields to the monoalkylated products (> 90%). For electron-rich derivatives (**XI.47** - **XI.49**), an incomplete conversion was found and unreacted starting material remained present. Finally, the heteroaromatic building block (**XI.50**), did not react.

As aliphatic aldehydes give rise to overalkylation, an extended optimization procedure is necessary. In order to find the optimal conditions to introduce a small alkyl chain using the reductive alkylation strategy, acetaldehyde was used as a test case. By reducing the amounts of reagent, in combination with shorter reaction times, several experiments were set up (**Scheme XI–14**).

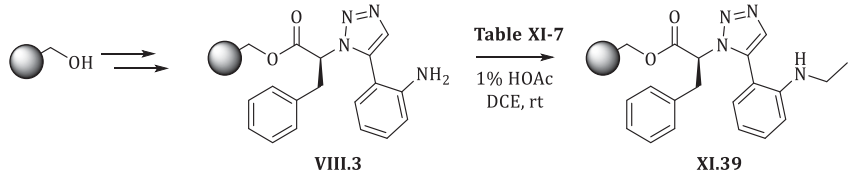

VIII.3 XI.39

Scheme XI–14: Reductive alkylation - acetaldehyde

Table XI-7: Conditions applied in Scheme XI–14

entry	conditions			XI.39 (%)[a]
	acetaldehyde	$NaBH(OAc)_3$	reaction time	
1	3 eq	4 eq	18h	1
2	1 eq	1.25 eq	1h	4
3	1 eq	1.25 eq	2h	10
4	1 eq	1.25 eq	3h	17
5	1 eq	1 eq	3h	18
6	1 eq	1 eq	6h	36
7	1 eq	1 eq	8h	51
8	1 eq	1 eq	2x 8h	43

[a] Crude yield determined via LC-MS analysis (214 nm)

In **Table XI-7**, the results of the test reactions for monoalkylation are presented. Due to the unhindered nature of acetaldehyde, there is a high tendency for overalkylation. The maximum yield of monoalkylated intermediate **XI.39** was achieved upon using 1 eq acetaldehyde and 1 eq of $NaBH(OAc)_3$ for 8h, yielding 51% of the desired intermediate **XI.39** (entry **7**).

4. Test case: Cyclization/release of *N*-benzylated precursors

In section **XI.E.2**, the reductive alkylation with benzaldehyde was optimized. By using 3 equivalents of benzaldehyde and 4 equivalents of $NaBH(OAc)_3$ a conversion of 96% into the monoalkylated intermediate **XI.38**, was achieved. As no or minimal cyclization/release

occurred during the standard TFA/H_2O (95/5) cleavage, further experiments performed in order to increase the amount of cyclized compound **XI.51,** while minimizing the amount of uncyclized precursor **XI.52** (**Scheme XI–15**).

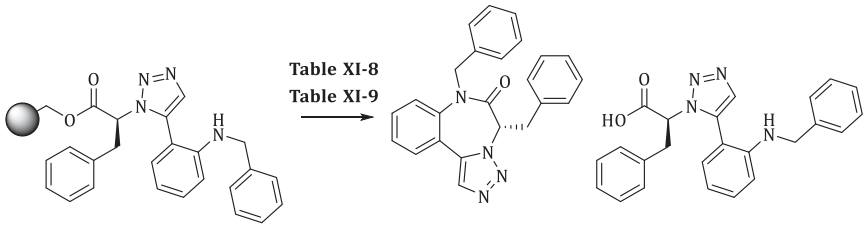

Scheme XI–15: Cyclization/release test reaction for XI.38

Table XI-8: Cyclization/release test reaction for XI.38 - Conventional heating

entry	conditions	crude purity of XI.51 (%)[a]	remarks
1	TFA/H_2O (1/1), rt, 2h	18%	**XI.51** + open product **XI.52**
2	TFA/H_2O (1/99), rt, 2h	43%	**XI.51** + open product **XI.52**
3	TFA/CH_2Cl_2 (1/1), rt, 15 min	5%	**XI.51** + open product **XI.52**
4	TFA/CH_2Cl_2 (1/1), 60°C, 15 min	6%	**XI.51** + open product **XI.52**
5	TFA/DCE (1/1), rt, 15 min	<1%	open product **XI.52**
6	TFA/DCE (1/1), 60°C, 15 min	3%	**XI.51** + open product **XI.52**
7	TFA/DCE (1/99), rt, 24h	31%	**XI.51** + open product **XI.52**
8	TFA/DCE (1/99), 60°C, 24h	38%	**XI.51** + open product **XI.52**
9	HOAc/CH_2Cl_2 (1/1), rt, 24h	57%	**XI.51**
10	HOAc/DCE (1/1), rt, 24h	67%	**XI.51**
11	HOAc/DCE (1/1), 60°C, 72h	72%	**XI.51**
12	1M KOtBu, THF, rt, 24h	<1%	no desired reaction
13	1M KOtBu, THF, 60°C, 24h	<1%	no desired reaction

[a] Crude purity determined via LC-MS analysis (214 nm)

In **Table XI-8**, the results are presented for different cyclization/release test conditions. Generally, it can be seen that applying different ratios of trifluoroacetic acid (entries **1** - **8**) yield a mixture of intermediate **XI.52** and cyclized product **XI.51**. By applying a weaker acid, acetic acid (entries **9** - **11**), open product release is avoided and hence only cyclized product **XI.51** is detected, apart from side products. Entry **11**, with an increased cleavage temperature

of 60°C, shows a selective formation of the desired compound **XI.51** with a crude purity of 72%.

Apart from acid-catalyzed ring formation, base-promoted cyclization was tested by adding potassium tert-butoxide in THF (1M) (entries **12** - **13**). Unfortunately, no desired cyclization occurred after applying these conditions.

As entry **11** shows the selective formation of the seven-membered ring after applying HOAc/DCE (1/1) at 60°C for 72 h, microwave heating was tested in order to reduce the time for this cyclization/release step. In order to toggle the possible microwave effect, experiments were done with and without "power max"[iii].

Table XI-9: Cyclization/release test reaction for XI.38 - Microwave heating

entry	conditions	crude purity of XI.51 (%)[a]	remarks
1	HOAc/DCE (1/1), 60°C, 15 min, power max off	52%	**XI.51**
2	HOAc/DCE (1/1), 60°C, 15 min, power max on	46%	**XI.51**
3	HOAc/DCE (1/1), 60°C, 1h, power max on	53%	**XI.51**

[a] Crude purity determined via LC-MS analysis (214 nm)

As can be seen in **Table XI-9**, microwave heating does not improve nor drastically affect the desired selectivity of the applied cyclization/release strategy. Entries **1** - **3** show a moderate crude purity, in an acceptable time scale without releasing the open form intermediate **XI.51**. Unfortunately, due to the limited apparatus capacity, this technique cannot be used for library synthesis as it does not allow large scale reaction nor automation. Therefore, further library synthesis will be performed with conventional heating.

5. Test case: Cyclization/release of ethylated compounds

Taken into account the insights provided in previous section and the limited amounts of intermediate **XI.39,** only three test reactions were performed to examine the effectiveness of the cyclization/release conditions found in section **XI.E.4** (**Scheme XI–16).**

[iii] After applying a fixed set temperature, the reaction vessel is continuously and deliberately cooled by passing air or nitrogen along the reaction vessel. As the microwave apparatus wants to reach the set point, applying microwave energy for a longer time is required to attain the set temperature. Eventually, this 'extended' microwave power can be absorbed by the reaction vessel content.

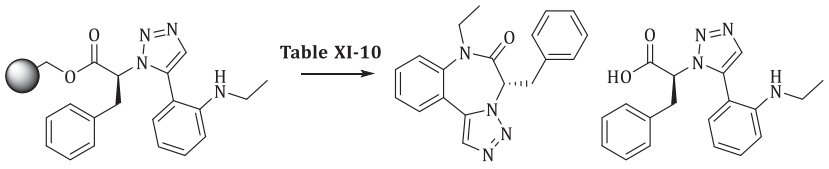

Scheme XI–16: Cyclization/release test reaction for XI.39

Table XI-10: Cyclization/release test reaction for XI.39 – Conventional heating

entry	conditions	crude purity of XI.53 (%)[a]	remarks
1	TFA/H_2O (1/1), rt, 2u	20%	**XI.53 +** open product **XI.54**
2	HOAc/DCE (1/1), rt, 72h	1%	**XI.53**
3	HOAc/DCE (1/1), 60°C, 72h	48%	**XI.53**

[a] Crude purity determined via HPLC-MS analysis (214 nm)

As can be seen from **Table XI-10**, test reactions with acetic acid in dichloroethane at elevated temperatures allow selective formation of the cyclized product in 48% crude purity without concomitant cleavage of precursor **XI.54**, next to the presence of side products.

6. Proof of principle library

A small (2x2) proof of principle library was synthesized, in order to verify the optimized conditions for large scale reactions. Two amino acids were chosen, Fmoc-Gly-OH (**VI.25**) and Fmoc-Phe-OH (**VI.28**). As side chain source, acetaldehyde and benzaldehyde had to be taken, as the conditions optimized in previous section only account for these substrates. The cyclization/release strategy, was performed with HOAc/DCE (1/1) for 72 h at 60°C. The full reaction sequence is presented in **Scheme XI–17**. The results for this initial library are illustrated in **Table XI-11** and **Figure XI-4**. It can be seen that the method provided by the reductive alkylation and the subsequent cyclization/release yields very low amounts of the desired compounds. Subsequent treatment of the beads with TFA/H_2O (95/5) showed that final product is still present on the beads therefore accounting for an ineffective cyclization/release.

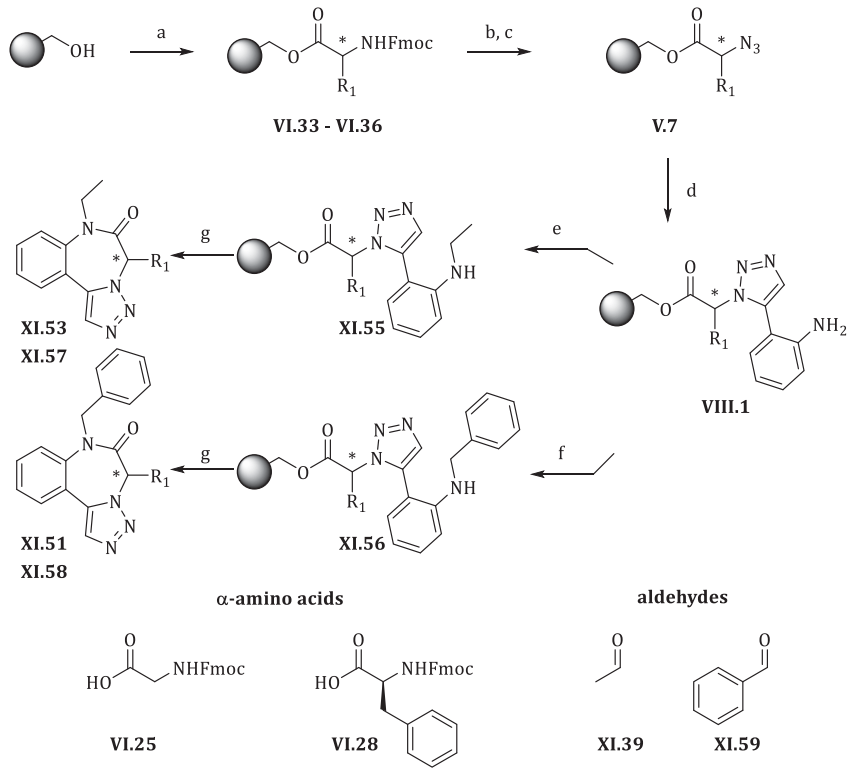

a) 1) 2 eq Fmoc-AA-OH, 2 eq DIC, 0,2 eq DMAP, CH_2Cl_2, rt, 2x 24h 2) Ac_2O, CH_2Cl_2, DIPEA (1/1/3) b) 20 v/v% 4-Me-piperidine/DMF, rt, 2x 10 min. c) 1,2 eq imidazole-1-sulfonyl azide hydrochloride, 2 eq TEA, 1 mol% $CuSO_4.5H_2O$, THF/H_2O (1/1), rt, 24h. d) 3 eq 2-ethynylaniline, 10 mol% C_p*$RuCl(PPh_3)_2$, toluene, 60°C, 6h. e) 1 eq acetaldehyde, 1 eq $NaBH(OAc)_3$, 1% HOAc, DCE, rt, 8h. f) 3 eq benzaldehyde, 4 eq $NaBH(OAc)_3$, 1% HOAc, DCE, rt, 18h. g) HOAc/DCE (1/1), 60°C, 72h.

Scheme XI–17: Synthesis scheme for solid-phase reductive alkylation

Table XI-11: Results for the proof of principle library presented in Scheme XI-17

entry	compound	R_1	R_5	isolated yield (%)
1	**XI.51**	CH_2Ph	CH_2Ph	1
2	**XI.53**	CH_2Ph	CH_2CH_3	1
3	**XI.57**	H	CH_2CH_3	16
4	**XI.58**	H	CH_2Ph	8

In section **XI.5.F**, another cyclization/release strategy will be explored by changing the resin type, therefore influencing the nucleophilicity of the linker attachment point.

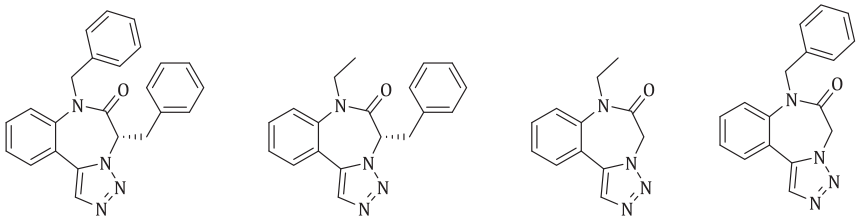

Figure XI-4: Proof of principle library after employing a reductive alkylation strategy

F. Solid-phase synthesis using HMPS resin

As the cyclization/release of monoalkylated intermediates, synthesized *via* Mitsunobu-Fukuyama conditions (see section **XI.B**) or *via* reductive alkylation (see section **XI.E**) proceeds in very low yields along with undesired cleavage of the acyclic precursor, the decision was made to elaborate a strategy using a different resin other than Wang's resin.

The choice for a hydroxymethylpolystyrene resin (HMPS, **Figure XI-5**) was made, as it shares the same polymer matrix (and solvent swelling properties) yet requires very different cleavage conditions. HMPS is very closely related to Merrifield's resin as the modified polystyrene bears nucleophilic hydroxyl groups instead of a classical nucleofuge (e.g. for Merrifield, chlorine). The difference with Wang resin lays in the absence of the acid-sensitive 4-alkoxybenzyl linker, which prevents the use of strong acid-catalyzed cyclization conditions without provoking undesired cleavage of the acyclic precursor. HMPS-resin requires stronger acids for cleavage, because of the formation of a less stabilized carbokation as compared to Wang resin.

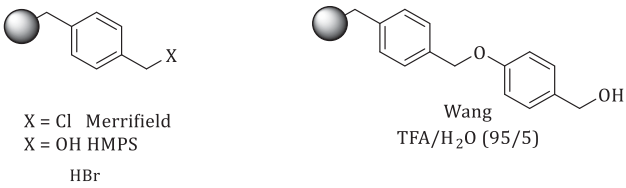

Figure XI-5: Three concerning resin-types and their standard cleavage conditions.

The optimized conditions for *N*-alkylation *via* Mitsunobu-Fukuyama alkylation and reductive alkylation were repeated on HMPS resin (**Scheme XI–18**). The cyclization/release was further investigated on this resin (**Table XI-12** and **Table XI-13**).

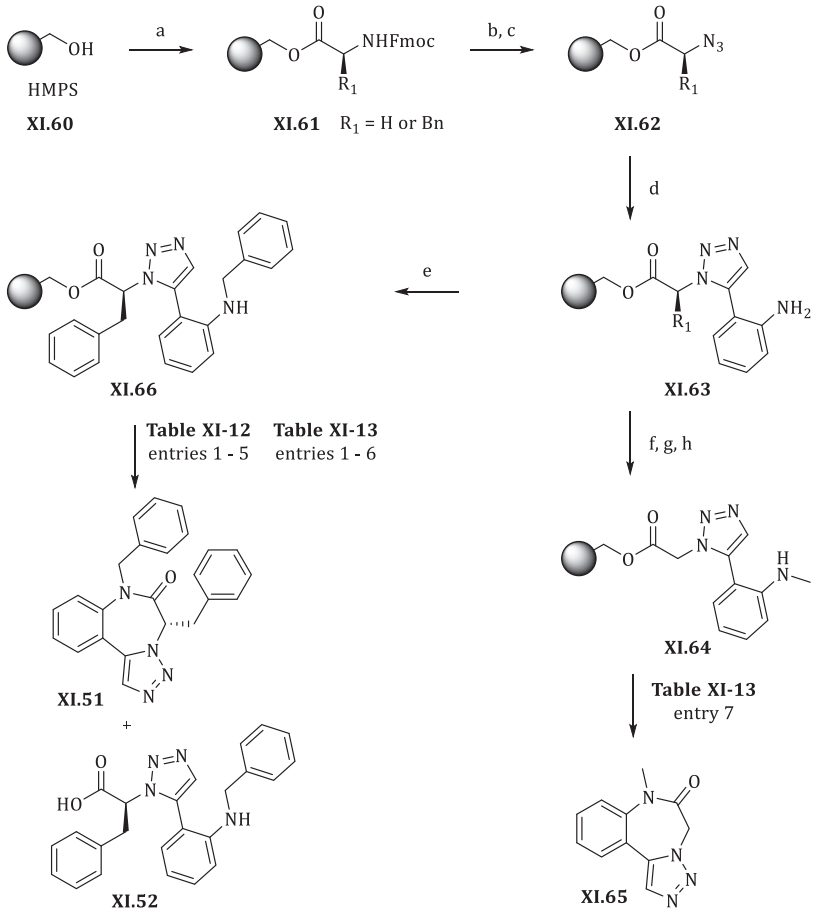

a) 1) 2 eq Fmoc-AA-OH, 2 eq DIC, 0,2 eq DMAP, CH_2Cl_2, rt, 2x 24h 2) Ac_2O, CH_2Cl_2, DIPEA (1/1/3) b) 20 v/v% 4-Me-piperidine/DMF, rt, 2x 10 min. c) 1,2 eq imidazole-1-sulfonyl azide hydrochloride, 2 eq TEA, 1 mol% $CuSO_4.5H_2O$, THF/H_2O (1/1), rt, 24h. d) 3 eq 2-ethynylaniline, 10 mol% C_p*RuCl(PPh_3)$_2$, toluene, 60°C, 6h. e) 3 eq benzaldehyde, 4 eq $NaBH(OAc)_3$, 1% HOAc, DCE, rt, 18h f) 10 eq *o*-NsCl, 20 eq pyridine, 1 eq DMAP, DCE, 70°C, 2x 5u. g) 10 eq R_5OH, 5 eq DIAD, 5 eq PPh_3, DCE, rt, 3x 2u. h) 2.5 eq DBU, 5 eq β-mercaptoethanol, DMF, rt, 2x 30min.

Scheme XI–18: *N*-Alkylation strategies employed on HMPS resin

Table XI-12: Cyclization/release test reaction for XI.66 – Conventional heating

entry	conditions	crude purity of XI.51 (%)[a]	remarks
1	TFA/CH_2Cl_2 (1/1), rt, 8h	13%	**XI.51** + open product **XI.52**
2	TFA/CH_2Cl_2 (1/9), rt, 8h	3%	**XI.51** + open product **XI.52**
3	TFA/CH_2Cl_2 (1/1), 60°C, 8h	17%	**XI.51** + open product **XI.52**
4	TFA/CH_2Cl_2 (1/9), 60°C, 8h	21%	**XI.51** + open product **XI.52**
5	TFA (100%), rt, 8h	26%	**XI.51** + open product **XI.52**

[a] Crude purity determined via LC-MS analysis (214 nm)

Table XI-12 shows the results of the cyclization/release strategy for HMPS resin bound intermediate **XI.66**. Entries **1** - **5** represent test conditions with trifluoroacetic acid in different ratios at room temperature and 60°C. Using TFA as an acid still liberates the uncyclized carboxylic acid as side product next to the desired seven-membered ring, although the cyclization/release is generally cleaner.

In **Table XI-13**, the results for microwave assisted cyclization/release test reactions are represented. Out of desperation to find efficient conditions for cyclization/release, simple heating was employed. Entries **1** - **4** show microwave assisted heating in DMF to respectively 130°C and 150°C[11]. To our surprise, prolonged microwave heating is able to cyclize the intermediates to the desired *N*-alkylated products. In order to avoid DMF as solvent, two test conditions with dichloroethane (entries **5** and **6**) were performed in order verify their outcome. Cyclization upon microwave heating could not be repeated.

Nonetheless, the reaction condition presented in entry **4** was also applied to **XI.64** synthesized *via* the Mitsunobu-Fukuyama method (entry **7**) . The obtained crude purity is certainly not satisfactory hence questioning this method for its wide applicability in library synthesis.

Table XI-13: Cyclization/release test reaction for XI.66 and XI.64 – Microwave heating

entry	conditions	crude purity (%)
1	DMF, 130°C, 15 min, powermax off	45%[a]
2	DMF, 130°C, 15 min, powermax on	49%[a]
3	DMF, 150°C, 20 min, powermax off	42%[a]
4	DMF, 150°C, 20 min, powermax on	39%[a]
5	HOAc/DCE (1/1), 100°C, 15 min, powermax on	15%[a]
6	DCE, 80°C, 15 min, powermax on	0%[a]
7	DMF, 150°C, 20 min, powermax on	10%[b]

[a] Crude purity of **XI.51** determined via LC-MS analysis (214 nm)

[b] Crude purity of **XI.65** determined via LC-MS analysis (214 nm)

Moreover, microwave-assisted test reactions investigating the cyclization/release of Wang-bound intermediates were performed. The monoalkylated intermediates **XI.25** - **XI.27** were synthesized *via* the Mitsunobu-Fukuyama strategy on Wang resin. A prolonged microwave heating in DMF was employed (**Table XI-14**).

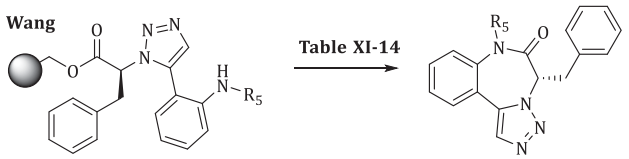

Scheme XI–19: Cyclization/release test reactions for XI.25 – XI.27 – Microwave heating

Table XI-14: Conditions applied in Scheme XI–19

entry	compound	conditions	crude purity (%)[a]
1	**XI.28**	DMF, 130°C, 20 min, powermax off	<1%
2	**XI.29**	DMF, 130°C, 20 min, powermax off	<1%
3	**XI.30**	DMF, 130°C, 20 min, powermax off	<1%

[a] Crude purity determined via LC-MS analysis (214 nm)

As can be seen from **Table XI-14**, only trace amounts of cyclized product were detected for all three intermediates synthesized *via* the Mitsunobu-Fukuyama strategy next to unidentifiable side products.

G. *N*-alkylation: Critical overview/review

In **Scheme XI-20**, a general overview is given for the explored approaches in the course of this chapter. **Pathway A** (**Scheme XI-20**) comprised the Mitsunobu-Fukuyama strategy, which started with the introduction of the nosyl protecting/activating group on **VIII.3**. If **VIII.3** was treated twice with 10 eq o-NsCl, 20 eq pyridine at 70°C for 5 hours, a maximum yield of 61% was achieved. Despite the desired result, few remarks should be made. First of all, the necessity for high excess of reagents makes this protecting step very (atom) inefficient. Moreover, adding a base at elevated temperatures could invoke racemization of the chiral center present in the molecule. At last, the obtained yield is considered low for a protecting step. An effort to introduce the nosyl group *via* a protected 2-ethynylaniline building block (**XI.34**) failed in the RuAAC due to a low yield and regioselectivity.

Nonetheless, the Mitsunobu-Fukuyama alkylation step was performed with three alkylating agents, MeOH, EtOH and iPrOH. The standard conditions yielded moderate to high conversion for the primary alcohols, a more comprehensive reaction monitoring is required for alkylation with secondary alcohols.

The subsequent removal of the nosyl-protecting group proceeded quantitatively to the secondary amine which was subjected to different cyclization/release conditions. Due to the induced sterical hindrance, this cyclization step was troublesome. The applied conditions failed in selectivity and efficacy.

Pathway B (**Scheme XI-20**) represents the reductive alkylation strategy. An optimization was performed in order to maximize the ratio of *N*-monoalkylated intermediate **XI.38 - XI.39**. An extensive study gave the insight that problems arise if non-sterically hindered (aliphatic) aldehydes are used. Initially, this work focused on acetaldehyde and benzaldehyde leading to conditions where the yield was maximized (**XI.38** 96%, **XI.39** 51%). Taken into account that scaffold decoration requires robust conditions, this reductive alkylation strategy fails due the case-specific optimization process.

Thanks to the higher conversion of the reductive alkylation for benzaldehyde, more test reactions for the cyclization/release strategy could be employed. The detrimental formation of the open product could not be avoided. Only a prolonged shaking of HOAc/DCE (1/1) at elevated temperatures gave the best results (72% crude purity).

In order to avoid the open product intermediate release, the resin type was changed into HMPS resin, allowing harsher cleavage conditions. Here, it was seen that the open product formation remained problematic. Surprisingly, a thermal activation in DMF with microwave conditions enabled the desired cleavage for small scale reactions.

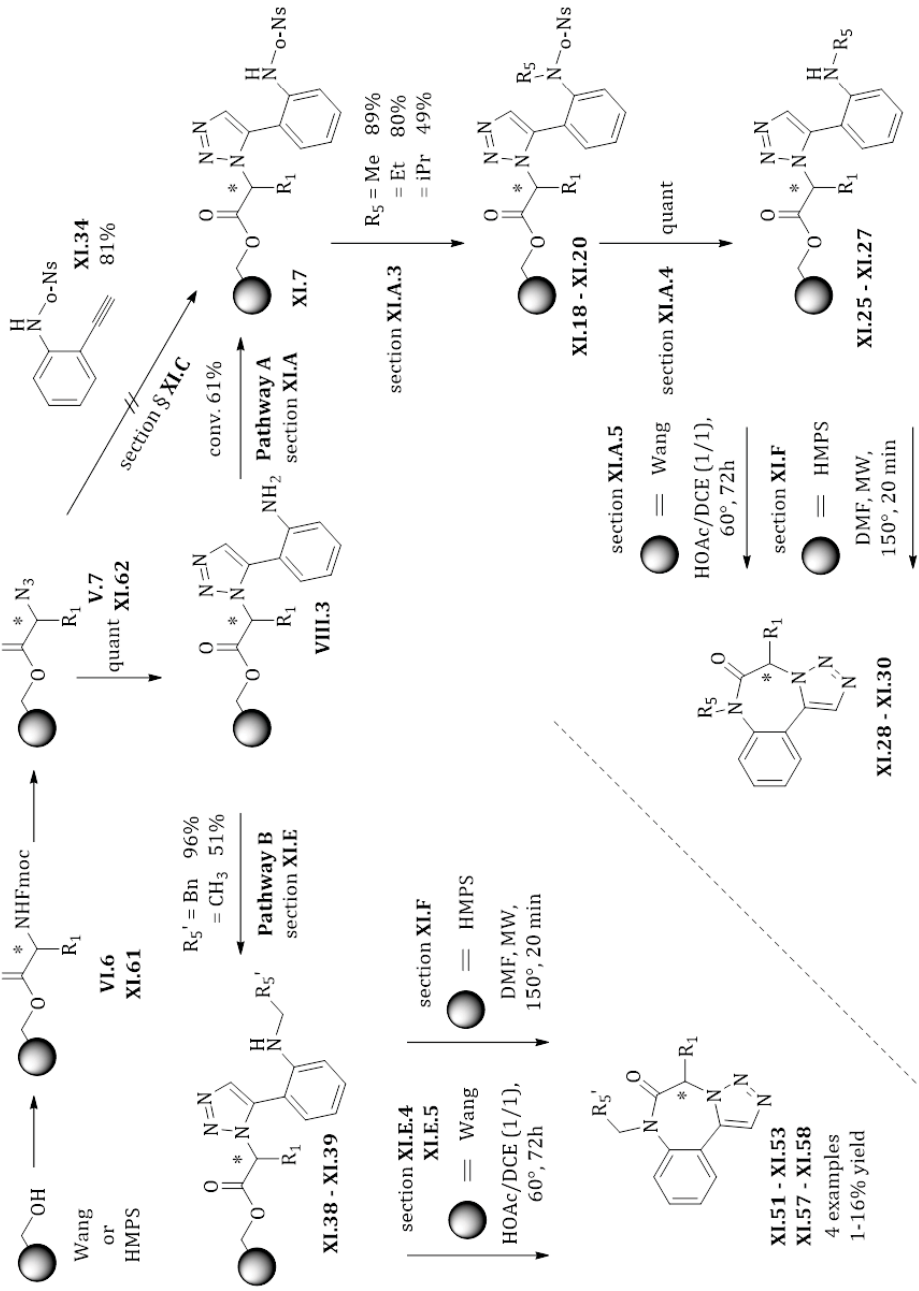

Scheme XI–20: General overview of the attempts towards *N*-alkylation

Overviewing the attempts towards the introduction of diversity on the nitrogen *via* a solid-phase approach, the general applied strategies remained problematic and unsatisfactory for a good solid-phase practice. A last endeavor was tried by forsaking the synthesis on the polymer matrix and performing the alkylation in solution-phase after cyclization/release of the non-*N*-diversified compound **IX.1**.

H. Third approach: *N*-alkylation in solution

1. Proof of principle

In order to avoid the observed cyclization/release problems after *N*-monoalkylation on solid-phase, *N*-alkylation after cyclization/release in solution was investigated. This strategy encompasses addition of a base (i.c. 2 eq KOH) and an alkylating agent (i.c. alkyl iodides) to the non-alkylated scaffold hence provoking racemization of N-alkylated products. Synthesis of a proof of principle library was performed by adding different halides (**Scheme XI.21**, **XI.67** – **XI.71**) to two scaffold molecules derived from two protected amino acids, Fmoc-Gly-OH (**VI.25**) and Fmoc-Phe-OH (**VI.28**).

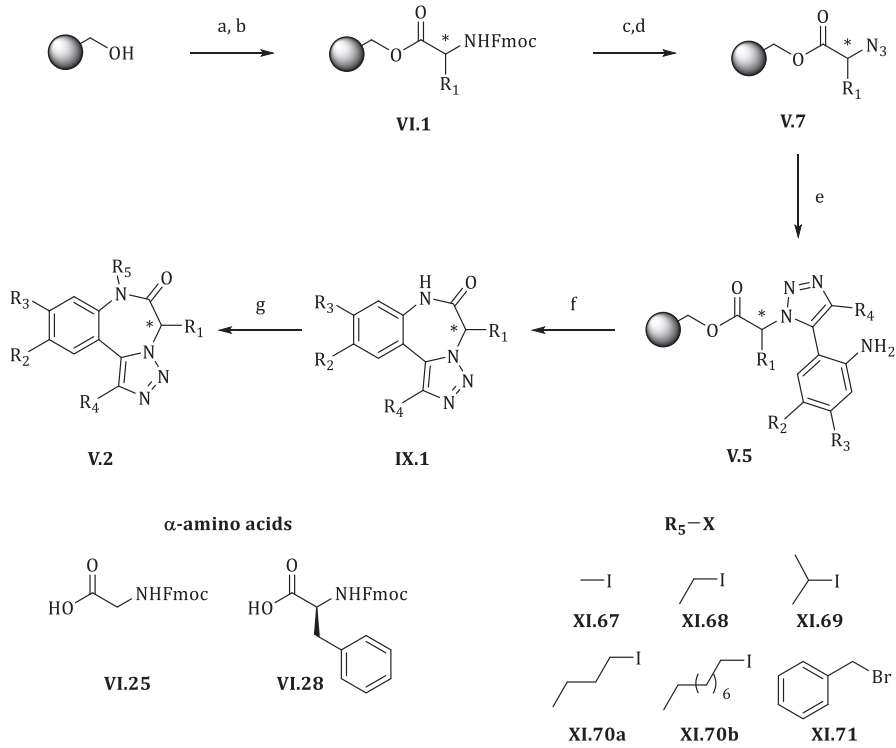

a) 2 eq Fmoc-AA-OH, 2 eq DIC, 0,2 eq DMAP, CH_2Cl_2, rt, 2x 24h b) Ac_2O, CH_2Cl_2, DIPEA (1/1/3) c) 1) 20 v/v% 4-Me-piperidine/DMF, rt, 2x 10 min. d) 1,2 eq imidazole-1-sulfonyl azide hydrochloride, 2 eq TEA, 1 mol% $CuSO_4.5H_2O$, THF/H_2O (1/1), rt, 24h. e) 3 eq 2-ethynylaniline, 10 mol% C_p*RuCl(PPh_3)$_2$, toluene, 60°C, 6h. f) HOAc/CH_2Cl_2 (1/1), rt, 24h. g) 4 eq **XI.67 - XI.71,** 2 eq KOH, THF, rt, 5h.

Scheme XI–21: Parallel synthesis of *N*-alkylated compounds – Proof of principle

As can be seen from **Table XI-15**, the proof of principle library counts nine members, which were all synthesized in good to excellent yields. Entries **3** and **7**, accounting for an isopropyl group, resulted in the lowest yields, explained by the sterical hindrance during the S_N2-alkylation step. This strategy enabled *N*-alkylation in a fast and easy way in order to give access to a future library synthesis of fully diversified scaffolds. In order to assess the degree of racemization of compounds **XI.28 – XI.30** and **XI.74 - XI.75** shown in **Table XI-16**, an extensive amount of method optimizations for chiral seperation were performed. Unfortunately for **XI.28** and **XI.29** no chiral separation could be observed on six different columns. For **XI.74 - XI.75**, no relevant enantiomeric excess could be observed, therefore we can generally assume full racemization during *N*-alkylation

Table XI-15: Members of the proof of principle library

entry	compound	R_1	R_5	isolated yield[a] (%)	overall yield (%)
1	**XI.65**	H	CH_3	88	39
2	**XI.57**	H	CH_2CH_3	89	35
3	**XI.72**	H	$CH(CH_3)_2$	50	22
4	**XI.73**	H	CH_2Ph	79	48
5	**(*rac*)-XI.28**	CH_2Ph	CH_3	81	44
6	**(*rac*)-XI.29**	CH_2Ph	CH_2CH_3	81	44
7	**(*rac*)-XI.30**	CH_2Ph	$CH(CH_3)_2$	41	22
8	**(*rac*)-XI.74**	CH_2Ph	$(CH_2)_3CH_3$	59	32
9	**(*rac*)-XI.75**	CH_2Ph	$(CH_2)_9CH_3$	55	30

[a]isolated yield of the alkylation step

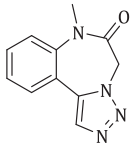

XI.65
alkylation step: **88%**
overall yield: **39%**

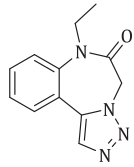

XI.57
alkylation step: **89%**
overall yield: **35%**

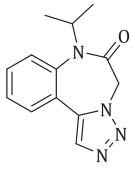

XI.72
alkylation step: **50%**
overall yield: **22%**

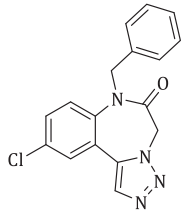

XI.73
alkylation step: **79%**
overall yield: **48%**

Figure XI-6: Members of the proof of principle library

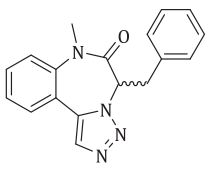

(*rac*)-XI.28
alkylation step: **81%**
overall yield: **44%**

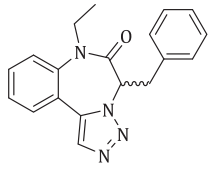

(*rac*)-XI.29
alkylation step: **81%**
overall yield: **44%**

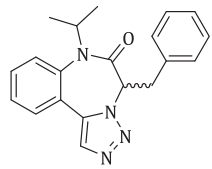

(*rac*)-XI.30
alkylation step: **41%**
overall yield: **22%**

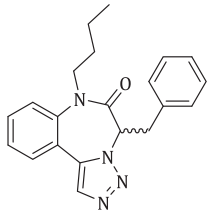

(*rac*)-XI.74
alkylation step: **59%**
overall yield: **32%**

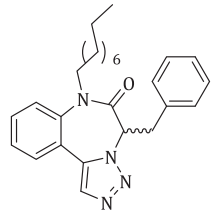

(*rac*)-XI.75
alkylation step: **55%**
overall yield: **30%**

Figure XI-7: Members of the proof of principle library

Table XI-16: Degree of racemization upon *N*-alkylation in solution

entry	compound	R_1	R_5	ratio	remarks
1	**(*rac*)-XI.28**	CH_2Ph	CH_3	N/A	N/A
2	**(*rac*)-XI.29**	CH_2Ph	CH_2CH_3	N/A	N/A
3	**(*rac*)-XI.30**	CH_2Ph	$CH(CH_3)_2$	52:48	A
4	**(*rac*)-XI.74**	CH_2Ph	$(CH_2)_3CH_3$	50:50	A
5	**(*rac*)-XI.75**	CH_2Ph	$(CH_2)_9CH_3$	48:42	A

Chromatographic conditions:

A: *n*-hexane – EtOH 90:10 Chiralcel AS-H

N/A: not available, chiral separation could not be achieved

2. Combinatorial synthesis

According to our intention to create a library of a fully diversified scaffold, compounds synthesized in section **IX.C.7** were subjected to the conditions described above and alkylated in a parallel fashion in solution-phase.

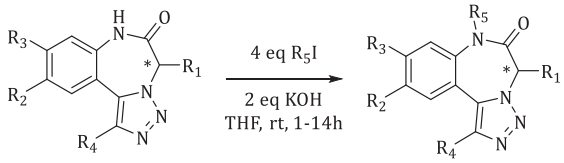

IX.1 **V.2**

Scheme XI–22: General *N*-alkylation procedure

To a first extent, small alkyl groups (ethyl and *n*-butyl) were chosen as alkylating groups. Eight different non-alkylated molecules synthesized in section **IX.C.7** were deprotonated and alkylated resulting in a library of 16 compounds presented in **Table XI-17** - **Table XI-18** and **Figure XI.8** - **Figure XI-9.**

Table XI-17: Library members XI.76 – XI.83

entry	compound	isolated yield[a] (%)	overall yield (%)
1	**(*rac*)-XI.76**	49	29
2	**(*rac*)-XI.77**	67	46
3	**(*rac*)-XI.78**	64	39
4	**(*rac*)-XI.79**	64	34
5	**(*rac*)-XI.80**	68	51
6	**(*rac*)-XI.81**	73	54
7	**(*rac*)-XI.82**	30	11
8	**(*rac*)-XI.83**	45	19

[a]isolated yield of the alkylation step

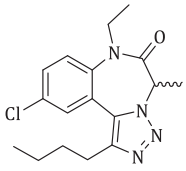

(*rac*)-XI.76

alkylation step: **49%**
overall yield: **29%**

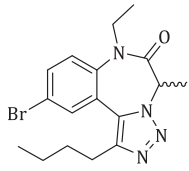

(*rac*)-XI.77

alkylation step: **67%**
overall yield: **46%**

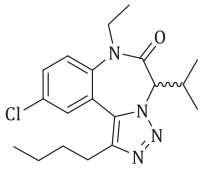

(*rac*)-XI.78

alkylation step: **64%**
overall yield: **39%**

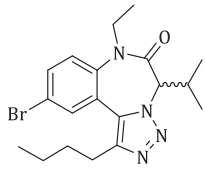

(*rac*)-XI.79

alkylation step: **64%**
overall yield: **34%**

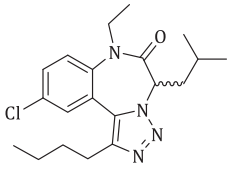

(*rac*)-XI.80

alkylation step: **68%**
overall yield: **51%**

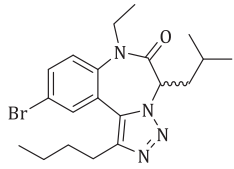

(*rac*)-XI.81

alkylation step: **73%**
overall yield: **54%**

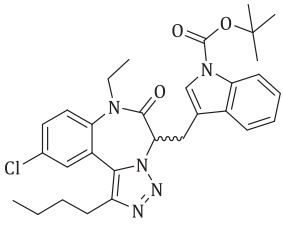

(*rac*)-XI.82

alkylation step: **30%**
overall yield: **11%**

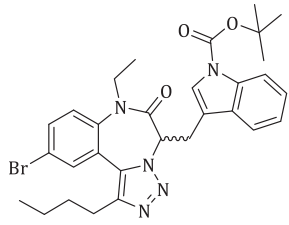

(*rac*)-XI.83

alkylation step: **45%**
overall yield: **19%**

Figure XI-8: Library members XI.76 – XI.83

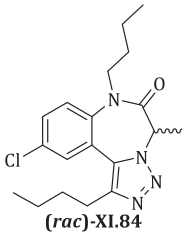

(*rac*)-XI.84
alkylation step: **73%**
overall yield: **43%**

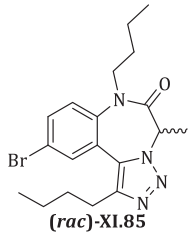

(*rac*)-XI.85
alkylation step: **42%**
overall yield: **29%**

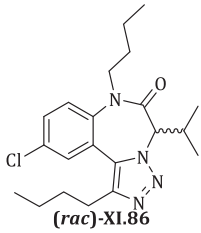

(*rac*)-XI.86
alkylation step: **62%**
overall yield: **38%**

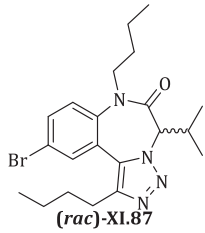

(*rac*)-XI.87
alkylation step: **72%**
overall yield: **38%**

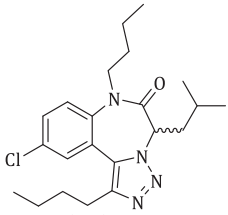

(*rac*)-XI.88
alkylation step: **61%**
overall yield: **46%**

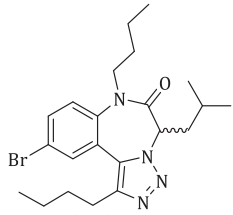

(*rac*)-XI.89
alkylation step: **63%**
overall yield: **47%**

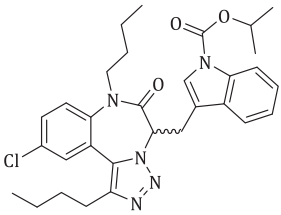

(*rac*)-XI.90
alkylation step: **83%**
overall yield: **30%**

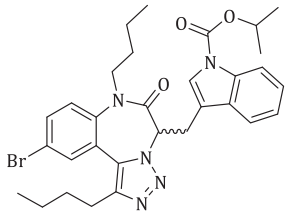

(*rac*)-XI.91
alkylation step: **47%**
overall yield: **21%**

Figure XI-9: Library members XI.84 – XI.91

Table XI-18: Library members XI.84 – XI.91

entry	compound	isolated yield[a] (%)	overall yield (%)
1	**(*rac*)-XI.84**	73	43
2	**(*rac*)-XI.85**	42	29
3	**(*rac*)-XI.86**	62	38
4	**(*rac*)-XI.87**	72	38
5	**(*rac*)-XI.88**	61	46
6	**(*rac*)-XI.89**	63	47
7	**(*rac*)-XI.90**	83	30
8	**(*rac*)-XI.91**	47	21

[a]isolated yield of the alkylation step

A close analogue of clobazam **I.24**, a commercial anxiolytic and anticonvulsant agent, was synthesized by methylating compound **IX.77**, giving **XI.92** (**Table XI-19, Figure XI-10**).

Table XI-19: Library members XI.92 – XI.93

entry	compound	alkylation yield (%)	overall yield (%)
1	**XI.92**	83	30
2	**XI.93**	30	21

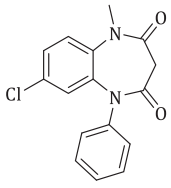

I.24
clobazam

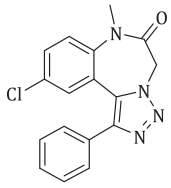

XI.92
alkylation step: **83%**
overall yield: **30%**

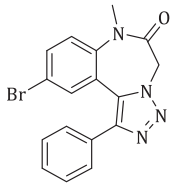

XI.93
alkylation step: **47%**
overall yield: **21%**

Figure XI-10: Library members XI.92 – XI.93

As can be seen from **Table XI-17** - **Table XI-18** and **Figure XI-8** - **Figure XI-9**, all alkylation reactions can be performed with good yields. In combination with the solid-phase synthesis of the non-alkylated scaffolds, sixteen fully diversified compounds were synthesized in acceptable yields. Chiral HPLC analysis of a selection of synthesized compounds indicated the anticipated racemization during the *N*-alkylation step. Further investigations for racemization-free *N*-alkylation in solution or on solid-phase is required.

REFERENCES

[1] Bazzini, P.; Wermuth, C.G. Specific substituents groups. In The practice of Medicinal Chemistry; Wermuth, C. G., Ed.; Elsevier: London, 2008; pp. 431-432.

[2] a) Swamy, K. C. K.; Kumar, N. N. B.; Balaraman, E.; Kumar, K. V. P. P. *Chem Rev* **2009**, *109*, 2551–2651. b) Kan, T.; Fukuyama, T. *Chem. Commun*. **2004**, 353–359. c) Reichwein, J. F.; Liskamp, R. M. J. *Tetrahedron Lett*. **1998**, *39*, 1243-1246. d) Guisado, C.; Waterhouse, J. E.; Price, W. S.; Jorgensen, M. R.; Miller, A. D. *Org. Biomol. Chem*., **2005**, *3*, 1049–1057. e) Olsen, C. A.; Jørgensen, M. R.; Witt, M.; Mellor, I. R.; Usherwood, P. N. R.; Jaroszewski, J. W.; Franzyk, H.; *Eur. J. Org. Chem.* **2003**, 3288-3299. f) Olsen, C. A.; Witt, M.; Hansen, S. H.; Jaroszewski, J. W.; Franzyk, H. *Tetrahedron*, **2005**, *61*, 6046-6055. g) Hone, N. D.; Payne, L. J. *Tetrahedron Lett* **2000**, *41*, 6149-6152. h) Fukuyama, T.; Cheung, M.; Jow, C. K.; Hidai, Y.; Kan, T. *Tetrahedron Lett* **1997**, *38*, 5831-5834. i) Fukuyama, T.; Jow, C. K.; Cheung, M. *Tetrahedron Lett* **1995**, *36*, 6373.

[3] Green, T. W.; Wuts, P. G. M.; *Protective Groups in Organic Synthesis,* Wiley-Interscience, New York, **1999**, 855

[4] Mitsunobu, O. *Synthesis* **1981**, *1*, 1-28.

[5] Kan, T.; Kobayashi, H.; Fukuyama, T *Synlett* **2002**, *8*, 1338.

[6] a) Leggio, A.; Di Gioia, M. L.; Perri, F.; Liguori, A. *Tetrahedron* **2007**, *63*, 8164-8173. b) Di Gioia, M. L.; Leggio, A.; Le Pera, A.; Liguori, A.; Napoli, A.; Siciliano, C.; Sindona, G. *J. Org. Chem*. **2003**, *68*, 7416-7421.

[7] a) Jönsson, D. *Tetrahedron Lett.* **2002**, *43*, 4793–4796. b) Jönsson, D.; Unden, A. *Tetrahedron Lett.* **2002**, *43*, 3125–3128. c) Abdel-Magid, A. F.; Mehrman, S. J. *Org. Process Res. Dev.* **2006**, *10*, 971-1031.

[8] For an excellent review on this topic and reagent ($NaBH(OAc)_3$): Abdel-Magid, A. F.; Mehrman, S. *Org. Process Res. Dev.* **2006**, *10,* 971-1031.

[9] Abdel-Magid, A. F.; Carson, K. G.; Harris, B. D.; Maryanoff, C. A.; Shah, R. D. *J. Org. Chem*. **1996**, *61*, 3849-3862.

[10] For an excellent review on this topic and reagent ($NaBH_3CN$): Olsen, C.A.; Franzyk, H.; Jaroszewski, J. W. *Synthesis* **2005**, 2631-2653.

[11] Perez, R.; Beryozkina, T.; Zbruyev, O. I.; Haas, W.; Kappe, C. O. *J. Comb. Chem.* **2002**, *4*, 501-510.

XII. Conclusions and future perspectives

A. Introduction

The concepts of bioisosterism led to the initial concept of replacing a *cis*-amide bond present in 1,5-benzodiazepine-2,4-diones (**V.1, Figure XII-1)** by a scaffold based on the 1,5-fused triazole moiety (i.c. [1,2,3]triazolo[1,5-*d*]benzo[1,4]diazepine-2-ones **V.2**). The foundation of this idea was explained by the structural and electronic similarities between a *cis*-amide bond and the 1,5-regioisomer of the 1,2,3-triazole moiety as depicted in **Figure XII-1**.

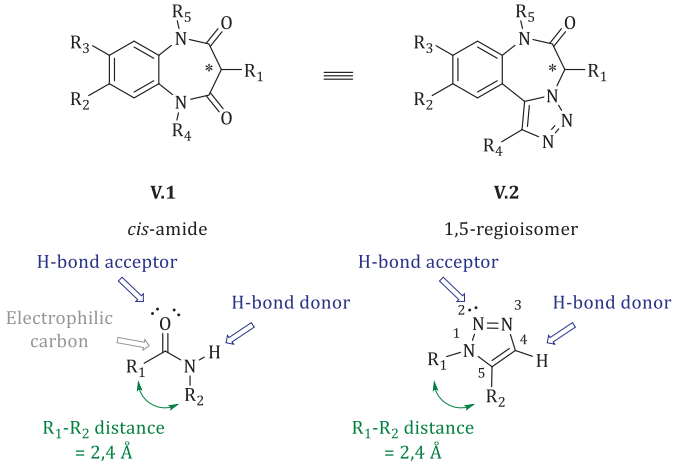

Figure XII-1: Structural and electronic evaluation of a *cis*-amide bond versus the 1,5-regioisomer of a 1,2,3-triazole moiety

Thanks to the advantages of solid-supported library synthesis, this work aimed to build an adequate solid-phase synthesis for [1,2,3]triazolo[1,5-*d*]benzo[1,4]diazepine-2-ones **V.2** as mimics of 1,5-benzodiazepine-2,4-diones **V.1**. With respect to the need for a straightforward synthesis, throughout this work, a high applicability of building blocks, high throughput synthesis and broad suitability of chosen reaction conditions were of fundamental importance in order to promote an rapid exploration of the chemical space around **V.2**. Essentially, our work can be summarized in **Figure XII-2.**

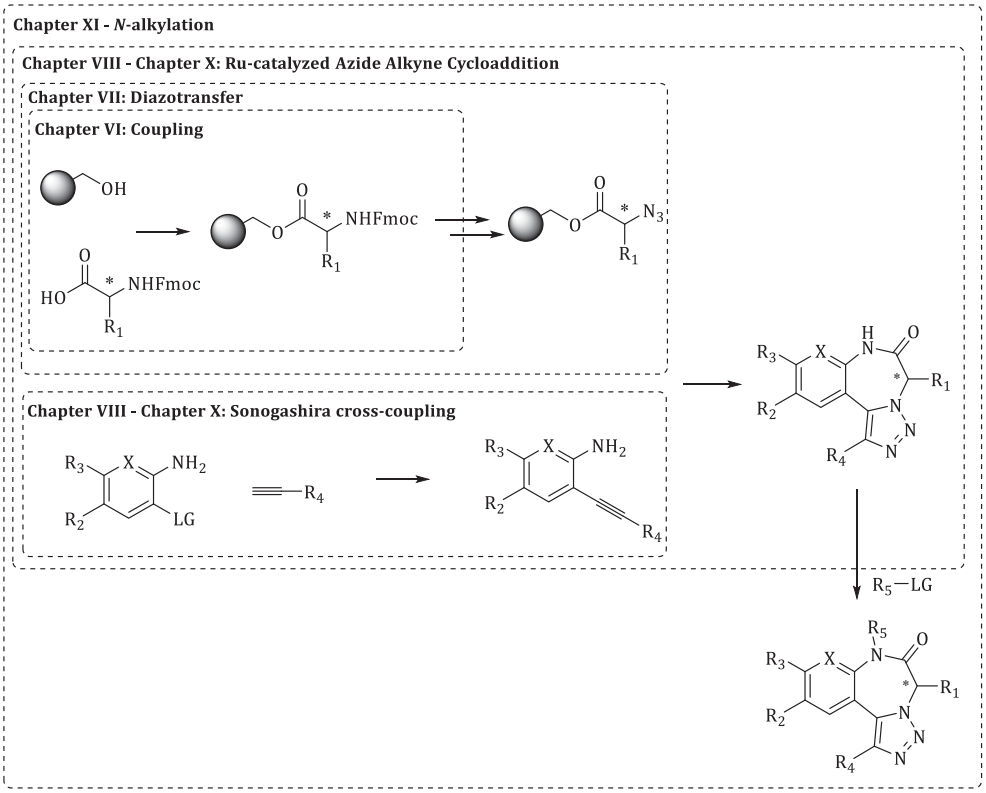

Figure XII-2: General representation of our research

Each of the following sections of this chapter will depict fundamental steps taken in this work and in order to attain an optimal understanding, references are made to the specific topics for further reading.

B. Coupling

In the preliminary phase of this research, α-amino acids were chosen as the preferred primary building blocks because of their inherently interesting characteristics: an amine source for diazotransfer at a later stage, and the presence of an amino acid side chain accounting for the first diversity point (R_1) of the envisioned scaffold. In combination with scaffold design on solid support, the first synthesis step encompassed a coupling step to Wang resin. In this work only natural and commercially available enantiomerically pure α-amino acids were used (**VI.25-VI.32, Scheme XII-1**). DMAP promoted coupling between preactived *O*-acylisourea derivatives and the alcohol residue of Wang resin, resulted in a solid-phase bound Fmoc-protected α-amino acid with coupling efficiencies varying between 88% and 97% (see section **VI.C**). The latter can be determined with a straightforward UV measurement thanks to the Fmoc-protecting group and the adduct formed upon cleavage. A consecutive treatment of the solid-phase with a capping reagent ensuring blocking any remaining alcohol moieties. Treatment of the solid-phase bound carbamate protected amino acids with 4-Me-piperidine in DMF according to standard SPOS conditions, afforded resin-bound amino acids with a free amino group.

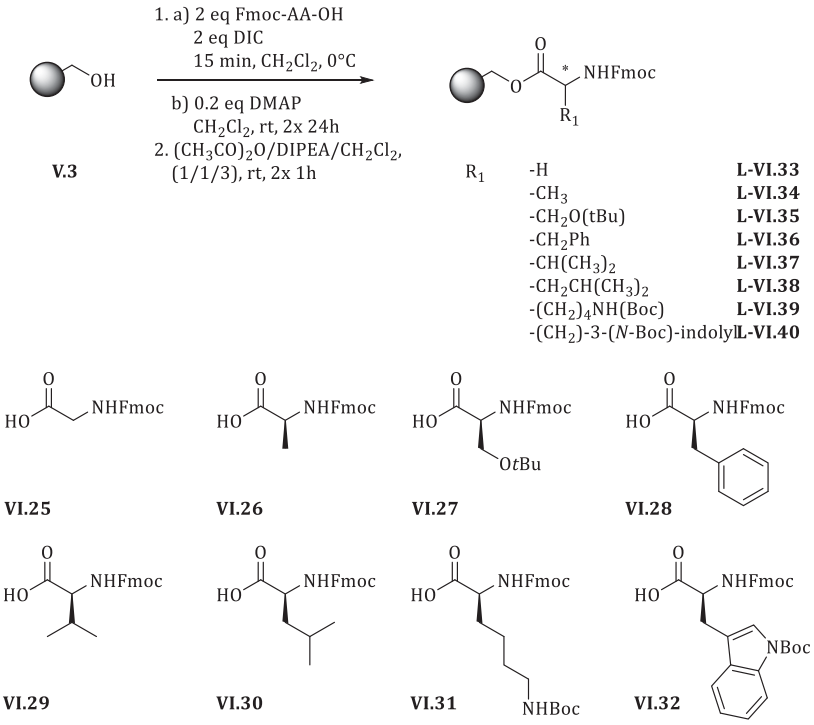

Scheme XII-1: Overview of the α-amino acids coupling reaction on Wang resin

C. Diazotransfer

In the quest to include a triazole moiety in the intended scaffold, the presence of an azide group is crucial. Literature provided various possible transformations for incorporating a reactive azide moiety. Taken into account the need for a solid-phase strategy, available building blocks and the requirement for conserving enantiomeric purity, the diazotransfer reaction appeared to be the most interesting option. Further investigating this topic also implied the need for a safe diazotransfer reagent and cautious handling of the reaction products. Literature provided imidazole-1-sulfonyl azide hydrochloride (**VII.11**) as an effective and safe reagent for in solution conversion of amines to the corresponding azides.

With respect to the physical properties of the chosen solid-phase, to a first extent, the applicability of the diazotransfer reaction was explored. After selecting the most effective conditions for our application, more insights on the enantiomeric purity of the obtained compounds was investigated, leading to the observation that no epimerization took place. Eventually, the solid-phase bound α-amino acids were readily converted into solid-phase bound azides. Thanks to the inherent benefits of solid-phase chemistry safe handling of azide reaction products was guaranteed.

Importantly, considering all safety aspects and careful handling, several multi-gram batches of diazotransfer reagent **VII.11** were synthesized according to **Scheme XII-2**.

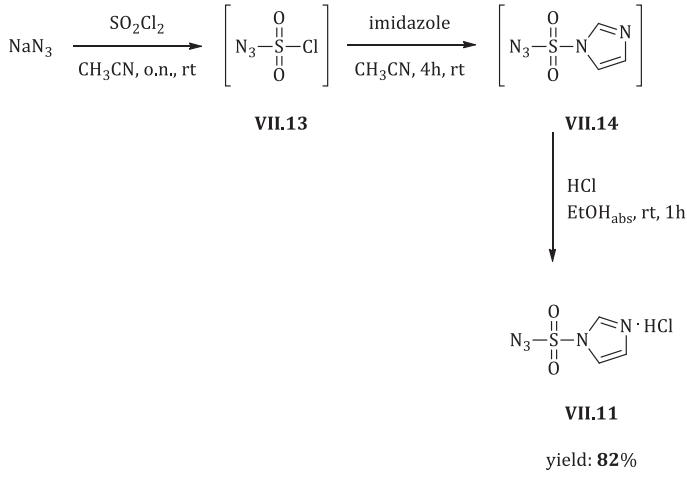

Scheme XII-2: Synthesis of imidazole-1-sulfonyl azide hydrochloride VII.11

The imidazole-1-sulfonyl azide hydrochloride (**VII.11**) obtained could be stored for over 24 months at -18°C . Throughout this research, this diazotransfer reagent was extensively used to convert unprotected resin-bound enantiomerically pure amines into the corresponding solid-bound azides **VII.28-VII.35**. The conditions presented enable an enantiomerically pure amine-to-azide conversion (see Scheme **XII-3**).

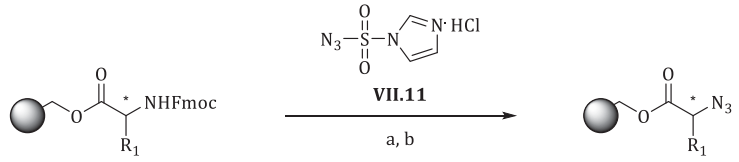

R_1			R_1		
	H	**L-VI.33**		H	**L-VII.28**
	(S)-CH_3	**L-VI.34**		(S)-CH_3	**L-VII.29**
	(S)-$CH_2O(t\text{Bu})$	**L-VI.35**		(S)-$CH_2O(t\text{Bu})$	**L-VII.30**
	(S)-Bn	**L-VI.36**		(S)-Bn	**L-VII.31**
	(R)-Bn	**D-VI.36**		(R)-Bn	**D-VII.31**
	(S)-$CH(CH_3)_2$	**L-VI.37**		(S)-$CH(CH_3)_2$	**L-VII.32**
	(S)-$CH_2CH(CH_3)_2$	**L-VI.38**		(S)-$CH_2CH(CH_3)_2$	**L-VII.33**
	(S)-$(CH_2)_4$NHBoc	**L-VI.39**		(S)-$(CH_2)_4$NHBoc	**L-VII.34**
	(S)-(CH_2)-3-(*N*-Boc)-indolyl	**L-VI.40**		(S)-(CH_2)-3-(*N*-Boc)-indolyl	**L-VII.35**

a) 20 v/v% 4-Me-piperidine/DMF, rt, 2x 10 min b) 1.2 eq imidazole-1-sulfonyl azide hydrochloride **(VII.11)**, 2 eq TEA, 1 mol% $CuSO_4.5H_2O$, THF/H_2O, rt, 24h.

Scheme XII-3: Overview of the resin-bound α-amino acids submitted to a diazotransfer reaction

D. Ru-catalyzed Azide Alkyne Cycloaddition (RuAAC)

Structural and electronic similarities between a *cis*-amide bond and a 1,5-disubsttuted triazole moiety (see chapter **III**) led to the concept of incorporating this mimic into the benzodiazepine-based scaffold design. Actual synthesis of this moiety on the solid-phase was performed *via* a Ru-catalyzed Azide Alkyne Cycloaddition (RuAAC). Thanks to this reaction, a straightforward, fast and regioselective formation of an 1,5-disubstituted triazole moiety could be achieved.

A test case using commercially available 2-ethynylaniline (**VIII.2**, **Scheme XII-4**) and solid-phase bound L-2-azido-3-phenylpropanoic acid **VII.31** led to interesting results. Apart from the exclusive formation of the 1,5-disubstituted triazole moiety, the acid promoted cleavage reaction to liberate the target molecule from the solid-phase directly yielded the desired cyclized scaffold. The test reaction for the RuAAC followed by cleavage under standard SPOS conditions are summarized in **Scheme XII-4**.

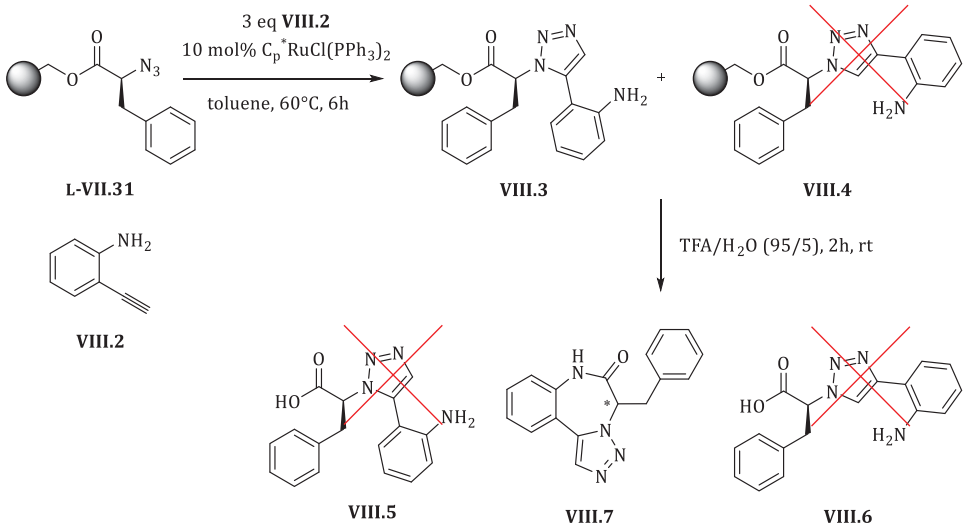

Scheme XII-4: RuAAC followed by 'cyclization/release' yielding VIII.7

As the standard release conditions also liberated side products from the resin, these conditions were fine-tuned in order to achieve a maximum crude purity to facilitate high-throughput synthesis and consecutive purification prior to biological screening. The optimal and mild cyclization/release conditions were $HOAc/CH_2Cl_2$ for 24h at room temperature. A proof of principle library with different Wang resin-bound α-azido acid building blocks and 2-ethynylaniline was prepared. Determination of the enantiomeric purity of final compounds showed the followed set of reactions to be racemization-free. Therefrom, it could be concluded that the reaction sequence did not provoke possible racemization of the stereogenic center.

In addition to the commercially available 2-ethynylaniline (**VIII.2**), several other 2-ethynylaniline building blocks **VIII.33 – VIII.37** were prepared *via* a Sonogashira cross-coupling reaction and a consecutive TMS removal step (see **Scheme XII-5, Table XII-1**). Compound **VIII.45** was synthesized in a six step process starting from 3-iodophenol (see **Scheme XII-6).**

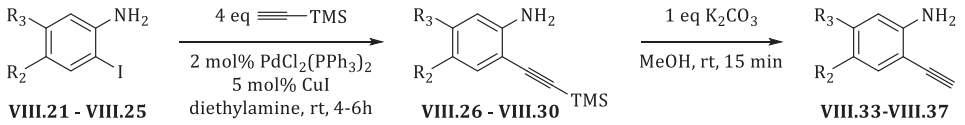

Scheme XII-5: Synthesis of 2-ethynylaniline building blocks VIII.33 – VIII.37

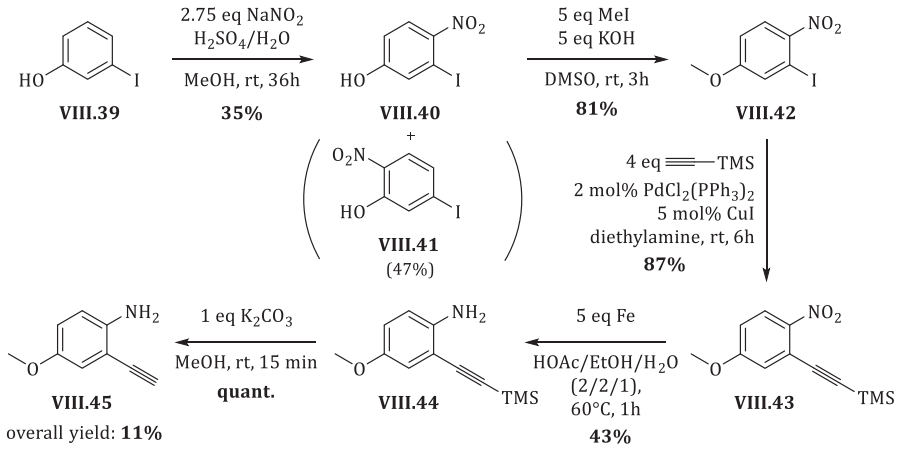

Scheme XII-6: Synthesis 2-ethynyl-4-methoxyaniline building block VIII.45

Table XII-1: Overall yields of 2-ethynylaniline building block VIII.33 – VIII.37 and VIII.45

entry	compound	R_2	R_3	overall yield (%)
1	**VIII.33**	Cl	H	88
2	**VIII.34**	H	Cl	77
3	**VIII.35**	Br	H	86
4	**VIII.36**	CN	H	87
5	**VIII.37**	NO_2	H	82
6	**VIII.45**	OMe	H	11[a]

[a] over six steps

The six 2-ethynylaniline building blocks **VIII.33 – VIII.37** and **VIII.45** were then used in combinatorial synthesis with seven α-amino acid building blocks yielding a total of thirty-six[i] compounds **VIII.47-VIII.82.** Section **VIII.2** discusses all compounds made in further detail.

[i] Not all possible combinations were synthesized, due to *ad hoc* unavailability of building blocks.

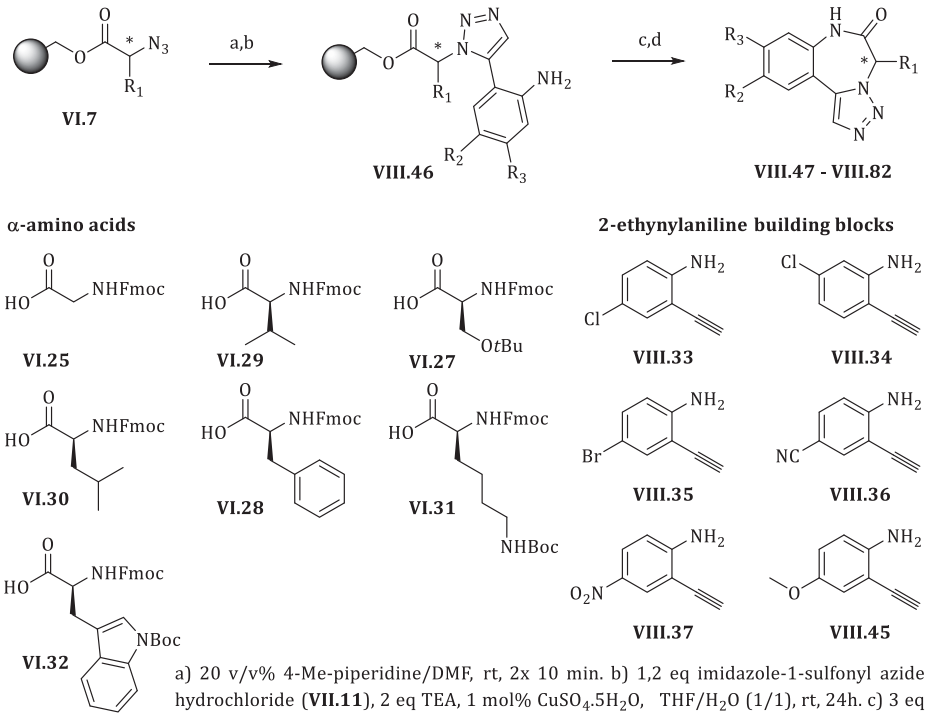

a) 20 v/v% 4-Me-piperidine/DMF, rt, 2x 10 min. b) 1,2 eq imidazole-1-sulfonyl azide hydrochloride (**VII.11**), 2 eq TEA, 1 mol% $CuSO_4.5H_2O$, THF/H_2O (1/1), rt, 24h. c) 3 eq **VIII.33 - VIII.37** or **VIII.45**, 10 mol% C_p*$RuCl(PPh_3)_2$, toluene, 60°C, 6h. d) $HOAc/CH_2Cl_2$ (1/1), rt, 24h.

Scheme XII-7: Combinatorial synthesis

From the yields presented in **Table VIII-7 – VIII-13,** it can be concluded that strong electron withdrawing groups (e.g. NO_2, CN) render the cyclization/release more difficult, resulting in significantly lower yields under the established conditions, whereas the sterical hindrance induced by the first diversity point (R_1) does not drastically impede the final synthesis step. In **Figure XII-3**, as an illustration of the statement above, a set of compounds are presented with the obtained isolated yields.

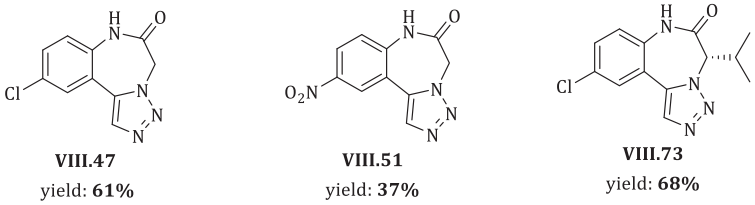

Figure XII-3: Selected compounds indicating trends towards cyclization/release

To a further extent, this research involved the modification of the triazole to afford 1,4,5-trisubstituted triazole moieties. Apart from prescribed *post*-solid-phase modifications of

compounds **VIII.47-VIII.82**, we aimed for an incorporation of internal alkynes into the synthesis scheme. The latter involved both building block synthesis and optimization of the RuAAC towards the preferred regioisomer of the 1,4,5-trisubstituted triazole moiety. Building blocks (**IX.13 – IX.16**, **IX.31**, **IX.42 – IX.47**) were readily synthesized *via* a Sonogashira cross-coupling between commercially available 2-iodoanilines and an excess of a terminal acetylene. In order to allow electron-donating ring substituents, such as an alkoxy moiety, a more elaborate synthesis was required in order to achieve the desired compounds **IX.51** and **IX.54**.

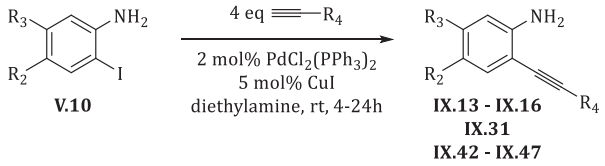

Scheme XII-8: Standard Sonogashira cross-coupling procedure

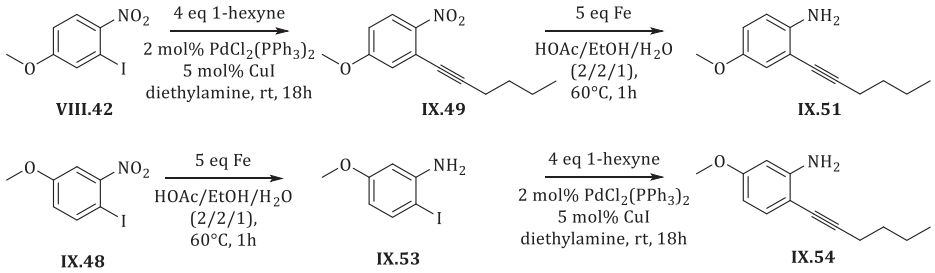

Scheme XII-9: Synthesis of 2-hexynyl-4-methoxyaniline (IX.51) and 2-hexynyl-5-methoxyaniline (IX.54)

Compounds **IX.13-IX.16** were used in an optimization procedure in order to gain more insight in the regioselectivity of the RuAAC with asymmetrical internal alkynes (see section **IX.C**). From the results obtained in this section, it can be concluded that the presence of the aniline strongly promotes the formation of the intended 1,5-regioisomer. Additionally, for **IX.31** with a more balanced electron density on both alkynyl carbons, a lower regioselectivity was observed during the RuAAC.

Table XII-2: Overall yields of 2-alkynylaniline building blocks IX.13 – IX.16, IX.31, IX.42 – IX.47, IX.51 and IX.54

entry	compound	R_2	R_3	R_4	yield (%)
1	**IX.13**	H	H	$(CH_2)_3CH_3$	94
2	**IX.14**	H	H	$(CH_2)_2Ph$	82
3	**IX.15**	H	H	CH_2Ph	98
4	**IX.16**	H	H	Ph	95
5	**IX.31**	H	H	*p*-NH_2-Ph	85
6	**IX.42**	Cl	H	$(CH_2)_3CH_3$	97
7	**IX.43**	Br	H	$(CH_2)_3CH_3$	93
8	**IX.44**	H	Cl	$(CH_2)_3CH_3$	98
9	**IX.45**	Cl	H	$(CH_2)_2OH$	95
10	**IX.46**	Cl	H	Ph	92
11	**IX.47**	Br	H	Ph	94
12	**IX.51**	OMe	H	$(CH_2)_3CH_3$	48
13	**IX.54**	H	OMe	$(CH_2)_3CH_3$	54

From a proof of principle library with three α-amino acids and four internal alkyne building blocks **IX.13-IX.16**, verifying the effectiveness of the cyclization/release conditions, it could be concluded that compounds containing building block **IX.15** produced too low amounts for further characterization. At a later stage, this building block with this specific alkyne modification was excluded from the combinatorial synthesis strategy which was performed according to **Scheme XII-8** with eight α-amino acids and seven internal alkyne building blocks (**IX.42 - IX.43, IX.45 - IX.47, IX.51** and **IX.54**) yielding twenty-five compounds[ii].

[ii] Not all combinations were made. Building block **IX.44** was not included due to time limitations.

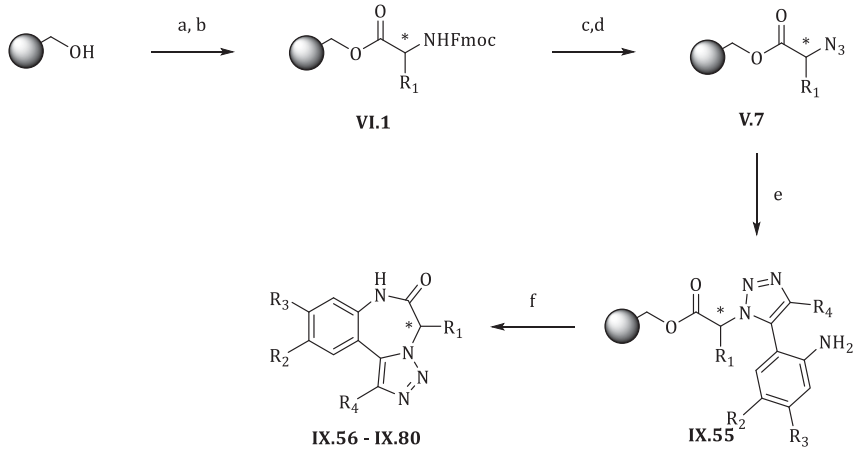

α-amino acids

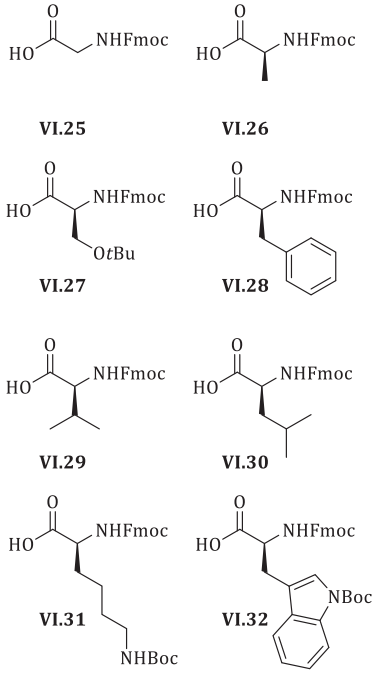

2-ethynylaniline building blocks

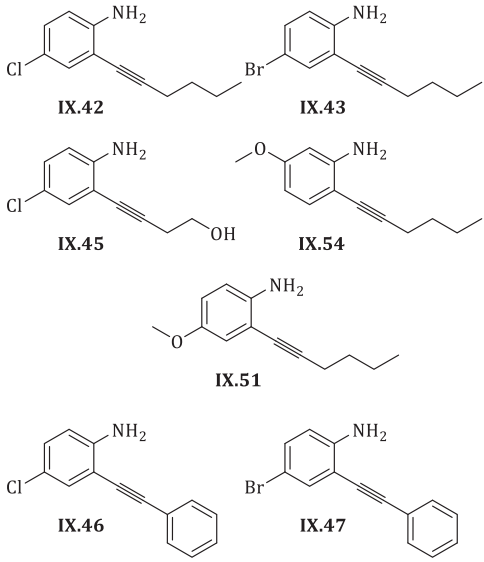

a) 2 eq Fmoc-AA-OH, 2 eq DIC, 0,2 eq DMAP, CH_2Cl_2, rt, 2x 24h b) Ac_2O, CH_2Cl_2, DIPEA (1/1/3) c) 1) 20 v/v% 4-Me-piperidine/DMF, rt, 2x 10 min. d) 1,2 eq imidazole-1-sulfonyl azide hydrochloride, 2 eq TEA, 1 mol% $CuSO_4.5H_2O$, THF/H_2O (1/1), rt, 24h. e) 3 eq alkyne, **§IX.6** f) HOAc/CH_2Cl_2 (1/1), rt, 24h.

Scheme XII-10

E. Bioisosteric replacement

In order to achieve some insights in the applicability of the synthesis scheme towards the inclusion of a pyridine motif instead of a benzene motif as central element in the scaffold, a set of 3-alkynyl-aminopyridine **X.6-X.9** building blocks were synthesized in good yields. A proof of principle library was constructed in order to achieve early understanding on the synthesis behavior. In total, five compounds (**X.11-X.15, Figure XII-4**) were synthesized in considerably lower yields (9-26%) compared to the yield observed earlier with 2-alkynylaniline building blocks. As the RuAAC proceeded smoothly, the lower yields are attributed to a disfavored cyclization/release due to protonation of 2-aminopyridine intermediates resulting in a non-nucleophilic ammonium derivative. Solutions for this problem are addressed in section **XI.F.**

Table XII-3: Overall yields for 3-alkynyl-aminopyridine X.6-X.8 building blocks

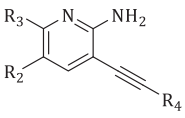

X.6 - X.9

entry	compound	R_2	R_3	R_4	yield (%)
1	**X.6**	H	H	H	76
2	**X.7**	Br	H	H	92
3	**X.8**	H	H	$(CH_2)_3CH_3$	87
4	**X.9**	H	H	Ph	99

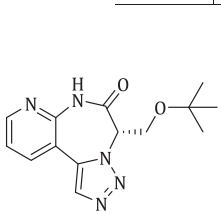

X.11
yield: **9%**

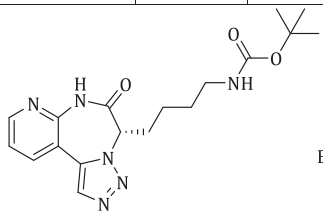

X.12
yield: **13%**

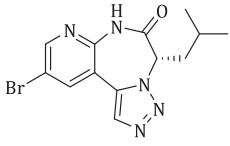

X.13
yield: **26%**

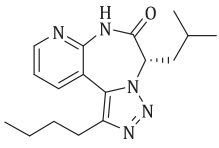

X.14
yield: **22%**

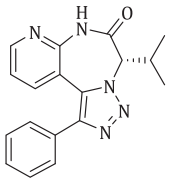

X.15
yield: **19%**

Figure XII-4: [1,2,3]triazolo[1,5-*d*]pyrido[3,2-*f*][1,4]diazepin-2-ones: proof of principle library results

F. *N*-alkylation

A final possibility for introducing diversity on the scaffold moiety was investigated by exploring *N*-alkylation before or after cyclization/release. Initially, we aimed for a comprehensive strategy including *N*-monoalkylation on solid-phase by performing an alkylation *via* a Mitsunobu-Fukuyama strategy (see section **XI.B** and section **XI.C**) or *via* a reductive alkylation (see section **XI.D**). Both methods failed due to low efficiency. Moreover, the *N*-monoalkylation impeded the cyclization/release, therefore disabling scaffold formation.

In more detail, as illustrated as **Pathway A** in **Scheme XII-11**, the Mitsunobu-Fukuyama strategy for this scaffold design required a high excess of different reagents in order to protect the aniline functionality with the required nosyl activating/protecting group. After a straightforward alkylation step with three different alcohols and the successive nosyl removal, the cyclization/release strategy appeared to be problematic. Additionally, we investigated the RuAAC with *o*-Ns protected building blocks which failed in efficiency.

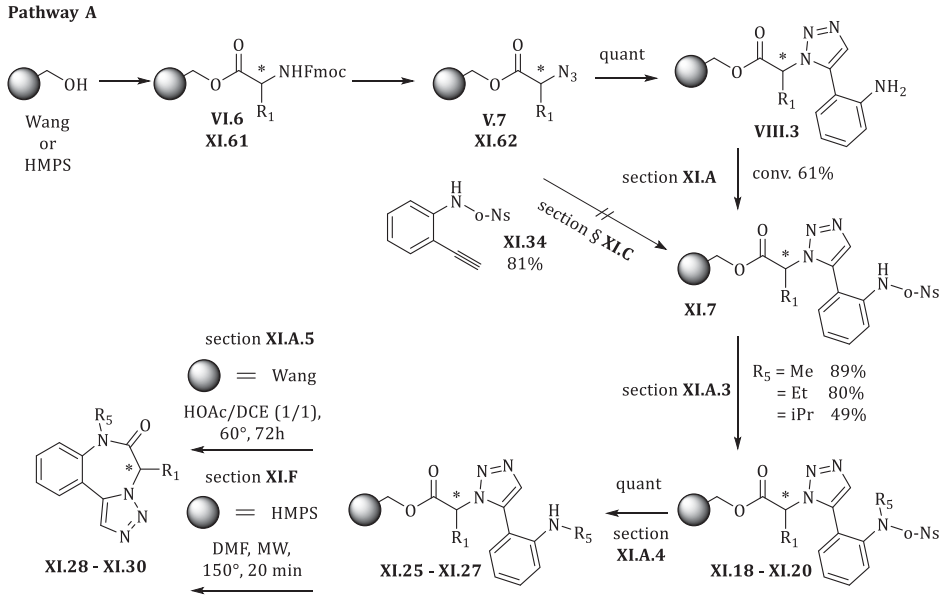

Scheme XII-11: Mitsunobu-Fukuyama strategy aiming *N*-monoalkylation on solid-phase

As an alternative, **Pathway B** in **Scheme XII-12** shows a reductive alkylation which was performed using different aldehydes leading to conditions in which *N*-monoalkylation occurred. However, a solution for a selective and effective cyclization/release could not be developed.

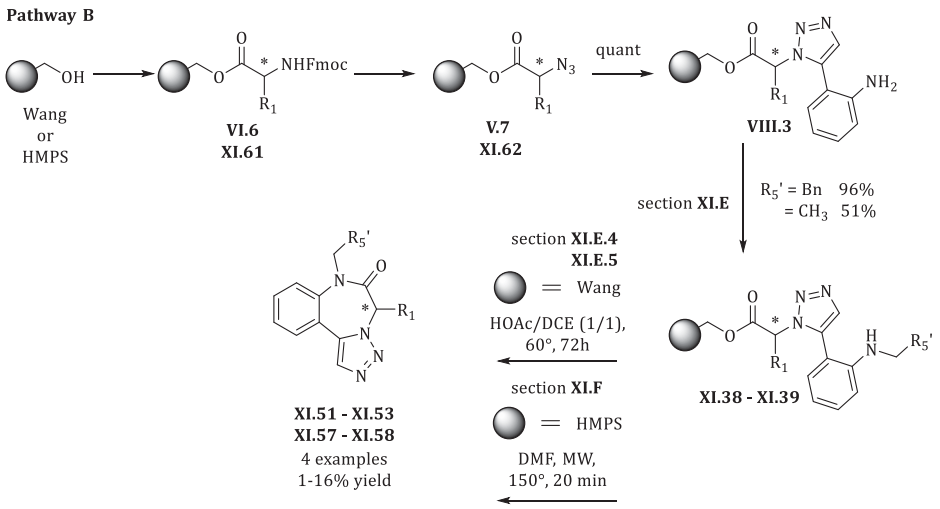

Scheme XII-12: Reductive alkylation strategy aiming *N*-monoalkylation on solid-phase

Despite many efforts to accomplish a complete solid-phase strategy, both routes were abandoned (see section **XI.G**) and *N*-alkylation was performed in solution with different alkyl halides upon addition of a base (**Scheme XII-13**). As a compromise, racemization of the final compounds was allowed under these conditions. With respect to the final purpose of this work, preliminary biological screening in a future stage of this research theme in our laboratory, racemization was not perceived as a disadvantage. After employing a parallel synthesis, twenty-seven *N*-alkylated compounds were synthesized and characterized.

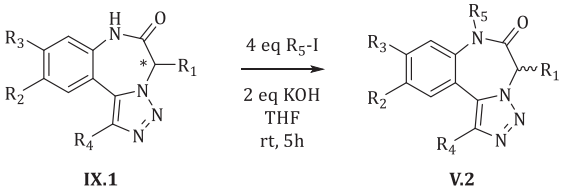

Scheme XII-13: *N*-alkylation in solution-phase

G. Recent literature report

After finishing the practical work of this PhD research project, Molteni[1] published a report on the synthesis of [1,2,3]triazole[1,5-*d*]benzo[1,4]diazepin-2-ones **V.2.** By using a Huisgen cycloaddition reaction to construct the triazolobenzodiazepine core, a small set of derivatives **XII.1-XII.5** was prepared as illustratated in **Scheme XII-14** and **Table XII-4**.

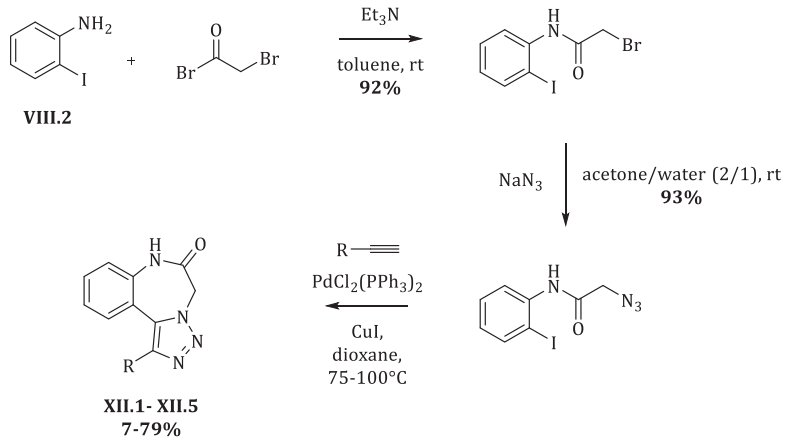

Scheme XII-14: In solution synthesis of [1,2,3]triazole[1,5-*d*]benzo[1,4]diazepines XII.1-XII.5 reported by Molteni

Table XII-4: Results for a in solution synthesis of [1,2,3]triazole[1,5-*d*]benzo[1,4]diazepines XII.1-XII.5 obtained by Molteni

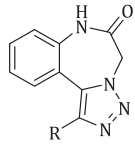

XII.1- XII.5

entry	compound	R	yield (%)
1	**XII.1**	Ph	60
2	**XII.2**	COOMe	35
3	**XII.3**	CH_2OH	37
4	**XII.4**	$(CH_2)_3OH$	79
5	**XII.5**	CH(OH)Ph	7

From the results above and especially entries **1**,**3** and **4**, it can be concluded that comparable yields can be obtained both in solution and on solid-phase. The synthesis of Molteni is more concise and scaffold-oriented. Nonetheless, library synthesis would be more favored by a solid-phase approach allowing a more high throughput strategy.

H. Future perspectives

Further exploration of the chemical space is needed to perform a well-thought decoration of the scaffold based on future preliminary *in vitro* screening results. **Figure XII-3** and **Figure XII-4** illustrate different non-exhaustive ways for further diversifying the targeted scaffold starting from the basic concepts established in this work.

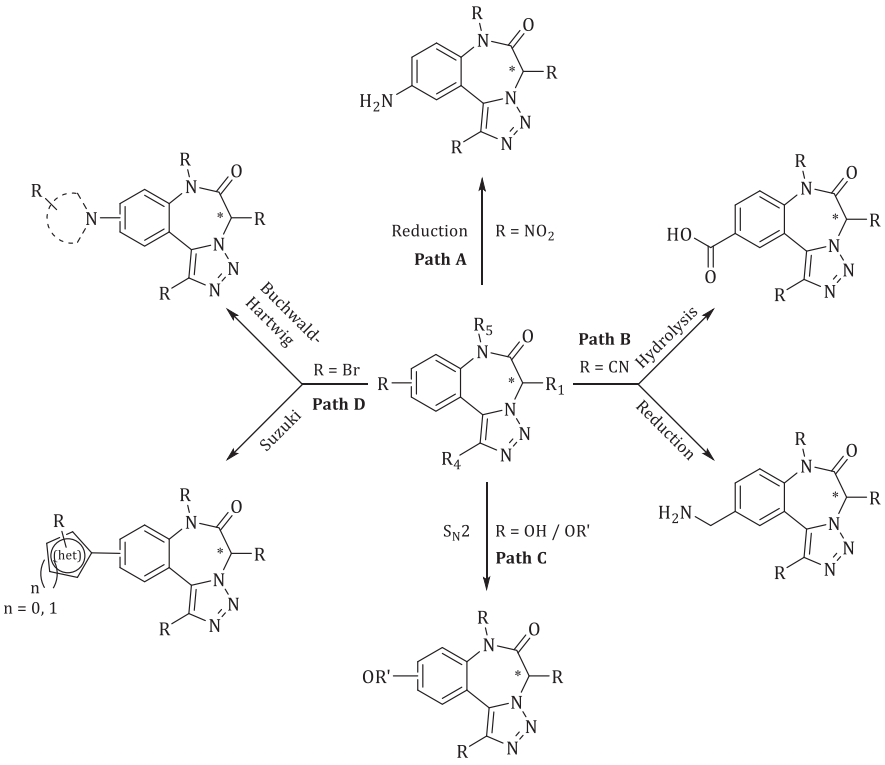

Figure XII-5 Future perspectives regarding variations of the aromatic moiety

Path A and **B** illustrate the introduction of respectively a nitro and cyano functionalities into the scaffold moiety, which could be transformed into reactive groups upon reduction or hydrolysis. Both steps can be undertaken in order to reduce lipophilicity *via* a reaction with a polar chain.

Path C (*O*-alkylation) can preferably be part of well-considered building block synthesis before the solid-phase chemistry strategy.

Path D can both be performed as a *post*-modification of the synthesized scaffold bearing a bromine on the aromatic ring or can be introduced *via* suitable building block synthesis. Thanks to the broad scope of both the Suzuki coupling and the Buchwald-Hartwig coupling, respectively a plethora of (hetero)aromatic groups and amine bearing functionalities could be incorporated onto the scaffold molecule, enabling and inducing specific receptor interactions.

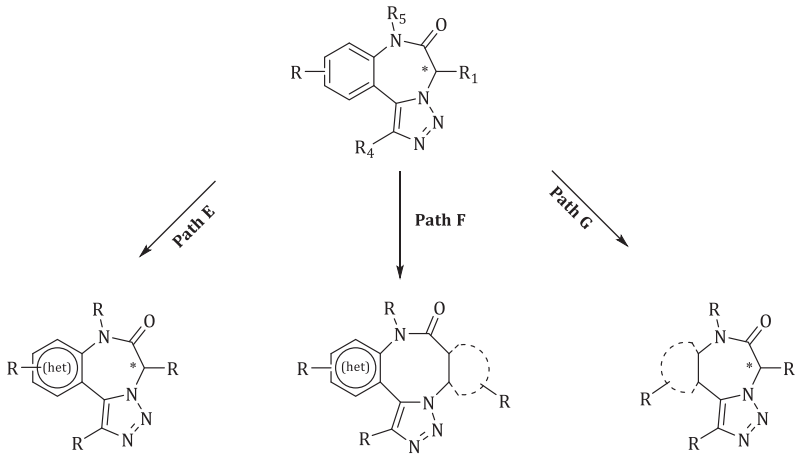

Figure XII-6: Profound scaffold modifications resulting in new classes of benzodiazepine motives

Path E describes the introduction of different heteroaromatic moieties in order to attain new scaffold molecules. Preliminary observations in chapter **X** clearly indicated the possible successes and problems to overcome.

Path F extends the predominant idea of constructing a seven-membered diazepine ring, as introducing (cyclic) β-amino acids would enable the synthesis of an eight-membered diazocine ring equivalent. In combination with (hetero)aromatic building blocks, this would lead to completely new scaffolds.

At last, **Path G**, suggests the idea of a saturated diazepine triazole mimic based on the proposed synthesis above. Starting from diversified aminoalcohols, a combination of an amine and alkyne moiety in a alicyclic system would enable cyclization/release, leading to new diazepine motives.

REFERENCES

[1] Molteni, G. *Heterocycles* **2013**, *87*, 1765-1773.

PART 4: SUPPORTING INFORMATION

XIII. Analytical information

A. General

All solid-phase reactions were carried out by using custom-made peptide reactions vessels, with or without an *in*-line filter, or automatically on a Mettler-Toledo Bohdan Miniblock™ High capacity shaking and washing station. Reagents were purchased from Aldrich, Novabiochem, Acros or TCI and used without purification. Solvents were used without drying unless noted otherwise. Dioxane, diethyl ether (Et_2O) and tetrahydrofuran (THF) were distilled from sodium/benzophenone and toluene from sodium. 1,2-Dichloroethane (DCE), dichloromethane (CH_2Cl_2), 2,3,5-collidine, pyridine and trietylamine (NEt_3) were distilled from calcium hydride.

Solid-phase reactions were monitored *via* LC-MS analyses upon cleavage of an aliquot of the reacted beads with TFA/H_2O (95/5) for two hours at room temperature and subsequent azeotropic evaporation of the supernatant with acetonitrile (3x). The residue was used for LC-MS sample preparation.

Reactions in solution were monitored by thin layer chromatography (TLC) on 0.25mm Macherey-Nagel SIL G-25 UV254 silica gel plates. Visualization occurred by UV-light (254 nm) and/or by staining in a molybdene solution (0.4 g $Ce(SO_4)_2$, 10 g $(NH_4)_6Mo_7O_{24}$ $4H_2O$, 200 ml H_2O and 10 ml conc. H_2SO_4) or a permanganate solution (3 g $KMnO_4$, 20 g K_2CO_3, 5 ml 5% aqueous NaOH and 300 ml H_2O).

Solid-phase reactions under microwave irradiation were performed with a CEM Focussed Microwave Synthesis system, model Discover in specifically designed reaction vessels.

All compounds were characterized by ^1H NMR and ^{13}C NMR spectroscopy. Nuclear Magnetic Resonance spectra were recorded on a 300 MHz Bruker Avance or 500 MHz Bruker DRX500 instrument. All ^1H NMR are reported in δ units, parts per million (ppm), and were measured relative to tetramethylsilane (TMS) using the residual solvent signal as a reference, while coupling constants (J) are noted in Hz. All ^{13}C NMR are recorded with a coupled proton test. The residual ^1H and ^{13}C signals are for $CDCl_3$ (7.26 ppm or 77.00 ppm), for CD_3OD (3.31 ppm

or 49.15 ppm) for benzene (7.16 ppm or 128.06 ppm) and for acetone-d_6 (2.05 ppm or 29.84 ppm). The following abbreviations were used to explain the multiplicities: s = singlet, d = doublet, t = triplet, q = quartet, m = multiplet, dd = doublet of doublets, dt = doublet of triplets. Peaks were assigned with the aid of homonuclear (^{1}H-^{1}H) correlation spectroscopy (COSY) and heteronuclear (^{1}H-^{13}C) correlation spectroscopy (HMQC and HMBC) when required. In the case of distinct signals for atropisomers present, the assignment will diversify by annotating A to the major atropisomer and B to the minor atropisomer.

All IR spectra were taken on a Perkin – Elmer 1000 FTIR with HATR module. Peaks are annotated with a relative intensity with following abbreviations: w = weak, m = medium, s = strong. UV-VIS spectra were recorded with a Hitachi U-2010 UV-VIS spectrophotometer.

All LC-MS analysis were performed with an Agilent 1100 Series HPLC with ES-single quad MS detector (type VL) on a reversed phase column (Phenomenex Luna C18 (2) 5µm/250mm x 4,6mm, conditions **1-4** or Phenomenex Kinetex 5µm/150mm x 4,6mm, condition **5**) with an injection volume of 25µL (concentration: 1 mg/ml), a flow of 1 ml/min at a temperature of 35°C. Different mobile phase conditions were employed during this research.

Mobile phase **condition 1**: A: 5mM NH_4OAc in H_2O B: CH_3CN

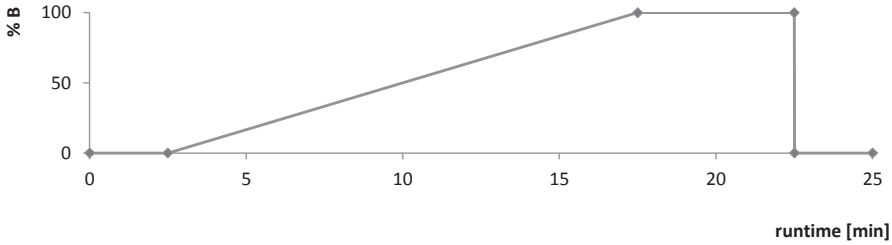

Mobile phase **condition 2**: A: 5mM NH_4OAc in H_2O B: CH_3CN

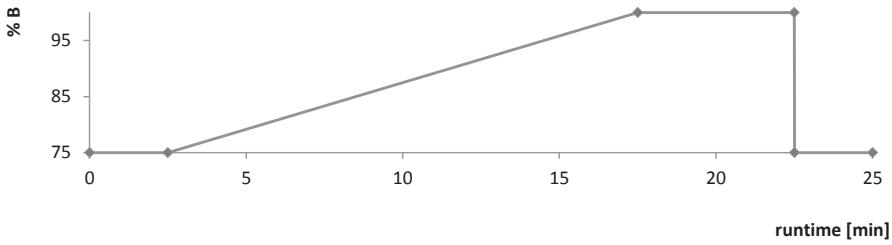

Mobile phase **condition 3**: A: 5mM NH_4OAc in H_2O B: CH_3CN

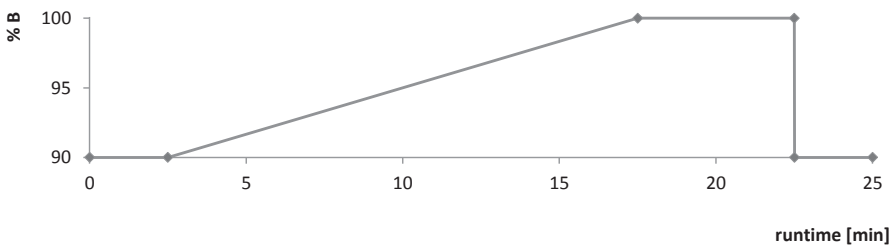

Mobile phase **condition 4**: A: 5mM NH_4OAc in H_2O B: CH_3CN

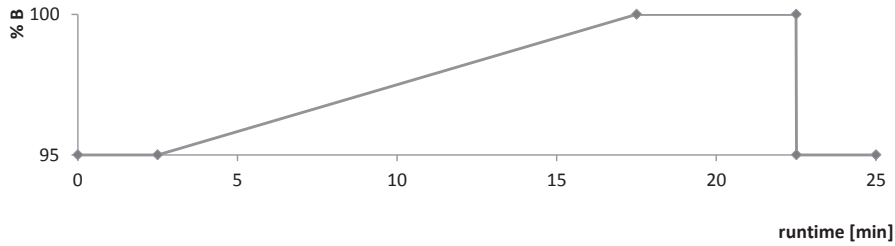

Mobile phase **condition 5**: A: 5mM NH_4OAc in H_2O B: CH_3CN

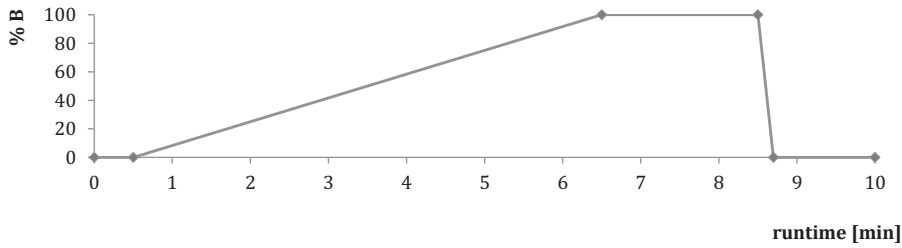

Mobile phase **condition 6**: A: 5mM NH_4OAc in H_2O B: CH_3CN

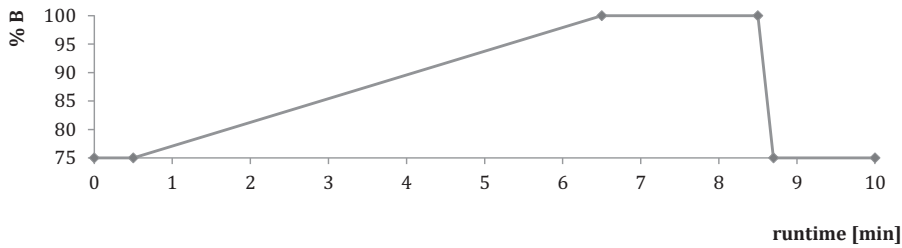

Chiral HPLC analysis was performed with an Agilent 1100 Series with a DAD detector employing a Chiralcel OD-H or AS-H column and an eluent flow of 1 mL/min at 35°C. Specific eluent conditions were determined with a racemic mixture of the specific compound.

All high resolution LC-MS analysis were performed with an Agilent 6220A Time Of Flight MS detector coupled with an Agilent 1100 Series HPLC system.

Melting point (if available) were determined *via* a Kofler bench which is calibrated by using a compound with a comparable melting point.

XIV. Coupling

A. Coupling of Fmoc-AA-OH to Wang resin V.3

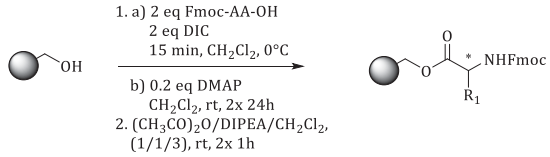

V.3	R_1 =	-H	**L-VI.33**
		$-CH_3$	**L-VI.34**
		$-CH_2O(t\text{Bu})$	**L-VI.35**
		$-CH_2Ph$	**L-VI.36**
		$-CH(CH_3)_2$	**L-VI.37**
		$-CH_2CH(CH_3)_2$	**L-VI.38**
		$-(CH_2)_4NHBoc$	**L-VI.39**
		$-(CH_2)$-3-indoyl-*N*(Boc)	**L-VI.40**

General procedure **P.01**: Fmoc-AA-OH (2 eq) was preactivated to an *O*-acylisourea by a dropwise addition of DIC (2 eq) to an ice-cooled suspension of the Fmoc-AA-OH in dry dichloromethane (0.1M) under Ar atmosphere. After 15 minutes, this preactivated mixture was carefully added to the prewashed Wang resin in a reaction vessel (1 eq) by using a minimal volume of extra dry solvent. Afterwards, DMAP (0.2 eq) was added to the reaction mixture. After 24 hours of shaking, the resin was filtered and washed with 3x DMF, 3x MeOH, 3x (dry) dichloromethane. This coupling reaction was repeated. After this second treatment, the residual alcohol functionalities were inactivated or capped by treating the resin twice with AcOAc/DIPEA/dichloromethane (1/1/3) for 2 hours with an intermediate washing procedure (3x DMF, 3x MeOH, 3x dichloromethane). At last, the resin was dried extensively under

reduced pressure. Whereupon, the loading of the resin was determined *via* a standard Fmoc determination using UV-VIS analysis.

B. Deprotection of Fmoc-protecting group

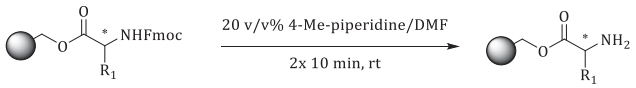

R_1 =			R_1 =		
	-H	**L-VI.33**		-H	**L-VI.41**
	$-CH_3$	**L-VI.34**		$-CH_3$	**L-VI.42**
	$-CH_2O(tBu)$	**L-VI.35**		$-CH_2O(tBu)$	**L-VI.43**
	$-CH_2Ph$	**L-VI.36**		$-CH_2Ph$	**L-VI.44**
	$-CH(CH_3)_2$	**L-VI.37**		$-CH(CH_3)_2$	**L-VI.45**
	$-CH_2CH(CH_3)_2$	**L-VI.38**		$-CH_2CH(CH_3)_2$	**L-VI.46**
	$-(CH_2)_4NHBoc$	**L-VI.39**		$-(CH_2)_4NHBoc$	**L-VI.47**
	-(CH_2)-3-indoyl-*N*(Boc)	**L-VI.40**		-(CH_2)-3 indoyl-*N*(Boc)	**L-VI.48**

General procedure **P.02**: The resin was treated twice with a solution of 4-Me-piperidine in DMF (20 v/v%) for 15 minutes at room temperature, with an intermediate washing step (3x DMF, 3x MeOH, 3x dichloromethane, 2x DMF). After completion of the second treatment the resin is washed with 3x DMF, 3x MeOH, 3x dichloromethane and dried extensively under reduced pressure.

XV. Diazotransfer

A. Synthesis of imidazole-1-sulfonyl azide hydrochloride (VII.11)

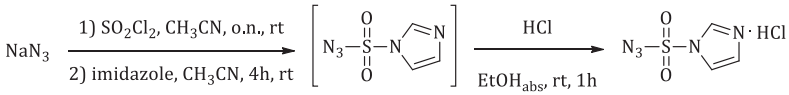

VII.14 **VII.11**

Sodium azide (26.01 g, 400 mmol, 1 eq) is added portionwise to an ice-cooled solution of acetonitrile (400 mL, 1M). After agitation for 15 minutes at 0°C, sulfurylchloride (32.4 mL, 400 mmol, 1 eq) is added dropwise to the suspension for a time period of 40 minutes. After maintaining the temperature at 0°C for 15 minutes, the ice bath is removed and the reaction mixture is stirred for an additional 12 hours overnight at room temperature.

Subsequently, the mixture is cooled to 0°C and imidazole (52.8 g, 800 mmol, 2 eq) is added portionwise to the solution whereupon the ice bath is removed and the reaction continues for 4 hours at room temperature. After this time the reaction mixture is transferred in a separation funnel and diluted with EtOAc (800 mL). The organic phase is washed with 10% NaCl-solution (2x 800 mL), saturated $NaHCO_3$-solution (2x 800mL) and saturated brine solution (2x 800 mL). The washed organic phase is dried over $MgSO_4$.

Meanwhile, acetyl chloride (43 mL, 602.5 mmol, 1.5 eq) is added dropwise to an ice-cooled solution of EtOH (150 mL) over 1 hour and after this time, the mixture is stirred for an additional 3 hours while maintaining the temperature at 0°C.

After filtering off $MgSO_4$ from the organic phase, the formed HCl-solution is added dropwise to the dried organic phase at 0°C while stirring gently, resulting in the formation of white crystals. Upon addition of the dry HCl-EtOH solution, this mixture is stirred at very low speed for one hour at 0°C. Subsequently, the white crystals **VII.11** are filtered off, washed with EtOAc and dried *in vacuo*.

Yield: 82%. imidazole-1-sulfonyl azide hydrochloride (68.81 g, 328.2 mmol).
White crystals.
Molecular weight: 209.61 Da.
^{1}H NMR (300 MHz, D_2O): δ 7.64 (d, J = 1.0Hz, 1H), 8.05 (d, J = 1.0Hz, 1H), 9.45 (s, 1H).
^{13}C NMR (75 MHz, D_2O): δ 120.2 (CH), 122.9 (CH), 137.6 (CH).
HATR (cm^{-1}): 3101 (m), 3056 (m), 2987 (w), 2911 (w), 2490 (m), 2426 (m), 2364 (m), 2312 (m), 2169 (s), 1914 (w), 1581 (m), 1507 (m), 1455 (m), 1425 (s), 1321 (w), 1298 (m), 1229 (s), 1187 (s), 1152 (s), 1137 (s), 1102 (s), 1068 (s), 982 (m), 968 (m), 900 (m), 837 (s), 776 (s), 762 (s), 630 (s).

B. Optimization procedure: diazotransfer reaction

1. Influence of the solvent

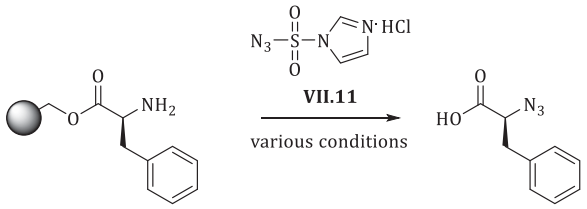

VI.36 **VII.10**

After pouring solid-phase bound L-phenylalanine (**VI.36**, 0.06584 mmol, 1 eq) in a 1 mL closed reaction vessel, imidazole-1-sulfonyl azide hydrochloride (**VII.11**, 16.5 mg, 0.07901 mmol, 1.2 eq) was added to the vessel, followed by solvent according to **Table XV-1.** Subsequently, standard solutions of $CuSO_4.5H_2O$ in MeOH and H_2O were made to ease the process of adding Cu(II) catalyst (**Table XV-2**). For entries 1, 4, 5 and 6, $CuSO_4.5H_2O$ was added in one portion.

After adding solvent and Cu(II)-catalyst, triethylamine (18.2 µL, 0.1317 mmol, 2 eq) was added. Reactions were put into the Mettler-Toledo Bohdan Miniblock™ high capacity shaking and washing station for 24 hours. After reaction time, the beads were isolated and washed with DMF (3x 2 mL), MeOH (3x 2 mL) and dichloromethane (3x 2 mL).

Cleavage: After drying *in vacuo*, an aliquot of the resin was transferred into a 1 mL closed reaction vessel and 1 mL TFA/H_2O (95/5) was added, after two hours shaking the

supernatant was isolated, the beads washed with dichloromethane (3x 2 mL) and the supernatant was evaporated under reduced pressure with acetonitrile. LC-MS analysis (condition 1) at 214 nm was used to determine the conversion of the amine into azide. The remaining beads were used for a qualitative IR analysis.

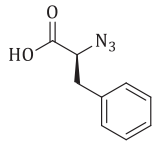

VII.10

Molecular weight: 191.19 Da.
LC-(ESI)MS (condition 1): t_R = 10.4 min, $[M- H]^-$: 190.1 (100%).
HATR (cm^{-1}): 3058 (w), 3025 (w), 2922 (w), 2851 (w), 2107 (s), 1736 (s), 1677 (m), 1611 (m), 1600 (m), 1584 (m), 1512 (s), 1492 (s), 1452 (s), 1379 (m), 1303 (m), 1223 (s), 1172 (s), 1113 (w), 1082 (w), 1016 (m), 909 (w), 874 (w), 821 (s), 756 (s), 697 (s), 621 (w).

Table XV-1: Solvent conditions optimization procedure

entry	CH_2Cl_2	MeOH	DMF	THF	Standard solution	$CuSO_4.5H_2O$
1	660 µL					0.2 mg
2	595 µL				65 µL Solution **1**	
3	530 µL	65µL			65 µL Solution **2**	
4			660 µL			0.2 mg
5	66 µL		594 µL			0.2 mg
6				660 µL		0.2 mg
7				594 µL	65 µL Solution **2**	
8				530 µL	130 µL Solution **3**	
9				460 µL	200 µL Solution **4**	
10				400 µL	265 µL Solution **5**	
11				330 µL	330 µL Solution **6**	
12				265 µL	400 µL Solution **7**	
13				200 µL	460 µL Solution **8**	
14				130 µL	530 µL Solution **9**	
15				65 µL	594 µL Solution **10**	
16				0 µL	660 µL Solution **11**	

Table XV-2: Concentration standard solutions $CuSO_4.5H_2O$ in MeOH (entry 1) or H_2O (entries 2-11)

Solution	$CuSO_4.5H_2O$ in MeOH (100 mL)
1	2.500 g/L
Solution	**$CuSO_4.5H_2O$ in H_2O (100 mL)**
2	2.500 g/L
3	1.250 g/L
4	0.833 g/L
5	0.625 g/L
6	0.500 g/L
7	0.416 g/L
8	0.357 g/L
9	0.313 g/L
10	0.278 g/L
11	0.250 g/L

2. Influence of the base

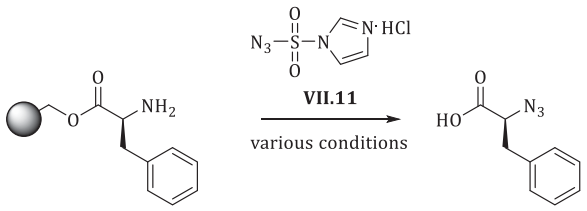

VI.36 **VII.10**

A standard solution of $CuSO_4.5H_2O$ in H_2O (10 mL, 0.500 g/L) was made in order to ease the addition of Cu(II)-catalyst to the test reaction.

Two test reactions were set up by pouring solid-phase bound L-phenylalanine (**VI.36**, 0.06584 mmol, 1 eq) in two 1 mL closed reaction vessels, imidazole-1-sulfonyl azide hydrochloride (**VII.11**, 16.5 mg, 0.07901 mmol, 1.2 eq) was added to the vessels, followed by 330 µL THF and 330 µL standard solution of $CuSO_4.5H_2O$ in H_2O for each vessel.

Subsequently, one test reaction was treated with triethylamine (18.2 µL, 0.1317 mmol, 2 eq) and the other with diisopropylethylamine (23.0 µL, 0.1317 mmol, 2 eq). Both reactions were

put into the Mettler-Toledo Bohdan Miniblock™ high capacity shaking and washing station for 24 hours. After reaction time, the beads were isolated and washed with DMF (3x 2 mL), MeOH (3x 2 mL) and dichloromethane (3x 2 mL).

Cleavage: After drying *in vacuo*, an aliquot was transferred into a 1 mL closed reaction vessel and 1 mL TFA/H_2O (95/5) was added, after two hours shaking the supernatant was isolated, the beads washed with dichloromethane (3x 2 mL) and the supernatant was evaporated under reduced pressure with acetonitrile. LC-MS analysis (condition 1) at 214 nm was used to determine the conversion of the amine into azide.

3. Influence of equivalents of diazotransfer reagent VII.11, base and reaction temperature

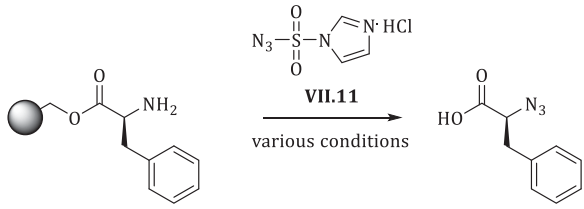

VI.36 **VII.10**

Four test reactions (**Table XV-3**, entries **1-4**) were set up by pouring solid-phase bound L-phenylalanine (**VI.36,** 0.06584 mmol, 1 eq) in four 1 mL closed reaction vessels. To each reaction vessel imidazole-1-sulfonyl azide hydrochloride (**VII.11**, 16.5 mg, 0.07901 mmol, 1.2 eq) or (**VII.11**, 27.5 mg, 0.1317 mmol, 2 eq) was added to the vessels, followed by 330 µL THF and 330 µL standard solution **6** of $CuSO_4.5H_2O$ in H_2O prepared in previous section.

Subsequently, the test reactions were treated with triethylamine (18.2 µL, 0.1317 mmol, 2 eq) or (27.3 µL, 0.1975 mmol, 3 eq). Two test reactions were put into the Mettler-Toledo Bohdan Miniblock™ high capacity shaking and washing station for 24 hours at 50°C. The remaining other two reactions were shaken at room temperature for 24 hours. After reaction time, the beads were isolated and washed with DMF (3x 2 mL), MeOH (3x 2 mL) and dichloromethane (3x 2 mL).

Cleavage: After drying *in vacuo*, an aliquot was transferred into a 1 mL closed reaction vessel and 1 mL TFA/H_2O (95/5) was added, after two hours shaking the supernatant was isolated, the beads washed with dichloromethane (3x 2 mL) and the supernatant was evaporated under reduced pressure with acetonitrile. LC-MS analysis (condition 1) at 214 nm was used to determine the conversion of the amine into azide.

Table XV-3: Conditions optimizing equivalents of VII.11 and reaction temperature

entry	VII.11	TEA	T (°C)
1	1.2 eq	2 eq	25
2	2 eq	3 eq	25
3	1.2 eq	2 eq	50
4	2 eq	3 eq	50

4. Determination of epimerization during diazotransfer reaction

In order to verify the enantiomeric purity of the diazotransfer reaction, eight tripeptides were synthesized. In the following paragraphs, the focus lays on the synthesis of two azido tripeptides which eventually led to a successful HPLC separation.

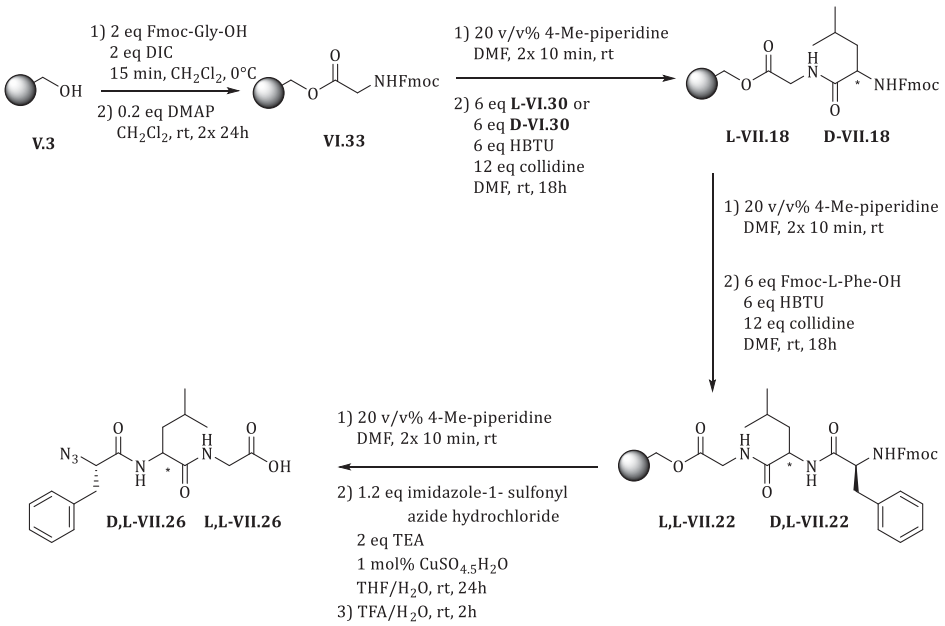

Scheme XV-1: Synthesis of azido tripeptides L,L-VII.26 and D,L-VII.26

- Coupling of Fmoc-Gly-OH:

Following general procedure **P.01.** After the capping procedure, the resin is dried extensively and the loading is verified *via* Fmoc-deprotection determination method. **Loading:** 0.5037 $mmol.g^{-1}$.

- Coupling of Fmoc-L-Leu-OH **L-VI.30** and Fmoc D-Leu-OH **D-VI.30** to **VI.33**

Activation: The α-amino acids are separately preactivated by adding HBTU (57.3 mg, 0.1511 mmol, 6 eq) to Fmoc-L-Leu-OH (**L-VI.30,** 53.4 mg, 0.1511 mmol, 6 eq) or Fmoc-D-Leu-OH (**D-VI.29**, 53.4 mg, 0.1511 mmol, 6 eq) and collidine (40 µL, 0.3022 mmol, 12 eq) in 300 µL DMF (1M). This pre-activation reaction is shaken for 10 minutes at room temperature.

Coupling: Two batches of Fmoc-Gly-OH on Wang resin **VI.33** (50 mg, 0.02519 mmol, 1 eq) are deprotected *via* general procedure **P.02**. After this deprotection the resin is washed with DMF (3x 1 mL). The coupling reaction is initiated by adding the preactivated mixture to the resin. After 18 hours of shaking at room temperature, the reaction was stopped and washed with DMF (3x 1 mL), MeOH (3x 1 mL), dichloromethane (3x 1 mL) and DMF (3x 1mL).

- Coupling of Fmoc-L-Phe-OH (**L-VI.28**)

Activation: This activation procedure is performed twice in order to synthesize two tripeptides **L,L-VII.22** and **D,L-VII.22**. For each tripeptide, Fmoc-L-Phe-OH (58.6 mg, 0.1511 mmol, 6 eq) is preactivated upon addition of HBTU (57.3 mg, 0.1511 mmol, 6 eq) and collidine (40 µL, 0.3022 mmol, 12 eq) in 300 µL DMF (1M). This pre-activation reaction is shaken for 10 minutes at room temperature.

Coupling: Two dipeptides **L,L-VII.22** and **D,L-VII.22** (0.02519 mmol, 1 eq) are deprotected *via* general procedure **P.02**. After this deprotection step, both dipeptides are washed with DMF (3x 1 mL). The coupling reaction of the third α-amino acids is started by adding the preactivated mixture of Fmoc-L-Phe-OH to the resin. After 18 hours of shaking at room temperature, the reaction was stopped and washed with DMF (3x 1 mL), MeOH (3x 1 mL), dichloromethane (3x 1 mL).

- Diazotransfer on tripeptides **L,L-VII.22** and **D,L-VII.22**

The two batches loaded with tripeptide **L,L-VII.22** and **D,L-VII.22** were Fmoc-deprotected by the standard protocol **P.02**. Subsequently they were washed with THF/H_2O (1/1) (2x 1 mL). After draining the washing solvent, imidazole-1-sulfonyl azide hydrochloride (**VII.11**, 6.3 mg, 0.03022 mmol, 1.2 eq) , 125 µL THF, 125 µL $CuSO_4.5H_2O$ in H_2O solution (0.500 g/L) and TEA (7 µL, 0.05036, 2 eq) were added to both batches. According to the optimized procedure, the reaction proceeded for 24 hours at room temperature. After this time, the beads were filtered off and washed with DMF (3x 1 mL), MeOH (3x 1 mL) and dichloromethane (3x 1 mL).

Cleavage: After drying of the beads *in vacuo*, an aliquot of the two batches **L,L-VII.26** and **D,L-VII.26** was treated with TFA/H_2O (95/5) in order to verify the effectiveness of the performed sequences. After two hours of cleavage at room temperature the supernatant is evaporated azeotropically with acetonitrile (3x 2 mL). The residues of both cleavage reactions were used to prepare samples for LC-MS analysis. Additionally, a third artificial mixture of both residues was made is order to use this sample to obtain HPLC separation. After optimization of the

HPLC eluent conditions with the co-injected sample, the ratio of epimerization could be determined by analyzing the chromatograms for each tripeptide individually.

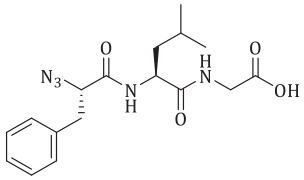

L,L-VII.26

Molecular weight: 361.40 Da.
LC-(ESI)MS (condition 1): t_R = 12.0 min $[M+H^+]^+$: 362.10 (100%).
Crude purity (214 nm): 85%.

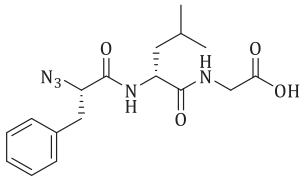

D,L-VII.26

Molecular weight: 361.40 Da.
LC-(ESI)MS (condition 1): t_R = 11.9 min $[M+H^+]^+$: 362.10 (100%).
Crude purity (214 nm): 70%.

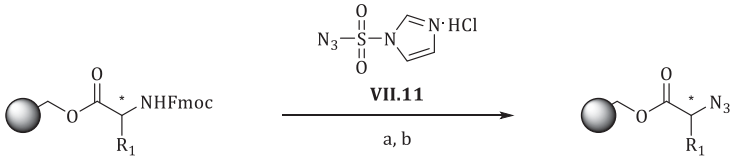

a) 20 v/v% 4-Me-piperidine/DMF, rt, 2x 10 min b) 1.2 eq imidazole-1-sulfonyl azide hydrochloride **(VII.11)**, 2 eq TEA, 1 mol% $CuSO_4.5H_2O$, THF/H_2O, rt, 24h.

R_1 =	-H	**VI.33**	R_1 =	-H	**VII.42**
	$-CH_3$	**VI.34**		$-CH_3$	**VII.43**
	$-CH_2O(t\text{Bu})$	**VI.35**		$-CH_2O(t\text{Bu})$	**VII.44**
	$-CH_2Ph$	**VI.36**		$-CH_2Ph$	**VII.45**
	$-CH(CH_3)_2$	**VI.37**		$-CH(CH_3)_2$	**VII.46**
	$-CH_2CH(CH_3)_2$	**VI.38**		$-CH_2CH(CH_3)_2$	**VII.47**
	$-(CH_2)_4NHBoc$	**VI.39**		$-(CH_2)_4NHBoc$	**VII.48**
	$-(CH_2)$-3-indoyl-N(Boc)	**VI.40**		$-(CH_2)$-3-indoyl-N-(Boc)	**VII.49**

General procedure **P.03** : Before starting the diazotransfer reaction, the resin (1 eq), prepared via general procedure **P.01** - **P.02**, is washed twice with THF/H_2O (1/1). Imidazole-1-sulfonyl azide hydrochloride (**VII.11**, 1.2 eq) is added to the resin. Then, THF (0.05M) and a standard solution of $CuSO_4.5H_2O$ (0.500 g/L) in milli-Q H_2O (0.05M) is added to the resin. Eventually, this leads to an addition of 0.01 eq $CuSO_4.5H_2O$ and an Wang-AA-NH_2 concentration of 0.1M in THF/H_2O (1/1). At last, triethylamine (2 eq) is added to the vessel. After shaking for 24 hours, the resin is filtered and washed with 3x DMF, 3x MeOH and 3x dichloromethane and dried under reduced pressure.

5. Combinatorial chemistry

Solid-phase bound azido acetic acid **VII.28**

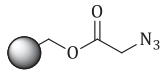

VII.28

Molecular weight: 101.06 Da.

LC-(ESI)MS: N/A[1]

HATR (cm^{-1}): 3024 (w), 2921 (w), 2851 (m), 2105 (s), 1739 (s), 1681 (w), 1602 (m), 1584 (m), 1511 (m), 1492 (m), 1451 (m), 1422 (w), 1377 (w), 1298 (w), 1222 (s), 1171 (s), 1112 (w), 1069 (w), 1030 (m), 1015 (m), 965 (w), 906 (w), 820 (s), 757 (s), 697 (s).

Solid-phase bound (*S*)-2-azido propanoic **VII.29**

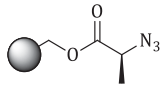

VII.29

Molecular weight: 115.09 Da.

LC-(ESI)MS: N/A[2]

HATR (cm^{-1}): 3050 (w), 3025 (w), 2921 (w), 2099 (s), 1736 (s), 1677 (m), 1611 (m), 1600 (m), 1584 (m), 1512 (m), 1492 (m), 1451 (m), 1377 (m), 1302 (w), 1222 (s), 1172 (s), 1112 (w), 1088 (w), 1016 (s), 962 (w), 821 (s), 757 (s), 697 (s).

[1] **VII.28** is not UV active nor detected in MS
[2] **VII.29** is not UV active nor detected in MS

Solid-phase bound (*S*)-2-azido-3-(tert-butoxy)propanoic acid **VII.30**

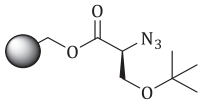

VII.30

Molecular weight: 187.20 Da.
LC-(ESI)MS: N/A[3]
HATR (cm^{-1}): 3059 (w), 3025 (w), 2922 (m), 2846 (w), 2102 (s), 1741 (s), 1678 (s), 1601 (m), 1578 (w), 1512 (m), 1492 (s), 1452 (s), 1364 (m), 1296 (m), 1225 (s), 1170 (s), 1088 (w), 1065 (m), 1028 (m), 907 (w), 873 (w), 822 (m), 756 (s), 696 (s), 620 (w).

Solid-phase bound (*S*)-2-azido-3-phenyl-propanoic acid **VII.31**

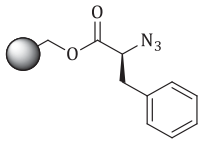

VII.31

Molecular weight: 191.19 Da.
LC-(ESI)MS (condition 1): t_R = 10.4 min, $[M- H]^-$: 190.1 (100%).
HATR (cm^{-1}): 3058 (w), 3025 (w), 2922 (w), 2851 (w), 2107 (s), 1736 (s), 1677 (m), 1611 (m), 1600 (m), 1584 (m), 1512 (s), 1492 (s), 1452 (s), 1379 (m), 1303 (m), 1223 (s), 1172 (s), 1113 (w), 1082 (w), 1016 (m), 909 (w), 874 (w), 821 (s), 756 (s), 697 (s), 621 (w).

Solid-phase bound (*S*)-2-azido-3-methylbutanoic acid **VII.32**

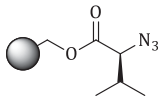

VII.32

Molecular weight: 143.14 Da.
LC-(ESI)MS: N/A[4]
HATR (cm^{-1}): 3054 (s) (m), 3025 (s), 2922 (s), 2846 (s), 2103 (s), 1736 (s), 1679 (m), 1611 (m), 1584 (m), 1512 (s), 1493 (s), 1451 (s), 1377 (m), 1303 (m), 1222 (s), 1172 (s), 1114 (w), 1016 (s), 908 (w), 821 (s), 757 (s), 697 (s).

[3] **VII.30** is not UV active nor detected in MS
[4] **VII.32** is not UV active not detected in MS

Solid-phase bound (*S*)-2-azido-4-methylpentanoic acid **VII.33**

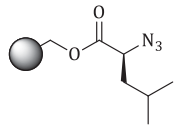

VII.33

Molecular weight: 157.17Da.
LC-(ESI)MS (condition 5): t_R = 3.6 min, [M- H]$^-$: 156.1 (100%).
HATR (cm^{-1}): 3059 (w), 3025 (w), 2922 (w), 2846 (w), 2109 (s), 1736 (s), 1678 (m), 1611 (m), 1603 (m), 1584 (w), 1512 (m), 1492 (m), 1451 (m), 1427 (m), 1378 (m), 1360 (m), 1303 (m), 1222 (s), 1172 (s), 1114 (w), 1016 (s), 908 (w), 821 (s), 757 (s), 697 (s).

Solid-phase bound (*S*)-2-azido-6-((tert-butoxycarbonyl)amino)hexanoic acid **VII.34**

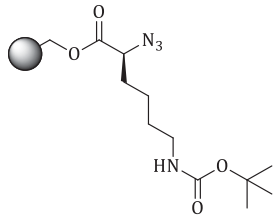

VII.34

Molecular weight: 272.30 Da.
LC-(ESI)MS (condition 5): t_R = 1.2 min, [M- H-Boc]$^-$: 171.2 (100%).
HATR (cm^{-1}): 3416 (w, broad), 3025 (w), 2922 (m), 2850 (w), 2104 (s), 1736 (s), 1711 (s), 1677 (s), 1611 (m), 1584 (w), 1512 (s), 1493 (s), 1452 (s), 1364 (m), 1302 (m), 1223 (s), 1170 (s), 1113 (m), 1016 (s), 908 (w), 822 (s), 758 (s), 698 (s).

Solid-phase bound (*S*)-2-azido-3-(1-(tert-butoxycarbonyl)-3-indolyl)propanoic acid **VII.35**

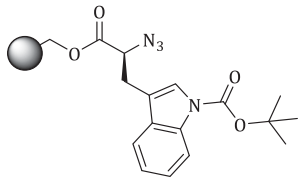

VII.35

Molecular weight: 330.34 Da.
LC-(ESI)MS (condition 5): t_R = 3.8 min, [M- H-Boc]$^-$: 229.1 (100%).
HATR (cm^{-1}): 3025 (w), 2922 (m), 2852 (w), 2105 (m), 1732 (s), 1678 (m), 1611 (m), 1581 (m), 1512 (m), 1493 (m), 1452 (s), 1369 (s), 1308 (m), 1223 (s), 1158 (s), 1113 (m), 1086 (m), 1017 (s), 821 (m), 765 (s), 746 (s), 698 (s).

C. Recent and ongoing important developments

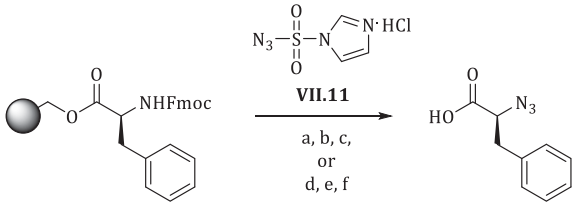

VI.36 **VII.10**

a) 20 v/v% 4-Me-piperidine/DMF, rt, 2x 15 min b) 3 eq **VII.11,** 4.5 eq DIPEA, DMF c) TFA/H_2O (95/5), rt, 2h.
d) 20 v/v% 4-Me-piperidine/DMF, rt, 2x 15 min e) 3 eq **VII.11,** 4.5 eq DIPEA, 1 mol% $CuSO_4.5H_2O$, DMF f) TFA/H_2O (95/5), rt, 2h.

Scheme XV-2: Late stage optimization

Solid-phase bound Fmoc-protected L-phenylalanine (**VI.36**, 50.0 mg, 0.0285 mmol, 1 eq) is poured into six solid-phase vessels. The Fmoc-group is removed *via* standard procedure **P.02**. Afterwards, the six vessels are divided in two groups. To the first three vessels imidazole-1-sulfonyl azide hydrochloride (**VII.11**, 17.9 mg, 0.0855 mmol, 3 eq), DMF (400 µL) and DIPEA (22.3 µL, 0.1283 mmol, 4.5 eq) are added to the vessels. These reactions put in a Mettler-Toledo Bohdan Miniblock™ high capacity shaking and washing station and after respectively 15, 30 and 60 minutes, the reactions are stopped and washed with DMF (3x 1 mL), MeOH (3x 1 mL) and dichloromethane (3x 1mL). For setting up the test reactions of the second group of vessels, a standard solution of $CuSO_4.5H_2O$ (2.5 mg/mL) in DMF is prepared. Subsequently, imidazole-1-sulfonyl azide hydrochloride (**VII.11**, 17.9 mg, 0.0855 mmol, 3 eq), $CuSO_4.5H_2O$ in DMF (300 µL), DMF (100 µL) and DIPEA (22.3 µL, 0.1283 mmol, 4.5 eq) are added to the vessels. Again, these vessels are shaken for respectively 15, 30 and 60 minutes. After these

reaction times, the beads are washed with DMF (3x 1 mL), MeOH (3x 1 mL) and dichloromethane (3x 1mL).

Cleavage: From all six reaction vessels, an aliquot of the resin is treated with TFA/H_2O (95/5) for two hours at room temperature. After isolation and evaporation of the supernatant, an LC-MS sample is prepared.

XVI. 1,3-Dipolar cycloaddition

A. Test reactions for introducing 1,5-disubstituted 1,2,3-triazole moiety

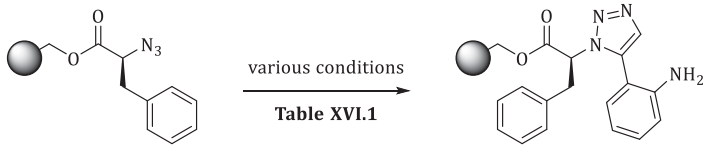

VII.31 **VIII.3**

Solid-phase bound L-2-azido-phenylpropanoic acid **VII.31** was prepared *via* general procedure **P.01-P.03**. To six 1 mL closed reaction vessels (**VII.31**, 0.03408 mmol, 1 eq) was added and combined with Ru(II)-catalyst (**Table XVI-1**), toluene (0.1M) and 2-ethynylaniline (**VIII.2,** 19 µL, 0.1022 mmol, 3 eq) in that specific order. The reactions are shaken at room temperature or at 60°C for six hours. After completion, each test reaction is washed with warm toluene (60°C, 3x 1 mL), DMF (3x 1 mL), MeOH (3x 1 mL) and dichloromethane (3x 1 mL).

Table XVI-1: Conditions applied for test reaction of RuAAC

entry	conditions				
	loading	catalyst	solvent	T	reaction time
1	5 mol%	$C_p^*RuCl(PPh_3)_2$	toluene	60°C	6h
2	10 mol%	$C_p^*RuCl(PPh_3)_2$	toluene	60°C	6h
3	5 mol%	$C_p^*RuCl(PPh_3)_2$	toluene	rt	6h
4	10 mol%	$C_p^*RuCl(PPh_3)_2$	toluene	rt	6h
5	5 mol%	$C_p^*RuCl(COD)$	toluene	rt	6h
6	10 mol%	$C_p^*RuCl(COD)$	toluene	rt	6h

Cleavage: All test reactions are cleaved from the resin with TFA/H_2O (95/5) for two hours at room temperature. After this time, the beads are filtered off and the washed with dichloromethane (3x 1 mL). The filtrate is evaporated azeotropically with acetonitrile (3x 1 mL) and subsequently used for LC-MS sample preparation.

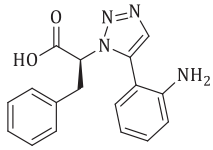

VIII.5

Brutoformula: $C_{17}H_{16}N_4O_2$
Molecular weight: 308.33 Da.
Not detected.

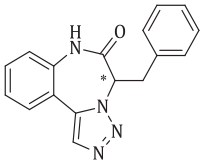

VIII.7

Brutoformula: $C_{17}H_{18}N_4O$
Molecular weight: 290.32 Da.
LC-(ESI)MS (condition 1): t_R = 14.4 min $[M+H^+]^+$: 291.1 (100%).

General procedure **P.04**: The resin (1 eq) is transferred into a reaction vessel and $C_p^*RuCl(PPh_3)_2$ (0.10 eq) is added, followed by an addition of toluene (0.1M) and 2-ethynylaniline (3 eq) building block. After 6 hours of shaking at 60°C the resin is filtered off and washed extensively with warm toluene (60°C, 3x), DMF (3x), MeOH (3x) and dichloromethane (3x). Afterwards, the resin is dried under reduced pressure.

B. Base-catalyzed cyclization/release

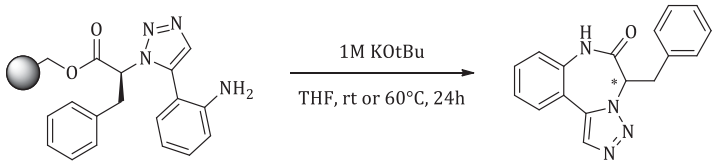

VIII.3 **VIII.7**

Solid-phase bound intermediate **VIII.3** is prepared *via* general procedure **P.01-P.04** and dried extensively *in vacuo*. Two closed 1 mL vessels are filled with **VIII.3** (0.0341 mmol, 1 eq). To these two vessels 1 ml of 1M KOtBu in THF is added. The cleavage reaction is set up for 24 hours of shaking at room temperature or 60°C. After this reaction time, the supernatant is isolated and the remaining beads are washed with THF (3x 1 mL). Then, the organic phase is evaporated under reduced pressure and afterwards diluted in EtOAc (1 mL). This solution is transferred into a separation funnel and washed with saturated $NaHCO_3$-solution (2x 1mL). The aqueous layers are washed with EtOAc (1 mL). The combined organic layers are dried with $MgSO_4$ for 20 minutes and after filtration of the drying salt, the organic phase is evaporated under reduced pressure. After drying, an LC-MS sample is prepared and analyzed for the crude purity.

An aliquot of the remaining resin is treated with 95% TFA in H_2O solution in order to verify the effectiveness of the performed cyclization/release strategy.

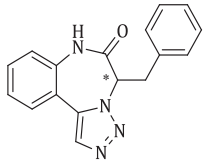

VIII.7

Brutoformula: $C_{17}H_{18}N_4O$
Molecular weight: 290.32 Da.
LC-(ESI)MS (condition 1): t_R = 14.4 min $[M+H^+]^+$: 291.1 (100%).

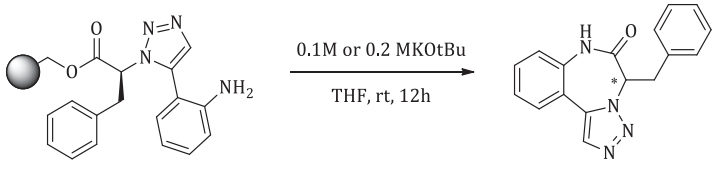

VIII.3 **VIII.7**

Solid-phase bound intermediate **VIII.3** is prepared *via* general procedure **P.01-P.04** and dried extensively *in vacuo*. Two closed 1 mL vessels are filled with **VIII.3** (0.0341 mmol, 1 eq). To the first vessel 900 µL of dry THF is added and secondly 100 µL of 1M KOtBu in THF. To the second vial, 800 µL of dry THF is added and secondly 200 µL of 1M KOtBu in THF. Both dilutions led to a final concentration of respectively 0.1M and 0.2M of KOtBu.

The cleavage reaction is set up for 24 hours of shaking at room temperature. The work up of this procedure is identical to one represented in previous section.

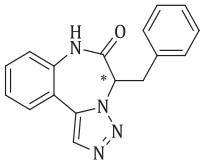

VIII.7

Brutoformula: $C_{17}H_{18}N_4O$
Molecular weight: 290.32 Da.
LC-(ESI)MS (condition 1): t_R = 14.4 min $[M+H^+]^+$: 291.1 (100%).

C. Acid-catalyzed cyclization/release

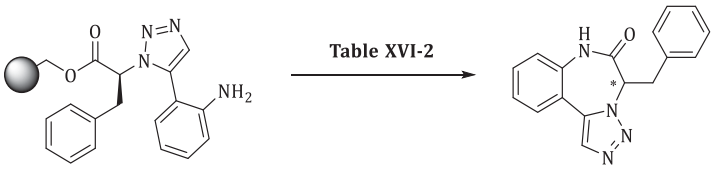

VIII.3 **VIII.7**

Solid-phase bound intermediate **VIII.3** is prepared *via* general procedure **P.01-P.04** and dried extensively *in vacuo*. To twelve 1mL closed vials, intermediate **VIII.3** (25 mg, 0.01836 mmol, 1 eq) is added. To each vial, a 500 µL of an acidic solution is added (solutions 1-12, **Table XVI-2**). The reactions are shaken for 24 hours at room temperature. After this reaction time, the supernatant is isolated and concentrated under reduced pressure. In order to fully evaporate the vials containing TFA (vials 1-8), acetonitrile is added (2x 1 mL). For the vials containing HOAc (vials 9-12), toluene (2x 1 mL) is added. After further concentration under reduced pressure, the test reactions are dried *in vacuo* and each residue is used to prepare an LC-MS sample. The remaining resin is transferred again into twelve closed 1 mL vessels and treated with 1 mL TFA/H_2O (95/5) at room temperature in order to verify the efficacy of the performed test reactions. After 2 hours, the supernatant is isolated and evaporated azeotropically upon addition of acetonitrile (3x 1mL) under reduced pressure. The obtained residues are used for LC-MS sample preparation.

Table XVI-2: Acid-catalyzed cyclization/release test reactions

Solution	TFA	HOAc	CH_2Cl_2	DCE
1	100 µL	-	9900 µL	-
2	200 µL	-	9800 µL	-
3	500 µL	-	9500 µL	-
4	1 mL	-	9 mL	-
5	100 µL	-	-	9900 µL
6	200 µL	-	-	9800 µL
7	500 µL	-	-	9500 µL
8	1 mL	-	-	9 mL
9	-	5 mL	5 mL	-
10	-	6 mL	4 mL	-
11	-	7 mL	3 mL	-
12	-	8 mL	2 mL	-

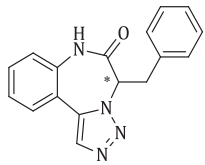

VIII.7

Brutoformula: $C_{17}H_{18}N_4O$
Molecular weight: 290.32 Da.
LC-(ESI)MS (condition 1): t_R = 14.4 min $[M+H^+]^+$: 291.1 (100%).

General procedure **P.05**: The resin (1 eq) is transferred into a reaction vessel and is treated with a solution of HOAc/dichloromethane (1/1) (substrate at final concentration of 0.1M) for 24 hours at room temperature. Afterwards the supernatant is isolated and the resin washed with dichloromethane (3x). After azeotropic evaporation with toluene (3x), the residue is dried under reduced pressure to remove traces of toluene. Further purification is done by flash chromatography yielding the desired compound.

D. Proof of principle library

[1,2,3]triazolo[1,5-*d*][1,4]benzodiazepin-2-one VIII.12

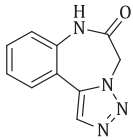

VIII.12

Following general procedure **P.01 - P.05**: [1,2,3]triazolo[1,5-*d*][1,4]benzodiazepin-2-one (**VIII.12**, 60.1 mg, 0.3003 mmol).

Yield: 44%.
Light-brown solid.
R_F: 0.12 (hexane/EtOAc: 4/6).
Molecular weight: 200.20 Da.
^{1}H NMR (500 MHz, acetone-d_6) δ 5.18 (s, 2H), 7.35 (td, J = 1.1Hz/7.7Hz, 1H), 7.39 (dd, J = 1.0Hz/8.2Hz, 1H), 7.53-7.56 (m, 1H), 7.75 (dd, J = 1.1Hz/7.7Hz, 1H), 8.04 (s, 1H), 9.63 (s broad, 1H).
^{13}C NMR (125 MHz, acetone-d_6) δ 53.0 (CH_2), 118.6 (C), 123.2 (CH), 126.1 (CH), 130.0 (CH), 131.6 (CH), 132.2 (CH), 136.1 (C), 136.1 (C), 167.0 (C).
HATR (cm^{-1}): 3209 (m), 3085 (m), 2931 (m), 2485 (w), 2232 (w), 2134 (w), 2008 (m), 1677 (s), 1485 (m), 1465 (w), 1449 (w), 1408 (m), 1392 (m), 1245 (w), 1230 (w), 1200 (m), 1137 (m), 1011 (w), 979 (w), 881 (w), 881 (w), 756 (m).
LC-(ESI)MS (condition 1): t_R = 10.8 min $[M+H^+]^+$: 201.1 (100%). **Purity** (214 nm): 97%.
HRMS (ESI) calcd for $C_{10}H_9N_4O^+$ $[M+H^+]^+$: 201.0771 found: 201.0775.

(*S*)-3-methyl[1,2,3]triazolo[1,5-*d*][1,4]benzodiazepin-2-one VIII.13

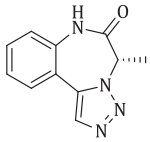

VIII.13

Following general procedure **P.01 - P.05**: (*S*)-3-methyl[1,2,3]triazolo[1,5-*d*][1,4]benzodiazepin-2-one (**VIII.13**, 54.6 mg, 0.2549 mmol).

Yield: 39%.
Light-brown solid.
R_F: 0.09 (dichloromethane/acetone: 95/5).
Molecular weight: 214.22 Da.

^{1}H NMR (300 MHz, DMSO-d_6) δ 1.70 (d, J = 7.0Hz, 3H), 5.12 (q, J = 7.0Hz, 1H), 7.27-7.35 (m, 2H), 7.53 (td, J = 1.4Hz/7.7Hz, 1H), 7.70 (dd, J = 1.4Hz/7.7Hz, 1H), 8.17 (s, 1H), 10.71 (s broad, 1H).
^{13}C NMR (75 MHz, DMSO-d_6) δ 12.7 (CH_3), 56.6 (CH), 117.4 (C), 122.0 (CH), 124,9 (CH), 128.9 (CH), 130.7 (CH), 131.7 (CH), 134.9 (C), 135.0 (C), 167.7 (C).
HATR (cm^{-1}): 3198 (m), 3078 (m), 2904 (m), 1746 (w), 1687 (s), 1617 (w), 1587 (m), 1560 (w), 1482 (s), 1447 (w), 1411 (m), 1385 (s), 1302 (w), 1264 (s), 1247 (m), 1176 (m), 1118 (m), 1095 (m), 1021 (m), 973 (m), 851 (m), 822 (m), 754 (s), 624 (m).
LC-(ESI)MS (condition 1): t_R = 11.7 min $[M+H^+]^+$: 215.1 (100%). **Purity** (214 nm): 91%.
HRMS (ESI) calcd for $C_{11}H_{11}N_4O^+$ $[M+H^+]^+$: 215.0927 found: 215.0932.

(*S*)-3-(tert-Butoxymethyl)[1,2,3] triazolo[1,5-*d*][1,4]benzodiazepin-2-one VIII.14

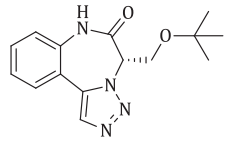

VIII.14

Following general procedure **P.01 - P.05**: (*S*)-3-(tert-Butoxymethyl)[1,2,3]triazolo[1,5-*d*][1,4]benzodiazepin-2-one (**VIII.14**, 76.0 mg, 0.2654 mmol).

Yield: 57%.
Light-yellow oil.
R_F: 0.13 (hexane/EtOAc: 6/4).
Molecular weight: 286.33 Da.
^{1}H NMR (300MHz, acetone-d_6) δ 0.91 (s, 9H), 3.84-3.94 (m, 2H), 5.50 (app s broad, 1H), 7.31(td, J = 1.3Hz/7.7Hz, 1H), 7.35-7.38 (m, 1H), 7.47-7.53 (m, 1H), 7.76 (dd, J = 1.3Hz/7.7Hz, 1H), 8.07 (s, 1H), 9.76 (s broad, 1H).
^{13}C NMR (75 MHz, acetone-d_6) δ 27.1 (CH_3), 60.9 (C), 66.0 (CH), 74.3 (CH_2), 118.4 (C), 122.4 (CH), 125.6 (CH), 129.4 (CH), 131.4 (CH), 132.5 (CH), 135.8 (C), 135.9 (C), 167.6 (C).
HATR (cm^{-1}): 3235 (m), 3117 (m), 2973 (m), 2930 (m), 2179 (w), 1937 (w), 1679 (s), 1612 (m), 1589 (m), 1486 (s), 1389 (s), 1364 (s), 1247 (m), 1230 (m), 1190 (s), 1098 (s), 1023 (w), 969 (w), 899 (m), 823 (m), 761 (s), 732 (s), 703 (m).
LC-(ESI)MS (condition 1): t_R = 14.4 min $[M+H^+]^+$: 287.0 (100%). **Purity** (214 nm): 97%.
HRMS (ESI) calcd for $C_{15}H_{19}N_4O_2^+$ $[M+H^+]^+$: 287.1503 found: 287.1495.

(*S*)-3-(*N*-(tert-butyloxycarbonyl)-butylamino)[1,2,3]triazolo[1,5-*d*][1,4]benzodiazepin-2-one VIII.15

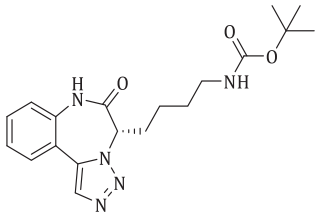

VIII.15

Following general procedure **P.01 - P.05**: (*S*)-3-(*N*-(tert-butyloxycarbonyl)-butylamino)[1,2,3]triazolo[1,5-*d*][1,4]benzodiazpin-2-one (**VIII.15**, 81.4 mg, 0.2191 mmol).

Yield: 45%.
White solid.
R_F: 0.16 (hexane/EtOAc: 4/6). 0.05 (hexane/EtOAc: 8/2).
Molecular weight: 371.43 Da.
^{1}H NMR (300MHz, CD_3OD) δ 1.16-1.15 (m, 13H), 1.86-2.06 (m, 2H), 2.90-2.95 (m, 2H), 5.30 (t, *J* = 7.3Hz, 1H), 7.26 (d, *J* = 8.1Hz, 1H), 7.33 (t, *J* = 7.3Hz, 1H), 7.52 (t, *J* = 7.3Hz, 1H), 7.73 (d, *J* = 7.9Hz, 1H), 8.09 (s, 1H).
^{13}C NMR (75 MHz, CD_3OD) δ 23.9 (CH_3), 28.8 (CH_2), 28.9 (CH_2), 30.1 (CH_2), 40.8 (CH_2), 65.6 (CH), 118.3 (C), 122.9 (CH), 126.6 (CH), 129.9 (CH), 132.3 (C), 132.9 (CH), 135.9 (C), 136.3 (C), 169.4 (C).
LC-(ESI)MS (condition 1): t_R = 14.5 min $[M+H^+]^+$: 372.0 (20%). **Purity** (214 nm): 95%.
HRMS (ESI) calcd for $C_{19}H_{24}N_5O_3^+$ $[M-H^+]^-$: 370.1885 found: 370.1895.

(*S*)-3-benzyl[1,2,3]triazolo[1,5-*d*][1,4]benzodiazepin-2-one (*S*)-VIII.16

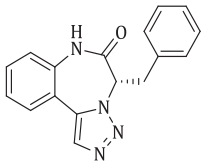

(*S*)-VIII.16

Following general procedure **P.01 - P.05**: (*S*)-3-benzyl[1,2,3]triazolo[1,5-*d*][1,4]benzodiazepin-2-one (**(*S*)-VIII.16**, 87.1 mg, 0.300 mmol).

Yield: 54%.
White solid.
%ee: 95%.

R_F: 0.26 (hexane/acetone: 6/4). 0.07 (hexane/acetone: 8/2).
Molecular weight: 290.32 Da.
^{1}H NMR (300MHz, acetone-d_6) δ 3.28-3.44 (m, 2H), 5.49-5.54 (m, 1H), 7.13-7.24 (m, 5H), 7.36-7.45 (m, 2H), 7.55-7.60 (m, 1H), 7.80 (dd, 1.5Hz/7.7Hz, 1H), 8.04 (s, 1H), 9.75 (s broad, 1H).
^{13}C NMR (75 MHz, acetone-d_6) δ 34.5 (CH_2), 65.7 (CH), 118.6 (C), 122.8 (CH), 126.1 (CH), 127.8 (CH), 129.2 (CH), 129.7 (CH), 130.1 (CH), 131.8 (CH), 132.6 (CH), 135.5 (C), 135.8 (C), 136.7 (C), 167.6 (C).
HATR (cm^{-1}): 3080 (m), 2923 (m), 2358 (m), 2206 (w), 2067 (w), 2010 (w), 1682 (s), 1612 (m), 1587 (m), 1506 (w),1486 (s), 1452 (m), 1426 (m), 1380 (s), 1246 (m), 1219 (m), 1117 (m), 1027 (w), 976 (w), 948 (w), 839 (w), 759 (s), 744 (s), 700 (s), 667 (w).
LC-(ESI)MS (condition 1): t_R = 14.5 min $[M+H^+]^+$: 291.0 (100%). **Purity** (214 nm): 95%.
HRMS (ESI) calcd for $C_{17}H_{15}N_4O^+$ $[M+H^+]^+$: 291.1240 found: 291.1238.

(*R*)-3-benzyl[1,2,3]triazolo[1,5-*d*][1,4]benzodiazepin-2-one (*R*)-VIII.16

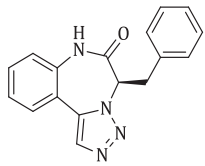

(*R*)-VIII.16

Following general procedure **P.01 - P.05**: (*S*)-3-benzyl[1,2,3]triazolo[1,5-*d*][1,4]benzodiazepin-2-one (**(*R*)-VIII.16**, 93.3 mg, 0.3214 mmol).

Yield: 55%.
White solid.
%ee: 96%.
R_F: 0.07 (hexane/acetone: 8/2).
Molecular weight: 290.32 Da.
^{1}H NMR (300MHz, DMSO-d_6) δ 3.16-3.35 (m, 2H), 5.47 (t, J = 7.5Hz, 1H), 7.08-7.23 (m, 5H), 7.33-7.37 (m, 2H), 7.55-7.60 (m, 1H), 7.77(d, J = 7.7Hz, 1H), 8.17 (s, 1H), 10.84 (s broad, 1H).
^{13}C NMR (75 MHz, DMSO-d_6) δ 33.1 (CH_2), 64.3 (CH), 117.0 (C), 121.9 (CH), 125.1 (CH), 126.8 (CH), 128.3 (CH), 128.8 (CH), 129.1 (CH), 130.9 (CH), 132.0 (CH), 134.4 (C), 134.7 (C), 135.6 (C), 166.5 (C).
HATR (cm^{-1}): 3198 (m), 3082 (m), 2981 (m), 2898 (m), 1798 (w), 1721 (w), 1682 (s), 1506 (w), 1486 (m), 1388 (m), 1276 (w), 1261 (m), 1196 (w), 1081 (m), 1026 (m), 796 (m), 757 (m), 698 (m), 667 (m).
LC-(ESI)MS (condition 1): t_R = 14.5 min $[M+H^+]^+$: 291.0 (100%). **Purity** (214 nm): 99%.
HRMS (ESI) calcd for $C_{17}H_{15}N_4O^+$ $[M+H^+]^+$: 291.1240 found: 291.1243.

E. Sonogashira cross-coupling reaction

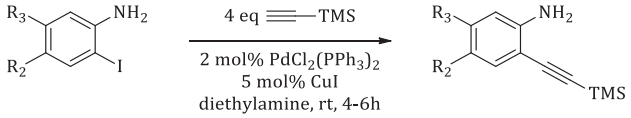

VIII.21 – VIII.25 **VIII.26 – VIII.30**

General procedure **P.06**: $PdCl_2(PPh_3)_2$ (0.02 eq) and CuI (0.05 eq) are dissolved in diethylamine (0.1M). After dropwise addition of trimethylsilylacetylene (4 eq), the 2-iodoaniline substrate **VIII.21 – VIII.25** (1 eq) is added in one portion. The reaction is stirred for four till six hours under Ar atmosphere at room temperature and followed by TLC (eluent: dichloromethane) until completion. Afterwards, the reaction mixture is diluted with EtOAc and after filtration of the formed salt, the filtrate is carefully evaporated under reduced pressure. Further purification is achieved by flash chromatography, leading to the desired 2-trimethylsilylethynylanilines **VIII.26** – **VIII.30**.

4-chloro-2-(trimethylsilyl)ethynylaniline VIII.26

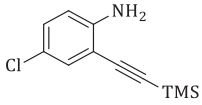

VIII.26

Following general procedure **P.06**: 4-chloro-2-iodoaniline (1.997 g, 7.879 mmol, 1 eq). trimethylsilylacetylene (4.5 mL, 31.52 mmol, 4 eq). $PdCl_2(PPh_3)_2$ (111 mg, 0.1581 mmol, 0.02 eq). CuI (75 mg, 0.3940 mmol, 0.05 eq). diethylamine (79 mL).

Yield: 95%. 4-chloro-2-(trimethylsilyl)ethynylaniline (**VIII.26,** 1.669 g, 7.486 mmol).
Red-brown oil.
R_F: 0.65 (dichloromethane). 0.49 (hexane/acetone 7/3).
Molecular weight: 223.77 Da.
^{1}H NMR (300 MHz, acetone-d_6) δ 0.23 (s, 9H), 5.14 (s broad, 2H), 6.76 (d, J = 8.9Hz, 1H), 7.07 (dd, J = 2.5Hz/8.9Hz, 1H), 7.16 (d, J = 2.5Hz, 1H).
^{13}C NMR (75 MHz, acetone-d_6) δ 0.0 (CH_3), 100.9 (C), 101.6 (C), 108.8 (C), 116.2 (CH), 120.7 (C), 130.7 (CH), 131.6 (CH), 149.6 (C).
HATR (cm^{-1}): 3478 (w), 3372 (w), 2957 (w), 2901 (w), 2151 (m), 1613 (m), 1485 (s), 1403 (m), 1299 (m), 1248 (s), 1145 (w), 1085 (w), 902 (s), 837 (s), 810 (s), 760 (s), 698 (m).
LC-(ESI)MS (condition 2): t_R = 10.1 min $[M+H^+]^+$: 224.0 (100%) **Purity** (214 nm): 98%.
HRMS (ESI) calcd for $C_{11}H_{15}ClNSi^+$ $[M+H^+]^+$: 224.0657 found: 224.0651.

5-chloro-2-(trimethylsilyl)ethynylaniline VIII.27

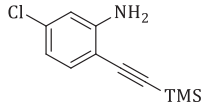

VIII.27

Following general procedure **P.06**: 5-chloro-2-iodoaniline (2.004 g, 7.906 mmol, 1 eq). trimethylsilylacetylene (4.5 mL, 31.62 mmol, 4 eq). $PdCl_2(PPh_3)_2$ (111 mg, 0.1581 mmol, 0.02 eq). CuI (75 mg, 0.3953 mmol, 0.05 eq). diethylamine (79 mL).

Yield: 92%. 5-chloro-2-(trimethylsilyl)ethynylaniline (**VIII.27**, 1.621 g, 7.273 mmol).
Red-brown oil.
R_F: 0.76 (dichloromethane).
Molecular weight: 223.77 Da.
^{1}H NMR (300 MHz, acetone-d_6) δ 0.23 (s, 9H), 5.24 (s broad, 2H), 6.56 (app dd, J = 1.5Hz/8.3Hz, 1H), 6.80 (app d, J = 1.5Hz, 1H), 7.17 (d, J = 8.3Hz, 1H).
^{13}C NMR (75 MHz, acetone-d_6) δ 0.0 (CH_3), 100.5 (C), 101.9 (C), 106.3 (C), 114.1 (CH), 117.0 (CH), 134.0 (CH), 135.9 (C), 151.8 (C).
HATR (cm^{-1}): 3483 (w), 3390 (w), 2961 (w), 2145 (m), 1612 (s), 1555 (m), 1484 (m), 1421 (m), 1308 (w), 1249 (s), 1204 (m), 1134 (w), 1093 (w), 912 (w), 840 (s), 798 (s), 758 (s), 680 (m), 626 (w).
LC-(ESI)MS (condition 2): t_R = 10.1 min $[M+H^+]^+$: 224.0 (100%). **Purity** (214 nm): 99%.
HRMS (ESI) calcd for $C_{11}H_{15}ClNSi^+$ $[M+H^+]^+$: 224.0657 found: 224.0655.

4-bromo-2-(trimethylsilyl)ethynylaniline VIII.28

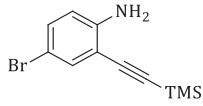

VIII.28

Following general procedure **P.06**: 4-bromo-2-iodoaniline (2.001 g, 6.716 mmol, 1 eq). trimethylsilylacetylene (3.8 mL, 26.86 mmol, 4 eq). $PdCl_2(PPh_3)_2$ (94 mg, 0.1343 mmol, 0.02 eq). CuI (64 mg, 0.3358 mmol, 0.05 eq). diethylamine (67 mL).

Yield: 99%. 4-bromo-2-(trimethylsilyl)ethynylaniline (**VIII.28**, 1.775 g, 6.649 mmol).
Red-brown oil.
R_F: 0.71 (dichloromethane).
Molecular weight: 268.23 Da.
^{1}H NMR (300 MHz, acetone-d_6) δ 0.24 (s, 9H), 5.14 (s broad, 2H), 6.71 (d, J = 8.7Hz, 1H), 7.18 (dd, J = 2.3Hz/8.7Hz, 1H), 7.30 (d, J = 2.3Hz, 1H).

^{13}C NMR (75 MHz, acetone-d_6) δ 0.0 (CH_3), 101.0 (C), 101.4 (C), 107.3 (C), 109.3 (C), 116.5 (CH), 133.4 (CH), 134.4 (CH), 149.7 (C).
HATR (cm^{-1}): 3480 (w), 3384 (w), 2955 (w), 2904 (w), 2145 (m), 1702 (w), 1610 (m), 1480 (s), 1402 (m), 1304 (m), 1248 (s), 1153 (m), 1082 (w), 886 (s), 840 (s), 812 (s), 759 (s), 701 (w).
LC-(ESI)MS (condition 2): t_R = 11.0 min $[M+H^+]^+$: 268.1 (100%). **Purity** (214 nm): 98%.
HRMS (ESI) calcd for $C_{11}H_{15}BrNSi^+$ $[M+H^+]^+$: 268.0152 found: 268.0149.

4-amino-3-((trimethylsilyl)ethynyl)benzonitrile VIII.29

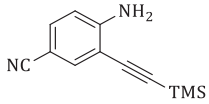

VIII.29

Following general procedure **P.06**: 4-amino-3-iodobenzonitrile (0.997 g, 4.085 mmol, 1 eq). trimethylsilylacetylene (2.3 mL, 16.34 mmol, 4 eq). $PdCl_2(PPh_3)_2$ (57 mg, 0.0817 mmol, 0.02 eq). CuI (37 mg, 0.2043 mmol, 0.05 eq). diethylamine (41 mL).

Yield: 91%. 4-amino-3-(trimethylsilyl)ethynylbenzonitrile (**VIII.29**, 795 mg, 3.717 mmol).
Light yellow solid.
R_F: 0.18 (hexane/acetone: 8/2).
Molecular weight: 214.34 Da.
^{1}H NMR (300 MHz, acetone-d_6) δ 0.24 (s, 9H), 5.87 (s broad, 2H), 6.86 (d, J = 8.5Hz, 1H), 7.39 (dd, J =1.9Hz/8.5Hz, 1H), 7.54 (d, J = 1.9Hz, 1H).
^{13}C NMR (75 MHz, acetone-d_6) δ 0.0 (CH_3), 99.2 (C), 100.4 (C), 114.8 (C), 114.9 (CH), 119.8 (C), 134.2 (CH), 137.0 (CH), 153.9 (C).
HATR (cm^{-1}): 3477 (w), 3362 (m), 3210 (w), 2958 (w), 2896 (w), 2220 (s), 2146 (s), 1618 (s), 1555 (w), 1498 (s), 1417 (m), 1325 (m), 1248 (s), 1163 (w), 1141 (w), 941 (w), 898 (w), 839 (s), 760 (m), 703 (w).
LC-(ESI)MS (condition 2): t_R = 6.3 min $[M+H^+]^+$: 215.1 (100%). **Purity** (214 nm): 98%.
HRMS (ESI) calcd for $C_{12}H_{13}N_2Si^-$ $[M-H^+]^-$: 213.0853 found: 213.0855.

4-nitro-2-(trimethylsilyl)ethynylaniline VIII.30

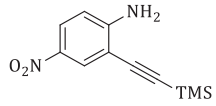

VIII.30

Following general procedure **P.06**: 2-iodo-4-nitroaniline (1.996 g, 7.560 mmol, 1 eq). trimethylsilylacetylene (4.3 mL, 30.24 mmol, 4 eq). $PdCl_2(PPh_3)_2$ (106 mg, 0.1512 mmol, 0.02 eq). CuI (72 mg, 0.3780 mmol, 0.05 eq). diethylamine (76 mL).

Yield: 94%. 4-nitro-2-(trimethylsilyl)ethynylaniline (**VIII.30**, 1.663 g, 7.106 mmol).
Bright yellow solid.
R_f: 0.57 (dichloromethane).
Molecular weight: 234.33 Da.
^{1}H NMR (300 MHz, acetone-d_6) δ 0.26 (s, 9H), 6.26 (s broad, 2H), 6.88 (d, J = 9.0Hz, 1H), 7.98 (dd, J = 2.6Hz/9.0Hz, 1H), 8.08 (d, J = 2.6Hz, 1H).
^{13}C NMR (75 MHz, acetone-d_6) δ 0.1 (CH_3), 100.2 (C), 101.8 (C), 106.8 (C), 113.8 (CH), 126.9 (CH), 129.3 (CH), 138.0 (C), 155.9 (C).
HATR (cm^{-1}): 3479 (w), 3368 (m), 3217 (w), 3075 (w), 2959 (w), 2146 (m), 1616 (s), 1570 (m), 1493 (s), 1304 (s), 1526 (s), 1205 (s), 1152 (m), 1089 (m), 938 (w), 903 (w), 820 (s), 754 (s).
LC-(ESI)MS (condition 2): t_R = 7.4 min $[M+H^+]^+$: 235.1 (100%). **Purity** (214 nm): 98%.
HRMS (ESI) calcd for $C_{11}H_{15}N_2O_2Si^+$ $[M+H^+]^+$: 235.0897 found: 235.0892.

F. Deprotection of TMS group

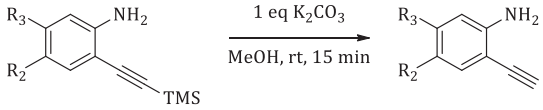

VIII.26 – VIII.30 **VIII.33 – VIII.37**

General procedure **P.07**: 2-trimethylsilylethynylanilines **VIII.30 – VIII.37** (1 eq) are dissolved in MeOH (0.1M) and potassium carbonate (1 eq) is added in one portion. The reaction is monitored via TLC until completion. After 15 minutes, the deprotection was finished and the reaction mixture was evaporated under reduced pressure. Further purification was performed by flash chromatography yielding 2-ethynylaniline building blocks **VIII.33 – VIII.37**.

4-chloro-2-ethynylaniline VIII.33

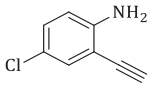

VIII.33

Following general procedure **P.07**: 4-chloro-2-(trimethylsilyl)ethynylaniline **VIII.26** (1.503 g, 6.717 mmol, 1 eq). potassium carbonate (928 mg, 6.717 mmol, 1 eq). MeOH (67 mL).

Yield: 93%. 4-chloro-2-ethynylaniline (**VIII.33**, 947 mg, 6.247 mmol).
Overall yield: 88%.
Light-yellow solid.
R_F: 0.52 (dichloromethane). 0.17 (hexane/acetone: 9/1).
Molecular weight: 151.59 Da.
^{1}H NMR (300 MHz, acetone-d_6) δ 3.97 (s, 1H), 5.18 (s broad, 2H), 6.77 (d, J = 8.7Hz, 1H), 7.08 (dd, J = 2.5Hz/8.7Hz, 1H), 7.19 (d, J = 2.5Hz, 1H).
^{13}C NMR (75 MHz, acetone-d_6) δ 80.1 (C), 85.1 (CH), 107.9 (C), 116.2 (CH), 120.7 (C), 130.7 (CH), 132.0 (CH), 149.8 (C).
HATR (cm^{-1}): 3475 (w), 3383 (w), 3284 (m), 2100 (w), 1613 (s), 1592 (w), 1485 (s), 1406 (m), 1302 (m), 1249 (m), 1185 (w), 1148 (m), 1086 (m), 879 (m), 813 (m), 767 (w).
LC-(ESI)MS (condition 1): t_R = 16.3 min $[M\text{-}H^+]^-$: 151.0 (100%). **Purity** (214 nm): 93%.
HRMS (ESI) calcd for $C_8H_7ClN^+$ $[M+H^+]^+$: 152.0262 found: 152.0263.

5-chloro-2-ethynylaniline VIII.34

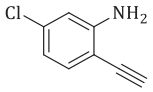

VIII.34

Following general procedure **P.07**: 5-chloro-2-(trimethylsilyl)ethynylaniline **VIII.27** (1.598 g, 7.141 mmol, 1 eq). potassium carbonate (987 mg, 7.141 mmol, 1 eq). MeOH (71 mL).

Yield: 84%. 5-chloro-2-ethynylaniline (**VIII.34**, 909 mg, 5.998 mmol).
Overall yield: 77%.
Light-yellow solid.
R_F: 0.62 (dichloromethane).
Molecular weight: 151.59 Da.
^{1}H NMR (300 MHz, acetone-d_6) δ 3.91 (s, 1H), 5.27 (s broad, 2H), 6.57 (dd, J = 1.9Hz/8.3Hz, 1H), 6.81 (d, J = 1.9Hz, 1H), 7.20 (d, J = 8.3Hz, 1H).
^{13}C NMR (75 MHz, acetone-d_6) δ 80.4 (C), 84.8 (CH), 105.4 (C), 114.2 (CH), 117.0 (CH), 134.3 (CH), 135.9 (C), 151.9 (C).

HATR (cm^{-1}): 3473 (w), 3379 (w), 3284 (m), 2098 (w), 1612 (s), 1558 (m), 1484 (s), 1423 (s), 1310 (w), 1256 (m), 1219 (m), 1191 (w), 1137 (w), 1096 (m), 1057 (w), 910 (s), 847 (m), 798 (s), 734 (w), 667 (m).
LC-(ESI)MS (condition 1): t_R = 16.4 min $[M\text{-}H^+]^-$: 151.0 (100%). **Purity** (214 nm): 96%.
HRMS (ESI) calcd for $C_8H_6ClN^-$ $[M\text{-}H^+]^-$: 150.0116 found: 150.0119.

4-bromo-2-ethynylaniline VIII.35

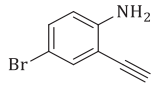

VIII.35

Following general procedure **P.07**: 4-bromo-2-(trimethylsilyl)ethynylaniline **VIII.28** (1.751 g, 5.870 mmol, 1 eq). potassium carbonate (811 mg, 5.870 mmol, 1 eq). MeOH (59 mL).

Yield: 87%. 4-bromo-2-ethynylaniline (**VIII.35**, 1.001 g, 5.107 mmol).
Overall yield: 86%.
Light-yellow solid.
R_F: 0.18 (hexane/acetone 9/1). 0.59 (dichloromethane).
Molecular weight: 196.04 Da.
^{1}H NMR (300 MHz, acetone-d_6) δ 3.96 (s, 1H), 5.20 (s broad, 2H), 6.74 (d, J = 8.6Hz, 1H), 7.20 (dd, J = 2.3Hz/8.6Hz, 1H), 7.33 (d, J = 2.3Hz, 1H).
^{13}C NMR (75 MHz, acetone-d_6) δ 80.0 (C), 85.2 (CH), 107.2 (C), 108.5 (C), 116.6 (CH), 133.5 (CH), 134.8 (CH), 150.1 (C).
HATR (cm^{-1}): 3474 (w), 3373 (w), 3283 (m), 2106 (w), 1616 (s), 1558 (w), 1483 (s), 1402 (m), 1304 (m), 1254 (m), 1185 (w), 1152 (m), 1079 (w), 883 (m), 865 (m), 812 (s), 759 (w), 668 (w).
LC-(ESI)MS (condition 1): t_R = 16.6 min $[M+H^+]^+$: 196.0 (100%). **Purity** (214 nm): 92%.
HRMS (ESI) calcd for $C_8H_5BrN[M\text{-}H^+]^-$: 193.9611 found: 193.9602.

4-amino-3-ethynylbenzonitril VIII.36

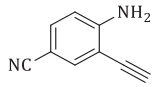

VIII.36

Following general procedure **P.07**: 4-amino-3-(trimethylsilyl)ethynylbenzonitrile **VIII.29** (500 mg, 2.333 mmol, 1 eq). potassium carbonate (322 mg, 2.333 mmol, 1 eq). MeOH (23 mL).

Yield: 96%. 4-amino-3-ethynylbenzonitril (**VIII.36**, 318 mg, 2.237 mmol).
Overall yield: 87%.
Light brown solid.

R_F: 0.12 (hexane/acetone: 8/2).
Molecular weight: 142.16 Da.
^{1}H NMR (300 MHz, acetone-d_6) δ 4.01 (s, 1H), 5.93 (s broad, 2H), 6.88 (d, J = 8.7Hz, 1H), 7.41 (dd, J = 1.7Hz/8.7Hz, 1H), 7.58 (d, J = 1.7Hz, 1H).
^{13}C NMR (75 MHz, acetone-d_6) δ 79.1 (C), 85.6 (CH), 99.1 (C), 106.9 (C), 114.9 (CH), 119.8 (C), 134.3 (CH), 137.3 (CH), 154.1 (C).
HATR (cm^{-1}): 3470 (m), 3360 (s), 3280 (m), 3212 (m), 3055 (w), 2217 (s), 2101 (m), 1909 (w), 1803 (w), 1702 (w), 1627 (s), 1504 (s), 1420 (m), 1325 (m), 1276 (m), 1238 (m), 1223 (m), 1163 (m), 1137 (w), 1055 (w), 903 (m), 832 (m), 816 (m), 782 (w), 739 (m), 695 (s).
LC-(ESI)MS (condition 1): t_R = 13.9 min $[M+H^+]^+$: 143.0 (100%). **Purity** (214 nm): 98%.
HRMS (ESI) calcd for $C_9H_7N_2^+$ $[M+H^+]^+$: 143.0604 found: 143.0607.

4-nitro-2-ethynylaniline VIII.37

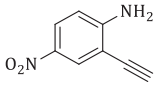

VIII.37

Following general procedure **P.07**: 4-nitro-2-(trimethylsilyl)ethynylaniline **VIII.30** (1.420 g, 6.060 mmol, 1 eq). potassium carbonate (837 mg, 6.060 mmol, 1 eq). MeOH (61 mL).

Yield: 87%. 4-nitro-2-ethynylaniline (**VIII.37**, 854 mg, 5.272 mmol).
Overall yield: 82%.
Yellow solid.
R_F: 0.52 (dichloromethane).
Molecular weight: 162.15 Da.
^{1}H NMR (300 MHz, acetone-d_6) δ 4.08 (s, 1H), 6.34 (s broad, 2H), 6.88 (d, J = 9.0Hz, 1H), 8.00 (dd, J = 2.6Hz/9.0Hz, 1H), 8.12 (d, J = 2.6Hz, 1H).
^{13}C NMR (75 MHz, acetone-d_6) δ 79.0 (C), 85.8 (CH), 105.8 (C), 113.9 (CH), 127.7 (CH), 129.6 (CH), 138.0 (C), 156.3 (C).
HATR (cm^{-1}): 3473 (m), 3368 (m), 3247 (m), 1632 (m), 1568 (w), 1489 (s), 1431 (w), 1320 (s), 1184 (w), 1145 (w), 1088 (w), 913 (w), 824 (w), 752 (w), 723 (w).
LC-(ESI)MS (condition 1): t_R = 14.8 min $[M+H^+]^+$: 163.0 (100%). **Purity** (214 nm): 96%.
HRMS (ESI) calcd for $C_8H_5N_2O_2^-$ $[M-H^+]^-$: 161.0357 found: 161.0355.

3-iodo-4-nitrophenol VIII.43

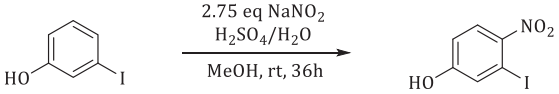

VIII.39 **VIII.40**

A solution of 3-iodophenol (**VIII.39**, 5.900 g, 26.81 mmol) in methanol (10 mL) was slowly added to a vigorously stirred solution of concentrated sulfuric acid (3.7 mL, 70 mmol) and sodium nitrite (6.30 g, 74 mmol) in water (10 mL) in an ice-cooled bad, maintaining the temperature at 0°C. The reaction was followed by TLC (eluent: hexane/ethyl acetate: 8/2) until completion. After 36 h the reaction mixture was diluted with ethyl acetate (20 mL) and the separated aqueous layer was extracted with ethyl acetate (3x 20 mL). The combined organic phases were then washed with brine (1x 50 mL) before being dried ($MgSO_4$), filtered, and concentrated under reduced pressure to yield a dark-brown oil. Further purification was performed with flash chromatography (eluent: hexane/ethyl acetate: 9/1) affording a brown solid which was dried under reduced pressure.

Yield: 35%. 3-iodo-4-nitrophenol (**VIII.40**, 2.488 g, 9.389 mmol).
Brown solid.
R_F: 0.09 (hexane/ethyl acetate: 9/1).
Molecular weight: 265.00 Da.
^{1}H NMR (300 MHz, acetone-d_6) δ 7.96 (dd, J = 8.9Hz, 1H), 7.57 (d, J = 2.5Hz, 1H), 7.04 (dd, J = 2.5Hz/8.9Hz, 1H), 9.88 (s broad, 1H).
^{13}C NMR (75 MHz, acetone-d_6)[1] δ 116.2 (CH), 130.7 (CH), 131.9 (CH).
HATR (cm^{-1}): 3368 (m broad), 3094 (m), 1596 (s), 1578 (s), 1510 (s), 1471 (m), 1453 (m), 1426 (m), 1331 (s), 1291 (s), 1248 (s), 1225 (s), 1125 (m), 1053 (w), 1024 (m), 877 (m), 829 (m), 779 (m), 748 (m), 684 (w), 662 (w), 623 (w).
LC-(ESI)MS (condition 3): t_R = 5.2 min $[M\text{-}H^+]^-$: 263.9 (100%). **Purity** (214 nm): 92%.
HRMS (ESI) calcd for $C_6H_3INO_3^-$: 263.9163 $[M\text{-}H^+]^-$ found: 263.9168.

2-Iodo-4-methoxy-1-nitrobenzene VIII.42

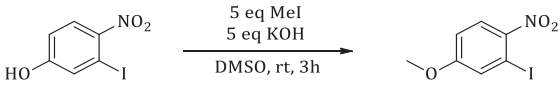

VIII.40 **VIII.42**

An ice-cooled solution of 3-iodo-4-nitrophenol (**VIII.40**, 1.976 g, 7.457 mmol, 1 eq) and potassium hydroxide (2.091 g, 37.28 mmol, 5 eq) in DMSO (24 mL) was stirred for 5 minutes and afterwards treated with iodomethane (2.100 mL, 37.28 mmol, 5 eq). The reaction was monitored by TLC (hexane/acetone: 9/1) and was completed after 3 hours. After a dilution with H_2O (24 mL), the mixture was poured into a separation funnel and EtOAc (24 mL) was added. The organic phase was separated and the remaining aqueous phase extracted with EtOAc (3x 24 mL). The combined organic phases were washed with H_2O (50 mL) and brine solution (50 mL). After drying with $MgSO_4$, the solvent was evaporated *in vacuo*. Resulting in crude product which was purified *via* flash chromatography (hexane/acetone: 95/5) affording 2-iodo-4-methoxy-1-nitrobenzene (**VIII.42**) as a yellow solid.

Yield: 81%. 2-Iodo-4-methoxy-1-nitrobenzene (**VIII.42**, 1.683 g, 6.031 mmol)

[1] Quaternary signals not visible

Yellow solid.
R_F: 0.19 (hexane/ethyl acetate: 9/1). 0.14 (hexane/acetone: 95/5).
Molecular weight: 279.03 Da.
^{1}H NMR (300 MHz, acetone-d_6) δ 3.95 (s, 3H), 7.15 (dd, J = 2.6Hz/9.0Hz, 1H), 7.62 (d, J = 2.6Hz, 1H), 8.00. (d, J = 9.0Hz, 1H),
^{13}C NMR (75 MHz, acetone-d_6) δ 56.8 (CH_3), 88.6 (C), 115.3 (CH), 127.6 (CH), 128.1 (CH), 163.6 (C).
HATR (cm^{-1}): 3095 (w), 2938 (w), 2839 (w), 1584 (s), 1573 (s), 1510 (s), 1475 (s), 1435 (m), 1332 (s), 1281 (s), 1229 (s), 1182 (m), 1125 (m), 1018 (s), 980 (m), 866 (m), 848 (m), 814 (m), 746 (m), 684 (w), 661 (w), 615 (m).
LC-(ESI)MS (condition 1): t_R = 6.2 min $[M+H^+]^+$: 280.1 (100%). **Purity** (214 nm): 96%.

4-methoxy-2-trimethylsilyl-1-nitrobenzene VIII.43

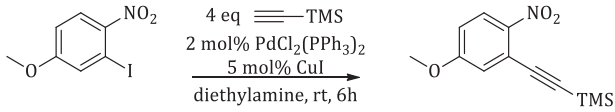

VIII.42 **VIII.43**

Following general procedure **P.06**: 2-iodo-4-methoxy-1-nitrobenzene (**VIII.42**, 1.500 g, 5.376 mmol, 1 eq). trimethylsilylacetylene (3.0 mL, 21.5 mmol, 4 eq). $PdCl_2(PPh_3)_2$ (75.3 mg, 0.1075 mmol, 0.02 eq). CuI (51.2 mg, 0.2688 mmol, 0.05 eq). diethylamine (54 mL).

Yield: 87%. 4-methoxy-2-trimethylsilyl-1-nitrobenzene (**VIII.43**, 1.166 g, 4.676 mmol).
Light-brown crystalline solid.
R_F: 0.35 (hexane/acetone: 8/2). 0.18 (hexane/acetone: 95/5).
Molecular weight: 249.34 Da.
^{1}H NMR (300 MHz, acetone-d_6) δ 0.25 (s, 9H), 3.95 (s, 3H). 7.11-7.17 (m, 2H), 8.11 (d, J = 9.0Hz, 1H).
^{13}C NMR (75 MHz, acetone-d_6) δ -0.40 (CH_3), 56.7 (CH_3), 100.8 (C), 103.2 (C), 116.2 (CH), 119.9 (CH), 120.7 (C), 127.9 (CH), 163.9 (C).
HATR (cm^{-1}): 3367 (m), 3088 (m), 2925 (w), 1697 (w), 1596 (s), 1578 (s), 1525 (s), 1471 (m), 1454 (m), 1368 (m), 1333 (s), 1293 (s), 1249 (s), 1229 (s), 1187 (m), 1125 (m), 1053 (w), 1023 (w), 878 (m), 848 (w), 829 (w), 778 (m), 748 (w), 686 (w), 624 (w).
LC-(ESI)MS (condition 1): t_R = 22.073 min $[M+ H^+]^+$: 250.1 (100%). **Purity** (214 nm): 94%.
HRMS (ESI) calcd for $C_{12}H_{16}NO_3Si^+$: 250.0894 $[M+ H^+]^+$ found: 250.0897.

4-methoxy-2-trimethylsilylaniline VIII.44

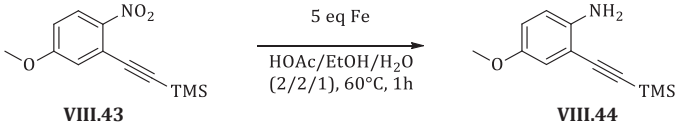

VIII.43 **VIII.44**

To a solution of 4-methoxy-2-trimethylsilyl-1-nitrobenzene **VIII.43** (1.000 g, 4.010 mmol, 1 eq) in $EtOH_{abs}$ (5.3 mL) in a pressure tube, H_2O (2.7 mL) and HOAc (5.3 mL) are added. This solution is agitated for 5 minutes in order to dissolve the substrate. Then, Fe (1.119 g, 20.05 mmol, 5 eq) is poured into the solution. The reaction is heated in an oil bath to 60°C, whereupon H_2 bubbles are visible. After one hour the reaction is completed (monitoring *via* TLC) and the reaction mixture is filtered over a Celite filter. After rinsing the formed Fe-aggregates on the Celite filter with EtOAc (2x 15 mL), the liquid mixture is evaporated. HOAc and H_2O are removed *via* an azeotropic evaporation with toluene (3x 10 mL). The resulting dark brown solid is further purified *via* flash chromatography (hexane/acetone: 95/5) affording 4-methoxy-2-trimethylsilylaniline **VIII.44** as a yellow oil.

Yield: 43%. 4-methoxy-2-trimethylsilylaniline (**VIII.44**, 378.1 mg, 1.723 mmol).
Yellow oil.
R_F: 0.32 (hexane/acetone: 8/2).
Molecular weight: 219.36 Da.
^{1}H NMR (300 MHz, acetone-d_6) δ 0.23 (s, 9H), 3.68 (s, 3H), 4.61 (s broad, 2H), 6.68-6.76 (m, 3H).
^{13}C NMR (75 MHz, acetone-d_6) δ 0.1 (CH_3), 55.9 (CH_3), 103.4 (C), 107.8 (C), 116.0 (CH), 116.3 (CH), 118.7 (CH), 145.0 (C), 151.9 (C).
LC-(ESI)MS (condition 1): t_R = 21.7 min $[M+H^+]^+$: 220.1 (100%).
HRMS (ESI) calcd for $C_{12}H_{18}NOSi^+$: 220.1152 $[M+H^+]^+$ found: 220.1153.

4-methoxy-2-ethynylaniline VIII.45

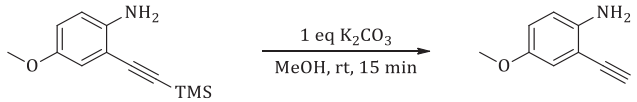

VIII.44 **VIII.45**

Following general procedure **P.07**: 4-methoxy-2-trimethylsilylaniline (**VIII.44**, 378.1 mg, 1.723 mmol, 1 eq). potassium carbonate (238 mg, 1.723 mmol, 1 eq). MeOH (17 mL).

Yield: 100%. 4-methoxy-2-ethynylaniline (**VIII.45**, 253 mg, 1.719 mmol).
Yellow solid.
R_F: 0.09 (hexane/acetone: 8/2)
Molecular weight: 147.17 Da.
^{1}H NMR (300 MHz, acetone-d_6) δ 3.68 (s, 3H). 3.85 (s, 1H), 4.61 (s broad, 2H), 6.71 (d, J = 8.9Hz, 1H), 6.77 (dd, J = 2.8Hz/8.9Hz, 1H), 6.82 (d, J = 2.8Hz).
^{13}C NMR (75 MHz, acetone-d_6) δ 55.8 (CH_3), 81.7 (C), 83.7 (CH), 107.0 (C), 116.3 (CH), 116.6 (CH), 118.4 (CH), 144.8 (C), 151.8 (C).
HATR (cm^{-1}): 3451 (w), 3362 (w), 3280 (m), 2939 (w), 2832 (w), 2096 (w), 1601 (m), 1498 (s), 1465 (m), 1420 (m), 1331 (w), 1276 (m), 1244 (s), 1154 (m), 1138 (m), 1035 (s), 924 (w), 854 (w), 817 (m), 792 (w), 668 (w), 612 (w).
HRMS (ESI) calcd for $C_9H_{10}NO^+$: 148.0757 $[M+H^+]^+$ found: 148.0757.

G. Combinatorial library

8-chloro[1,2,3]triazolo[1,5-*d*][1,4]benzodiazepin-2-one VIII.47

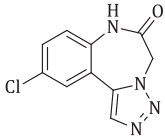

VIII.47

Following general procedure **P.01 - P.05**: 8-chloro[1,2,3]triazolo[1,5-*d*][1,4]benzodiazepin-2-one (**VIII.47**, 96.1 mg, 0.4096 mmol).

Yield: 61%.
White solid.
R_F: 0.26 (hexane/acetone: 6/4).
Mp: 254°C.
Molecular weight: 234.64 Da.
^{1}H NMR (300 MHz, acetone-d_6) δ 5.22 (s, 2H), 7.41 (d, J = 8.9Hz, 1H), 7.55 (dd, J = 2.5Hz/8.9Hz, 1H), 7.79 (d, J = 2.5Hz, 1H), 8.15 (s, 1H), 9.73 (s broad, 1H).
^{13}C NMR (75 MHz, acetone-d_6) δ 53.1 (CH_2), 120.2 (C), 125.0 (CH), 129.3 (CH), 130.6 (C), 131.4 (CH), 132.8 (CH), 134.9 (C), 135.0 (C), 166.9 (C).
HATR (cm^{-1}): 3202 (w), 3083 (w), 2959 (m), 2924 (m), 2360 (w), 1684 (s), 1583 (m), 1533 (w), 1484 (s), 1447 (m), 1394 (s), 1374 (s), 1330 (s), 1291 (m), 1247 (m), 1224 (m), 1203 (m), 1119 (m), 1096 (m), 1034 (m), 981 (m), 956 (w), 840 (s), 817 (s), 752 (w), 730 (m), 697 (w), 681 (w).
LC-(ESI)MS (condition 1): t_R = 12.4 min $[M+H^+]^+$: 235.0 (100%). **Purity** (214 nm): 97%.
HRMS (ESI) calcd for $C_{10}H_6ClN_4O^-$ $[M-H^+]^-$: 233.0236 found: 233.0235.

9-chloro[1,2,3]triazolo[1,5-*d*][1,4]benzodiazepin-2-one VIII.48

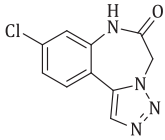

VIII.48

Following general procedure **P.01 - P.05**: 9-chloro[1,2,3]triazolo[1,5-*d*][1,4]benzodiazepin-2-one (**VIII.48**, 95.4 mg, 0.4066 mmol).

Yield: 60%.
Light-brown solid.

R_F: 0.28 (hexane/acetone: 6/4).
Molecular weight: 234.64 Da.
^{1}H NMR (300 MHz, acetone-d_6) δ 5.23 (s, 2H), 7.39 (dd, J = 2.3Hz/8.5Hz, 1H), 7.45 (d, J = 2.3Hz, 1H), 7.77 (d, J = 8.5Hz, 1H), 8.07 (s, 1H), 9.70 (s broad, 1H).
^{13}C NMR (75 MHz, acetone-d_6) δ 53.0 (CH_2), 117.4 (C), 122.9 (CH), 126.0 (CH), 131.5 (CH), 132.5 (CH), 135.3 (C), 136.4 (C), 166.9 (C).
HATR (cm^{-1}): 3189 (w), 3093 (w), 3030 (m), 2922 (w), 2848 (w), 2312 (w), 2227 (w), 1677 (s), 1602 (m), 1575 (s), 1554 (m), 1501 (m), 1472 (m), 1403 (m), 1376 (m), 1327 (m), 1269 (m), 1241 (m), 1216 (w), 1192 (w), 1111 (s), 1022 (w), 961 (m), 908 (w), 856 (w), 816 (s), 744 (w), 722 (w), 696 (w).
LC-(ESI)MS (condition 1): t_R = 12.4 min $[M+H^+]^+$: 235.0 (100%). **Purity** (214 nm): 93%.
HRMS (ESI) calcd for $C_{10}H_6ClN_4O^-$ $[M-H^+]^-$:233.0236 found: 233.0237.

8-bromo[1,2,3]triazolo[1,5-*d*][1,4]benzodiazepin-2-one VIII.49

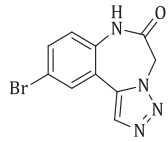

VIII.49

Following general procedure **P.01 - P.05**: 8-bromo[1,2,3]triazolo[1,5-*d*][1,4]benzodiazepin-2-one **VIII.49** (95.6 mg, 0.3425 mmol).

Yield: 51%.
White solid.
R_F: 0.22 (hexane/acetone: 6/4). 0.07 (hexane/acetone: 8/2).
Molecular weight: 279.09 Da.
^{1}H NMR (300 MHz, acetone-d_6) δ 5.23 (s, 2H), 7.34 (d, J = 8.7Hz, 1H), 7.68 (dd, J = 2.5Hz/8.7Hz, 1H), 7.93 (d, J = 2.5Hz, 1H), 8.15 (s, 1H), 9.71 (s broad, 1H).
^{13}C NMR (75 MHz, acetone-d_6) δ 53.1 (CH_2), 118.1 (C), 120.6 (C), 125.2 (CH), 132.2 (CH), 132.8 (CH), 134.3 (CH), 134.9 (C), 135.4 (C), 166.9 (C).
HATR (cm^{-1}): 3220 (w), 3109 (w), 2926 (m), 2866 (w), 2238 (w), 1686 (s), 1599 (w), 1482 (m), 1445 (m), 1398 (m), 1370 (m), 1287 (w), 1244 (w), 1221 (w), 1186 (w), 1112 (w), 1032 (w), 984 (w), 835 (m), 817 (m), 730 (m), 693 (w).
LC-(ESI)MS (condition 1): t_R = 12.7 min $[M+H^+]^+$: 277.0 (100%). **Purity** (214 nm): 98%.
HRMS (ESI) calcd for $C_{10}H_6BrN_4O^-$ $[M-H^+]^-$: 276.9730 found: 276.9729.

8-cyano[1,2,3]triazolo[1,5-*d*][1,4]benzodiazepin-2-one VIII.50

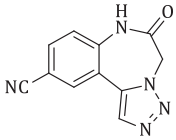

VIII.50

Following general procedure **P.01 - P.05**: 8-cyano[1,2,3]triazolo[1,5-*d*][1,4]benzodiazepin-2-one (**VIII.50**, 80.2 mg, 0.3561 mmol).

Yield: 53%.
Light-brown solid.
R_F: 0.20 (hexane/acetone: 6/4).
Molecular weight: 225.21 Da.
^{1}H NMR (300 MHz, acetone-d_6) δ 5.30 (s, 2H), 7.57 (d, J = 8.5Hz, 1H), 7.91 (dd, J = 1.9Hz/8.5Hz, 1H), 8.21 (s, 1H), 8.23 (d, J = 8.5Hz, 1H), 9.90 (s broad, 1H).
^{13}C NMR (75 MHz, acetone-d_6) δ 53.2 (CH_2), 109.3 (C), 118.4 (C), 119.2 (C), 124.0 (CH), 133.2 (CH), 134.4 (CH), 134.6 (CH), 134.7 (C), 139.6 (C), 166.8 (C).
HATR (cm^{-1}): 3112 (w), 3035 (w), 2921 (s), 2859 (m), 2364 (w), 2291 (w), 2228 (s), 1687 (s), 1677 (s), 1610 (s), 1585 (s), 1495 (s), 1450 (m), 1416 (s), 1375 (s), 1304 (m), 1248 (m), 1233 (m), 1199 (m), 1120 (m), 1032 (w), 991 (w), 923 (w), 903 (w), 869 (w), 838 (s), 798 (m), 724 (w), 695 (w).
LC-(ESI)MS (condition 1): t_R = 11.0 min $[M+H^+]^+$: 226.0 (100%). **Purity** (214 nm): 89%.
HRMS (ESI) calcd for $C_{11}H_6N_5O^-$ $[M-H^+]^-$: 224.0578 found: 224.0576.

8-nitro[1,2,3]triazolo[1,5-*d*][1,4]benzodiazepin-2-one VIII.51

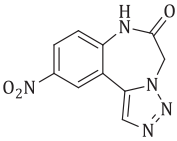

VIII.51

Following general procedure **P.01 - P.05**: 8-nitro[1,2,3]triazolo[1,5-*d*][1,4]benzodiazepin-2-one (**VIII.51**, 60.9 mg, 0.2484 mmol).

Yield: 37%.
Light-brown solid.
R_F: 0.20 (hexane/acetone: 6/4).
Molecular weight: 245.19 Da.

^{1}H NMR (300 MHz, acetone-d_6) δ 5.23 (s, 2H), 7.35 (d, J = 8.9Hz, 1H), 7.68 (dd, J = 2.5Hz/8.7Hz, 1H), 7.93 (d, J = 2.5Hz, 1H), 8.15 (s, 1H), 9.71 (s broad, 1H).
^{13}C NMR (75 MHz, acetone-d_6) δ 53.1 (CH_2), 118.1 (C), 120.6 (C), 125.2 (CH), 132.2 (CH), 132.8 (CH), 134.3 (CH), 134.9 (C), 135.4 (C), 166.9 (C).
HATR (cm^{-1}): 3323 (w), 3230 (w), 3110 (w), 2958 (w), 2924 (w), 1694 (s), 1670 (m), 1584 (m), 1525 (m), 1496 (m), 1409 (m), 1340 (s), 1323 (s), 1260 (m), 1226 (m), 1119 (m), 1030 (w), 980 (w), 907 (w), 839 (w), 800 (w), 748 (w), 695 (w).
LC-(ESI)MS (condition 1): t_R = 11.7 min $[M\text{-}H^+]^-$: 244.0 (100%). **Purity** (214 nm): 88%.
HRMS (ESI) calcd for $C_{10}H_6N_5O_3^-$ $[M\text{-}H^+]^-$: 244.0476 found: 244.0474.

(*S*)-3-benzyl-8-chloro[1,2,3]triazolo[1,5-*d*][1,4]benzodiazepin-2-one VIII.52

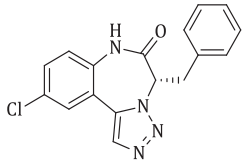

VIII.52

Following general procedure **P.01 - P.05**: (*S*)-3-benzyl-8-chloro[1,2,3]triazolo[1,5-*d*][1,4]benzodiazepin-2-one (**VIII.52**, 135.4 mg, 0.4169 mmol).

Yield: 75%.
White solid.
R_F: 0.39 (hexane/acetone: 6/4). 0.10 (hexane/acetone: 8/2).
Molecular weight: 324.76 Da.
^{1}H NMR (300 MHz, acetone-d_6) δ 3.33-3.48 (m, 2H), 5.52-5.58 (m, 1H), 7.14-7.24 (m, 5H), 7.44 (d, J = 8.9Hz, 1H), 7.58 (dd, J = 2.5Hz/8.9Hz, 1H), 7.85 (d, J = 2.5Hz, 1H), 8.15 (s, 1H), 9.79 (s broad, 1H).
^{13}C NMR (75 MHz, acetone-d_6) δ 34.5 (CH_2), 65.6 (CH), 120.2 (C), 124.50 (CH), 127.8 (CH), 129.0 (CH), 129.2 (CH), 130.1 (CH), 130.7 (C), 131.5 (CH), 133.2 (CH), 134.4 (C), 134.7 (C), 136.6 (C), 167.3 (C).
HATR (cm^{-1}): 3205 (w), 3090 (w), 2955 (w), 1684 (s), 1484 (s), 1455 (w), 1399 (m), 1365 (m), 1222 (w), 1244 (w), 1117 (w), 1090 (w), 976 (w), 827 (w), 750 (w), 699 (w).
LC-(ESI)MS (condition 1): t_R = 15.6 min $[M+H^+]^+$: 325.0 (100%). **Purity** (214 nm): 94%.
HRMS (ESI) calcd for $C_{17}H_{14}ClN_4O^+$ $[M+H^+]^+$: 325.0851 found: 325.0827.

(*S*)-3-Benzyl-9-chloro[1,2,3]triazolo[1,5-*d*][1,4]benzodiazepin-2-one VIII.53

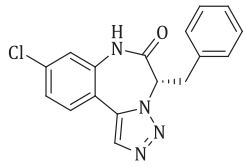

VIII.53

Following general procedure **P.01 - P.05**: (*S*)-3-Benzyl-9-chloro[1,2,3]triazolo[1,5-*d*][1,4]benzodiazepin-2-one (**VIII.53**, 102.9 mg, 0.3168 mmol).

Yield: 57%.
White solid.
R_F: 0.39 (hexane/acetone: 6/4). 0.10 (hexane/acetone: 8/2).
Molecular weight: 324.76 Da.
^{1}H NMR (300 MHz, acetone-d_6) δ 3.32-3.48 (m, 2H), 5.54-5.59 (m, 1H), 7.13-7.24 (m, 5H), 7.41 (dd, J = 2.1Hz/8.3Hz, 1H), 7.48 (d, J = 2.1Hz, 1H), 7.83 (d, J = 8.3Hz, 1H), 8.07 (s, 1H), 9.80 (s broad, 1H).
^{13}C NMR (75 MHz, acetone-d_6) δ 34.6 (CH_2), 65.6 (CH), 117.4 (C), 122.4 (CH), 126.0 (CH), 127.8 (CH), 129.2 (CH), 130.1 (CH), 131.2 (CH), 132.9 (CH), 134.8 (C), 136.6 (C), 136.6 (C), 137.0 (C), 167.4 (C).
HATR (cm^{-1}): 3227 (w), 3121 (w), 3065 (w), 2974 (s), 1687 (m), 1606 (m), 1584 (m), 1480 (m), 1400 (m), 1362 (m), 1266 (m), 1215 (m), 1120 (m), 1027 (w), 976 (m), 873 (m), 820 (m), 734 (s), 699 (s).
LC-(ESI)MS (condition 1): t_R = 15.6 min $[M+H^+]^+$: 325.0 (100%). **Purity** (214 nm): 95%.
HRMS (ESI) calcd for $C_{17}H_{14}ClN_4O^+$ $[M+H^+]^+$: 325.0851 found: 325.0818.

(*S*)-3-Benzyl-8-bromo[1,2,3]triazolo[1,5-*d*][1,4]benzodiazepin-2-one VIII.54

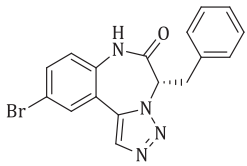

VIII.54

Following general procedure **P.01 - P.05**: (*S*)-3-Benzyl-8-bromo[1,2,3]triazolo[1,5-*d*][1,4]benzodiazepin-2-one (**VIII.54**, 106.7 mg, 0.2890 mmol).

Yield: 52%.
White solid.
R_F: 0.39 (hexane/acetone: 6/4). 0.10 (hexane/acetone: 8/2).

Molecular weight: 369.22 Da.
^{1}H NMR (300 MHz, acetone-d_6) δ 3.33-3.48 (m, 2H), 5.53-5.58 (m, 1H), 7.13-7.24 (m, 5H), 7.37 (d, J = 8.7Hz, 1H), 7.71 (dd, J = 2.3Hz/8.7Hz, 1H), 7.98 (d, J = 2.3Hz, 1H), 8.15 (s, 1H), 9.80 (s broad, 1H).
^{13}C NMR (75 MHz, acetone-d_6) δ 34.6 (CH_2), 65.6 (CH), 118.2 (C), 120.6 (C), 124.7 (CH), 127.8 (CH), 129.2 (CH), 130.1 (CH), 131.9 (CH), 133.2 (CH), 134.3 (C), 134.5 (CH), 135.1 (C), 136.6 (C), 167.3 (C).
HATR (cm^{-1}): 3205 (w), 3129 (w), 2961 (w), 1686 (s), 1483 (s), 1454 (w), 1438 (w), 1397 (m), 1364 (m), 1241 (w), 1224 (w), 1117 (w), 1079 (w), 1029 (w), 974 (w), 880 (w), 826 (w), 746 (w), 700 (w).
LC-(ESI)MS (condition 1): t_R = 15.8 min $[M+H^+]^+$: 369.0 (100%). **Purity** (214 nm): 96%.
HRMS (ESI) calcd for $C_{17}H_{14}BrN_4O^+$ $[M+H^+]^+$: 369.0346 found: 369.0346.

(*S*)-3-Benzyl-8-cyano[1,2,3]triazolo[1,5-*d*][1,4]benzodiazepin-2-one VIII.55

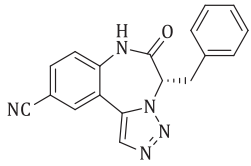

VIII.55

Following general procedure **P.01 - P.05**: (*S*)-3-Benzyl-8-cyano[1,2,3]triazolo[1,5-*d*][1,4]benzodiazepin-2-one (**VIII.55**, 98.1 mg, 0.3112 mmol).

Yield: 56%.
Light-brown solid.
R_F: 0.26 (hexane/acetone: 6/4). 0.05 (hexane/acetone: 8/2).
Molecular weight: 315.33 Da.
^{1}H NMR (300 MHz, acetone-d_6) δ 3.32-3.47 (m, 2H), 5.61-5.67 (m, 1H), 7.15-7.24 (m, 5H), 7.60 (d, J = 8.5Hz, 1H), 7.92 (dd, J = 1.9Hz/8.5Hz, 1H), 8.21 (s, 1H), 8.28 (d, J = 1.9Hz, 1H), 10.08 (s broad, 1H).
^{13}C NMR (75 MHz, acetone-d_6) δ 34.9 (CH_2), 65.9 (CH), 109.3 (C), 118.5 (C), 119.1 (C), 123.5 (CH), 127.9 (CH), 129.3 (CH), 130.1 (CH), 133.6 (CH), 134.1 (CH), 134.8 (CH), 136.4 (C), 139.3 (C), 167.3 (C).
HATR (cm^{-1}): 3217 (w), 3080 (w), 2927 (s), 2227 (w), 1687 (s), 1614 (m), 1589 (m), 1495 (m), 1455 (m), 1435 (m), 1398 (m), 1363 (m), 1251 (w), 1209 (w), 1120 (w), 1080 (w), 983 (w), 895 (w), 832 (m), 736 (s), 700 (s).
LC-(ESI)MS (condition 1): t_R = 14.4 min $[M+H^+]^+$: 316.0 (100%). **Purity** (214 nm): 89%.
HRMS (ESI) calcd for $C_{18}H_{14}N_5O^+$ $[M+H^+]^+$: 316.1193 found: 316.1198.

(*S*)-3-Benzyl-8-nitro[1,2,3]triazolo[1,5-*d*][1,4]benzodiazepin-2-one VIII.56

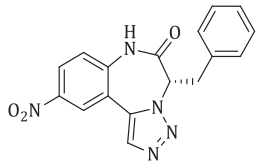

VIII.56

Following general procedure **P.01 - P.05**: (*S*)-3-Benzyl-8-nitro[1,2,3]triazolo[1,5-*d*][1,4]benzodiazepin-2-one (**VIII.56**, 87.6 mg, 0.2612 mmol).

Yield: 47%.
Light-brown solid.
R_F: 0.33 (hexane/acetone: 6/4). 0.05 (hexane/acetone: 8/2).
Molecular weight: 335.32 Da.
^{1}H NMR (300 MHz, acetone-d_6) δ 3.37-3.52 (m, 2H), 5.67-5.73 (m 1H), 7.18-7.25 (m, 5H), 7.67 (d, J = 9.0Hz, 1H), 8.33 (s, 1H), 8.41 (dd, J = 2.5Hz/9.0Hz, 1H), 8.68 (d, J = 2.5.Hz, 1H), 10.20 (s broad, 1H).
^{13}C NMR (75 MHz, acetone-d_6) δ 35.0 (CH_2), 65.9 (CH), 118.7 (C), 123.6 (CH), 125.4 (CH), 126.4 (CH), 127.9 (CH), 129.3 (CH), 130.1(CH), 133.9 (CH), 134.1 (CH), 136.3 (C), 140.9 (C), 145.2 (C), 167.3 (C).
HATR (cm^{-1}): 3230 (w), 3112 (w), 2972 (w), 1697 (s), 1620 (w), 1585 (m), 1528 (m), 1488 (m), 1454 (w), 1403 (w), 1337 (s), 1247 (w), 1234 (w), 1120 (w), 1102 (w), 973 (w), 905 (w), 841 (w), 748 (m), 699 (w).
LC-(ESI)MS (condition 1): t_R = 14.9 min $[M+H^+]^+$: 336.0 (100%). **Purity** (214 nm): 91%.
HRMS (ESI) calcd for $C_{17}H_{14}N_5O_3^+$ $[M+H^+]^+$ 336.1091 found: 336.1093.

(*S*)-3-Benzyl-8-methoxy[1,2,3]triazolo[1,5-*d*][1,4]benzodiazepin-2-one VIII.57

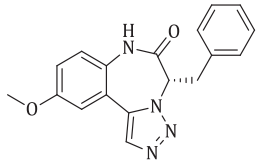

VIII.57

Following general procedure **P.01 - P.05**: (*S*)-3-benzyl-8-methoxy[1,2,3]triazolo[1,5-*d*][1,4]benzodiazepin-2-one (**VIII.57**, 92.1 mg, 0.2875 mmol).

Yield: 63%.
White solid.

R_F: 0.05 (hexane/acetone: 8/2). 0.18 (hexane/acetone: 7/3).
Molecular weight: 320.35 Da.
^{1}H NMR (300 MHz, acetone-d_6) δ 3.31-3.46 (m, 2H), 3.90 (s, 3H), 5.46 (t, J = 7.3Hz, 1H), 7.13-7.21 (m, 6H), 7.32 (d, J = 2.8Hz, 1H), 7.33 (d, J = 9.1Hz, 1H), 8.07 (s, 1H), 9.55 (s broad, 1H).
^{13}C NMR (75 MHz, acetone-d_6) δ 34.2 (CH_2), 56.1 (CH_3), 65.6 (CH), 113.3 (CH), 118.3 (CH), 119.8 (C), 124.4 (CH), 127.7 (CH), 129.1 (C), 129.2 (CH), 130.1 (CH), 132.7 (CH), 136.9 (C), 157.9 (C), 167.3 (C).
HATR (cm^{-1}): 3457 (w), 3219 (w), 2125 (w), 2969 (w), 2940 (w), 1681 (s), 1618 (m), 1557 (w), 1500 (s), 1455 (m), 1439 (m), 1408 (m), 1378 (m), 1296 (m), 1283 (m), 1233 (m), 1217 (m), 1179 (m), 1114 (m), 1078 (w), 1029 (m), 977 (m), 829 (m), 776 (w), 747 (m), 699 (m), 608 (w).
LC-(ESI)MS (condition 1): t_R = 18.2 min $[M+H^+]^+$: 321.1 (100%). **Purity** (214 nm): 98%.
HRMS (ESI) calcd for $C_{18}H_{17}N_4O_2^+$: 321.1346 $[M+H^+]^+$ found: 321.1351.

(*S*)-3-(tert-Butoxymethyl)-8-chloro[1,2,3]triazolo[1,5-*d*][1,4]benzodiazepin-2-one VIII.58

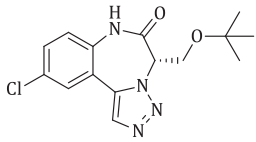

VIII.58

Following general procedure **P.01 - P.05**: (*S*)-3-(tert-Butoxymethyl)-8-chloro[1,2,3]triazolo[1,5-*d*][1,4]benzodiazepin-2-one (**VIII.58** ,114.6 mg, 0.3573 mmol).

Yield: 73%.
White solid.
R_F: 0.43 (hexane/acetone: 6/4). 0.13 (hexane/acetone: 8/2).
Molecular weight: 320.77 Da.
^{1}H NMR (300 MHz, acetone-d_6) δ 0.92 (s, 9H), 3.82-4.03 (m, 2H), 5.53 (app s broad, 1H), 7.38 (d, J = 8.7Hz, 1H), 7.51 (dd, J = 2.3Hz/8.7Hz, 1H), 7.81 (d, J = 2.3Hz, 1H), 8.17 (s, 1H).
^{13}C NMR (75 MHz, acetone-d_6) δ 27.0 (CH_3), 61.6 (CH_2), 74.4 (CH), 120.1 (C), 124.1 (CH), 128.6 (CH), 130.1 (C), 131.1 (CH), 133.1 (CH), 134.7 (C), 135.1 (C), 167.4 (C).
HATR (cm^{-1}): 3195 (w), 3125 (w), 3084 (w), 2977 (m), 2932 (m), 2871 (m), 1701 (s), 1686 (s), 1588 (w), 1484 (s), 1444 (w), 1401 (m), 1364 (s), 1345 (m), 1289 (w), 1259 (w), 1236 (m), 1226 (m), 1186 (m), 1120 (m), 1102 (m), 1069 (s), 1027 (w), 981 (w), 913 (w), 890 (m), 847 (m), 817 (m), 758 (w), 743 (w), 687 (w).
LC-(ESI)MS (condition 1): t_R = 15.5 min $[M+H^+]^+$: 321.1 (100%). **Purity** (214 nm): 91%.
HRMS (ESI) calcd for $C_{15}H_{18}ClN_4O_2^+$ $[M+H^+]^+$: 321.1113 found: 321.1112.

(*S*)-3-(tert-butoxymethyl)-9-chloro[1,2,3]triazolo[1,5-*d*][1,4]benzodiazepin-2-one VIII.59

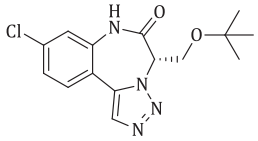

VIII.59

Following general procedure **P.01 - P.05**: (*S*)-3-(tert-butoxymethyl)-9-chloro[1,2,3]triazolo[1,5-*d*][1,4]benzodiazepin-2-one (**VIII.59**, 115.2 mg, 0.3591 mmol).

Yield: 73%.
White solid.
R_F: 0.40 (hexane/acetone: 6/4). 0.13 (hexane/acetone: 8/2).
Molecular weight: 320.77 Da.
^{1}H NMR (300 MHz, acetone-d_6) δ 0.90 (s, 9H), 3.81-4.01 (m, 2H), 5.55 (app s broad, 1H), 7.34 (dd, J = 2.1Hz/8.3Hz, 1H), 7.41 (d, J = 2.1Hz, 1H), 7.79 (d, J = 8.3Hz, 1H), 8.09 (s, 1H), 9.77 (s broad, 1H).
^{13}C NMR (75 MHz, acetone-d_6) δ 27.0 (CH_3), 61.6 (C), 66.2 (CH), 74.4 (CH_2), 117.3 (C), 121.9 (CH), 125.4 (CH), 130.8 (CH), 132.8 (CH), 135.2 (C), 136.1 (C), 137.0 (C), 167.6 (C).
HATR (cm^{-1}): 3218 (w), 3110 (w), 2973 (m), 2873 (w), 1681 (s), 1609 (m), 1582 (s), 1555 (w), 1480 (m), 1445 (w), 1402 (m), 1364 (s), 1247 (m), 1212 (m), 1189 (s), 1102 (s), 1022 (w), 985 (w), 968 (m), 944 (w), 904 (w), 873 (m), 857 (m), 814 (s), 734 (s), 701 (m), 664 (m).
LC-(ESI)MS (condition 1): t_R = 15.5 min $[M+H^+]^+$: 321.0 (100%). **Purity** (214 nm): 97%.
HRMS (ESI) calcd for $C_{15}H_{18}ClN_4O_2^+$ $[M+H^+]^+$: 321.1113 found: 321.1114.

***(S)*-3-(tert-butoxymethyl)-8-bromo[1,2,3]triazolo[1,5-*d*][1,4]benzodiazepin-2-one VIII.60**

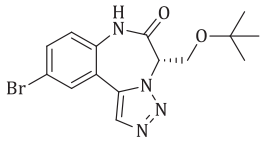

VIII.60

Following general procedure **P.01 - P.05**: *(S)*-3-(tert-butoxymethyl)-8-bromo[1,2,3]triazolo[1,5-*d*][1,4]benzodiazepin-2-one (**VIII.60**, 94.7 mg, 0.2593 mmol).

Yield: 53%.
White solid.
R_F: 0.35 (hexane/acetone: 6/4). 0.10 (hexane/acetone: 8/2).
Molecular weight: 365.22 Da.

^{1}H NMR (300 MHz, acetone-d_6) δ 0.92 (s, 9H), 3.82-4.01 (m, 2H), 5.54 (app s broad, 1H), 7.30 (d, J = 8.7Hz, 1H), 7.64 (dd, J = 2.3Hz/8.7Hz, 1H), 7.95 (d, J = 2.3Hz, 1H), 8.18 (s, 1H), 9.74 (s broad, 1H).
^{13}C NMR (75 MHz, acetone-d_6) δ 27.0 (CH_3), 61.6 (C), 74.4 (CH_2), 117.6 (C), 120.5 (C), 124.3 (CH), 131.5 (CH), 133.1 (CH), 134.0 (CH), 134.9 (C), 135.2 (C), 167.5 (C).
HATR (cm^{-1}): 3269 (w), 2112 (w), 2973 (w), 2930 (w), 2871 (w), 1688 (s), 1618 (m), 1587 (m), 1528 (m), 1490 (m), 1445 (w), 1406 (w), 1365 (m), 1328 (s), 1274 (m), 1240 (m), 1190 (m), 1108 (m), 984 (w), 906 (w), 872 (m), 840 (m), 746 (m), 733 (m), 696 (w), 665 (w).
LC-(ESI)MS (condition 1): t_R = 15.7 min $[M+H^+]^+$: 365.0 (100%). **Purity** (214 nm): 99%.
HRMS (ESI) calcd for $C_{15}H_{18}BrN_4O_2^+$ $[M+H^+]^+$: 365.0608 found: 365.0606.

(S)-3-(tert-butoxymethyl)-8-cyano[1,2,3]triazolo[1,5-*d*][1,4]benzodiazepin-2-one VIII.61

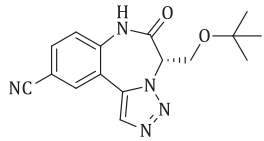

VIII.61

Following general procedure **P.01 - P.05**: *(S)*-3-(tert-butoxymethyl)-8-cyano[1,2,3]triazolo[1,5-*d*][1,4]benzodiazepin-2-one (**VIII.61**, 76.2 mg, 0.2447 mmol).

Yield: 50%.
Light-brown solid.
R_F: 0.31 (hexane/acetone: 6/4). 0.08 (hexane/acetone: 8/2).
Molecular weight: 311.34 Da.
^{1}H NMR (300 MHz, acetone-d_6) δ 0.85 (s, 9H), 3.82 (dd, J = 4.3Hz/10.2Hz, 1H), 4.02 (dd, J = 4.9Hz/10.2Hz, 1H), 5.68 (app s broad, 1H), 7.51 (d, J = 8.5Hz, 1H), 7.85 (dd, J = 2.0Hz/8.5Hz, 1H), 8.26 (app s, 2H), 10.07 (s broad, 1H).
^{13}C NMR (75 MHz, acetone-d_6) δ 26.9 (CH_3), 66.5 (CH_2), 74.4 (CH), 108.6 (C), 118.6 (C), 119.3 (C), 123.0 (CH), 133.4 (CH), 134.3 (CH), 134.8 (C) 139.4 (C), 167.8 (C).
HATR (cm^{-1}): 3215 (w), 3124 (w), 3048 (w), 2977 (m), 2921 (w), 2871 (w), 2233 (m), 1682 (s), 1613 (m), 1592 (m), 1496 (s), 1446 (w), 1400 (m), 1365 (s), 1294 (w), 1259 (m), 1231 (m), 1188 (s), 1099 (s), 1026 (w), 981 (w), 897 (w), 834 (m), 733 (s), 703 (m).
LC-(ESI)MS (condition 1): t_R = 14.2 min $[M+H^+]^+$: 312.1 (100%). **Purity** (214 nm): 99%.
HRMS (ESI) calcd for $C_{16}H_{18}N_5O_2^+$ $[M+H^+]^+$: 312.1455 found: 312.1456.

(*S*)-3-(tert-butoxymethyl)-8-nitro[1,2,3]triazolo[1,5-*d*][1,4]benzodiazepin-2-one VIII.62

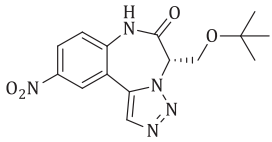

VIII.62

Following general procedure **P.01 - P.05:** (*S*)-3-(tert-butoxymethyl)-8-nitro[1,2,3]triazolo[1,5-*d*][1,4]benzodiazepin-2-one **VIII.62** (40.5 mg, 0.1222 mmol).

Yield: 25%.
Light-brown solid.
R_F: 0.45 (hexane/acetone: 6/4). 0.14 (hexane/acetone: 8/2).
Molecular weight: 331.33 Da.
^{1}H NMR (300 MHz, acetone-d_6) δ 0.85 (s, 9H), 3.84 (dd, *J* = 4.3Hz/10.3Hz, 1H), 3.94 (dd, *J* = 4.7Hz/10.3Hz, 1H), 5.71 (app s broad, 1H), 7.57 (d, *J* = 9.0Hz, 1H), 8.33 (dd, *J* = 2.6Hz/9.0Hz, 1H), 8.35 (s, 1H), 8.62 (d, *J* = 2.6Hz, 1H), 10.18 (s broad, 1H).
^{13}C NMR (75 MHz, acetone-d_6) δ 26.9 (CH_3), 62.8 (C), 66.5 (CH), 74.5 (CH_2), 119.0 (C), 123.0 (CH), 124.7 (CH), 126.0 (CH), 133.8 (CH), 134.8 (C), 141.1 (C), 144.8 (C), 167.7 (C).
HATR (cm^{-1}): 3200 (w), 3119 (w), 3078 (w), 2971 (m), 2932 (w), 2886 (w), 1684 (s), 1575 (w), 1480 (m), 1436 (w), 1396 (m), 1365 (s), 1290 (w), 1237 (m), 1221 (m), 1183 (m), 1122 (m), 1069 (s), 1024 (w), 978 (w), 915 (w), 885 (m), 842 (m), 818 (m), 781 (w), 736 (w), 698 (w), 667 (w).
LC-(ESI)MS (condition 1): t_R = 14.8 min $[M+H^+]^+$: 332.1 (100%). **Purity** (214 nm): 93%.
HRMS (ESI) calcd for $C_{15}H_{18}N_5O_4^+$ $[M+H^+]^+$: 332.1353 found: 332.1361.

(*S*)-3-(*N*-(tert-butyloxycarbonyl)-indolylmethyl)-8-chloro[1,2,3]triazolo[1,5-*d*][1,4]-benzodiazepin-2-one VIII.63

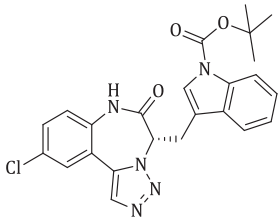

VIII.63

Following general procedure **P.01 - P.05:** (*S*)-3-(*N*-(tert-butyloxycarbonyl)-indolylmethyl)-8-chloro[1,2,3]triazolo[1,5-*d*][1,4]benzodiazepin-2-one (**VIII.63**, 203.7 mg, 0.4390 mmol).

Yield: 86%.
White solid.
R_F: 0.33 (hexane/acetone: 6/4). 0.12 (hexane/acetone: 8/2).
Molecular weight: 463.92 Da.
^{1}H NMR (300 MHz, acetone-d_6) δ 1.65 (s, 9H), 3.58 (d, J = 7.3Hz, 2H), 5.74 (t, J = 7.3Hz, 1H), 7.18 (td, J = 1.1Hz/7.9Hz, 1H), 7.25-7.33 (m, 2H), 7.41-7.51 (m, 3H), 7.69 (d, J = 2.4Hz, 1H), 8.03 (d, J = 8.1 Hz, 1H), 8.15 (s, 1H).
^{13}C NMR (75 MHz, acetone-d_6) δ 25.1 (C), 28.2 (CH_3), 84.4 (CH_2), 115.1 (C), 115.8 (CH), 119.5 (CH), 123.4 (CH), 124.3 (CH), 125.2 (CH), 125.8 (CH), 126.8 (C), 128.8 (CH), 130.9 (C), 131.3 (CH), 133.2 (C), 167.7 (C).
HATR (cm^{-1}): 3220 (w), 3124 (w), 2974 (w), 1729 (s), 1683 (s), 1610 (w), 1590 (w), 1484 (m), 1451 (s), 1368 (s), 1308 (m), 1254 (s), 1227 (m), 1154 (s), 1121 (m), 1084 (s), 1040 (w), 1017 (m), 974 (m), 907 (w), 878 (w), 854 (m), 828 (m), 762 (s), 744 (s), 669 (w).
LC-(ESI)MS (condition 1): t_R = 18.4 min $[M+H^+]^+$: 464.1 (100%). **Purity** (214 nm): 99%.
HRMS (ESI) calcd for $C_{24}H_{21}ClN_5O_3^-$ $[M-H^+]^-$: 462.1338 found: 464.1348.

(*S*)-3-(*N*-(tert-butyloxycarbonyl)-indolylmethyl)-9-chloro[1,2,3]triazolo[1,5-*d*][1,4]-benzodiazepin-2-one VIII.64

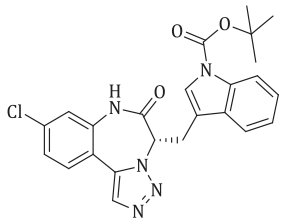

VIII.64

Following general procedure **P.01 - P.05:** (*S*)-3-(*N*-(tert-butyloxycarbonyl)-indolylmethyl)-9-chloro[1,2,3]triazolo[1,5-*d*][1,4]benzodiazepin-2-one (**VIII.64**, 240.1 mg, 0.5175 mmol).

Yield: 94%.
White solid.
R_F: 0.44 (hexane/acetone: 6/4). 0.10 (hexane/acetone: 8/2).
Mp: 162°C.
Molecular weight: 463.92 Da.
^{1}H NMR (300 MHz, acetone-d_6) δ 1.62 (s, 9H), 3.57 (d, J = 7.1Hz, 2H), 5.75 (t, J = 7.1Hz, 1H), 7.16 (app td, J = 1Hz/7.5Hz, 1H), 7.22-7.32 (m, 3H), 7.40 (s, 1H), 7.46 (d, J = 7.5Hz, 1H), 7.66 (d, J = 8.2Hz, 1H), 8.01 (d, J = 8.1 Hz, 1H), 8.06 (s, 1H), 9.86 (s broad, 1H).
^{13}C NMR (75 MHz, acetone-d_6) δ 25.1 (C), 28.2 (CH_3), 64.5 (CH), 84.4 (CH_2), 115.3 (C), 115.8 (CH), 119.5 (CH), 122.2 (CH), 123.4 (CH), 125.2 (CH), 125.8 (CH), 130.9 (C), 131.0 (CH), 132.9 (CH), 134.9 (C), 136.4 (C), 167.7 (C).
HATR (cm^{-1}): 3217 (w), 3152 (w), 3106 (w), 2968 (m), 2934 (w), 1730 (s), 1682 (s), 1609 (m), 1583 (m), 1479 (s), 1451 (s), 1392 (s), 1367 (s), 1311 (m), 1253 (m), 1220 (m), 1154 (s),

1120 (m), 1086 (s), 1042 (w), 1017 (m), 979 (m), 946 (w), 882 (m), 857 (m), 822 (s), 744 (s), 701 (w), 666 (w).
LC-(ESI)MS (condition 1): t_R = 18.4 min $[M\text{-}H^+]^-$: 464.1 (100%). **Purity** (214 nm): 97%.
HRMS (ESI) calcd for $C_{24}H_{21}ClN_5O_3^-$ $[M\text{-}H^+]^-$: 462.1338 found: 462.1345.

(S)-8-bromo-3-(*N*-(tert-butyloxycarbonyl)-indolylmethyl)[1,2,3]triazolo[1,5-*d*][1,4]-benzodiazepin-2-one VIII.65

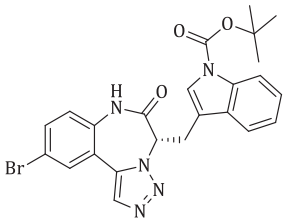

VIII.65

Following general procedure **P.01 - P.05:** *(S)*-8-bromo-3-(*N*-(tert-butyloxycarbonyl)-indolylmethyl)[1,2,3]triazolo[1,5-*d*][1,4]benzodiazepin-2-one (**VIII.65**, 209.3 mg, 0.4117 mmol).

Yield: 75%.
White solid.
%ee: 99%.
R_F: 0.44 (hexane/acetone: 6/4). 0.08 (hexane/acetone: 8/2).
Mp: 170°C.
Molecular weight: 508.37 Da.
^{1}H NMR (300 MHz, acetone-d_6) δ 1.63 (s, 9H), 3.58 (d, J = 7.2Hz, 1H), 5.76 (t, J = 7.2Hz, 1H), 7.16 (t, J = 7.2Hz, 1H), 7.25 (m, 2H), 7.41-7.44 (m, 2H), 7.57 (dd, J = 2.3Hz/8.3Hz, 1H), 7.81 (d, J = 2.3Hz, 1H), 8.02 (d, J = 8.3Hz, 1H), 8.15 (s, 1H), 9.88 (s broad, 1H).
^{13}C NMR (75 MHz, acetone-d_6) δ 25.1 (C), 28.2 (CH_3), 64.4 (CH), 84.3 (CH_2), 115.1 (C), 115.7 (CH), 117.9 (C), 119.4 (CH), 120.0 (C), 123.2 (CH), 124.3 (CH), 125.1 (CH), 125.7 (CH), 130.8 (C), 131.6 (CH), 133.1 (CH), 134.1 (CH), 134.5 (C), 134.6 (C), 135.9 (C), 149.9 (C), 167.6 (C).
HATR (cm^{-1}): 3217 (w), 3116 (w), 3096 (w), 2975 (w), 2364 (w), 2323 (w), 2162 (w), 1732 (s), 1682 (s), 1612 (w), 1581 (w), 1480 (m), 1452 (m), 1368 (s), 1307 (m), 1252 (s), 1224 (m), 1154 (s), 1122 (m), 1087 (s), 1017 (m), 973 (m), 853 (m), 824 (s), 744 (s), 745 (s), 697 (w).
LC-(ESI)MS (condition 1): t_R = 18.6 min $[M+H^+]^+$: 508.0 (100%). **Purity** (214 nm): 97%.
HRMS (ESI) calcd for $C_{24}H_{21}BrN_5O_3^-$ $[M\text{-}H^+]^-$: 506.0833 found: 506.0833.

(*S*)-8-cyano-3-(*N*-(tert-butyloxycarbonyl)-indolylmethyl)[1,2,3]triazolo[1,5-*d*][1,4]-benzodiazepin-2-one VIII.66

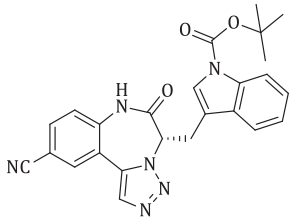

VIII.66

Following general procedure **P.01 - P.05:** (*S*)-8-cyano-3-(*N*-(tert-butyloxycarbonyl)-indolylmethyl)[1,2,3]triazolo[1,5-*d*][1,4]benzodiazepin-2-one (**VIII.66**, 87.3 mg, 0.1921 mmol).

Yield: 35%.
Light-brown solid.
R_F: 0.38 (hexane/acetone: 6/4). 0.04 (hexane/acetone: 8/2).
Mp: 178°C.
Molecular weight: 454.48 Da.
^{1}H NMR (300 MHz, acetone-d_6) δ 1.65 (s, 9H), 3.58 (d, J = 6.8Hz, 2H), 5.86 (t, J = 7.0Hz, 1H), 7.17 (app td, J =1.1Hz/7.5Hz, 1H), 7.26 (td, J = 1.1Hz/7.1Hz, 1H), 7.37 (m, 3H), 7.76 (dd, J = 1.9Hz/8.5Hz, 1H), 7.99 (m, 2H), 8.19 (s, 1H), 10.06 (s broad, 1H).
^{13}C NMR (75 MHz, acetone-d_6) δ 26.0 (C), 28.2 (CH_3), 65.0 (CH), 84.5 (CH_2), 108.9 (C), 114.9 (C), 115.7 (CH), 118.4 (C), 118.5 (C), 119.4 (CH), 123.0 (CH), 123.4 (CH), 125.2 (CH), 126.0(CH), 130.8 (C), 133.5 (CH), 133.6 (CH), 134.3 (CH), 134.4 (C), 135.9 (C), 138.8 (C), 149.9 (C), 167.9 (C).
HATR (cm^{-1}): 3217 (w), 3126 (w), 3045 (w), 2977 (w), 2225 (m), 1733 (s), 1682 (s), 1614 (m), 1587 (m), 1492 (m), 1454 (s), 1410 (m), 1371 (s), 1305 (m), 1254 (s), 1233 (m), 1154 (s), 1115 (m), 1088 (s), 1075 (m), 1016 (m), 976 (m), 913 (m), 880 (w), 833 (s), 800 (m), 759 (s), 745 (s), 688 (w).
LC-(ESI)MS (condition 1): t_R = 17.0 min $[M+H^+]^+$: 455.0 (100%). **Purity** (214 nm): 97%.
HRMS (ESI) calcd for $C_{25}H_{21}N_6O_3^-$ $[M-H^+]^-$: 453.1681 found: 453.1689.

(*S*)-3-(*N*-(tert-butyloxycarbonyl)-indolylmethyl)-8-nitro[1,2,3]triazolo[1,5-*d*][1,4]-benzodiazepin-2-one VIII.67

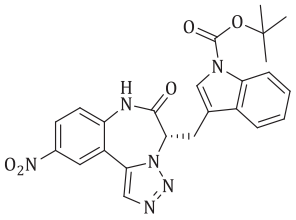

VIII.67

Following general procedure **P.01 - P.05:** (*S*)-3-(*N*-(tert-butyloxycarbonyl)-indolylmethyl)-8-nitro[1,2,3]triazolo[1,5-*d*][1,4]benzodiazepin-2-one (**VIII.67**, 98.1 mg, 0.2069 mmol).

Yield: 13%.
Brown solid.
R_F: 0.32 (hexane/acetone: 6/4).
Mp: 157°C.
Molecular weight: 474.47 Da.
^{1}H NMR (300 MHz, acetone-d_6) δ 1.64 (s, 9H), 3.54-3.67 (m, 2H), 5.90 (t, J = 6.6Hz, 1H), 7.17 (td, J = 1.3Hz/7.6Hz, 1H), 7.25 (td, J = 1.3Hz/7.6Hz, 1H), 7.37 (m, 3H), 7.93 (d, J = 8.3Hz, 1H), 8.22 (dd, J = 2.6Hz/8.9Hz, 1H), 8.27 (s, 1H), 8.32 (d, J = 2.6Hz, 1H), 10.15 (s broad, 1H).
^{13}C NMR (75 MHz, acetone-d_6) δ 26.3 (C), 28.2 (CH_3), 65.1 (CH), 85.6 (CH_2), 114.8 (C), 115.7 (CH), 118.1 (C), 119.4 (CH), 122.9 (CH), 123.4 (CH), 124.8 (CH), 125.3 (CH), 125.9 (CH), 126.2 (CH), 130.9 (C), 133.8 (CH), 134.5 (C), 135.9 (C), 140.4 (C), 144.7 (C), 149.9 (C), 168.0 (C).
HATR (cm^{-1}): 3240 (w), 3112 (w), 2970 (w), 2925 (w), 1727 (s), 1693 (s), 1621 (w), 1586 (m), 1528 (m), 1489 (m), 1451 (m), 1369 (s), 1337 (s), 1309 (s), 1274 (m), 1256 (s), 1228 (m), 1155 (s), 1085 (m), 1018 (w), 976 (w), 905 (w), 852 (m), 840 (m), 765 (m), 745 (m), 691 (w), 665 (w).
LC-(ESI)MS (condition 1): t_R = 17.4 min $[M+H^+]^+$: 475.1 (75%), $[M+H^+-t\text{Bu}]^+$: 419.1 (100%); **Purity** (214 nm): 90%.
HRMS (ESI) calcd for $C_{24}H_{21}N_6O_5^-$ $[M-H^+]^-$: 473.4613, found: 473.4618.

(*S*)-3-isobutyl-8-chloro[1,2,3]triazolo[1,5-*d*][1,4]benzodiazepin-2-one VIII.68

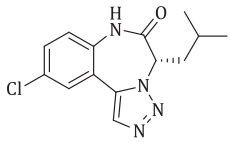

VIII.68

Following general procedure **P.01 - P.05:** (*S*)-3-isobutyl-8-chloro[1,2,3]triazolo[1,5-*d*][1,4]benzodiazepin-2-one (**VIII.68**, 109.1 mg, 0.3752 mmol).

Yield: 63%.
Light-brown solid.
%ee: 97%.
R_F: 0.45 (hexane/acetone: 6/4).
Mp: 198°C.
Molecular weight: 290.75 Da.
^{1}H NMR (300 MHz, acetone-d_6) δ 0.80 (d, J = 6.6Hz, 3H), 0.90 (d, J = 6.6Hz, 3H), 1.45 (septet, J = 6.6Hz, 1H), 1.81-1.86 (m, 2H), 5.46 (t, J = 7.9Hz, 1H), 7.41 (d, J = 8.9Hz, 1H), 7.54 (dd, J = 2.4Hz/8.9Hz, 1H), 7.82 (d, J = 2.4Hz, 1H), 8.19 (s, 1H), 9.85 (s broad, 1H).
^{13}C NMR (75 MHz, acetone-d_6) δ 22.0 (CH_3), 22.4 (CH_3), 25.5 (CH), 37.6 (CH_2), 63.7 (C), 119.7 (C), 124.2 (CH), 128.8 (CH), 130.5 (C), 131.4 (CH), 133.4 (CH), 134.1 (C), 134.4 (C), 168.2 (C).
HATR (cm^{-1}): 3219 (w), 3148 (w), 3096 (w), 2955 (m), 2924 (m), 2874 (w), 1682 (s), 1584 (w), 1484 (s), 1440 (m), 1392 (s), 1368 (s), 1336 (m), 1296 (m), 1248 (m), 1216 (m), 1160 (m), 1119 (m), 1039 (w), 978 (m), 941 (w), 882 (m), 864 (m), 824 (s), 751 (s), 696 (w).
LC-(ESI)MS (condition 1): t_R = 15.7 min $[M+H^+]^+$: 291.0 (100%). **Purity** (214 nm): 95%.
HRMS (ESI) calcd for $C_{14}H_{14}ClN_4O^-$ $[M-H^+]^-$: 289.0862 found: 289.0862.

(*S*)-3-isobutyl-9-chloro[1,2,3]triazolo[1,5-*d*][1,4]benzodiazepin-2-one VIII.69

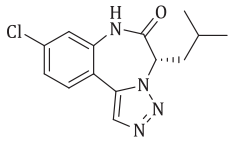

VIII.69

Following general procedure **P.01 - P.05:** (*S*)-3-isobutyl-9-chloro[1,2,3]triazolo[1,5-*d*][1,4]benzodiazepin-2-one (**VIII.69**, 130.4 mg, 0.4485 mmol).

Yield: 75%.
Light-brown solid.
R_F: 0.45 (hexane/acetone: 6/4).

Mp: 175°C.
Molecular weight: 290.75 Da.
^{1}H NMR (300 MHz, acetone-d_6) δ 0.80 (d, J =6.8Hz, 3H), 0.90 (d, J =6.8Hz, 3H), 1.45 (septet, J = 6.8Hz, 1H), 1.81-1.86 (m, 2H), 5.47 (t, J = 7.9Hz, 1H), 7.36 (dd, J = 2.1Hz/8.4Hz, 1H), 7.45 (d, J = 2.1Hz, 1H), 7.80 (d, J = 8.4Hz, 1H), 8.11 (s, 1H), 9.84 (s broad, 1H).
^{13}C NMR (75 MHz, acetone-d_6) δ 22.0 (CH_3), 22.4 (CH_3), 25.5 (CH), 37.6 (CH_2), 63.7 (C), 119.9 (C), 122.2 (CH), 125.8 (CH), 131.0 (C), 133.0 (CH), 134.4 (CH), 136.4 (C), 136.7 (C), 168.2 (C).
HATR (cm^{-1}): 3217 (w), 3093 (w), 2960 (m), 2950 (m), 2217 (w), 1687 (s), 1608 (w), 1582 (m), 1479 (m), 1450 (m), 1391 (s), 1367 (s), 1342 (m), 1284 (m), 1248 (m), 1216 (m), 1167 (m), 1120 (s), 1100 (m), 1016 (w), 976 (m), 903 (w), 871 (m), 830 (s), 767 (m), 745 (m), 694 (w).
LC-(ESI)MS (condition 1): t_R = 15.7 min $[M+H^+]^+$: 291.0 (100%). **Purity** (214 nm): 93%.
HRMS (ESI) calcd for $C_{14}H_{14}ClN_4O^-$ $[M-H^+]^-$: 289.0862 found: 289.0864.

(*S*)-3-isobutyl-8-bromo[1,2,3]triazolo[1,5-*d*][1,4]benzodiazepin-2-one VIII.70

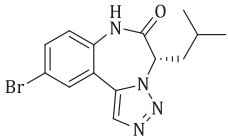

VIII.70

Following general procedure **P.01 - P.05:** (*S*)-3-isobutyl-8-bromo[1,2,3]triazolo[1,5-*d*][1,4]benzodiazepin-2-one (**VIII.70**, 119.9 mg, 0.3577 mmol).

Yield: 60%.
White solid.
R_F: 0.45 (hexane/acetone: 6/4).
Mp: 234°C.
Molecular weight: 335.20 Da.
^{1}H NMR (300 MHz, acetone-d_6) δ 0.82 (d, J = 6.8Hz, 3H), 0.91 (d, J = 6.6Hz, 3H), 1.47 (septet, J = 6.6Hz, 1H), 1.84 (m, 2H), 5.42-5.47 (m, 1H), 7.5 (d, J = 8.7Hz, 1H), 7.68 (dd, 2.3Hz/8.7Hz, 1H), 7.95 (d, J = 2.3Hz, 1H), 8.19 (s, 1H), 9.77 (s broad, 1H).
^{13}C NMR (75 MHz, acetone-d_6) δ 22.0 (CH_3), 22.4 (CH_3), 25.6 (CH), 37.6 (CH_2), 63.7 (C), 118.0 (C), 120.1 (C), 124.5 (CH), 131.7 (CH), 133.4 (CH), 134.0 (C), 134.4 (CH), 135.0 (C), 168.1 (C).
HATR (cm^{-1}): 3217 (w), 3144 (w), 3091 (w), 3035 (w), 2959 (w), 2919 (w), 2868 (w), 2368 (w), 1682 (s), 1581 (w), 1481 (s), 1438 (w), 1392 (s), 1368 (s), 1337 (m), 1296 (w), 1251 (w), 1217 (m), 1160 (w), 1120 (m), 1042 (w), 977 (m), 886 (m), 865 (m), 824 (s), 760 (m), 732 (m), 699 (w).
LC-(ESI)MS (condition 1): t_R = 16.0 min $[M+H^+]^+$: 335.0 (100%). **Purity** (214 nm): 95%.
HRMS (ESI) calcd for $C_{14}H_{14}BrN_4O^-$ $[M-H^+]^-$: 333.0356 found: 333.0357.

(*S*)-3-isobutyl-8-cyano[1,2,3]triazolo[1,5-*d*][1,4]benzodiazepin-2-one VIII.71

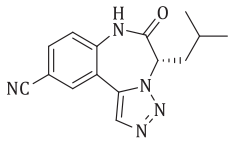

VIII.71

Following general procedure **P.01 - P.05:** (*S*)-3-isobutyl-8-cyano[1,2,3]triazolo[1,5-*d*][1,4]benzodiazepin-2-one (**VIII.71**, 98.1 mg, 0.3484 mmol).

Yield: 59%.
White solid.
R_F: 0.38 (hexane/acetone: 6/4).
Mp: 239°C.
Molecular weight: 281.31 Da.
^{1}H NMR (300 MHz, acetone-d_6) δ 0.80 (d, J =6.6Hz, 3H), 0.90 (d, J =6.6Hz, 3H), 1.45 (septet, J = 6.6Hz, 1H), 1.81-1.87 (m, 2H), 5.52 (t, J = 7.9Hz, 1H), 7.56 (d, J = 8.5Hz, 1H), 7.89 (dd, J = 1.9Hz/8.5Hz 1H), 8.26 (app s, 2H), 10.12 (s broad, 1H).
^{13}C NMR (75 MHz, acetone-d_6) δ 21.9 (CH_3), 22.4 (CH_3), 25.5 (CH), 37.8 (CH_2), 63.8 (C), 109.1 (C), 118.4 (C), 118.7 (C), 123.3 (CH), 133.8 (CH), 133.9 (CH), 134.6 (CH), 139.1 (C), 168.1 (C).
HATR (cm^{-1}): 3187 (w), 3101 (w), 3035 (w), 2959 (m), 2919 (m), 2867 (w), 2360 (w), 2338 (w), 2224 (m), 1677 (s), 1619 (w), 1589 (m), 1489 (m), 1445 (w), 1403 (s), 1378 (s), 1350 (m), 1310 (w), 1286 (w), 1239 (w), 1188 (w), 1121 (m), 1067 (w), 1039 (w), 976 (m), 903 (m), 845 (s), 793 (m), 764 (m), 691 (m).
LC-(ESI)MS (condition 1): t_R = 14.3 min $[M+H^+]^+$: 282.1 (100%). **Purity** (214 nm): 96%.
HRMS (ESI) calcd for $C_{15}H_{14}N_5O^-$ $[M-H^+]^-$: 280.1204 found: 280.1204.

(*S*)-3-isobutyl-8-nitro[1,2,3]triazolo[1,5-*d*][1,4]benzodiazepin-2-one VIII.72

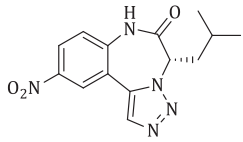

VIII.72

Following general procedure **P.01 - P.05:** (*S*)-3-isobutyl-8-nitro[1,2,3]triazolo[1,5-*d*][1,4]benzodiazepin-2-one (**VIII.72**, 56.1 mg, 0.1890 mmol).

Yield: 32%.
White solid.
R_F: 0.34 (hexane/acetone: 6/4).

Mp: 198°C.
Molecular weight: 301.30 Da.
^{1}H NMR (300 MHz, acetone-d_6) δ 0.81 (d, J = 6.6Hz, 3H), 0.91 (d, J = 6.6Hz, 3H), 1.46 (septet, J = 6.6Hz, 1H), 1.79-1.95 (m, 2H), 5.53 (app td, J = 8.2Hz, 1H), 7.63 (d, J = 8.9Hz, 1H), 8.36 (m, 2H), 8.62 (d, J = 2.5Hz, 1H), 10.21 (s broad, 1H).
^{13}C NMR (75 MHz, acetone-d_6) δ 21.9 (CH_3), 22.4 (CH_3), 25.5 (CH), 37.9 (CH_2), 63.8 (CH), 118.4 (C), 123.4 (CH), 125.2 (CH), 126.3 (CH), 133.8 (C), 134.0 (CH), 140.8 (C), 145.0 (C), 168.1 (C).
HATR (cm^{-1}): 3110 (w), 2958 (m), 2924 (m), 1691 (s), 1622 (w), 1585 (m), 1528 (m), 1488 (m), 1408 (w), 1363 (m), 1340 (s), 1235 (w), 1165 (w), 1122 (w), 1095 (w), 976 (w), 908 (w), 852 (w), 842 (w), 747 (w), 733 (w), 694 (w).
LC-(ESI)MS (condition 1): t_R = 15.0 min $[M+H^+]^+$: 302.1 (100%). **Purity** (214 nm): 96%.
HRMS (ESI) calcd for $C_{15}H_{14}N_5O_3^-$ $[M-H^+]^-$: 300.1102 found: 300.1101.

(*S*)-8-chloro-3-isopropyl[1,2,3]triazolo[1,5-*d*][1,4]benzodiazepin-2-one VIII.73

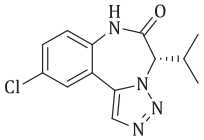

VIII.73

Following general procedure **P.01 - P.05:** (*S*)-8-chloro-3-isopropyl[1,2,3]triazolo[1,5-*d*][1,4]benzodiazepin-2-one (**VIII.73**, 125.8 mg, 0.4546 mmol).

Yield: 68%.
White solid.
R_F: 0.41 (hexane/acetone: 6/4). 0.08 (hexane/acetone: 8/2).
Mp: 216°C.
Molecular weight: 276.72 Da.
^{1}H NMR (300 MHz, acetone-d_6) δ 0.58 (d, J = 6.6Hz, 3H), 1.05 (d, J = 6.6Hz, 3H), 1.88-2.03 (m, 1H), 5.13 (d, J = 11.6Hz, 1H), 7.40 (d, J = 8.6Hz, 1H), 7.51 (dd, J = 2.4Hz/8.6Hz, 1H), 7.82 (d, J = 2.4Hz, 1H), 8.23 (s, 1H), 9.89 (s broad, 1H).
^{13}C NMR (75 MHz, acetone-d_6) δ 18.8 (CH_3), 19.1 (CH_3), 28.7 (CH), 72.9 (CH), 109.3 (C), 124.0 (CH), 128.6 (CH), 130.4 (C), 131.4 (CH), 133.5 (CH), 133.9 (C), 167.6 (C).
HATR (cm^{-1}): 3217 (w), 3126 (w), 3085 (w), 2967 (m), 2924 (m), 1687 (s), 1586 (w), 1484 (s), 1460 (m), 1430 (w), 1400 (s), 1360 (s), 1248 (m), 1223 (m), 1173 (w), 1112 (m), 1039 (w), 977 (m), 920 (w), 873 (m), 816 (s), 760 (m), 732 (w), 696 (w), 671 (w).
LC-(ESI)MS (condition 1): t_R = 14.7 min $[M+H^+]^+$: 277.0 (100%). **Purity** (214 nm): 95%.
HRMS (ESI) calcd for $C_{13}H_{12}ClN_4O^-$ $[M-H^+]^-$: 275.0705 found: 275.0709.

(*S*)-9-chloro-3-isopropyl[1,2,3]triazolo[1,5-*d*][1,4]benzodiazepin-2-one VIII.74

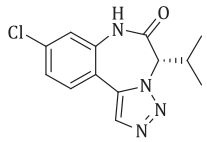

VIII.74

Following general procedure **P.01 - P.05:** (*S*)-9-chloro-3-isopropyl[1,2,3]triazolo[1,5-*d*][1,4]benzodiazepin-2-one (**VIII.74**, 127.9 mg, 0.4622 mmol).

Yield: 69%.
White solid.
R_F: 0.42 (hexane/acetone: 6/4). 0.08 (hexane/acetone: 8/2).
Mp: 236°C.
Molecular weight: 276.72 Da.
^{1}H NMR (300 MHz, acetone-d_6) δ 0.58 (d, J = 6.4Hz, 3H), 1.05 (d, J = 6.4Hz, 3H), 1.91-2.03 (m, 1H), 5.11 (d, J = 11.7Hz, 1H), 7.34 (dd, J = 2.1Hz/8.3Hz, 1H), 7.45 (d, J = 2.1Hz, 1H), 7.81 (d, J = 8.3Hz, 1H), 8.13 (s, 1H), 9.81 (s broad, 1H).
^{13}C NMR (75 MHz, acetone-d_6) δ 18.8 (CH_3), 19.1 (CH_3), 28.7 (CH), 72.9 (CH), 116.6 (C), 122.0 (CH), 125.8 (CH), 130.9 (CH), 133.2 (CH), 133.9 (C), 136.3 (C), 136.5 (C), 167.7 (C).
HATR (cm^{-1}): 3352 (m), 3120 (w), 3066 (w), 2973 (w), 2924 (w), 2874 (w), 1675 (s), 1607 (m), 1583 (s), 1554 (w), 1479 (s), 1458 (m), 1442 (w), 1391 (s), 1368 (m), 1352 (m), 1331 (m), 1279 (m), 1254 (m), 1207 (m), 1170 (w), 1105 (m), 1026 (w), 983 (m), 967 (m), 933 (w), 872 (m), 856 (s), 818 (s), 744 (m), 712 (s), 668 (w).
LC-(ESI)MS (condition 1): t_R = 14.7 min $[M+H^+]^+$: 277.0 (100%). **Purity** (214 nm): 98%.
HRMS (ESI) calcd for $C_{13}H_{12}ClN_4O^-$ $[M-H^+]^-$: 275.0705 found: 275.0705.

(*S*)-8-bromo-3-isopropyl[1,2,3]triazolo[1,5-*d*][1,4]benzodiazepin-2-one VIII.75

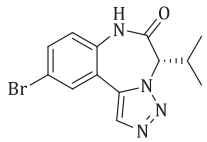

VIII.75

Following general procedure **P.01 - P.05**: (*S*)-8-bromo-3-isopropyl[1,2,3]triazolo[1,5-*d*][1,4]benzodiazepin-2-one (**VIII.75**, 157.0 mg, 0.4888 mmol).

Yield: 73%.
%ee: >99%.
R_F: 0.42 (hexane/acetone: 6/4). 0.09 (hexane/acetone: 8/2).

Mp: 239°C.
Molecular weight: 321.17 Da.
^{1}H NMR (300 MHz, acetone-d_6) δ 0.57 (d, J = 6.6Hz, 3H), 1.04 (d, J = 6.6Hz, 3H), 1.88-2.02 (m, 1H), 5.13 (d, J = 11.6Hz, 1H), 7.34 (d, J = 8.8Hz, 1H), 7.64 (dd, J = 2.2Hz/8.8Hz, 1H), 7.95 (d, J = 2.2Hz, 1H), 8.22 (s, 1H), 9.87 (s broad, 1H).
^{13}C NMR (75 MHz, acetone-d_6) δ 18.8 (CH_3), 19.1 (CH_3), 28.7 (CH), 72.9 (CH), 117.9 (C), 119.6 (C), 124.2 (CH), 131.5 (CH), 133.4 (C), 133.5 (CH), 133.3 (CH), 133.3 (C), 167.7 (C).
HATR (cm^{-1}): 3212 (w), 3129 (w), 3096 (w), 3045 (w), 2966 (m), 2929 (m), 1692 (s), 1584 (w), 1480 (s), 1398 (s), 1353 (s), 1309 (w), 1244 (w), 1224 (w), 1168 (w), 1119 (m), 1080 (w), 1035 (w), 976 (m), 943 (w), 918(w), 891(m), 856(m), 815(s), 736(m), 691(w), 666(w).
LC-(ESI)MS (condition 1): t_R = 14.9 min $[M+H^+]^+$: 321.0 (100%). **Purity** (214 nm): 93%.
HRMS (ESI) calcd for $C_{13}H_{12}BrN_4O^-$ $[M-H^+]^-$: 319.0200 found: 319.0203.

(*S*)-8-cyano-3-isopropyl[1,2,3]triazolo[1,5-*d*][1,4]benzodiazepin-2-one VIII.76

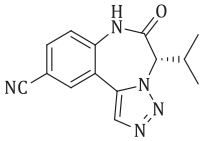

VIII.76

Following general procedure **P.01 - P.05**: (*S*)-8-cyano-3-isopropyl[1,2,3]triazolo[1,5-*d*][1,4]benzodiazepin-2-one (**VIII.76**, 46.8 mg, 0.1755 mmol).

Yield: 26%.
R_F: 0.33 (hexane/acetone: 6/4). 0.07(hexane/acetone: 8/2).
Molecular weight: 267.28 Da.
^{1}H NMR (300 MHz, acetone-d_6) δ 0.59 (d, J = 6.6Hz, 3H), 1.06 (d, J = 6.6Hz, 3H), 1.90-2.01 (m, 1H), 5.16 (d, J = 11.5Hz, 1H), 7.56 (d, J = 8.5Hz, 1H), 7.89 (dd, J = 2.1Hz/8.5Hz, 1H), 8.27 (d, J = 2.1Hz, 1H), 8.29 (s, 1H), 10.11 (s broad, 1H).
^{13}C NMR (75 MHz, acetone-d_6) δ 18.8 (CH_3), 19.1 (CH_3), 29.1 (CH), 72.9 (CH), 109.1 (C), 118.4 (C), 123.1 (CH), 133.2 (C), 133.8 (CH), 134.0 (CH), 134.7 (CH), 138.7 (C), 167.5 (C).
HATR (cm^{-1}): 3216 (w), 3114 (w), 3082 (w), 3032 (w), 2967 (w), 2931 (w), 2229 (m), 1685 (s), 1614 (m), 1590 (m), 1497 (s), 1467 (m), 1445 (m), 1402 (m), 1358 (s), 1247 (m), 1229 (m), 1206 (m), 1121 (w), 1100 (w), 977 (w), 888 (w), 836 (m), 698 (w), 865 (w), 607 (w).
LC-(ESI)MS (condition 1): t_R = 13.2 min $[M-H^+]^-$: 266.0 (100%). **Purity** (214 nm): 96%.
HRMS (ESI) calcd for $C_{14}H_{12}N_5O^-$ $[M-H^+]^-$: 266.1047 found: 266.1043.

***(S)*-3-isopropyl-8-nitro[1,2,3]triazolo[1,5-*d*][1,4]benzodiazepin-2-one VIII.77**

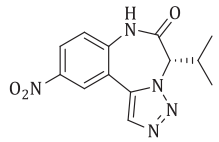

VIII.77

Following general procedure **P.01 - P.05:** *(S)*-3-isopropyl-8-nitro[1,2,3]triazolo[1,5-*d*][1,4]benzodiazepin-2-one (**VIII.77**, 38.1 mg, 0.1327 mmol).

Yield: 9%.
Light-brown solid.
R_F: 0.13 (hexane/acetone: 8/2).
Molecular weight: 287.27 Da.
^{1}H NMR (300 MHz, acetone-d_6) δ 0.61 (d, J =6.6Hz, 3H), 1.06 (d, J =6.6Hz, 3H), 1.93-2.01 (m, 1H), 5.18 (d, J = 11.7Hz, 1H), 7.63 (d, J = 9.0Hz, 1H), 8.35 (dd, J = 2.6Hz/9.0Hz, 1H), 8.38 (s, 1H), 8.63 (d, J = 2.6Hz, 1H), 10.22 (s broad, 1H).
^{13}C NMR (75 MHz, acetone-d_6) δ 18.8 (CH_3), 19.1 (CH_3), 29.2 (CH), 73.0 (CH), 118.0 (C), 123.2 (CH), 125.1 (CH), 126.4 (CH), 133.3 (C), 134.3 (CH), 140.3 (C), 145.0 (C), 167.5 (C).
HATR (cm^{-1}): 3235 (w), 3111 (w), 2969 (w), 1693 (s), 1615 (w), 1585 (m), 1528 (m), 1489 (m), 1395 (w), 1370 (w), 1340 (s), 1262 (w), 1231 (w), 1118 (w), 975 (w), 910 (w), 849 (w), 834 (w), 747 (w), 738 (w).
LC-(ESI)MS (condition 1): t_R = 13.9 min $[M+H^+]^+$: 288.1 (100%). **Purity** (214 nm): 80%.
HRMS (ESI) calcd for $C_{15}H_{12}N_5O_3^-$ $[M-H^+]^-$: 286.0946 found: 286.0946.

(*S*)-3-isopropyl-8-methoxy[1,2,3]triazolo[1,5-*d*][1,4]benzodiazepin-2-one VIII.78

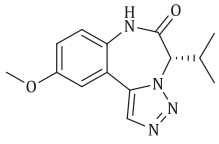

VIII.78

Following general procedure **P.01 - P.05**: (*S*)-3-isopropyl-8-methoxy[1,2,3]triazolo[1,5-*d*] benzodiazepin-2-one (**VIII.78**, 68.6 mg, 0.2519 mmol).

Yield: 38%.
Light-yellow solid.
R_F: 0.07 (hexane/acetone: 8/2). 0.23 (hexane/acetone: 7/3).
Molecular weight: 272.30 Da.

^{1}H NMR (300 MHz, acetone-d_6) δ 0.57 (d, J = 6.6Hz, 3H), 1.04 (d, J = 6.6Hz, 3H), 1.92-2.03 (m, 1H), 3.87 (s, 3H), 5.07 (d, J = 11.5Hz, 1H), 7.10 (dd, J = 2.8Hz/9.1Hz, 1H), 7.30-7.33 (m, 2H), 8.13 (s, 1H), 9.61 (s broad, 1H).
^{13}C NMR (75 MHz, acetone-d_6) δ 18.8 (CH_3), 19.1 (CH_3), 28.4 (CH), 56.0 (CH_3), 73.0 (CH), 113.0 (CH), 118.0 (CH), 118.9 (C), 123.8 (CH), 128.4 (C), 133.1 (CH), 134.6 (C), 157.6 (C), 167.7 (C).
HATR (cm^{-1}): 3480 (w), 3204 (w), 3089 (w), 2965 (m), 2934 (m), 1676 (s), 1618 (m), 1557 (w), 1500 (s), 1464 (m), 1441 (m), 1409 (m), 1373 (m), 1346 (m), 1295 (m), 1282 (m), 1233 (s), 1216 (m), 1181 (w), 1144 (w), 1118 (w), 1029 (m), 975 (m), 920 (w), 889 (w), 827 (m), 734 (m), 698 (m), 613 (m).
LC-(ESI)MS (condition 1): t_R = 17.2 min $[M+H^+]^+$: 273.1 (100%).
HRMS (ESI) calcd for $C_{14}H_{17}N_4O_2^+$: 273.1346 $[M+H^+]^+$ found: 273.1337.

(*S*)-8-chloro-3-(4-(tert-butyloxycarbonyl)-aminobutyl)[1,2,3]triazolo[1,5-*d*][1,4]benzodiazepin-2-one VIII.79

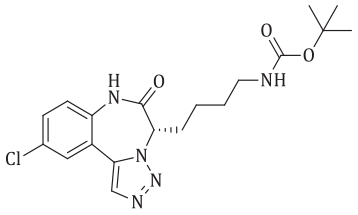

VIII.79

Following general procedure **P.01 - P.05**: (*S*)-8-chloro-3-(4-(tert-butyloxycarbonyl)-aminobutyl))[1,2,3]triazolo[1,5-*d*][1,4]benzodiazepin-2-one (**VIII.79**, 149.3 mg, 0.3678 mmol).

Yield: 55%.
White solid.
R_F: 0.35 (hexane/acetone: 6/4). 0.04 (hexane/acetone: 8/2).
Mp: 194°C.
Molecular weight: 405.88 Da.
^{1}H NMR (300 MHz, acetone-d_6) δ 1.26-1.32 (m, 2H), 1.37 (s, 9H), 1.42-1.52 (m, 2H), 2.04-2.08 (m, 2H), 3.00 (q, J = 6.4Hz/6.3Hz, 2H), 5.32 (t, J = 8.1Hz, 1H), 5.90 (s broad, 1H), 7.42 (dd, J = 8.7Hz, 1H), 7.56 (dd, J = 2.4Hz/8.7Hz, 1H), 7.82 (d, J = 2.4Hz, 1H), 8.19 (s, 1H), 9.77 (s broad, 1H).
^{13}C NMR (75 MHz, acetone-d_6) δ 23.6 (C), 28.6 (CH_3), 29.9 (CH_2), 40.5 (CH_2), 64.7 (CH), 78.3 (CH_2), 119.9 (C), 124.3 (CH), 124.4 (CH), 128.9 (CH), 130.5 (C), 131.4 (CH), 133.3 (CH), 134.2 (C), 134.6 (C), 156.6 (C), 168.0 (C).
HATR (cm^{-1}): 3276 (w), 3202 (w), 3105 (w), 2938 (m), 2868 (w), 1680 (s), 1584 (w), 1487 (s), 1448 (m), 1404 (s), 1368 (s), 1336 (m), 1247 (m), 1224 (m), 1168 (m), 1143 (w), 1120 (w), 1087 (w), 1049 (w), 1008 (w), 977 (m), 954 (w), 881 (w), 848 (m), 823 (m), 775 (w), 767 (w), 723 (w), 691 (w).

LC-(ESI)MS (condition 1): t_R = 15.5 min $[M+H^+\text{-Boc}]^+$: 306.1 (100%), $[M\text{-}H^+]^-$: 404.1 (100%).
Purity (214 nm): 97%.
HRMS (ESI) calcd for $C_{19}H_{23}ClN_5O_3^-$ $[M\text{-}H^+]^-$: 404.1495 found: 404.1501.

(S)-9-chloro-3-(4-(tert-butyloxycarbonyl)-aminobutyl)[1,2,3]triazolo[1,5-*d*][1,4]benzodiazepin-2-one VIII.80

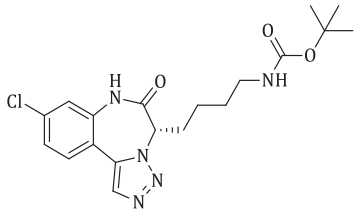

VIII.80

Following general procedure **P.01 - P.05:** *(S)*-9-chloro-3-(4-(tert-butyloxycarbonyl)-aminobutyl)[1,2,3]triazolo[1,5-d][1,4]benzodiazepin-2-one (**VIII.80**, 186.0 mg, 0.4583 mmol).

Yield: 69%.
R_F: 0.35 (hexane/acetone: 6/4). 0.04 (hexane/acetone: 8/2).
Mp: 116°C.
Molecular weight: 405.88 Da.
^{1}H NMR (300 MHz, acetone-d_6) δ 1.27-1.32 (m, 2H), 1.37 (s, 9H), 1.42-1.55 (m, 2H), 1.98-2.17 (m, 2H), 2.97-3.04 (m, 2H), 5.35 (t, *J* = 7.3Hz, 1H), 5.95 (s broad, 1H), 7.37 (dd, *J* = 2.1Hz/8.3Hz, 1H), 7.47 (d, *J* = 2.1Hz, 1H), 7.80 (d, *J* = 8.3Hz, 1H), 8.12 (s, 1H), 9.88 (s broad, 1H).
^{13}C NMR (75 MHz, acetone-d_6) δ 23.5 (C), 28.6 (CH_3), 29.8 (CH_2), 40.4 (CH_2), 64.6 (CH), 78.3 (CH_2), 117.0 (C), 122.2 (CH), 125.8 (CH), 131.0 (CH), 132.9 (CH), 134.4 (C), 136.4 (C), 136.7 (C), 156.6 (C), 168.1 (C).
HATR (cm^{-1}): 3229 (w), 3060 (w), 2935 (w), 2868 (w), 1692 (s), 1608 (m), 1582 (m), 1550 (m), 1513 (m), 1479 (m), 1392 (s), 1364 (m), 1310 (m), 1276 (m), 1248 (m), 1216 (m), 1166 (s), 1125 (m), 1099 (m), 991 (w), 974 (w), 865 (w), 812 (m), 737 (w), 697 (w).
LC-(ESI)MS (condition 1): t_R = 15.5 min $[M+H^+\text{-Boc}]^+$: 306.1 (100%), $[M\text{-}H^+]^-$: 404.0 (100%).
Purity (214 nm): 97%.
HRMS (ESI) calcd for $C_{19}H_{23}ClN_5O_3^-$ $[M\text{-}H^+]^-$: 404.1495, found: 404.1500.

***(S)*-8-bromo-3-(4-(tert-butyloxycarbonyl)-aminobutyl)[1,2,3]triazolo[1,5-*d*][1,4]benzodiazepin-2-one VIII.81**

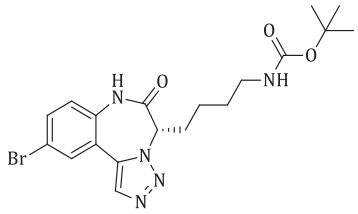

VIII.81

Following general procedure **P.01 - P.05:** *(S)*-8-bromo-3-(4-(tert-butyloxycarbonyl)-aminobutyl)[1,2,3]triazolo[1,5-*d*][1,4]benzodiazepin-2-one (**VIII.81**, 162.8 mg, 0.3615 mmol).

Yield: 55%.
White solid.
Mp: 180°C.
R_F: 0.33 (hexane/acetone: 6/4). 0.03 (hexane/acetone: 8/2).
Molecular weight: 450.33 Da.
^{1}H NMR (300 MHz, $CDCl_3$) δ 1.15-1.33 (m, 2H), 1.37 (s, 9H), 1.42-1.52 (m, 2H), 1.99-2.15 (m, 1H), 2.97-3.03 (m, 2H), 5.28-5.34 (m, 1H), 5.94 (s broad, 1H), 7.36 (dd, *J* = 2.1Hz/8.5Hz, 1H), 7.46 (d, *J* = 2.1Hz, 1H), 7.80 (d, *J* = 8.3Hz, 1H), 8.11 (s, 1H), 9.88 (s broad, 1H).
^{13}C NMR (75 MHz, acetone-d_6) δ 23.5 (C), 28.6 (CH_3), 29.8 (CH_2), 40.4 (CH_2), 64.6 (CH), 78.3 (CH_2), 117.0 (C), 122.2 (C), 125.8 (CH), 131.0 (CH), 133.0 (CH), 134.4 (C), 136.4 (CH), 136.7 (C), 156.6 (C), 168.1 (C).
HATR (cm^{-1}): 3276 (w), 3106 (w), 2937 (w), 2874 (w), 2360 (w), 2328 (w), 1682 (s), 1586 (w), 1485 (m), 1450 (m), 1403 (s), 1368 (s), 1336 (m), 1247 (m), 1220 (m), 1167 (s), 1142 (m), 1119 (m), 1087 (w), 1046 (w), 1011 (w), 976 (w), 883 (w), 847 (m), 822 (m), 775 (m), 739 (w), 691 (w).
LC-(ESI)MS (condition 1): t_R = 15.7 min $[M\text{-}H^+]^-$: 448.0 (100%). **Purity** (214 nm): 99%.
HRMS (ESI) calcd for $C_{19}H_{23}BrN_5O_3^-$ $[M\text{-}H^+]^-$: 448.0990, found: 448.1001.

***(S)*-8-nitro-3-(4-(tert-butyloxycarbonyl)-aminobutyl)[1,2,3]triazolo[1,5-*d*][1,4]benzodiazepin-2-one VIII.82**

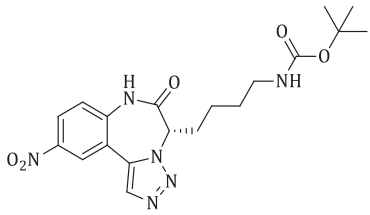

VIII.82

Following general procedure **P.01 - P.05:** *(S)*-8-nitro-3-(4-(tert-butyloxycarbonyl)-aminobutyl)[1,2,3]triazolo[1,5-*d*][1,4]benzodiazepin-2-one (**VIII.82**, 73.9 mg, 0.1775 mmol).

Yield: 27%.
White solid.
R_F: 0.17 (hexane/acetone: 7/3).
Mp: 192°C.
Molecular weight: 416.43 Da.
^{1}H NMR (300 MHz, $CDCl_3$) δ 1.24-1.25 (m, 2H), 1.39-1.52 (m, 11H), 1.84-2.07 (m, 1H), 2.99-3.05 (m, 2H), 5.46-5.51 (m, 1H), 7.40 (d, *J* = 8.9Hz, 1H), 8.08 (s, 1H), 8.33 (dd, *J* = 2.6Hz/8.9Hz, 1H), 8.52 (d, *J* = 2.6Hz, 1H), 9.67 (s broad, 1H).
^{13}C NMR (75 MHz, $CDCl_3$) δ 22.7 (CH_2), 28.4 (CH_3), 28.7 (CH_2), 29.1 (CH_2), 39.8 (CH_2), 64.4 (CH), 117.2 (C), 122.3 (CH), 124.4 (CH), 125.9 (CH), 132.5 (C), 133.3 (CH), 138.6 (C), 144.5 (C), 168.1 (C).
HATR (cm^{-1}): 3341(w), 3225(w), 3112(w), 2970(w), 2930(w), 1691(s), 1585(w), 1526(m), 1488(m), 1455(m), 1364(m), 1339(s), 1271(m), 1248(m), 1167(s), 1044(w), 976(w), 906(w), 845(m), 748(w), 693(w), 667(w).
LC-(ESI)MS (condition 1): t_R = 15.0 min $[M\text{-}H^+]^-$: 415.1 (100%). **Purity** (214 nm): 87%.
HRMS (ESI) calcd for $C_{19}H_{23}N_6O_5^-$ $[M\text{-}H^+]^-$: 415.1735, found: 415.1738.

XVII. Synthesis of 1,4,5-trisubstituted triazoles

A. Building block synthesis

2-(1-hexynyl)aniline IX.13

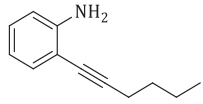

IX.13

Following general procedure **P.06**: 2-iodoaniline (2.000 g, 9.131 mmol, 1 eq). 1-hexyne (4.200 mL, 36.56 mmol, 4 eq). $PdCl_2(PPh_3)_2$ (128.0 mg, 0.1826 mmol, 0.02 eq). CuI (86.9 mg, 0.4565 mmol, 0.05 eq). diethylamine (91 mL).

Yield: 94%. 2-(1-hexynyl)aniline (**IX.13**, 1.487 g, 8.583 mmol).
Orange-yellow oil.
Molecular weight: 173.25 Da.
R_F: 0.19 (hexane/acetone: 95/5).
^{1}H NMR (300 MHz, acetone-d_6) δ 0.92 (t, J = 7.2Hz, 3H), 1.42-1.63 (m, 4H), 2.46 (t, J = 7.0Hz, 2H), 4.85 (s broad, 2H), 6.52 (dt, J = 1.1Hz/7.5Hz, 1H), 6.71 (d, J = 8.1Hz, 1H),7.02 (t, J = 8.1Hz, 1H), 7.12 (dd, J = 1.3Hz/7.6Hz, 1H).
^{13}C NMR (75 MHz, acetone-d_6) δ 13.9 (CH_3), 19.6 (CH_2), 22.6 (CH_2), 31.8 (CH_2), 78.1 (C), 95.7 (C), 108.9 (C), 114.5 (CH), 117.2 (CH), 129.5 (CH), 132.4 (CH), 149.9 (C).
HATR (cm^{-1}): 3464 (w), 3373 (w), 2954 (m), 2929 (m), 2868 (m), 1611 (s), 1579 (w), 1490 (s), 1453 (s), 1377 (w), 1304 (m), 1271 (w), 1158 (w), 935 (w), 749 (s), 679 (w).
LC-(ESI)MS (condition 1): t_R = 18.7 min $[M+H^+]^+$: 174.1 (100%). **Purity** (214 nm): 96%.

HRMS (ESI) calcd for $C_{12}H_{16}N^+$: 174.1277 $[M+H^+]^+$ found: 174.1281.

2-(4-phenylbutynyl)aniline IX.14

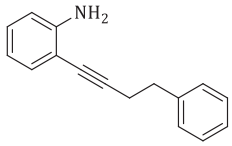

IX.14

Following general procedure **P.06**: 2-iodoaniline (1.000 g, 4.464 mmol, 1 eq). 4-phenyl-1-butyne (1.25 mL, 8.528 mmol, 2 eq). $PdCl_2(PPh_3)_2$ (63 mg, 0.08928 mmol, 0.02 eq). CuI (43 mg, 0.2232 mmol, 0.05 eq). diethylamine (45 mL).

Yield: 82%. 2-(4-phenylbutynyl)aniline (**IX.14**, 0.810 g, 3.660 mmol).
Light-yellow viscous oil.
Molecular weight: 221.30 Da.
R_F: 0.31 (hexane/acetone: 8/2).
^{1}H NMR (300 MHz, acetone-d_6) δ 7.35-7.27 (m, 4H), 7.17-7.23 (m, 1H), 7.10(dd, J = 1.5Hz/7.7Hz, 1H), 7.02 (td, J = 1.6Hz/7.5Hz, 1H), 6.68 (dd, J = 0.8Hz/8.1Hz, 1H), 6.52 (td, J = 1.1Hz/7.5Hz, 1H), 4.73 (s broad, 2H), 2.89-2.94 (m, 2H), 2.74-7.29 (m, 2H).
^{13}C NMR (75 MHz, acetone-d_6) δ 150.0 (C), 141.7 (C), 132.4 (CH), 129.6 (CH), 129.4 (CH), 129.1 (CH), 127.0 (CH), 117.1 (CH), 114.5 (CH), 108.5 (C), 95.0 (C), 78.9 (C), 35.7 (CH_2), 22.1 (CH_2).
HATR (cm^{-1}): 3468(w), 3374(w), 3059(w), 3026(w), 2925(w), 2858(w), 1611(s), 1570(w), 1491(s), 1453(s), 1428(w), 1339(w), 1307(m), 1265(m), 1156(m), 1076(w), 1030(w), 933(w), 908(w), 746(s), 699(s).
LC-(ESI)MS (condition 1): t_R = 18.6 min $[M+H^+]^+$: 222.1 (100%). **Purity** (214 nm): 96%.
HRMS (ESI) calcd for $C_{16}H_{16}N^+$: 222.1277 $[M+H^+]^+$ found: 222.1280.

2-(3-phenylpropynyl)aniline IX.15

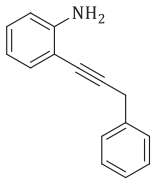

IX.15

Following general procedure **P.06**: 2-iodoaniline (300 mg, 1.369 mmol, 1 eq). 3-phenyl-1-propyne (680 µL, 5.476 mmol, 4 eq). $PdCl_2(PPh_3)_2$ (19 mg, 0.027438 mmol, 0.02 eq). CuI (13 mg, 0.06845 mmol, 0.05 eq). diethylamine (13 mL).

Yield: 98%. 2-(3-phenylpropynyl)aniline (**IX.15**, 278.1 mg, 1.342 mmol).
Light-brown reddish viscous oil.
Molecular weight: 207.27 Da.
R_F: 0.28 (hexane/acetone: 8/2).
^{1}H NMR (300 MHz, acetone-d_6) δ 7.44-7.46 (m, 2H), 7.33-7.38 (m, 2H), 7.23-7.26 (m, 1H), 7.22 (dd, J = 1.5Hz/7.7Hz, 1H), 7.04 (td, J = 1.5Hz/7.5Hz, 1H), 6.73 (dd, J = 0.8Hz/8.3Hz, 1H), 6.54 (td, J = 1.1Hz/7.5Hz, 1H), 4.94 (s broad, 2H), 3.91 (s, 2H).
^{13}C NMR (75 MHz, acetone-d_6) δ 150.2 (C), 138.2 (C), 132.6 (CH), 129.9 (CH), 129.4 (CH), 129.3 (CH), 128.7 (CH), 127.3 (CH), 117.2 (CH), 114.7 (CH), 108.3 (C), 93.3 (C), 80.2 (C), 26.1 (CH_2).
HATR (cm^{-1}): 3463(w), 3372(m), 3059(w), 3026(w), 2885(w), 1611(s), 1490(s), 1452(s), 1416(m), 1335(w), 1306(m), 1259(m), 1182(w), 1156(m), 1073(w), 1028(w), 975(w), 936(w), 852(w), 832(w), 741(s), 731(s), 699(s).
LC-(ESI)MS (condition 1): t_R = 18.2 min $[M+H^+]^+$: 208.1 (100%). **Purity** (214 nm): 94%.
HRMS (ESI) calcd for $C_{15}H_{14}N^+$: 208.1121 $[M+H^+]^+$ found 208.1124.

2-(phenylethynyl)aniline IX.16

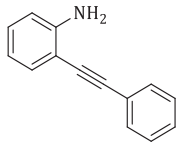

IX.16

Following general procedure **P.06**: 2-iodoaniline (1.500 g, 6.849 mmol, 1 eq). phenylacetylene (1.50 mL, 13.67 mmol, 2 eq). $PdCl_2(PPh_3)_2$ (96 mg, 0.1370 mmol, 0.02 eq). CuI (65.3 mg, 0.3425 mmol, 0.05 eq). diethylamine (69 mL).

Yield: 95%. 2-(phenylethynyl)aniline (**IX.16**, 1.257 g, 6.505 mmol)
Yellow solid.
Molecular weight: 193.24 Da.
R_F: 0.17 (pentane/ether: 98/2).
^{1}H NMR (300 MHz, acetone-d_6) δ 7.54-7.58 (m, 2H), 7.33-7.42 (m, 3H), 7.28 (dd, J = 1.3Hz/7.7Hz, 1H), 7.10 (t, J = 7.8Hz, 1H), 6.79 (d, J = 8Hz, 1H), 6.61(td, J = 0.8Hz/7.3Hz, 1H), 5.12 (s broad, 2H).
^{13}C NMR (75 MHz, acetone-d_6) δ 150.3 (C), 132.7 (CH), 132.1 (CH), 130.6 (CH), 130.2 (CH), 129.3 (CH), 129.0 (CH), 124.5 (C), 117.3 (CH), 114.9 (CH), 107.5 (C), 94.9 (C), 87.3 (C).

HATR (cm^{-1}): 3466(m), 3369(m), 3050(w), 3030(w), 2206(w), 1612(s), 1566(w), 1494(s), 1482(s), 1453(s), 1312(s), 1259(m), 1152(m), 1069(w), 1025(w), 940(w), 914(w), 859(w), 748(s), 690(s).
LC-(ESI)MS (condition 1): t_R = 18.0 min $[M+H^+]^+$: 194.1 (100%). **Purity** (214 nm): 91%.
HRMS (ESI) calcd for $C_{14}H_{12}N^+$: 194.0964 $[M+H^+]^+$ found: 194.0962.

B. Regioselectivity of IX.13 in RuAAC

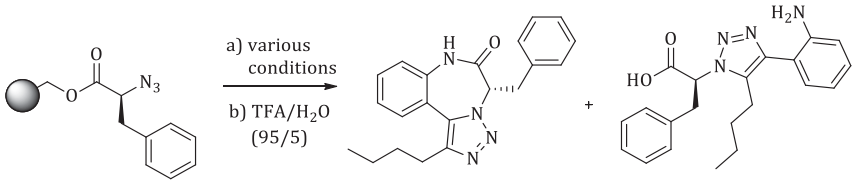

VII.31 **IX.23** **IX.24**

Solid-phase bound (L)-2-azido phenylpropanoic acid **VII.31** is prepared *via* standard procedure **P.01** - **P.03** and dried extensively under reduced pressure. To eight vials solid-phase bound intermediate **VII.31** (0.06584 mmol, 1 eq) and 2-hexynylaniline **IX.13** (63.6 mg, 0.3292 mmol, 5 eq) are added. Meanwhile, four standard solutions of $C_p^*RuCl(PPh_3)_2$ (7.5 mg/mL) and $C_p^*RuCl(COD)$ (3.6 mg/mL) are made in toluene and dioxane. Four samples are treaded with toluene (700 µL, 0.094M), the other four are treated with dioxane (700 µL, 0.094M). The reaction vials are shaken for 6 hours at the appropriate temperature according to design of the test library.

For each solvent and temperature, four additional vials are filled with solid-phase bound intermediate **VII.31** (0.06584 mmol, 1 eq) and 2-hexynylaniline **IX.13** (63.6 mg, 0.3292 mmol, 5 eq) and 700 µL of toluene or 700 µL of dioxane is added. As no catalyst is added to these vials, these vials are blank runs.

The test reactions are put at the appropriate temperatures together with the other eight samples.

Cleavage: After 6 hours of reaction time, the beads are isolated and washed with toluene (3x 1 mL, rt or 60°C) or dioxane (3x 1 mL, rt or 60°C). Temperature according to the reaction conditions. The washing step continues with DMF (3x 1 mL), MeOH (3x 1 mL) and dichloromethane (3x 1mL). After drying of the beads *in vacuo*, an aliquot of the sample is cleaved *via* standard protocol with TFA/H_2O (95/5) for 2 hours at room temperature and after isolating the supernatans and evaporation, the residue is used for LC-MS sample preparation.

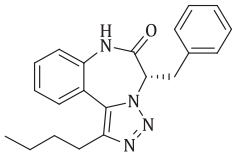

IX.23

Brutoformula: $C_{21}H_{22}N_4O$
Molecular weight: 346.43 Da.
LC-(ESI)MS (condition 1): t_R = 17.0 min $[M+H^+]^+$: 347.2 (100%).

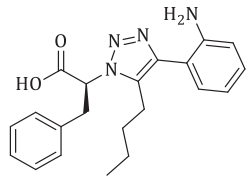

IX.24

Brutoformula: $C_{21}H_{24}N_4O_2$
Molecular weight: 363.43 Da.
LC-(ESI)MS (condition 1): not detected

C. Regioselectivity of IX.14 in RuAAC

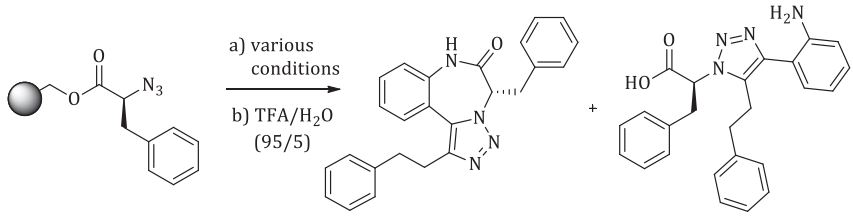

VII.31 **IX.25** **IX.26**

Procedure according to section **XVII.B** internal alkyne **IX.14** (72.8 mg, 0.3292 mmol, 5 eq).

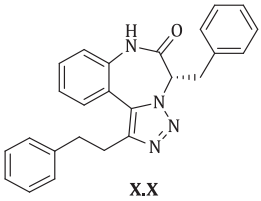

X.X

IX.25

Brutoformula: $C_{25}H_{22}N_4O$
Molecular weight: 394.47 Da.
LC-(ESI)MS (condition 1): t_R = 17.3 min $[M+H^+]^+$: 395.2 (100%).

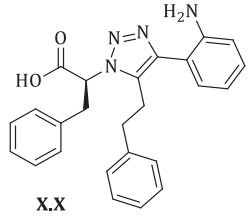

X.X

IX.26

Brutoformula: $C_{25}H_{24}N_4O_2$
Molecular weight: 412.48 Da.
LC-(ESI)MS (condition 1): t_R = 13.9 min $[M+H^+]^+$: 413.1 (100%).

D. Regioselectivity of IX.15 in RuAAC

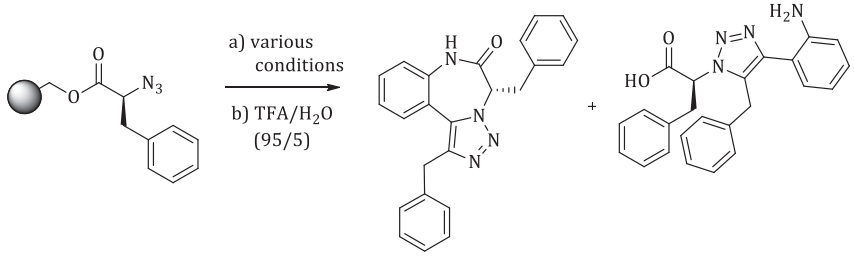

VII.31 **IX.27** **IX.28**

Procedure according to section **XVII.B** internal alkyne **IX.15** (68.2 mg, 0.3292 mmol, 5 eq).

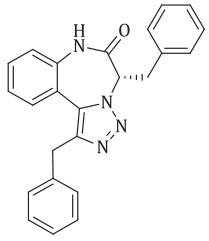

IX.27

Brutoformula: $C_{24}H_{20}N_4O$
Molecular weight: 380.44 Da.
LC-(ESI)MS (condition 1): t_R = 16.9 min $[M\text{-}H^+]^-$: 381.1 (100%).

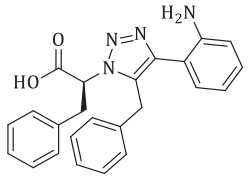

IX.28

Brutoformula: $C_{24}H_{22}N_4O_2$
Molecular weight: 398.46 Da.
LC-(ESI)MS (condition 1): t_R = 13.4 min $[M+H^+]^+$: 399.1 (100%).

E. Regioselectivity of IX.16 in RuAAC

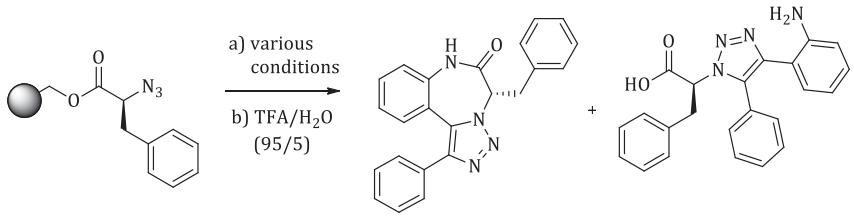

VII.31 **IX.29** **IX.30**

Procedure according to section **XVII.B** internal alkyne **IX.16** (63.6 mg, 0.3292 mmol, 5 eq).

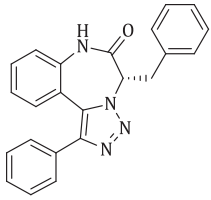

IX.29

Brutoformula: $C_{23}H_{18}N_4O$
Molecular weight: 366.42 Da.
LC-(ESI)MS (condition 1): t_R = 17.0 min $[M+H^+]^+$: 367.1 (100%).

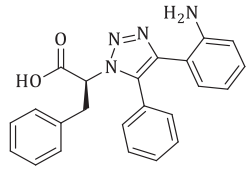

IX.30

Brutoformula: $C_{23}H_{20}N_4O_2$
Molecular weight: 384.43 Da.
LC-(ESI)MS (condition 1): t_R = 13.4 min $[M+H^+]^+$: 385.1 (100%).

2-(4-aminophenyl)ethynylaniline IX.31

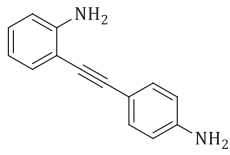

IX.31

Following general procedure **P.06**: 2-iodoaniline (500.0 mg, 2.273 mmol, 1 eq). 4-ethynylaniline (1.095 g, 9.092 mmol, 4 eq). $PdCl_2(PPh_3)_2$ (31.9 mg, 0.04546 mmol, 0.02 eq). CuI (22.5 mg, 0.1136 mmol, 0.05 eq). diethylamine (22 mL).

Yield: 85%. 2-(4-aminophenyl)ethynylaniline (**IX.31,** 402.5 mg, 1.933 mmol).
Yellow crystals.
R_F: 0.17 (hexane/acetone 7/3).
Molecular weight: 208.26 Da.
^{1}H NMR (300 MHz, acetone-d_6) δ 4.83-5.00 (m broad, 4H), 6.62-6.63 (m, 1H), 6.71-6.76 (m, 2H), 6.93-7.04 (m, 2H), 7.32-7.35 (m, 1H), 7.46-7.49 (m, 1H), 7.54-7.59 (m, 2H).
HATR (cm^{-1}): 3441 (w), 3352 (m), 3213 (w), 3030 (w), 2971 (w), 2203 (w), 2019 (w), 1697 (w), 1605 (s), 1512 (s), 1500 (s), 1488 (m), 1454 (m), 1351 (m), 1294 (m), 1257 (m), 1178 (m), 1156 (m), 1145 (m), 1056 (w), 1029 (w), 1011 (w), 939 (w), 826 (s), 783 (m), 748 (s), 694 (m), 625 (w).
LC-(ESI)MS (condition 1): t_R = 15.7 min $[M+H^+]^+$: 209.1. **Purity** (214 nm): 98%.

F. Regioselectivity of IX.31 in RuAAC

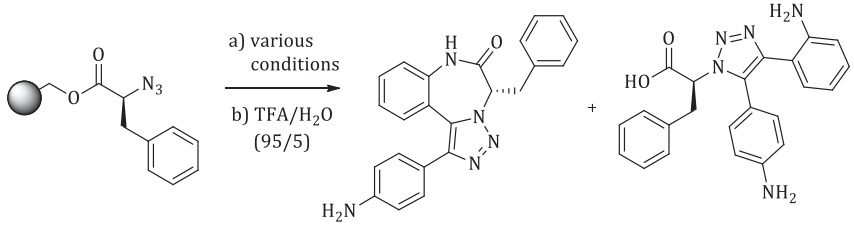

VII.31 **IX.32** **IX.33**

Procedure according to section **XVII.B**: only test reactions were performed in toluene: internal alkyne **IX.31** (68.6 mg, 0.3292 mmol, 5 eq).

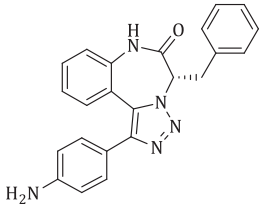

XI.32

Brutoformula: $C_{23}H_{19}N_5O$
Molecular weight: 381.43 Da.
LC-(ESI)MS (condition 1): t_R = 14.9 min $[M\text{-}H^+]^-$: 382.1 (100%).

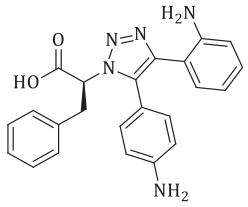

XI.33

Brutoformula: $C_{23}H_{21}N_5O$
Molecular weight: 399.45 Da.
LC-(ESI)MS (condition 1): t_R = 12.0 min $[M+H^+]^+$: 400.1 (100%).

General procedure **P.08**: The resin (1 eq) is transferred into a reaction vessel and $C_p^*RuCl(COD)$ (0.10 eq) is added, followed by an addition of toluene (0.1M) and 2-ethynylaniline (3 eq) building block. After 6 hours of shaking at room temperature the resin is filtered off and washed extensively with toluene (3x), DMF (3x), MeOH (3x) and dichloromethane (3x). Afterwards, the resin is dried under reduced pressure.

G. Proof of principle library

(*S*)-6-butyl-3-(4-(tert-butyloxycarbonyl)-aminobutyl)[1,2,3]triazolo[1,5-*d*][1,4]benzodiazepin-2-one IX.35

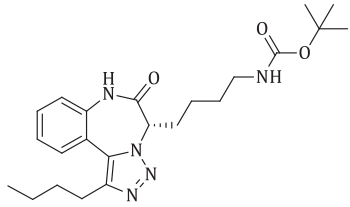

IX.35

Following general procedure **P.01** – **P.05**: (*S*)- 6-butyl-3-(4-(tert-butyloxycarbonyl)-aminobutyl)[1,2,3]triazolo[1,5-*d*][1,4]benzodiazepin-2-one (**IX.35**, 121.4 mg, 0.2840 mmol).

Yield: 51%.
Brown solid.
Molecular weight: 427.54 Da.
R_F: 0.21 (hexane/acetone: 8/2).
^{1}H NMR (500 MHz, acetone-d_6) δ 0.88 (t, J = 7.4Hz, 3H), 1.38-1.51 (m, 17H), 1.73 (sextet, J = 7.5Hz, 2H), 2.82-2.92 (m, 2H), 2.95-3.05 (m broad, 2H), 4.75-5.45 (m broad, 1H), 5.92 (s broad, 1H), 7.40-7.44 (m, 2H), 7.55 (t, J = 7.4Hz, 1H), 7.70 (d, J = 7.7Hz, 1H), 9.63 (s broad, 1H).
^{13}C NMR (125 MHz, acetone-d_6) δ 14.1 (CH_3), 23.1 (CH_2), 23.8 (CH_2), 25.8 (CH_2), 28.6 (CH_3), 32.1 (CH_2), 40.6 (CH_2), 78.3 (CH_2), 122.9 (CH), 125.9 (CH), 129.5 (CH), 131.1 (CH), 156.6 (C).
HATR (cm^{-1}): 3354 (w), 3227 (w), 2956 (m), 2930 (m), 2868 (w), 1687 (s), 1587 (w), 1555 (w), 1521 (w), 1481 (m), 1456 (w), 1390 (w), 1365 (m), 1276 (w), 1250 (w), 1170 (m), 1048 (w), 1013 (w), 863 (w), 766 (w), 650 (w).
LC-(ESI)MS (condition 1): t_R = 16.7 min $[M+H^+]^+$: 428.2 (100%). **Purity** (214 nm): >90%.
HRMS (ESI) calcd for $C_{23}H_{32}N_5O_3^-$: 426.2511 $[M-H^+]^-$ found: 426.2517.

(*S*)-6-(2-phenylethyl)-3-(4-(tert-butyloxycarbonyl)-aminobutyl)[1,2,3]triazolo[1,5-*d*][1,4]benzodiazepin-2-one IX.36

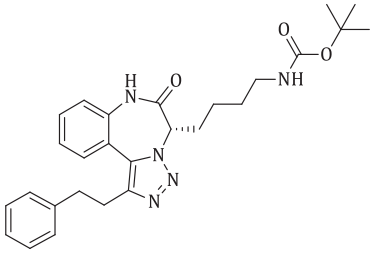

IX.36

Following general procedure **P.01 – P.03, P.08** and **P.05**: (*S*)-6-(2-phenylethyl)-3-(4-(tert-butyloxycarbonyl)-aminobutyl)[1,2,3]triazolo[1,5-*d*][1,4]benzodiazepin-2-one (**IX.36,** 173.1 mg, 0.3640 mmol).

Yield: 83%.
Brown solid.
Molecular weight: 475.58 Da.
R_F: 0.11 (hexane/acetone: 8/2).
^{1}H NMR (500 MHz, acetone-d_6) δ 1.13-1.74 (m, 15H), 2.90-3.21 (m, 6H), 4.55-5.67 (m broad, 1H), 5.89 (s broad, 1H), 7.11-7.15 (m, 3H), 7.30 (t, J = 7.6Hz, 2H), 7.36 (d, J = 8.0Hz, 1H), 7.56 (d, J = 7.6Hz, 1H), 7.50 (t, J = 8.0Hz, 1H), 9.54 (s broad, 1H).
^{13}C NMR (125 MHz, acetone-d_6) δ 23.7 (C), 28.4 (CH_2), 28.6 (CH_3), 35.8 (CH_2), 40.6 (CH_2), 78.3 (CH_2), 114.0 (C), 122.9 (CH, weak), 125.8 (CH), 126.9 (CH), 129.1 (CH), 129.3 (CH), 129.4 (CH, weak), 131.1 (CH), 142.3 (C), 156.6 (C).
HATR (cm^{-1}): 3354 (w), 3214 (w), 3055 (w), 2976 (w), 2929 (w), 2864 (w), 1682 (s), 1603 (w), 1587 (w), 1508 (w), 1481 (m), 1453 (m), 1429 (w), 1390 (m), 1364 (m), 1264 (m), 1249 (m), 1227 (w), 1165 (m), 1070 (w), 1049 (w), 1029 (w), 1012 (w), 948 (w), 865 (w), 763 (w), 734 (w), 699 (w), 651 (w).
LC-(ESI)MS (condition 1): t_R = 17.0 min $[M+H^+]^+$: 476.3 (100%). **Purity** (214 nm): >90%.
HRMS (ESI) calcd for $C_{27}H_{32}N_5O_3^-$: 474.2511 $[M-H^+]^-$ found: 474.2514.

(*S*)-6-benzyl-3-(4-(tert-butyloxycarbonyl)-aminobutyl)[1,2,3]triazolo[1,5-*d*][1,4]-benzodiazepin-2-one IX.37

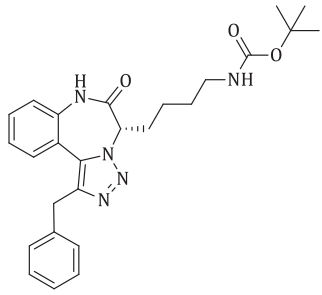

IX.37

Following general procedure **P.01** – **P.05**: (*S*)-6-benzyl-3-(4-(tert-butyloxycarbonyl)-aminobutyl)[1,2,3]triazolo[1,5-*d*][1,4]benzodiazepin-2-one (**IX.37**, 51.7 mg, 0.1115 mmol).

Yield: 20%.
Brown solid.
Molecular weight: 461.56 Da.
R_F: 0.08 (hexane/acetone: 8/2).
^{1}H NMR (300 MHz, acetone-d_6) δ 1.26-1.67 (m, 15H), 1.75-2.50 (m broad, 2H), 2.92-3.16 (m, 2H), 4.06-5.56 (m broad, 1H), 5.91 (s broad, 1H), 7.25 (t, J = 7.9Hz, 1H), 7.35-7.49 (m, 5H), 7.56 (d, J = 8.5Hz, 1H), 7.59-7.64 (m, 2H), 9.73 (s broad, 1H).
^{13}C NMR (75 MHz, acetone-d_6) δ 23.9 (C), 28.6 (CH_3), 30.6 (CH_2), 35.8 (CH_2), 40.6 (CH_2), 78.3 (CH_2), 123.0 (CH), 125.8 (CH), 126.8 (CH), 129.1 (CH), 129.3 (CH), 131.1 (CH), 142.2 (C).
HATR (cm^{-1}): 3333 (w), 3228 (w), 2971 (w), 2928 (w), 2863 (w), 1682 (s), 1587 (w), 1519 (w), 1508 (w), 1496 (w), 1482 (m), 1453 (w), 1423 (w), 1389 (w), 1364 (m), 1272 (w), 1250 (w), 1230 (w), 1168 (m), 765 (w), 731 (m), 697 (w), 646 (w), 619 (w).
LC-(ESI)MS (condition 1): t_R = 16.7 min $[M+H^+]^+$: 462.2 (100%). **Purity** (214 nm): >90%.
HRMS (ESI) calcd for $C_{26}H_{30}N_5O_3^-$: 460.2354 $[M-H^+]^-$ found: 460.2361.

(*S*)-6-phenyl-3-(4-tert-butyloxycarbonyl)-aminobutyl)[1,2,3]triazolo[1,5-*d*][1,4]benzodiazepin-2-one IX.38

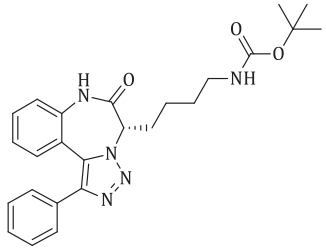

IX.38

Following general procedure **P.01** – **P.03, P.08** and **P.05**: (*S*)-6-phenyl-3-(4-(tert-butyloxycarbonyl)-aminobutyl)[1,2,3]triazolo[1,5-*d*][1,4]benzodiazepin-2-one (**IX.38,** 162.8 mg, 0.3638 mmol).

Yield: 84%.
Brown solid.
Molecular weight: 447.53 Da.
R_F: 0.21 (hexane/acetone: 7/3).
^{1}H NMR (300 MHz, acetone-d_6) δ 1.28-1.67 (m, 15H), 2.90-3.10 (m broad, 2H), 4.40-5.55 (m broad, 1H), 7.25 (t, J = 7.9Hz, 1H), 7.36-7.49 (m, 5H), 7.54-7.64 (m, 3H), 9.73 (s broad, 1H).
^{13}C NMR (75 MHz, acetone-d_6) δ 23.9 (CH_2), 28.6 (CH_3), 40.6 (CH_2), 125.7 (CH), 128.6 (CH), 129.1 (CH), 129.5 (CH), 130.4 (CH),131.7 (CH) ,132.2 (C), 165.9 (C).
HATR (cm^{-1}): 3359 (w), 3233 (w), 2974 (w), 2930 (w), 2868 (w), 1684 (s), 1607 (w), 1587 (w), 1508 (w), 1478 (m), 1448 (w), 1390 (w), 1364 (m), 1269 (w), 1250 (w), 1167 (m), 1023 (w), 984 (w), 866 (w), 765 (m), 733 (m), 698 (m), 650 (w).
LC-(ESI)MS (condition 1): t_R = 16.7 min $[M+H^+]^+$: 448.2 (100%). **Purity** (214 nm): >90%.
HRMS (ESI) calcd for $C_{25}H_{28}N_5O_3^-$: 446.2198 $[M-H^+]^-$ found: 446.2203.

(*S*)-6-butyl-3-benzyl[1,2,3]triazolo[1,5-*d*][1,4]benzodiazepin-2-one IX.23

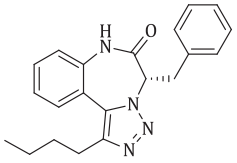

IX.23

Following general procedure **P.01** – **P.05**: (*S*)-6-butyl-3-benzyl[1,2,3]triazolo[1,5-*d*][1,4]benzodiazepin-2-one (**IX.23**, 140.0 mg, 0.4041 mmol).

Yield: 57%.
Brown solid.
Molecular weight: 346.43 Da.
R_F: 0.11 (hexane/acetone: 85/15).
^{1}H NMR (500 MHz, acetone-d_6) δ 0.90 (t, J = 7.4Hz, 3H), 1.34 (sextet, J = 7.4Hz, 2H), 1.71 (sextet, J = 7.7Hz, 2H), 2.83 (t, J = 7.7Hz, 2H), 3.10-3.80 (m, 2H), 5.15-5.65 (m, 1H), 7.18-7.33 (m, 5H), 7.41-7.44 (m, 2H), 7.55-7.58 (m, 1H), 7.71-7.72 (m, 1H) 9.63 (s broad, 1H).
^{13}C NMR (125 MHz, acetone-d_6) δ 14.1 (CH_3), 23.0 (CH_2), 25.7 (CH_2), 32.0 (CH_2), 123.2 (CH), 126.1 (CH), 127.7 (CH), 129.2 (CH), 129.6 (CH), 130.3 (CH), 131.2 (CH), 168.1 (C).
HATR (cm^{-1}): 3219 (w), 3085 (w), 3028 (w), 2955 (w), 2928 (w), 2869 (w), 1684 (s), 1607 (w), 1586 (w), 1496 (m), 1481 (m), 1455 (w), 1427 (w), 1380 (w), 1310 (w), 1258 (w), 1224 (w), 1077 (w), 1048 (w), 763 (w), 698 (m), 650 (w).
LC-(ESI)MS (condition 1): t_R = 17.0 min $[M+H^+]^+$: 347.2 (100%). **Purity** (214 nm): 96%.
HRMS (ESI) calcd for $C_{21}H_{21}N_4O^-$: 345.1721 $[M-H^+]^-$ found: 345.1728.

(*S*)-6-(2-phenylethyl)-3-benzyl[1,2,3]triazolo[1,5-*d*][1,4]benzodiazepin-2-one IX.25

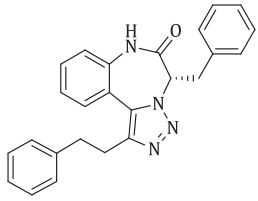

IX.25

Following general procedure **P.01** – **P.03, P.08** and **P.05**: (*S*)-6-(2-phenylethyl)-3-benzyl[1,2,3]triazolo[1,5-*d*][1,4]benzodiazepin-2-one (**IX.25**, 161.8 mg, 0.4102 mmol).

Yield: 58%.
Brown solid.
Molecular weight: 394.47 Da.
R_F: 0.09 (hexane/acetone: 8/2).
^{1}H NMR (300 MHz, acetone-d_6) δ 2.85-3.03 (m, 4H), 3.30-3.80 (m broad, 2H), 5.10-5.55 (m broad, 1H), 7.15-7.25 (m, 5H), 7.29-7.41 (m, 4H), 7.42-7.50 (m, 2H), 7.51-7.64 (m, 3H), 9.86 (s broad, 1H).
^{13}C NMR (75 MHz, acetone-d_6) δ 28.3 (CH_2), 35.8 (CH_2), 126.0 (CH), 126.8 (CH), 127.6 (CH), 129.1 (CH), 129.2 (CH), 129.3 (CH), 129.5 (CH), 130.2 (CH), 131.2 (CH), 142.2 (C).

HATR (cm^{-1}): 3214 (w), 3060 (w), 3027 (w), 2961 (w), 2925 (w), 2863 (w), 2143 (w), 1681 (s), 1603 (w), 1586 (w), 1495 (w), 1480 (m), 1453 (w), 1427 (m), 1383 (s), 1361 (m), 1315 (w), 1263 (w), 1224 (w), 1199 (w), 1191 (w), 1124 (w), 1074 (w), 1049 (w), 1030 (w), 940 (w), 844 (m), 762 (m), 748 (m), 698 (s), 650 (w).
LC-(ESI)MS (condition 1): t_R = 17.2 min $[M+H^+]^+$: 395.2 (100%). Purity (214 nm): 96%.
HRMS (ESI) calcd for $C_{25}H_{21}N_4O^-$: 393.1721 $[M-H^+]^-$ found: 393.1723.

(*S*)-6-phenyl-3-benzyl[1,2,3]triazolo[1,5-*d*][1,4]benzodiazepin-2-one IX.29

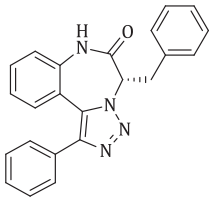

IX.29

Following general procedure **P.01** – **P.03, P.08** and **P.05**: (*S*)-6-phenyl-3-benzyl[1,2,3]triazolo[1,5-*d*][1,4]benzodiazepin-2-one (**IX.29**, 169.1 mg, 0.4615 mmol).

Yield: 64%.
Brown solid.
Molecular weight: 366.42 Da.
R_F: 0.12 (hexane/acetone: 8/2).
^{1}H NMR (300 MHz, acetone-d_6) δ 3.20-4.30 (m broad, 2H), 5.00-5.80 (m broad, 1H), 7.15-7.25 (m, 5H), 7.29-7.41 (m, 4H), 7.42-7.50 (m, 2H), 7.51-7.64 (m, 3H), 9.86 (s broad, 1H).
^{13}C NMR (75 MHz, acetone-d_6) δ 123.7 (CH), 125.9 (CH), 127.8 (CH), 128.6 (CH), 129.0 (CH), 129.1 (CH), 129.4 (CH), 130.2 (CH), 130.5 (CH), 131.9 (CH), 132.0 (C), 136.8 (C), 144.8 (C), 168.1 (C).
HATR (cm^{-1}): 3209 (w), 3063 (w), 3028 (w), 1684 (s), 1605 (w), 1586 (w), 1478 (m), 1454 (w), 1425 (w), 1383 (w), 1354 (w), 1261 (w), 1224 (w), 1075 (w), 1023 (w), 985 (w), 764 (m), 747 (w), 736 (w), 697 (m), 635 (w).
LC-(ESI)MS (condition 1): t_R = 17.0 min $[M+H^+]^+$: 367.1 (100%). **Purity** (214 nm): 93%.
HRMS (ESI) calcd for $C_{23}H_{17}N_4O^-$: 365.1408 $[M-H^+]^-$ found: 365.1410.

(*S*)-6-butyl-3-(tert-butoxymethyl)[1,2,3]triazolo[1,5-*d*][1,4]benzodiazepin-2-one IX.39

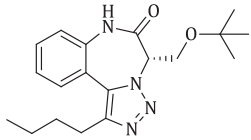

IX.39

Following general procedure **P.01** – **P.05**: (*S*)-6-butyl-3-(tert-butoxymethyl)[1,2,3]triazolo[1,5-*d*][1,4]benzodiazepin-2-one (**IX.39**, 165.4 mg, 0.4830 mmol).

Yield: 63%.
Brown solid.
Molecular weight: 342.44 Da.
R_F: 0.12 (hexane/acetone: 85/15).
^{1}H NMR (500 MHz, acetone-d_6) δ 0.88(t, J = 7.4Hz, 3H), 1.04 (s, 9H), 1.37 (sextet, J = 7.4Hz, 2H), 1.70 (sextet, J = 7.6Hz, 2H), 2.85 (t, J = 7.6Hz, 2H), 3.75-4.18 (m broad, 2H), 5.04-5.45 (m broad, 1H), 7.37-7.40 (m, 2H), 7.52 (t, J = 7.7Hz, 1H), 7.67 (d, J = 7.3Hz, 1H), 9.59 (s broad, 1H).
^{13}C NMR (125 MHz, acetone-d_6) δ 14.0 (CH_3), 23.0 (CH_2), 25.8 (CH_2), 27.3 (CH_3), 32.0 (CH_2), 74.2 (CH_2), 123.1 (CH), 125.8 (CH), 129.5 (CH), 131.0 (CH), 167.6 (C).
HATR (cm^{-1}): 3223 (w), 3095 (w), 2965 (w), 2930 (w), 2871 (w), 1682 (s), 1612 (w), 1588 (w), 1480 (m), 1427 (w), 1363 (m), 1308 (w), 1258 (w), 1235 (w), 1192 (m), 1124 (w), 1089 (m), 1023 (w), 986 (w), 950 (w), 894 (w), 852 (w), 765 (m), 734 (m), 701 (w), 650 (w).
LC-(ESI)MS (condition 1): t_R = 17.1 min $[M+H^+]^+$: 343.2 (100%). **Purity** (214 nm): 96%.
HRMS (ESI) calcd for $C_{19}H_{25}N_4O_2^-$: 341.1983 $[M-H^+]^-$ found: 341.1990.

(*S*)-6-(2-phenylethyl)-3-(tert-butoxymethyl)[1,2,3]triazolo[1,5-*d*][1,4]benzodiazepin-2-one IX.40

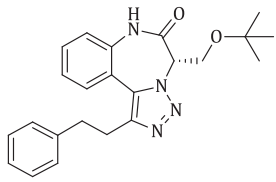

IX.40

Following general procedure **P.01** – **P.03, P.08** and **P.05**: (*S*)-6-butyl-3-(tert-butoxymethyl)[1,2,3]triazolo[1,5-*d*][1,4]benzodiazepin-2-one (**IX.40**, 96.4 mg, 0.2469 mmol).

Yield: 32%.
Brown oil.
Molecular weight: 390.48 Da.
R_F: 0.12 (hexane/acetone: 8/2).
^{1}H NMR (500 MHz, acetone-d_6) δ 1.04 (s, 9H), 3.02-3.12 (m, 2H), 3.12-3.21 (m, 2H), 3.60-4.43 (m, 2H), 5.12-5.50 (m, 1H), 7.13-7.25 (m, 5H), 7.34-7.39 (m, 2H), 7.51-7.55 (m, 2H), 9.59 (s broad, 1H).
^{13}C NMR (125 MHz, acetone-d_6) δ 27.3 (CH3), 28.3 (C), 35.7 (CH2), 55.4 (CH_2), 74.2 (CH_2), 119.2 (C), 122.9 (CH), 125.7 (CH), 126.7 (CH), 129.0 (CH), 129.2 (CH), 129.4 (CH), 131.0 (CH), 136.2 (C), 142.0 (C), 144.5 (C), 167.6 (C).
HATR (cm^{-1}): 3219 (w), 3087 (w), 3059 (w), 3033 (w), 2971 (m), 2928 (w), 2873 (w), 2356 (m), 2340 (m), 1684 (s), 1588 (w), 1558 (w), 1540 (w), 1522 (w), 1481 (m), 1453 (w), 1427 (w), 1363 (m), 1258 (w), 1235 (w), 1192 (m), 1090 (m), 1025 (w), 948 (w), 894 (w), 852 (w), 763 (w), 748 (m), 699 (m), 668 (m), 650 (w).
LC-(ESI)MS (condition 1): t_R = 17.3 min $[M+H^+]^+$: 391.2 (100%). **Purity** (214 nm): 90%.
HRMS (ESI) calcd for $C_{23}H_{25}N_4O_2^-$: 389.1993 $[M-H^+]^-$ found: 389.1990.

(*S*)-6-phenyl-3-(tert-butoxymethyl)[1,2,3]triazolo[1,5-*d*][1,4]benzodiazepin-2-one IX.41

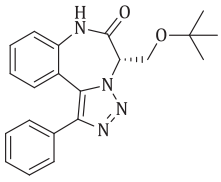

IX.41

Following general procedure **P.01** – **P.03, P.08** and **P.05**: (*S*)-6-phenyl-3-(tert-butoxymethyl)[1,2,3]triazolo[1,5-*d*][1,4]benzodiazepin-2-one (**IX.41**, 127.2 mg, 0.3510 mmol).

Yield: 46%.
Brown solid.
Molecular weight: 362.42 Da.
R_F: 0.17 (hexane/acetone: 8/2).
^{1}H NMR (300 MHz, acetone-d_6) δ 1.08 (s, 9H), 3.76-4.40 (m broad, 2H), 5.00-5.50 (m broad, 1H), 7.21 (t, J = 7.6Hz, 1H), 7.36-7.46 (m, 5H), 7.51-7.57 (m, 1H), 7.59-7.62 (m, 2H), 9.73 (s broad, 1H).
^{13}C NMR (75 MHz, acetone-d_6) δ 25.8 (C), 27.4 (CH_3), 59.0 (CH_2), 74.4 (CH), 123.5 (CH), 125.7 (CH), 128.6 (CH), 129.1 (CH), 129.5 (CH), 130.4 (CH), 131.7 (CH), 132.2 (C), 167.6 (C).

HATR (cm^{-1}): 3218 (w), 2972 (m), 2935 (w), 1687 (s), 1607 (w), 1587 (w), 1506 (w), 1478 (m), 1447 (w), 1425 (w), 1362 (m), 1258 (w), 1234 (w), 1192 (m), 1145 (w), 1088 (m), 1022 (w), 983 (w), 951 (w), 894 (w), 851 (w), 764 (m), 735 (m), 698 (m), 650 (w), 620 (w).
LC-(ESI)MS (condition 1): t_R = 17.0 min $[M+H^+]^+$: 363.2 (100%). **Purity** (214 nm): 96%.
HRMS (ESI) calcd for $C_{21}H_{21}N_4O_2^-$: 361.1670 $[M-H^+]^-$ found: 361.1679.

H. Building block synthesis

4-chloro-2-(1-hexynyl)aniline IX.42

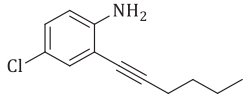

IX.42

Following general procedure **P.06**: 4-chloro-2-iodoaniline (2.000 g, 7.890 mmol, 1 eq). 1-hexyne (3.625 mL, 31.56 mmol, 4 eq). $PdCl_2(PPh_3)_2$ (110.6 mg, 0.1578 mmol, 0.02 eq). CuI (75.1 mg, 0.3945 mmol, 0.05 eq). diethylamine (79 mL).

Yield: 97%. 4-chloro-2-hexynylaniline (**IX.42**, 1.589 g, 7.653 mmol).
Red oil.
Molecular weight: 207.70 Da.
R_F: 0.38 (hexane/acetone: 8/2). 0.59 (hexane/acetone: 6/4).
^{1}H NMR (300 MHz, acetone-d_6) δ 0.91 (t, J = 7.2Hz, 3H), 1.41-1.63 (m, 4H), 2.47 (t, J = 7.0Hz, 2H), 5.02 (s broad, 2H), 6.72 (d, J = 8.7Hz, 1H), 7.00 (dd, J = 2.4Hz/8.7Hz, 1H), 7.10 (d, J = 2.4Hz, 1H).
^{13}C NMR (75 MHz, acetone-d_6) δ 13.8 (CH_3), 19.6 (CH_2), 22.6 (CH_2), 31.6 (CH_2), 76.9 (C), 97.2 (C), 110.2 (C), 115.8 (CH), 120.7 (C), 129.4 (CH), 131.5 (CH), 148.9 (C).
HATR (cm^{-1}): 3457 (w), 3430 (w), 3382 (w), 2956 (m), 2930 (m), 2870 (w), 1612 (m), 1590 (m), 1488 (w), 1464 (s), 1427 (w), 1408 (m), 1378 (w), 1306 (m), 1248 (m), 1147 (m), 1088 (m), 1061 (w), 972 (w), 949 (w), 912 (w), 877 (m), 810 (s), 777 (w), 716 (m), 689 (m), 652 (m).
LC-(ESI)MS (condition 1): t_R = 19.8 min $[M+H^+]^+$: 208.1 (100%). **Purity** (214 nm): 95%.
HRMS (ESI) calcd for $C_{12}H_{15}ClN^+$: 208.0888 $[M+H^+]^+$ found: 208.0890.

4-bromo-2-(1-hexynyl)aniline IX.43

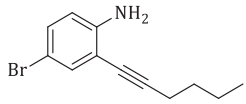

IX.43

Following general procedure **P.06**: 4-bromo-2-iodoaniline (3.000 g, 10.10 mmol, 1 eq). 1-hexyne (4.665 mL, 40.40 mmol, 4 eq). $PdCl_2(PPh_3)_2$ (141.6 mg, 0.202 mmol, 0.02 eq). CuI (96.9 mg, 0.505 mmol, 0.05 eq). diethylamine (101 mL).

Yield: 93%. 4-bromo-2-(1-hexynyl)aniline (**IX.43**, 2.368 g, 9.391 mmol).
Yellow oil.
Molecular weight: 252.15 Da.
R_F: 0.40 (hexane/acetone: 8/2). 0.59 (hexane/acetone: 6/4).
^{1}H NMR (300 MHz, acetone-d_6) δ 0.92 (t, J = 7.2Hz, 3H), 1.41-1.63 (m, 4H), 2.47 (t, J = 7.2Hz, 2H), 5.05 (s broad, 2H), 6.66 (d, J = 8.9Hz, 1H), 7.13 (dd, J = 2.5Hz/8.9Hz, 1H), 7.23 (d, J = 2.5Hz, 1H).
^{13}C NMR (75 MHz, acetone-d_6) δ 13.9 (CH_3), 19.4 (CH_2), 19.6 (CH_2), 31.6 (CH_2), 76.8 (C), 97.3 (C), 107.4 (C), 110.8 (C), 116.3 (CH), 132.2 (CH), 134.3 (CH), 149.3 (C).
HATR (cm^{-1}): 3475 (w), 3379 (w), 2959 (m), 2930 (m), 2870 (w), 1610 (s), 1484 (s), 1470 (w), 1404 (m), 1301 (m), 1249 (w), 1149 (m), 1078 (w), 948 (w), 879 (m), 809 (m), 705 (w), 634 (w).
LC-(ESI)MS (condition 1): t_R = 19.9 min $[M+H^+]^+$: 253.2 (100%). **Purity** (214 nm): 96%.
HRMS (ESI) calcd for $C_{12}H_{15}BrN^+$: 252.0382 $[M+H^+]^+$ found: 252.0385.

5-chloro-2-(1-hexynyl)aniline IX.44

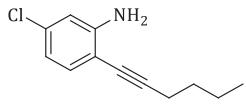

IX.44

Following general procedure **P.06**: 5-chloro-2-iodoaniline (2.000 g, 7.890 mmol, 1 eq). 1-hexyne (3.625 mL, 31.56 mmol, 4 eq). $PdCl_2(PPh_3)_2$ (110.6 mg, 0.1578 mmol, 0.02 eq). CuI (75.1 mg, 0.3945 mmol, 0.05 eq). diethylamine (79 mL).

Yield: 98%. 5-chloro-2-hexynylaniline (**IX.44**, 1.606 g, 7.732 mmol).
Red oil.
Molecular weight: 207.70 Da.
R_F: 0.44 (hexane/acetone: 8/2). 0.59 (hexane/acetone: 6/4).

^{1}H NMR (300 MHz, acetone-d_6) δ 0.91 (t, J = 7.2Hz, 3H), 1.41-1.62 (m, 4H), 2.46 (t, J = 7.0Hz, 2H), 5.14 (s broad, 2H), 6.53 (dd, J = 2.1Hz/8.1Hz, 1H), 6.76 (d, J = 2.1Hz, 1H), 7.11 (d, J = 8.1Hz, 1H).
^{13}C NMR (75 MHz, acetone-d_6) δ 13.8 (CH_3), 19.6 (CH_2), 22.6 (CH_2), 31.7 (CH_2), 77.0 (C), 96.8 (C), 107.6 (C), 113.9 (CH), 116.9 (CH), 133.7 (CH), 134.6 (C), 151.2 (C).
HATR (cm^{-1}): 3476 (w), 3383 (w), 2956 (m), 2929 (m), 2860 (w), 1610 (s), 1560 (m), 1488 (s), 1464 (m), 1421 (s), 1378 (w), 1362 (w), 1327 (w), 1303 (m), 1268 (m), 1240 (m), 1134 (w), 1093 (m), 1060 (m), 1006 (w), 987 (w), 959 (w), 943 (m), 902 (m), 845 (m), 796 (s), 744 (w), 652 (w).
LC-(ESI)MS (condition 1): t_R = 19.7 min $[M+H^+]^+$: 208.1 (100%). Purity (214 nm): 96%.
HRMS (ESI) calcd for $C_{12}H_{15}ClN^+$: 208.0888 $[M+H^+]^+$ found: 208.0890.

4-chloro-2-(butyn-4-ol)aniline IX.45

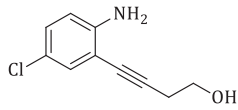

IX.45

Following general procedure **P.06**: 4-chloro-2-iodoaniline (3.000 g, 11.83 mmol, 1 eq). 3-butyn-1-ol (3.583 mL, 47.92 mmol, 4 eq). $PdCl_2(PPh_3)_2$ (165.8 mg, 0.2366 mmol, 0.02 eq). CuI (113.6 mg, 0.5915 mmol, 0.05 eq). diethylamine (118 mL).

Yield: 95%. 4-chloro-2-(butyn-4-ol)aniline (**IX.45**, 2.198 g, 11.23 mmol).
Yellow solid.
Molecular weight: 195.65 Da.
R_F: 0.06 (hexane/acetone: 8/2). 0.33 (hexane/acetone: 6/4).
^{1}H NMR (300 MHz, acetone-d_6) δ 2.65 (t, J = 6.6Hz, 2H), 3.75 (q, J = 5.8Hz/6.6Hz, 2H), 4.00 (t, J = 5.8Hz, 1H), 5.11 (s broad, 2H), 6.72 (d, J = 8.7Hz, 1H), 7.01 (dd, J = 2.6Hz/8.7Hz, 1H), 7.10 (d, J = 2.6Hz, 1H).
^{13}C NMR (75 MHz, acetone-d_6) δ 24.5 (CH_2), 61.4 (CH_2), 77.8 (C), 94.9 (C), 109.9 (C), 115.8 (CH), 120.5 (C), 121.6 (C), 129.5 (CH), 131.3 (CH), 149.2 (C).
HATR (cm^{-1}): 3352 (m, br), 2942 (w), 2897 (w), 1698 (w), 1615 (m), 1488 (s), 1410 (m), 1332 (m), 1307 (m), 1249 (m), 1181 (m), 1149 (m), 1088 (m), 1045 (m), 911 (w), 880 (w), 847 (w), 814 (m), 721 (w), 654 (w).
LC-(ESI)MS (condition 1): t_R = 14.3 min $[M+H^+]^+$: 196.0. **Purity** (214 nm): 92%.
HRMS (ESI) calcd for $C_{10}H_{11}ClNO^+$: 196.0524 $[M+H^+]^+$ found: 196.0526.

4-chloro-2-(2-phenyl)ethynylaniline IX.46

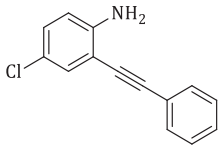

IX.46

Following general procedure **P.06**: 4-chloro-2-iodoaniline (5.645 g, 22.27 mmol, 1 eq). phenylacetylene (4.900 mL, 44.61 mmol, 2 eq). $PdCl_2(PPh_3)_2$ (312.6 mg, 0.4454 mmol, 0.02 eq). CuI (212.1 mg, 1.113 mmol, 0.05 eq). diethylamine (220 mL).

Yield: 92%. 4-chloro-2-(2-phenyl)ethynylaniline (**IX.46,** 5.070 g, 20.49 mmol).
Yellow solid.
R_F: 0.46 (hexane/acetone: 7/3). 0.29 (hexane/acetone: 8/2).
Molecular weight: 227.69 Da.
^{1}H NMR (700 MHz, acetone-d_6) δ 5.27 (s broad, 2H), 6.81 (d, J = 8.6Hz, 1H), 7.10 (dd, J = 2.6Hz/8.8Hz, 1H), 7.30 (d, J = 2.4Hz, 1H), 7.35-7.40 (m, 3H), 7.58-7.59 (m, 2H).
^{13}C NMR (175 MHz, acetone-d_6) δ 85.8 (C), 95.8 (C), 108.8 (C), 116.2 (CH), 120.9 (C), 123.8 (C), 129.2 (CH), 129.2 (CH), 130.3 (CH), 131.5 (CH), 132.1 (C), 148.9 (C).
HATR (cm^{-1}): 3485 (m), 3387 (m), 3058 (w), 2200 (w), 1607 (s), 1493 (s), 1492 (s), 1482 (s), 1442 (m), 1410 (m), 1309 (m), 1281 (w), 1248 (m), 1150 (w), 1083 (w), 1070 (w), 1024 (w), 912 (m), 897 (m), 811 (s), 740 (s), 718 (m), 688 (s), 656 (m).
LC-(ESI)MS (condition 1): t_R = 19.1 min $[M+H^+]^+$: 228.1 (100%). **Purity** (214 nm): 96%.
HRMS (ESI) calcd for $C_{14}H_{11}ClN^+$: 228.0575 $[M+H^+]^+$ found: 228.0569.

4-bromo-2-(2-phenyl)ethynylaniline IX.47

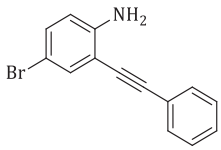

IX.47

Following general procedure **P.06**: 4-bromo-2-iodoaniline (2.000 g, 6.713 mmol, 1 eq). phenylacetylene (1.475 mL, 13.43 mmol, 2 eq). $PdCl_2(PPh_3)_2$ (94.1 mg, 0.1343 mmol, 0.02 eq). CuI (63.8 mg, 0.3356 mmol, 0.05 eq). diethylamine (67 mL).

Yield: 94%. 4-bromo-2-(2-phenyl)ethynylaniline (**IX.47,** 1.717 g, 6.309 mmol).

Yellow solid.
Molecular weight: 272.14 Da.
R_F: 0.18 (hexane/acetone: 8/2).
^{1}H NMR (700 MHz, acetone-d_6) δ 5.33 (s broad, 2H), 6.76 (d, J = 8.8Hz, 1H), 7.21 (dd, J = 2.4Hz/8.8Hz, 1H), 7.37-7.41 (m, 4H), 7.57-7.59 (m, 2H).
^{13}C NMR (175 MHz, acetone-d_6) δ 85.7 (C), 95.9 (C), 107.4 (C), 109.5 (C), 116.7 (CH), 124.0 (C), 129.3 (CH), 129.3 (CH), 132.2 (CH), 133.2 (CH), 134.5 (CH), 149.6 (C).
HATR (cm^{-1}): 3476 (m), 3380 (m), 3056 (w), 2212 (w), 1610 (s), 1491 (s), 1479 (s), 1442 (m), 1405 (m), 1308 (m), 1280 (m), 1250 (m), 1152 (m), 1070 (w), 1027 (w), 913 (w), 884 (m), 810 (m), 754 (s), 688 (s), 635 (m).
LC-(ESI)MS (condition 1): t_R = 19.3 min $[M+H^+]^+$: 272.1 (100%). **Purity** (214 nm): 98%.
HRMS (ESI) calcd for $C_{14}H_{11}BrN^+$: 272.0069 $[M+H^+]^+$ found: 272.0059.

2-(hexynyl)-4-methoxy-1-nitrobenzene IX.49

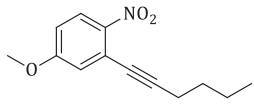

IX.49

Following general procedure **P.06**: 2-iodo-4-methoxy-1-nitrobenzene (**VIII.42**, 0.455 g, 1.631 mmol, 1 eq). 1-hexyne (0.745 mL, 6.523 mmol, 4 eq). $PdCl_2(PPh_3)_2$ (22.9 mg, 0.0326 mmol, 0.02 eq). CuI (15.5 mg, 0.815 mmol, 0.05 eq). diethylamine (16 mL).

Yield: 93%. 2-(hexynyl)-4-methoxy-1-nitrobenzene (**IX.49**, 354.0 mg, 1.518 mmol).
Greenish oil.
Molecular weight: 233.26 Da.
R_F: 0.13 (hexane/acetone: 99/1).
^{1}H NMR (300 MHz, acetone-d_6) δ 0.92 (t, J = 7.2Hz, 3H), 1.43-1.64 (m, 4H), 2.47 (t, J = 6.8Hz, 2H), 3.90 (s, 3H), 6.98-7.04 (m, 2H), 8.03 (d, J = 9.1Hz, 1H).
^{13}C NMR (75 MHz, acetone-d_6) δ 13.8 (CH_3), 19.8 (CH_2), 22.5 (CH_2), 31.1 (CH_2), 56.5 (CH_3), 73.5 (C), 77.2 (C), 99.4 (C), 114.9 (CH), 119.6 (CH), 121.9 (C), 127.6 (CH), 163.6 (C).
LC-(ESI)MS (condition 1): t_R = 21.0 min $[M+H^+]^+$: 234.1 (100%).
HRMS (ESI) calcd for $C_{13}H_{16}NO_3^+$: 234.1125 $[M+H^+]^+$ found: 234.1129.

2-(hexynyl)-5-methoxy-1-nitrobenzene IX.50

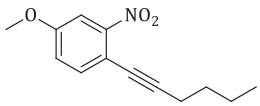

IX.50

Following general procedure **P.06**: 4-iodo-3-nitroanisole (1.500 g, 5.376 mmol, 1 eq). 1-hexyne (2.450 mL, 21.04 mmol, 4 eq). $PdCl_2(PPh_3)_2$ (75.4 mg, 0.1072 mmol, 0.02 eq). CuI (51.1 mg, 0.2688 mmol, 0.05 eq). diethylamine (54 mL).

Yield: 96%. 2-(hexynyl)-5-methoxy-1-nitrobenzene (**IX.50**, 1.202 g, 5.153 mmol).
Yellow oil.
Molecular weight: 233.26 Da.
R_F: 0.39 (hexane/acetone: 9/1).
^{1}H NMR (300 MHz, acetone-d_6) δ 0.92 (t, J = 7.4Hz, 3H), 1.42-1.62 (m, 4H), 2.44 (t, J = 7.0Hz, 2H), 3.92 (s, 3H), 7.23 (dd, J = 2.8Hz/8.7Hz, 1H), 7.50 (d, J = 2.8Hz, 1H), 7.53(d, J = 8.7Hz, 1H).
^{13}C NMR (75 MHz, acetone-d_6) δ 13.8 (CH_3), 19.6 (CH_2), 22.5 (CH_2), 31.3 (CH_2), 56.5 (CH_3), 76.1 (C), 96.9 (C), 109.8 (CH), 111.3 (C), 120.1 (CH), 136.3 (CH), 160.1 (C).
HATR (cm^{-1}): 3105 (w), 2957 (w), 2932 (w), 2871 (w), 2230 (w), 2067 (w), 1618 (m), 1560 (m), 1527 (s), 1497 (s), 1461 (m), 1440 (m), 1344 (s), 1306 (s), 1296 (s), 1271 (s), 1223 (s), 1184 (w), 1140 (w), 1105 (w), 1074 (w), 1032 (m), 947 (w), 907 (w), 857 (m), 828 (m), 801 (s), 759 (m), 680 (w), 658 (w).
LC-(ESI)MS (condition 1): t_R = 19.3 min $[M+H^+]^+$: 234.1 (100%). **Purity** (214 nm): 97%.
HRMS (ESI) calcd for $C_{13}H_{16}NO_3^+$: 234.1125 $[M+H^+]^+$ found: 234.1127.

2-hexynyl-4-methoxyaniline IX.51

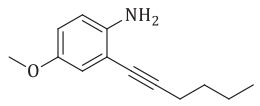

IX.51

To a solution of 2-hexyn-4-methoxy-1-nitrobenzene (**IX.49**, 354.0 mg, 1.518 mmol, 1 eq) in $EtOH_{abs}$ (2.0 mL) in a pressure tube, H_2O (1.0 mL) and HOAc (2.0 mL) are added. This solution is agitated for 5 minutes in order to dissolve the substrate. Then, Fe (424 mg, 7.590 mmol, 5 eq) is poured into the solution. The reaction is heated in an oil bath to 60°C, whereupon H_2 bubbles are visible. After one hour the reaction is completed (monitoring *via* TLC) and the reaction mixture is filtered over a Celite filter. After rinsing the formed Fe-aggregates on the Celite filter with EtOAc (2x 15 mL), the liquid mixture is evaporated. HOAc and H_2O are

removed *via* an azeotropic evaporation with toluene (3x 10 mL). The resulting dark brown viscuous oil is further purified *via* flash chromatography (hexane/acetone: 9/1) affording 2-hexynyl-4-methoxyaniline **IX.51** as a red oil.

Yield: 52%. 2-hexynyl-4-methoxyaniline (**IX.51,** 160.0 mg, 0.7871 mmol).
Red oil.
Molecular weight: 203.28 Da.
R_F: 0.29 (hexane/acetone: 8/2).
^{1}H NMR (300 MHz, acetone-d_6) δ 0.94 (t, J = 7.4Hz, 3H), 1.42-1.63 (m, 4H), 2.46 (t, J = 7.0Hz, 2H), 3.67 (s, 3H), 4.49 (s broad, 2H), 6.64-6.68 (m, 2H), 6.70-6.72 (m, 1H).
^{13}C NMR (75 MHz, acetone-d_6) δ 13.8 (CH_3), 19.6 (CH_2), 22.6 (CH_2), 31.8 (CH_2), 55.7 (CH_3), 78.3 (C), 95.6 (C), 115.9 (CH), 116.5 (CH), 116.9 (CH), 144.2 (C), 152.0 (C).
HATR (cm^{-1}): 3456 (w), 3362 (w), 2955 (m), 2931 (m), 2870 (w), 2832 (w), 1599 (m), 1552 (w), 1498 (s), 1464 (m), 1422 (m), 1378 (w), 1332 (w), 1318 (w), 1279 (m), 1268 (m), 1245 (m), 1200 (m), 1169 (m), 1106 (w), 1038 (m), 869 (w), 850 (w), 813 (m), 770 (w), 741 (w), 685 (w).
LC-(ESI)MS (condition 1): t_R = 21.4 min $[M+H^+]^+$: 204.1. **Purity** (214 nm): 90%.
HRMS (ESI) calcd for $C_{13}H_{18}NO^+$: 204.1383 $[M+H^+]^+$ found: 204.1382.

2-hexyl-5-methoxyaniline IX.52

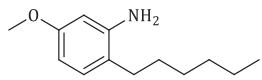

IX.52

To a solution of 2-hexyn-5-methoxy-1-nitrobenzene (**IX.50**, 500.0 mg, 2.143 mmol, 1 eq) in $EtOH_{abs}$ (2.85 mL) in a pressure tube, H_2O (1.45 mL) and HOAc (2.85 mL) are added. This solution is agitated for 5 minutes in order to dissolve the substrate. Then, Fe (600.0 mg, 10.72 mmol, 5 eq) is poured into the solution. The reaction is heated in an oil bath to 60°C, whereupon H_2 bubbles are visible. After 15 minutes the reaction is completed (monitoring *via* TLC) and the reaction mixture is filtered over a Celite filter. After rinsing the formed Fe-aggregates on the Celite filter with EtOAc (2x 15 mL), the liquid mixture is evaporated. HOAc and H_2O are removed *via* an azeotropic evaporation with toluene (3x 10 mL). The resulting dard red viscuous oil is further purified *via* flash chromatography (hexane/acetone: 95/5) affording 2-hexyl-4-methoxyaniline **IX.52** as white crystals.

Yield: 65%. 2-hexyl-5-methoxyaniline (**IX.52**, 289.2 mg, 1.395 mmol).
R_F: 0.20 (hexane/acetone: 9/1).
White crystals.

Molecular weight: 207.31 Da.
^{1}H NMR (300 MHz, acetone-d_6) δ 0.86-0.91 (m, 3H), 1.27-1.38 (m, 4H), 1.60-1.70 (m, 2H), 2.83-2.86 (m, 4H), 3.75 (s, 3H), 6.16 (dd, J = 2.5Hz/8.9Hz, 1H), 6.27 (d, J = 2.5Hz, 1H), 7.07 (s broad, 2H), 7.72 (d, J = 9.0 Hz, 1H).
^{13}C NMR (75 MHz, acetone-d_6) δ 14.3 (CH_3), 23.2 (CH_2), 25.6 (CH_2), 33.3 (CH_2), 39.3 (CH_2), 55.4 (CH_3), 99.7 (CH), 104.4 (CH), 112.8 (C), 134.0 (CH), 154.7 (C), 168.0 (C).
HATR (cm^{-1}): 3459 (w), 3332 (w), 2954 (w), 2925 (w), 2869 (w), 2067 (w), 1616 (s), 1584 (s), 1542 (m), 1505 (w), 1462 (w), 1443 (w), 1372 (w), 1304 (w), 1242 (m), 1223 (m), 1200 (m), 1181 (m), 1158 (m), 1142 (m), 1094 (w), 1029 (w), 974 (w), 946 (w), 828 (w), 787 (w).
LC-(ESI)MS (condition 5): t_R = 6.7 min $[M+H^+]^+$: 208.1. **Purity** (214 nm): 93%.

2-iodo-5-methoxyaniline IX.53

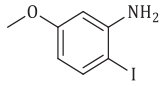

IX.53

To a solution of commercial 2-iodo-5-methoxy-1-nitrobenzene (**IX.48**, 1.000 mg, 3.584 mmol, 1 eq) in $EtOH_{abs}$ (4.8 mL) in a pressure tube, H_2O (2.4 mL) and HOAc (4.8 mL) are added. This solution is agitated for 5 minutes in order to dissolve the substrate. Then, Fe (1.002 mg, 17.92 mmol, 5 eq) is poured into the solution. The reaction is heated in an oil bath to 60°C, whereupon H_2 bubbles are visible. After one hour the reaction is completed (monitoring *via* TLC) and the reaction mixture is filtered over a Celite filter. After rinsing the formed Fe-aggregates on the Celite filter with EtOAc (2x 15 mL), the liquid mixture is evaporated. HOAc and H_2O are removed *via* an azeotropic evaporation with toluene (3x 10 mL). The resulting dark brown solid is further purified *via* flash chromatography (hexane/acetone: 99/1) affording 2-hexynyl-4-methoxyaniline **IX.53** as a light-red oil.

Yield: 63%. 2-iodo-3-methoxyaniline (**IX.53**, 461.1 mg, 1.851 mmol).
Light-red oil.
Molecular Weight: 249.05 Da.
R_F: 0.36 (hexane/acetone: 8/2).
^{1}H NMR (300 MHz, acetone-d_6) δ 3.69 (s, 3H), 4.82 (s broad, 2H), 6.08 (dd, J = 2.8Hz/8.7Hz, 1H), 6.44 (d, J = 2.8Hz, 1H), 7.43 (d, J = 8.7Hz, 1H).
^{13}C NMR (75 MHz, acetone-d_6) δ 55.3 (CH_3), 72.8 (C), 100.6 (CH), 106.4 (CH), 139.7 (CH), 149.8 (C), 162.1 (C).
HATR (cm^{-1}): 3455 (w), 3362 (w), 3199 (w), 2998 (w), 2958 (w), 2935 (w), 2833 (w), 1662 (w), 1608 (s), 1590 (s), 1567 (s), 1484 (s), 1463 (m), 1442 (m), 1427 (m), 1415 (m), 1331

(m), 1295 (s), 1267 (m), 1256 (m), 1207 (s), 1168 (s), 1147 (m), 1084 (w), 1040 (m), 1000 (s), 955 (m), 824 (m), 776 (m), 730 (w), 685 (w), 655 (w), 630 (w).
LC-(ESI)MS (condition 1): t_R = 16.0 min $[M+H^+]^+$: 249.9 (100%). **Purity** (214 nm): 94%.
HRMS (ESI) calcd for $C_7H_9INO^+$: 249.9723 $[M+H^+]^+$ found: 249.9721.

2-hexynyl-5-methoxyaniline IX.54

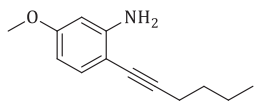

IX.54

Following general procedure **P.06**: 2-iodo-3-methoxyaniline (400.0 mg, 1.606 mmol, 1 eq). 1-hexyne (733 µL, 6.424 mmol, 4 eq). $PdCl_2(PPh_3)_2$ (22.5 mg, 0.03212 mmol, 0.02 eq). CuI (15.3 mg, 0.08031 mmol, 0.05 eq). diethylamine (16 mL).

Yield: 92%. 2-(1-hexynyl)-3-methoxyaniline (**IX.54**, 300.2 mg, 1.477 mmol).
Yellow oil.
Molecular weight: 203.28 Da.
R_F: 0.29 (hexane/acetone: 8/2). 0.16 (hexane/acetone: 9/1). 0.09 (hexane/acetone: 95/5).
^{1}H NMR (300 MHz, acetone-d_6) δ 0.93 (t, J = 7.2Hz, 3H), 1.41-1.61 (m, 4H), 2.43 (t, J = 7.0Hz, 2H), 3.69 (s, 3H), 4.88 (s broad, 2H), 6.14 (dd, J =2.6Hz/8.5Hz, 1H), 6.29 (d, J = 2.6Hz, 1H), 7.03 (d, J = 8.5Hz, 1H).
^{13}C NMR (75 MHz, acetone-d_6) δ 13.9 (CH_3), 19.6 (CH_2), 22.6 (CH_2), 31.9 (CH_2), 55.2 (CH), 78.1 (C), 94.0 (C), 99.5 (CH), 101.8 (C), 103.9 (CH), 133.5 (CH), 151.3 (C), 161.5 (C).
HATR (cm^{-1}): 3474 (w), 3375 (w), 2956 (m), 2931 (m), 2871 (w), 2835 (w), 2035 (w), 1616 (s), 1568 (m), 1505 (s), 1465 (m), 1449 (m), 1378 (w), 1336 (w), 1297 (m), 1265 (m), 1250 (m), 1209 (s), 1169 (m), 1138 (m), 1076 (w), 1031 (m), 960 (w), 932 (w), 830 (m), 795 (m), 745 (w), 635 (w).
LC-(ESI)MS (condition 1): t_R = 18.2 min $[M+H^+]^+$: 204.1 (100%). **Purity** (214 nm): 93%.
HRMS (ESI) calcd for $C_{13}H_{18}NO^+$: 204.1383 $[M+H^+]^+$ found: 204.1383.

I. Combinatorial library synthesis:

(*S*)-6-butyl-8-chloro-3-methyl[1,2,3]triazolo[1,5-*d*][1,4]benzodiazepin-2-one IX.56

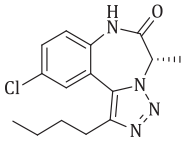

IX.56

Following general procedure **P.01** – **P.05**: (S)-6-butyl-8-chloro-3-methyl[1,2,3]triazolo[1,5-d][1,4]benzodiazepin-2-one (**IX.56**, 92.0 mg, 0.3025 mmol).

Yield: 59%.
White solid.
Molecular weight: 304.11 Da.
R_F: 0.34 (hexane/acetone: 6/4).
^{1}H NMR (700 MHz, acetone-d_6) δ 0.90 (t, J = 7.5Hz, 3H), 1.35-1.40 (m, 2H), 1.66-1.77 (m, 2H), 1.84 (m broad, 3H), 2.86 (t, J = 7.9Hz, 2H), 5.11 (m broad, 1H), 7.43 (d, J = 8.8Hz, 1H), 7.56 (8.8Hz, 1H), 7.65 (d, J = 2.2Hz, 1H), 9.66 (s broad, 1H).
^{13}C NMR (176 MHz, acetone-d_6) δ 14.0 (CH_3), 23.0 (CH_2), 25.5 (CH_2), 32.0 (CH_2), 121.6 (C), 125.0 (CH), 128.8 (CH), 130.5 (C), 130.9 (CH), 135.6 (C), 145.7 (C), 169.0 (C).
HATR (cm^{-1}): 3501(s), 3430(s), 3194(m), 3064(m), 2954(s), 2900(m), 2866(m), 1679(s), 1646(s), 1555(w), 1478(s), 1430(s), 1408(s), 1389(s), 1345(m), 1277(s), 1248(m), 1219(m), 1196(m), 1149(m), 1129(m), 1094(s), 1057(m), 1029(m), 1007(m), 909(w), 874(m), 832(s), 800(s), 769(m), 711(m), 673(w).
LC-(ESI)MS (condition 1): t_R = 16.3 min $[M+H^+]^+$: 305.1 (100%). **Purity** (214 nm): 99%.
HRMS (ESI) calcd for $C_{15}H_{18}ClN_4O^+$: 305.1164 $[M+H^+]^+$ found: 305.1160.

(*S*)-3-benzyl-6-butyl-8-chloro[1,2,3]triazolo[1,5-*d*][1,4]benzodiazepin-2-one IX.57

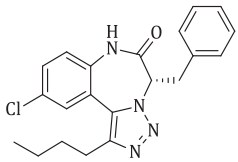

IX.57

Following general procedure **P.01** – **P.05**: (*S*)-3-benzyl-6-butyl-8-chloro[1,2,3]triazolo[1,5-*d*][1,4]benzodiazepin-2-one (**IX.57**, 64.6 mg, 0.1699 mmol).

Yield: 34%.
Light-brown solid.
Molecular weight: 380.14 Da.
R_F: 0.57 (hexane/acetone: 1/1).
^{1}H NMR (300 MHz, acetone-d_6) δ 0.88 (t, J = 7.4Hz, 3H), 1.35 (sextet, J = 7.4Hz, 2H), 1.65-1.75 (m, 2H), 2.84 (t, J = 7.5Hz, 2H), 3.38-3.66 (m broad, 2H), 5.32-5.46 (m broad, 1H), 7.16-7.30 (m broad, 5H), 7.45 (d, J = 8.7Hz, 1H), 7.58 (d, J = 2.5Hz,/8.7Hz, 1H), 7.69 (app d, 1H), 9.69 (s broad, 1H).
^{13}C NMR (75 MHz, acetone-d_6) δ 14.0 (CH_3, A), 14.2 (CH_3, B), 22.9 (CH_2, A+B), 25.5 (CH_2, A+B), 31.8 (CH_2, A+B), 100.4 (C, A+B), 124.9 (CH, A+B), 127.6 (CH, A+B), 128.8 (CH, A), 129.2 (CH, A), 129.3 (CH, B), 129.5 (CH, B), 130.5 (CH, A+B), 130.7 (C), 131.0 (CH, A+B), 167.8 (C, A+B).
HATR (cm^{-1}): 3205 (w), 3088 (w), 2953 (w), 2870 (w), 1685 (s), 1484 (m), 1456 (m), 1436 (m), 1400 (m), 1350 (m), 1357 (m), 1362 (m), 1309 (w), 1277 (w), 1223 (w), 1203 (w), 1107 (w), 1079 (w), 1034 (w), 877 (w), 827 (m), 740 (m), 723 (m), 701 (m), 670 (w).
LC-(ESI)MS (condition 1): t_R = 18.3 min $[M+H^+]^+$: 381.1 (100%). **Purity** (214 nm): 94%.
HRMS (ESI) calcd for $C_{21}H_{22}ClN_4O^+$: 381.1477 $[M+H^+]^+$ found: 381.1476.

(*S*)-3-(tert-Butoxymethyl)-6-butyl-8-chloro[1,2,3]triazolo[1,5-*d*][1,4]benzodiazepin-2-one IX.58

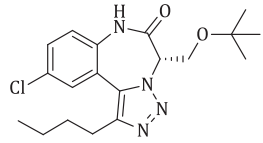

IX.58

Following general procedure **P.01** – **P.05**: (*S*)-3-(tert-Butoxymethyl)-6-butyl-8-chloro[1,2,3]triazolo[1,5-*d*][1,4]benzodiazepin-2-one (**IX.58,** 56.4 mg, 0.1499 mmol).

Yield: 31%.
White solid.
Molecular weight: 376.17 Da.
R_F: 0.19 (hexane/acetone: 8/2).
^{1}H NMR (300 MHz, acetone-d_6) δ 9.69 (s broad, 1H), 7.65 (d, J = 2.5Hz, 1H), 7.54 (dd, J = 2.5Hz/8.7Hz, 1H), 7.40 (d, 8.7Hz, 1H), 5.30-5.61 (m broad, 1H), 3.95-4.08 (m broad, 2H), 2.88 (app t, J = 7.5Hz, 2H), 1.67-1.77 (m, 2H), 1.38 (sextet, J = 7.3Hz, 2H), 1.02 (s, 9H), 0.88-0.92 (t, J = 7.3Hz, 3H).
^{13}C NMR (75 MHz, acetone-d_6) δ 167.6 (C, A+B), 145.9 (C, A+B), 135.3 (C, A+B), 130.8 (CH, A+B), 130.4 (C, A+B), 128.6 (CH, A+B), 124.0 (CH, A+B), 121.2 (C, A+B), 74.3 (CH, A+B), 59.6

(CH_2, broad, A+B), 32.2 (CH_2, B), 31.8 (CH_2, B), 27.3 (CH_3, A+B), 25.7 (CH_2, A+B), 23.2 (CH_2, B), 23.0 (CH_2, A), 14.3 (CH_3, B), 14.0 (CH_3, A).
HATR (cm^{-1}): 3207 (w), 3132 (w), 3085 (w), 2960 (m), 2934 (m), 2861 (m), 1690 (s), 1481 (s), 1466 (s), 1405 (m), 1363 (s), 1342 (m), 1313 (w), 1292 (w), 1275 (m), 1233 (m), 1215 (m), 1178 (m), 1155 (w), 1098 (m), 1077 (s), 1032 (m), 966 (w), 953 (w), 889 (m), 875 (s), 856 (m), 832 (s), 809 (m), 794 (m), 749 (m), 733 (m), 723 (m), 709 (w), 683 (w), 673 (w).
LC-(ESI)MS (condition 1): t_R = 18.5 min $[M+H^+]^+$: 377.1 (100%). **Purity** (214 nm): 99%.
HRMS (ESI) calcd for $C_{19}H_{26}ClN_4O_2^+$: 377.1739 $[M+H^+]^+$ found: 377.1734.

(*S*)-6-butyl-3-(*N*-(tert-butyloxycarbonyl)-indolylmethyl)-8-chloro[1,2,3]triazolo[1,5-*d*][1,4]benzodiazepin-2-one IX.59

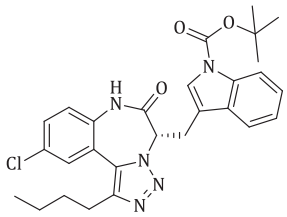

IX.59

Following general procedure **P.01** – **P.05**: (*S*)-6-butyl-3-(*N*-(tert-butyloxycarbonyl)-indolylmethyl)-8-chloro[1,2,3]triazolo[1,5-*d*][1,4]benzodiazepin-2-one (**IX.59,** 106.0 mg, 0.2038 mmol).

Yield: 36%.
White solid.
Molecular weight: 520.02 Da.
R_F: 0.39 (hexane/acetone: 6/4).
^{1}H NMR (700 MHz, acetone-d_6) δ 0.89 (t, J = 7.5Hz, 3H), 1.33-1.39 (m, 2H), 1.64 (s, 9H), 1.68-1.72 (m, 2H), 2.80-2.86 (m, 2H), 3.69 (m broad, 2H), 5.52 (m broad, 1H), 7.17 (t, J = 7.5Hz, 1H), 7.26 (t, J = 7.5Hz, 1H), 7.37-7.83 (m, 5H), 8.04 (app d, J = 7.5Hz, 1H), 9.78 (s broad, 1H).
^{13}C NMR (176 MHz, acetone-d_6) δ 14.0 (CH_3), 22.9 (CH_2), 25.4 (CH_2), 28.2 (CH_3), 31.8 (CH_2), 84.3 (CH), 115.8 (CH), 119.7 (CH), 123.6 (CH), 125.1 (CH), 125.7 (CH), 128.7 (CH), 130.5 (C), 130.9 (CH), 136.0 (C), 150.0 (C), 168.1 (C).
HATR (cm^{-1}): 3210(w), 3123(w), 2956(m), 2930(m), 2870(w), 1731(s), 1687(s), 1608(w), 1479(s), 1452(s), 1369(s), 1308(m), 1256(s), 1228(m), 1156(s), 1087(m), 1031(w), 1017(w), 880(w), 855(w), 826(w), 766(m), 745(m).
LC-(ESI)MS (condition 1): t_R = 20.7 min $[M+H^+]^+$: 520.1 (100%). **Purity** (214 nm): 99%.
HRMS (ESI) calcd for $C_{28}H_{31}ClN_5O_3^+$: 520.2110 $[M+H^+]^+$ found: 520.2113.

(*S*)-6-butyl-3-isobutyl-8-chloro[1,2,3]triazolo[1,5-*d*][1,4]benzodiazepin-2-one IX.60

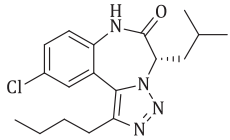

IX.60

Following general procedure **P.01** – **P.05**: (*S*)-6-butyl-3-isobutyl-8-chloro[1,2,3]triazolo[1,5-*d*][1,4]benzodiazepin-2-one (**IX.60**, 121.6 mg, 0.3506 mmol).

Yield: 75%.
White solid.
Molecular weight: 346.85 Da.
R_F: 0.22 (hexane/acetone: 8/2).
^{1}H NMR (300 MHz, acetone-d_6) δ 0.71-0.92 (m, 9H), 1.15-1.95 (m broad, 7H), 2.86 (t, J = 7.7Hz, 2H), 4.50-5.89 (m broad, 1H), 7.43 (d, J = 8.7Hz, 1H), 7.55 (dd, J = 2.5Hz/8.7Hz, 1H), 7.66 (d, J = 2.5Hz, 1H), 9.70 (s broad, 1H).
^{13}C NMR (75 MHz, acetone-d_6) δ 14.0 (CH_3), 22.1 (CH_3), 22.6 (CH_3), 22.9 (CH_2), 25.6 (CH_2), 25.6 (CH), 31.8 (CH_2), 124.6 (CH), 128.6 (CH), 130.4 (C), 130.9 (CH), 168.7 (C).
HATR (cm^{-1}): 3222 (m), 3131 (w), 2956 (m), 2930 (m), 2869 (m), 1681 (s), 1583 (w), 1556 (w), 1478 (s), 1401 (m), 1366 (m), 1304 (m), 1270 (m), 1245 (m), 1218 (m), 1173 (m), 1135 (m), 1100 (m), 1030 (m), 955 (w), 940 (w), 905 (w), 876 (m), 825 (m), 792 (m), 754 (m), 745 (m), 672 (w).
LC-(ESI)MS (condition 1): t_R = 18.6 min $[M+H^+]^+$: 347.1 (100%). **Purity** (214 nm): 98%.
HRMS (ESI) calcd for $C_{18}H_{24}ClN_4O^+$: 347.1633 $[M+H^+]^+$ found: 347.1633.

(*S*)-6-butyl-8-chloro-3-isopropyl[1,2,3]triazolo[1,5-*d*][1,4]benzodiazepin-2-one IX.61

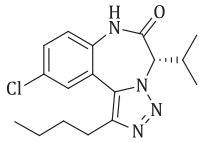

IX.61

Following general procedure **P.01** – **P.05**: (*S*)-6-butyl-8-chloro-3-isopropyl[1,2,3]triazolo[1,5-*d*][1,4]benzodiazepin-2-one (**IX.61**, 101.9 mg, 0.3061 mmol).

Yield: 61%.
White solid.

Molecular weight: 332.83 Da.
R_F: 0.19 (hexane/acetone: 8/2).
^{1}H NMR (300 MHz, acetone-d_6) δ 0.83 (d broad, J = 5.5Hz, 3H), 0.90 (t, J = 7.2Hz, 3H), 1.03 (d broad, J = 6.6Hz, 3H), 1.32-1.44 (m, 2H), 1.65-1.81 (m, 2H), 1.91 (m broad, 1H), 2.90 (app t, J = 7.9Hz, 2H), 5.02 (app d, J = 11.5Hz, 1H), 7.42 (d, 8.7Hz, 1H), 7.53 (dd, J = 2.3Hz/8.7Hz, 1H), 7.66 (d, J = 2.3Hz, 1H), 9.74 (s broad, 1H),
^{13}C NMR (75 MHz, acetone-d_6) δ 14.0(CH), 19.0 (CH_3), 19.1 (CH_3), 23.0 (CH_2), 25.7 (CH_2), 28.1 (CH), 31.7 (CH_2), 73.5 (CH), 120.5 (C), 124.3 (CH), 128.4 (CH), 130.4 (C), 130.9 (CH), 134.6 (C), 146.5 (C), 168.2 (C).
HATR (cm^{-1}): 3204 (w), 3124 (w), 2954 (m), 2896 (m), 2870 (m), 1686 (s), 1582 (w), 1550 (w), 1485 (s), 1473 (m), 1461 (m), 1429 (w), 1401 (m), 1380 (m), 1351 (m), 1310 (m), 1269 (w), 1247 (w), 1221 (m), 1167 (w), 1146 (w), 1118 (w), 1104 (w), 1083 (w), 1033 (m), 971 (w), 952 (w), 925 (w), 883 (m), 849 (m), 821 (s), 749 (w), 729 (m), 696 (w), 670 (m).
LC-(ESI)MS (condition 1): t_R = 17.9 min $[M+H^+]^+$: 331.1 (100%). **Purity** (214 nm): 97%.
HRMS (ESI) calcd for $C_{17}H_{22}ClN_4O^+$: 333.1477 $[M+H^+]^+$ found: 331.1477.

(*S*)-6-butyl-3-(*N*-(tert-butyloxycarbonyl)-aminobutyl)-8-chloro[1,2,3]triazolo[1,5-*d*][1,4]benzodiazepin-2-one IX.62

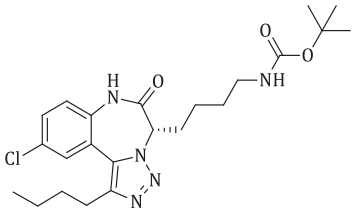

IX.62

Following general procedure **P.01** – **P.05**: (*S*)-6-butyl-3-(*N*-(tert-butyloxycarbonyl)-aminobutyl)-8-chloro[1,2,3]triazolo[1,5-*d*][1,4]benzodiazepin-2-one (**IX.62**, 135.5 mg, 0.2932 mmol).

Yield: 58%.
White solid.
Molecular weight: 461.22 Da.
R_F: 0.10 (hexane/acetone: 8/2).
^{1}H NMR (300 MHz, acetone-d_6) δ 7.66 (s broad, 1H), 7.65 (d, J = 2.5Hz, 1H), 7.55 (dd, J = 2.5Hz/8.7Hz, 1H), 7.41 (d, J = 8.7Hz, 1H), 5.89 (s broad, 1H), 5.15 (s broad, 1H), 2.95-3.05 (m, 2H), 2.86 (app t, J = 7.5Hz, 2H), 1.8-2.5 (m broad, 2H), 1.66-1.77 (m, 2H), 1.31-1.56 (m, 15H).
^{13}C NMR (75 MHz, acetone-d_6) δ 168.5 (C), 156.6 (C), 130.9 (CH), 130.5 (C), 128.7 (CH), 124.7 (CH), 78.3 (CH), 40.5 (CH_2), 31.8 (CH_2), 28.6 (CH_3), 25.6 (CH_2), 23.7 (CH_2), 23.0 (CH_2), 14.0 (CH_3).

HATR (cm^{-1}): 3353 (m), 3208 (w), 3130 (w), 2957 (m), 2933 (m), 2867 (m), 1687 (s), 1521 (s), 1480 (s), 1464 (m), 1402 (m), 1389 (m), 1364 (s), 1283 (m), 1282 (m), 1247 (m), 1229 (m), 1170 (m), 1128 (m), 1101 (m), 1081 (w), 1048 (w), 1035 (m), 1022 (m), 1002 (m), 952 (w), 935 (w), 921 (w), 872 (m), 824 (s), 806 (m), 782 (m), 762 (m), 725 (m), 706 (w), 673 (w).
LC-(ESI)MS (condition 1): t_R = 18.0, M+ H^+ - Boc: 362.1 (100%). **Purity** (214 nm): 99%.
HRMS (ESI) calcd for $C_{23}H_{33}N_5O_3^+$: 462.2266 $[M+H^+]^+$ found: 462.2264.

(*S*)-6-butyl-8-bromo-3-methyl[1,2,3]triazolo[1,5-*d*][1,4]benzodiazepin-2-one IX.63

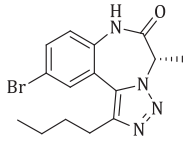

IX.63

Following general procedure **P.01** – **P.05**: (*S*)-6-butyl-8-bromo-3-methyl[1,2,3]triazolo[1,5-*d*][1,4]benzodiazepin-2-one (**IX.63,** 123.8 mg, 0.3545 mmol).

Yield: 69%.
Light-brown solid.
Molecular weight: 349.22 Da.
R_F: 0.34 (hexane/acetone: 6/4).
^{1}H NMR (300 MHz, acetone-d_6) δ 0.92 (t, J = 7.3Hz, 3H), 1.39 (sextet, J = 7.5Hz, 2H), 1.68-1.76 (m, 2H), 1.85 (app d broad, 3H), 2.87 (t, J = 7.5Hz, 3H), 5.13 (s broad, 1H), 7.38 (d, J = 8.7Hz, 1H), 7.71 (dd, J = 2.5/8.7Hz, 1H), 7.80 (d, J = 2.5Hz, 1H), 9.64 (s broad, 1H).
^{13}C NMR (75 MHz, acetone-d_6) δ 12.7 (CH_3, weak), 14.0 (CH_3), 23.0 (CH_2), 25.5 (CH_2), 31.9 (CH_2), 118.0 (C), 125.2 (CH), 131.8 (CH), 133.8 (CH), 134.9 (C), 168.9 (C).
HATR (cm^{-1}): 3209(w), 3125(w), 3102(w), 2955(m), 2940(m), 2871(w), 1691(s), 1476(s), 1432(w), 1399(w), 1384(m), 1367(w), 1348(w), 1296(w), 1277(m), 1258(w), 1246(w), 1216(m), 1188(m), 1142(w), 1130(w), 1085(m), 1057(w), 1029(w), 1009(w), 954(w), 906(w), 878(m), 818(s), 777(m), 753(m), 728(m), 700(m), 690(m), 667(s).
LC-(ESI)MS (condition 1): t_R = 16.5 min $[M+H^+]^+$: 349.1 (100%). **Purity** (214 nm): 99%.
HRMS (ESI) calcd for $C_{15}H_{18}BrN_4O^+$: 349.0656 $[M+H^+]^+$ found: 349.0656.

(*S*)-3-benzyl-6-butyl-8-bromo[1,2,3]triazolo[1,5-*d*][1,4]benzodiazepin-2-one IX.64

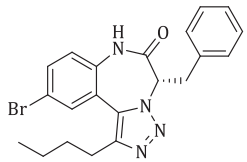

IX.64

Following general procedure **P.01** – **P.05**: (*S*)-3-benzyl-6-butyl-8-bromo[1,2,3]triazolo[1,5-*d*][1,4]benzodiazepin-2-one (**IX.64**, 70.3 mg, 0.1653 mmol).

Yield: 33%.
White solid.
Molecular weight: 425.32 Da.
R_F: 0.19 (hexane/acetone: 8/2).
^{1}H NMR (300 MHz, acetone-d_6) δ 0.90 (t, J = 7.4Hz, 3H), 1.30-1.42 (m, 2H), 1.64-1.74 (m, 2H), 2.85 (t, J = 7.4Hz, 2H), 3.51 (app s broad, 2H), 5.40 (app s broad, 1H), 7.13-7.33 (m, 5H), 7.37 (d, 8.7Hz, 1H), 7.71 (dd, J = 2.3Hz/8.7Hz, 1H), 7.82 (app d broad, J = 1.9Hz, 1H), 9.69 (s broad, 1H).
^{13}C NMR (75 MHz, acetone-d_6) δ 14.0 (CH_3), 22.9 (CH_2), 25.5 (CH_2), 31.8 (CH_2), 118.2 (C), 125.1 (CH), 127.7 (CH), 129.2 (CH), 130.3 (CH), 131.7 (CH), 134.0 (CH), 147.8 (C), 167.8 (C).
HATR (cm^{-1}): 3203 (w), 3134 (w), 3082 (w), 2951 (m), 2925 (m), 2856 (m), 1685 (s), 1479 (m), 1454 (m), 1397 (m), 1360 (m), 1355 (m), 1311 (w), 1274 (w), 1223 (w), 1200 (w), 1138 (w), 1082 (w), 1030 (w), 881 (w), 827 (m), 737 (m), 701 (m), 667 (w).
LC-(ESI)MS (condition 1): t_R = 18.5 min $[M+H^+]^+$: 425.1 (100%). **Purity** (214 nm): 98%.
HRMS (ESI) calcd for $C_{21}H_{22}BrN_4O^+$: 425.0972 $[M+H^+]^+$ found: 425.0969.

(*S*)-8-bromo-3-(tert-Butoxymethyl)-6-butyl[1,2,3]triazolo[1,5-*d*][1,4]benzodiazepin-2-one IX.65

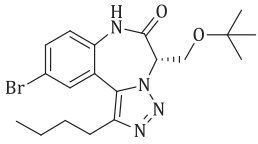

IX.65

Following general procedure **P.01** – **P.05**: (*S*)-8-bromo-3-(tert-Butoxymethyl)-6-butyl[1,2,3]triazolo[1,5-*d*][1,4]benzodiazepin-2-one (**IX.65**, 66.7 mg, 0.1583 mmol).

Yield: 29%.
White solid.
Molecular weight: 421.33 Da.
R_F: 0.23 (hexane/acetone: 8/2).
^{1}H NMR (700 MHz, acetone-d_6) δ 0.91 (t, J = 7.5Hz, 3H), 1.02 (s, 9H), 1.38 (sextet, J = 7.5Hz, 2H), 1.72 (quintet, J = 7.5Hz, 2H), 2.86 (t, J = 7.5Hz, 2H), 3.95 (app s broad, 2H), 5.31 (s broad, 1H), 7.34 (d, J = 8.8Hz, 1H), 7.67 (dd, J = 2.2Hz/8.8Hz, 1H), 7.79 (d, J = 2.2Hz, 1H), 9.69 (s broad, 1H).
^{13}C NMR (176 MHz, acetone-d_6) δ 14.0 (CH_3), 23.0 (CH_2), 25.7 (CH_2), 27.3 (CH_3), 31.8 (CH_2), 58.6 (CH_2, weak), 74.3 (CH), 117.8 (C), 121.5 (C), 124.9 (CH), 131.6 (CH), 133.7 (CH), 135.7 (C), 146.0 (C), 167.6 (C).
HATR (cm^{-1}): 3204 (m), 3128 (m), 3083 (w), 2959 (m), 2931 (m), 2856 (m), 1691 (s), 1479 (s), 1466 (m), 1435 (w), 1404 (m), 1363 (s), 1342 (m), 1312 (w), 1292 (w), 1275 (w), 1234 (m), 1191 (m), 1155 (w), 1123 (w), 1077 (s), 1029 (m), 966 (w), 886 (m), 876 (m), 855 (m), 831 (m), 808 (m), 790 (w), 758 (w), 745 (w), 732 (w), 713 (w), 706 (w), 682 (w), 668 (w).
LC-(ESI)MS (condition 1): t_R = 18.7 min $[M+H^+]^+$: 421.1 (100%). **Purity** (214 nm): 99%.
HRMS (ESI) calcd for $C_{19}H_{26}BrN_4O_2^+$: 421.1234 $[M+H^+]^+$ found: 421.1232.

(*S*)-8-bromo-6-butyl-3-(*N*-(tert-butyloxycarbonyl)-indolylmethyl)[1,2,3]triazolo[1,5-*d*][1,4]benzodiazepin-2-one IX.66

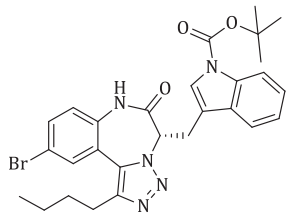

IX.66

Following general procedure **P.01** – **P.05**: (*S*)-8-bromo-6-butyl-3-(*N*-(tert-butyloxycarbonyl)-indolylmethyl)[1,2,3]triazolo[1,5-*d*][1,4]benzodiazepin-2-one (**IX.66,** 128.3 mg, 0.2273 mmol).

Yield: 45%.
White solid.
Molecular weight: 564.47 Da.
R_F: 0.41 (hexane/acetone: 6/4).
^{1}H NMR (300 MHz, acetone-d_6) δ 0.90 (t, J = 7.4Hz, 3H), 1.31-1.43 (m, 2H), 1.67-1.75 (m, 2H), 2.78-2.85 (m, 2H), 3.65 (app s broad, 2H), 5.53 (app s broad, 1H), 7.18 (app td, J =

1.0Hz/7.7Hz, 1H), 7.25-7.34 (m, 2H), 7.40-7.58 (m, 2H), 7.64-7.70 (m, 2H), 8.05 (d, *J* = 8.3Hz, 1H), 9.72 (s broad, 1H).
^{13}C NMR (75 MHz, acetone-d_6) δ 14.0 (CH_3), 22.9 (CH_2), 25.6 (CH_2), 28.2 (CH_3), 31.9 (CH_2), 84.4 (CH_2), 115.8 (CH), 118.0 (C), 119.7 (CH), 123.3 (C), 125.0 (CH), 125.2 (CH), 125.8 (CH), 131.0 (C), 131.6 (CH), 133.9 (CH), 136.0 (C), 168.0 (C).
HATR (cm^{-1}): 3205 (w), 3114 (w), 2955 (m), 2929 (m), 2870 (w), 1730 (s), 1685 (s), 1608 (w), 1476 (s), 1452 (s), 1368 (s), 1308 (m), 1270 (m), 1255 (s), 1227 (m), 1155 (s), 1085 (s), 1017 (m), 879 (w), 855 (w), 824 (m), 765 (m), 744 (s), 702 (w), 667 (w).
LC-(ESI)MS (condition 1): t_R = 20.8 min $[M+H^+]^+$: 564.1 (100%). **Purity** (214 nm): 96%.
LC-(ESI)MS (condition 2): t_R = 11.8 min $[M+H^+]^+$: 564.1 (100%). **Purity** (214 nm): 96%.
HRMS (ESI) calcd for $C_{28}H_{31}BrN_5O_3^+$: 564.1605 $[M+H^+]^+$ found: 564.1604.

(*S*)-8-bromo-6-butyl-3-isobutyl[1,2,3]triazolo[1,5-*d*][1,4]benzodiazepin-2-one IX.67

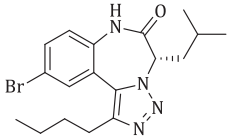

IX.67

Following general procedure **P.01** – **P.05**: (*S*)-8-bromo-6-butyl-3-isobutyl[1,2,3]triazolo[1,5-*d*][1,4]benzodiazepin-2-one (**IX.67,** 144.7 mg, 0.3700 mmol).

Yield: 74%.
Light-brown solid.
Molecular weight: 391.11 Da.
R_F: 0.22 (hexane/acetone: 8/2).
^{1}H NMR (300 MHz, acetone-d_6) δ 0.74-0.94 (m, 9H), 1.01-2.02 (m broad, 7H), 2.87 (t, *J* = 7.7Hz, 2H), 5.08-5.72 (m broad, 1H), 7.36 (d, *J* = 8.7Hz, 1H), 7.70 (dd, *J* = 2.3Hz/8.7Hz, 1H), 7.80 (d, *J* = 2.3Hz, 1H), 9.68 (s broad, 1H).
^{13}C NMR (75 MHz, acetone-d_6) δ 14.0 (CH_3), 22.1 (CH_3), 22.6 (CH_3), 25.6 (CH_2), 23.0 (CH_2), 25.7 (CH), 31.8 (CH_2), 118.0 (C), 124.9 (CH), 131.6 (CH), 133.9 (CH).
HATR (cm^{-1}): 3211 (w), 3121 (w), 2955 (m), 2929 (m), 2869 (m), 1682 (s), 1580 (w), 1477 (m), 1394 (m), 1367 (m), 1300 (m), 1272 (m), 1221 (m), 1170 (w), 1138 (w), 1113 (w), 1090 (w), 1075 (w), 1029 (w), 880 (m), 823 (m), 735 (m), 667 (w).
LC-(ESI)MS (condition 1): t_R = 18.9 min $[M+H^+]^+$: 391.1 (100%). **Purity** (214 nm): 99%.
HRMS (ESI) calcd for $C_{18}H_{24}BrN_4O^+$: 391.1128 $[M+H^+]^+$ found: 391.1127.

(*S*)-8-bromo-6-butyl-3-isopropyl[1,2,3]triazolo[1,5-*d*][1,4]benzodiazepin-2-one IX.68

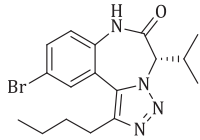

IX.68

Following general procedure **P.01 – P.05**: (*S*)-8-bromo-6-butyl-3-isopropyl[1,2,3]triazolo[1,5-*d*][1,4]benzodiazepin-2-one (**IX.68,** 101.2 mg, 0.2682 mmol).

Yield: 53%.
Light-yellow solid.
Molecular weight: 377.28 Da.
R_F: 0.23 (hexane/acetone: 8/2). 0.53 (hexane/acetone: 6/4).
^{1}H NMR (300 MHz, acetone-d_6) δ 0.51 (d broad, 3H), 0.78 (t, J = 7.5Hz, 3H), 0.91 (d, J = 6.6Hz, 3H), 1.33-1.20 (m, 2H), 1.69-1.51 (m, 2H), 1.79 (m broad, 1H), 2.77 (t, J = 7.7Hz, 2H), 4.89 (app d broad, J = 11.5Hz, 1H), 7.24 (d, J = 8.7Hz, 1H), 7.55 (dd, J = 2.3Hz/8.7Hz, 1H), 7.68 (d, J = 2.3Hz, 1H), 9.58 (s broad, 1H).
^{13}C NMR (75 MHz, acetone-d_6) δ 14.0 (CH_3). 19.0 (CH_3), 19.1 (CH_3), 23.0 (CH_2), 25.7 (CH_2), 28.1 (CH), 31.8 (CH_2), 73.5 (CH), 117.9 (C), 120.8 (C), 124.5 (CH), 131.4 (CH), 133.9 (CH), 135.0 (C), 146.6 (C), 168.2 (C).
HATR (cm^{-1}): 3213 (w), 3125 (w), 3084 (w), 2958 (m), 2930 (m), 2871 (m), 1685 (s), 1577 (w), 1479 (s), 1396 (m), 1380 (m), 1349 (m), 1267 (w), 1222 (m), 1167 (w), 1115 (w), 1079 (w), 1028 (w), 923 (w), 872 (m), 847 (m), 823 (m), 708 (m), 694 (w), 667 (w).
LC-(ESI)MS (condition 1): t_R = 18.0 min $[M+H^+]^+$: 377.1 (100%). **Purity** (214 nm): 99%.
HRMS (ESI) calcd for $C_{17}H_{22}BrN_4O^+$: 377.0972 $[M+H^+]^+$ found: 377.0966.

(*S*)-8-bromo-6-butyl-3-(*N*-(tert-butyloxycarbonyl)-aminobutyl)[1,2,3]triazolo[1,5-*d*][1,4]benzodiazepin-2-one IX.69

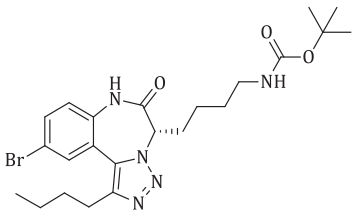

IX.69

Following general procedure **P.01** – **P.05**: (*S*)-8-bromo-6-butyl-3-(*N*-(tert-butyloxycarbonyl)-aminobutyl)[1,2,3]triazolo[1,5-*d*][1,4]benzodiazepin-2-one (**IX.69,** 161.3 mg, 0.3185 mmol).

Yield: 63%.
White solid.
Molecular weight: 506.44 Da.
R_F: 0.10 (hexane/acetone: 8/2).
^{1}H NMR (500 MHz, acetone-d_6) δ 0.90 (t, J = 7.4Hz, 3H), 1.22-1.55 (m, 15H), 1.68-1.74 (m, 2H), 2.84-2.86 (m, 2H), 2.94-3.06 (m broad, 2H), 4.83-5.54 (m broad, 1H), 5.90 (s broad, 1H), 7.35 (d, J = 8.7Hz, 1H), 7.68 (dd, J = 2.4Hz/8.7Hz, 1H), 7.79 (d, J = 2.4Hz, 1H), 9.70 (s broad, 1H).
^{13}C NMR (125 MHz, acetone-d_6) δ 14.1 (CH_3), 23.0 (CH_2), 25.6 (CH_2), 28.6 (CH_3), +/- 29.8 (CH_2), 29.8 (CH_2), 31.9 (CH_2), 40.6 (CH_2), 78.4 (CH_2, weak), 118.0 (C), 125.0 (CH), 131.7 (CH), 133.9 (CH), 156.7 (C), 168.6 (C).
HATR (cm^{-1}): 3362 (w), 3213 (w), 3150 (w), 2950 (m), 2930 (m), 2869 (m), 1690 (s), 1517 (m), 1478 (m), 1393 (m), 1364 (m), 1271 (m), 1250 (m), 1169 (m), 1086 (w), 1029 (w), 869 (w), 823 (w), 780 (w), 735 (w), 668 (w).
LC-(ESI)MS (condition 1): t_R = 18.3 min [M+ H^+-Boc]$^+$: 406.1 (100%). **Purity** (214 nm): 99%.
LC-(ESI)MS (condition 2): t_R = 8.5 min [M+H^+-Boc]$^+$: 406.1 (100%). **Purity** (214 nm): 99%.
HRMS (ESI) calcd for $C_{23}H_{33}BrN_5O_3^+$: 506.1761 [M+H^+]$^+$ found: 506.1762.

(*S*)-8-chloro-6-(2-hydroxyethyl)-3-methyl[1,2,3]triazolo[1,5-*d*][1,4]benzodiazepin-2-one IX.70

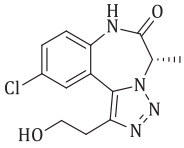

IX.70

Following general procedure **P.01** – **P.05**: (*S*)-8-chloro-6-(2-hydroxyethyl)-3-methyl[1,2,3]triazolo[1,5-*d*][1,4]benzodiazepin-2-one (**IX.70,** 92.5 mg, 0.3160 mmol).

Yield: 62%.
Light-brown solid.
Molecular weight: 292.72 Da.
R_F: 0.16 (hexane/acetone: 6/4).
^{1}H NMR (500 MHz, acetone-d_6) δ 1.94 (s broad, 3H), 3.00 (t, J = 6.3Hz, 2H), 3.96 (m, 2H), 4.04-(t, J = 5.2Hz, 1H), 5.09 (s broad, 1H), 7.40 (d, J = 8.7Hz, 1H), 7.55 (dd, J = 2.5Hz/8.7Hz, 1H), 8.04 (d, J = 2.5Hz, 1H), 9.64 (s broad, 1H).
^{13}C NMR (125 MHz, acetone-d_6) δ 29.5 (CH_2), 62.0 (CH_2, m), 62.1 (CH_2, M), 85.1 (CH, weak), 121.5 (C), 124.9 (CH), 129.4 (CH), 130.6 (C), 131.0 (CH), 135.6 (C), 143.7 (C), 168.9 (C).

HATR (cm^{-1}): 3427 (m broad), 3213 (m), 3198 (m), 2926 (m), 1694 (s), 1480 (s), 1446 (m), 1395 (m), 1383 (m), 1363 (m), 1273 (m), 1218 (m), 1186 (m), 1120 (m), 1099 (m), 1054 (m), 953 (w), 910 (w), 818 (m), 771 (w), 734 (w), 695 (w).
LC-(ESI)MS (condition 1): t_R = 11.8 min $[M+H^+]^+$: 293.1 (100%). **Purity** (214 nm): 97%.
HRMS (ESI) calcd for $C_{13}H_{14}ClN_4O_2^+$: 293.0800 $[M+H^+]^+$ found: 293.0795.

(*S*)-3-benzyl-8-chloro-6-(2-hydroxyethyl)[1,2,3]triazolo[1,5-*d*][1,4]benzodiazepin-2-one IX.71

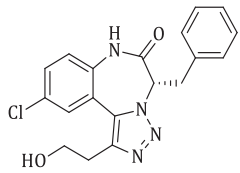

IX.71

Following general procedure **P.01** – **P.05**: (*S*)-3-benzyl-8-chloro-6-(2-hydroxyethyl)[1,2,3]triazolo[1,5-*d*][1,4]benzodiazepin-2-one (**IX.71**, 76.5 mg, 0.1669 mmol).

Yield: 51%.
White solid.
Molecular weight: 368.82 Da.
R_F: 0.10 (hexane/acetone: 7/3).
^{1}H NMR (300 MHz, acetone-d_6) δ 3.00 (t, J = 6.2H, 2H), 3.31-4.08 (m broad, 5H), 5.15-5.70 (m broad, 1H), 7.13-7.44 (m, 6H), 7.57 (dd, J = 2.5Hz/8.7Hz, 1H), 8.07 (s broad, 1H), 9.70 (s broad, 1H).
^{13}C NMR (75 MHz, acetone-d_6) δ 29.5 (CH_2), 61.8 (CH_2, m), 61.9 (CH_2), 119.0 (C), 124.8 (CH), 127.6 (CH), 129.2 (CH), 129.4 (CH), 130.3 (CH), 130.7 (C), 131.1 (CH), 135.4 (C), 167.7 (C).
HATR (cm^{-1}): 3387 (w), 3203 (m), 3084 (m), 2928 (m), 1682 (s), 1604 (w), 1584 (w), 1479 (s), 1454 (m), 1396 (m), 1366 (m), 1314 (m), 1266 (m), 1224 (m), 1173 (w), 1134 (w), 1095 (w), 1045 (m), 953 (w), 880 (m), 821 (m), 735 (m), 698 (m), 671 (w).
LC-(ESI)MS (condition 1): t_R = 14.3 min $[M+H^+]^+$: 369.1 (100%). **Purity** (214 nm): 94%.
HRMS (ESI) calcd for $C_{19}H_{18}ClN_4O_2^+$: 365.1375 $[M+H^+]^+$ found: 369.1115.

(*S*)-8-bromo-3-(tert-Butoxymethyl)-6-(2-hydroxyethyl)[1,2,3]triazolo[1,5-*d*][1,4]-benzodiazepin-2-one IX.72

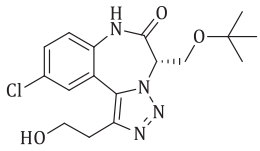

IX.72

Following general procedure **P.01** – **P.05**: (*S*)-8-bromo-3-(tert-Butoxymethyl)-6-(2-hydroxyethyl)[1,2,3]triazolo[1,5-*d*][1,4]benzodiazepin-2-one (**IX.72**, 59.7 mg, 0.1636 mmol).

Yield: 34%.
White solid.
Molecular weight: 364.83 Da.
R_F: 0.13 (hexane/acetone: 7/3).
^{1}H NMR (700 MHz, acetone-d_6) δ 1.03 (s broad, 9H), 3.03 (m, 2H), 3.82-4.25 (m, 5H), 4.91-5.85 (m broad, 1H), 7.39 (d, J = 8.4Hz, 1H), 7.53 (dd, J = 2.2Hz/8.4Hz, 1H), 8.03 (d, J= 2.2Hz, 1H), 9.70 (s broad, 1H).
^{13}C NMR (175 MHz, acetone-d_6) δ23.2 (C), 27.3 (CH_3), 29.5 (CH_2), 61.9 (CH_2), 74.3 (CH_2), 121.0 (C), 124.6 (CH, weak), 129.2 (CH), 130.4 (C), 130.9 (CH), 135.3 (C), 143.9 (C), 167.5 (C).
HATR (cm^{-1}): 3412(w), 3221(w), 2971(m), 2931(m), 2876(w), 1689(s), 1480(m), 1403(m), 1364(m), 1271(w), 1231(m), 1191(m), 1094(m), 1052(m), 892(w), 826(w), 720(w).
LC-(ESI)MS (condition 1): t_R = 14.0 min $[M+H^+]^+$: 365.1 (100%). **Purity** (214 nm): 93%.
HRMS (ESI) calcd for $C_{17}H_{22}ClN_4O_3^+$: 365.1375 $[M+H^+]^+$ found: 365.1374.

(*S*)-3-(*N*-(tert-butyloxycarbonyl)-indolylmethyl)-8-chloro-6-(2-hydroxyethyl)[1,2,3] triazolo[1,5-*d*][1,4]benzodiazepin-2-one IX.73

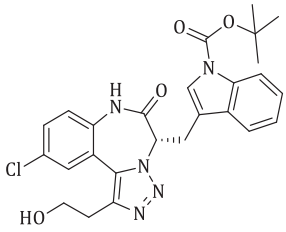

IX.73

Following general procedure **P.01** – **P.05**: (*S*)-8-bromo-6-butyl-3-(*N*-(tert-butyloxycarbonyl)-indolylmethyl)[1,2,3]triazolo[1,5-*d*][1,4]benzodiazepin-2-one (**IX.73,** 112.2 mg, 0.2209 mmol)

Yield: 43%.
White solid.
Molecular weight: 507.97 Da.
R_F: 0.27 (hexane/acetone: 6/4).
^{1}H NMR (500 MHz, acetone-d_6) δ 1.64 (s, 9H), 3.00 (t, J = 6.3Hz, 2H), 3.13-4.40 (m broad, 2H), 3.93-3.97 (m, 2H), 4.02 (t, J = 5.0Hz, 1H), 5.11-5.87 (m broad, 1H), 7.18 (t, J = 7.1Hz, 1H), 7.27 (t, J = 8.2Hz, 1H), 7.37 (d, J = 8.7Hz, 1H), 7.41-7.93 (m broad, 2H), 7,52 (dd, J = 2.4Hz/8.7Hz, 1H), 7.98 (d, J = 2.4Hz, 1H), 8.05 (d, J = 8.2Hz, 1H), 9.75 (s broad, 1H).
^{13}C NMR (125 MHz, acetone-d_6) δ 23.2 (C), 28.2 (CH_3), 61.8 (CH_2, weak), 61.9 (CH_2), 84.4 (CH_2), 115.2 (C), 115.8 (CH), 119.8 (CH, broad), 123.3 (CH), 124.7 (CH, broad), 126.2 (CH), 125.8 (CH, weak), 129.3 (CH, weak), 130.4 (C), 131.0 (CH), 136.0 (C), 150.1 (C), 167.9 (C).
HATR (cm^{-1}): 3422 (m broad), 3213 (m), 3124 (m), 2970 (m), 2929 (m), 1727 (s), 1684 (s), 1608 (w), 1580 (w), 1535 (w), 1478 (m), 1451 (s), 1368 (s), 1308 (m), 1254 (s), 1227 (m), 1154 (s), 1085 (s), 1050 (m), 1017 (m), 936 (w), 906 (w), 881 (w), 854 (m), 826 (m), 765 (m), 735 (s), 702 (m), 672 (w).
LC-(ESI)MS (condition 1): t_R = 17.3 min $[M+H^+]^+$: 508.2 (100%). **Purity** (214 nm): 94%.
HRMS (ESI) calcd for $C_{26}H_{27}ClN_5O_4^+$: 508.1746 $[M+H^+]^+$ found: 508.1749.

(*S*)-3-isobutyl-8-chloro-6-(2-hydroxyethyl)[1,2,3]triazolo[1,5-*d*][1,4]benzodiazepin-2-one IX.74

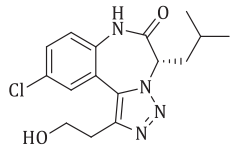

IX.74

Following general procedure **P.01** – **P.05**: (*S*)-3-isobutyl-8-chloro-6-(2-hydroxyethyl)[1,2,3]triazolo[1,5-*d*][1,4]benzodiazepin-2-one (**IX.74,** 131.5 mg, 0.3928 mmol).

Yield: 70%.
White solid.
Molecular weight: 334.80 Da.
R_F: 0.27 (hexane/acetone: 6/4).
^{1}H NMR (500 MHz, acetone-d_6) δ 0.71-0.95 (m, 6H), 2.20-3.15 (m, 4H), 3.97 (t, J = 6.3Hz, 2H), 4.15 (s broad, 1H), 4.73-5.72 (m, 1H), 7.41 (d, J = 8.7Hz, 1H), 7.53 (dd, J = 2.5Hz/8.7Hz, 1H), 8.03 (app d, J = 2.2Hz, 1H), 9.79 (s broad, 1H).

^{13}C NMR (125 MHz, acetone-d_6) δ 22.5 (CH_3, broad), 25.6 (CH_3, broad), 29.4 (CH_2), 41.9 (CH_2, weak), 55.4 (CH_2, weak), 61.9 (CH_2), 65.6 (CH, weak), 124.4 (CH, weak), 129.1 (CH, broad), 130.5 (C), 131.0 (CH).
HATR (cm^{-1}): 3382 (m broad), 3212 (w), 3125 (w), 2956 (m), 2901 (m), 2870(m), 1684 (s), 1602 (w), 1585 (w), 1540 (w), 1479 (s), 1396 (s), 1367 (m), 1300 (m), 1264 (m), 1221 (m), 1169 (m), 1137 (m), 1101 (m), 1047 (m), 956 (w), 880 (m), 858 (m), 823 (m), 733 (m), 701 (m), 671 (w).
LC-(ESI)MS (condition 1): t_R = 14.1 min $[M+H^+]^+$: 335.1 (100%). **Purity** (214 nm): 99%.
HRMS (ESI) calcd for $C_{16}H_{20}ClN_4O_2^+$: 335.1263 $[M+H^+]^+$ found: 335.1266.

(*S*)-8-chloro-6-(2-hydroxyethyl)-3-isopropyl[1,2,3]triazolo[1,5-*d*][1,4]benzodiazepin-2-one IX.75

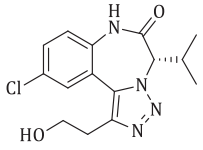

IX.75

Following general procedure **P.01** – **P.05**: (*S*)-8-chloro-6-(2-hydroxyethyl)-3-isopropyl[1,2,3]triazolo[1,5-*d*][1,4]benzodiazepin-2-one (**IX.75,** 92.9 mg, 0.2896 mmol).

Yield: 51%.
White solid.
Molecular weight: 320.77 Da.
R_F: 0.24 (hexane/acetone: 6/4).
^{1}H NMR (700 MHz, acetone-d_6) δ 0.62 (s broad, 3H), 1.03 (d, J = 5.7Hz, 3H), 1.90 (s broad, 1H), 2.91-2.97 (m, 2H), 3.99 (m, 2H), 4.14 (t, J = 4.8Hz, 1H), 5.05 (app d, J = 9.7Hz, 1H), 7.41 (d, J = 8.8Hz, 1H), 7.53 (dd, J = 2.2Hz/8.8Hz, 1H), 8.05 (d, J = 2.2Hz, 1H), 9.82 (s broad, 1H).
^{13}C NMR (176 MHz, acetone-d_6) δ 18.9 (CH_3), 19.1 (CH_3), 28.1 (CH), 29.5 (CH_2), 61.7 (CH_2,B), 61.8 (CH_2,A), 73.5 (CH), 120.2 (C), 124.2 (CH), 128.9 (CH), 129.8 (C), 130.4 (C), 131.0 (CH), 134.0 (C), 144.5 (C), 168.2 (C).
HATR (cm^{-1}): 3387 (m broad), 3223 (w), 2963 (m), 2890 (m), 2821 (m), 1681 (s), 1482 (m), 1398 (m), 1372 (m), 1269 (w), 1222 (m), 1168 (w), 1102 (m), 1050 (m), 958 (w), 920 (m), 877 (m), 830 (m), 736 (m), 700 (w), 672 (w).
LC-(ESI)MS (condition 1): t_R = 13.1 min $[M+H^+]^+$: 321.1 (100%). **Purity** (214 nm): 97%.
HRMS (ESI) calcd for $C_{15}H_{18}ClN_4O_2^+$: 321.1113 $[M+H^+]^+$ found: 321.1110.

(*S*)-3-(*N*-(tert-butyloxycarbonyl)-aminobutyl)-8-chloro-6-(2-hydroxyethyl)[1,2,3] triazolo[1,5-*d*][1,4]benzodiazepin-2-one IX.76

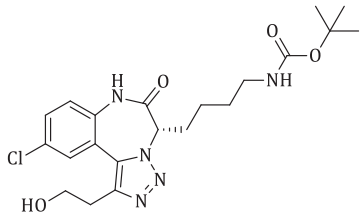

IX.76

Following general procedure **P.01** – **P.05**: (*S*)-3-(*N*-(tert-butyloxycarbonyl)-aminobutyl)-8-chloro-6-(2-hydroxyethyl)[1,2,3]triazolo[1,5-*d*][1,4]benzodiazepin-2-one (**IX.76,** 140.5 mg, 0.3123 mmol).

Yield: 62%.
Bright-yellow solid.
Molecular weight: 449.93 Da.
R_F: 0.16 (hexane/acetone: 6/4).
^{1}H NMR (500 MHz, acetone-d_6) δ 1.19-1.57 (m, 15H), 2.93-3.11 (m broad, 4H), 3.94-4.03 (m, 3H), 4.55-5.55 (m broad, 1H), 5.89 (s broad, 1H), 7.40 (d, J = 8.7Hz, 1H), 7.54 (dd, J = 2.5Hz/8.7Hz, 1H), 8.03 (d, J = 2.5Hz, 1H), 9.66 (s broad, 1H).
^{13}C NMR (75 MHz, acetone-d_6) δ 23.7 (C), 28.6 (CH_3), 29.5 (CH_2), 40.5 (CH_2, broad), 54.9 (CH_2, weak), 61.9 (CH_2), 78.3 (CH_2, weak), 124.6 (CH, broad), 129.2 (CH), 130.5 (C), 130.9 (CH), 156.6 (C), 168.4 (C).
HATR (cm^{-1}): 3347 (m broad), 3225 (m), 3134 (m), 3048 (m), 2931 (m), 2876 (m), 1682 (s), 1584 (m), 1517 (w), 1479 (s), 1454 (m), 1395 (m), 1365 (s), 1269 (m), 1249 (m), 1226 (m), 1166 (s), 1100 (m), 1049 (m), 952 (m), 862 (m), 824 (m), 779 (m), 734 (s), 701 (m), 672 (w).
LC-(ESI)MS (condition 1): t_R = 14.3 min $[M+H^+]^+$: 450.0 (100%). **Purity** (214 nm): 97%.
HRMS (ESI) calcd for $C_{21}H_{29}ClN_5O_4^+$: 450.1903 $[M+H^+]^+$ found: 450.1900.

8-chloro-6-phenyl[1,2,3]triazolo[1,5-*d*][1,4]benzodiazepin-2-one IX.77

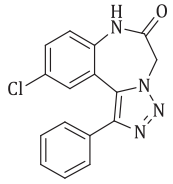

IX.77

Following general procedure **P.01** – **P.03, P.08** and **P.05**: 8-chloro-6-phenyl[1,2,3]triazolo[1,5-*d*][1,4]benzodiazepin-2-one (**IX.77,** 75.7 mg, 0.2436 mmol).

Yield: 46%.
Light-brown solid.
Molecular weight: 310.74 Da.
R_F: 0.19 (hexane/acetone: 7/3).
^{1}H NMR (300 MHz, acetone-d_6) δ 2.81 (s broad, 3H), 5.21 (s, 2H), 7.39-7.49 (m, 5H), 7.56 (dd, *J* = 2.5Hz/8.7Hz, 1H), 7.61-7.65 (m, 2H), 9.73 (s broad, 1H).
^{13}C NMR (75 MHz, acetone-d_6) δ 53.2 (CH_2), 120.9 (C), 125.7 (CH), 128.5 (CH), 129.6 (CH), 129.7 (CH), 130.4 (C), 131.5 (CH), 131.7 (C), 135.8 (C), 167.3 (C).
HATR (cm^{-1}): 3218 (w), 3143 (w), 3065 (w), 2964 (w), 2932 (w), 1697 (s), 1482 (m), 1444 (w), 1391 (m), 1362 (m), 1297 (w), 1285 (w), 1221 (w), 1181 (w), 1153 (w), 1117 (w), 1094 (w), 1044 (w), 990 (w), 966 (w), 921 (w), 885 (w), 868 (w), 825 (m), 775 (m), 742 (m), 698 (m).
LC-(ESI)MS (condition 1): t_R = 15.3 min $[M+H^+]^+$: 311.1 (100%). **Purity** (214 nm): 99%.
HRMS (ESI) calcd for $C_{16}H_{12}ClN_4O^+$: 311.0694 $[M+H^+]^+$ found: 311.0690.

8-bromo-6-phenyl[1,2,3]triazolo[1,5-*d*][1,4]benzodiazepin-2-one IX.78

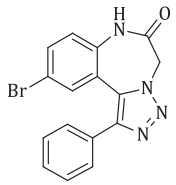

IX.78

Following general procedure **P.01** – **P.03, P.08** and **P.05**: 8-bromo-6-phenyl[1,2,3]triazolo[1,5-*d*][1,4]benzodiazepin-2-one (**IX.78,** 92.1 mg, 0.2593 mmol).

Yield: 49%.
Light-brown solid.
Molecular weight: 355.19 Da.
R_F: 0.17 (hexane/acetone: 7/3).
^{1}H NMR (300 MHz, acetone-d_6) δ 2.83 (s broad, 3H), 5.21 (s, 2H), 7.38-7.48 (m, 4H), 7.53 (d, *J* = 2.3Hz, 1H), 7.62-7.71 (m, 3H), 9.75 (s broad, 1H).
^{13}C NMR (75 MHz, acetone-d_6) δ 53.2 (CH_2), 117.9 (C), 121.2 (C), 125.9 (CH), 128.4 (CH), 129.4 (CH), 129.6 (CH), 131.6 (C), 132.7 (CH), 134.4 (CH), 136.3 (C), 167.3 (C).
HATR (cm^{-1}): 3407 (w, broad), 3216 (w), 3127 (w), 3057 (w), 2969 (m), 2940 (m), 1693 (s), 1605 (w), 1583 (w), 1478 (m), 1445 (m), 1385 (m), 1361 (m), 1288 (m), 1220 (m), 1179 (m), 1139 (m), 1082 (w), 1048 (w), 988 (m), 885 (w), 824 (m), 775 (m), 741 (m), 698 (m).

LC-(ESI)MS (condition 1): t_R = 15.4 min $[M+H^+]^+$: 357.1 (100%). **Purity** (214 nm): 99%.
HRMS (ESI) calcd for $C_{16}H_{12}BrN_4O^+$: 355.0189 $[M+H^+]^+$ found: 355.0186.

(*S*)-6-butyl-8-methoxy-3-isopropyl[1,2,3]triazolo[1,5-*d*][1,4]benzodiazepin-2-one IX.79

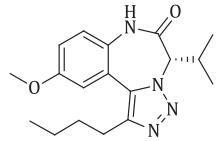

IX.79

Following general procedure **P.01** – **P.05**: (*S*)-6-butyl-8-methoxy-3-isopropyl[1,2,3]triazolo[1,5-*d*][1,4]benzodiazepin-2-one (**IX.79,** 52.4 mg, 0.1596 mmol).

Yield: 42%
White solid.
R_F: 0.15 (hexane/acetone: 8/2). 0.28 (hexane/acetone: 7/3)
Molecular weight: 328.41 Da.
^{1}H NMR (300 MHz, acetone-d_6) δ 0.61 (app d, J = 5.1Hz, 3H), 0.90 (t, J = 7.4Hz, 3H), 1.01 (d, J = 6.6Hz, 3H), 1.33-1.45 (m, 2H), 1.65-1.79 (m, 2H), 1.82-1.97 (m broad, 1H), 2.90 (t, J = 7.7Hz, 2H), 3.88 (s, 3H), 4.97 (app dd broad, J = 10.9Hz, 1H), 7.10 (dd, J = 2.8Hz/8.7Hz, 1H), 7.14 (d, J = 2.8Hz, 1H), 7.32 (d, J = 8.7Hz, 1H), 9.31 (s broad, 1H).
^{13}C NMR (75 MHz, acetone-d_6) δ 14.1 (CH_3), 19.1 (CH_3), 19.2 (CH_3), 23.1 (CH_2), 26.0 (CH_2), 27.8 (CH_2), 32.0 (CH_2), 56.0 (CH_3), 73.7 (CH, broad), 113.2 (CH), 117.2 (CH), 124.1 (CH), 129.0 (C), 152.9 (C), 157.6 (C).
HATR (cm^{-1}): 3209 (w), 3099 (w), 2959 (m), 2930 (m), 2872 (m), 1678 (s), 1617 (w), 1555 (w), 1498 (s), 1465 (m), 1409 (m), 1372 (m), 1337 (m), 1294 (m), 1232 (m), 1214 (m), 1175 (w), 1114 (w), 1038 (m), 1026 (w), 929 (w), 851 (m), 826 (m).
LC-(ESI)MS (condition 1): t_R = 16.2 min $[M+H^+]^+$: 329.2 (100%). **Purity** (214 nm): 90%.
HRMS (ESI) calcd for $C_{18}H_{25}N_4O_2^+$: 329.1972 $[M+H^+]^+$ found: 329.1969.

(*S*)-6-butyl-9-methoxy-3-isopropyl[1,2,3]triazolo[1,5-*d*][1,4]benzodiazepin-2-one IX.80

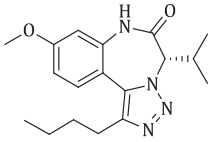

IX.80

Following general procedure **P.01** – **P.05**: (*S*)-6-butyl-9-methoxy-3-isopropyl[1,2,3]triazolo[1,5-*d*][1,4]benzodiazepin-2-one (**IX.80**, 88.1 mg, 0.2682 mmol).

Yield: 34%.
Yellow oil.
Molecular weight: 328.41 Da.
R_F: 0.06 (hexane/acetone: 8/2). 0.23 (hexane/acetone: 7/3).
^{1}H NMR (300 MHz, acetone-d_6) δ 0.61 (app d, J = 6.0Hz, 3H), 0.87 (t, J = 7.5Hz, 3H), 1.02 (d, J = 6.7Hz, 3H), 1.30-1.43 (m, 2H), 1.62-1.79 (m, 2H), 1.81-2.02 (m broad, 1H), 2.85 (t, J = 7.5Hz, 2H), 3.87 (s, 3H), 4.98 (app dd broad, J = 11.3Hz, 1H), 6.96 (m, 2H), 7.57-7.62 (m, 1H).
^{13}C NMR (75 MHz, acetone-d_6) δ 14.1 (CH_3, A), 14.3 (CH_3, B), 19.0 (CH3), 19.2 (CH_3), 23.0 (CH_2, A), 23.2 (CH_2, B), 25.9 (CH_2), 27.8 (CH, broad), 32.0 (CH_2, A), 32.2 (CH, B), 55.9 (CH_3), 73.4 (CH, weak), 107.4 (CH), 111.4 (C), 111.9 (CH), 130.4 (CH), 137.0 (C), 145.2 (C), 161.9 (C), 168.4 (C).
HATR (cm^{-1}): 3226 (w), 3121 (w), 2960 (m), 2933 (m), 2871 (m), 1684 (s), 1618 (m), 1587 (m), 1563 (m), 1515 (m), 1479 (m), 1464 (m), 1399 (m), 1364 (m), 1336 (m), 1285 (m), 1249 (m), 1221 (m), 1202 (m), 1169 (m), 1141 (m), 1125 (w), 1046 (w), 1012 (w), 993 (w), 946 (w), 851 (m), 820 (m), 699 (w), 675 (w), 612 (w).
LC-(ESI)MS (condition 1): t_R = 16.4 min $[M+H^+]^+$: 329.2 (100%). **Purity** (214 nm): 96%.
HRMS (ESI) calcd for $C_{18}H_{25}N_4O_2^+$: 329.1972 $[M+H^+]^+$ found: 329.1966.

XVIII.Synthesis of [1,2,3]triazolo[1,5-*d*][3,2-*f*]pyrido[1,4]diazepin-2-ones

A. Building block synthesis

2-amino-3-(trimethylsilyl)ethynylpyridine X.4

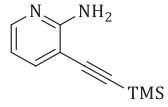

X.4

Following general procedure **P.06**: 2-amino-3-iodopyridine (4,036 g, 18.34 mmol, 1 eq). Trimethylsilylacetylene (7.775 mL, 55.03 mmol, 4 eq). $PdCl_2(PPh_3)_2$ (257.6 mg, 0.3669 mmol, 0.02 eq). CuI (174.9 mg, 0.9172 mmol, 0.05 eq). diethylamine (183 mL).

Yield: 94%. 2-amino-3-(trimethylsilyl)ethynylpyridine (**X.4**, 3.281 g, 17.24 mmol).
Yellow solid.
Molecular weight: 190.32 Da.
R_F: 0.40 (hexane/acetone: 7/3).
^{1}H NMR (300 MHz, acetone-d_6) δ 0.24 (s, 9H), 5.69 (s broad, 2H), 6.56 (dd, J = 4.9Hz/7.5Hz, 1H), 7.50 (dd, J = 1.9Hz/7.5Hz, 1H), 7.96 (dd, J = 1.9Hz/4.9Hz, 1H).
^{13}C NMR (75 MHz, acetone-d_6) δ 0.0 (CH_3), 100.7 (C), 101.6 (C), 102.7 (C), 113.3 (CH), 140.5 (CH), 149.3 (CH), 160.8 (C).
HATR (cm^{-1}): 3469 (w), 3385 (w), 3300 (w), 3168 (w), 2959 (w), 2143 (m), 1619 (m), 1604 (m), 1569 (w), 1449 (m), 1249 (m), 1201 (m), 892 (w), 843 (s), 787 (w), 762 (m), 703 (w), 653 (w).
LC-(ESI)MS (condition 1): t_R = 17.3 min [M+ H^+]: 191.1 **Purity** (214 nm): 98%.

HRMS (ESI) calcd for $C_{10}H_{15}N_2Si^+$: 191.0999 [M+ H^+], found: 191.1004.

2-amino-5-bromo-3-(trimethylsilyl)ethynylpyridine X.5

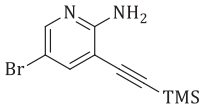

X.5

Following general procedure **P.06**: 2-amino-5-bromo-3-iodopyridine (900.0 mg, 3.011 mmol, 1 eq). Trimethylsilylacetylene (1.700 mL, 12.04 mmol, 4 eq). $PdCl_2(PPh_3)_2$ (42.0 mg, 0.06022 mmol, 0.02 eq). CuI (28 mg, 0.1506 mmol, 0.05 eq). diethylamine (30 mL).

Yield: 90%. 2-amino-5-bromo-3-(trimethylsilyl)ethynylpyridine (**X.5**, 730.4 mg, 2.713 mmol).
Light-yellow solid.
Molecular weight: 269.21 Da.
R_F: 0.31 (dichloromethane).
^{1}H NMR (300 MHz, acetone-d_6) δ 0.24 (s, 9H), 5.89 (s broad, 2H), 7.63 (d, J = 2.5 Hz, 1H), 8.01 (d, J = 2.5Hz, 1H).
^{13}C NMR (75 MHz, acetone-d_6) δ 0.0 (CH_3), 99.9 (C), 102.5 (C), 104.7 (C), 105.9 (C), 142.1 (CH), 149.7 (CH), 159.6 (C).
HATR (cm^{-1}): 3456 (w), 3296 (w), 3162 (w), 2957 (w), 2150 (m), 1715 (w), 1626 (s), 1548 (m), 1458 (s), 1398 (w), 1247 (m), 1194 (m), 1099 (w), 1055 (w), 913 (m), 901 (m), 837 (s), 790 (w), 763 (m), 704 (w), 646 (w).
LC-(ESI)MS (condition 5): t_R = 7.1 min [M+ H^+]:269.1 (100%). **Purity** (214 nm): 99%.
HRMS (ESI) calcd for $C_{10}H_{14}BrN_2Si^+$: 269.0104 [M+ H^+], found: 269.0105.

2-amino-3-ethynylpyridine X.6

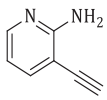

X.6

Following general procedure **P.07**: 2-amino-3-(trimethylsilyl)ethynylpyridine **X.4** (809.1 mg, 4.251 mmol, 1 eq). Potassium carbonate (587.5 mg, 4.250 mmol, 1 eq). MeOH (43 mL).

Yield: 76%. 2-amino-3-ethynylpyridine (**X.6**, 381.0 mg, 3.225 mmol).
Overall yield: 71%.
Light-brown solid.
R_F: 0.22 (hexane/acetone: 7/3).

Molecular weight: 118.14 Da.
^{1}H NMR (300 MHz, acetone-d_6) δ 3.96 (s, 1H), 5.82 (s broad, 2H), 6.57 (dd, J = 4.9Hz/7.5Hz, 1H), 7.54 (dd, J = 1.7Hz/7.5Hz, 1H), 7.99 (dd, J = 1.7Hz/4.9Hz, 1H).
^{13}C NMR (75 MHz, acetone-d_6) δ 80.1 (C), 84.9 (CH), 101.9 (C), 113.2 (CH), 141.0 (CH), 149.3 (CH), 161.0 (C).
HATR (cm^{-1}): 3462 (s), 3286 (m), 3239 (s), 3162 (m), 2980 (w), 1620 (s), 1568 (m), 1463 (s), 1449 (s), 1294 (w), 1251 (m), 1186 (w), 1142 (w), 1079 (w), 950 (w), 800 (w), 787 (w), 770 (w), 730 (w), 708 (w).
LC-(ESI)MS (condition 1): t_R = 11.9 min [M+ H^+]:119.1 (100%). **Purity** (214 nm): 99%.
HRMS (ESI) calcd for $C_7H_7N_2^+$: 119.0604 [M+ H^+], found: 119.0606.

2-amino-5-bromo-3-ethynylpyridine X.7

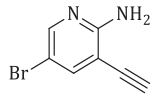

X.7

Following general procedure **P.07**: 2-amino-5-bromo-3-(trimethylsilyl)ethynylpyridine **X.5** (606.0 mg, 2.251 mmol, 1 eq). Potassium carbonate (311.0 mg, 2.251 mmol, 1 eq). MeOH (23 mL).

Yield: 92%. 2-amino-5-bromo-3-ethynylpyridine (**X.7,** 406.2 mg, 2.062 mmol).
Overall yield: 83%
Light-yellow solid.
Molecular weight: 197.03 Da.
R_F: 0.22 (dichloromethane).
^{1}H NMR (300 MHz, acetone-d_6) δ 4.07 (s, 1H), 5.94 (s broad, 2H), 7.67 (d, J = 2.4Hz, 1H), 8.02 (d, J = 2.4Hz, 1H).
^{13}C NMR (75 MHz, acetone-d_6) δ 86.4 (CH), 105.9 (C), 121.4 (C), 142.6 (CH), 149.9 (CH).
HATR (cm^{-1}): 3456(m), 3291(m), 3138(m), 1626(s), 1555(m), 1457(s), 1397(m), 1244(m), 1178(w), 898(m), 765(w), 665(m), 650(m).
LC-(ESI)MS (condition 5): t_R = 5.3 min [M+ H^+]: 197.1 (100%). **Purity** (214 nm): 97%.
HRMS (ESI) calcd for $C_7H_6N_2^+$: 196.9709 [M+ H^+], found: 196.9706.

2-amino-3-hexynylpyridine X.8

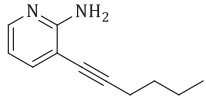

X.8

Following general procedure **P.06**: 2-amino-3-iodopyridine (1.000 g, 4.545 mmol, 1 eq). 1-hexyn (2.100 mL, 18.18 mmol, 4 eq). $PdCl_2(PPh_3)_2$ (63.8 mg, 0.0909 mmol, 0.02 eq). CuI (43.3 mg, 0.227 mmol, 0.05 eq). diethylamine (45 mL).

Yield: 87%. 2-amino-3-hexynylpyridine (**X.8**, 689.2 mg, 3.955 mmol).
Dark-red oil.
Molecular weight: 174.24 Da.
R_F: 0.61 (hexane/acetone: 6/4). 0.22 (hexane/acetone: 8/2).
^{1}H NMR (300 MHz, acetone-d_6) δ 0.93 (t, J = 7.4Hz, 3H), 1.41-1.63 (m, 4H), 2.47 (t, J = 7.2Hz, 2H), 5.65 (s broad, 2H), 6.51-6.55 (m, 1H), 7.44 (dd, J = 1.9Hz/7.5Hz, 1H), 7.91 (dd, J = 1.9Hz/5.1Hz, 1H).
^{13}C NMR (75 MHz, acetone-d_6) δ 13.8 (CH_3), 19.6 (CH_2), 22.6 (CH_2), 31.6 (CH_2), 76.7 (C), 97.0 (C), 104.2 (C), 113.2 (CH), 140.0 (CH), 148.1 (CH), 160.6 (C).
HATR (cm^{-1}): 3472 (w), 3292 (m), 3166 (m), 2956 (m), 2930 (m), 2870 (m), 1707 (m), 1604 (s), 1570 (m), 1452 (s), 1378 (m), 1355 (m), 1328 (m), 1302 (m), 1275 (m), 1247 (m), 1222 (m), 1119 (w), 1075 (w), 1005 (w), 787 (m), 766 (s), 745 (m), 722 (w), 695 (w).
LC-(ESI)MS (condition 1): t_R = 16.7 min [M+ H^+]: 175.1 **Purity** (214 nm): 98%.

2-amino-3-phenylethynylpyridine X.9

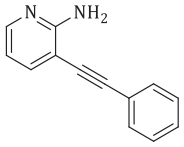

X.9

Following general procedure **P.06**: 2-amino-3-iodopyridine (1.000 g, 4.545 mmol, 1 eq). phenylacetylene (1.500 mL, 13.64 mmol, 4 eq). $PdCl_2(PPh_3)_2$ (63.8 mg, 0.0909 mmol, 0.02 eq). CuI (43.3 mg, 0.227 mmol, 0.05 eq). diethylamine (45 mL).

Yield: 99%. 2-amino-3-phenylethynylpyridine (**X.9,** 872.0 mg, 4.490 mmol).
Yellow solid.
Molecular weight: 194.23 Da.
R_F: 0.50 (hexane/acetone: 6/4). 0.16 (hexane/acetone: 8/2).
^{1}H NMR (300 MHz, acetone-d_6) δ 5.84 (s broad, 2H), 7.37-7.42 (m, 4H), 7.57-7.61 (m, 4H).
^{13}C NMR (75 MHz, acetone-d_6) δ 95.5 (C), 113.5 (CH, broad), 129.9 (C), 129.4 (CH), 132.3 (CH), 140.5 (CH), 149.7 (CH, broad), 160.5 (C).
HATR (cm^{-1}): 3466 (m), 3390 (w), 3292 (m), 3233 (w), 3141 (m), 3065 (m), 2919 (w), 1633 (s), 1600 (m), 1578 (m), 1563 (m), 1485 (m), 1465 (m), 1453 (m), 1337 (w), 1293 (w), 1245 (m), 1069 (w), 787 (m), 764 (m), 751 (m), 685 (m).
LC-(ESI)MS (condition 1): t_R = 16.1 min [M+ H^+]: 195.1 **Purity** (214 nm): 96%.

HRMS (ESI) calcd for $C_{13}H_{11}N_2^+$: 195.0917 [M+ H^+], found: 195.0920.

B. Proof of principle library

(*S*)-3-(tert-butoxymethyl)[1,2,3]triazolo[1,5-*d*][3,2-*f*]pyrido[1,4]diazepin-2-one X.11

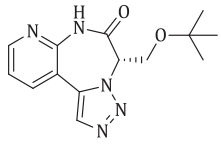

X.11

Following general procedure **P.01 – P.05**: (*S*)-3-(tert-butoxymethyl)[1,2,3]triazolo[1,5-*d*][3,2-*f*]pyrido[1,4]diazepin-2-one (**X.11**, 11.4 mg, 0.03968 mmol).

Yield: 9%.
White solid.
Molecular weight: 287.32 Da.
R_F: 0.09 (hexane/acetone 8/2).
^{1}H NMR (300 MHz, acetone-d_6) δ 0.81 (s, 9H), 3.77-4.04 (m, 2H), 5.72-5.75 (m, 1H), 7.33(dd, *J* = 4.9Hz/7.7Hz, 1H, 1H), 8.16 (s, 1H), 8.22 (dd, *J* = 1.8Hz/7.7Hz, 1H), 8.50 (dd, *J* = 1.9Hz/4.9Hz, 1H), 10.01 (s broad, 1H).
^{13}C NMR (75 MHz, acetone-d_6) δ 26.9 (CH_3), 63.6 (C), 67.0 (CH), 74.3 (CH_2), 120.9 (CH), 133.4 (CH), 137.8 (CH), 150.4 (CH), 168.1 (C).
LC-(ESI)MS (condition 1): t_R = 13.0 min [M+ H^+]: 288.1 (100%). **Purity** (214 nm): 95%.
HRMS (ESI) calcd for $C_{14}H_{18}N_5O_2^+$: 288.1455 [M+ H^+], found: 288.1443.

(*S*)-3-(*N*-(tert-butyloxycarbonyl)-amino)[1,2,3]triazolo[1,5-*d*][3,2-*f*]pyrido[1,4]diazepin-2-one X.12

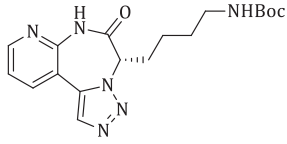

X.12

Following general procedure **P.01 – P.05**: (*S*)-3-(*N*-(tert-butyloxycarbonyl)-aminobutyl)[1,2,3]triazolo[1,5-*d*][3,2-*f*]pyrido[1,4]diazepin-2-one (**X.12**, 27.6 mg, 0.07411 mmol).

Yield: 13%.
Light-brown solid.
Molecular weight: 372.42 Da.
R_F: 0.12 (hexane/acetone 65/35).
^{1}H NMR (300 MHz, acetone-d_6) δ 1.25-1.52 (m, 15H), 3.00 (q, J = 6.6Hz, 2H), 5.43 (app dd, J = 6.8Hz/9.0Hz, 1H), 5.92 (s broad, 1H), 7.40 (dd, J = 4.7Hz/7.7Hz, 1H), 8.18 (s, 1H), 8.27 (dd, J = 1.7Hz/7.7Hz, 1H), 8.57 (dd, J = 1.7Hz/4.7Hz, 1H), 9.97 (s broad, 1H).
^{13}C NMR (75 MHz, acetone-d_6) δ 23.5 (CH_2), 28.6 (CH_3), 40.5 (CH_2), 55.5 (CH_2), 65.3 (CH), 121.3 (CH), 133.7 (CH), 138.5 (CH), 151.2 (CH), 162.2 (C).
HATR (cm^{-1}): 3362 (w), 3093 (w), 2975 (m), 2927 (m), 2869 (m), 1689 (s), 1606 (w), 1579 (m), 1519 (m), 1456 (m), 1413 (m), 1385 (m), 1366 (m), 1343 (m), 1270 (m), 1250 (m), 1171 (m), 1116 (w), 968 (w), 865 (w), 808 (w), 764 (w).
LC-(ESI)MS (condition 1): t_R = 13.430 min, [M-Boc+H$^+$]$^+$: 273.1 (100%).

(*S*)-3-isobutyl-9-bromo[1,2,3]triazolo[1,5-*d*][3,2-*f*]pyrido[1,4]diazepin-2-one X.13

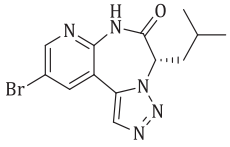

X.13

Following general procedure **P.01 – P.05**: (*S*)-3-isobutyl-9-bromo[1,2,3]triazolo[1,5-*d*][3,2-*f*]pyrido[1,4]diazepin-2-one (**X.13**, 45.4 mg, 0.1350 mmol).

Yield: 26%.
White solid.
R_F: 0.15 (hexane/acetone: 8/2).
Molecular weight: 336.19 Da.
^{1}H NMR (300 MHz, acetone-d_6) δ 0.82 (d, J = 6.6Hz, 3H), 0.93 (d, J = 6.6Hz, 3H), 1.44 (sextet, J = 6.6Hz, 1H), 1.85 (t, J = 7.5Hz, 2H), 5.57 (app t, J = 7.9Hz, 1H), 8.25 (s, 1H), 8.45 (d, J = 2.3Hz, 1H), 8.60 (d, J = 2.3Hz, 1H), 10.11 (s broad, 1H).
^{13}C NMR (75 MHz, acetone-d_6) δ 21.9 (CH_3), 22.4 (CH_3), 25.5 (CH), 38.4 (CH_2), 64.0 (CH), 114.6 (C), 115.7 (C), 132.2 (C), 134.4 (CH), 140.2 (CH), 151.6 (CH), 168.0 (C).
HATR (cm^{-1}): 3211 (w), 3124 (w), 2958 (m), 2925 (m), 1691 (s), 1566 (w), 1491 (m), 1472 (m), 1417 (m), 1391 (m), 1367 (m), 1337 (m), 1215 (w), 1119 (w), 1036 (w), 973 (w), 901 (w), 836 (w), 767 (w).
LC-(ESI)MS (condition 5): t_R = 5.537 min, [M+ H$^+$]: 336.0 (100%). **Purity** (214 nm): 95%.
HRMS (ESI) calcd for $C_{13}H_{15}BrN_5O^+$: 336.0454 [M+ H$^+$], found: 336.0454.

(*S*)-6-butyl-3-isobutyl[1,2,3]triazolo[1,5-*d*][3,2-*f*]pyrido[1,4]diazepin-2-one X.14

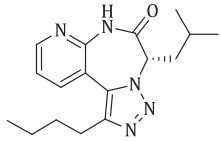

X.14

Following general procedure **P.01 – P.05**: (*S*)-6-butyl-3-isobutyl-[1,2,3]triazolo[1,5-*d*][3,2-f]pyrido[1,4]diazepin-2-one (**X.14**, 43.3 mg, 0.1381 mmol).

Yield: 22%.
Green solid.
Molecular weight: 313.40 Da.
R_F: 0.13 (hexane/acetone: 8/2).
^{1}H NMR (300 MHz, acetone-d_6) δ 0.80-0.95 (m, 9H), 1.30-1.42 (m, 2H), 1.45-1.61 (m, 1H), 1.65-1.76 (m, 2H), 1.78-1.90 (m, 2H), 2.84 (t, *J* = 7.5Hz, 2H), 5.31-5.48 (m, 1H), 7.41-7.45 (m, 1H), 8.17 (dd, *J* = 1.1Hz/7.7Hz, 1H), 8.49-8.65 (m broad, 1H), 10.08 (s broad, 1H).
^{13}C NMR (75 MHz, acetone-d_6) δ 14.0 (CH_3), 22.0 (CH_3), 22.5 (CH_3), 23.0 (CH_2), 25.6 (CH), 25.7 (CH_2), 31.9 (CH_2), 37.4 (CH_2, broad), 114.0 (C), 121.2 (CH, broad), 138.2 (CH), 146.8 (C), 148.2 (C), 150.5 (CH), 168.9 (C).
LC-(ESI)MS (condition 1): t_R = 12.9 min [M+ H^+]: 314.2 (100%). **Purity** (214 nm): 92%.

(*S*)-6-phenyl-3-isopropyl[1,2,3]triazolo[1,5-*d*][3,2-*f*]pyrido[1,4]diazepin-2-one X.15

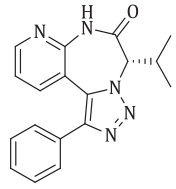

X.15

Following general procedure **P.01 – P.05**: (*S*)-6-phenyl-3-isopropyl[1,2,3]triazolo[1,5-*d*][3,2-*f*]pyrido[1,4]diazepin-2-one (**X.15**, 39.5 mg, 0.1237 mmol).

Yield: 19%.
White Solid.
Molecular weight: 319.36 Da.
R_F: 0.11 (hexane/acetone: 8/2).

^{1}H NMR (300 MHz, acetone-d_6) δ 0.59 (d, J = 6.4Hz, 3H), 0.94 (d, J = 6.4Hz, 3H), 1.70-1.74 (m, 1H), 5.03 (d, J = 11.7Hz, 1H), 6.49 (dd, J = 4.9Hz/7.5Hz, 2H), 7.11 (dd, J = 4.9Hz/7.9Hz, 1H), 7.45-7.48 (m, 1H), 7.71 (dd, J = 1.7Hz/7.7Hz, 1H), 7.86-7.88 (m, 2H), 8.40 (dd, J = 1.7Hz/4.9Hz, 1H), 9.68 (s broad, 1H).
^{13}C NMR (75 MHz, acetone-d_6) δ 19.0 (CH_3), 19.2 (CH_3), 28.9 (CH), 73.5 (CH), 113.4 (CH), 120.9 (CH), 138.8 (CH), 140.5 (CH), 149.2 (CH), 151.3 (CH), 168.2 (C).
HATR (cm^{-1}): 3474 (w), 3318 (w), 3180 (w), 3055 (w), 2963 (w), 2922 (m), 2852 (w), 1683 (s), 1610 (s), 1573 (s), 1490 (m), 1450 (s), 1418 (m), 1371 (m), 1293 (w), 1262 (w), 1237 (s), 1146 (w), 1118 (w), 1073 (w), 1026 (w), 982 (w), 916 (w), 842 (w), 756 (s), 733 (m), 692 (s), 651 (w), 600 (w).
LC-(ESI)MS (condition 1): t_R = 15.0 min [M+ H^+]: 320.1 (100%). **Purity** (214 nm): 97%.
HRMS (ESI) calcd for $C_{18}H_{18}N_5O^+$: 320.1506 [M+ H^+], found: 320.1514.

XIX. *N*-Alkylation

A. First approach: Mitsunobu-Fukuyama alkylation

1. Induction of a nosyl group: test cases

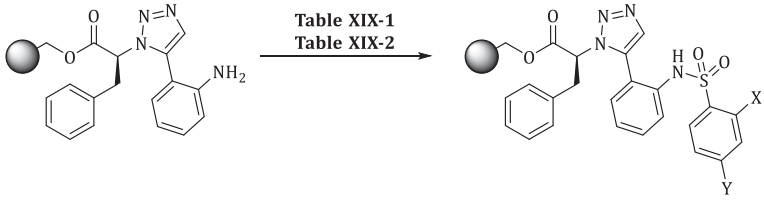

VIII.3

$X = NO_2$; Y = H	**XI.7**
X = H; $Y = NO_2$	**XI.8**
$X = NO_2$; $Y = NO_2$	**XI.9**

Resin bound intermediate **VIII.3** is prepared *via* procedure **P.01** – **P.04** and dried extensively under reduced pressure. Intermediate **VIII.3** (**Table XIX-1** and **Table XIX-2**, 1 eq) is poured in closed 1 mL vials and dry solvent (**Table XIX-1** and **Table XIX-2**) is added. Each vessel is treated with protective reagent (**Table XIX-1 and Table XIX-2**), DMAP (**Table XIX-1 and Table XIX-2**) if necessary and collidine or pyridine (**Table XIX-1 and Table XIX-2**). Depending on the specific conditions, the vessels are shaken for one, two or five hours at room temperature or at 70°C and after this reaction time, the resin is isolated and washed with DMF (3x 1 mL), MeOH (3x 1 mL) and dry dichloromethane (3x 1 mL). After drying *in vacuo*, this procedure is repeated. The analysis of this reaction is performed after treating the reacted beads with TFA/H_2O (95/5) for 2 hours at room temperature and after evaporation of supernatans (upon addition of acetonitrile) an LC-MS analysis is performed to gain insight on the formed products.

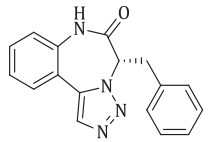

VIII.17

Brutoformula: $C_{17}H_{14}N_4O$
Molecular weight: 290.32 Da.
LC-(ESI)MS (condition 1): t_R = 14.4 min $[M+H^+]^+$: 291.1 (100%).

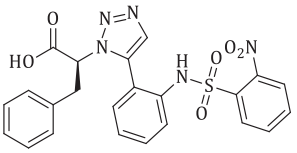

XI.7

Brutoformula: $C_{23}H_{19}N_5O_6S$
Molecular weight: 493.49 Da.
LC-(ESI)MS (condition 1): t_R = 13.2 min $[M+H^+]^+$: 494.0 (100%).

Table XIX-1: Various conditions for Nosyl protection (equivalents)

entry	conditions							
	N.6 [eq]	*o*-NsCl [eq]	*p*-NsCl [eq]	DNCl [eq]	collidine [eq]	CH_2Cl_2[M]	T	reaction time
1	1	5	-	-	10	0.1	rt	2x 1h
2	1	-	5	-	10	0.1	rt	2x 1h
3	1	-	-	5	10	0.1	rt	2x 1h

entry	conditions							
	N.6 [eq]	*o*-NsCl [eq]	pyridine [eq]	collidine [eq]	DMAP [eq]	solvent [M]	T	reaction time
4	1	2	2		0.2	0.05	rt	1h
5	1	2	2		0.2	0.05	70°C	1h
6	1	5	5		0.5	0.05	70°C	1h
7	1	5	10		0.5	0.02	rt	5h
8	1	5		10	0.5	0.02	rt	5h
9	1	10	20		1	0.02	rt	5h
10	1	10		20	1	0.02	rt	5h
11	1	5	10		0.5	0.02	70°C	5h
12	1	5		10	0.5	0.02	70°C	5h
13	1	10	20		1	0.02	70°C	5h
14	1	10		20	1	0.02	70°C	5h
15	1	10	20		1	0.02	70°C	2x 5h

Table XIX-2: Various conditions for Nosyl protection (amounts)

entry	conditions								
	VIII.3 [mmol]	*o*-NsCl [mg]	*p*-NsCl [mg]	DNCl [mg]	collidine [µL]	CH_2Cl_2[µL]	T	reaction time
1	0.03670	40.7	-	-	49.0	375	rt	2x 1h
2	0.03670	-	40.7	-	49.0	375	rt	2x 1h
3	0.03670	-	-	48.9	49.0	375	rt	2x 1h

entry	conditions								
	VIII.3 [mmol]	*o*-NsCl [mg]	pyridine [µL]	collidine [µL]	DMAP [mg]	solvent [µL]	T	reaction time
1	0.01568	7.0	2.5	-	0.4	310	rt	1h
2	0.01568	7.0	2.5	-	0.4	310	70°C	1h
3	0.01568	17.4	6.3	-	1.0	310	70°C	1h
4	0.01729	17.4	14	-	1.0	860	rt	5h
5	0.01729	17.4	-	23	1.0	860	rt	5h
6	0.01729	38.4	28	-	2.0	860	rt	5h
7	0.01729	38.4	-	46	2.0	860	rt	5h
8	0.01729	17.4	14	-	1.0	860	70°C	5h
9	0.01729	17.4	-	23	1.0	860	70°C	5h
10	0.01729	38.4	28	-	2.0	860	70°C	5h
11	0.01729	38.4	-	46	2.0	860	70°C	5h
12	0.05763	128.0	93	-	6.7	2850	70°C	2x 5h

2. Introduction of *o*-Nosyl group

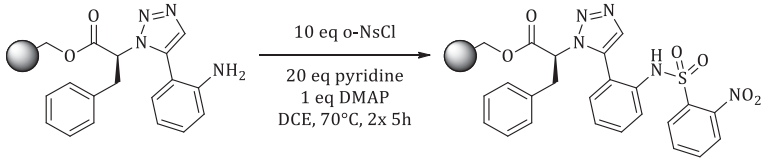

VIII.3 **XI.7**

General procedure **P.09**: Solid-phase bound intermediate **VIII.3** (0.2140 mmol, 1 eq) is synthesized *via* procedure **P.01** – **P.04** and dried extensively under reduced pressure. Afterwards intermediate **VIII.3** is prepared for the nosylation step by a pre-swelling step with dry dichloromethane twice for 5 minutes (2x 5 mL). The swollen beads are isolated and dry dichloromethane (10.70 mL, 0.02M) is added. *o*-NsCl (472.9 mg, 2.140 mmol, 10 eq), DMAP (24.0 mg, 0.2140 mmol, 1 eq) and dry pyridine (345 µL, 4.280 mmol, 20 eq) are added to the mixture. The reaction mixture is shaken for 5 hours at 70°C. Afterwards the beads are filtered off and washed with DMF (3x 10 mL), MeOH (3x 10 mL) and dry CH_2Cl_2 (4x 10 mL). The beads are treated a second time by the procedure described above.

Cleavage: After the second reaction, an aliquot of the beads is cleaved with a 95% TFA-solution in H_2O for two hours at room temperature. This solution is isolated and evaporated under reduced pressure upon addition of acetonitrile and used for LC-MS sample preparation. If begin product remains it is expected to be detected as ringclosed product **VIII.17** as cyclization/release occurs during the cleavage step.

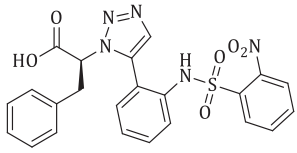

XI.7

Brutoformula: $C_{23}H_{19}N_5O_6S$
Conversion: 61%.
Molecular weight: 493.49 Da.
LC-(ESI)MS (condition 1): t_R = 13.2 min $[M+H^+]^+$: 494.0 (100%).

3. Mitsunobu-Fukuyama alkylation

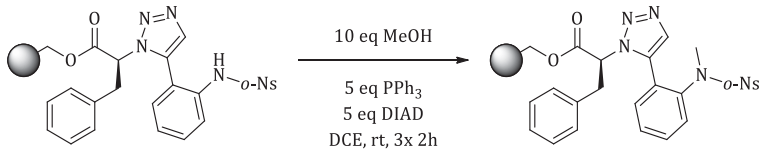

XI.7 **XI.18**

General procedure **P.10**: Intermediate **XI.7** (114 mg, 0.06793 mmol, 1 eq) is dried under reduced pressure and afterwards pre-swollen in dry dichloroethane (2x 1 mL). After isolating the beads, 700 µL of dry dichloroethane (0.1M) is added. Subsequently, triphenylphosphine (89 mg, 0.3397 mmol, 5 eq), MeOH (28 µL, 0.6793 mmol, 10 eq) and DIAD (67 µL, 0.3396, 5 eq) are added to the beads and the reaction proceeds for 2 hours at room temperature. After two hours, the beads are isolated and washed with DMF (3x 2mL), MeOH (3x 2 mL) and dry dichloroethane (3x 2 mL).

Cleavage: An aliquot of resin is cleaved with TFA/H_2O (95/5) for 2 hours at room temperature. After two hours this mixture is isolated and evaporated azeotropically with acetonitrile. An LC-MS sample is prepared for reaction monitoring. This whole procedure is repeated twice in order to obtain three alkylation cycles with intermediate yield determination.

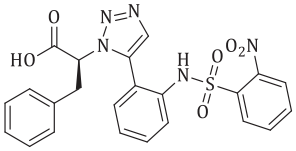

Brutoformula: $C_{23}H_{19}N_5O_6S$
Molecular weight: 493.49 Da.
LC-(ESI)MS (condition 1): t_R = 13.2 min [M-H^+]-: 492.0 (100%).

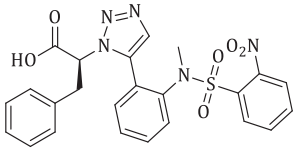

Brutoformula: $C_{24}H_{21}N_5O_6S$
Molecular weight: 507.52 Da.
LC-(ESI)MS (condition 1): t_R = 12.7 min [M-H^+]$^-$: 506.0 (100%).

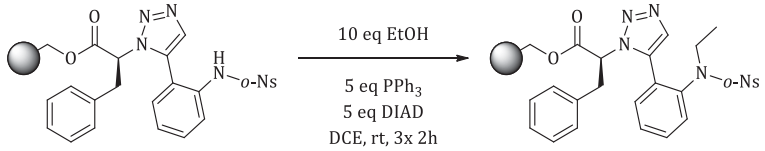

XI.7 **XI.19**

Following general procedure **P.10**: Intermediate **XI.7** (114 mg, 0.06793 mmol, 1 eq), EtOH (40 µL, 0.6793 mmol, 10 eq), DIAD (67 µL, 0.3396, 5 eq) and 700 µL dichloroethane.

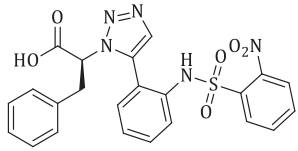

Brutoformula: $C_{23}H_{19}N_5O_6S$
Molecular weight: 493.49 Da.
LC-(ESI)MS (condition 1): t_R = 13.2 min [M-H$^+$]-: 492.0 (100%).

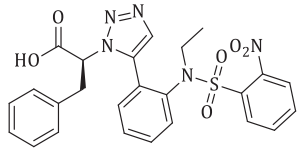

Brutoformula: $C_{25}H_{23}N_5O_6S$
Molecular weight: 521.54 Da.
LC-(ESI)MS (condition 1): t_R = 12.9 min [M-H$^+$]$^-$: 520.0 (100%).

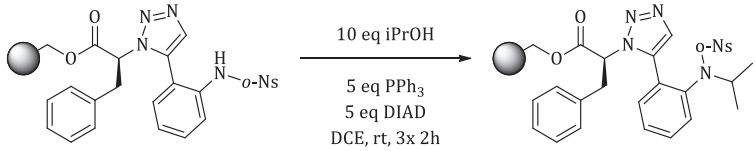

XI.7 **XI.20**

Following general procedure **P.10**: Intermediate **XI.7** (114 mg, 0.06793 mmol, 1 eq), iPrOH (52 µL, 0.6793 mmol, 10 eq), DIAD (67 µL, 0.3396, 5 eq) and 700 µL dichloroethane.

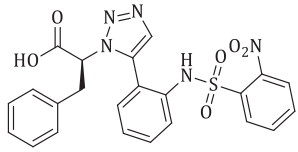

Brutoformula: $C_{23}H_{19}N_5O_6S$
Molecular weight: 493.49 Da.
LC-(ESI)MS (condition 1): t_R = 13.2 min [M-H$^+$]-: 492.0 (100%).

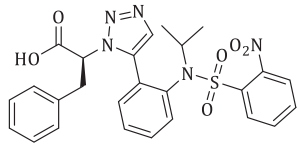

Brutoformula: $C_{26}H_{25}N_5O_6S$
Molecular weight: 535.57 Da.
LC-(ESI)MS (condition 1): t_R = 13.1 min [M-H$^+$]$^-$: 534.0 (100%).

4. Nosyl cleavage

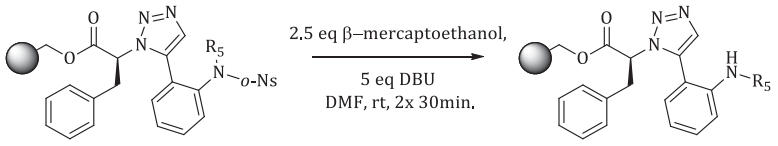

$R_5 = CH_3$	**XI.18**	$R_5 = CH_3$	**XI.25**
$R_5 = CH_2CH_3$	**XI.19**	$R_5 = CH_2CH_3$	**XI.26**
$R_5 = CH(CH_3)_2$	**XI.20**	$R_5 = CH(CH_3)_2$	**XI.27**

General procedure **P.11**: Resin bound intermediates **XI.18** (0.06793 mmol, 1 eq), **XI.19** (0.06793 mmol, 1 eq) and **XI.20** (0.06793 mmol, 1 eq) are separately Nosyl-deprotected upon addition of β-mercaptoethanol and DBU in DMF. To the beads, DMF (675 µL, 0.1M), DBU (51 µL, 0.3395 mmol, 5 eq) and β-mercaptoethanol (70 µL, 0.1698 mmol, 2.5 eq) are added. The deprotection is carried out for 30 minutes. After this time, the beads are isolated and washed with DMF (3x 2 mL), MeOH (3x 2 mL), CH_2Cl_2 (3x 2 mL) and DMF (3x 2 mL). After this washing step, this deprotection is repeated once. The effectiveness of this deprotection is verified upon LC-MS analysis after cleaving an aliquot of the reacted beads with TFA/H_2O (95/5).

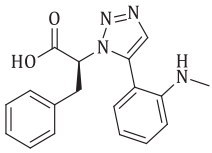

XI.31

Brutoformula: $C_{18}H_{17}N_4O_2$
Molecular weight: 322.36 Da.
LC-(ESI)MS (condition 1): t_R = 12.0 min
$[M+H^+]^+$: 323.1 (100%).

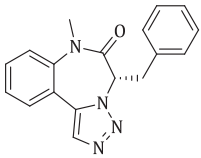

XI.28

Brutoformula: $C_{18}H_{16}N_4O$
Molecular weight: 304.35 Da.
LC-(ESI)MS (condition 1): t_R = 15.5 min
$[M+H^+]^+$: 305.1 (100%).
Crude purity: <5%

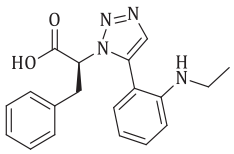

XI.32

Brutoformula: $C_{18}H_{17}N_4O_2$
Molecular weight: 336.38 Da.
LC-(ESI)MS (condition 1): t_R = 12.4 min
$[M+H^+]^+$: 337.1 (100%).

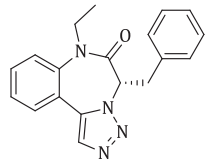

XI.29

Brutoformula: $C_{19}H_{18}N_4O$
Molecular weight: 318.37 Da.
LC-(ESI)MS (condition 1): t_R = 13.1 min
$[M+H^+]^+$: 319.1 (100%).
Crude purity: <1%

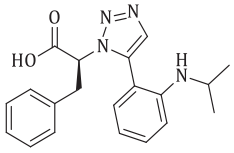

XI.33

Brutoformula: $C_{18}H_{17}N_4O_2$
Molecular weight: 336.38 Da.
LC-(ESI)MS (condition 1): t_R = 12.8 min
$[M+H^+]^+$: 351.1 (100%).

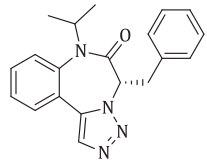

XI.30

Brutoformula: $C_{20}H_{20}N_4O$
Molecular weight: 332.40 Da.
LC-(ESI)MS (condition 1): not detected

B. Mitsunobu-Fukuyama: Second strategy

1. Solution-phase synthesis of XI.37

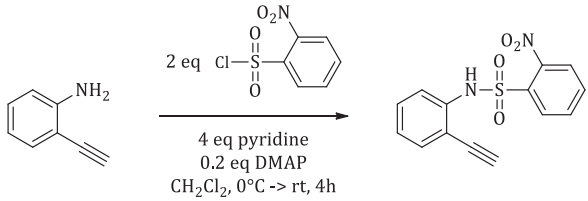

VIII.2 **XI.34**

To an ice-cooled solution of *o*-NsCl (378 mg, 1.709 mmol, 2 eq) in dry dichloromethane (850 µL, 0.1M), dry pyridine (275 µL, 3.419 mmol, 4 eq) and DMAP (20.8 mg, 0.1709 mmol, 0.2 eq)

are added resulting in a bright-yellow solution. After five minutes, 2-ethynylaniline (**VIII.2**, 97 µL, 0.8547 mmol, 1 eq) is added dropwise to this ice-cooled solution. After 20 minutes, the ice bath is removed and the reaction runs at room temperature. The reaction is followed by TLC (hexane/acetone: 6/4) until completion. After four hours, the reaction mixture is diluted with 10 mL of dichloromethane and transferred into a separation funnel. The reaction mixture is consecutively washed with 2M HCl solution (2x 10 mL), H_2O (1x 10 mL) and saturated brine solution (2x 10 mL). Afterwards, the organic phase is dried over $MgSO_4$ for 25 minutes and after filtration of the salt, the organic phase is evaporated under reduced pressure resulting in a dark red solid. Further purification was done *via* flash chromatography (eluent: hexane/acetone: 8/2).

Yield: 81%. *N*-(2-ethynylphenyl)-2-nitrobenzenesulfonamide (209.3 mg, 0.6927 mmol)
Dark-red solid.
R_F: 0.27 (hexane/acetone: 6/4).
Molecular weight: 302.30 Da.
^{1}H NMR (300 MHz, acetone-d_6) δ 3.91 (s, 1H), 7.22 (td, J = 1.1Hz/7.7 Hz, 1H), 7.42-7.47 (m, 2H), 7.62-7.65 (m, 1H), 7.79-7.85 (m, 1H), 7.90-8.03 (m, 4H), 8.44 (s broad, 1H).
^{13}C NMR (75 MHz, acetone-d_6) δ 86.1 (CH), 116.5 (C), 123.6 (CH), 126.4 (CH), 126.6 (CH), 130.4 (CH), 131.6 (CH), 133.7 (CH), 133.8 (CH),135.7 (CH),138.6 (C).
LC-(ESI)MS (condition 1): t_R = 16.5 min $[M+H^+]^+$: 303.0 (100%). **Purity:** 91%.

2. Click-reaction of XI.37 with VII.31

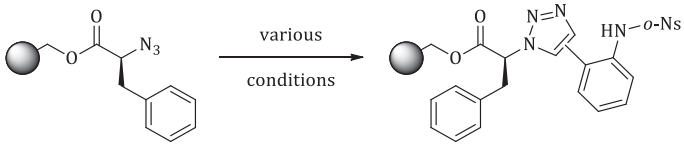

VII.31

1,4-regioisomer **XI.35**
1,5-regioisomer **XI.7**

In order to verify the effectiveness and regioselectivity of the 1,3-dipolar cycloaddition with **XI.34**, four test reactions are set up. To solid-phase bound (*S*)-2-azido-phenyl propanoic acid (**VII.31**, 0.02545 mmol, 1 eq) Nosyl-protected 2-ethynylaniline (**XI.34**, 38.5 mg, 0.1273 mmol, 5 eq) and toluene (250 µL, 0.1M) are added in a sealed cap vessel. Subsequently $C_p^*RuCl(PPh_3)_2$ (2.0 mg, 0.002545 mmol, 0.1 eq) or $C_p^*RuClCOD$ (1.0 mg, 0.002545 mmol, 0.1 eq) are added as Ru(II)-catalyst. The reaction is shaken for 3 hours at 60°C or for 14 hours at room temperature. After this reaction time the beads are isolated and washed extensively with DMF (3x 1 mL), MeOH (3x 1 mL) and dichloromethane (3x 1 mL). The beads are subsequently subjected to a 95% TFA solution in H_2O for two hours at room temperature. Afterwards this solution is isolated and concentrated *in vacuo* upon addition of acetonitrile.

LC-MS samples are prepared and LC-MS analysis is used for reaction monitoring at the specific conditions.

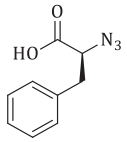

VII.10

Brutoformula: $C_9H_9N_3O_2$
Molecular weight: 191.91 Da..
LC-(ESI)MS (condition 1): t_R = 9.3 min [M-H$^+$]$^-$: 190.0 (100%).

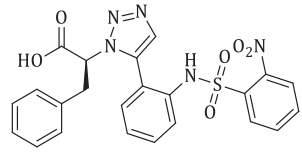

XI.7

Brutoformula: $C_{23}H_{18}N_5O_6S$
Molecular weight: 493.49 Da.
LC-(ESI)MS (condition 1): t_R = 13.3 min [M-H$^+$]$^-$: 492.0 (100%).

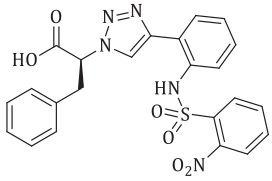

XI.35

Brutoformula: $C_{23}H_{18}N_5O_6S$
Molecular weight: 493.49 Da.
LC-(ESI)MS (condition 1): t_R = 13.5 min [M-H$^+$]$^-$: 492.0 (100%).

C. Second approach: Reductive alkylation

1. Reductive alkylation - benzaldehyde

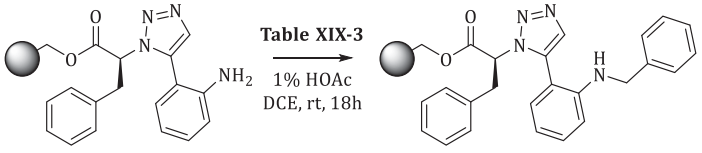

VIII.3 **XI.38**

The aniline intermediate **VIII.3** (prepared *via* procedure **P.01** – **P.04**, 0.03219 mmol, 1 eq) undergoes a reductive alkylation with benzaldehyde into the monoalkylated intermediate **XI.38**. Test reactions are performed with varying amounts of benzaldehyde (**Table XIX-3**, 3 eq, 6 eq and 10 eq) combined with $NaBH(OAc)_3$ (**Table XIX-3**, 2 eq, 4 eq, 6 eq) in dry

dichloroethane with 1% of HOAc. After 18 hours of reaction, the beads are isolated and washed with DMF (3x), MeOH (3x) and dichloromethane (3x). An aliquot of the beads is used for LC-MS analysis upon a cleavage reaction with TFA/H_2O (95/5).

Table XIX-3: Various conditions for reductive alkylation optimization for benzaldehyde

entry	conditions			
	benzaldehyde [eq]	$NaBH(OAc)_3$ [eq]	benzaldehyde [µl]	$NaBH(OAc)_3$ [mg]
1	3 eq	2 eq	10 µL	14.0 mg
2	6 eq	2 eq	20 µL	14.0 mg
3	10 eq	2 eq	30 µL	14.0 mg
4	3 eq	4 eq	10 µL	28.0 mg
5	6 eq	4 eq	20 µL	28.0 mg
6	10 eq	4 eq	30 µL	28.0 mg
7	3 eq	6 eq	10 µL	42.0 mg
8	6 eq	6 eq	20 µL	42.0 mg
9	10 eq	6 eq	30 µL	42.0 mg

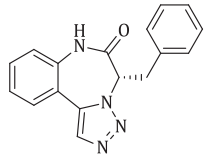

(*S*)-VIII.16

Brutoformula: $C_{17}H_{14}N_4O$
Molecular weight: 290.32 Da.
LC-(ESI)MS (condition 1): t_R = 14.5 min
$[M+H^+]^+$: 291.1 (100%).

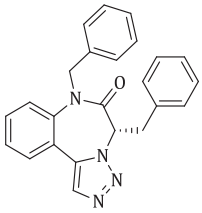

XI.51

Brutoformula: $C_{24}H_{20}N_4O$
Molecular weight: 380.44 Da.
LC-(ESI)MS (condition 1): t_R = 17.9 min
$[M+H^+]^+$: 381.1 (100%).

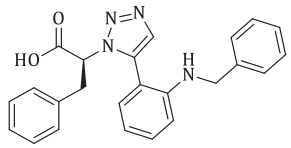

XI.52

Brutoformula: $C_{24}H_{22}N_4O_2$
Molecular weight: 398.46 Da.
LC-(ESI)MS (condition 1): t_R = 13.8 min
$[M+H^+]^+$: 399.1 (100%).

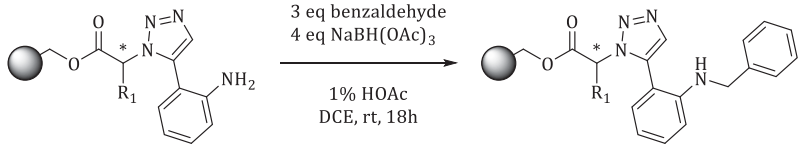

VIII.1 **XI.56**

General procedure **P.12:** Reductive alkylation benzaldehyde

The resin is prepared *via* general procedure **P.01** – **P.04**. Solid-phase bound aniline (1 eq, **VIII.1**) is dried extensively and treated with dry dichloroethane twice for 10 minutes. Afterwards, dichloroethane (0.05 M), HOAc 1 v/v% and benzaldehyde (3 eq) are added to the mixture. At last, $NaBH(OAc)_3$ (4 eq) is poured into the reaction vessel. The reaction is set up for 18 hours at room temperature for 18 hours. After this reaction time, the beads are isolated and washed extensively with DMF (1x), MeOH (3x), DMF (3x), MeOH (3x) and dichloromethane (3x). This advanced washing step is required in order to fully remove $NaBH(OAc)_3$ traces.

2. Scope of the reductive alkylation

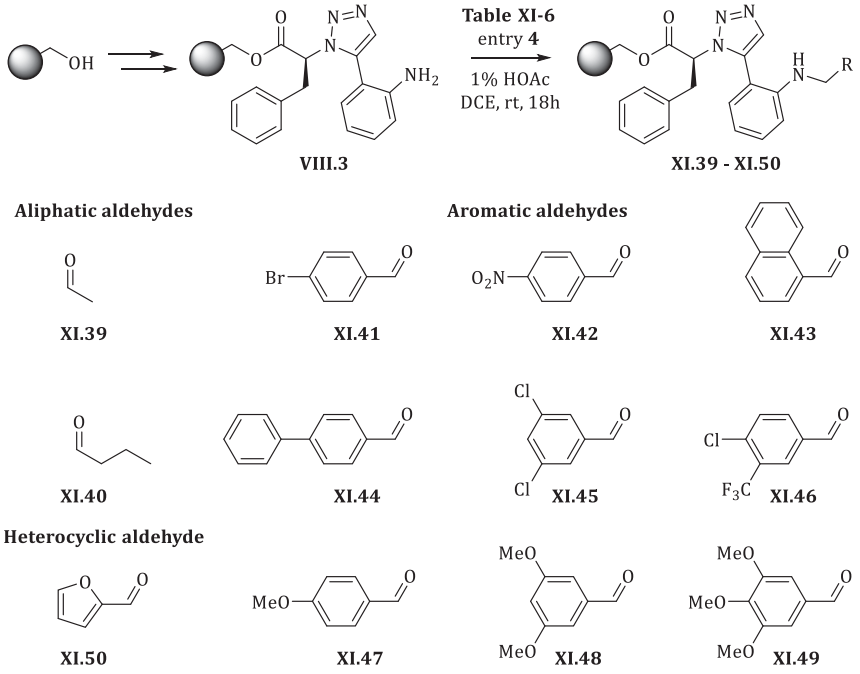

Scheme XIX-1: Scope of the reductive alkylation

The scope of the reductive alkylation was verified by applying the optimized conditions (General procedure **P.12**) to solid-phase bound intermediate **VIII.3** (prepared via procedure **P.01** – **P.04**, 0.01390 mmol, 1 eq) with aldehyde (**Table XIX-4**, 0.04170 mmol, 3 eq) and $NaBH(OAc)_3$ (12.0 mg, 0.05560 mmol, 4 eq) in dry dichloroethane (150 µL, 0.1M) with 1% HOAc for 18 hours. After the reaction time, the beads were isolated and washed with DMF (3x), MeOH (3x) and dichloromethane (3x). An aliquot of the resin was used to cleave with TFA/H_2O (95/5) for two hours at room temperature and the residue was used for LC-MS sample preparation.

Table XIX-4: Amounts for XI.42-XI-52

entry	conditions	
1	**XI.42**	2.3 µL
2	**XI.43**	4.5 µL
3	**XI.44**	5.0 µL
4	**XI.45**	6.3 mg
5	**XI.46**	6.5 mg
6	**XI.47**	7.6 mg
7	**XI.48**	7.3 mg
8	**XI.49**	6.0 µL
9	**XI.50**	5.0 µL
10	**XI.51**	6.9 mg
11	**XI.52**	8.1 mg

3. Test case: Cyclization/release of *N*-benzylated precursors

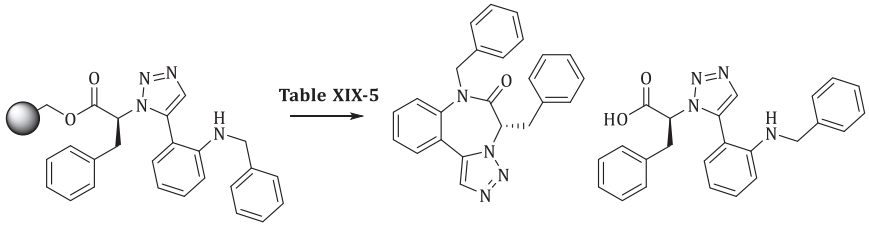

XI.38 **XI.51** **XI.52**

Intermediate **XI.38** is prepared *via* general procedure **P.12** and dried extensively under reduced pressure. This resin is divided in 16 reaction vessels (13 closed 1 mL vials and 3 microwave vessels). To each vessel, a reaction medium is added according to **Table XIX-5**. The test reactions are put at the designated temperature for a specific time (see **Table XIX-5**). Afterwards the supernatans is isolated and evaporated upon addition of respectively acetonitrile (2x 1 mL) for entries **1** - **8** and toluene (2x 1 mL) for entries **9** – **11** and **14** – **16**. An extractive workup for entries **12** – **13** with $NaHCO_3$ is performed. Upon evaporation, the residues are used for LC-MS sample preparation.

Table XIX-5: Test conditions applied for cyclization/release on intermediate XI.38

entry	conditions
1	TFA/H_2O (1/1), rt, 2h
2	TFA/H_2O (1/99), rt, 2h
3	TFA/CH_2Cl_2 (1/1), rt, 15 min
4	TFA/CH_2Cl_2 (1/1), 60°C, 15 min
5	TFA/DCE (1/1), rt, 15 min
6	TFA/DCE (1/1), 60°C, 15 min
7	TFA/DCE (1/99), rt, 24h
8	TFA/DCE (1/99), 60°C, 24h
9	HOAc/CH_2Cl_2 (1/1), rt, 24h
10	HOAc/DCE (1/1), rt, 24h
11	HOAc/DCE (1/1), 60°C, 72h
12	1M KOtBu, THF, rt, 24h
13	1M KOtBu, THF, 60°C, 24h
14	HOAc/DCE (1/1), 60°C, 15 min, power max off, stirring low.
15	HOAc/DCE (1/1), 60°C, 15 min, power max on, stirring low.
16	HOAc/DCE (1/1), 60°C, 1h, power max on, stirring low.

4. Optimization procedure for acetaldehyde

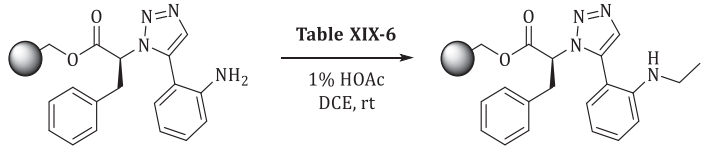

VIII.3 **XI.39**

After preparing intermediate **VIII.3** via general procedure **P.01 – P.04**, this resin (0.03219 mmol, 1 mmol) is added to a closed 1 mL vial, subsequently dichloroethane (0.1M), HOAc (1 v/v%), acetaldehyde (**Table XIX-6**) and $NaBH(OAc)_3$ (**Table XIX-6**) are added. After shaking, the beads are isolated and washed with DMF (3x), MeOH (3x) and dichloromethane (3x). An

aliquot of the reacted beads are cleaved via standard protocol (TFA/H_2O 95/5) and after evaporation, the residue is used for LC-MS sample preparation.

Table XIX-6: Various conditions for reductive alkylation optimization for acetaldehyde

entry	conditions				
	acetaldehyde [eq]	$NaBH(OAc)_3$ [eq]	acetaldehyde [µl]	$NaBH(OAc)_3$ [mg]	reaction time
1	3 eq	4 eq	5.4	27.2	18h
2	1 eq	1.25 eq	1.8	8.5	1h
3	1 eq	1.25 eq	1.8	8.5	2h
4	1 eq	1.25 eq	1.8	8.5	3h
5	1 eq	1 eq	1.8	6.8	3h
6	1 eq	1 eq	1.8	6.8	6h
7	1 eq	1 eq	1.8	6.8	8h
8	1 eq	1 eq	1.8	6.8	2x 8h

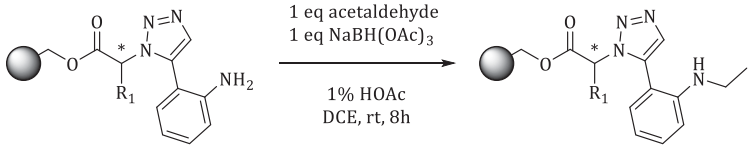

VIII.1 **XI.55**

General procedure **P.13**: Reductive alkylation acetaldehyde

The resin is prepared *via* general procedure **P.01** – **P.04**. Solid-phase bound aniline (1 eq, **VIII.1**) is dried extensively and treated with dry dichloroethane twice for 10 minutes. Afterwards, dichloroethane (0.05 M), HOAc 1 v/v% and acetaldehyde (1 eq) are added to the mixture. At last, $NaBH(OAc)_3$ (1 eq) is poured into the reaction vessel. The reaction is set up at room temperature for 8 hours. After this reaction time, the beads are isolated and washed extensively with DMF (1x), MeOH (3x), DMF (3x), MeOH (3x) and dichloromethane (3x). This advanced washing step is required in order to fully remove $NaBH(OAc)_3$ traces.

5. Test case: Cyclization/release of *N*-ethylated precursors

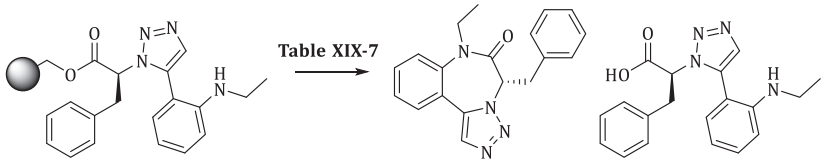

XI.39 **XI.53** **XI.54**

Intermediate **XI.39** is prepared *via* general procedure **P.13** and dried extensively under reduced pressure. This resin is poured in three closed 1 mL vials. To each vessel, a reaction medium is added according to **Table XIX-7**. The test reactions are put at the designated temperature for a specific time (see **Table XIX-7**). Afterwards the supernatans is isolated and evaporated upon addition of respectively acetonitrile (2x 1 mL) for entry **1** and toluene (2x 1 mL) for entries **2 – 3**. Upon evaporation, the residues are used for LC-MS sample preparation.

Table XIX-7: Test conditions applied for cyclization/release on intermediate XI.39

entry	conditions
1	TFA/H_2O (1/1), rt, 2u
2	HOAc/DCE (1/1), rt, 72h
3	HOAc/DCE (1/1), 60°C, 72h

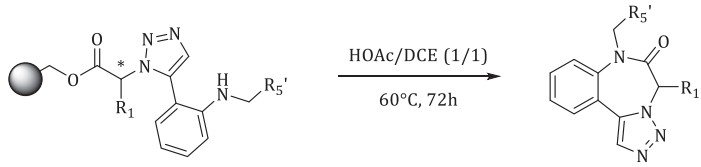

XI.55-XI.56 **XI.51 XI.53 XI.57 XI.58**

General procedure **P.14**: Cyclization/release for alkylated intermediates

The resin is prepared *via* general procedure **P.01 – P.04** and **P.12** or **P.13.** After extensive drying, the resin is poured into a pressure tube and dry dichloroethane is added. Subsequently, an equal volume of HOAc is added to the pressure tube as well. The reaction proceeds at 60°C for three days. Afterwards the supernatans is isolated and the beads are washed with dichloromethane. The filtrate is evaporated upon addition of toluene (3x) in order to fully remove HOAc traces. Further purification can be performed with flash chromatography.

6. Proof of principle library

1-ethyl[1,2,3]triazolo[1,5-*d*][1,4]benzodiazepin-2-one XI.57

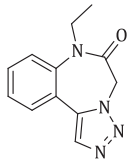

XI.57

Following general procedure **P.01** - **P.04, P.13** - **P.14** 1-ethyl[1,2,3]triazolo[1,5-*d*][1,4]benzodiazepin-2-one **XI.57** (16.8 mg, 0.07365 mmol).

Yield: 16%.
White solid.
R_F: 0.13 (dichloromethane/acetone 95/5)
Molecular weight: 228.10 Da.
^{1}H NMR (300 MHz, benzene-d_6) δ 0.65 (t, J = 7Hz, 3H), 3.46 (app s broad, 2H), 3.61-3.54 (m broad, 2H), 6.74-6.95 (m, 4H), 7.68 (s, 1H).
^{13}C NMR (75 MHz, benzene-d_6) δ 12.9 (CH_3), 44.5 (CH_2), 51.7 (CH_2), 127.6 (C), 127.9 (C), 123.6 (CH), 125.8 (CH), 129.5 (CH), 130.0 (CH), 130.8 (CH), 139.0 (C), 164.3 (C).
LC-(ESI)MS (condition 1): t_R = 12.8 min $[M+H^+]^+$: 229.1 (100%). **Purity** (214 nm): 99%.
HRMS (ESI) calcd for $C_{12}H_{13}N_4O^+$: 229.1084 $[M+H^+]^+$ found: 229.1087.

1-benzyl[1,2,3]triazolo[1,5-*d*][1,4]benzodiazepin-2-one XI.58

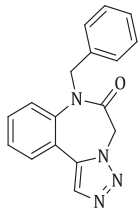

XI.58

Following general procedure **P.01** - **P.04, P.12** and **P.14** 1-benzyl[1,2,3]triazolo[1,5-*d*][1,4]benzodiazepin-2-one **XI.58** (10.7 mg, 0.03688 mmol).

Yield: 8%.
White solid.
R_F: 0.11(hexane/acetone: 6/4)
Molecular weight: 290.12 Da.

^{1}H NMR (300 MHz, benzene-d_6) δ 2.49-5.41 (m, 2H), 4.66 (s broad, 2H), 6.67 (td, J = 1.3Hz/7.5Hz, 1H), 6.78-6.91 (m, 8H), 7.64 (s, 1H).
^{13}C NMR (75 MHz, benzene-d_6) δ 51.5 (CH_2), 52.7 (CH_2), 121.5 (C), 123.7 (CH), 126.0 (CH), 127.1 (CH), 127.4 (CH), 128.6 (CH), 129.4 (CH), 130.0 (CH), 130.8 (CH), 134.5 (C), 137.0 (C), 139.1 (C), 165.0 (C).
LC-(ESI)MS (condition 1): t_R = 14.8 min $[M+H^+]^+$: 291.1 (100%). **Purity** (214 nm): 99%.

D. Solid-phase synthesis using HMPS resin

1. Synthesis of XI.66 on HMPS resin

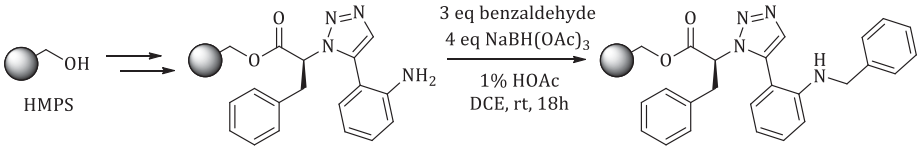

XI.60 **XI.61** **XI.66**

HMPS resin is coupled with Fmoc-(L)-Phe-OH according to general procedure **P.01**. After loading determination (loading: 0.5870 mmol.g^{-1}), the Fmoc-group is removed *via* standard conditions (**P.02**). Subsequently a diazotransfer reaction is performed by following general procedure **P.03** and the resulting azide is converted into 1,5-disubstituted triazole moiety according to procedure **P.04**. Afterwards, a reductive alkylation with benzaldehyde is done by following procedure **P.12**.

Cleavage: An aliquot of resin is cleaved with TFA/H_2O (95/5) for two hours at room temperature. After this time, the beads are filtered off and the washed with dichloromethane (3x 1 mL). The filtrate is evaporated azeotropically with acetonitrile (3x 1 mL) and subsequently used for LC-MS sample preparation.

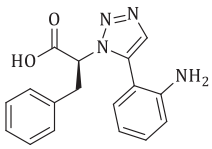

VIII.5

Brutoformula: $C_{17}H_{16}N_4O_2$
Molecular weight: 308.33 Da.
LC-(ESI)MS (condition 1): t_R = 11.6 min $[M+H^+]^+$: 309.1 (100%).

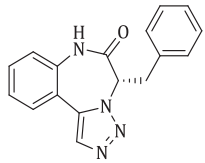

(*S*)-VIII.16

Brutoformula: $C_{17}H_{18}N_4O$
Molecular weight: 290.32 Da.
LC-(ESI)MS (condition 1): t_R = 14.4 min $[M+H^+]^+$: 291.1 (100%).

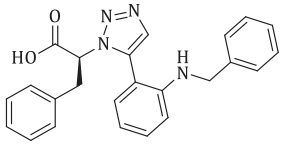

XI.52

Brutoformula: $C_{24}H_{22}N_4O_2$
Molecular weight: 398.46 Da.
LC-(ESI)MS (condition 1): t_R = 13.8 min $[M+H^+]^+$: 399.1 (100%).

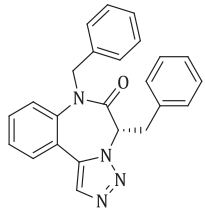

XI.51

Brutoformula: $C_{24}H_{20}N_4O$
Molecular weight: 380.44 Da.
Not detected.

2. Cyclization/release on HMPS-resin for intermediate XI.66

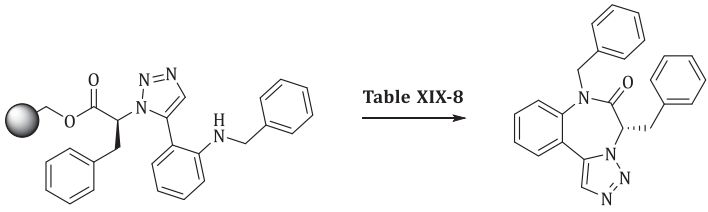

XI.66 **XI.51**

To twelve vials (closed 1 mL vials or microwave vessels), resin **XI.66** (20 mg, 1 eq) is added. To each of these vials a reaction medium is added according to **Table XIX-8**. Entries **1 – 5** are put into the shaker for eight hours, while entries **6 – 12** are used for microwave assisted cleavage conditions.

After the specific reaction time, the supernatans is isolated. For entries **1 – 5**, acetonitrile (2x 1mL) is added to assist azeotropic evaporation. For entries **6 – 9** and **12**, upon addition of H_2O (8mL) an extraction is performed with pentane (3x 10mL). For entry **10**, toluene (2x 1 mL) is added to fully remove HOAc. After evaporation, all residues are used for LC-MS preparation.

Table XIX-8: Test conditions applied for cyclization/release on intermediate XI.66

entry	conditions
1	1 mL TFA/CH_2Cl_2 (1/1), rt, 8h
2	1 mL TFA/CH_2Cl_2 (1/9), rt, 8h
3	1 mL TFA/CH_2Cl_2 (1/1), 60°C, 8h
4	1 mL TFA/CH_2Cl_2 (1/9), 60°C, 8h
5	1 mL TFA (100%), rt, 8h
6	1 mL DMF, 130°C, 15 min, powermax off, stirring low.
7	1 mL DMF, 130°C, 15 min, powermax on, stirring low.
8	1 mL DMF, 150°C, 20 min, powermax off, stirring low.
9	1 mL DMF, 150°C, 20 min, powermax on, stirring low.
10	1 mL HOAc/DCE (1/1), 100°C, 15 min, powermax on, stirring low.
11	1 mL DCE, 80°C, 15 min, powermax on, stirring low.
12	1 mL DMF, 150°C, 20 min, powermax off, stirring low.

3. Synthesis of XI.65 on HMPS resin and cyclization/release

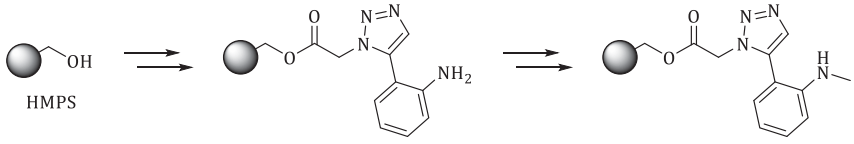

XI.60 **XI.61** **XI.64**

HMPS resin is coupled with Fmoc-Gly-OH according to general procedure **P.01**. After loading determination (loading: 0.6403 $mmol.g^{-1}$), the Fmoc-group is removed *via* standard conditions (**P.02**). Subsequently a diazotransfer reaction is performed by following general procedure **P.03** and the resulting azide is converted into 1,5-disubstituted triazole moiety according to procedure **P.04**. Afterwards, a o-Ns activating group is introduced according general procedure **P.09**. After employing a Mitsunobu-Fukuyama alkylation with MeOH (**P.10**), the o-Ns group is removed according to **P.12.**

Cleavage: Intermediate **XI.64** (100 mg, 1 eq) is transferred in a microwave vessel. After adding 3 mL of DMF, the vessel is put in the microwave apparatus and a temperature of 150°C for 20 minutes with powermax on are applied. Afterwards, the supernatans is isolated, extracted with pentane (3x 4 mL) and the organic phase is evaporated. The residue is used for LC-MS analysis.

E. Third approach: *N*-alkylation in solution-phase

1. *N*-alkylation in solution-phase

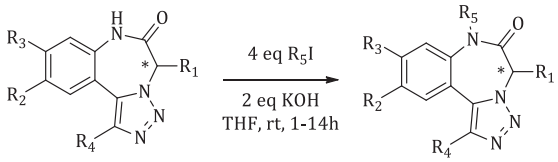

IX.1 **V.2**

General procedure **P.15**: After dissolving compound **IX.1** (1 eq) in THF in a closed 1 mL vessel, subsequently potassium hydroxide (2 eq) and alkyl halide (4 eq) are added to the mixture. The reaction is followed by TLC upon completion. After completion the mixture is transferred in a 5 mL flask and evaporated under reduced pressure. Then, this residue is loaded on silica and purified via flash chromatography.

1-methyl[1,2,3]triazolo[1,5-*d*][1,4]benzodiazepin-2-XI.65

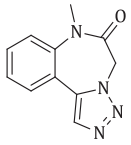

XI.65

Following general procedure **P.15**: [1,2,3]triazolo[1,5-*d*][1,4]benzodiazepin-2-one (**VIII.12**, 20.6 mg, 0.09991 mmol, 1 eq). methyliodide (26 µL, 0.3996 mmol, 4 eq). potassium hydroxide (11.2 mg, 0.1998 mmol, 2 eq). THF (1.0 mL).

Yield: 88%. 1-methyl[1,2,3]triazolo[1,5-*d*][1,4]benzodiazepin-2-one (**XI.65**, 18.8 mg, 0.08776 mmol).
Overall yield: 39%.
White solid.
R_F: 0.06 (hexane/acetone: 8/2). 0.23 (hexane/acetone: 6/4).

Molecular weight: 214.22 Da.
^{1}H NMR (500 MHz, acetone-d_6, **278K**) δ 3.35 (s, 3H), 4.79-5.03 (m, 1H), 5.18-5.42 (m, 1H), 7.40-7.47 (m, 1H), 7.62-7.64 (m, 2H), 7.70-7.72 (m, 1H), 8.04 (s, 1H).
^{1}H NMR (300 MHz, acetone-d_6, **298K**) δ 3.35 (s, 3H), 5.10 (s broad, 2H), 7.40-7.47 (m, 1H), 7.62-7.72 (m, 3H), 8.04 (s, 1H).
^{1}H NMR (500 MHz, acetone-d_6, **313K**) δ 3.36 (s, 3H), 5.10 (s, 2H), 7.40-7.44 (m, 1H), 7.62-7.65 (m, 2H), 7.69-7.71 (m, 1H), 8.02 (s, 1H).
^{13}C NMR (75 MHz, acetone-d_6, **298K**) δ 37.3 (CH_3), 52.7 (CH_2), 120.1 (C), 121.1 (C), 124.6 (CH), 126.9 (CH), 130.2 (CH), 131.6 (CH), 135.7 (C), 141.3 (C), 166.5 (C).
HATR (cm^{-1}): 3452 (w, broad), 3127 (w), 3031 (w), 2946 (w), 1659 (s), 1609 (w), 1582 (w), 1488 (m), 1475 (m), 1438 (m), 1426 (m), 1374 (s), 1305 (w), 1290 (w), 1264 (m), 1247 (m), 1196 (w), 1149 (w), 1119 (m), 1046 (m), 972 (m), 957 (w), 924 (w), 824 (m), 771 (m), 738 (w), 655 (w).
LC-(ESI)MS (condition 1): t_R = 11.8 min $[M+H^+]^+$: 215.1 (100%). **Purity** (214 nm): 97%.
HRMS (ESI) calcd for $C_{11}H_{11}N_4O^+$: 215.0927 $[M+H^+]^+$ found: 215.0926.

1-ethyl[1,2,3]triazolo[1,5-*d*][1,4]benzodiazepin-2-one XI.57

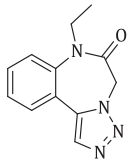

XI.57

Following general procedure **P.15**: [1,2,3]triazolo[1,5-*d*][1,4]benzodiazepin-2-one (**VIII.12**, 25.6 mg, 0.1279 mmol, 1 eq). ethyliodide (40 µL, 0.5116 mmol, 4 eq). potassium hydroxide (14.4 mg, 0.2558 mmol, 2 eq). THF (1.2 mL).

Yield: 89%. 1-ethyl[1,2,3]triazolo[1,5-*d*][1,4]benzodiazepin-2-one (**XI.57**, 26.0 mg, 0.1139 mmol).
Overall yield: 35%.
White solid.
R_F: 0.05 (hexane/acetone: 8/2). 0.30 (hexane/acetone: 6/4).
Molecular weight: 228.25 Da.
^{1}H NMR (500 MHz, acetone-d_6, **223K**) δ 1.00 (t, J = 7.1Hz, 3H), 3.74-3.81 (m, 1H), 4.02-4.09 (m, 1H), 4.87-4.90 (m, 1H), 5.29-5.31 (m, 1H), 7.46 (td, J = 1.3Hz/7.6Hz, 1H), 7.66 (td, J = 1.5Hz/7.4Hz, 1H), 7.72-7.73 (m, 2H), 8.14 (s, 1H).
^{1}H NMR (300 MHz, acetone-d_6, **298K**) δ 1.00 (t, J = 7.0Hz, 3H), 3.95 (m broad, 2H), 5.06 (m broad, 2H), 7.45 (td, J = 1.3Hz/7.1Hz, 1H), 7.63 (td, J = 1.5Hz/7.0Hz , 1H), 7.68-7.73 (m, 2H), 8.05 (s, 1H).

^{1}H NMR (500 MHz, acetone-d_6, **328K**) δ 1.01 (t, J = 7.1Hz, 3H), 3.96 (app s broad, 2H), 5.06 (s broad, 2H), 7.43-7.46 (m, 1H), 7.62-7.72 (m, 3H), 8.04 (s, 1H).
^{13}C NMR (75 MHz, acetone-d_6, **298K**) δ 13.4 (CH_3), 45.2 (CH_2), 53.0 (CH_2), 122.4 (C), 125.2 (CH), 127.2 (CH), 130.4 (CH), 131.5 (CH), 131.7 (CH), 135.7 (C), 140.0 (C), 165.5 (C).
HATR (cm^{-1}): 3077 (m), 2909 (m), 2490 (w), 2014 (m), 1922 (w), 1671 (s), 1612 (m), 1581 (m), 1563 (m), 1484 (s), 1449 (m), 1429 (m), 1405 (s), 1390 (s), 1276 (m), 1261 (m), 1244 (m), 1165 (w), 1103 (m), 1016 (m), 977 (m), 952 (m), 795 (s), 758 (s), 739 (m), 668 (m).
LC-(ESI)MS (condition 1): t_R = 12.9 min $[M+H^+]^+$: 229.1 (100%). **Purity** (214 nm): 99%.
HRMS (ESI) calcd for $C_{12}H_{13}N_4O^+$: 229.1084 $[M+H^+]^+$ found: 229.1087.

1-isopropyl[1,2,3]triazolo[1,5-*d*][1,4]benzodiazepin-2-one XI.72

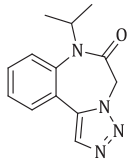

XI.72

Following general procedure **P.15**: [1,2,3]triazolo[1,5-*d*][1,4]benzodiazepin-2-one (**VIII.12**, 19.6 mg, 0.09791 mmol, 1 eq). isopropyliodide (40 µL, 0.3916 mmol, 4 eq). potassium hydroxide (11.0 mg, 0.1958 mmol, 2 eq). THF (975 µL).

Yield: 50%. 1-isopropyl[1,2,3]triazolo[1,5-*d*][1,4]benzodiazepin-2-one (**XI.72**, 11.9 mg, 0.04912 mmol).
Overall yield: 22%
White solid.
R_F: 0.13 (hexane/acetone: 7/3).
Molecular weight: 242.28 Da.
^{1}H NMR (300 MHz, acetone-d_6) δ 1.15 (d broad, J = 7.0Hz, 3H), 1.40 (d broad, J = 6.7Hz, 3H), 4.35 (septet, J = 7.0Hz, 1H), 4.75-4.79 (m, 1H), 5.18-5.23 (m, 1H), 7.45-7.50 (m, 1H), 7.58-7.71 (m, 3H), 8.05 (s, 1H).
^{13}C NMR (75 MHz, acetone-d_6) δ 20.3 (CH_3), 21.9 (CH_3), 53.6 (CH_2), 54.4 (CH), 126.5 (CH), 127.8 (CH), 128.8 (C), 130.4 (CH), 131.1 (CH), 131.3 (CH).
HATR (cm^{-1}): 2970 (m), 2925 (m), 1673 (s), 1650 (m), 1631 (m), 1608 (w), 1508 (w), 1483 (w), 1457 (w), 1438 (w), 1394 (w), 1363 (m), 1268 (w), 1243 (w), 1134 (w), 1106 (w), 996 (w), 968 (w), 817 (w), 768 (w).
LC-(ESI)MS (condition 1): t_R = 13.4 min $[M+H^+]^+$: 243.1 (100%). **Purity** (214 nm): 98%.
HRMS (ESI) calcd for $C_{13}H_{15}N_4O^+$: 243.1240 $[M+H^+]^+$ found: 243.1243.

1-benzyl-8-chloro[1,2,3]triazolo[1,5-*d*][1,4]benzodiazepin-2-one XI.73

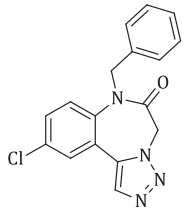

XI.73

Following general procedure **P.15**: 8-chloro[1,2,3]triazolo[1,5-*d*][1,4]benzodiazepin-2-one (**VIII.47,** 28.0 mg, 0.1197 mmol, 1 eq). benzylbromide (56 µL, 0.4788 mmol, 4 eq). potassium hydroxide (13.4 mg, 0.2394 mmol, 2 eq). THF (1.2 mL).

Yield: 79%. 1-benzyl-8-chloro[1,2,3]triazolo[1,5-*d*][1,4]benzodiazepin-2-one (**XI.73**, 30.6 mg, 0.09442 mmol).
Overall yield: 48%.
White solid.
R_F: 0.11 (hexane/acetone: 8/2). 0.38 (hexane/acetone: 6/4).
Molecular weight: 324.08 Da.
^{1}H NMR (300 MHz, acetone-d_6) δ 5.04-5.45 (m broad, 4H), 6.95-6.98 (m, 2H), 7.14-7.21 (m, 3H), 7.54 (dd, J = 2.5Hz/8.9Hz, 1H), 7.66-7.70 (m, 2H), 8.11 (s, 1H).
^{13}C NMR (75 MHz, acetone-d_6) δ 52.8 (CH_2), 52.9 (CH_2), 124.2 (C), 127.3 (CH), 127.8 (CH), 128.1 (CH), 129.3 (CH), 129.7 (CH), 131.3 (CH), 132.0 (C), 132.2 (CH), 134.7 (C), 137.7 (C), 138.8 (C), 166.2 (C).
HATR (cm^{-1}): 3435 (w, br), 3059 (w), 3029 (w), 2936 (w), 1676 (s), 1604 (w), 1483 (m), 1452 (m), 1427 (m), 1404 (m), 1374 (m), 1334 (m), 1292 (m), 1261 (m), 1241 (m), 1217 (m), 1105 (m), 1080 (m), 1017 (m), 975 (m), 918 (w), 881 (w), 829 (m), 802 (m), 734 (m), 697 (m), 672 (m), 642 (w).
LC-(ESI)MS (condition 1): t_R = 15.8 min $[M+H^+]^+$: 325.1 (100%). **Purity** (214 nm): 96%.
HRMS (ESI) calcd for $C_{17}H_{14}ClN_4O^+$: 325.0851 $[M+H^+]^+$ found: 325.0854.

***(rac)*-3-benzyl-1-methyl[1,2,3]triazolo[1,5-*d*][1,4]benzodiazepin-2-one (*rac*)-XI.28**

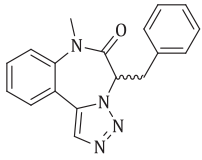

(*rac*)-XI.28

Following general procedure **P.15**: *(S)*-3-benzyl[1,2,3]triazolo[1,5-*d*][1,4]benzodiazepin-2-one (***(S)*-VIII.16**, 25.1 mg, 0.08646 mmol, 1 eq). methyliodide (21 µL, 0.3458 mmol, 4 eq). potassium hydroxide (9.8 mg, 0.1729 mmol, 2 eq). THF (850 µL).

Yield: 81%. *(rac)*-3-benzyl-1-methyl[1,2,3]triazolo[1,5-*d*][1,4]benzodiazepin-2-one (**(*rac*)-XI.28**, 21.3 mg, 0.06999 mmol).
Overall yield: 44%.
White solid.
Molecular weight: 304.34 Da.
R_F: 0.39 (hexane/acetone: 6/4). 0.11 (hexane/acetone: 8/2).
^{1}H NMR (300 MHz, acetone-d_6) δ 3.35 (s broad, 3H), 3.56-4.20 (m broad, 2H), 4.61-5.49 (m broad, 0.76H, A), 5.55-6.32 (m broad, 0.24H, B), 6.67-7.95 (m, 9H), 8.03 (s, 1H).
^{13}C NMR (75 MHz, acetone-d_6) δ 124.8 (CH, broad), 127.0 (CH), 127.5 (CH, broad), 129.1 (CH), 129.9 (CH), 130.5 (CH, broad), 131.7 (CH), 167.1 (C).
HATR (cm^{-1}): 3452 (w, br), 3071 (w), 3030 (w), 2942 (w), 1674 (s), 1606 (m), 1582 (w), 1480 (m), 1454 (m), 1418 (m), 1375 (m), 1298 (w), 1252 (w), 1223 (w), 1192 (w), 1126 (m), 1085 (w), 1049 (w), 970 (m), 835 (w), 768 (m), 699 (m), 656 (w), 612 (w).
LC-(ESI)MS (condition 1): t_R = 15.5 min $[M+H^+]^+$: 305.1 (100%). **Purity** (214 nm): 96%.
HRMS (ESI) calcd for $C_{18}H_{17}N_4O^+$: 305.1397 $[M+H^+]^+$ found: 305.1405.

(rac)-3-benzyl-1-ethyl[1,2,3]triazolo[1,5-*d*][1,4]benzodiazepin-2-one (*rac*)-XI.29

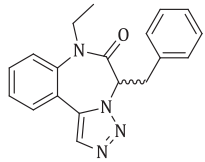

(*rac*)-XI.29

Following general procedure **P.15**: *(S)*-3-benzyl[1,2,3]triazolo[1,5-*d*][1,4]benzodiazepin-2-one (***(S)*-VIII.16**, 28.5 mg, 0.09817 mmol, 1 eq). ethyliodide (32 µL, 0.3926 mmol, 4 eq). potassium hydroxide (11.0 mg, 0.1963 mmol, 2 eq). THF (1.0 mL).

Yield: 81%. *(rac)*-3-benzyl-1-ethyl[1,2,3]triazolo[1,5-*d*][1,4]benzodiazepin-2-one (**(*rac*)-XI.29**, 25.3 mg, 0.07947 mmol).
Overall yield: 44%.
White solid.
Molecular weight: 318.37 Da.
R_F: 0.38 (hexane/acetone: 6/4). 0.13 (hexane/acetone: 8/2).
^{1}H NMR (500 MHz, acetone-d_6) δ 0.86 (t, J = 7.3Hz, 2.4H, A), 1.10 (t, J = 7.0Hz, 0.6H, B), 2.74-2.91 (ABX, J_{AX} = 9.8Hz, J_{BX} = 8.2Hz, J_{AB} = 13.7Hz, 0.4H, B), 3.67-3.74 (m, 0.8H, A), 3.86-4.01 (m,

2H, A+B), 4.09-4.16 (m, 0.8H, B). 5.00 (t, *J* = 7.0Hz, 0.8H, A), 5.82 (t, *J* = 9.2 Hz, 0.2H, B), 6.97 (app d, *J* = 7.0Hz, 0.4H, B), 7.14-7.23 (m, 3H, A+B), 7.43-7.46 (m, 2.4H, A), 7.52 (t, *J* = 7.3Hz, 0.2H, B), 7.61-7.69 (m, 2.4H, A), 7.72 (t, *J* = 7.3Hz, 0.2H, B), 7.80-7.85 (m, 0.4H, B), 8.07 (s, 0.8H, A), 8.12 (s, 0.2H, B).

^{13}C NMR (75 MHz, acetone-d_6) δ 13.2 (CH_3, A), 14.3 (CH_3, B), 32.7 (CH_2, A), 34.8 (CH_2, B), 45.2 (CH_2, A), 46.7 (CH_2, B), 61.7 (CH, A), 68.4 (CH, B), 123.1 (C), 124.4 (CH, B), 125.3 (CH, B), 127.3 (CH, A+B), 129.0 (CH, A), 129.4 (CH, B), 129.8 (CH, B), 130.2 (CH, A+B), 130.6 (CH, A), 131.5 (CH, B), 131.8 (CH, A), 135.9 (C), 138.5 (C), 140.1 (C), 166.0 (C).

HATR (cm^{-1}): 3476 (w, br), 3330 (w), 2974 (w), 2934 (w), 1671 (s, br), 1606 (m), 1579 (w), 1557 (w), 1495 (m), 1475 (m), 1454 (m), 1430 (m), 1415 (m), 1389 (m), 1359 (m), 1305 (m), 1244 (m), 1217 (m), 1191 (m), 1131 (m), 1112 (m), 1086 (m), 1066 (w), 1052 (w), 1029 (w), 969 (m), 915 (w), 890 (w), 831 (w), 799 (w), 866 (m), 765 (s), 732 (s), 698 (s), 655 (m), 621 (w).

LC-(ESI)MS (condition 1): t_R = 16.2 min $[M+H^+]^+$: 319.1 (100%). **Purity** (214 nm): 98%.

HRMS (ESI) calcd for $C_{19}H_{19}N_4O^+$: 319.1553 $[M+H^+]^+$ found: 319.1560.

(rac)-3-benzyl-1-isopropyl[1,2,3]triazolo[1,5-*d*][1,4]benzodiazepin-2-one (*rac*)-XI.30

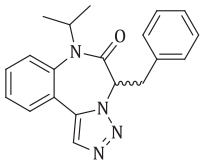

(*rac*)-XI.30

Following general procedure **P.15**: *(S)*-3-benzyl[1,2,3]triazolo[1,5-*d*][1,4]benzodiazepin-2-one , (**(*S*)-VIII.16**, 50.2 mg, 0.1729 mmol, 1 eq). isopropyliodide (69 µL, 0.6916 mmol, 4 eq). potassium hydroxide (19.4 mg, 0.3458 mmol, 2 eq). THF (1.750 mL).

Yield: 41%. *(rac)*-3-benzyl-1-isopropyl[1,2,3]triazolo[1,5-*d*][1,4]benzodiazepin-2-one (**(*rac*)-XI.30**, 23.6 mg, 0.07100 mmol).

Overall yield: 22%.

White solid.

Molecular weight: 332.40 Da.

R_F: 0.44 (hexane/acetone: 6/4). 0.14 (hexane/acetone: 8/2).

^{1}H NMR (700 MHz, acetone-d_6) δ 1.07 (d, *J* = 7.0Hz, 2.3H, A), 1.22 (d, *J* = 7.0Hz, 0.7H, B), 1.33 (d, *J* = 7.0Hz, 2.3H, A), 1.40 (d, *J* = 6.6Hz, 0.7H, B), 2.68-2.84 (ABX, J_{AX} = 8.8Hz, J_{BX} = 9.3Hz, J_{AB} = 13.7Hz, 0.5H, B), 3.85-3.96 (ABX, J_{AX} = 6.6Hz, J_{BX} = 7.0Hz, J_{AB} = 14.5Hz, 1.5H, A), 4.38 (septet, *J* = 6.6Hz, 1H, A+B), 4.93 (t, *J* = 7.0Hz, 0.75Hz, A), 5.74 (t, *J* = 9.3Hz, 0.25H, B), 6.96 (app d, *J* = 7.1Hz, 0.5H, B), 7.13-7.22 (m, 3H, A+B), 7.40-7.41 (m, 1.5H, A), 7.46-7.49 (m, 0.75H, A), 7.54

(td, *J* = 0.9Hz/7.5Hz, 0.25H, B), 7.60 (m, 1.5H, A), 7.66 (app dd, *J* = 0.9Hz/7.5Hz, 0.75H, A), 7.71 (td, *J* = 1.4Hz/8.4Hz, 0.25H, B), 7.76 (d, *J* = 8.4Hz, 0.25H), 7.80 (dd, *J* = 1.3Hz/7.5Hz, 0.50H, B), 8.03 (s, 0.75H, A), 8.06 (s, 0.25H, B).

^{13}C NMR (176 MHz, acetone-d_6) δ 20.2 (CH_3, B). 20.3 (CH_3, A), 21.7 (CH_3, B), 21.8 (CH_3, A), 32.6 (CH_2, A), 34.9 (CH_2, B), 54.3 (CH, A), 55.8 (CH, B), 62.3 (CH, A), 69.1 (CH, B), 122.8 (C), 124.0 (C), 125.9 (CH, B), 126.6 (CH, A), 127.3 (CH, A+B), 127.9 (CH, B), 127.9 (CH, A), 129.0 (CH, A+B), 129.4 (CH, A), 129.7 (CH, B), 130.2 (CH, A), 130.3 (CH, B), 130.6 (CH, A), 131.1 (CH, A), 131.3 (CH, A), 131.5 (CH,B), 132.1 (CH,B), 135.8 (C, B), 138.6 (C, A), 139.0 (C, B), 139.6 (C, A), 167.0 (C).

HATR (cm^{-1}): 3401 (w, br), 3054 (w), 3026 (w), 2973 (w), 2936 (w), 1673 (s), 1606 (m), 1580 (w), 1495 (m), 1478 (m), 1454 (m), 1416 (m), 1394 (m), 1368 (m), 1340 (m), 1317 (m), 1240 (m), 1215 (m), 1179 (m), 1125 (m), 1100 (m), 1084 (m), 1033 (w), 971 (m), 833 (w), 768 (m), 751 (m), 737 (m), 699 (m), 658 (w), 625 (w).

LC-(ESI)MS (condition 1): t_R = 17.0 min $[M+H^+]^+$: 333.1 (100%). Purity (214 nm): 94%.

HRMS (ESI) calcd for $C_{20}H_{21}N_4O^+$: 333.1710 $[M+H^+]^+$ found: 333.1716.

(rac)-3-benzyl-1-butyl[1,2,3]triazolo[1,5-*d*][1,4]benzodiazepin-2-one (*rac*)-XI.74

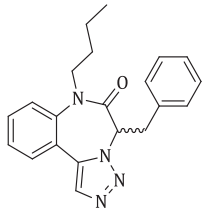

(*rac*)-XI.74

Following general procedure **P.15**: *(S)*-3-benzyl[1,2,3]triazolo[1,5-*d*][1,4]benzodiazepin-2-one (**(*S*)-VIII.16**, 40.5 mg, 0.1395 mmol, 1 eq). butyliodide (63 µL, 0.5560 mmol, 4 eq). potassium hydroxide (15.6 mg, 0.2780 mmol, 2 eq). THF (1.400 mL).

Yield: 59%. *(rac)*-3-benzyl-1-butyl[1,2,3]triazolo[1,5-*d*][1,4]benzodiazepin-2-one (**(*rac*)-XI.74**, 28.5 mg, 0.08227 mmol).

Overall yield: 32%.

White solid.

Molecular weight: 346.43 Da.

R_F: 0.48 (hexane/acetone: 6/4). R_F: 0.16 (hexane/acetone: 8/2).

^{1}H NMR (700 MHz, acetone-d_6) δ 0.67 (t, *J* = 7.5Hz, 2.4H, A), 0.72-0.74 (m, 0.6H, B), 0.85-1.05 (m, 2H, A+B), 1.11-1.45 (m, 2H, A+B), 2.73-2.76 (m, 0.2H, B), 2.91-2.94 (m, 0.2H, B), 3.62-3.66 (m, 0.8H, A), 3.77-3.82 (m, 0.2H, B), 3.90-3.98 (m, 1.6H, A), 4.19-4.23 (m, 0.2H, B), 4.27-4.33 (m, 0.8H, A), 5.00 (t, J = 7.0Hz, 0.8H, A), 5.84-5.86 (m, 0.2H, B), 6.95-6.96 (m, 0.2H, B), 7.15-7.23 (m, 3H, A+B), 7.43-7.46 (m, 2.6H, 3A+B), 7.52-7.54 (m, 0.2H, B), 7.63 (t, *J* = 7.5Hz, 0.8H,

A), 7.68 (t, *J* = 8.8Hz, 1.6H, 2A), 7.72-7.74 (m, 0.2H, B), 7.80-7.84 (m, 0.4H, 2B), 8.05 (s, 0.8H, A), 8.08 (s, 0.2H, B).
^{13}C NMR (175 MHz, acetone-d_6) δ 13.7 (CH_3, A), 14.3 (CH_3, B), 20.0 (CH_2, A), 20.3 (CH_2, B), 30.3 (CH_2, A), 30.4 (CH_2, B), 32.8 (CH_2, A), 34.9 (CH_2, B), 49.3 (CH_2, A), 50.4 (CH_2, B), 61.7 (CH, A), 68.5 (CH, B), 123.3 (C), 124.7 (C), 125.0 (CH, B), 125.6 (CH, A), 127.4 (CH, 2A+B), 128.1 (CH, B), 129.0 (CH, 2A+B), 129.4 (CH, B), 129.7 (CH, B), 130.2 (CH, A), 130.7 (CH, A+B), 131.4 (CH, A), 131.7 (CH, A), 132.0 (CH, B), 132.3 (CH, B), 135.9 (C), 138.6 (C), 140.1 (C), 166.6 (C).
HATR (cm^{-1}): 3408 (w, broad), 3029 (w), 2958 (m), 2931 (m), 2871 (m), 1673 (s), 1606 (m), 1579 (m), 1496 (w), 1478 (m), 1455 (m), 1431 (m), 1415 (m), 1389 (m), 1300 (w), 1240 (m), 1215 (m), 1137 (w), 1113 (w), 1086 (w), 1030 (w), 1011 (w), 969 (m), 828 (w), 766 (m), 751 (m), 699 (m), 656 (w), 622 (w).
LC-(ESI)MS (condition 1): t_R = 17.7 min $[M+H^+]^+$: 347.1 (100%). **Purity** (214 nm): 99%.
HRMS (ESI) calcd for $C_{21}H_{23}N_4O^+$: 347.1866 $[M+H^+]^+$ found: 347.1872.

(rac)-3-benzyl-1-decyl[1,2,3]triazolo[1,5-*d*][1,4]benzodiazepin-2-one (*rac*)-XI.75

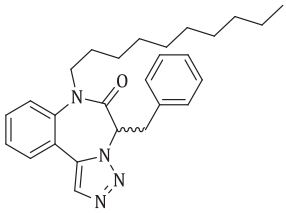

(*rac*)-XI.75

Following general procedure **P.15**: *(S)*-3-benzyl[1,2,3]triazolo[1,5-*d*][1,4]benzodiazepin-2-one (**(*S*)-VIII.16**, 48.0 mg, 0.1653 mmol, 1 eq). decyliodide (152 µL, 0.6612 mmol, 4 eq). potassium hydroxide (19.6 mg, 0.3306 mmol, 2 eq). THF (1.650 mL).

Yield: 55%. (*rac)*-3-benzyl-1-decyl[1,2,3]triazolo[1,5-*d*][1,4]benzodiazepin-2-one (**(*rac*)-XI.75**, 39.1 mg, 0.09081 mmol).
Overall yield: 30%.
White solid.
Molecular weight: 430.59 Da.
R_F: 0.51 (hexane/acetone: 6/4). 0.25 (hexane/acetone: 8/2).
^{1}H NMR (700 MHz, acetone-d_6) δ 0.87 (t, J = 7.5Hz, 3H), 0.97-1.33 (m, 16H), 2.73-2.76 (m, 0.2H, B), 2.90-2.94 (m, 0.2H, B), 3.62-3.66 (m, 0.8H, A), 3.77-3.83 (m, 0.2H, B), 3.90-3.98 (m, 1.6H, A), 4.20-4.24 (m, 0.2H, B), 4.28-4.33 (m, 0.8H, A), 5.00 (t, J = 7.0Hz, 0.8H, A), 5.84-5.86 (app t, 0.2H, B), 6.95-6.96 (app d, 0.2H, B), 7.15-7.23 (m, 3H, A+B), 7.43-7.46 (m, 2.6H, 3A+B), 7.52-7.54 (m, 0.2H, B), 7.63 (t, *J* = 7.9Hz, 0.8H, A), 7.67-7.70 (m, 1.6H, 2A), 7.72-7.74 (m, 0.2H, B), 7.80-7.84 (app dd, 0.4H, 2B), 8.05 (s, 0.8H, A), 8.07 (s, 0.2H, B).

^{13}C NMR (175 MHz, acetone-d_6) δ 14.4 (CH_3, A+B), 23.3 (CH_2, A+B), 26.8 (CH_2, A), 27.0 (CH_2, B), 28.1 (CH_2, A+B), 29.6 (CH_2, A+B), 30.0 (CH_2, A+B), 32.6 (CH_2, A), 32.8 (CH_2, A+B), 34.9 (CH_2, B), 49.4 (CH_2, A), 50.5 (CH_2, B), 61.7 (CH_2, A), 68.5 (CH_2, B), 123.3 (C), 125.1 (CH, B), 125.6 (CH, A), 127.4 (CH, 2A+B), 128.1 (CH, B), 129.0 (CH, 2A+B), 129.4 (CH, B), 129.7 (CH, B), 130.3 (CH, A), 130.7 (CH, A+B), 131.4 (CH, A), 131.7 (CH, A), 132.1 (CH, B), 132.3 (CH, B), 135.9 (C), 138.6 (C), 140.1 (C), 166.6 (C).

HATR (cm^{-1}): 3065 (w), 3030 (w), 2923 (s), 2852 (m), 1676 (s), 1606 (m), 1579 (w), 1496 (w), 1478 (m), 1456 (m), 1432 (m), 1415 (w), 1388 (m), 1306 (w), 1242 (m), 1191 (w), 1112 (w), 1083 (w), 1030 (w), 1010 (w), 969 (m), 826 (w), 766 (m), 750 (m), 698 (m), 656 (w), 623 (w).

LC-(ESI)MS (condition 1): t_R = 21.6 min $[M+H^+]^+$: 431.2 (100%). **Purity** (214 nm): 97%. **HRMS (ESI)** calcd for $C_{27}H_{35}N_4O^+$: 431.2805 $[M+H^+]^+$ found: 431.2815.

(rac)-6-butyl-8-chloro-1-ethyl-3-methyl[1,2,3]triazolo[1,5-*d*][1,4]benzodiazepin-2-one (*rac*)-XI.76

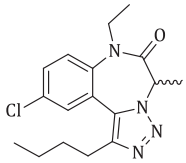

(*rac*)-XI.76

Following general procedure **P.15**: *(S)*-6-butyl-8-chloro-3-methyl[1,2,3]triazolo[1,5-*d*][1,4]benzodiazepin-2-one (**IX.56,** 20.7 mg, 0.06791 mmol, 1 eq). ethyliodide (22 µL, 0.2716 mmol, 4 eq). potassium hydroxide (7.6 mg, 0.1358 mmol, 2 eq). THF (680 µL).

Yield: 49%. *(rac)*-6-butyl-8-chloro-1-ethyl-3-methyl[1,2,3]triazolo[1,5-*d*][1,4]benzodiazepin-2-one (**(*rac*)-XI.76,** 11.1 mg, 0.03335 mmol).

Overall yield: 29%.

White solid.

Molecular weight: 332.83 Da.

R_F: 0.15 (hexane/acetone: 8/2).

^{1}H NMR (500 MHz, acetone-d_6) δ 0,83-0,89 (m, 5.8H, A+B), 1.00 (t, J = 7.1Hz, 0.2H, B), 1.24-1.35 (m, 2H, A+B), 1.66 (quintet, J = 7.5Hz, 2H, A+B), 1.90 (d, J = 6.8Hz, 3H, A+B), 2.85-2.94 (m, 2H, A+B), 3.67 (sextet, J = 7.1Hz, 0.95H, A), 3.77 (sextet, J = 6.9Hz, 0.05H, B), 4.18-4.25 (m, 1H, A+B), 4.85-4.89 (q, J = 6.9Hz, 0.95H, A), 5.66-5.70 (q, J = 7.8Hz, 0.05H, B), 7.62-7.65 (m, 2H, A+B), 7.71 (d, J = 10.0Hz, 1H, A+B).

^{13}C NMR (125 MHz, acetone-d_6) δ 12.1 (CH_3, A+B), 13.1 (CH_3, A+B), 13.9 (CH_3, A), 14.9 (CH_3, B), 22.7 (CH_2, A+B), 25.3 (CH_2, A+B), 31.9 (CH_2, A+B), 44.8 (CH_2, A), 45.6 (CH_2, B), 56.0 (CH,

A+B), 125.8 (C), 126.7 (CH, B), 127.4 (CH, A), 128.8 (CH, B), 128.9 (CH, A), 130.3 (C), 131.0 (CH, A+B), 131.9 (C), 139.2 (C), 145.2 (C), 167.3 (C).
HATR (cm^{-1}): 2955 (m), 2919 (m), 2869 (w), 1678 (s), 1603 (m), 1476 (m), 1444 (m), 1408 (m), 1382 (m), 1268 (m), 1241 (m), 1184 (m), 1124 (m), 1100 (m), 1090 (w), 1054 (w), 1036 (w), 904 (w), 880 (w), 829 (m), 800 (w).
LC-(ESI)MS (condition 5): t_R = 6.5 min $[M+H^+]^+$: 333.1 (100%). **Purity** (214 nm): 99%.
HRMS (ESI) calcd for $C_{17}H_{22}ClN_4O^+$: 333.1477 $[M+H^+]^+$ found: 333.1475.

(rac)-8-bromo-6-butyl-1-ethyl-3-methyl[1,2,3]triazolo[1,5-*d*][1,4]benzo-diazepin-2-one (*rac*)-XI.77

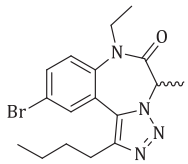

(*rac*)-XI.77

Following general procedure **P.15**: *(S)*-8-bromo-6-butyl-3-methyl[1,2,3]triazolo[1,5-*d*][1,4]benzodiazepin-2-one (**IX.63,** 20.4 mg, 0.05842 mmol, 1 eq). ethyliodide (19.0 µL, 0.2337 mmol, 4 eq). potassium hydroxide (6.6 mg, 0.1168 mmol, 2 eq). THF (590 µL).

Yield: 67%. *(rac)*-8-bromo-6-butyl-1-ethyl-3-methyl[1,2,3]triazolo[1,5-*d*][1,4]benzodiazepin-2-one (**(*rac*)-XI.77,** 14.8 mg, 0.03923 mmol).
Overall yield: 46%.
White solid.
Molecular weight: 377.28 Da.
R_F: 0.15 (hexane/acetone: 8/2).
^{1}H NMR (300 MHz, acetone-d_6) δ 0.83-0.90 (m, 5.7H, A+B), 1.00 (t, J = 7.2Hz, 0.3H, B), 1.23-1.38 (m, 2H, A+B), 1.61-1.71 (m, 2H, A+B), 1.90 (d, J = 6.8Hz, 3H), 2.87-2.91 (m, 2H, A+B), 3.61-3.79 (m, 1H, A+B), 4.15-4.27 (m, 1H, A+B), 4.88 (q, J = 6.8Hz, 0.9H, A), 5.66 (q, J = 7.7Hz, 0.1H), 7.63-7.66 (m, 1H, A+B), 7.75-7.80 (m, 2H, A+B).
^{13}C NMR (75 MHz, acetone-d_6) δ 12.1 (CH_3), 13.1 (CH_3), 13.9 (CH_3), 22.7 (CH_2), 25.3 (CH_2), 31.9 (CH_2), 44.8 (CH_2), 55.9 (CH), 119.6 (C), 125.9 (C), 127.6 (CH), 131.9 (CH), 134.0 (CH), 139.7 (C), 142.5 (C), 145.2 (C), 167.2 (C).
HATR (cm^{-1}): 2955 (w), 2925 (w), 2871 (w), 1681 (s), 1597 (w), 1474 (m), 1407 (m), 1382 (m), 1270 (w), 1241 (m), 1184 (w), 1124 (w), 1086 (w), 1052 (w), 1026 (w), 898 (w), 882 (w), 826 (w), 777 (w), 664 (w).
LC-(ESI)MS (condition 5): t_R = 6.6 min $[M+H^+]^+$: 378.0 (100%). **Purity** (214 nm): 97%.
HRMS (ESI) calcd for $C_{17}H_{22}BrN_4O^+$: 377.0971 $[M+H^+]^+$ found: 377.0970.

***(rac)*-6-butyl-8-chloro-1-ethyl-3-isopropyl[1,2,3]triazolo[1,5-*d*][1,4]benzodiazepin-2-one (*rac*)-XI.78**

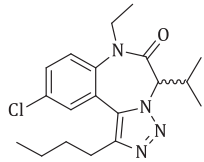

(*rac*)-XI.78

Following general procedure **P.15**: *(S)*-6-butyl-8-chloro-3-isopropyl[1,2,3]triazolo[1,5-*d*][1,4]benzodiazepin-2-one (**IX.61**, 19.8 mg, 0.05949 mmol, 1 eq). ethyliodide (19.0 µL, 0.2380 mmol, 4 eq). potassium hydroxide (6.8 mg, 0.1190 mmol, 2 eq). THF (600 µL).

Yield: 64%. *(rac)*-6-butyl-8-chloro-1-ethyl-3-isopropyl[1,2,3]triazolo[1,5-*d*][1,4]benzodiazepin-2-one (**(*rac*)-XI.78**, 13.7 mg, 0.03796 mmol).
Overall yield: 39%.
White solid.
Molecular weight: 360.88 Da.
R_F: 0.40 (hexane/acetone: 8/2).
^{1}H NMR (500 MHz, acetone-d_6) δ 0.60 (d, J = 6.6Hz, 2.25H, A), 0.80 (t, J = 7.1Hz, 0.75H, B), 0.86 (m, 3H, A+B), 0.94 (d, J = 6.6Hz, 2.25H, A), 1.04 (t, J = 7.1Hz, 2.25H, A), 1.14 (d, J = 6.6Hz, 0.75H, B), 1.16 (d, J = 6.6Hz, 0.75H, B), 1.22-1.39 (m, 2H, A+B), 1.55-1.76 (m, 2.75H, A+B), 2.88 (t, J = 7.3Hz, 0.5H, B), 2.91 (t, J = 7.6Hz, 1.5H, B), 3.14-3.21 (m, 0.25H, B), 3.59-3.66 (m, 0.25H, B), 3.77-3.84 (m, 0.75H, A), 4.12-4.24 (m, 1H, A+B), 4.36 (d, J = 10.7Hz, 0.25H, B), 5.08 (d, J = 11.8Hz, 0.75H, A), 7.61-7.62 (m, 1H, A+B), 7.66-7.69 (m, 1H, A+B), 7.71-7.73 (m, 1H, A+B).
^{13}C NMR (125 MHz, acetone-d_6) δ 12.9 (CH_3, B), 13.3 (CH_3, A), 13.9 (CH_3, B), 14.0 (CH_3, A), 19.0 (CH_3, A), 19.1 (CH_3, A), 19.8 (CH_3, B), 20.1 (CH_3, B), 22.7 (CH_2, B), 22.8 (CH_2, A), 25.2 (CH_2, B), 25.4 (CH_2, A), 26.3 (CH, B), 27.9 (CH, A), 31.8 (CH_2, B), 31.9 (CH_2, A), 44.8 (CH_2, A), 45.8 (CH_2, B), 65.8 (CH, B), 74.3 (CH, A), 124.2 (C, A), 125.8 (C, B), 126.5 (CH, A), 127.5 (CH, B), 128.4 (C, A), 128.7 (CH, A), 129.0 (CH, B), 130.8 (C, B), 131.2 (CH, B), 131.3 (CH, A), 131.8 (C, A), 131.9 (C, B), 138.2 (C, A), 139.5 (C, B), 144.7 (C, B), 146.0 (C, A), 165.5 (C, B), 166.9 (C, A).
HATR (cm^{-1}): 2956 (s), 2930 (m), 2871 (m), 1678 (s), 1474 (s), 1408 (s), 1368 (w), 1298 (m), 1246 (m), 1210 (m), 1177 (m), 1131 (m), 1130 (w), 1030 (w), 881 (w), 826 (w), 804 (w).
LC-(ESI)MS (condition 2): t_R = 8.1 min $[M+H^+]^+$: 361.1 (100%). **Purity** (214 nm): 96%.
HRMS (ESI) calcd for $C_{19}H_{26}ClN_4O^+$: 361.1790 $[M+H^+]^+$ found: 361.1790.

***(rac)*-8-bromo-6-butyl-1-ethyl-3-isopropyl[1,2,3]triazolo[1,5-*d*][1,4]benzodiazepin-2-one (*rac*)-XI.79**

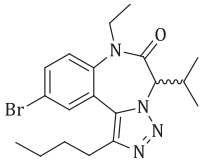

(*rac*)-XI.79

Following general procedure **P.15**: *(S)*-8-bromo-6-butyl-3-isopropyl[1,2,3]triazolo[1,5-*d*][1,4]benzodiazepin-2-one (**IX.68**, 20.2 mg, 0.05354 mmol, 1 eq). ethyliodide (17.0 µL, 0.2142 mmol, 4 eq). potassium hydroxide (6.0 mg, 0.1071 mmol, 2 eq). THF (540 µL).

Yield: 64%. *(rac)*-8-bromo-6-butyl-1-ethyl-3-isopropyl[1,2,3]triazolo[1,5-*d*][1,4]benzodiazepin-2-one (**(*rac*)-XI.79**, 13.9 mg, 0.03431 mmol).
Overall yield: 34%.
White solid.
Molecular weight: 405.11 Da.
R_F: 0.36 (hexane/acetone: 8/2).
^{1}H NMR (300 MHz, acetone-d_6) δ 0.60 (d, J = 6.4Hz, 2.25H, A), 0.80 (t, J = 7.1Hz, 0.75H, B), 0.83-0.88 (m, 3.0H, A+B), 0.94 (d, J = 6.6Hz, 2.25H, A), 1.05 (t, J = 7.2Hz, 2.25H, A), 1.14 (d, J = 6.6Hz, 0.75H,B), 1.16 (d, J = 6.6Hz, 0.75H, B), 1.24-1.38 (m, 2H, A+B), 1.53-1.74 (m, 2.75H, A+B), 2.88 (t, J = 7.7Hz, 0.5H, B), 2.92 (t, J = 7.7Hz, 1.5H, A), 3.11-3.23 (m, 0.25H, B), 3.57-3.68 (m, 0.25H, B), 3.75-3.86 (m, 0.75H, A), 4.09-4.25 (m, 1H, A+B), 4.36 (d, J = 10.6Hz, 0.25H, B), 5.08 (d, J = 11.9Hz, 0.75H, A), 7.63-7.67 (m, 1H, A+B), 7.75-7.82 (m, 2H, A+B).
^{13}C NMR (75 MHz, acetone-d_6) δ 12.9 (CH_3, B), 13.3 (CH_3, A), 13.9 (CH_3, B), 13.9 (CH_3, A), 19.0 (CH_3, A), 19.1 (CH_3, A), 19.8 (CH_3, B), 20.1 (CH_3, B), 22.7 (CH_2, B), 22.7 (CH_2, A), 25.2 (CH_2, B), 25.4 (CH_2, A), 26.3 (CH, B), 27.9 (CH, A), 31.8 (CH_2, A), 31.9 (CH_2, B), 44.8 (CH_2, B), 45.8 (CH_2, A), 65.7 (CH, B), 74.3 (CH, A), 119.5 (C, A), 119.7 (C, B), 124.4 (C, A), 126.1 (C, B), 126.7 (CH, A), 127.7 (CH, B), 131.6 (CH, A), 131.9 (CH, B), 134.2 (CH, B), 134.3 (CH, A), 138.7 (C, B), 140.0 (C, A), 165.5 (C, B), 166.9 (C, A).
HATR (cm^{-1}): 2959 (m), 2936 (m), 2871 (w), 1670 (s), 1597 (w), 1549 (w), 1476 (m), 1407 (m), 1371 (m), 1305 (m), 1268 (m), 1242 (m), 1173 (w), 1142 (w), 1118 (w), 1087 (w), 1054 (w), 1026 (w), 941 (w), 882 (w), 856 (w), 825 (w), 776 (m), 705 (w), 671 (w).
LC-(ESI)MS (condition 2): A: t_R = 8.5 min $[M+H^+]^+$: 407.1 (100%), 405.1 (100%). **Purity** (214 nm): 96%.
LC-(ESI)MS (condition 2): B: t_R = 12.9 min $[M+H^+]^+$: 407.1 (100%), 405.1 (100%). **Purity** (214 nm): 3%.
HRMS (ESI) calcd for $C_{19}H_{26}BrN_4O^+$: 405.1285 $[M+H^+]^+$ found: 405.1284.

***(rac)*-6-butyl-8-chloro-1-ethyl-3-isobutyl[1,2,3]triazolo[1,5-*d*][1,4]benzodiazepin-2-one (*rac*)-XI.80**

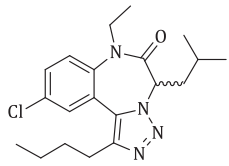

(*rac*)-XI.80

Following general procedure **P.15**: *(S)*-6-butyl-8-chloro-3-isobutyl[1,2,3]triazolo[1,5-*d*][1,4]benzodiazepin-2-one (**IX.60**, 25.0 mg, 0.07208 mmol, 1 eq). ethyliodide (23.0 µL, 0.2883 mmol, 4 eq). potassium hydroxide (8.2 mg, 0.1442 mmol, 2 eq). THF (720 µL).

Yield: 68%. *(rac)*-6-butyl-8-chloro-1-ethyl-3-isobutyl[1,2,3]triazolo[1,5-*d*][1,4]benzodiazepin-2-one (**(*rac*)-XI.80**, 18.4 mg, 0.04908 mmol).
Overall yield: 51%.
White solid.
Molecular weight: 374.91 Da.
R_F: 0.36 (hexane/acetone: 8/2).
^{1}H NMR (300 MHz, acetone-d_6) δ 0.62 (d, J = 6.2Hz, 0.9H, B), 0.70-0.81 (m, 10.2H, A+B), 0.89 (app t, J = 7.0Hz, 0.9H, B), 1.07-1.33 (m, 2.9H, A+B), 1.48-1.62 (m, 2H, A+B), 1.67-1.81 (m, 0.7H, A), 2.18-2.46 (m, 1.4H, A), 2.74-2.81 (m, 2H, A+B), 3.49-3.59 (m, 0.7H, A), 3.60-3.71 (m, 0.3H, B), 4.00-4.14 (m, 1H, A+B), 4.57-4.62 (app t, J = 7.15Hz, 0.7H, A), 5.45-5.51 (app t, J = 7.5Hz, 0.3H, B), 7.49-7.55 (m, 2H, A+B), 7.57-7.61 (m, 1H, A+B).
^{13}C NMR (75 MHz, acetone-d_6) δ 13.1 (CH_3, A), 13.2 (CH_3, B), 13.9 (CH_3, A+B), 22.0 (CH_3, B), 22.2 (CH_3, B), 22.7 (CH_3, A), 22.7 (CH_2, A+B), 22.9 (CH, A), 25.3 (CH_2, A), 25.4 (CH_2, B), 25.5 (CH, A), 26.2 (CH, B), 31.8 (CH_2, B), 31.9 (CH_2, A), 35.2 (CH_2, A), 37.4 (CH_2, B), 45.0 (CH_2, A), 45.7 (CH_2, B), 58.4 (CH, A), 66.4 (CH, B), 124.4 (C, B), 125.6 (C, A), 126.7 (CH, B), 127.4 (CH, A), 128.6 (CH, B), 129.0 (CH, A), 130.6 (C, B), 131.1 (CH, A), 131.3 (CH, B), 131.9 (C, A), 138.4 (C, B), 139.3 (C, A), 145.1 (C, A), 146.1 (C, B), 166.5 (C, A), 167.5 (C, B).
HATR (cm^{-1}): 2956 (m), 2932 (m), 2870 (w), 1679 (s), 1476 (m), 1408 (m), 1369 (m), 1297 (w), 1268 (w), 1244 (w), 1216 (w), 1178 (w), 1126 (w), 1103 (w), 1089 (w), 1032 (w), 954 (w), 881 (w), 824 (w), 802 (w), 673 (w).
LC-(ESI)MS (condition 2): t_R = 9.4 min $[M+H^+]^+$: 375.1 (100%). **Purity** (214 nm): 91%.
HRMS (ESI) calcd for $C_{20}H_{28}ClN_4O^+$: 375.1946 $[M+H^+]^+$ found: 375.1946.

***(rac)*-8-bromo-6-butyl-1-ethyl-3-isobutyl[1,2,3]triazolo[1,5-*d*][1,4]benzodiazepin-2-one (*rac*)-XI.81**

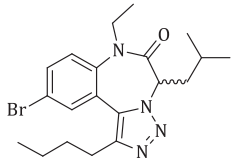

(*rac*)-XI.81

Following general procedure **P.15**: *(S)*-8-bromo-6-butyl-3-isobutyl[1,2,3]triazolo[1,5-*d*][1,4]benzodiazepin-2-one (**IX.67**, 25.0 mg, 0.06389 mmol, 1 eq). ethyliodide (20.5 μL, 0.2556 mmol, 4 eq). potassium hydroxide (7.2 mg, 0.1278 mmol, 2 eq). THF (640 μL).

Yield: 73%. *(rac)*-8-bromo-6-butyl-1-ethyl-3-isobutyl[1,2,3]triazolo[1,5-*d*][1,4]benzodiazepin-2-one (**(*rac*)-XI.81,** 19.6 mg, 0.04674 mmol).
Overall yield: 54%.
White solid.
Molecular weight: 419.36 Da.
R_F: 0.36 (hexane/acetone: 8/2).
^{1}H NMR (300 MHz, acetone-d_6) δ 0.74 (d, J = 6.2Hz, 0.75H, B), 0.82-0.93 (m, 10.5H, A+B), 1.02 (t, J = 7.0Hz, 0.75H, B), 1.19-1.46 (m, 2.75H, A+B), 1.60-1.74 (m, 2H, A+B), 1.80-1.93 (m, 0.75H, A), 2.30-2.58 (m, 1.5H, A), 2.86-2.93 (m, 2H, A+B), 3.61-3.72 (m, 0.75H, A), 3.73-3.83 (m, 0.25H, B), 4.12-4.26 (m, 1H, A+B), 4.72 (t, J = 7.0Hz, 0.75H, A), 5.60 (app t, J = 7.4Hz, 0.25H, B), 7.62-7.67 (m, 1H, A+B), 7.75-7.80 (m, 2H, A+B).
^{13}C NMR (75 MHz, acetone-d_6) δ 13.1 (CH_3, A), 13.2 (CH_3, B), 13.9 (CH_3, A+B), 22.0 (CH_3, B), 22.2 (CH_3, B), 22.7 (CH_3, A), 22.7 (CH_2, A+B), 22.9 (CH, A), 25.3 (CH_2, A), 25.4 (CH_2, B), 25.5 (CH, A), 26.2 (CH, B), 31.8 (CH_2, B), 31.9 (CH_2, A), 35.2 (CH_2, A), 37.4 (CH_2, B), 45.0 (CH_2, A), 45.7 (CH_2, B), 58.4 (CH, A), 66.4 (CH, B), 119.5 (C, B), 119.6 (C, A), 124.7 (C, B), 125.9 (C, A), 126.6 (CH, B), 127.6 (CH, A), 128.5 (C, B), 130.5 (C, A), 131.6 (CH, B), 131.9 (CH, A), 134.1 (CH, A), 134.2 (CH, B), 138.9 (C, B), 139.7 (C, A), 145.1 (C, A), 146.1 (C, B), 166.5 (C, A), 167.4 (C, B).
HATR (cm^{-1}): 2956 (m), 2925 (m), 2870 (w), 1726 (w), 1680 (s), 1475 (m), 1407 (m), 1368 (m), 1297 (w), 1271 (w), 1243 (w), 1216 (w), 1179 (w), 1126 (m), 1089 (w), 1030 (w), 952 (w), 881 (w), 822 (w), 802 (w), 780 (w).
LC-(ESI)MS (condition 1): t_R = 20.2 min $[M+H^+]^+$: 421.1 (100%), 419.1 (100%).
LC-(ESI)MS (condition 2): t_R = 10.0 min $[M+H^+]^+$: 421.1 (100%), 419.1 (100%).
HRMS (ESI) calcd for $C_{20}H_{26}BrN_4O^-$: 417.1295 ($M - H^+$), found: 417.1292.

***(rac)*-6-butyl-8-chloro-1-ethyl-3-(*N*-(tert-butyloxycarbonyl)-indolylmethyl)[1,2,3] triazolo[1,5-*d*][1,4]benzodiazepin-2-one (*rac*)-XI.82**

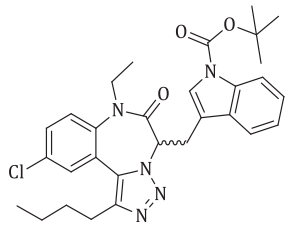

(*rac*)-XI.82

Following general procedure **P.15**: *(S)*-6-butyl-8-chloro-3-(*N*-(tert-butyloxycarbonyl)-indolylmethyl)[1,2,3]triazolo[1,5-*d*][1,4]benzodiazepin-2-one (**IX.59**, 24.3 mg, 0.04673 mmol, 1 eq). ethyliodide (15.0 µL, 0.1869 mmol, 4 eq). potassium hydroxide (5.2 mg, 0.09346 mmol, 2 eq). THF (500 µL).

Yield: 30%. *(rac)*-6-butyl-8-chloro-1-ethyl-3-(*N*-(tert-butyloxycarbonyl)-indolylmethyl) [1,2,3]triazolo[1,5-*d*][1,4]benzodiazepin-2-one (**(*rac*)-XI.82**, 7.7 mg, 0.01405 mmol).
Overall yield: 11%.
White solid.
Molecular weight: 548.07 Da.
R_F: 0.13 (hexane/acetone: 9/1). 0.25 (hexane/acetone: 8/2). 0.58 (hexane/acetone: 6/4).
^{1}H NMR (500 MHz, acetone-d_6) δ 0.83-0.88 (m, 5.55H, A+B), 1.04 (t, J = 7.0Hz, 0.45H, B), 1.23-1.36 (m, 2H, A+B), 1.63-1.67 (m, 11H, A+B), 2.90 (t, J = 7.5Hz, 2H, A+B), 2.93-3.12 (ABX, J_{AX} = 9.2Hz, J_{BX} = 8.0Hz, J_{AB} = 15.1Hz, 0.30H, B), 3.62-3.69 (m, 0.85H, A), 3.79-3.86 (m, 0.15H, B), 3.94-4.05 (ABX, J_{AX} = 7.3Hz, J_{BX} = 6.9Hz, J_{AB} = 15.1Hz, 1.7H, A), 4.09-4.15 (m, 0.15, B), 4.20-4.27 (m, 0.85H, A), 5.10 (app t, J = 7.2Hz, 0.85H, A), 5.93 (app t, J = 8.3Hz, 0.15H, B), 7.17 (t, J = 7.9Hz, 0.85H, A), 7.21 (t, J = 7.9Hz, 0.15H, B), 7.26 (t, J = 7.3Hz, 0.85H, A), 7.30-7.34 (m, 0.15H, B), 7.57-7.60 (m, 1.7H, A), 7.69-7.79 (m, 3.30H, A+B), 8.05-8.07 (m, 1H, A+B).
^{13}C NMR (125 MHz, acetone-d_6) δ 13.0 (CH_3, A), 13.3 (CH_3, B), 13.9 (CH_3, A), 14.0 (CH_3, B), 22.1 (CH_2, broad, A+B), 22.7 (CH_2, A), 22.8 (CH_2, B), 24.9 (C, A+B), 25.3 (CH_2, A), 25.4 (CH_2, B), 28.2 (CH_3, A+B), 31.8 (CH_2, A), 31.9 (CH_2, B), 45.0 (CH_2, A), 46.1 (CH_2, B), 60.2 (CH, A), 67.4 (CH, B), 84.3 (CH_2, A), 84.5 (CH_2, B), 114.9 (C, B), 115.8 (CH, A), 115.9 (CH, B), 116.9 (C, A), 119.4 (CH, B), 120.2 (CH, A), 123.2 (CH, A), 123.4 (CH, B), 124.6 (C, B), 125.1 (CH, A), 125.1 (CH, B), 125.4 (CH, B), 125.5 (C, A), 125.9 (CH, A), 126.7 (CH, B), 127.5 (CH, A+B), 128.9 (CH, B), 129.0 (CH, A), 130.5 (C, A+B), 131.2 (C, A), 131.3 (C, A+B), 131.5 (CH, B), 132.1 (C, A), 132.4 (C, B), 138.5 (C, B), 139.1 (C, A), 145.3 (C, A), 150.2 (C, B), 166.2 (C, A), 166.6 (C, B).

HATR (cm^{-1}): 2956 (m), 2925 (m), 2863 (w), 1731 (s), 1682 (s), 1476 (m), 1452 (s), 1409 (m), 1368 (s), 1308 (m), 1255 (m), 1225 (m), 1157 (s), 1083 (m), 1016 (m), 854 (w), 824 (w), 766 (w), 746 (w).
LC-(ESI)MS (condition 6): t_R = 4.5 min $[M+H^+]^+$: 548.2 (100%). **Purity** (214 nm): 99%.
HRMS (ESI) calcd for $C_{30}H_{35}ClN_5O_3^+$: 548.2422 $[M+H^+]^+$ found: 548.2421.

(*rac*)-8-bromo-6-butyl-1-ethyl-3-(*N*-(tert-butyloxycarbonyl)-indolylmethyl)[1,2,3]-triazolo[1,5-*d*][1,4]benzodiazepin-2-one (*rac*)-XI.83

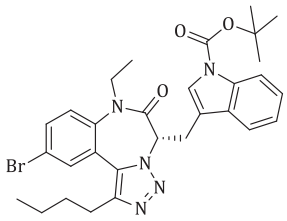

(*rac*)-XI.83

Following general procedure **P.15**: *(S)*-8-bromo-6-butyl-3-(*N*-(tert-butyloxycarbonyl)-indolylmethyl)[1,2,3]triazolo[1,5-*d*][1,4]benzodiazepin-2-one (**IX.66**, 26.7 mg, 0.04730 mmol, 1 eq). ethyliodide (15.2 µL, 0.1892 mmol, 4 eq). potassium hydroxide (5.4 mg, 0.09460 mmol, 2 eq). THF (500 µL).

Yield: 45%. (*rac*)-8-bromo-6-butyl-1-ethyl-3-(*N*-(tert-butyloxycarbonyl)-indolylmethyl) [1,2,3]triazolo[1,5-*d*][1,4]benzodiazepin-2-one (**(*rac*)-XI.83**, 12.6 mg, 0.02126 mmol).
Overall yield: 19%.
White solid.
Molecular weight: 592.53 Da.
R_F: 0.13 (hexane/acetone: 9/1). 0.25 (hexane/acetone: 8/2). 0.58 (hexane/acetone: 6/4).
^{1}H NMR (500 MHz, acetone-d_6) δ 0.83-0.88 (m, 5.55H, A+B), 1.03 (t, *J* = 7.0Hz, 0.45H, B), 1.23-1.36 (m, 2H, A+B), 1.63 (s, 9H, A+B), 1.64-1.67 (m, 2H, A+B), 2.90 (t, J = 7.3Hz, 2H, A+B), 2.94-3.13 (ABX, J_{AX} = 9.2Hz, J_{BX} = 7.9Hz, J_{AB} = 15.0Hz, 0.30H, B), 3.62-3.69 (m, 0.85H, A), 3.79-3.86 (m, 0.15H, B), 3.94-4.05 (ABX, J_{AX} = 7.2Hz, J_{BX} = 6.9Hz, J_{AB} = 15.0Hz, 1.7H, A), 4.07-4.14 (m, 0.15, B), 4.19-4.27 (m, 0.85H, A), 5.12 (app t, *J* = 7.0Hz, 0.85H, A), 5.93 (app t, *J* = 8.2Hz, 0.15H, B), 7.17 (t, *J* = 7.9Hz, 0.85H, A), 7.21 (t, *J* = 7.9Hz, 0.15H, B), 7.26 (t, *J* = 7.3Hz, 0.85H, A), 7.30-7.34 (m, 0.15H, B), 7.57-7.61 (m, 1.7H, A), 7.70-7.74 (m, 2H, A+B), 7.77 (d, *J* = 2.3Hz, 1H, A+B), 7.82-7.86 (m, 0.30H, B), 8.05-8.07 (m, 1H, A+B).
^{13}C NMR (125 MHz, acetone-d_6) δ 13.0 (CH_3, A), 13.3 (CH_3, B), 13.9 (CH_3, A), 14.0 (CH_3, B), 22.0 (CH_2, B), 22.1 (CH_2, A), 22.7 (CH_2, A), 22.8 (CH_2, B), 24.9 (C, A+B), 25.3 (CH_2, A), 25.4 (CH_2, B), 28.2 (CH_3, A+B), 31.8 (CH_2, A), 31.9 (CH_2, B), 45.0 (CH_2, A), 46.1 (CH_2, B), 60.2 (CH, A), 67.4

(CH, B), 84.3 (CH_2, broad, A+B), 114.9 (C, B), 115.8 (CH, A), 115.9 (CH, B), 116.9 (C, A), 119.4 (CH, B), 119.7 (C, B), 119.8 (C, B), 120.2 (CH, A), 123.2 (CH, A), 123.4 (CH, B), 124.4 (C, B), 125.1 (CH, A), 125.1 (CH, B), 125.4 (C, B), 125.8 (C, A), 125.9 (CH, A), 126.9 (CH, B), 127.7 (CH, A), 130.4 (C, A+B), 131.3 (C, A+B), 131.9 (CH, B), 131.9 (CH, A), 134.2 (CH, A), 134.4 (CH, B), 136.0 (C, A+B), 139.0 (C, B), 139.6 (C, A), 145.3 (C, A), 146.2 (C, B), 150.0 (C, B), 150.2 (C, A), 166.2 (C, A), 166.6 (C, B).

HATR (cm^{-1}): 2956 (m), 2931 (m), 2869 (w), 1732 (s), 1684 (s), 1474 (m), 1452 (m), 1407 (m), 1370 (s), 1308 (m), 1255 (m), 1226 (m), 1157 (s), 1084 (m), 1016 (m), 854 (w), 818 (w), 764 (m), 746 (m).

LC-(ESI)MS (condition 6): t_R = 4.8 min $[M+H^+]^+$: 592.2 (100%). **Purity** (214 nm): 98%.

HRMS (ESI) $C_{30}H_{35}BrN_5O_3^+$: 592.1914 $[M+H^+]^+$ found: 592.1918.

(rac)-1-butyl 6-butyl-8-chloro-3-methyl[1,2,3]triazolo[1,5-*d*][1,4]benzodiazepin-2-one (*rac*)-XI.84

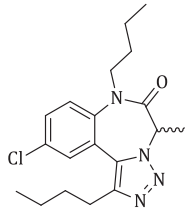

(*rac*)-XI.84

Following general procedure **P.15**: *(S)*-6-butyl-8-chloro-3-methyl[1,2,3]triazolo[1,5-*d*][1,4]benzodiazepin-2-one (**IX.56,** 19.8 mg, 0.06496 mmol, 1 eq). butyliodide (30 µL, 0.2598 mmol, 4 eq). potassium hydroxide (7.2 mg, 0.1299 mmol, 2 eq). THF (650 µL).

Yield: 73%. *(rac)*-1-butyl-6-butyl-8-chloro-3-methyl[1,2,3]triazolo[1,5-*d*][1,4]benzodiazepin-2-one (**(*rac*)-XI.84**, 17.1 mg, 0.04748 mmol).

Overall yield: 43%.

White solid.

Molecular weight: 360.17 Da.

R_F: 0.40 (hexane/acetone: 6/4).

^{1}H NMR (300 MHz, acetone-d_6) δ 0.64-0.71 (m, 3H, A+B), 0.79-0.95 (m, 5H, A+B), 1.05-1.41 (m, 4.14H, A+B), 1.61-1.71 (m, 2H, A+B), 1.90 (d, J = 6.8Hz, 2.86H, A), 2.87-2.94 (m, 2H, A+B), 3.55-3.71 (m, 1H, A+B), 4.29-4.40 (m, 1H, A+B), 4.88 (q, J = 6.8Hz, 0.95H, A), 5.69 (q, J = 7.7Hz, 0.05H, B), 7.61-7.68 (m, 2H, A+B), 7.69-7.76 (m, 1H, A+B).

^{13}C NMR (75 MHz, acetone-d_6) δ 12.2 (CH_3), 13.8 (CH_3), 14.2 (CH_3), 20.1 (CH_2), 22.9 (CH_2), 25.4 (CH_2), 30.2 (CH_2), 32.0 (CH_2), 48.8 (CH_2), 55.9 (CH), 125.7 (C), 127.6 (CH), 129.0 (CH), 131.0 (CH), 131.9 (C), 139.2 (C), 145.1 (C), 167.8 (C).

HATR (cm^{-1}): 2956 (m), 2931 (m), 2871 (w), 1682 (s), 1474 (m), 1407 (m), 1382 (w), 1340 (w), 1284 (w), 1240 (m), 1212 (w), 1202 (w), 1128 (w), 1102 (w), 1058 (w), 1030 (w), 951 (w), 880 (w), 824 (w), 808 (w), 668 (w, broad).
LC-(ESI)MS (condition 5): t_R = 7.1 min $[M+H^+]^+$: 361.1 (100%). **Purity** (214 nm): 98%.
HRMS (ESI) calcd for $C_{19}H_{26}ClN_4O^+$: 361.1790 $[M+H^+]^+$ found: 361.1790.

(rac)-8-bromo-1-butyl-6-butyl-3-methyl[1,2,3]triazolo[1,5-*d*][1,4]benzodiazepin-2-one (*rac*)-XI.85

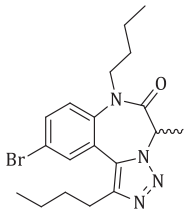

(*rac*)-XI.85

Following general procedure **P.15**: *(S)*-8-bromo-6-butyl-3-methyl[1,2,3]triazolo[1,5-*d*][1,4]benzodiazepin-2-one (**IX.63**, 20.2 mg, 0.05784 mmol, 1 eq). butyliodide (26 µL, 0.2314 mmol, 4 eq). potassium hydroxide (6.6 mg, 0.1157 mmol, 2 eq). THF (580 µL).

Yield: 42%. *N*-butyl-*(rac)*-8-bromo-14-butyl-3-methyl[1,2,3]triazolo[1,5-*d*][1,4]benzodiazepin-2-one (**(*rac*)-XI.85**, 15.7 mg, 0.03885 mmol).
Overall yield: 29%.
White solid.
Molecular weight: 404.12 Da.
R_F: 0.40 (hexane/acetone: 6/4).
^{1}H NMR (300 MHz, acetone-d_6) δ 0.64-0.72 (m, 3H, A+B), 0.80-0.98 (m, 5H, A+B), 1.08-1.40 (m, 4.12H, A+B), 1.61-1.71 (m, 2H, A+B), 1.90 (d, J = 6.8Hz, 2.88H, A), 2.90-2.92 (m, 2H, A+B), 3.56-3.70 (m, 1H, A+B), 4.30-4.40 (m, 1H, A+B), 4.88 (q, J = 6.8Hz, 0.95H, A), 5.69 (q, J = 7.7Hz, 0.05H, B), 7.64-7.69 (m, 1H, A+B), 7.75-7.82 (m, 2H, A+B).
^{13}C NMR (75 MHz, acetone-d_6) δ 12.2 (CH_3), 13.8 (CH_3), 14.0 (CH_3), 20.0 (CH_2), 22.9 (CH_2), 25.4 (CH_2), 30.2 (CH_2), 32.0 (CH_2), 48.7 (CH_2), 55.9 (CH), 119.6 (C), 126.0 (C), 127.8 (CH), 130.2 (C), 131.9 (CH), 134.0 (CH), 139.7 (C), 145.1 (C), 167.7 (C).
HATR (cm^{-1}): 2955 (m), 2929 (m), 2871 (w), 1681 (s), 1472 (m), 1407 (m), 1382 (m), 1361 (w), 1284 (w), 1259 (w), 1240 (m), 1211 (w), 1184 (w), 1129 (w), 1088 (w), 1058 (w), 1026 (w), 954 (w), 881 (w), 826 (w), 787 (w), 774 (w), 669 (w).
LC-(ESI)MS (condition 5): t_R = 7.2 min $[M+H^+]^+$: 405.1 (100%). **Purity** (214 nm): 99%.
HRMS (ESI) calcd for $C_{19}H_{26}BrN_4O^+$: 405.1285 $[M+H^+]^+$ found: 405.1285.

***(rac)*-1-butyl-6-butyl-8-chloro-3-isopropyl[1,2,3]triazolo[1,5-*d*][1,4]benzodiazepin-2-one (*rac*)-XI.86**

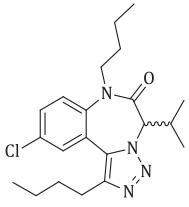

(*rac*)-XI.86

Following general procedure **P.15**: *(S)*-6-butyl-8-chloro-3-isopropyl[1,2,3]triazolo[1,5-*d*][1,4]benzodiazepin-2-one (**IX.61,** 19.8 mg, 0.05949 mmol, 1 eq). butyliodide (27 µL, 0.2377 mmol, 4 eq). potassium hydroxide (6.8 mg, 0.1190 mmol, 2 eq). THF (600 µL).

Yield: 62%. *(rac)*-1-butyl-6-butyl-8-chloro-3-isopropyl[1,2,3]triazolo[1,5-*d*][1,4]benzodiazepin-2-one (**(*rac*)-XI.86**, 14.3 mg, 0.03677 mmol).
Overall yield: 38%.
White solid.
Molecular weight: 388.93 Da.
R_F: 0.27 (hexane/acetone: 8/2).
^{1}H NMR (500 MHz, acetone-d_6) δ 0.59 (d, J = 6.6Hz, 2.25H, A), 0.67 (t, J = 7.3Hz, 0.75H, B), 0.70 (t, J = 7.4Hz, 2.25H, A), 0.86-0.89 (m, 3.5H, A+B), 0.90-1.10 (m, 3.75H, A+B), 1.13 (d, J = 6.6Hz, 0.75H, B), 1.16 (d, J = 6.6Hz, 0.75H, B), 1.18-1.46 (m, 4H, A+B), 1.52-1.73 (m, 2.75H, A+B), 2.87 (t, J = 7.7Hz, 0.5H, B), 2.92 (t, J = 7.7Hz, 1.5H, A), 3.14-3.21 (m, 0.25H, B), 3.54-3.59 (m, 0.25H, B), 3.67-3.72 (m, 0.75H, A), 4.28-4.37 (m, 1.25H, A+B), 5.08-5.10 (m, 0.75H, A), 7.61-7.65 (m, 1H, A+B), 7.67-7.68 (m, 1H, A+B), 7.72-7.75 (m, 1H, A+B).
^{13}C NMR (125 MHz, acetone-d_6) δ 13.8 (CH_3, A), 13.8 (CH_3, B), 14.0 (CH_3, A+B), 19.0 (CH_3, A), 19.2 (CH_3, A), 19.8 (CH_3, B), 20.1 (CH_2, B), 20.1 (CH_2, A), 20.2 (C_{H3}, B), 22.8 (CH_2, A), 22.9 (CH_2, B), 25.3 (CH_2, B), 25.5 (CH_2, A), 26.3 (CH, B), 28.0 (CH, A), 30.1 (CH2, A), 30.2 (CH_2, B), 31.9 (CH_2, A), 32.0 (CH_2, B), 48.8 (CH_2, B), 49.6 (CH_2, A), 65.7 (CH, B), 74.3 (CH, A), 124.5 (C, A), 125.9 (C, B), 127.0 (CH, A), 127.6 (CH, B), 128.4 (C, A+B), 128.7 (CH, A), 129.0 (CH, B), 131.2 (CH, B), 131.3 (CH, A), 131.9 (C, B), 132.0 (C, A), 138.2 (C, A), 139.6 (C, B), 144.7 (C, B), 146.0 (C, A), 166.0 (C, B), 167.4 (C, A).
HATR (cm^{-1}): 2957 (m), 2930 (m), 2871 (w), 1713 (w), 1668 (s), 1601 (w), 1552 (w), 1474 (m), 1408 (m), 1363 (m), 1301 (m), 1247 (m), 1218 (m), 1167 (w), 1143 (m), 1115 (m), 1029 (m), 946 (w), 881 (m), 854 (w), 825 (m), 803 (m), 715 (w), 674 (w).
LC-(ESI)MS (condition 2): A: t_R = 10.7 min $[M+H^+]^+$: 389.2 (100%). **Purity** (214 nm): 99.8%.
LC-(ESI)MS (condition 2): B: t_R = 11.9 $[M+H^+]^+$: 389.2 (100%). **Purity** (214 nm): 0.2%.
HRMS (ESI) calcd for $C_{21}H_{30}ClN_4O^+$: 389.2103 $[M+H^+]^+$ found: 389.2100.

***(rac)*-8-bromo-1-butyl-6-butyl-3-isopropyl[1,2,3]triazolo[1,5-*d*][1,4]benzodiazepin-2-one (*rac*)-XI.87**

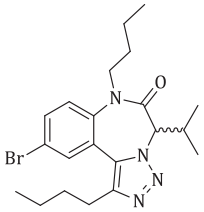

(*rac*)-XI.87

Following general procedure **P.15**: *(S)*-8-bromo-6-butyl-3-isopropyl[1,2,3]triazolo[1,5-*d*][1,4]benzodiazepin-2-one (**IX.68**, 20.5 mg, 0.05433 mmol, 1 eq). butyliodide (25 µL, 0.2173 mmol, 4 eq). potassium hydroxide (6.2 mg, 0.1088 mmol, 2eq). THF (550 µL).

Yield: 72%. *(rac)*-8-bromo-1-butyl-6-butyl-3-isopropyl[1,2,3]triazolo[1,5-*d*][1,4]benzodiazepin-2-one (**(*rac*)-XI.87**, 16.9 mg, 0.03911 mmol).
Overall yield: 38%.
Molecular weight: 432.15 Da.
R_F: 0.63 (hexane/acetone: 6/4).
^{1}H NMR (300 MHz, acetone-d_6) δ 0.60 (d, J = 6.5Hz, 2.40H, A), 0.68 (t, J = 7.3Hz, 0.72H, B), 0.71 (t, J = 7.4Hz, 2.42H, A), 0.87-0.91(m, 3H, A+B), 0.94 (d, J = 6.6Hz, 2.40H, A), 0.97-1.11 (m, 2H, A+B), 1.14 (d, J = 6.5Hz, 0.75H, B), 1.17 (d, J = 6.6Hz, 0.74H, B), 1.24-1.47 (m, 4H, A+B), 1.55-1.72 (m, 2.8H, A+B), 2.88 (t, J = 7.9Hz, 0.50H, B), 2.93 (t, J = 7.7Hz, 1.60H, A), 3.15-3.22 (m, 0.22H, B), 3.55-3.66 (m, 0.23H, B), 3.68-3.73 (m, 0.82H, A), 4.29-4.36 (m, 1H, A+B), 4.38 (d, J = 10.6Hz, 0.23H, B), 5.10(d, J = 11.8Hz, 0.78H, A), 7.65-7.68 (m, 1H, A+B), 7.75-7.78 (m, 1H, A+B), 7.81-7.82 (m, 1H, A+B).
^{13}C NMR (75 MHz, acetone-d_6) δ 13.8 (CH_3, A), 13.8 (CH_3, B), 14.0 (CH_3, A), 14.3 (CH_3, B), 19.0 (CH_3, A), 19.2 (CH_3, A), 19.8 (CH_3, B), 20.1 (CH_2, B), 20.1 (CH_2, A), 20.2 (CH_3, B), 22.8 (CH_2, A), 22.9 (CH_2, B), 25.3 (CH_2, B), 25.5 (CH_2, A), 26.3 (CH, B), 28.0 (CH, A), 30.1 (CH_2, A), 30.3 (CH_2, B), 31.9 (CH_2, A), 31.9 (CH_2, B), 48.7 (CH_2, B), 49.6 (CH_2, A), 65.7 (CH, B), 74.3 (CH, A), 119.6 (C), 124.8 (C, A), 126.2 (C, B), 127.2 (CH, A), 127.8 (CH, B), 128.3 (C, A), 130.8 (C, B), 131.6 (CH, A), 131.9 (CH, B), 134.1 (CH, B), 134.2 (CH, A), 138.6 (C, A), 140.0 (C, B), 144.7 (C, B), 146.0 (C, A), 166.0 (C, B), 167.4 (C, A).
HATR (cm^{-1}): 2958 (m), 2930 (m), 2871 (w), 1680 (w), 1670 (s), 1473 (m), 1406 (m), 1373 (w), 1302 (w), 1247 (w), 1214 (w), 1147 (w), 1117 (w), 1026 (w), 946 (w), 882 (w), 826 (w), 787 (w), 670 (w, broad).
LC-(ESI)MS (condition 2): A: t_R = 11.1 min $[M+H^+]^+$: 433.1 (100%). **Purity** (214 nm): 99%.
LC-(ESI)MS (condition 2): B: t_R = 16.9 min $[M+H^+]^+$: 433.1 (100%). **Purity** (214 nm): 1%.
HRMS (ESI) calcd for $C_{21}H_{30}BrN_4O^+$: 433.1598 $[M+H^+]^+$ found: 433.1592.

***(rac)*-1-butyl-6-butyl-8-chloro-3-isobutyl[1,2,3]triazolo[1,5-*d*][1,4]benzodiazepin-2-one (*rac*)-XI.88**

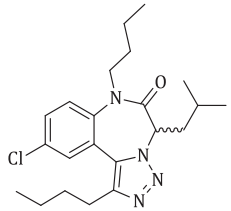

(*rac*)-XI.88

Following general procedure **P.15**: *(S)*-6-butyl-8-chloro-3-isobutyl[1,2,3]triazolo[1,5-*d*][1,4]benzodiazepin-2-one (**IX.60,** 19.2 mg, 0.05593 mmol, 1 eq). butyliodide (25 µL, 0.2237 mmol, 4 eq). potassium hydroxide (6.2 mg, 0.1119 mmol, 2 eq). THF (560 µL).

Yield: 61%. *(rac)*-1-butyl-6-butyl-8-chloro-3-isobutyl[1,2,3]triazolo[1,5-*d*][1,4]benzodiazepin-2-one (**(*rac*)-XI.88**, 13.7 mg, 0.03400 mmol).
Overall yield: 46%.
White solid.
Molecular weight: 402.96 Da.
R_F: 0.36 (hexane/acetone: 8/2).
^{1}H NMR (500 MHz, acetone-d_6) δ 0.66 (t, J = 7.4Hz, 2.1H, A), 0.69 (app t, J = 7.4Hz, 0.9H, B), 0.73 (d, J = 6.3Hz, 0.9H, B), 0.81-1.00 (m, 10.1H, A+B), 1.06-1.15 (m, 0.7H, A), 1.20-1.43 (m, 4.2H, A+B), 1.61-1.71(m, 2H, A+B), 1.81-1.89 (m, 0.7H, A), 2.31-2.37 (m, 0.7H, A), 2.50-2.56 (m, 0.7H, A), 2.87-2.94 (m, 2H, A+B), 3.57-3.62 (m, 0.7H, A), 3.65-3.70 (m, 0.3H, B), 4.31-4.37 (m, 1H, A+B), 4.72 (app t, J = 7.1Hz, 0.7H, A), 5.61 (app t, J = 7.3H, 0.3H, B), 7.62-7.68 (m, 2H, A+B), 7.71-7.74 (m, 1H, A+B).
^{13}C NMR (125 MHz, acetone-d_6) δ 13.7 (CH_3, B), 13.8 (CH_3, A), 14.0 (CH_3, A+B), 20.0 (CH_2, A), 20.1 (CH_2, B), 22.0 (CH_3, B), 22.2 (CH_3, B) 22.7 (CH_3, A), 22.8 (CH_2, B), 22.9 (CH_3, A), 22.9 (CH_2, A), 25.4 (CH_2, A), 25.5 (CH_2, B), 25.5 (CH, A), 26.2 (CH, B), 30.1 (CH_2, B), 30.2 (CH_2, A), 31.9 (CH_2, B), 32.0 (CH_2, A), 35.3 (CH_2, A), 37.4 (CH_2, B), 48.9 (CH_2, A), 49.5 (CH_2, B), 58.4 (CH, A), 66.4 (CH, B), 124.6 (C, B), 125.7 (C, A), 127.2 (CH, B), 127.6 (CH, A), 128.6 (CH, B), 129.0 (CH, A), 130.6 (C, A+B), 131.1 (CH, A), 131.3 (CH, B), 131.9 (C, A), 132.0 (C, B), 138.14 (C, B), 139.3 (C, A), 145.0 (C, A), 146.0 (C, B), 167.1 (C, A), 168.4 (C, B).
HATR (cm^{-1}): 2960 (m), 2932 (m), 2872 (w), 1670 (s), 1597 (w), 1555 (w), 1476 (m), 1409 (m), 1376 (m), 1329 (w), 1306 (m), 1268 (w), 1242 (m), 1141 (w), 1118 (w), 1028 (w), 935 (w), 882 (w), 820 (w), 786 (w).
LC-(ESI)MS (condition 5): t_R = 7.7 min $[M+H^+]^+$: 403.2 (100%). **Purity** (214 nm): 99%.
LC-(ESI)MS (condition 6): t_R = 3.6 min $[M+H^+]^+$: 403.2 (100%). **Purity** (214 nm): 99%.
HRMS (ESI) calcd for $C_{22}H_{32}ClN_4O^+$: 403.2259 $[M+H^+]^+$ found: 403.2254.

***(rac)*-8-bromo-1-butyl-6-butyl-3-isobutyl[1,2,3]triazolo[1,5-*d*][1,4]benzodiazepin-2-one (*rac*)-XI.89**

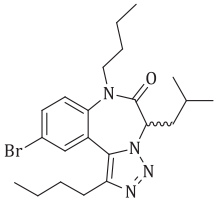

(*rac*)-XI.89

Following general procedure **P.15**: *(S)*-8-bromo-6-butyl-3-isobutyl[1,2,3]triazolo[1,5-*d*][1,4]benzodiazepin-2-one (**IX.67**, 20.0 mg, 0.05111 mmol, 1 eq). butyliodide (23 µL, 0.2044 mmol, 4 eq). potassium hydroxide (5.8 mg, 0.1022 mmol, 2 eq). THF (520 µL).

Yield: 63%. *(rac)*-8-bromo-1-butyl-6-butyl-3-isobutyl[1,2,3]triazolo[1,5-*d*][1,4]benzodiazepin-2-one (**(*rac*)-XI.89**, 14.4 mg, 0.03219 mmol).
Overall yield: 47%.
White solid.
Molecular weight: 447.41 Da.
R_F: 0.33 (hexane/acetone: 8/2).
^{1}H NMR (500 MHz, acetone-d_6) δ 0.67 (t, J = 7.4Hz, 2.25H, A), 0.70 (app t, J = 7.4Hz, 0.75H, B), 0.73 (d, J = 6.3Hz, 0.75H, B), 0.82-1.00 (m, 10.25H, A+B), 1.06-1.15 (m, 0.75H, A), 1.17-1.43 (m, 4H, A+B), 1.62-1.71(m, 2H, A+B), 1.81-1.89 (m, 0.75H, A), 2.31-2.37 (m, 0.75H, A), 2.50-2.55 (m, 0.75H, A), 2.87-2.93 (m, 2H, A+B), 3.57-3.63 (m, 0.75H, A), 3.65-3.70 (m, 0.25H, B), 4.30-4.37 (m, 1H, A+B), 4.72(app t, J = 7.4Hz, 0.75H, A), 5.61 (app t, J = 7.2H, 0.25H, B), 7.64-7.68 (m, 1H, A+B), 7.76-7.81 (m, 2H, A+B).
^{13}C NMR (125 MHz, acetone-d_6) δ 13.7 (CH_3, B), 13.8 (CH_3, A), 14.0 (CH_3, A+B), 20.0 (CH_2, B), 20.1 (CH_2, A), 22.0 (CH_3, B), 22.2 (CH_3, B), 22.7 (CH_3, A), 22.8 (CH_2, B), 22.9 (CH_3, A), 22.9 (CH_2, B), 25.4 (CH_2, A), 25.4 (CH_2, B), 25.5 (CH, A), 26.2 (CH, B), 30.1 (CH_2, A), 30.3 (CH_2, B), 31.9 (CH_2, B), 32.0 (CH_2, A), 35.3 (CH_2, A), 37.4 (CH_2, B), 48.9 (CH_2, A), 49.5 (CH_2, B), 58.4 (CH, A), 66.4 (CH, B), 119.6 (C, A+B), 124.9 (C, B), 126.0 (C, B), 127.3 (CH, B), 127.8 (CH, A), 128.5 (C, B), 130.5 (C, A), 131.6 (CH, B), 131.9 (CH, A), 134.1 (CH, A), 134.3 (CH, B), 138.8 (C, B), 139.8 (C, A), 145.0 (C, A), 145.2 (C, B), 167.1 (C, A), 167.9 (C, B).
HATR (cm^{-1}): 2956 (m), 2930 (m), 2870 (m), 1726 (w), 1679 (s), 1603 (w), 1468 (m), 1406 (m), 1367 (m), 1297 (w), 1245 (w), 1209 (m), 1172 (w), 1131 (w), 1086 (w), 1027 (w), 985 (w), 881 (w), 827 (w), 776 (w). M:
LC-(ESI)MS (condition 2): t_R = 12.6 min $[M+H^+]^+$: 447.1 (100%), 449.1 (100%). **Purity** (214 nm): 99%.

LC-(ESI)MS (condition 2): B: t_R = 18.1 min $[M+H^+]^+$: 447.1 (100%), 449.1 (100%). **Purity** (214 nm): 1%.
HRMS (ESI) calcd for $C_{22}H_{32}BrN_4O^+$: 447.1754 $[M+H^+]^+$ found: 447.1747.

(rac)-1-butyl-6-butyl-8-chloro-3-(*N*-(tert-butyloxycarbonyl)-indolylmethyl)[1,5-*d*][1,4]benzodiazepin-2-one (*rac*)-XI.90

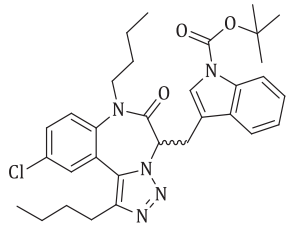

(*rac*)-XI.90

Following general procedure **P.15**: *(S)*-6-butyl-8-chloro-3-(*N*-(tert-butyloxycarbonyl)-indolylmethyl)[1,2,3]triazolo[1,5-*d*][1,4]benzodiazepin-2-one (**IX.59**, 27.0 mg, 0.05192 mmol, 1 eq). butyliodide (24.0 µL, 0.2077 mmol, 4 eq). potassium hydroxide (5.8 mg, 0.1038 mmol, 2 eq). THF (520 µL).

Yield: 83%. *(rac)*-1-butyl-6-butyl-8-chloro-3-(*N*-(tert-butyloxycarbonyl)-indolylmethyl)[1,5-*d*][1,4]benzodiazepin-2-one (**(*rac*)-XI.90**, 24.5 mg, 0.04259 mmol).
Overall yield: 30%.
White solid.
Molecular weight: 575.27 Da.
R_F: 0.48 (hexane/acetone: 6/4).
^{1}H NMR (500 MHz, acetone-d_6) δ 0.67-0.72 (m, 3H, A+B), 0.81-1.01 (m, 5H, A+B), 1.08-1.16 (m, 1H, A+B), 1.20-1.44 (m, 3H, A+B), 1.61-1.70 (m, 11H, A+B), 2.88-2.92 (m, 2H, A+B), 2.92-3.13 (ABX, J_{AB} = 15.3Hz, J_{AX} = 7.9Hz, J_{BX} = 9.3Hz, 0.2H, B), 3.57-3.62 (m, 0.8H, A), 3.70-3.75 (m, 0.2H, B), 3.95-4.06 (ABX, J_{AB} = 15.3Hz, J_{AX} = 6.8Hz, J_{BX} = 7.1Hz, 1.8H, A), 4.25-4.39 (m, 1H, A+B), 5.11 (app t, J = 7.1Hz, 0.8H, A), 5.96(app t, J = 7.9Hz, 0.2H, B), 7.17 (t, J = 7.1Hz, 0.8H, A), 7.21 (t, J = 7.2Hz, 0.2H, B), 7.25-7.35 (m, 1.2H, A+B), 7.60-7.75 (m, 4.8H, A+B), 7.81-8.09 (m, 1H, A+B).
^{13}C NMR (125 MHz, acetone-d_6) δ 13.8 (CH_3, A+B), 14.0 (CH, A+B), 20.0 (CH_2, A), 20.2 (CH_2, B), 22.2 (CH_2, A), 22.8 (CH_2, B), 22.9 (CH_2, A), 25.0 (CH_2, B), 25.4 (CH_2, A), 25.4 (CH_2, B), 28.2 (CH_3, A+B), 30.2 (CH_2, A+B), 31.9 (CH_2, A+B), 48.9 (CH_2, A), 49.9 (CH_2, B), 60.1 (CH, A), 67.4 (CH, B), 84.3 (CH_2, A), 84.5 (CH_2, B) 114.9 (C, B), 115.8 (CH, A), 115.9 (CH, B), 116.9 (C, A), 119.4 (CH, B), 120.2 (C, A), 123.2 (CH, A), 123.4 (CH, B), 124.4 (C, B), 125.0 (CH, A), 125.1 (CH, B), 125.4 (CH, B), 125.6 (C, A), 125.9 (CH, A), 127.3 (CH, B), 127.7 (CH, A), 128.9 (CH, B), 129.0 (CH, A), 130.5 (C, B), 131.2 (CH, A), 131.3 (C, A), 131.5 (CH, B), 132.1 (C, A), 132.2 (C, B), 136.0 (C,

A+B), 138.4 (C, B), 139.1 (C, A), 145.2 (C, A), 146.1 (C, B), 145.0 (C, B), 150.2 (C, A), 166.7 (C, A), 167.1 (C, B).
HATR (cm^{-1}): 2956 (m), 2930 (m), 2872 (w), 1731 (s), 1681 (s), 1611 (w), 1475 (m), 1452 (s), 1409 (m), 1370 (s), 1354 (m), 1308 (m), 1256 (s), 1224 (m), 1156 (s), 1083 (m), 1017 (w), 885 (w), 857 (w), 825 (w), 766 (m), 745 (m).
LC-(ESI)MS (condition 6): M: t_R = 5.6 min $[M+H^+]^+$: 576.1 (100%). **Purity** (214 nm): 99%.
HRMS (ESI) calcd for $C_{32}H_{39}ClN_5O_3^+$: 576.2736 $[M+H^+]^+$ found: 576.2733.

(rac)-8-bromo-1-butyl-6-butyl-3-(*N*-(tert-butyloxycarbonyl)-indolylmethyl)[1,5-*d*][1,4]benzodiazepin-2-one (*rac*)-XI.91

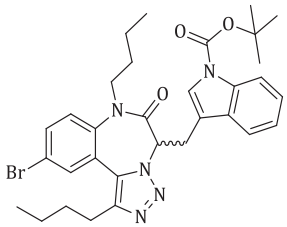

(*rac*)-XI.91

Following general procedure **P.15**: *(S)*-8-bromo-6-butyl-3-(*N*-(tert-butyloxycarbonyl)-indolylmethyl)[1,2,3]triazolo[1,5-*d*][1,4]benzodiazepin-2-one (**IX.66,** 25.3 mg, 0.04482 mmol, 1 eq). butyliodide (20 µL, 0.1793 mmol, 4 eq). potassium hydroxide (5.0 mg, 0.08964 mmol, 2 eq). THF (450 µL).

Yield: 47%. *(rac)*-8-bromo-1-butyl-6-butyl-3-(*N*-(tert-butyloxycarbonyl)-indolylmethyl)[1,5-*d*][1,4]benzodiazepin-2-one **(*rac*)-XI.91** (13.0 mg, 0.02095 mmol).
Overall yield: 21%.
White solid.
Molecular weight: 620.58 Da.
R_F: 0.50 (hexane/acetone: 6/4).
^{1}H NMR (500 MHz, acetone-d_6) δ 0.66-0.72 (m, 3H, A+B), 0.82-1.01 (m, 5H, A+B), 1.07-1.15 (m, 1H, A+B), 1.21-1.41 (m, 3H, A+B), 1.63-1.69 (m, 11H, A+B), 2.87-2.92 (m, 2H, A+B), 2.92-3.12 (ABX, J_{AB} = 15.1Hz, J_{AX} = 7.9Hz, J_{BX} = 9.2Hz, 0.2H, B), 3.56-3.61 (m, 0.8H, A), 3.69-3.74 (m, 0.2H, B), 3.94-4.05 (ABX, J_{AB} = 15.1Hz, J_{AX} = 6.8Hz, J_{BX} = 7.3Hz, 1.8H, A), 4.24-4.38 (m, 1H, A+B), 5.11 (app t, J = 6.9Hz, 0.8H, A), 5.95 (app t, J = 7.9Hz, 0.2H, B), 7.15-7.23 (m, 1H, A+B), 7.24-7.34 (m, 1.2H, A+B), 7.57-7.62 (m, 1.8H, A+B), 7.70-7.74 (m, 1.8H, A+B), 7.77-7.78 (m, 0.8H, A+B), 7.84-7.86 (m, 0.2H, B), 8.04-8.06 (m, 1H, A+B).
^{13}C NMR (125 MHz, acetone-d_6) δ 13.8 (CH_3, A+B), 14.0 (CH, A), 14.3 (CH, B), 20.1 (CH_2, A), 20.2 (CH_2, B), 22.2 (CH_2, A), 22.8 (CH_2, B), 22.9 (CH_2, A), 24.9 (CH_2, B), 25.4 (CH_2, A), 25.4 (CH_2, B), 28.2 (CH_3, A+B), 30.2 (CH_2, A+B), 31.9 (CH_2, A), 32.3 (CH_2, B), 48.9 (CH_2, A), 49.9 (CH_2, B),

60.1 (CH, A), 67.4 (CH, B), 84.3 (CH_2, A+B), 114.9 (C, B), 115.8 (CH, A), 115.9 (CH, B), 116.9 (C, A), 119.3 (CH, B), 119.8 (C, A), 119.8 (C, B), 120.2 (CH, A), 123.2 (CH, A), 123.4 (CH, B), 124.7 (C, B), 125.0 (CH, A), 125.1 (CH, B), 125.4 (CH, B), 125.9 (C, A), 125.9 (CH, A), 127.4 (CH, B), 127.9 (CH, A), 130.4 (C, A), 131.3 (C, B), 131.8 (CH, B), 132.0 (CH, A), 134.1 (CH, A), 134.4 (CH, B), 136.0 (C, B), 139.6 (C, A), 145.2 (C, A), 150.2 (C, B), 166.7 (C, A), 167.1 (C, B).
HATR (cm^{-1}): 2956 (m), 2930 (m), 2871 (w), 1731 (s), 1682 (s), 1605 (w), 1474 (m), 1452 (s), 1407 (m), 1369 (s), 1348 (m), 1308 (m), 1255 (s), 1224 (m), 1156 (s), 1083 (m), 1017 (w), 980 (w), 854 (w), 828 (w), 766 (m), 746 (m).
LC-(ESI)MS (condition 5): M: t_R = 5.8 min $[M+H^+]^+$: 621.1 (100%). **Purity** (214 nm): 95%.
HRMS (ESI) calcd for $C_{32}H_{39}BrN_5O_3^+$: 620.2231 $[M+H^+]^+$ found: 620.2228.

8-chloro-1-methyl-6-phenyl[1,2,3]triazolo[1,5-*d*][1,4]benzodiazepin-2-one XI.92

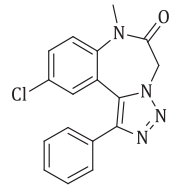

XI.92

Following general procedure **P.15**: 8-chloro-6-phenyl[1,2,3]triazolo[1,5-*d*][1,4]benzodiazepin-2-one (**IX.77**, 22.8 mg, 0.07337 mmol, 1 eq). methyliodide (18.3 µL, 0.2935 mmol, 4 eq). potassium hydroxide (8.2 mg, 0.1467 mmol, 2 eq). THF (750 µL).

Yield: 83%. 8-chloro-1-methyl-6-phenyl[1,2,3]triazolo[1,5-*d*][1,4]benzodiazepin-2-one (**XI.92,** 19.7 mg, 0.06066 mmol).
Overall yield: 30%.
White solid.
R_F: 0.13 (hexane/acetone: 7/3).
Molecular weight: 324.76 Da.
^{1}H NMR (300 MHz, acetone-d_6) δ 3.41 (s, 3H), 4.95-5.00 (m, 1H), 5.30-5.35 (m, 1H), 7.37-7.47 (m, 4H), 7.63 (dd, J = 2.6Hz/9.0Hz, 1H), 7.69-7.73 (m, 3H).
^{13}C NMR (75 MHz, acetone-d_6) δ 37.0 (CH_3), 53.0 (CH_2), 102.3 (C), 127.0 (CH), 128.2 (CH), 129.4 (CH), 129.6 (CH), 131.5 (CH), 166.5 (C).
HATR (cm^{-1}): 3059 (w), 2948 (w), 1682 (s), 1508 (w), 1482 (m), 1446 (w), 1415 (w), 1398 (w), 1360 (w), 1298 (w), 1259 (w), 1239 (w), 1115 (w), 1048 (w), 989 (w), 921 (w), 884 (w), 828 (w), 799 (w), 774 (w), 698 (w).
LC-(ESI)MS (condition 1): t_R = 16.3 min $[M+H^+]^+$: 325.1 (100%). Purity (214 nm): 94%.
HRMS calcd for $C_{17}H_{14}ClN_4O^+$: 325.0851 $[M+H^+]^+$, found: 325.0851.

8-bromo-1-methyl-6-phenyl[1,2,3]triazolo[1,5-*d*][1,4]benzodiazepin-2-one XI.93

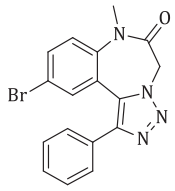

XI.93

Following general procedure **P.15**: 8-bromo-6-phenyl[1,2,3]triazolo[1,5-*d*][1,4]benzodiazepin-2-one (**IX.78,** 26.6 mg, 0.07489 mmol, 1 eq). methyliodide (18.6 µL, 0.2996 mmol, 4 eq). potassium hydroxide (8.4 mg, 0.1498 mmol, 2 eq). THF (750 µL).

Yield: 47%. 8-bromo-1-methyl-6-phenyl[1,2,3]triazolo[1,5-*d*][1,4]benzodiazepin-2-one (**XI.93,** 13.1 mg, 0.03548 mmol).
Overall yield: 21%.
White solid.
Molecular weight: 369.21 Da.
R_F: 0.35 (hexane/acetone: 6/4). 0.15 (hexane/acetone: 7/3) 0.07 (hexane/acetone: 8/2)
^{1}H NMR (300 MHz, acetone-d_6) δ 3.41 (s, 3H), 4.95-5.00 (m, 1H), 5.30-5.35 (m, 1H), 7.37-7.47 (m, 3H), 7.54 (d, *J* = 2.6Hz, 1H), 7.63-7.66 (d, *J* = 8.9Hz, 1H), 7.69-7.77 (m, 2H), 7.77 (dd, *J* = 2.3Hz/8.9Hz, 1H).
^{13}C NMR (75 MHz, acetone-d_6) δ 37.0 (CH_3), 53.0 (CH_2), 119.0 (C), 127.2 (CH), 128.2 (CH), 129.4 (CH), 129.7 (CH), 131.5 (C), 132.4 (CH), 134.4 (CH), 166.5 (C).
HATR (cm^{-1}): 2979 (w), 1681 (s), 1505 (w), 1480 (m), 1445 (w), 1422 (w), 1395 (m), 1359 (w), 1297 (w), 1258 (w), 1238 (w), 1217 (w), 1115 (w), 1046 (w), 987 (w), 918 (w), 885 (w), 824 (w), 773 (m), 698 (m).
LC-(ESI)MS (condition 1): t_R = 16.5 min $[M+H^+]^+$: 370.1 (100%). **Purity** (214 nm): 98%.
HRMS calcd for $C_{17}H_{14}BrN_4O^+$: 369.0345 $[M+H^+]^+$, found: 369.0354.

PART 5: APPENDIX

XX. Atropisomerism

A. Introduction

One of the major concerns of drug developers is to create compounds which are safe, stable and interact in a specific way with a biological receptor responsible for health defects. Besides the general characteristics of the substances, molecular chirality adds an additional level of complexity to the development of new active molecules. In their interactions with a receptor, enantiomers behave as distinct substances and therefore need to be treated as such. Classical chiral-center enantiomers have been shown to differ significantly in biological response and ADME(T) properties. The best known examples of enantiomers acting in a completely different way regarding toxicity and metabolism are thalidomide (**XX.1**, **Figure XX-1**) and perhexiline[1] (**XX.2**).

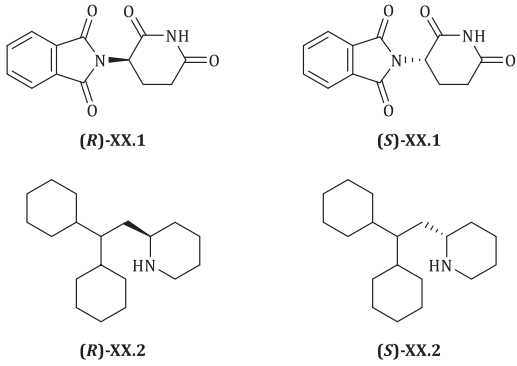

Figure XX-1: Thalidomide (XX.1) and perhexiline (XX.2) enantiomers

Another, and possibly more overlooked, form of drug chirality is that created by a hindered rotation around a single bond, resulting in an energy barrier high enough for separation of conformers. This phenomenon was first discovered and acknowledged by Christie and

Kenner[2] in 1922 after studying 6,6'-dinitro-2,2'-diphenic acid (**XX.4**, **Figure XX-2**). In 1933, Kuhn[3] introduced this new form of chirality as atropisomerism[i] which selectively referred to different enantiomers (i.e. atropisomers) in biaryl compounds. Much later, in 1983, a more general and arbitrary definition of atropisomers was given by Oki[4,5] as:

> *"conformers which, owing to steric or electronic constraints, interconvert slowly enough (by definition, with a half-life of > 1000s [ii]) that they can be isolated".*

Atropisomerism is not limited to drug-like compounds, it concerns a broad range of molecular systems including chiral catalysts (i.e. BINAP[6]), pesticides (i.e. polychlorinated biphenyls, PCB's[7]), agricultural products (metolachor[8]), liquid crystals[9], coolants and lubricants. There is a clear difference between classical chiral center based enantiomers **XX.3** and atropisomers **XX.4**, which can racemize respectively *via* bond cleavage and breaking, and *via* intramolecular dynamic processes involving bond rotation (**Figure XX-2**).

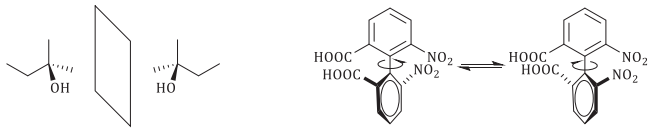

XX.3 **XX.4**

Figure XX-2: Difference between classical enantiomers and atropisomers

This dynamic process is highly time-dependent and influenced by sterical hindrance, electronic influences, temperature and solvent. Half-lives were introduced to define atropisomers according to their level of interconversion at a certain temperature. This enables a qualitative classification of atropisomeric compounds into three classes (**Figure XX-3**), based on the correlation of calculated energy barriers and rotation rates.

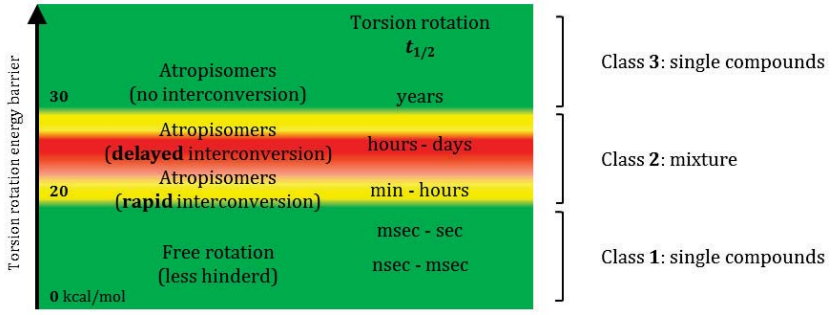

Figure XX-3: Classification of atropisomers based on torsion rotation energy barrier

[i] Atropisomerism is derived from the Greek word *atropos* meaning "without rotation"

[ii] Thus corresponding to a minimum free energy barrier $\Delta G^{\neq}$ calculated by the equation of Eyring equation at various temperatures (200K: $\Delta G^{\neq}$=61.6 kJ/mol, 300K: $\Delta G^{\neq}$=93.5 kJ/mol)

Class 1 compounds which possess fast axial rotation rates in the order of seconds or faster, show no axial chirality, do not have atropisomeric properties and have a rotational energy barrier of $\Delta E_{rot} < \sim 20$ kcal/mol. Compounds within this class occur as single, pure substances and no special precautions regarding atropisomerism have to be taken into account.

Compounds with a rotational energy barrier higher than $\Delta E_{rot} \sim 20$ kcal/mol exhibit a noticeable interconversion over time and are subdivided in two classes (2 and 3). Class 2 compounds have a delayed axial interconversion, characterized by a half-life from minutes to days or months. These rotational isomers are susceptible to racemization during assaying, analytical characterization and shelf storage, leading to inconveniencies regarding safety/efficacy of a drug. Employing class 2 atropisomers as drug is only appropriate if the mixture is used at equilibrium state and the toxicological profile is acceptable. Moreover, problems arise when the half-life of the rotamer is within the range of the *in vivo* elimination. A discrepancy in atropisomer-elimination could lead to an undesired imbalance of the concentration of the atropisomers concerned. Laquinimod (**XX.5**, **Figure XX-4**) is a drug currently in phase III clinical trials for the treatment of multiple sclerosis and other diseases such as Crohns disease. LaPlante and co-workers[1b] characterized this drug as a class 2 atropisomer, although no reports for mirror images were found, assuming that atropisomeric properties were overlooked. By means of a diastereoisomer mimic, LaPlante was able to clearly classify **XX.5** as an atropisomer using dynamic NMR techniques.[10]

Class 3 compounds have a rotational energy barrier which is higher than $\Delta E_{rot} \sim 30$ kcal/mol and therefore have a half-life on the order of years. These substances are stable over time and thus can be isolated as enantiomerically pure compounds. No precautions for drug formulation or drug dosage have to be taken into account. Afloqualone (**XX.6**, **Figure XX-4**) is a sedative hypnotic with a calculated rotational energy barrier of 35.7 kcal/mol. This compound belongs to the family of the Quaaludes, all members of which are Class 3 atropisomers, including commercially available metaqualone.[10]

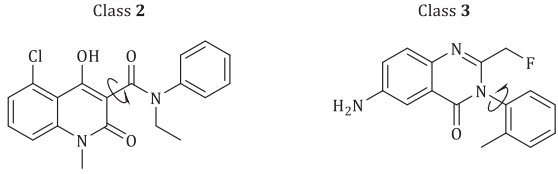

Figure XX-4: Laquinimod (XX.5) and Afloqualone (XX.6)

Ring inversion of diazepam has also been investigated by Gilman and co-workers[11]. An interconversion energy barrier of 17.6 kcal/mol was calculated. In a ^{1}H-NMR spectrum, the mixture of **XX.8** shows a distinct AB pattern for the C(3)-methylene protons indicating a slow interconversion on the NMR time scale. Compared to *N*-desmethyldiazepam (**XX.7**), with a calculated interconversion energy barrier of 12.3 kcal/mol, the C(3)-methylene protons appear as a singlet, indicating a rapid interconversion on the NMR time scale.

Increasing the size of the *N*-amide substituent from a hydrogen in **XX.7** to a *tert*-butyl group in **XX.10**, increases the interconversion energy barrier from 12 kcal/mol to more than 24 kcal/mol. Compound **XX.10** is a class 3 atropisomer, allowing separation and characterization of both enantiomers. As the latter **XX.10** is 100 times less active than diazepam itself, this illustrates the challenge to balance between stereoisomer stability and intrinsic potency in the case of medium-size ring atropisomers.[1]

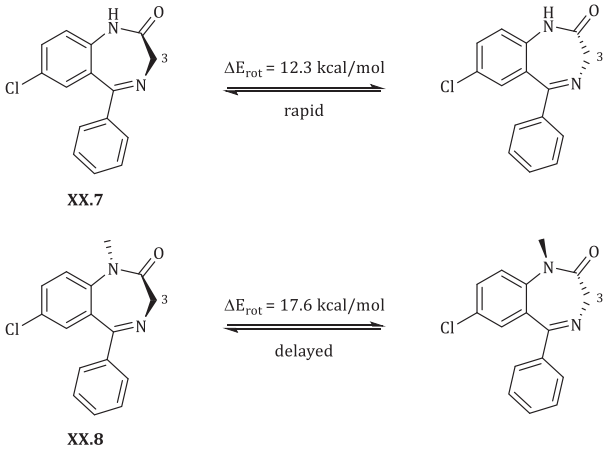

Figure XX-5: N-desmethyldiazepam (XX.7) and diazepam (XX.8)

Table XX -1: Ring inversion energy barriers

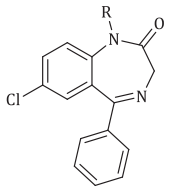

R	ΔE_{rot} [kcal/mol]
H **XX.7**	12
Me **XX.8**	17.6
*i*Pr **XX.9**	21.1
*t*Bu **XX.10**	>24

A link between interconversion energy barrier or Gibbs free activation energy ($\Delta G^{\neq}$) and the half-life of atropisomers at different temperatures can be derived *via* the equation of Eyring [1] assuming a first order reaction for the interconversion between both atropisomers. **Table XX-2** illustrates half-life times as function of the absolute temperature for different Gibbs free activation energies.

$$k = \kappa \frac{k_B . T}{h} e^{-\frac{\Delta G^{\neq}}{RT}} \quad [1]$$

k = rate constant for interconversion
κ = transmission coefficient
k_B = Boltzmann constant
T = absolute temperature
h = Plank's constant
$\Delta G^{\neq}$ = Gibbs free energy of activation
R = universal gas constant

$$\tau_{\frac{1}{2}} = \frac{\ln 2}{2\,k} \quad [2]$$

$\tau_{\frac{1}{2}}$= half-life time
k = rate constant for interconversion

Table XX-2: Half-life times for different free Gibbs activation energies in function of the absolute temperature

		$\Delta G^{\neq}$ [kcal/mol]			
		12	**17.6**	**21.1**	**24**
Temperature	223.15 K	0.0422 s	3.57 h	1.09 y	755 y
	248.15 K	$2.48 .10^{-3}$ s	3.53 min	2.96 d	2.91 y
	273.15 K	$2.43 .10^{-4}$ s	7.35 s	1.29 h	11.2 d
	310.15 K	$1.53 . 10^{-5}$ s	0.135 s	39.6 s	1.21 h
	323.15 K	$6.71 . 10^{-6}$ s	0.0412 s	9.58s	14.6 min

Table XX-2 clearly demonstrates the impact of increasingly sterically demanding groups on the half-life time at different temperatures. The need for detailed insights in the dynamics of atropisomeric compounds, specifically at 37°C or 310.15K has become of utmost importance to understand the biological behavior of a lead compound.

B. Dynamic NMR studies

Different techniques can be employed in order to investigate dynamic properties of compounds. Variable-temperature or dynamic NMR can be used to study atropisomeric processes. This can be done when the interconversion process is slow on the NMR time scale which can be translated into the following:

$$k = \frac{1}{t} << \pi \frac{\Delta \nu}{\sqrt{2}} \quad [3]$$

k = rate constant for interconversion
t = interconversion time
$\Delta \nu$ = difference in chemical shift (in Hz) between distinguished signals

In this case both atropisomers and their distinct proton nucleus environment can be observed and their ^{1}H NMR signals can be interpreted independently. This phenomenon is also referred to as *slow exchange*. If the separate ^{1}H NMR signals are converging as an average signal, interconversion between both atropisomers is fast, hence not allowing to identify the separate atropisomers and their distinct proton nucleus environment.

During this research, while characterizing synthesized *N*-alkylated compounds (see chapter **XI**), abnormally broad ^{1}H NMR signals were detected for NMR spectra recorded at room temperature. 2D NMR techniques (HSQC, HMBC, COSY and TOCSY) were employed to correlate these broadened signals with the specific protons. The broadened signals could be associated with spin systems 1 and 2 (see **Figure XX-6**).

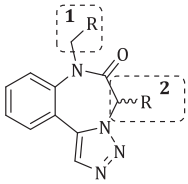

Figure XX-6: Spin systems 1 and 2 for *N*-alkylated compounds

The strong broadening of the peaks is related to an interchange between two conformers which cannot be detected separately at room temperature. This state is referred to as coalescence. By performing various ^{1}H NMR experiments at both higher and lower temperatures, a transition from slow to fast exchange can be observed.

In particular, for compound (**XI.57, Figure XX-7**) after recording a spectrum under standard conditions, identifying strong peak broadening and assigning the ^{1}H NMR signals, a more comprehensive study was undertaken to gain more insight in the dynamic properties of this molecule. An attempt for representing both atropisomeric structures is shown in **Figure XX-7.**

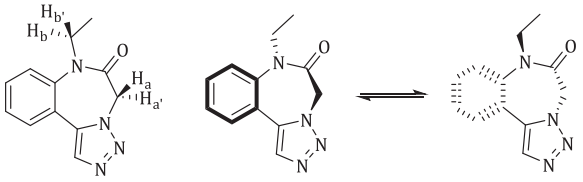

XI.57

Figure XX- 7: Compound XI.57 and illustration of possible atropisomers

In **Figure XX-8** a full ^{1}H NMR spectrum of compound **XI.57** is depicted, clearly illustrating the strongly broadened peaks which are related to H_a and H_b (assigned *via* 2D NMR techniques).

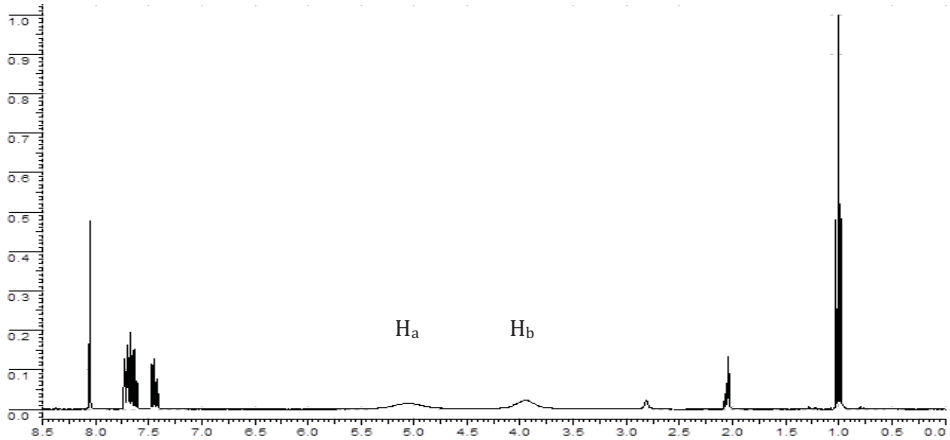

Figure XX- 8: Full ^{1}H NMR spectrum indicating strongly broadened signals for H_a and H_b (acetone-d_6, 298K, 300 MHz)

Thanks to an extensive dynamic NMR study performed at various temperatures (from 223K till 328K), **Figure XX-8** could be built up. The latter only focusses on the region 3.7-5.5 ppm which is impacted with broadened signals. When the sample temperature is decreased, a more distinct peak separation occurs which, upon further cooling, results in an equimolar presence of double doublets at 253K. From this temperature onwards, the conformers are in a state of slow exchange.

When the sample temperature is increased, the broad signals tend to become sharper, resulting in apparent singlets, as a consequence of fast exchange on the NMR-time scale and an averaged signal for both conformers. Dynamic NMR in combination with the Eyring equation would enable an estimation of the Gibbs free energy of activation.

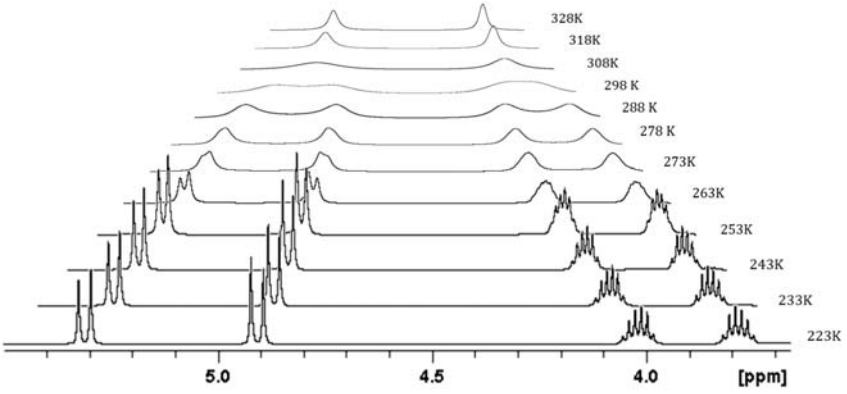

Figure XX- 9: NMR spectra at different temperatures for compound XI.57 (acetone-d_6, 500MHz)

In addition, for compounds **XI.65** and **XI.72** respectively equipped with a methyl and an isopropyl group, the ^{1}H NMR spectra at room temperature are represented in **Figure XX-10.** The latter clearly indicates for **XI.65** a lower Gibbs free energy of activation comparing to **XI.57,** as fast exchange is more predominant. For **XI.72**, a higher Gibbs free energy of activation is observed as this compound tends to be in slow exchange at room temperature. Further detailed temperature studies to estimate the Gibbs free energy of activation for **XI. 57**, **XI.65** and **XI.72** are required.

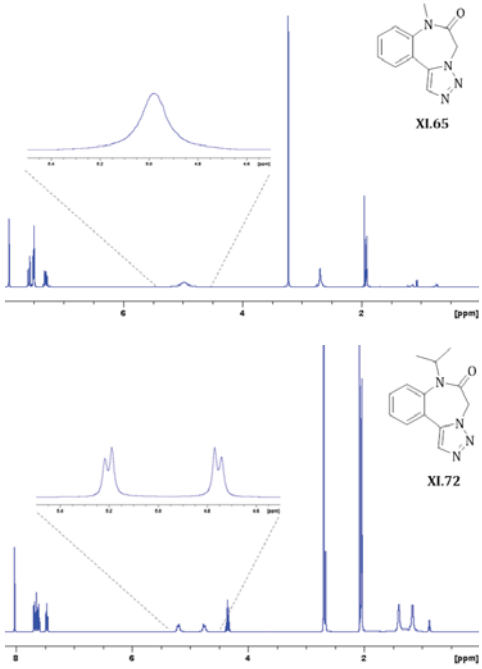

Figure XX- 10: Full and detailed ^{1}H spectra for XI.65 and XI.72 (acetone-d_6, 298K, 500MHz)

REFERENCES

[1] a) LaPlante, S. R.; Fader, L. D.; Fandrick, K. R.; Fandrick, D. R.; Hucke, O.; Kemper, R.; Miller, S. P. F.; Edwards, P. J. *J. Med. Chem* **2011**, *54*, 7005-7022. b) LaPlante, S. R.; Edwards, P. J.; Fader, L. D.; Jakalian, A.; Hucke, O. *ChemMedChem* **2011**, *6*, 505-513.

[2] Christie, G. H.; Kenner, J. *J. Chem. Soc.* **1922**, *121*, 614-620.

[3] Kuhn, R. in *Stereochemie* (Ed.: F. Freudenberg), Franz Deuticke, Leipzig, **1933**, pp. 803-824.

[4] Oki, M. *Top. Stereochem.* **1983**, *14*, 1.

[5] Bringmann, G.; Mortimer, J. P.; Keller, P. A.; Gresser, M. J.; Garner, J.; Breuning, M. *Angew. Chem. Int. Ed.* **2005**, *44*, 5384-5427.

[6] Noyori, R.; Takaya, H. Acc. Chem. Res. **1990** *23*, 345.

[7] a) Kania-Korwel, I.; El-Komy, M. H. M. E.; Veng-Pedersen, P.; Lehmler, H.-J. Environ. Sci. Technol. **2010**, *44*, 2828–2835. b) Jamshidi, A.; Hunter, S.; Hazrati, S.; Harrad, S. Environ. Sci. Technol. **2007**, *41*, 2153– 2158

[8] Dreikorn, B. A.; Jourdan, G. P.; Hall, H. R.; Deeter, J. B.; Jones, N. J. J. Agric. Food Chem. **1990**, *38*, 549– 552;

[9] Vizitiu, D.; Halden, B. J.; Lemieux, R. P. Chem. Commun. **1997**, 1123–1124.

[10] Supporting information of LaPlante, S. R.; Edwards, P. J.; Fader, L. D.; Jakalian, A.; Hucke, O. *ChemMedChem* **2011**, *6*, 505-513.

[11] Gilman, N. W.; Rosen, P.; Earley, J. V.; Cook, C.; Todaro, L. J. *J. Am. Chem. Soc.* **1990**, *112*, 3969-3979.

XXI. NMR Case Study

A. Introduction

A detailed assignment for the obtained NMR spectrum of compound **XI.81** will be made by means of analyzing recorded 1D NMR and 2D NMR spectra. As compound **XI.81** shows atropisomeric properties, a full assignment of both atropisomers will be pursued. At room temperature, compound **XI.81** interconverts between two conformers, whereas upon integration of the NMR signals a minor and major conformer can be identified. As a guide, capital letters (H and C) are used for the major atropisomer and lower case letters (h and c) are used for the minor conformer.

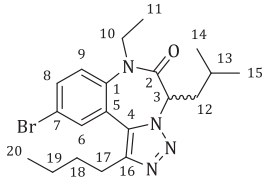

XI.81

In **Figure XXI.1** and **Figure XXI.2,** a full 1D NMR and C13 APT respectively recorded at 500 MHz and 176 MHz are presented. Labels are attached to each multiplet, which will be used to discuss and annotate the specific signals in detail. Even more, this complex fully diversified scaffold will be subdivided in four different spin systems to ease the assignment. A 2D TOCSY experiment (**Figure XXI.3**) enables the identification of each spin system and supports further elucidation.

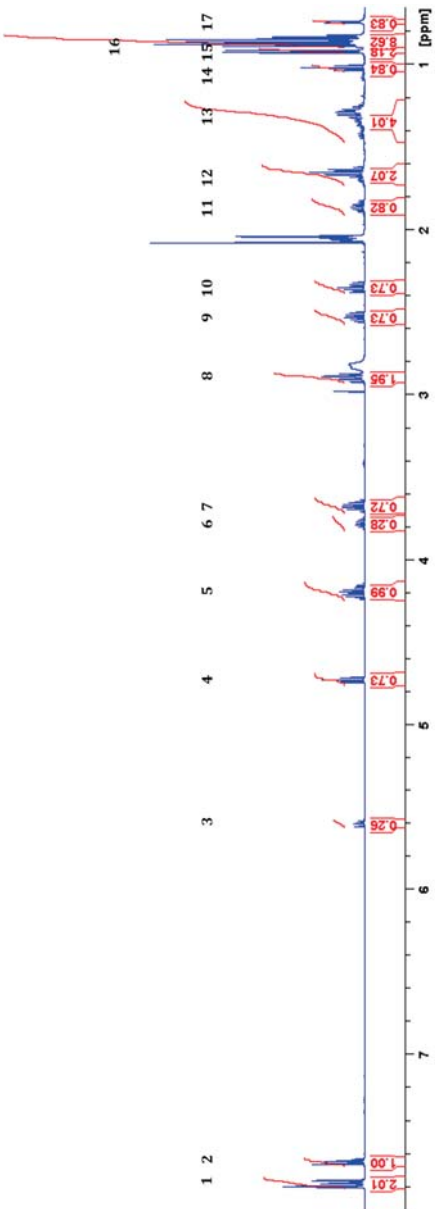

Figure XXI.1: Full 1D spectrum (500 MHz)

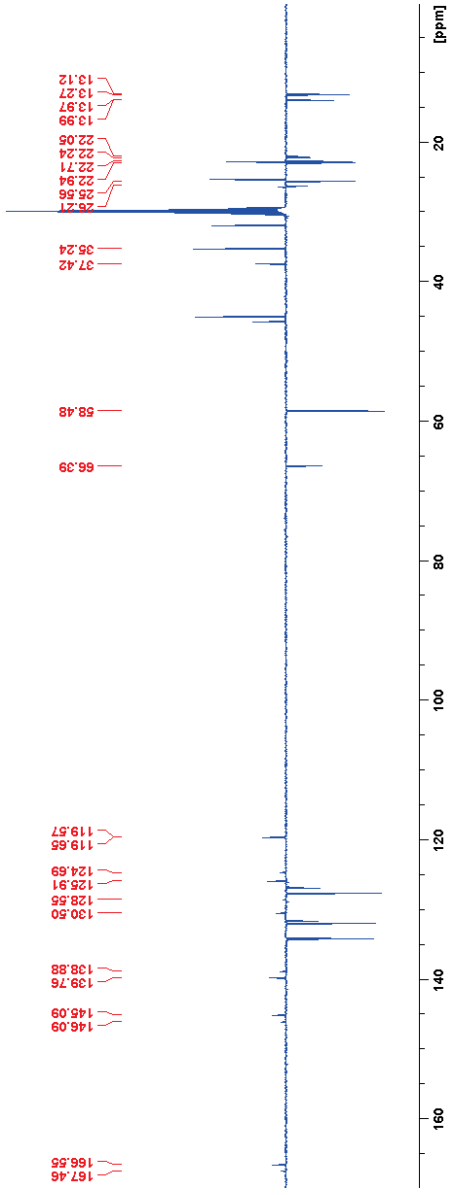

Figure XXI.2: Full C13 APT spectrum (176 MHz)

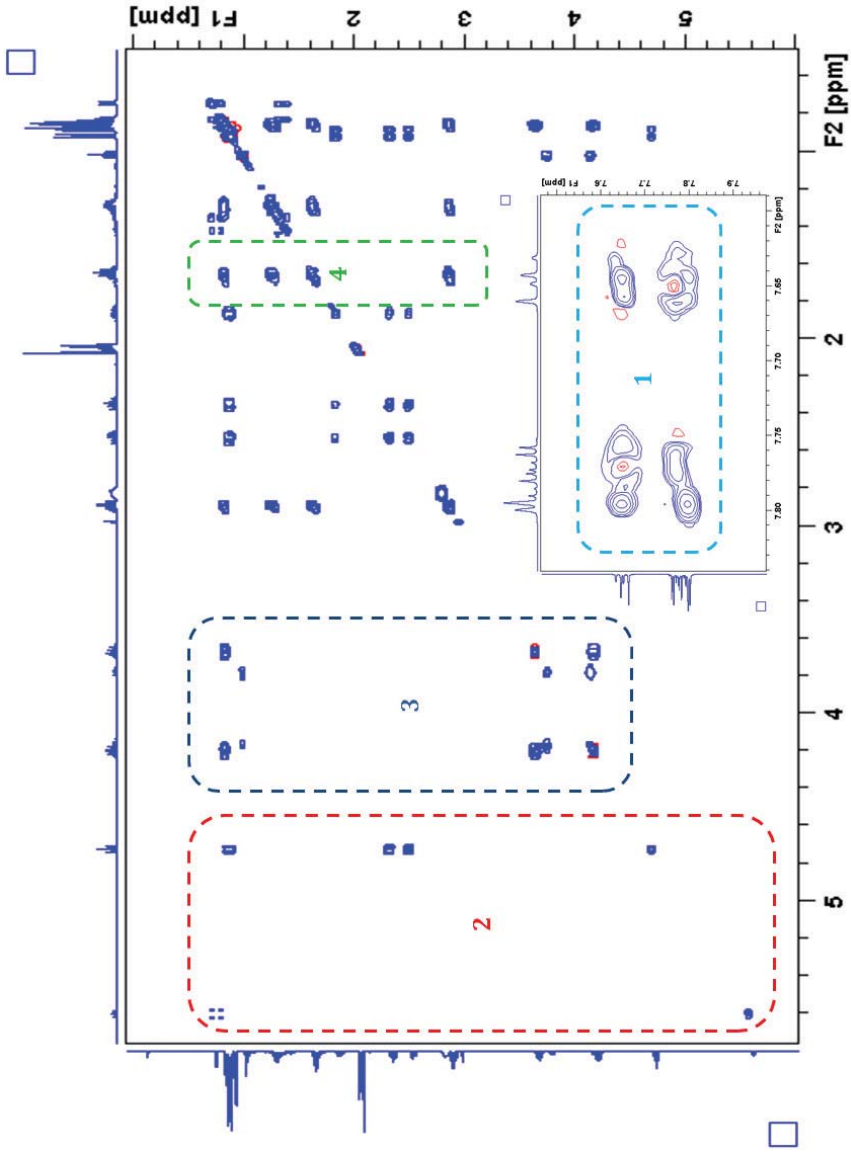

Figure XXI.3: Full 2D TOCSY spectrum with annotation of the selected spin systems

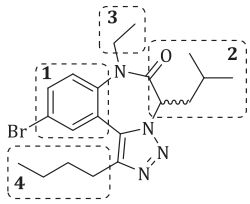

Spin system	Residue
1	Aromatic moiety
2	Amino acid side chain
3	Ethyl group
4	*n*-Butyl group

B. Spin system 1

Figure XXI.4 illustrates the aromatic region of the 1D NMR (7.60 – 7.85 ppm) where two aromatic multiplet regions can be observed: region 1 (**M1**, 7.75-7.80 ppm) integrating for two hydrogens and region 2 (**M2**, 7.63-7.66 ppm) integrating for one hydrogen. Whereas the sum is in correspondence with the number of aromatic hydrogens present in molecule **XI.81**, both atropisomers give overlap within the depicted regions.

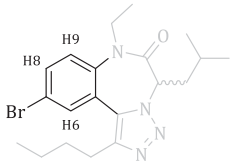

XI.81

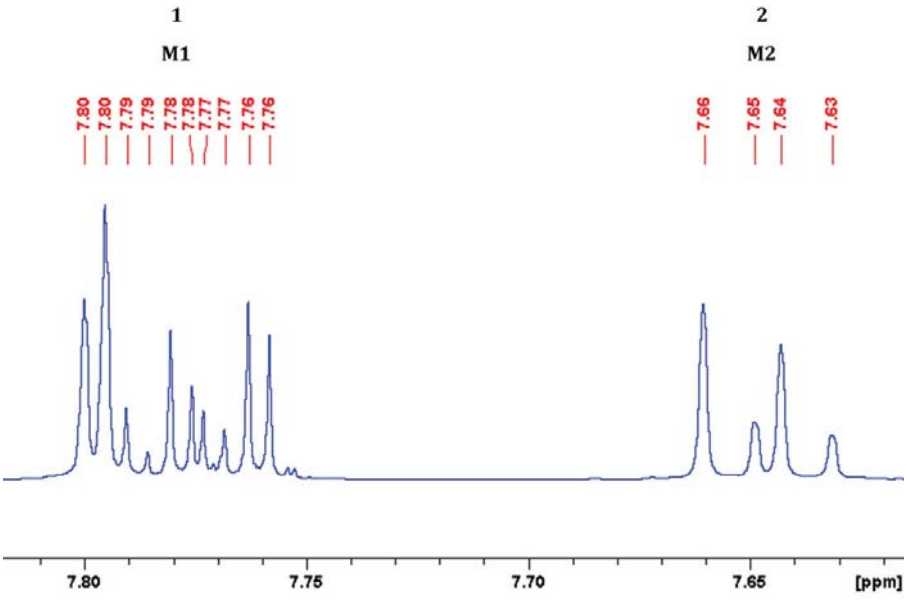

Figure XXI.4: Detail 1D NMR aromatic spin system

Label	multiplicity	ppm	Integration
1	m	7.80 - 7.76	2
2	m	7.66 - 7.63	1

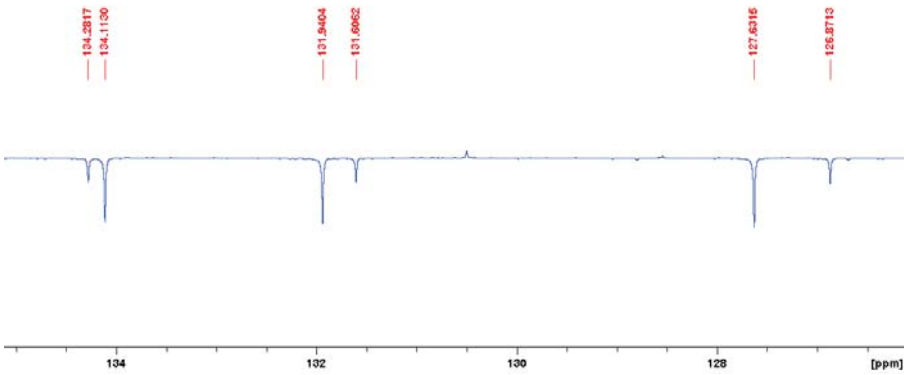

Figure XXI.5: Detail C13 APT aromatic spin system

Further analyzing **M1** gives arise to observe three underlying separate signals systems: d_1, dd_1 and dd_2. A schematic representation of these individual coupling systems is given in **Figure XXI.6**. Whereas d_1 integrates for (approx.) one and dd_1 and dd_2 together also integrate for one. In the d_1 system a coupling of 2.4Hz is measured, which is a typical value for meta coupled protons therefore assigning d_1 to H6 and h6 as both atropisomers have an identical chemical shift. As the two double doublets (dd_1 & dd_2), correspond to the signals of minor and the major atropisomer with both a J^2 coupling of 8.7Hz and a J^3 coupling of 2.4Hz an assignment for dd_1 as h8 and dd_2 as H8 is made.

Multiplet two (**M_2**) can be subdivided into two doublets (d_2 and d_3, see **Figure XXI.6**) both with a J^2 coupling of 8.7Hz, corresponding for a ortho coupling with another aromatic hydrogen. Taking into the account the doublet splitting pattern, the large coupling constant and the integration; an assignment for d_2 as H9 and for d_3 for h9 is made.

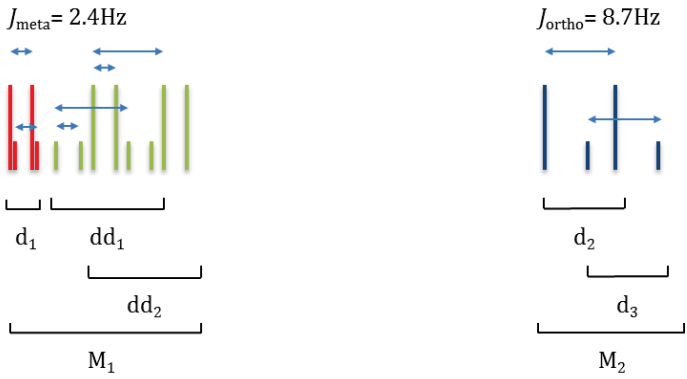

Figure XXI.6: Schematic representation of the aromatic region (7.60-7.85 ppm)

In **Figure XXI.5** (*vide supra*), a close-up for the aromatic CH region is presented where can be seen that both atropisomers give arise to separate APT signals. By using cross peak analysis in 2D HSQC (**Figure XXI.7**) a full identification of all CH carbons can be made.

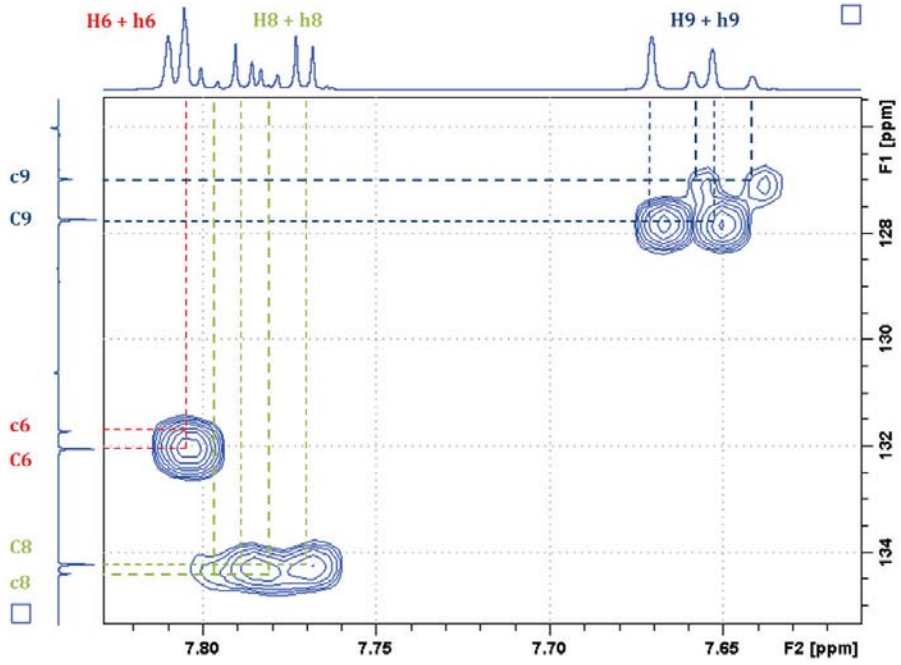

Figure XXI.7: 2D HSQC detail related to the aromatic region

C. Spin system 2

In **Figure XXI.8**, two signals can be recognized as spin systems corresponding to the minor and the major atropisomer of the hydrogen in position 3 as the chemical shift and integration values agree with the expected values for α-hydrogens of amino acids.

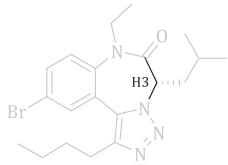

XI.81

More specifically, a double doublet for the minor conformer and an apparent triplet for the major conformer. By means of 2D HSQC cross peaks correlation (**Figure XXI.10**), the corresponding APT signals (**Figure XXI.9**) can be assigned for both atropisomers.

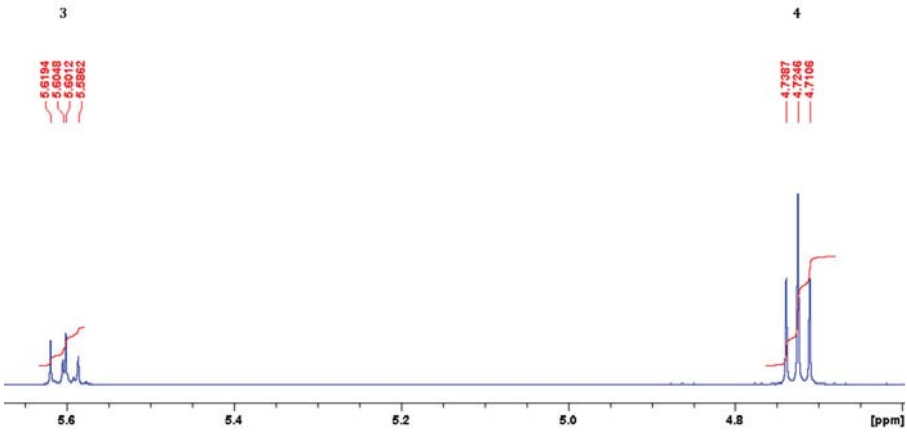

Figure XXI.8: Detail 1D NMR α-H amino acid region

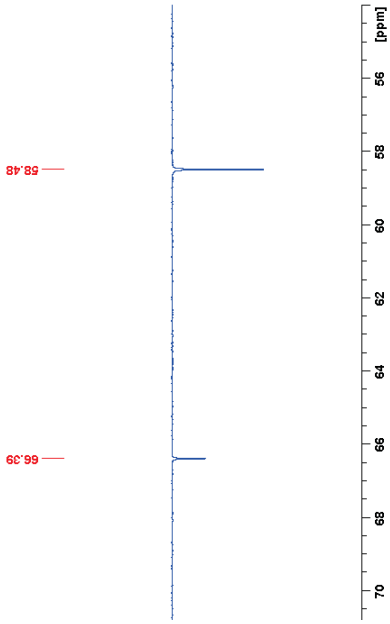

Figure XXI.9: Detail C13 APT 55-71 ppm

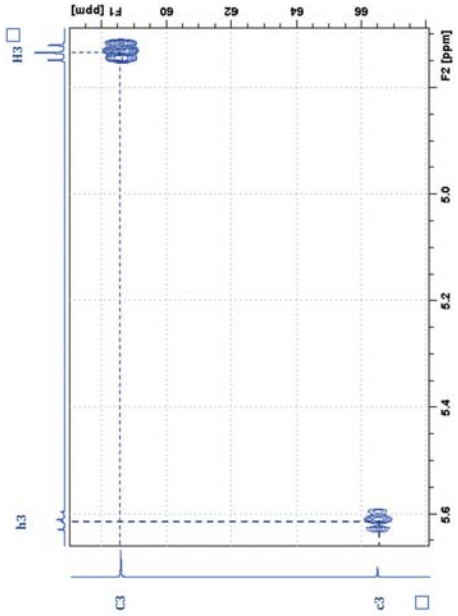

Figure XXI.10: 2D HSQC detail related to α-H amino acid region

In **Figure XXI.11**, a detailed view of 1D NMR region 1.20-2.60 ppm is given where four signals of interest can be recognized. In **Figure XXI.12** till **Figure XXI.13**, the details of 2D HSQC are given which enable us to see the bonded carbons. Whereas **Figure XXI.14** represents a detail of the concerning APT region.

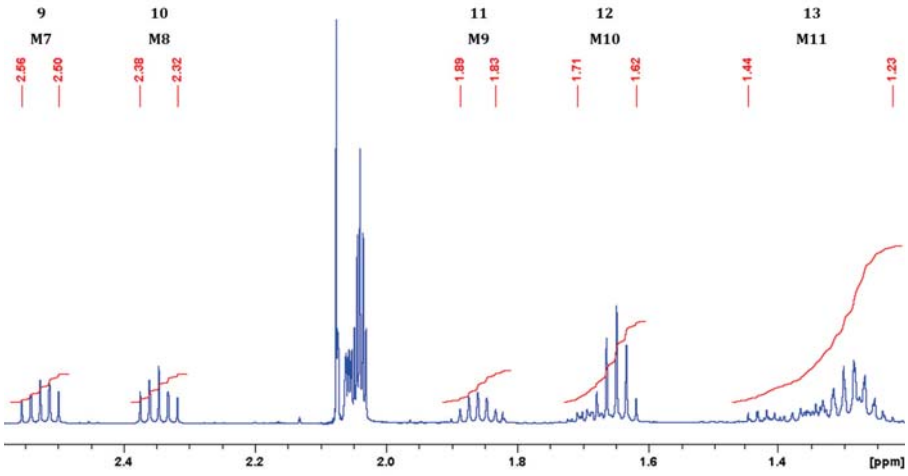

Figure XXI.11: Detail 1D NMR 1.20-2.60 ppm

Label	multiplicity	ppm	Integration
9	m	2.50 - 2.56	0.73
10	m	2.32 - 2.38	0.73
11	m	1.83 - 1.89	0.80
13	m	1.23 - 1.44	4.00

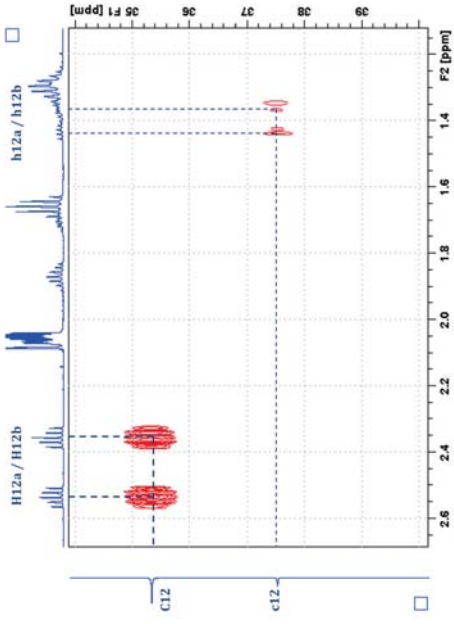

Figure XXI.12: 2D HSQC detail related to 9 and 13

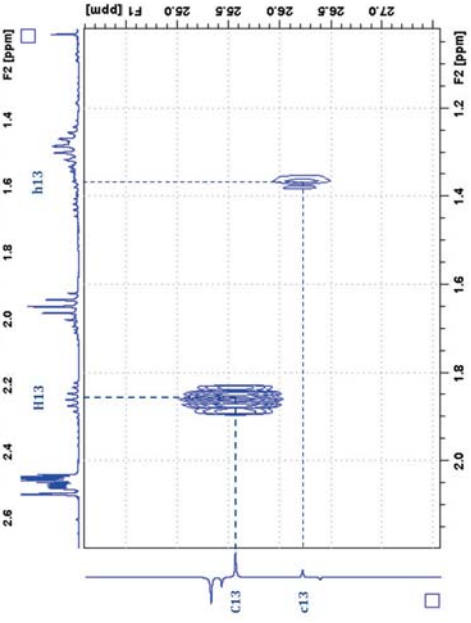

Figure XXI.13: 2D HSQC detail related to 11 and 13

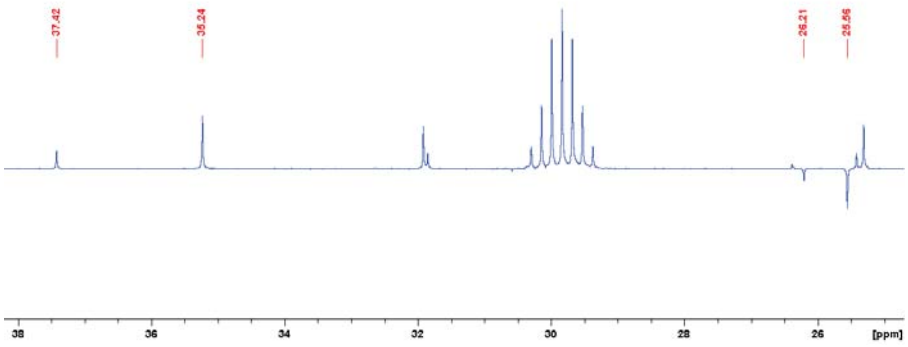

Figure XXI.14: Detail C13 APT related to region 9 - 11

In **Figure XXI.12**, it can be seen that region 9 and 10 are bound to the same carbon, more specifically they represent the major atropisomer of a CH_2-fragment. The minor conformer can be found within region 13. **Figure XXI.13**, shows the relation between region 11 and the bounded carbon(s). The presented cross peaks relate to the major and minor conformer of a CH-fragment in the molecule. In order to make the right assignment for these signals, a detailed 2D COSY representation given between region 9 and 10 and hydrogen three (H3) (**Figure XXI.15**) and between region 9 - 10 and region 11 (**Figure XXI.16**). A 2D COSY cross peak between region 9 and 10 and H3 leads to the assumption that the corresponding carbons are next to each other. Whereas **Figure XXI.16**, illustrates the close structural proximity between region 9 and 10 and region 11.

Taking into account these observations and integration values, region 9 and 10 are assigned to H12a and H12b. A distinction between both signals cannot be made. The corresponding minor atropisomer signals h12a and h12b are found in region 13. Region 11 is assigned to H13 for the major atropisomer, whereas region 13 also includes the minor atropisomer. A 2D TOCSY detail is given to give proof of the full coupling system (**Figure XXI.29**, *vide infra*), in the latter can also be seen that another coupling partner is found in region 16 which will be discussed later.

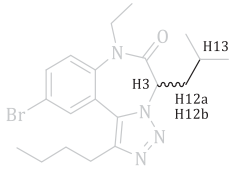

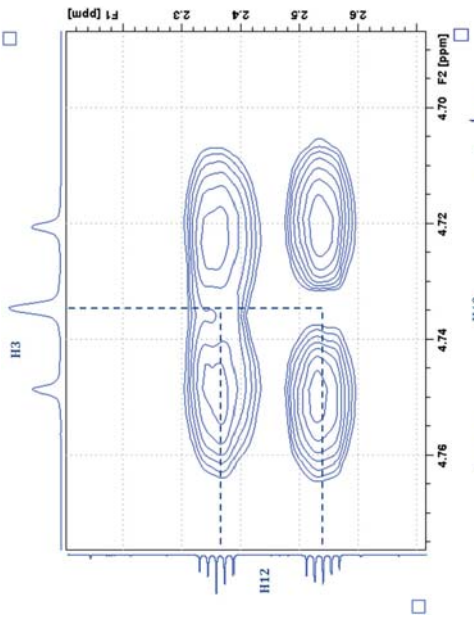

Figure XXI.15: 2D COSY detail related to 4 and 9-10

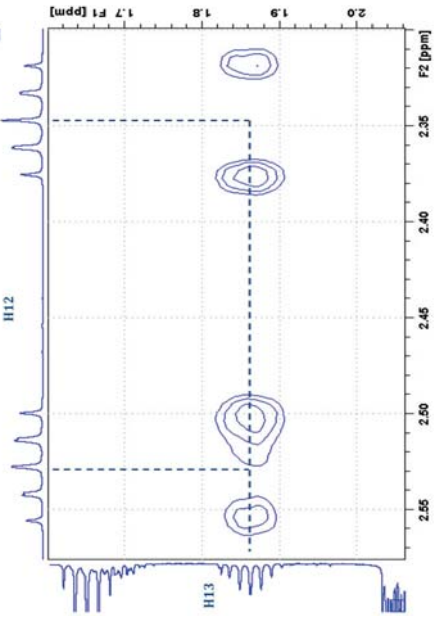

Figure XXI.16: 2D COSY detail related to 9-10 and 11

Moreover, for region 9 (2.31-2.37 ppm) and region 10 (2.50-2.55 ppm), both appearing as an identical multiplet, a complex splitting pattern is observed. The latter can be explained by a J^2 coupling with a geminal hydrogen and two J^3 scalar couplings with H3 and H13. A schematic representation of this splitting pattern shown in **Figure XXI.17**.

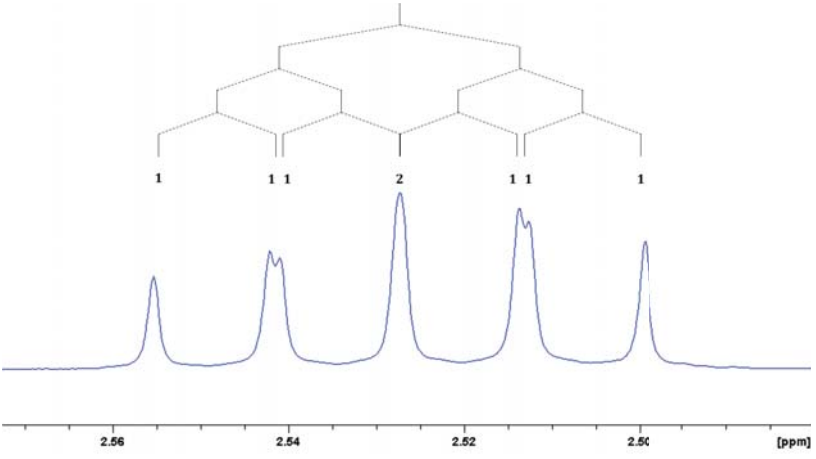

Figure XXI.17: Detail of region 9 and proposed splitting pattern

In **Figure XXI.18**, a detail is given for region 0.70-1.05 ppm whereas from left to right, regions 14 to 17 are denoted and respectively appear as a triplet (t_3), a doublet (d_4), a multiplet and doublet (d_7).

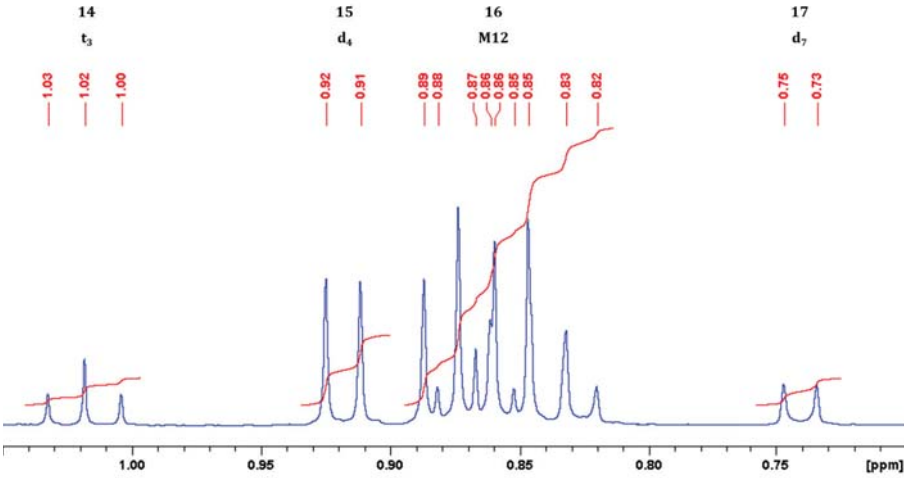

Figure XXI.18: Detail 1D NMR 0.70 – 1.05 ppm

Label	multiplicity	ppm	Integration
14	t	2.50 - 2.56	0.83
15	d	2.32 - 2.38	2.18
16	m	1.83 - 1.89	8.62
17	d	1.23 - 1.44	0.83

In **Figure XXI.19** till **Figure XXI.22** details of the 2D HSQC and 2D COSY are provided in order to obtain a better insight in the corresponding bounded carbons and the neighboring coupling partners. **Figure XXI.23** accounts for a detail of the related APT region.

In **Figure XXI.19** it can clearly be seen that four cross peaks are found between CH or CH_3 APT peaks and signals within the 1D region. More specifically, there are two cross peaks with two doublets and two with the multiplet region. In combination with the fact that they are no unassigned CH signals left and a 2D COSY cross peak to a nearby coupling partner, i.e. H13, anchors these signals as H14 and H15 but also h14 and h15.

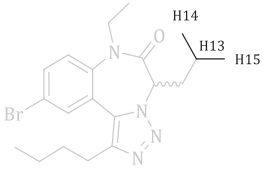

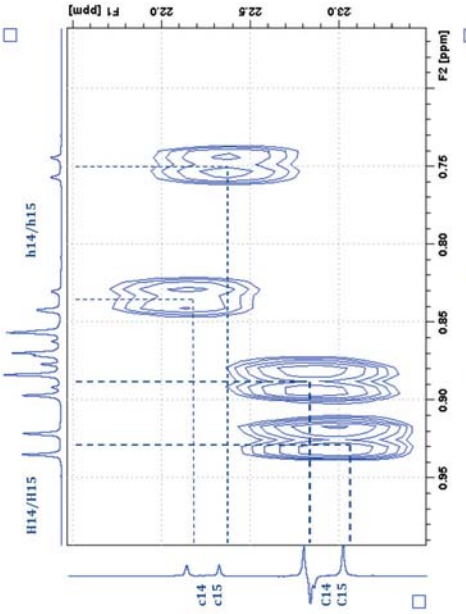

Figure XXI.19: 2D HSQC detail related to region 15 - 16

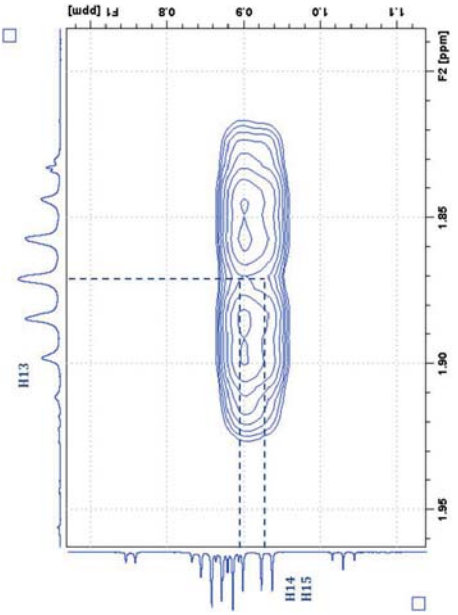

Figure XXI.20: 2D COSY detail correlation between region 11 and region 16

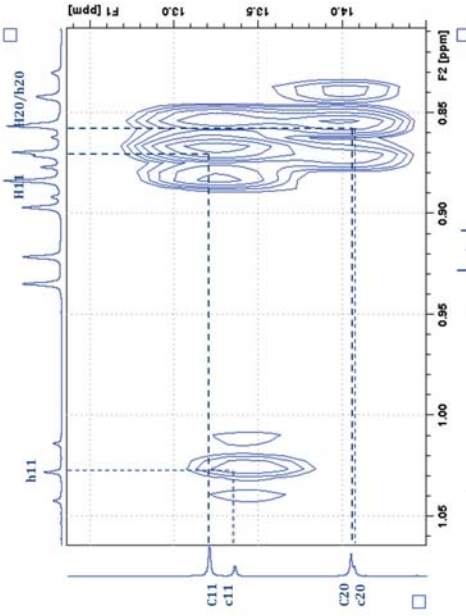

Figure XXI.21: 2D HSQC detail related to region 14 - 16

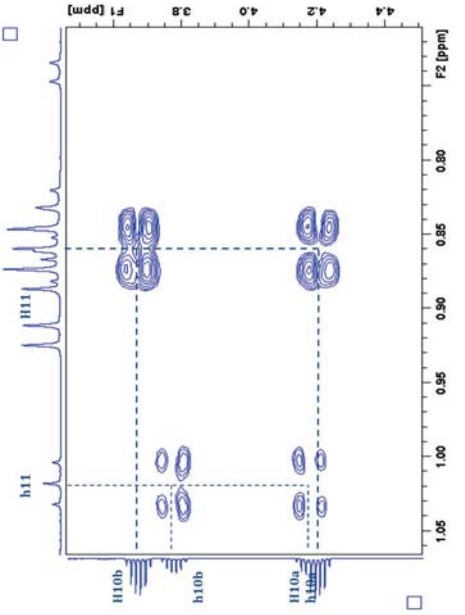

Figure XXI.22: 2D COSY detail correlation between region 14 – 16 and region 5 to 7

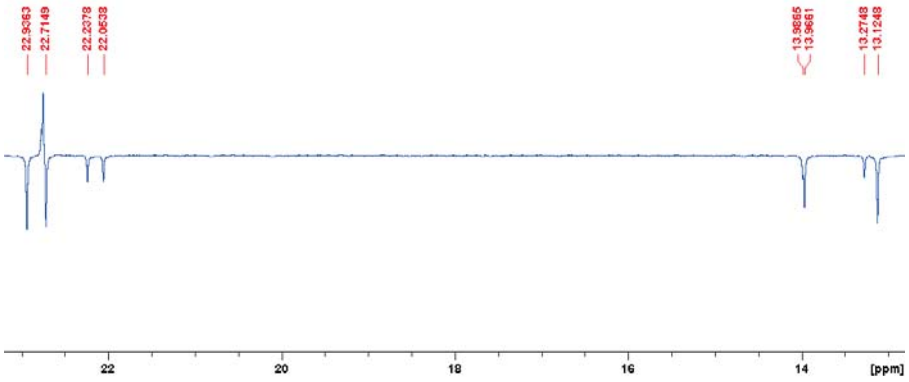

Figure XXI.23: Detail C13 APT related to region 14 to 17

Apart from these methyl signals, three other cross peaks are found to be located within this studied range in the 1D spectrum. Taken into account the integration value, one of these signals corresponds with for the minor atropisomer. **Figure XXI.22** shows 2D COSY cross peaks with signals within spin system 4, therefore assuming that these two triplets account for H11 and h11 (*vide infra*).

Even more, in **Figure XXI.24**, a 2D COSY cross peak is presented assuming the signal to be terminal methyl group from butyl chain in spin system 4.

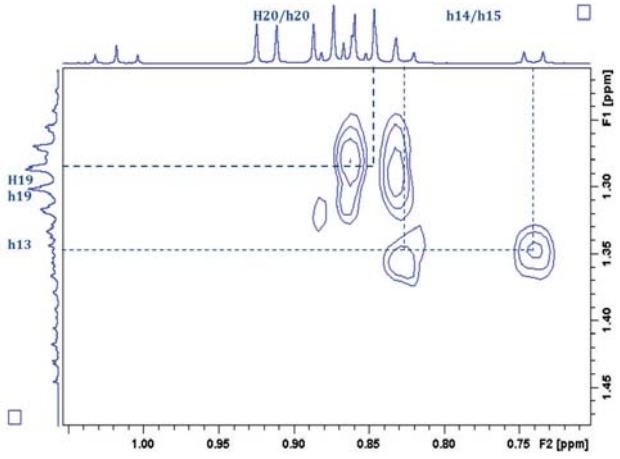

Figure XXI.24: 2D COSY detail related to region 16 – 17 and region 13

The provided knowledge presented above, enables a deeper analysis of the region 14 to 17 which shows a clear subdivision into specific signals (**Figure XXI.25**).

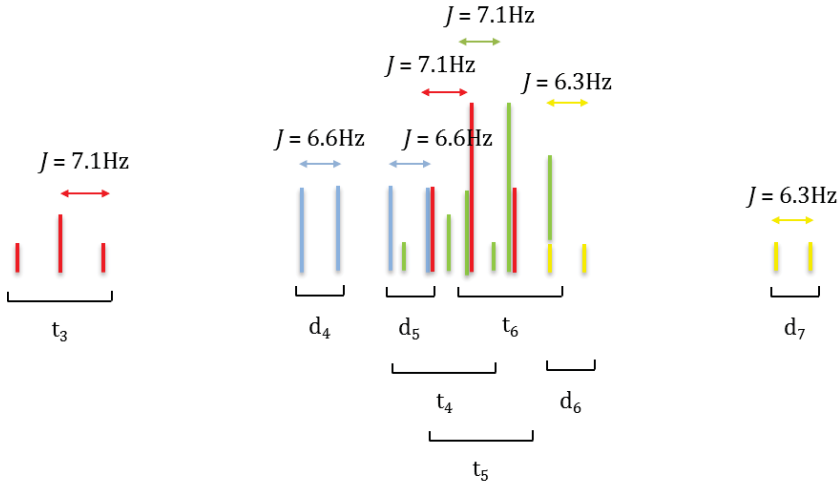

Figure XXI.25: Schematic representation of splitting pattern in region 14 to 17

multiplicity	ppm	integration	annotation
t_3	1.00 – 1.03	0.83	h11
d_4	0.91 – 0.92	2.18	H14 or H15
d_5			H14 or H15
t_4			h20
t_5	0.82 – 0.89	8.62	H11
t_6			H20
d_6			h14 or h15
d_7	0.73 - 0.75	0.83	h14 or h15

D. Spin system 3

In **Figure XXI.26**, a detailed view is given on the region 3.60-4.30 ppm whereas three regions 5, 6 and 7 can be seen as multiplets. In **Figure XXI.27** and **Figure XXI.28** a 2D HSQC and 2D COSY detail are presented, where can be seen that all 1D signals are bound to a CH_2-fragment. Furthermore, the 2D COSY detail reveals strong cross peaks with methyl fragments previously assigned as H11 and h11.

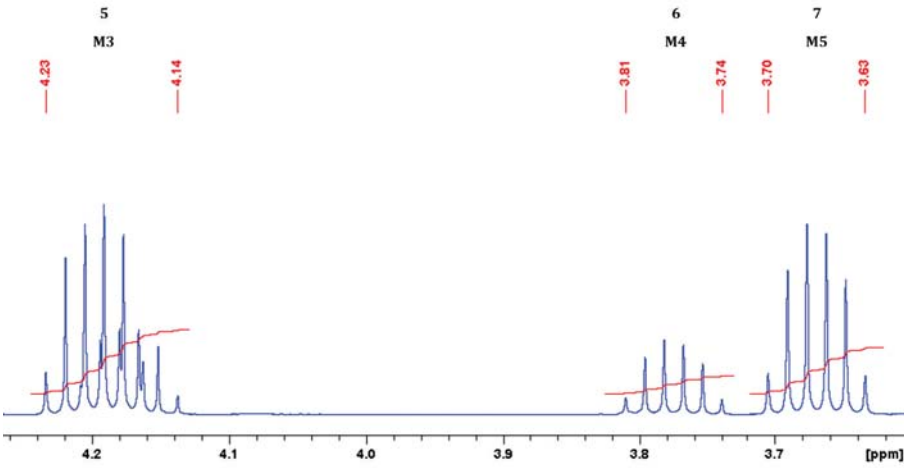

Figure XXI.26: Detail 1D NMR 3.60 – 4.25 ppm

Label	multiplicity	ppm	Integration
5	m	4.14 – 4.23	1.00
6	m	3.74 - 3.81	0.28
7	m	3.63 – 3.70	0.72

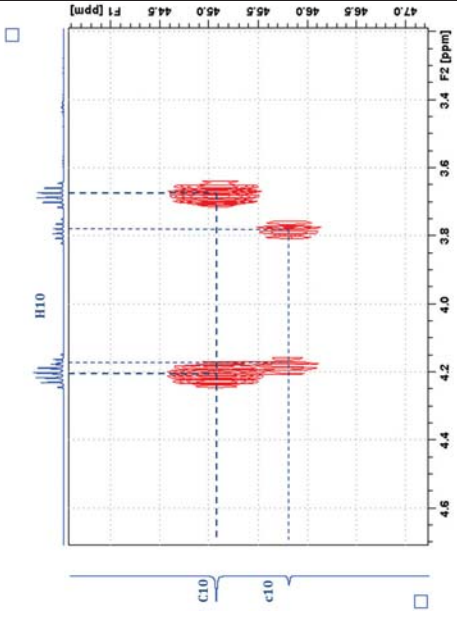

Figure XXI.27: 2D HSQC detail related to region 5 to 7

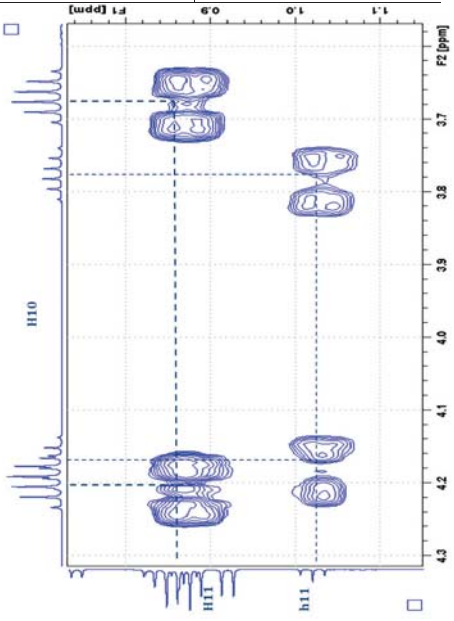

Figure XXI.28: 2D COSY detail related to region 5 to 7 and region 14 - 16

Figure XXI.29 represents a 2D TOCSY experiment which enables us to isolate different spin systems. It can be seen that spin system 3 only shows four cross peaks. In accordance to this observation, taken into account the knowledge provided by **Figure XXI.27** and **Figure XXI.28**, combined with the corresponding coupling value of approx. 7.0Hz, region 5 is assigned to both atropisomers of one hydrogen (H10a and h10a) on position 10. Region 6 and region 7 are respectively assigned to the minor and major atropisomer of another hydrogen present in position 10.

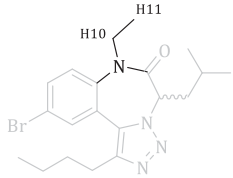

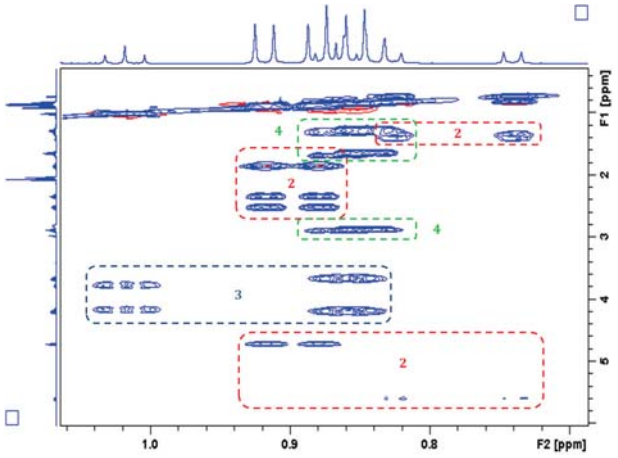

Figure XXI.29: 2D TOCSY detail appointing three spin systems regarding the aliphatic region

This assignment makes it possible to unveil the underlying splitting pattern behind the multiplets. Region 5 is build up by two apparent sextets and both region 6 and region 7 are two separate apparent sextets. In **Figure XXI.30**, a schematic representation is given for the suggested multiplicities. The occurring apparent sextets can be explained by an overlap of double quadruplets.

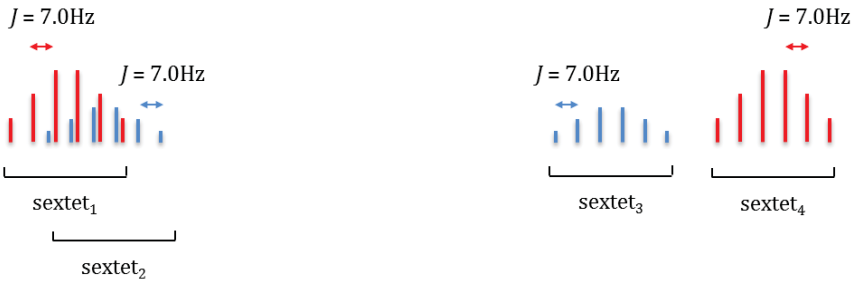

Figure XXI.30: Schematic representation of the region 5 to 7

E. Spin System 4

The data presented above and **Figure XXI.29** (*vide supra*) give proof of correlation between the remaining unassigned triplets (t_4 and t_5) in region 16 and H20. In **Figure XXI.31** a 2D COSY walkthrough is presented and in **Figure XXI.32** till **Figure XXI.37**, 2D COSY and 2D HSQC details are presented in order to determine the corresponding 1D signals from spin system 4.

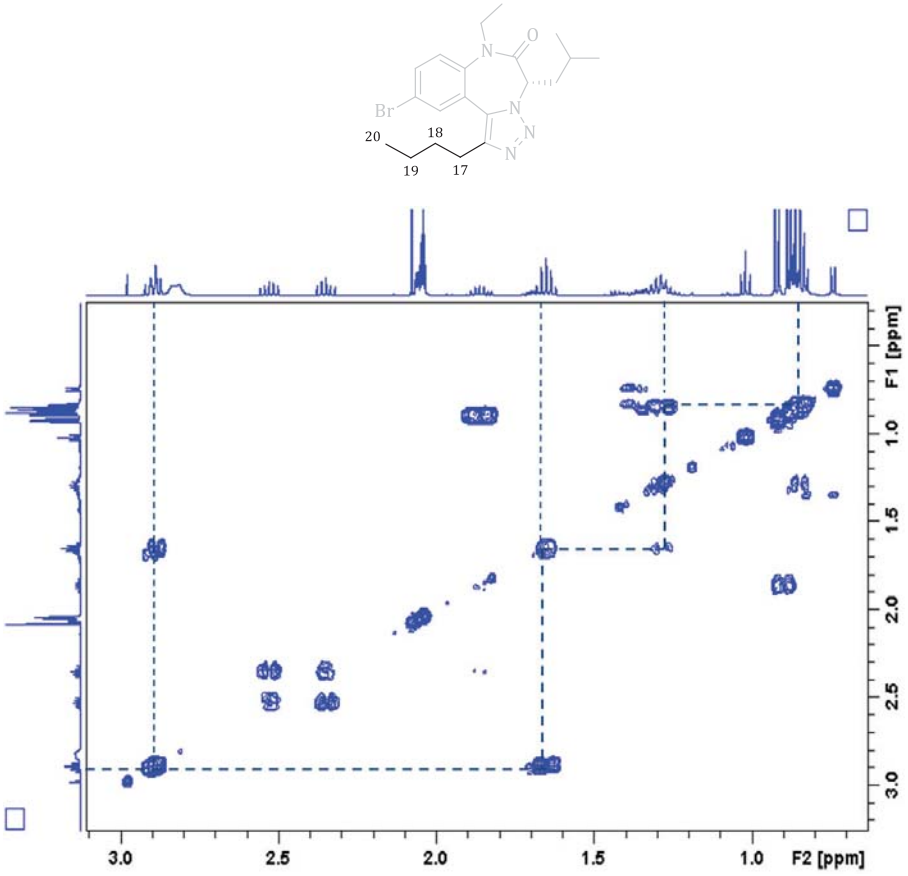

Figure XXI.31: 2D COSY walkthrough related to spin system 4

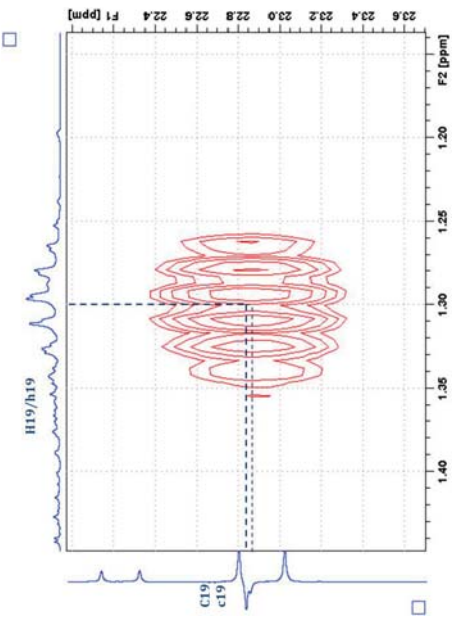

Figure XXI.32: 2D HSQC detail related to region 13

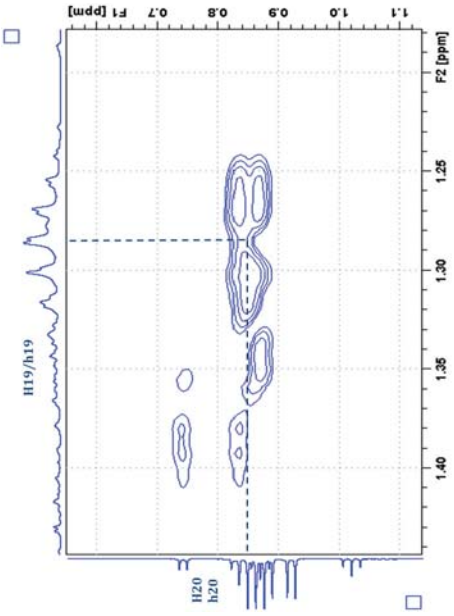

Figure XXI.33: 2D COSY detail related to region 13 and region 16

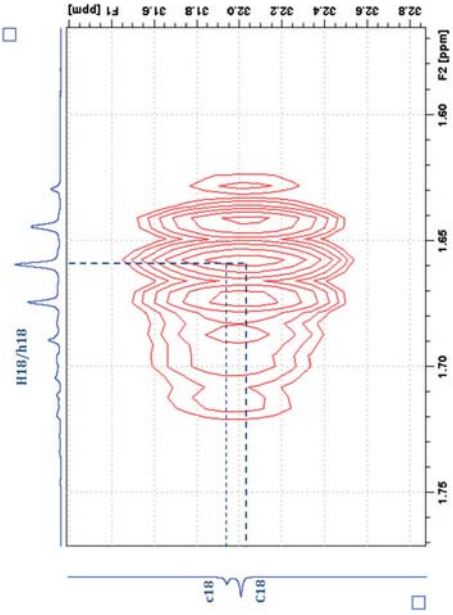

Figure XXI.34: 2D HSQC detail related to region 12

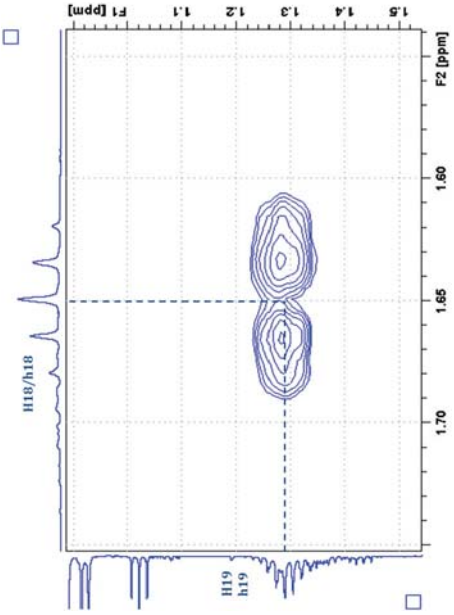

Figure XXI.35: 2D COSY detail related to region 12 and region 13

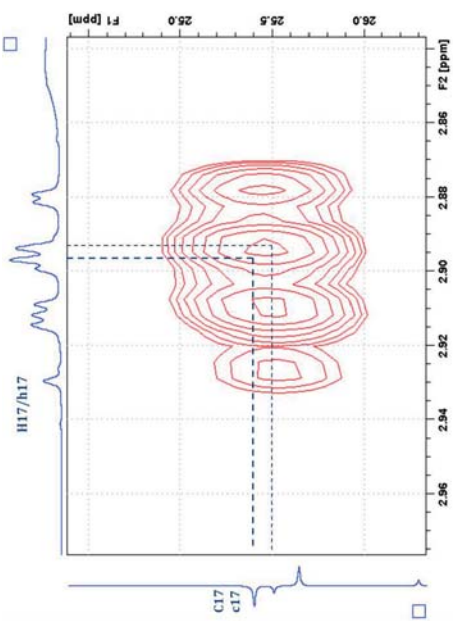

Figure XXI.36: 2D HSQC detail related to region 8

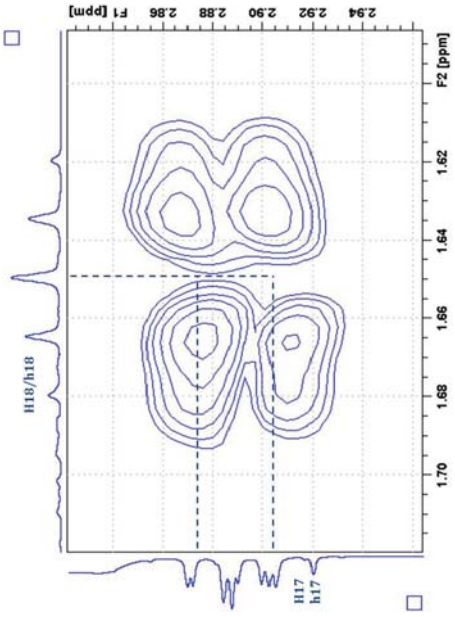

Figure XXI.37: 2D COSY detail related to region 12 and region 8

With respect to the presented data above, a full annotation for spin system 4 can be made as following region 8 is the signal of H17 and h17, region 12 is the signal of H18 and h18 and region 13 is the signal of H19 and h19.

F. Quaternary carbon assignment

Here below, in **Figure XXI.38**, a detailed view is given of the APT region containing quaternary carbon signals. Taking into account theoretical values, A can be assigned to the carbonyl carbon 2 and F to the bromine bearing carbon 7. The four remaining quaternary carbon signals are further studied *via* 2D HMBC experiments.

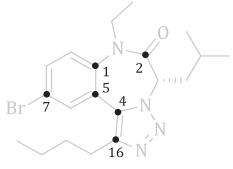

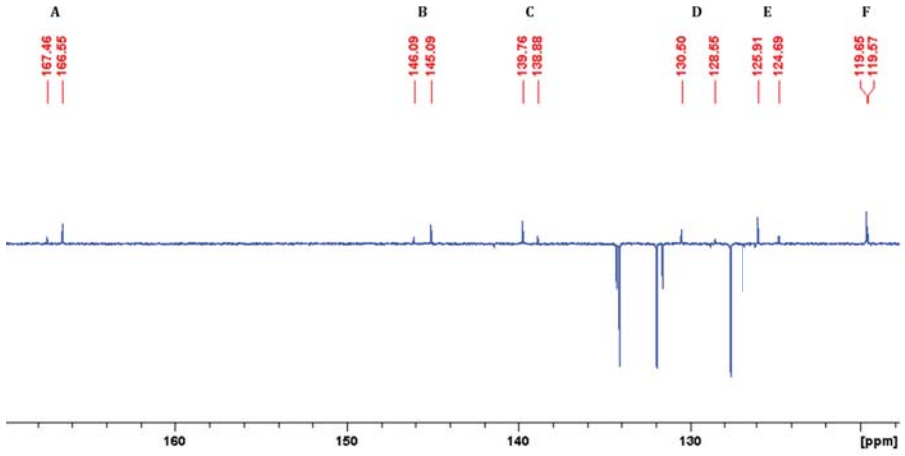

Figure XXI.38: Detail C13 APT quaternary carbon region

In **Figure XXI.39**, a 2D HMBC is depicted where strong cross peaks can be seen for both H17 and H18 and B, and for H17 and D. Therefore assigning, B to C16 and D to C4. In **Figure XXI.40** another 2D HMBC detail is presented which shows a strong cross peak between H9 (no H6 or H8) and E, even more H6/H8 cross peaks are found with C. Both observations lead to the assignment that E represents C5 and C corresponds with C1.

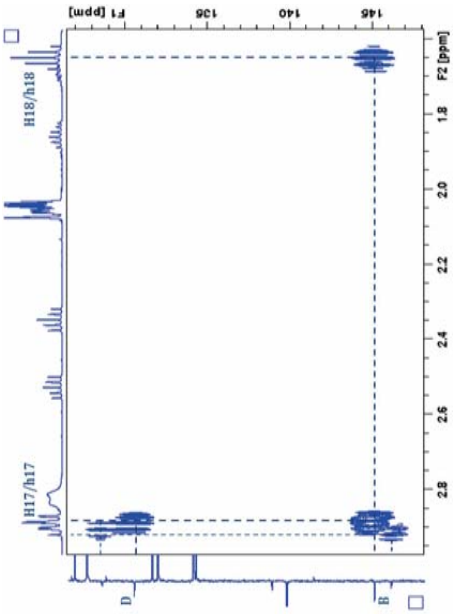

Figure XXI.39: 2D HMBC detail related to quaternary carbons B and D

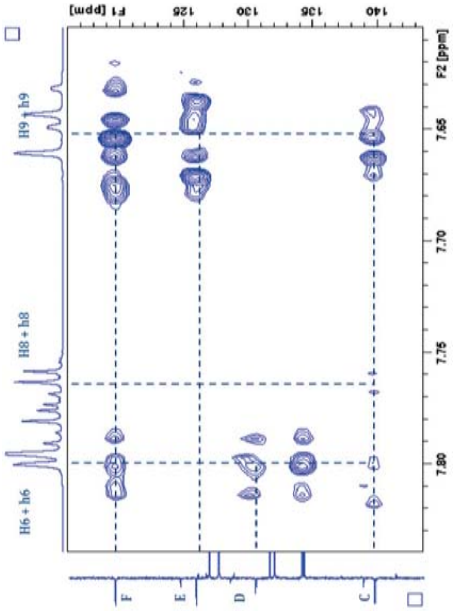

Figure XXI.40: 2D HMBC detail related to quaternary carbons C - F

G. Overview

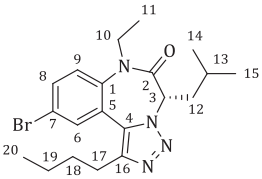

-

label	multiplicity	range (ppm)	integration	annotation
1	m	7.80 - 7.76	2	H6+h6 H8+h8
2	m	7.66 - 7.63	1	H9+h9
3	app t	5.62 - 5.59	0.26	h3
4	t	4.73 - 4.71	0.73	H3
5	m	4.23 - 4.14	1.00	H10a+h10a
6	app sextet	3.81 - 3.74	0.28	h10b
7	app sextet	3.70 - 3.63	0.72	H10b
8	m	2.92 - 2.87	1.95	H17
9	m	2.56 - 2.50	0.73	H12a
10	m	2.38 - 2.32	0.73	H12b
11	m	1.89 - 1.83	0.82	H13
12	m	1.71 - 1.62	2.07	H18+h18
13	m	1.44 - 1.23	4.00	H19+h19 h13 h12a h12b
14	t	1.03 - 1.00	0.84	h11
15	d	0.92 - 0.91	2.18	H14 or H15
16	m	0.89 - 0.82	8.62	H15 or H14 H20+h20 H11 h14 or h15
17	d	0.75 - 0.75	0.83	h15 or h14

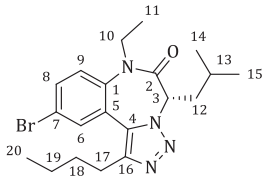

-

range (ppm)	annotation	range (ppm)	annotation
13.1	C11	58.5	C3
13.3	c11	66.4	c3
14.0	C20	119.6	c7
14.0	c20	119.7	C7
22.1	c14 or c15	124.7	c5
22.2	c15 or c14	125.9	C5
22.7	C14 or C15	126.9	c9
22.7	C19	127.6	C9
22.8	c19	128.6	c4
22.9	C15 or C14	130.5	C4
25.3	C17	131.6	c6
25.4	c17	131.9	C6
25.6	C13	134.1	C8
26.2	c13	134.3	c8
31.8	c18	138.9	c1
31.9	C18	139.8	C1
35.2	C12	145.1	C16
37.4	c12	146.1	c16
45.0	C10	166.6	C2
45.2	c10	167.5	c2